An examination of the impact of cellular age on leukaemic transformation to understand biological differences in paediatric and adult acute myeloid leukaemia

Shahzya Shahrin Chaudhury

MBBChir MA (Cantab) MRCP FRCPath

A thesis submitted in fulfilment of the requirements for a Doctor of Philosophy at the University of Glasgow

Institute of Cancer Sciences
College of Medical, Veterinary and Life Sciences
University of Glasgow

Submitted: February 2018

Abstract

Acute myeloid leukaemia (AML) is a heterogeneous disorder and patient age is an independent prognostic factor for clinical outcome. Treatment of paediatric AML is largely extrapolated from adult trial data, despite age related disease heterogeneity. Normal haemopoietic stem and progenitor cells (HSPCs) display differences in cellular behaviour and molecular landscape with age, which may influence leukaemic transformation. Using a murine model to represent infant (foetal liver (FL), childhood (3 week (w)), young adult (10w) and middle aged adult (>52w) age groups, the impact of HSPC age on oncogene mediated leukaemogenesis was investigated.

Assessment of transformation *in vitro* suggests that FL HSPCs are more resistant to leukaemia transformation. Using the NUP98-HOXA9 (NH9) fusion oncogene leukaemia model it was demonstrated that cells negative for cell surface lineage makers but expressing stem cell antigen 1 and cKit (LSKs) from all 4 ages transformed *in vitro*. However, a trend towards delayed transformation in FL-LSKs was observed. While post-foetal (3w, 10w and >52w) common myeloid progenitors (CMP) and granulocyte macrophage progenitors (GMP) also transformed, FL-CMPs and GMPs did not. Other oncogenes including the fusion oncogene AML1-ETO (A1E) and internal tandem duplications of the FLT3 gene (FLT3-ITD) also transformed FL-LSKs but consistently failed to transform FL-CMP and GMPs. This suggests that, independent of the oncogenic insult, foetal transformation relies on specific features of the LSK that are absent from FL committed myeloid progenitors.

These results were corroborated by *in vivo* data, showing that recipients transplanted with NH9 expressing LSKs derived from young (FL and 3w) donors were less susceptible to leukaemia with a longer latency to disease and incomplete penetrance compared to recipients transplanted with adult (10w and >52w) LSKs. This suggests that young stem cells possess foetal specific protective mechanisms, which prevent or delay the development of AML *in vivo*, regardless of self-renewal *in vitro*. Furthermore, despite pre-transplant expansion in myeloid conditions, a small proportion of young, but not adult pre-leukaemic

LSKs, gave rise to acute lymphoblastic leukaemia (ALL) or mixed phenotype acute leukaemia (MPAL) suggesting foetal/young LSKs retain a lymphoid bias that can overcome myeloid programmes. Both results from *in vivo* studies are in line with clinical data, showing a lower incidence of AML in childhood and predominance of ALL.

The observations from *in vitro* and *in vivo* data were complemented by gene expression analysis. Targeted gene expression analysis demonstrated the expression of multiple lineage pathways in young (FL and 3w) pre-leukaemic and leukaemic cells, while adult (10w and >52w) pre-leukaemic and leukaemic cells exhibited myeloid restricted transcription. In contrast, adult pre-leukaemic and leukaemic cells exhibited stem cell programmes, which have been implicated in aggressive disease. Upregulation of the BMP pathway in adult pre-leukaemic cells implicates a mechanistic role for the bone marrow microenvironment driving aggressive and myeloid restricted disease in adult LSKs. Global gene expression analysis using RNA-sequencing on *in vivo* generated AML cells mirrored these findings. This analysis revealed, in addition, apoptotic and tumour suppressive programmes were enriched in young-AML while pro-leukaemic programmes, including pathways related to the oncogene Myc, were enriched in adult-AML. Therefore, despite using the same oncogenic model to drive AML, cellular age discriminated disease at the transcriptional level and adult-AML expressed transcriptional programmes associated with a more aggressive disease.

The results of this thesis demonstrate that cellular age does indeed influence oncogene mediated transformability and leukaemia phenotype. Age defined transcriptional pathways that may impact pathogenesis, response to therapy and therapeutic targets have also been identified. In the era of personalised medicine in which a patient's mutational, transcriptional and epigenetic profile is considered when making therapy decisions, the consequence of cellular ontogeny on leukaemia biology should also inform treatment decisions. In particular, novel therapeutic targets must be specifically sought in the paediatric context as potential targetable dysregulated pathways in paediatric AML are not necessarily the same as adult AML.

Table of Contents

List of Tables

List of Figures

Acknowledgement

First and foremost I want to thank my primary supervisor, Dr Karen Keeshan, for all the guidance and support she has given me. I am indebted to your mentorship. I must also thank my co-supervisor, Prof Brenda Gibson, for her help in the clinical aspects of the project especially. Between you both I have had inspiring scientific and clinical role models and the knowledge I have gained from you I will take into my future career.

My colleagues in the Keeshan lab and Office 5 are the best group of people a person could hope to work with. I would like to thank all past and present members for their tutelage, support and banter. I must particularly mention Caitriona, Joana, Mara, Kai, Jenny and Chris, who became like a second family to me during my PhD.

The Paul O'Gorman Leukaemia Research Centre is an inspiring, friendly and fun place to work and I am thankful for all the friends I have made. I must especially thank Karen Dunn and Jennifer Cassels for their technical expertise.

This research would not have been possible without the funding from the Yorkhill Leukaemia and Cancer Research Fund, Yorkhill Children's Charity, Yorkhill Children's Foundation and Children with Cancer UK.

Finally, I want to thank my family, Dulal, Bilkish and Lameya, for their unwavering love and support.

Author's Declaration

I declare that except where explicit reference is made to the contribution of others, this thesis represents original work carried out by myself and has not been submitted for any other degree at the University of Glasgow or any other institution.

Signed name:

Printed name: SHAHZYA SHAHRIN CHAUDHURY

Abbreviations

5-FU	5-fluorouracil
7-AAD	7-aminoactinomycin-D
αMEM	α-Minimum Essential medium
ABC	ATP binding cassette
A1E	AML1-ETO
AGM	Aorta-gonad-mesonephros
AMKL	Acute megakaryoblastic leukaemia
AML	Acute myeloid leukaemia
ANGPT1	Angiopoietic-1
APL	Acute promyelocytic leukaemia
ALL	Acute lymphoblastic leukaemia
ASXL1	Additional sex combs like 1
ATO	Arsenic trioxide
ATRA	all-transretinoic-acid
B-ALL	B acute lymphoblastic leukaemia
BCRP1	Breakpoint cluster region pseudogene 1
BM	Bone marrow
BME	2-mercaptoethanol
BMI1	B lymphoma Mo-MLV insertion region 1
BMP	Bone morphogenetic protein
BMPR1A	BMP receptor 1a
BMT	Bone marrow transplant
bp	Base pair
BRDU	5-bromo-27-deoxyuridine
BRE	BMP responsive element
CAFC	Cobblestone-area forming cell
CAR	CXCL12 abundant reticular
CB	Cord blood
CBF	Core binding factor
CD	Cluster of differentiation
cDNA	Complementary DNA
C/EBP	CCAAT-enhancer binding protein

CFC	Colony forming cell
CLP	Common lymphoid progenitor
CML	Chronic myeloid leukaemia
CMP	Common myeloid progenitor
CN	Cytogenetically normal
CR	Complete remission
Cre	Cyclisation recombination recombinase
CRU	Competitive repopulating unit
CTV	CellTrace™ Violet
d	Day
DAPI	4',6-diamidino-2-phenylindole
DAVID	Database for Annotation, Visualization and Integrated Discovery
ddH_2O	Double distilled water
ddNTP	Chain terminating dideoxynucleotides
dNTP	Dideoxynucleotides
DDR	DNA damage response
DEG	Differentially expressed gene
DKK1	Dickkopf1
DLL	Delta-like
DMEM	Dulbecco's Modified Eagle medium
DMSO	dimethysulfoxide
DS	Down syndrome
E	Embryonic day (Eg. E14.5, embryonic day 14.5)
E2A	E box binding protein 2A
EBF	Early B cell factor
ECM	Extracellular matrix
EFS	Event free survival
EPCR	Endothelial protein receptor C
EPO	Erythropoietin
ES	Embryonic stem
ESLAM	$CD45^+EPCR^+CD48^-CD150^+$ HSCs
EtOH	Ethanol
ETP	Early thymocyte progenitor
ETV6	Ets variant 6

EV	Empty vector
Exo I	Exonuclease I
EZH2	Enhancer of zeste homolog 2
F	Phenylalanine
FAB	French-American-British
FACS	Fluorescence activated cell sorting
FBS	Foetal bovine serum
FC	Fold change
FDR	False discovery rate
FL	Foetal liver
fl	Floxed
FLT3	FMS-like tyrosine kinase 3
FLT3-ITD	Internal tandem duplications of FLT3
FMO	Fluorescence-minus-one
FOG-1	Friend of GATA1
FoxO	Forkhead box
FSC-A	Forward scatter-area
FSC-H	Forward scatter-height
Fz	Frizzled
γH2AX	Gamma-H2AX
G	Glycine
G-CSF	Granulocyte stimulating factor
GEMM	Granulocyte erythroid macrophage megakaryocyte
GEP	Gene expression profiling
GFI1	Growth factor independent 1
GFP	Green fluorescent protein
GM	Granulocyte macrophage
GMP	Granulocyte macrophage progenitor
GM-SCF	Granulocyte/macrophage stimulating factor
GO	Gemtuzumab ozogamicin
GPI	Glycosylphosphatidylinositol
GSEA	Gene Set Enrichment Analysis
GSK3ß	Glycogen synthase kinase 3 beta
Gy	Gray

^{3}H-Tdr	^{3}H-thymidine
h	Hours
H&E	Haematoxylin and eosin
H3K4me3	Tri-methylation of lysine 4 on histone H3
HEPES	4-(2-hydroxyethyl)-1-piperazineethanesulfonic acid
HERP	Hes related repressor protein
HES	Hairy-enhancer of split
Hh	Hedgehog
HMGA2	High Mobility Group AT-Hook 2
HOX	Homeobox
HPC	Haemopoietic progenitor cell
HSC	Haemopoietic stem cell
HSCT	Haemopoietic stem cell transplant
HSPC	Haemopoietic stem and progenitor cell
ICN	Intracellular notch
ID	Inhibitor of DNA binding
IDH	Isocitrate Dehydrogenase
IFC	Integrated fluidic circuit
IFN	Interferon
IHC	Immunohistochemistry
IL	Interleukin
IPS	Induced pluripotent stem
IRES	Internal ribosome entry site
ITD	Internal tandem duplication
JAG	Jagged
JM	Juxtamembrane
KEGG	Kyoto Encyclopedia of Genes and Genomes
KO	Knock out
LDA	Limiting dilution assay
L-Glut	L-glutamine
LIC	Leukaemia initiating cell
Lin	Lineage
LK	$Lin^{-}cKit^{+}$
LMPP	Lymphoid-primed multipotent progenitor

LRP	Low density lipoprotein receptor related protein
LSC	Leukaemia stem cell
LSK	$Lin^{-}Sca\text{-}1^{+}cKit^{+}$
LTC-IC	Long-term culture initiating cell
LT-HSC	Long term haemopoietic stem cell
m	Months
MA9	MLL-AF9
MACS	Magnetic activating cell sorting
M-CSF	Macrophage colony-stimulating factor
MDR1	Multidrug resistance protein 1
MDS	Myelodysplastic syndrome
MEP	Megakaryocyte erythroid progenitor
MFI	Median fluorescent intensity
min	Minutes
ML-DS	Myeloid leukaemia of Down syndrome
MLL	Mixed lineage leukaemia
MLL-PTD	Partial tandem duplication of the MLL gene
MLLr	MLL rearranged
MPAL	Mixed phenotype acute leukaemia
MPL	Thrombopoietin receptor
MPN	Myeloproliferative neoplasm
MPO	Myeloperoxidase
MPP	Multipotent progenitor
MMTV-tTA	Murine mammary tumour virus–tet-controlled transcriptional activator
MS	Median survival
MSC	Mesencymal stem cells
MSCV	Murine stem cell virus
MSigDB	Molecular Signatures Database
NES	Normalised enrichment score
NGS	Next generation sequencing
NH9	NUP98-HOXA9
NHEJ	Non-homologous end joining
NER	Nucleotide excision repair

NIH	National Institute of Health
NPM1	Nucleophosmin 1
NOD/SCID	Non-obese diabetic/severe combined immunodeficiency
NSD1	Nuclear receptor binding SET domain protein 1
NSG	Non obese diabetic severe combined immunodeficiency gamma
OS	Overall survival
PAX5	Paired box 5
PB	Peripheral blood
PBS	Phosphate buffered saline
PC1	First principle component
PC2	Second principle component
PCA	Principle component analysis
pIC	polyinosinic polycytidylic acid
PS	Penicillin/Streptomycin
PTCH	Patched
PTEN	Phosphatase and tensin homolog
PU.1	Purine box factor 1
qPCR	Quantitative polymerase chain reaction
RANKL	Receptor activator of nuclear factor κβ ligand
RARA	Retinoic acid receptor alpha
RARγ	Retinoic acid receptor gamma
Rb	Retinoblastoma
RBC	Red blood cell
RFS	Relapse free survival
rh	Recombinant human
Rho	Rhodamine-123
RIN	RNA integrity number
rm	Recombinant murine
RNA-seq	RNA sequencing
RPMI1640	Roswell Park Memorial Institute medium 1640
R-SMAD	Responsive SMAD
ROS	Reactive oxygen species
RR	Relapse rate
RT	Room temperature

s	Seconds
Sca-1	Stem cell antigen 1
SCF	Stem cell factor
SD	Standard deviation
SDF-1	Stromal derived factor 1
Sl	Steel
SLAM	Signalling lymphocyte activation molecule
SMO	Smoothened
SNP	Single nucleotide polymorphisms
SOX17	Sex determining region Y box 17
SP	Side population
SSC-A	Side scatter-area
ST-HSC	Short-term haemopoietic stem cell
SV	Streptavidin
T-ALL	T-acute lymphoblastic leukaemia
TAM	Transient abnormal myelopoiesis
TE	Tris-EDTA
TET2	Tet methylcytosine dioxygenase 2
TGFß	Transforming growth factor ß
Thy1.1	Thymocyte antigen 1.1
TPO	Thrombopoietin
T&T	Transduction and transplantation
US	Unstained
UT	Untransduced
w	week
W	ckit gene
WB	Wash buffer
WCC	White cell count
WES	Whole exome sequencing
WGS	Whole genome sequencing
WHO	World Health Organization
WT	Wild type
y	Years
YFP	Yellow fluorescent protein

1 Introduction

1.1 Haemopoiesis

Haemopoiesis refers to the formation of blood cellular components. Blood cells are derived from the haemopoietic stem cell (HSC), from which terminally differentiated effector cells for all haemopoietic lineages are formed. In order to maintain the haemopoietic system for life, haemopoiesis is tightly regulated. The term 'haemopoietic stem cell' was first used by Artur Pappenheim in the late 19th century to describe a common precursor from which red and white blood cells were derived. (Ramalho-Santos and Willenbring, 2007) The first experimental evidence of HSCs came from seminal work by Till and McCulloch in 1961. They demonstrated a population of clonogenic bone marrow (BM) cells that could generate multilineage colonies in the spleen of lethally irradiated recipients, termed the colony forming unit-spleen. Some of the cells from these colonies could be re-transplanted into lethally irradiated secondary recipients and reconstitute the immune system and were thus proposed to be HSCs. (Till and McCulloch, 1961) These cells demonstrated the 2 cardinal characteristics defining the HSC; the ability to self-renew and multilineage differentiation potential (multipotency). Since then developments in multicolour flow cytometry has allowed the prospective purification of haemopoietic stem and progenitor (HSPC) populations and *in vitro* and *in vivo* clonogenic assays have allowed their functional assessment and enumeration. Investigation of haemopoiesis has primarily been conducted in the murine system and correlated with human haemopoiesis. Murine models employing gene editing technology have greatly enhanced our understanding of haemopoiesis. Cyclisation recombination recombinase (Cre) from bacteriophage P1 recognises specific LoxP sequences and excises LoxP-flanked (floxed (fl)) DNA at high efficiency. (Sauer and Henderson, 1988) Conditional deletion with Cre-LoxP technology allows gene inactivation in a tissue-specific manner. Inducible systems in which *Cre* expression is activated by an exogenous ligand, such as tamoxifen or tetracycline, allows greater control over Cre mediated deletion and can circumvent embryonic and neonatal lethality in gene deletion models. Correlation of murine and human ages will be discussed in Section 3.1.1.

1.1.1 Haemopoietic hierarchy

Haemopoiesis is hierarchically organised with a small population of HSCs at the apex and terminally differentiated blood cells at the base. A summary of the haemopoiesis hierarchy is shown in Figure 1.1. When HSCs divide the daughter cells must decide their fate, to remain HSCs (self-renewal), differentiate or die by apoptosis. With each step down the haemopoietic hierarchy, cells lose self-renewal ability and become progressively more lineage restricted. Long-term repopulating HSCs (LT-HSC) retain unlimited self-renewal and multilineage ability. Experimentally, LT-HSCs are able to stably reconstitute all blood lineages in lethally irradiated recipients for >16 weeks (w). LT-HSCs differentiate to give rise to short-term reconstituting HSCs (ST-HSC). ST-HSCs retain multipotency but have limited self-renewal and are only able to reconstitute lethally irradiated recipients for 8w. (Morrison and Weissman, 1994) ST-HSCs further differentiate into a multipotent progenitor (MPP), which retain multipotency but demonstrate no or very brief self-renewal. (Morrison et al., 1997) Thereafter, MPPs differentiate into oligolineage haemopoietic progenitor cells (HPCs) that are progressively restricted in their lineage output and demonstrate no self-renewal capability. (Na Nakorn et al., 2002) The common lymphoid progenitor (CLP) is restricted to produce B-lymphoid, T-lymphoid and natural killer cells. The common myeloid progenitor (CMP) is restricted to produce myeloid and erythroid cells. CMPs further differentiate into the granulocyte macrophage progenitor (GMP) that gives rise to granulocytes and monocytes/macrophages, and the megakaryocyte erythroid progenitor (MEP) that gives rise to platelets and erythrocytes. (Akashi et al., 2000) Both CLP and CMP populations can give rise to dendritic cells. (Traver et al., 2000, Manz et al., 2001)

This pyramidal model of haemopoiesis has recently been challenged with the identification of the lymphoid-primed multipotent progenitor (LMPP). The LMPP has lymphoid, granulocyte and macrophage potential but lacks megakaryocyte and erythroid potential. This paradigm suggests that the MEP diverts early in haemopoiesis from the ST-HSC while CLP and GMPs are derived from the intermediate LMPP. (Adolfsson et al., 2005, Mansson et al., 2007) More recently, Notta *et al* have proposed a 2-tier model for adult haemopoiesis. In this model,

MPPs differentiate into unipotent progenitors, capable of producing a single cell type, while megakaryocytes differentiate directly from the HSC. Interestingly the authors suggest that for foetal haemopoiesis, blood cells develop via oligolineage progenitors. (Notta et al., 2016) However, while the pyramidal model may be a simplification of normal haemopoiesis, it serves as a useful operational paradigm and basis for experimental investigation.

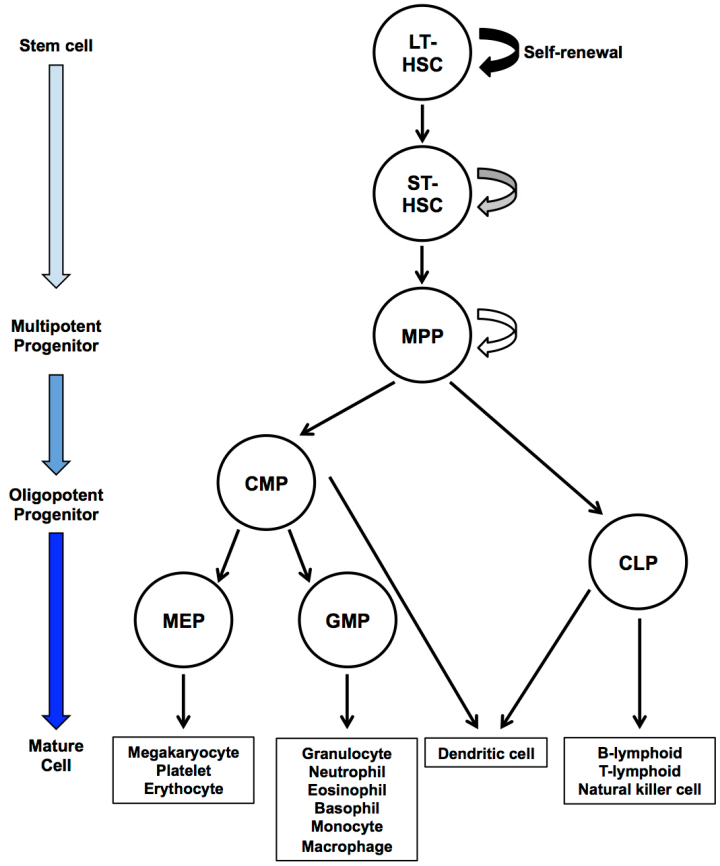

Figure 1.1 Haemopoietic hierarchy

Diagram depicting the haemopoietic hierarchy from stem cells to multipotent progenitors, to oligopotent progenitors to mature blood cells.

1.1.2 Defining and identifying HSC and progenitor populations

The study of HSPCs requires prospective isolation of HSPC populations. The identification of surface markers defining HSPC populations has progressed the study in this area. In murine BM, HSCs and MPPs are contained in a small population that lack cell surface lineage markers that are found on terminally differentiated cells. In addition, these lineage negative (Lin^-) cells also express the cell surface markers cKit and stem cell antigen 1 (Sca-1). cKit or cluster of

differentiation (CD) 117 is the receptor for the cytokine stem cell factor (SCF) and Sca-1 is a glycosylphosphatidylinositol (GPI) anchored cell surface protein whose biological function is largely unknown. The $Lin^{-}Sca\text{-}1^{+}cKit^{+}$ (LSK) cells comprise 0.1% of the BM. (Spangrude et al., 1988)

Additional cell surface marker combinations are employed to further classify HSCs and MPPs within the LSK compartment. The expression of surface thymocyte antigen 1.1 (Thy1.1) and FMS-like tyrosine kinase 3 (Flt3) can subdivide the LSK population. Thy1.1 or CD90 is a GPI anchored surface protein. Flt3 (also Flk-2) is the receptor kinase for the FLT3 ligand. Using this system, populations are defined as: LT-HSC $Thy^{lo}Flt3^{-}$, ST-HSC $Thy^{lo}Flt3^{+}$ and MPPs $Thy^{-}Flt3^{+}$. (Figure 1.2) (Christensen and Weissman, 2001) The expression of the signalling lymphocyte activation molecule (SLAM) family of receptors, CD150 and CD48 can subdivide LSKs into HSC, MPP and the progenitor populations HPC-1 (akin to the LMPP) and HPC-2 (akin to the MEP). Using this system, populations are defined as: HSC $CD150^{+}CD48^{-}$, MPP $CD150^{-}CD48^{-}$, HPC-1 $CD150^{-}CD48^{+}$ and HPC-2 $CD150^{+}CD48^{+}$. (Figure 1.2) (Kiel et al., 2005) The expression of the endothelial protein receptor C (EPCR) and the leukocyte common antigen CD45 on SLAM defined HSCs ($CD45^{+}EPCR^{+}CD150^{+}CD48^{-}$) further enriches for the LT-HSC (ESLAM). (Kent et al., 2009) Quiescent HSCs can also be defined based on their ability to efflux the dyes Rhodamine-123 (Rho) and Hoechst 33324. In the later case, when Hoechst 33324 stained cells are exposed to ultraviolet light and examined for 2 wavelength emissions, HSCs are found in the side population (SP) of dimly fluorescent cells, adjacent to the majority of BM or FL cell. Thus, HSC can be defined as $CD45^{dim}Lin^{-}Rho^{-}SP$. (Uchida et al., 2004)

The immunophenotype of oligolineage progenitors has also been devised. From within the $Lin^{-}cKit^{+}$ but $Sca\text{-}1^{-}$ (LK) population, CMP, GMP and MEP populations can be identified by the expression of surface CD34 and CD16/32. CD34 is a surface glycoprotein involved in cell-to-cell adhesion. CD16/32 or Fcγ receptor-II/III is involved in the humoral immune response. (Akashi et al., 2000) CLP are identified as Lin- cells with low expression of cKit and Sca-1. In addition, they express the receptor for interleukin (IL) 7 (IL7Rα). (Kondo et al., 2000) Thus, progenitor populations are defined as: CMP LK-$CD34^{+}CD16/32^{+}$, GMP LK-

$CD34^{+}CD16/32^{hi}$, MEP LK-$CD34^{-}CD16/32^{-}$ and CLP $Lin^{-}cKit^{lo}Sca\text{-}1^{lo}IL7R\alpha^{+}$. (Figure 1.2)

For the most part, cell surface markers defining adult HSPCs also apply to foetal stem and progenitor cells too. Apart from the expression of CD11b on foetal stem cells, foetal LSKs are functionally similar to adult LSKs in that they exhibit self-renewal and multilineage output in reconstitution studies. (Morrison et al., 1995) In addition, foetal CMP, GMP and MEPs defined as above exhibit similar lineage outputs and hierarchical organisation as their adult counterparts do. (Traver et al., 2001)

In acute myeloid leukaemia (AML), the leukaemia initiating event does not necessarily occur within the most primitive HSC. In fact, progenitors with limited or no self-renewal capability have been implicated as the cell of origin (see Section 3.1.2). Therefore, in this thesis, the most primitive population investigated is the heterogeneous LSK compartment, which contains LT-HSCs, ST-HSCs and MPPs. The myeloid committed progenitors CMP and GMP populations are also investigated.

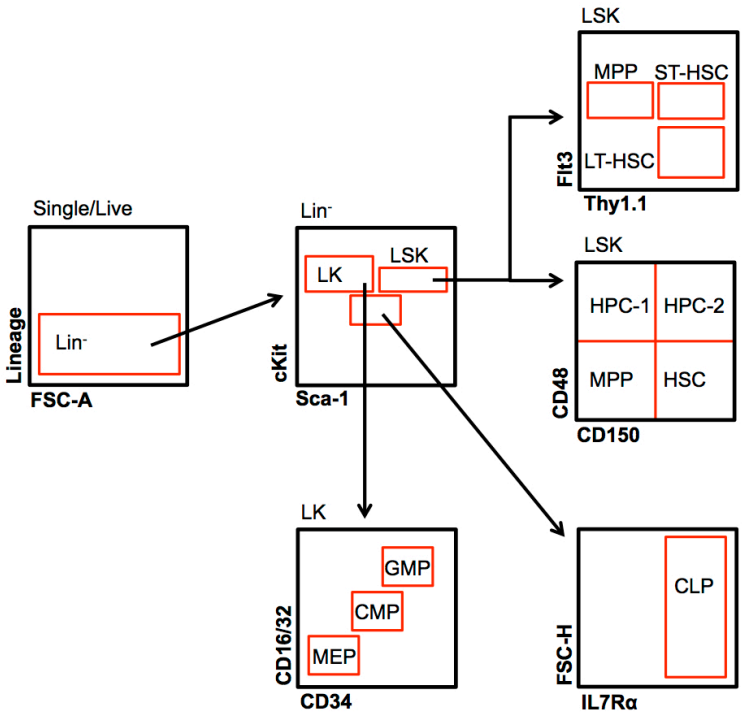

Figure 1.2 Immunophenotyping of HSPCs

Schematic showing multiparametric flow cytometry strategy for the identification of HSPCs based on surface marker expression.

1.1.2.1 Defining and identifying human HSC and progenitor populations

Human HSPCs have not been as well defined as they have been in the murine system. In 1984 Civin *et al* identified a surface marker found on 1-4% of BM cells that was highly enriched for *in vitro* colony forming cell (CFC) ability. The marker, initially called My10, was later identified as CD34. (Civin et al., 1984) In 1988 Berenson *et al* demonstrated that $CD34^+$ cells could fully reconstitute the haemopoietic compartment of lethally irradiated baboons, proving their ability to self-renew and their multipotency. (Berenson et al., 1988) Subsequently, reconstitution experiments using non-obese diabetic/severe combined immunodeficiency (NOD/SCID) mice allowed further characterisation and refinement of human HSCs. The expression of CD38 further delineates HSCs from committed progenitors. CD38 is a surface protein and functions in cell adhesion and signal transduction. Both foetal and adult HSCs reside within the $CD34^+CD38^-$ compartment while progenitors reside within the $CD34^+CD38^+$ compartment. (Bhatia et al., 1997) Committed myeloid progenitors have also been classified within the $CD34^+CD38^+$ compartment by differential expression of CD45RA and IL3Ra. Both foetal and adult progenitor populations are defined as: CMP

IL3Ra^{+}CD45RA^{-}, GMP IL3Ra^{+}CD45RA^{+} and MEP IL3Ra^{lo}CD45RA^{-}. (Manz et al., 2002) Foetal and adult CLPs on the other hand, reside in the CD34^{+}CD38^{-} compartment and can be either identified as CD34^{+}CD38^{-}CD10^{+}CD45RA^{+} or CD34^{+}CD38^{-}CD7^{+}. (Hoebeke et al., 2007, Hao et al., 2001, Galy et al., 1995)

1.1.3 Lineage determination

Differentiation down a lineage path occurs as a result of interplay between intrinsic temporal expression of key lineage determining transcription factors and exogenous cytokine signalling. The key transcription factors and cytokines involved in lineage determination are depicted in Figure 1.3.

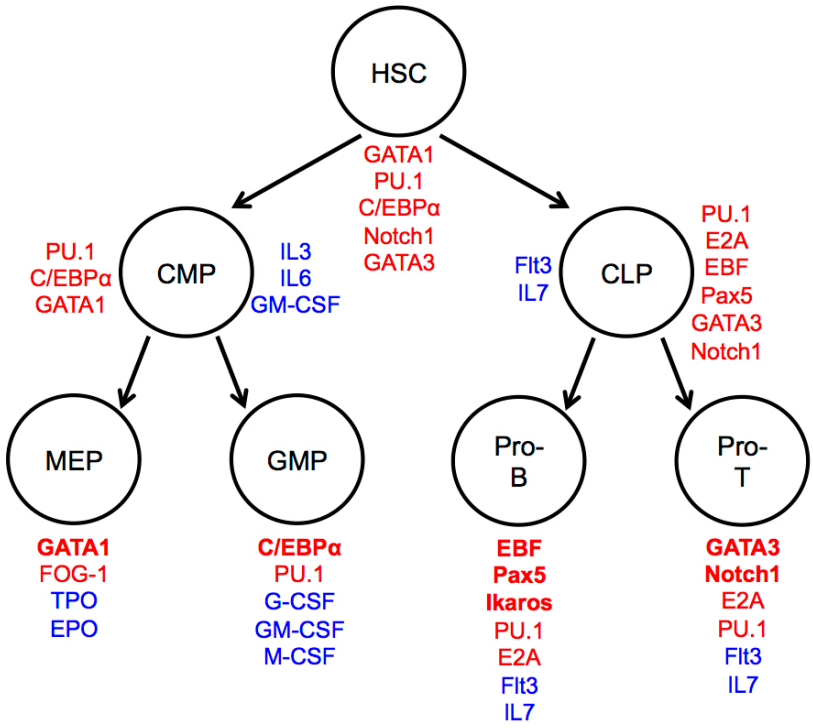

Figure 1.3 Key transcription factors and cytokines in lineage determination

Diagram showing the key transcription factors (red) and cytokines (blue) involved in murine progenitor lineage determination. The most important transcription factors for progenitor differentiation are shown in bold.

1.1.3.1 Myelopoiesis

The CMP differentiates to form mature granulocytes, monocytes, erythrocytes and platelets. Granulocytes comprise of neutrophils, eosinophils and basophils, which are all involved in the innate immune system. Monocytes mature into tissue macrophages and are involved in the inflammatory response. Haemoglobin

containing erythrocytes transport oxygen and carbon dioxide and platelets function to stop bleeding at sites of injury. Cell surface markers distinguishing myeloid cells include CD11b/Mac1 (granulocytes and macrophages), GR1 (granulocytes), F4/80 (macrophages), Ter119 (erythrocytes) and CD41 (platelets).

Cytokines important in myeloid differentiation include granulocyte colony stimulating factor (G-CSF), granulocyte/macrophage colony stimulating factor (GM-CSF), macrophage colony stimulating factor (M-CSF), IL3 and IL6, which are important for granulocytes and macrophage differentiation. Erythropoietin (EPO) is important for erythrocytosis and thrombopoietin (TPO) is important for megakaryocyte differentiation. Mice deficient for G-CSF display severe neutropenia. (Lieschke et al., 1994) However, mice deficient for GM-CSF and EPO display only minor perturbations in progenitor and terminally differentiated progeny, suggesting a degree of redundancy in cytokine mediated differentiation. (Stanley et al., 1994, Wu et al., 1995)

Transcription factors important for granulocyte and macrophage differentiation include purine box factor 1 (PU.1) and the CCAAT-enhancer binding protein (C/EBP) family of transcription factors, in particular C/EBPα. These factors cooperate to regulate the expression of myeloid cytokine receptors. (Friedman, 2002) Conditional deletion of *Pu.1* in adult BM results in complete loss of CMP and GMP progenitor populations. (Dakic et al., 2005) Conditional deletion or knock out (KO) of *Cebpa (Cebpa*$^{-/-}$*)* results in the absence of GMPs and a decrease in CMPs. (Zhang et al., 1997a) The transcription factors GATA1 and its co-factor, friend of GATA1 (FOG-1), are critical for both erythroid and megakaryocyte differentiation. *GATA1* deficient embryos cannot generate erythroid cells and die *in utero* due to severe anaemia. (Pevny et al., 1991) Conditional deletion of *Gata1* in megakaryocytes results in thrombocytopenia and deregulated megakaryocyte proliferation, revealing a critical role for GATA1 in megakaryocyte function. (Shivdasani et al., 1997) *FOG-1* deficient mice display partial erythroid arrest and complete failure of megakaryopoiesis. (Tsang et al., 1998)

In this thesis flow cytometry analysis is used to identify terminally differentiated myeloid cells by expression of the surface marker CD11b. Myeloid cells are further characterised with GR1 to detect granulocytes and F4/80 to detect monocytes/macrophages.

1.1.3.2 Lymphopoiesis

CLPs differentiate to form B and T-lymphoid precursors. Cytokines that are important in lymphoid determination include Flt3 ligand and IL7. The Flt3 receptor is first expressed on ST-HSCs and MPPs. Mice with mutated *Flt3* gene or deficient for Flt3 ligand display reduced B and T-lymphoid progenitors but normal HSC and CMP numbers, showing that Flt3 is specifically important in lymphopoiesis. (Mackarehtschian et al., 1995, Sitnicka et al., 2002) The expression of the IL7 receptor IL7Rα defines the CLP population immunophenotypically. Mice deficient for either *Il7* or *Il7ra* display severe defects in lymphoid differentiation. (Corcoran et al., 1998, Peschon et al., 1994) Mice deficient for both Flt3 ligand and *Il7ra* show complete absence of B-lymphopoiesis. (Sitnicka et al., 2003)

1.1.3.3 B-Lymphopoiesis

CLPs differentiate in the BM to form the early pro B-precursor, which ultimately differentiate into mature B-lymphoid cells. B-lymphoid cells function as the humoral component of the adaptive immune system, producing antibodies on exposure to pathogens. B-cell differentiation is reliant on the expression of key transcription factors: PU.1, Ikaros, early B cell factor (EBF), E box binding protein 2A (E2A) and paired box 5 (Pax5). (Georgopoulos et al., 1994, Scott et al., 1994, Bain et al., 1994, O'Riordan and Grosschedl, 1999, Nutt et al., 1999) Inactivation of any of these factors results in severe B-lymphoid deficiency. Cell surface markers used to detect B-lymphoid cells include B220 and CD19. B220 is expressed on all committed B-lymphoid precursors from the early pro-B stage. CD19 is expressed from the slightly later pro-B stage. Both B220 and CD19 expression is retained on mature B-cells. (Lyons and Parish, 1994) In this thesis both surface B220 and CD19 expression is used to identify B-lymphoid cells by flow cytometry.

1.1.3.4 T-Lymphopoiesis

Unlike myeloid and B-lymphoid cells, the primary site of T-lymphopoiesis is the thymus. Progenitors with T-lymphoid potential migrate to the thymus and differentiate into the early thymocyte progenitor (ETP). T-cell precursors express surface CD3 and retain CD3 expression on mature T-cells. T-lymphoid differentiation is characterised by the expression of CD4 and CD8 surface markers. ETPs differentiate into T-cell precursors which lack either CD4 or CD8 cells (double negative cells). They then differentiate into precursors that express both CD4 and CD8 (double positive cells). Finally, double positive cells differentiate into single positive $CD4^+$ T-helper cells or $CD8^+$ T-cytotoxic cells. Single positive cells leave the thymus and reside in peripheral organs. T-lymphoid differentiation is dependent on the transcription factors GATA3 and Notch1. Deficiency in either transcription factor results in an early block in T-cell maturation. (Schmitt et al., 2004, Ting et al., 1996) In this thesis surface marker expression of CD3, CD4 and CD8 is used to detect T-lymphoid cells by flow cytometry. Surface and intracellular CD3 expression is also identified by immunohistochemistry (IHC).

1.1.3.5 Lineage plasticity

In general, differentiation down a particular lineage is thought to be a 1-way process. However, there is evidence of reprogramming of lineage committed precursors and terminally differentiated cells. Ectopic expression of human CSF-R1 (the receptor for M-CSF) in murine pro-B cell lines results in a loss of all B-cell lineage markers. Furthermore, CSF-R1 expressing cells give rise to macrophage like cells. (Borzillo et al., 1990) Conditional deletion of *Pax5* in mature B-cells can induce conversion to macrophages or T-cells. (Cobaleda et al., 2007, Nutt et al., 1999) Forced expression of C/EBPα in B-precursor cells can reprogram them to macrophages. (Xie et al., 2004) It is likely that lineage committed progenitors do not de-differentiate under steady state conditions. However, during periods of stress it is conceivable that committed progenitors can switch lineage. The other situation in which this could occur is forced expression of abnormal lineage determining transcription factors by oncogenes,

which may be a mechanism for aberrant lineage expression and lineage switching in acute leukaemia.

1.2 Haemopoietic ageing

The previous section described how the haemopoietic system is maintained by a small number of highly specialised HSCs that are capable of self-renewal and have multilineage output potential. However, HSCs display differences in number, cell cycle status, lineage bias and molecular characteristics with age. While ageing is a continuous process, stages of haemopoietic ageing have been described. In the murine system, foetal stage is up to birth, neonatal up to 21 days (d) and juvenile is considered 3-6w. Young adult is considered 8w-6 months (m), middle-aged 10-15m and aged/old is considered 18-24m. (Flurkey et al., 2007, Dutta and Sengupta, 2016) The characteristics of each age group are summarised in Figure 1.4. Like haemopoiesis, haemopoietic ageing has been extensively investigated in the mouse, as a model for human haemopoietic ageing. The characteristics of ageing in the murine and, where available, the human system, will be described.

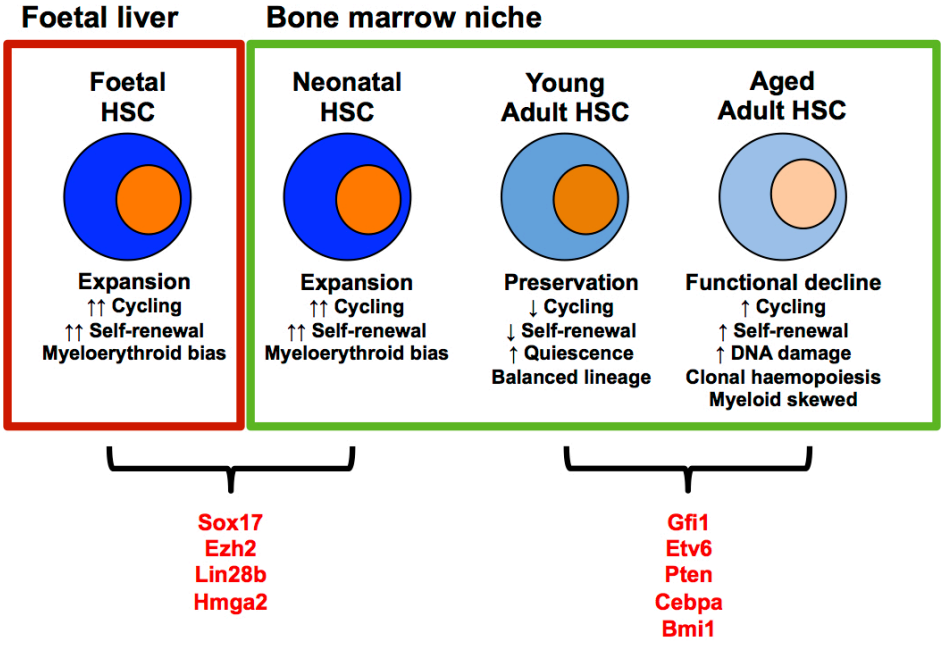

Figure 1.4 Changes in HSCs with age

Diagram showing the changes in HSC behaviour and location with age. Genetic regulators in young and adult HSCs are shown in red.

1.2.1 Foetal haemopoiesis and the development of the haemopoietic system

The function of the foetal HSC is to generate the haemopoietic system. Two waves of embryonic haemopoiesis are present: primary and definitive. The primary wave aims to quickly expand the number of erythroid cells to maximise oxygen transport. In mice, the primary wave occurs at embryonic (E) day 7.5 with the emergence of primitive erythroid restricted haemopoietic cells from the yolk sac. These cells do not have long-term repopulating ability. (Palis et al., 1999) The definitive stage aims to produce all lineages in the developing haemopoietic system and is associated with the emergence of the first engrafting HSC. The first HSCs with long-term multilineage engrafting potential in BM transplant (BMT) studies emerge from the ventral aspect of the aorta-gonad-mesonephros (AGM) at E10.5 in the murine system, and to a lesser degree from the yolk sac and placenta. (Medvinsky and Dzierzak, 1996, Gekas et al., 2005, Kumaravelu et al., 2002) They then migrate to the foetal liver (FL) where the HSC pool expands and differentiates to form progenitors and terminally differentiated blood cells. (Houssaint, 1981, Ikuta and Weissman, 1992) E14.5 is the age when the FL contains the highest proportion of HSCs. From E15 onwards, HSCs migrate from the FL to the BM, the definitive site of haemopoiesis in postnatal life. This migration is largely controlled by the CXCL12 (also known as stromal derived factor 1 (SDF-1)) ligand and its receptor CXCR4, which regulates HSC homing to the BM. At E15.5 the BM from wild type (WT) embryos is cellular with a predominance of myeloid and erythroid precursors. In contrast, BM from embryos haploinsufficient for CXCR4 is hypocellular with marked reduction in haemopoiesis. (Ma et al., 1998) Migration from the liver to the BM continues in the first 2w of life. Thereafter, HSCs remain in specialised regions of the BM termed the BM niche or microenvironment. (Schofield, 1978) The BM niche is described in more detail in Section 1.4.

Lineage tracing studies in mice have shown that haemopoietic cells detectable in adults are derived from HSCs generated prenatally. In a non-invasive technique for HSC labelling, *Cre* is under the control of the *Runx1* locus. Administration of tamoxifen results in ß-galactosidase labelling of *Runx1* expressing HSCs. HSCs labelled at E9.5 made a high contribution to blood cells generated 9-12m later in

the adult mouse. (Samokhvalov et al., 2007) In another study HSCs are labelled with yellow fluorescent protein (YFP), which can be detected by flow cytometry. Using the *SCL-Cre-YFP* model, *Cre* expression is limited to HSCs by the control of the stem cell enhancer of the stem cell leukaemia gene. Tamoxifen induces irreversible recombination, resulting in YFP labelling of HSCs. *SCL-Cre-YFP* foetuses were induced to express YFP at E14.5. Mice were either delivered and allowed to grow until 5m of age, or sacrificed at E14.5 and YFP^+ FL HSCs harvested and transplanted into adult recipients. At 5m, both groups showed 10% of all BM cells were YFP^+, denoting they had originated from a foetal HSC. (Gothert et al., 2005) Therefore, foetal HSCs can repopulate the adult BM compartment. Furthermore, foetal derived HSCs contribute to the adult BM compartment. As the percentage of YFP^+ cells was similar in the transplanted and non-transplanted group, this suggests that beyond E14.5, *de novo* generation of HSCs is rare. Therefore, studies of foetal HSC function have concentrated at the E14.5 stage, as it is at this age that large numbers of definitive HSCs are localised in the FL and directly contribute to adult haemopoiesis.

1.2.2 Differences in foetal and adult HSCs

1.2.2.1 Proliferative activity

In line with the expansion of HSCs seen in the FL, FL HSCs are highly cycling. 5-fluorouracil (5-FU) and ^{3}H-thymidine (^{3}H-Tdr) are both pharmacological agents that target actively cycling cells. BMT of E14.5 FL cells from pregnant females treated with 5-FU or E14.5 FL cells treated with ^{3}H-Tdr *in vitro* results in 1000 and 100 fold decrease in competitive repopulating units (CRU) respectively, compared to untreated controls, showing that the engrafting HSC from FL is in active cycle. In contrast, *in vitro* treatment with ^{3}H-Tdr has no effect on the number of CRUs from adult 10w BM. BMT of FL and BM from E14.5, 3w, 4w and adult 10w sorted by cell cycle status show that up to 3w of age, the engrafting cell is within the $G_1/S/G_2/M$ actively cycling compartment. At 4w and beyond, the engrafting cell is within the G_0 quiescent compartment. Thus, FL HSCs are actively cycling until 3w of age, after which there is an abrupt switch to a quiescent phenotype. (Bowie et al., 2006) Studies of cell cycle status show that near 100% of FL HSCs are in active cycle and divide every 1-2 days, compared to

adult HSCs that cycle every month or even more infrequently. (Nygren et al., 2006, Pietras et al., 2011) The highly proliferative nature of FL cells is also reflected in their transcriptional profile. FL and neonatal HSCs (up to 3w) exhibit higher expression of cell cycle and self-renewal regulating genes (e.g. *Ccnd2*, *Ikaros*, *MEF*, *Rae28*). In contrast, adult HSCs have higher expression of genes associated with HSC maintenance (e.g. *Atm*, *Ezh2*, *Gata2*, *Mel18*). (Bowie et al., 2007b)

This post-natal switch has not been investigated directly in human studies. However, measurement of telomere shortening as a surrogate for prior cell divisions suggests that HSCs in children rapidly divide in the first year of life. Thereafter, there is an abrupt decline in proliferation between 1-3 years (y) and a further decline after 13y to an adult rate of cell division. (Rufer et al., 1999, Sidorov et al., 2009) Interestingly, human cord blood (CB) $CD34^+$ are exclusively found to be in G_0/G_1 and not in $S/G_2/M$. (Wilpshaar et al., 2000) This may reflect some discrepancy in the cell cycle status of murine and human neonatal cells. Neonatal cycling HSCs may not be found in the $CD34^+$ compartment or cycling neonatal HSCs may not survive in the circulation.

1.2.2.2 Self-renewal

FL HSCs display exaggerated self-renewal, which can be demonstrated in repopulation studies. Rebel *et al* compared the reconstitution ability of FL from E14.5 foetuses and adult (10w) BM. Comparable donor HSC dose was achieved by calculating the number of CRUs present in each group. Donor reconstitution was assessed in peripheral blood (PB) at 4, 8 and 16w post BMT. At all time points, FL showed a higher percentage of donor derived reconstitution. (Rebel et al., 1996) Bowie *et al* assessed the repopulating ability of FL HSCs at E14.5 and BM HSCs from E18.5, 3w, 4w and 10w mice. BMT of FL HSCs showed superior repopulating capacity compared to 10w BM, FL recipients reaching maximal donor chimerism at 8w post BMT versus 24w in 10w BM recipients. Donor cells from E18.5 and 3w BM displayed similar reconstitution kinetics to FL, whereas 4w BM displayed similar kinetics to adult 10w BM, suggesting that between 3-4w of age, there is an abrupt switch from a foetal to an adult phenotype that is independent of microenvironment. (Bowie et al., 2007b) Similar to murine studies, human FL

(14-21w gestation) and CB also display enhanced repopulating ability compared to adult BM. BMT of Lin^- cells from FL generated more primitive $CD34^+CD38^-$ cells *in vivo* and long-term culture initiating cells (LTC-IC) *in vitro*, compared to CB, which in turn generated more than adult BM. (Holyoake et al., 1999)

1.2.2.3 Lineage output

As well as superior repopulating ability, FL HSCs exhibit different lineage outputs compared to adult BM. Lineage output assessed by CFC assay and flow cytometry of donor engrafted recipients, shows that donor FL type HSCs (E14.5, E18.5 and 3w) are myeloerythroid biased. Post BMT FL type HSCs produce a 2-fold higher contribution of myeloid cells to the total leukocyte progeny, compared to adult HSCs (4w and 10w). (Bowie et al., 2007b) Using single cell transplants of HSCs (defined as $CD45^{dim}Lin^-Rho^-SP$) from adult BM (8-12w), Dykstra *et al* identified 4 subtypes (α, ß, γ and ð) of murine HSC based on their contribution to myeloid and lymphoid cells in PB of primary recipients 16w post BMT. α-HSCs predominantly generated myeloid cells (granulocytes and monocytes), ß-HSCs generated myeloid and lymphoid (B and T) cells, γ-HSCs generated mainly lymphoid cells and few myeloid and ð-HSCs only produced lymphoid cells. Furthermore, α and ß-HSC were the only HSCs that had self-renewal properties and could serially engraft secondary recipients. (Dykstra et al., 2007) Similar single cell BMT experiments (using ESLAM defined HSCs), investigating foetal, neonatal and adult HSCs showed that these 4 HSC subtypes were present in foetal and neonatal mice. However, in E14.5 FL only 5% of HSCs were of α-subtype, compared to adult BM (8-12w) in which 27% were of α-subtype. This is despite the myeloid bias observed in the progeny cells of FL donor HSCs. By 3w, the α-HSC content of the BM was already very similar to that of adult BM, at 23%. In E18.5 mice the α-HSC content in BM mirrored that of the adult BM while in the FL it mirrored that of the E14.5 FL, suggesting that the increase in α-HSCs with increasing age is extrinsically determined by the BM microenvironment. (Benz et al., 2012)

1.2.2.4 Response to exogenous growth factors

Foetal HSCs exhibit different responses to exogenous factors compared to adult HSCs. SCF is a transmembrane growth factor that binds to cKit (CD117) on the surface of HSCs to promote self-renewal, proliferation and differentiation. FL and adult HSCs have comparable levels of surface cKit expression. (Ikuta and Weissman, 1992) However, response to SCF stimulation differs in FL and HSCs. Mice with mutations at the steel (*Sl*) locus (*Sl/Sl* mice) have no functional SCF and die at E15-16 from anaemia. While the absolute number of FL HSCs in *Sl/Sl* mice was 18-23% of WT littermate controls, the rate of HSC expansion between E13-E15 was comparable, suggesting that SCF is not required for foetal HSC development or FL expansion. (Ikuta and Weissman, 1992) Mice with mutations of the *cKit/W* gene lack functional cKit. The W^{41} mutation encodes a single amino acid change which results in attenuated SCF mediated cKit activation. *In vitro*, self-renewal divisions in FL and adult (10w) HSCs are dependent on cKit activation. However, FL HSCs respond to a 6-fold lower dose of SCF compared to adult HSCs. Furthermore FL HSCs from W^{41}/W^{41} mice exhibit reduced ability to repopulate primary recipients compared to WT FL HSCs. In fact, repopulation kinetics are comparable to WT adult HSCs, suggesting that a heightened response to SCF contributes to the increased self-renewal observed in FL-HSCs. (Bowie et al., 2007a)

1.2.2.5 Regulation of the foetal to adult HSC phenotype switch

As discussed above, FL HSCs are highly proliferative with enhanced self-renewal. This phenotype persists until 3w of age, even after HSCs have migrated to the BM. Thereafter, there is an abrupt switch in proliferative activity between 3 and 4w of age to a more quiescent adult phenotype. This suggests that cell intrinsic factors determine the foetal to adult phenotype switch rather than localisation in the BM microenvironment, which is also developing. Other feedback mechanisms informing the HSCs that haemopoietic and BM niche development is complete may trigger the foetal to adult phenotype switch. The 'master regulator' that triggers the phenotype switch at 3-4w has not been elucidated. Transcriptional studies have identified genes that are particularly crucial for either foetal or adult HSC function. Developmentally determined changes in the

expression of these genes are postulated to control the foetal to adult phenotype switch. The experimental models will be described in brief here and expanded in Section 5.1.2.2.

Genes important in adult HSC maintenance, self-renewal and quiescence include B lymphoma Mo-MLV insertion region 1 (*Bmi1*), Ets variant 6 (*Etv6*), *CEBPa* and growth factor independent 1 (*Gfi1*). (Park et al., 2003, Hock et al., 2004a, Hock et al., 2004b, Ye et al., 2013) Genes critical for foetal HSC generation, maintenance and self-renewal include sex determining region Y box 17 (*Sox17*), enhancer of zeste homolog 2 (*Ezh2*), *Lin28b* and high mobility group AT-hook 2 (*Hmga2*). (Kim et al., 2007, Mochizuki-Kashio et al., 2011, Copley et al., 2013) *Sox17* is highly expressed in foetal HSCs but expression declines after 4w. *Sox17*$^{-/-}$ embryos fail to develop HSCs and conditional deletion of *Sox17* in E14.5 and neonates results in a marked reduction in HSC number. Conditional deletion of *Sox17* in endothelial cells and HSCs can be achieved using the *Tie2-Cre* model. (Koni et al., 2001) Conditional deletion of *Sox17* in mice >4w old has no effect on HSC number or function, showing that *Sox17* is crucial for foetal HSC development but redundant for adult HSCs function. (Kim et al., 2007) EZH2 is a component of the polycomb repressive complex 2. Conditional deletion of *Ezh2* in haemopoietic and endothelial cells, using the *Tie2-Cre;Ezh2*$^{fl/fl}$ mouse model, results in embryonic death in mid-gestation due to anaemia, and significantly reduced numbers of HSCs in the FL at E14.5. In contrast, deletion of *Ezh2* in adult BM does not affect the reconstitution potential of adult HSCs, suggesting that *Ezh2* is required for foetal but not adult HSC maintenance. (Mochizuki-Kashio et al., 2011) LIN28B is an inhibitor of the *Let-7* family of inhibitory microRNAs that inhibit gene expression, including *Hmga2*. FL LSKs and HSCs display upregulation of *Lin28b* and its downstream target *Hmga2* compared to adult LSKs and HSCs, while the *Let-7* family is downregulated in FL populations. Overexpression of *Lin28b* or *Hmga2* in adult HSCs results in increased repopulating ability in primary and secondary recipients post BMT, similar to BMT with FL HSCs. Conversely, *Hmga2*$^{-/-}$ mice can generate HSCs but FL-HSCs displayed a 10-fold reduction in repopulating ability post BMT compared to WT FL HSC controls. (Copley et al., 2013)

1.2.3 Adult haemopoiesis and the maintenance of the haemopoietic system

Once the haemopoietic system has been established, it is the function of the post-foetal adult HSCs to maintain the haemopoietic system in that organism for life. Therefore, it is crucial that the genetic integrity of adult HSCs is maintained to ensure mutations are not passed onto progeny cells. Unlike foetal HSCs, adult HSCs are quiescent in order to minimise replicative errors. Concordant with this, adult HSC display attenuated self-renewal compared to FL HSC, resulting in an inferior repopulating ability post BMT. (Holyoake et al., 1999, Bowie et al., 2007b, Rebel et al., 1996) Furthermore, adult HSCs display a balanced myeloid and lymphoid output. (Bowie et al., 2007b)

1.2.3.1 Proliferative activity

One of the major mechanisms protecting HSC function and genomic integrity is that adult HSCs are largely quiescent. In contrast to the highly proliferative FL HSCs, only 5% of adult cells are in active cycle. Proliferative stress by serial transplantation results in HSC functional decline and eventual exhaustion. (Harrison and Astle, 1982, Siminovitch et al., 1964) LT-HSCs treated *in vitro* with the DNA polymerase inhibitor, aphidicolin, show strikingly impaired *in vivo* reconstitution ability with early onset BM failure and death of primary recipients. (Flach et al., 2014) In addition, *in vivo* replicative stress by treatment with polyinosinic polycytidylic acid (pIC), interferon (IFN) α, G-CSF, TPO or repeated venesection in adult (8-16w) mice causes LT-HSCs to enter cell cycle and is associated with an accumulation of DNA damage (measured by the comet tail assay). (Walter et al., 2015) Dormant HSCs express high levels of retinoic acid protein, a metabolite of vitamin A. Treatment of mice with the retinoid all-transretinoic-acid (ATRA), results in attenuated stress induced activation of HSCs. Conversely, absence of dietary vitamin A results in disrupted HSC re-entry into dormancy following inflammatory stress and loss of HSC number. (Cabezas-Wallscheid et al., 2017)

Frequency of HSC proliferation has been studied using label-retaining assays. DNA is labelled i*n vivo* using 5-bromo-27-deoxyuridine (BRDU) followed by a long chase period of up to 306d. Cells that retain BRDU labelling have cycled most

infrequently. Such studies have shown that 2 populations of adult HSCs exist that can be classified by their cycling frequency. An ‘active’ population, comprising of 90-95% of the HSC pool, cycles relatively frequently at a rate of once every 36d, suggesting these HSCs contribute to the steady state maintenance of haemopoietic cells. A ‘dormant’ population, comprising of 5-10% of the HSC pool, cycles extremely rarely at a rate of once every 145d or less. The dormant population is enriched for LT-HSCs, as evidenced by serial transplantation studies. Interestingly, *in vivo* stimulation by G-CSF or BM injury (by 5-FU or BRDU injection) stimulates dormant HSCs into cycle. However, upon repair of the blood system, activated HSCs return to a state of dormancy, suggesting dormant HSCs act as a reserve that can be relied on during periods of stress. (Wilson et al., 2008)

Conversely, quiescent HSCs display an attenuation of DNA damage response (DDR) and repair mechanisms, favouring the error-prone non-homologous end joining (NHEJ) DNA repair mechanism. (Mohrin et al., 2010) Therefore, while quiescence protects HSCs from replicative stress, other genotoxic stresses can result in DNA damage. However, upon entry into cell cycle, HSCs upregulate DDR mechanisms and repair DNA strand breaks, allowing for DNA repair before replication. (Beerman et al., 2014)

1.2.3.2 Other protective mechanisms in adult HSCs

Other mechanisms that aid the maintenance of genomic integrity of adult HSCs include prevention of telomere shortening, protection against oxidative stress, and expression of membrane transporters that expel toxic compounds from the intracellular compartment.

Both murine and human HSCs have active telomerase activity. (Hiyama et al., 1995, Morrison et al., 1996a) Loss of telomerase activity results in reduced HSC self-renewal with an attenuation of serial transplantation ability. (Allsopp et al., 2003) The presence of telomerase, coupled with the dormant nature of HSCs, prevents uncapping of telomeres and telomere shortening.

Reactive oxygen species (ROS) are chemically active by-products of oxygen metabolism that can cause cellular damage via oxidative mechanisms. To minimise ROS induced damage, adult HSCs reside in the hypoxic BM niche. (Mohyeldin et al., 2010) In addition, due to the low metabolic activity of HSCs, HSCs employ anaerobic glycolytic metabolism pathways to further reduce the generation of ROS. (Kocabas et al., 2012, Simsek et al., 2010) The oxidative stress response is regulated in part by the Forkhead box (FoxO) family of proteins. FoxO proteins are highly expressed in adult HSCs. *FoxO* deficient mice exhibit increased levels of ROS and display reduced self-renewal activity compared to WT controls. (Tothova and Gilliland, 2007) Therefore, the adult HSC employs various methods to protect against ROS induced damage.

ATP binding cassette (ABC) transporters are transmembrane proteins that efflux toxins out of the intracellular compartment, thus minimising toxic damage to the cell. (Holland and Blight, 1999) ABC transporters, such as breakpoint cluster region pseudogene 1 (BCRP1) and multidrug resistance protein 1 (MDR1), are highly expressed on HSCs at the protein and transcriptional level. Loss of *Bcrp1* in murine HSCs results in HSC depletion, reduced survival under hypoxic conditions and increased sensitivity to the chemotherapy agent mitoxantrone. (Zhou et al., 2001, Krishnamurthy et al., 2004)

1.2.3.3 Lineage output

BMT of single cells and single cell generated colonies from adult (10w) HSCs show that like FL, the dominant HSC is the ß-subtype (balanced myeloid and lymphoid potential). However, adult BM contains a higher proportion of α-HSCs (myeloid predominant). (Benz et al., 2012) Despite this, compared to BMT of FL HSCs, adult HSCs results in a balanced lineage output in primary and secondary recipients, in keeping with maintaining homeostatic blood production. (Bowie et al., 2007b)

1.2.3.4 Molecular regulation of adult HSC function

As alluded to above, genes important in adult HSC maintenance, self-renewal and quiescence are different to the genes important in foetal HSC function.

These include *Bmi1*, *Etv6*, *Cebpa* and *Gfi1*. (Park et al., 2003, Hock et al., 2004a, Hock et al., 2004b, Ye et al., 2013) BMI1 is a component of the polycomb repressor complex 1. *Bmi1*$^{-/-}$ mice show normal HSC development and numbers in the FL. However, at 4-5w, there is a 10-fold reduction in HSC number compared to WT and heterozygous controls, accompanied by an inability of total BM from 5w *Bmi1*$^{-/-}$ mice to initiate long term engraftment in primary recipients. (Park et al., 2003) *Etv6* is essential for adult HSC survival. Inducible Cre mediated conditional deletion of *Etv6* in adult (6-10w) mice is achieved by the administration of pIC using the *Mx-Cre* model. Following *Etv6* deletion, there is a gradual decline in LSK number to almost undetectable levels 4w post pIC administration. (Hock et al., 2004b) C/EBPα is a transcription factor that regulates granulopoiesis. In adult HSCs, C/EBPα is also a negative regulator of cell cycle and promotes quiescence. (Johnson, 2005) *CEBPa* gene expression levels increase with increasing age with a 2-fold increase in 4w HSCs compared to 2w HSCs. *CEBPa* KO in adult HSCs results in increased proliferation and repopulating ability compared to WT controls. Conversely, overexpression of *CEBPa* in foetal HSC induces quiescence. (Ye et al., 2013) The zinc-finger repressor GFI1 also regulates function and quiescence in adult HSCs. *Gfi*$^{-/-}$ mice develop HSCs normally, and phenotypically defined LSKs are higher in *Gfi*$^{-/-}$ 4w old mice compered to WT controls. However, LSK function is compromised with an inability to serially engraft secondary recipients. Limiting dilution assays (LDA) show a 200-fold reduction in functional HSCs in *Gfi*$^{-/-}$ compared to WT control. Furthermore, cell cycle analysis by *in vitro* incorporation of BRDU over a 3d period show that 67% of *Gfi*$^{-/-}$ LSKs have cycled over that time, compared to only 28% of WT LSKs. (Hock et al., 2004a)

1.2.4 Aged haemopoiesis and potential disorders of the haemopoietic system

With increasing age, changes are observed in the haemopoietic system. In humans, ageing (>60-70y) is associated with anaemia, defective lymphopoiesis, myeloid skewing and dysregulated innate immunity. (Guralnik et al., 2004, Shaw et al., 2013, Montecino-Rodriguez et al., 2013) In addition, the incidence of clonal disorders, including AML and myelodysplastic syndrome (MDS) rise exponentially after the age of 60y. (Howlader N, 2014, Chaudhury et al., 2015)

Studies of human and murine ageing (in mice >24m), have shown that with increasing age there is an increase in the relative and absolute numbers of phenotypic HSCs but impaired function, with reduced self-renewal capacity, myeloid skewing and an accumulation of DNA damage. This results in a haemopoietic system at risk of malignant transformation.

1.2.4.1 HSC number and function

Murine studies have attempted to characterise changes in the haemopoietic system with age. Comparing young adult (2-4m) and aged adult (>24m) murine BM, there is an increase in the absolute numbers of LSKs and LT-HSCs, resulting in a 2-10 fold increase in immunophenotypic HSCs in aged mice. (Morrison et al., 1996b, de Haan et al., 1997, Rossi et al., 2005) BMT of total BM from young and aged mice show a greater number of donor derived LT-HSCs in recipients transplanted with aged BM, showing that the expanded HSC pool in aged BM retains self-renewal properties. (Rossi et al., 2005) Furthermore, cell cycle assessments show that a greater proportion of aged HSCs are in active cycle (12.5%), while young adult HSCs are largely quiescent with only 3% in cycle. (de Haan et al., 1997, Morrison et al., 1996b) However, at the single cell level, aged HSCs display inferior repopulating ability compared to young adult HSCs. BMT of equal numbers of young or aged immunophenotypically defined LT-HSCs show inferior donor derived reconstitution of white cell count (WCC) in PB in recipients of aged LT-HSCs. (Rossi et al., 2005) Aged HSCs also display inferior reconstitution ability in serial transplantation studies. (Dykstra et al., 2011, Flach et al., 2014)

Similarly, changes in HSC number and function are observed in humans. Comparing BM from healthy young (20-35y) and aged (>65y) persons, aged BM contains more immunophenotypic HSCs (defined as $Lin^{-}CD34^{+}CD38^{-}CD90^{+}CD45RA^{-}$) within the $CD34^{+}$ compartment and of the entire BM mononuclear fraction. However, as with murine studies, aged HSCs displayed inferior repopulating ability *in vivo*. Mice engrafted with aged human HSCs show lower human $CD45^{+}$ chimerism at 16w compared to mice engrafted with young HSCs (1% versus 2%, respectively). (Pang et al., 2011) Furthermore, assessment of cell cycle status by using RNA (Pyronin Y) and DNA (Hoechst 33342) dyes, show

that a greater percentage of aged HSCs are in active cycle (20-35% versus 5-15% of young HSCs). As discussed above, loss of HSC quiescence is associated with functional decline. (Siminovitch et al., 1964, Harrison and Astle, 1982) Therefore, as the haemopoietic system ages, HSCs number and cell cycle activity increases, in order to compensate for their functional decline. However, on-going replication may itself contribute to loss of HSC function.

1.2.4.2 Lineage skewing

The lineage output of young and aged adult murine HSCs has been investigated by *in vivo* reconstitution assays. Compared to young adult donors, BMT of total BM and HSCs from aged donors results in myeloid biased reconstitution and impaired numbers of lymphoid progeny. (Rossi et al., 2005, Sudo et al., 2000, Dykstra et al., 2011, Beerman et al., 2010, Flach et al., 2014) In Section 1.2.3.3 we discussed how compared to FL HSCs, young adult (10w) BM contained more myeloid predominant α-HSCs. Single cell transplants of HSCs show that with increasing age there is a further increase in the proportion of α-HSCs such that α-HSCs make up 45% of all HSCs in BM aged >52w. (Benz et al., 2012) Gene expression profiling (GEP) by microarray of LT-HSCs from young adult (2-3m) and aged adult (22-24m) mice show that aged HSCs upregulate genes related to myeloid specification, while pathways relating to lymphoid specification are downregulated. (Rossi et al., 2005) Therefore, murine models show that the aged haemopoietic system is progressively myeloid restricted.

Myeloid skewing of aged HSCs is also observed in human studies. *In vitro* differentiation and *in vivo* repopulation studies comparing human HSCs from young (20-35y) and aged (>65y) BM show higher myeloid to lymphoid ratio of progeny from aged HSCs. (Pang et al., 2011) Thus, aged HSCs have myeloid biased output which likely contributes to the increased incidence of myeloid malignancies observed at older age.

1.2.4.3 DNA damage

Ageing is associated with the acquisition of DNA damage. DNA damage can be directly quantified by measurement of the phosphorylation of histone H2 family

member X (gamma-H2AX (γH2AX)) staining and alkaline comet tail moments; both markers of DNA double strand breaks. Murine HSCs display increased γH2AX staining and alkaline comet tail moments with age. (Beerman et al., 2014, Flach et al., 2014, Rossi et al., 2007b) Similarly, at baseline, human $CD34^+$ HSCs from CB have less γH2AX staining compared to adult BM up to the age of 50y, which in turn had less γH2AX staining than from adults older than 50y. (Rube et al., 2011) HSCs from mice with impaired DNA repair mechanism display impaired self-renewal and repopulating ability compared to WT control. (Rossi et al., 2007a) With the observation that DNA damage increases with age, it is postulated that an accumulation of DNA damage drives the impaired function and myeloid skewing observed in aged HSCs.

It is tempting to assume that aged HSCs have attenuated DDR and repair mechanisms, which result in an accumulation of DNA damage. Quiescent young (6-12w) and aged (22-30m) adult HSCs do show attenuated DDR and repair associated genes (compared to FL HSCs), and tend to employ the error prone NHEJ DNA repair mechanism. (Mohrin et al., 2010) However, upon entry into cell cycle, young and aged adult HSCs upregulate DDR and repair genes to levels similar to FL HSCs. This is associated with a decrease in DNA damage (measured by reduced γH2AX staining and alkaline comet tail moments). In fact, after entry into cell cycle, aged HSCs show similar DNA damage to young adult HSCs, suggesting that aged HSCs can effectively employ DNA repair mechanisms. (Beerman et al., 2014) DNA damage can be induced by ionising radiation. Both young and aged adult murine HSCs can effectively repair DNA damage accrued as a result of ionising radiation. However, aged HSCs do so more slowly. (Flach et al., 2014) Similarly, in human HSCs, both young adult (<50y) and aged adult (>50y) HSCs can effectively repair DNA damage resulting from ionising radiation, although both are inferior to CB derived HSCs. (Rube et al., 2011) Therefore, while DDR and repair are slower in adult and aged HSCs, the accumulation of DNA damage in aged HSCs cannot be fully explained by attenuated DDR and repair mechanisms.

Mechanisms of increased DNA damage in aged HSCs include replication stress and telomere shortening. Stimulation of HSCs into cycle is associated with an

accumulation of DNA damage. (Flach et al., 2014, Walter et al., 2015) Furthermore, despite the presence of telomerase in HSCs, repeated replication does result in telomere shortening in aged HSCs. Critical telomere shortening can lead to permanent cell cycle arrest (senescence). (Allsopp et al., 2003) As discussed above, aged HSCs are less quiescent than young adult HSCs. Increased proliferative activity in aged HSCs, therefore, may drive replication associated DNA damage.

The result of increasing DNA damage with age is an accumulation of mutations that have implications on HSC function and malignant transformability. Whole genome sequencing (WGS) of normal HSPCs from healthy individuals with ages ranging from birth to 70y show that the number of mutations in HSPCs increases with increasing age. (Welch et al., 2012) In addition to gross strand breaks, aged HSCs can acquire mutations in genes resulting in oncogenic potential. Specifically, acquired mutations in epigenetic modifiers such as DNA methyl transferase 3A (*DNMT3A*), tet methylcytosine dioxygenase 2 (*TET2*), additional sex combs like 1 (*ASXL1*) and isocitrate dehydrogenase 1 and 2 (*IDH1/2*) are increasingly prevalent in aged HSCs. Mutations in these genes result in alterations in the epigenetic landscape and drive clonal haemopoiesis, a recognised precursor to AML development. (Busque et al., 2012, Genovese et al., 2014, Jaiswal et al., 2014, Xie et al., 2014) Clonal haemopoiesis and the implication for leukaemogenesis are discussed in Section 1.3.6.4.

1.2.5 Ageing is associated with transcriptional and epigenetic dysregulation

As discussed above, aged HSCs exhibit increased proliferation, impaired repopulating ability and myeloid skewed lineage output. At a transcriptional level, compared to young adult (2-3m) murine HSCs, aged HSCs (22-24m) upregulate genes associated with cell signalling pathways, myeloid specification, stress response, inflammation and protein aggregation. Genes related to lymphoid specification, maintenance of genomic stability and chromatin remodelling are downregulated. (Rossi et al., 2005, Chambers et al., 2007) These studies and the fact that mutations in epigenetic regulators are common in aged HSCs suggest that the epigenetic landscape alters with increasing age.

Comprehensive integrated genomic analysis of HSCs from young adult (4m) and aged adult (24m) mice show changes in the transcriptome, DNA methylation and histone modification that contribute to increasing DNA instability with increasing age. Aged HSCs exhibit broader tri-methylation of lysine 4 on histone H3 (H3K4me3, an epigenetic marker of gene activation) peaks across HSC identity and self-renewal genes, suggesting activation of these pathways. In addition, aged HSCs show hypomethylation at binding sites of transcription factors important in self-renewal and oncogenesis. (Sun et al., 2014)

1.3 Acute myeloid leukaemia

The term leukaemia refers to any disorder in which there is an accumulation of malignant leukocytes in the BM. Chronic leukaemia results in the uncontrolled proliferation of mature leukocytes. Acute leukaemia is characterised by uncontrolled proliferation and differentiation block resulting in the accumulation of immature blasts. A diagnosis of acute leukaemia is made when blasts make up >20% of the nucleated cells in the BM or PB. Acute leukaemia can be either lymphoid or myeloid. (Swerdlow et al., 2008) Acute lymphoblastic leukaemia (ALL) results in the accumulation of lymphoblasts and is the most common cancer in childhood (defined as <18y) with an incidence of 4-5/100,000 per annum. (Cancer Research UK, 2016) Effective chemotherapy regimens have improved clinical outcomes, such that childhood ALL is cured in >95% of cases. (Vora et al., 2013) AML results in the accumulation of myeloblasts with an overall incidence rate in all ages of 5/100,000 per annum. AML is rare in childhood, accounting for only 15% of childhood leukaemia and 5% of childhood cancers. (Cancer Research UK, 2014) However, unlike ALL, outcomes for AML in childhood are less favourable, with a 5 year overall survival (OS) of 65-70% and relapse rate (RR) of 30-35%. (Creutzig et al., 2013, Chaudhury et al., 2015) Therefore, despite its rarity, AML represents a significant disease burden and challenge in the paediatric cancer population.

1.3.1 Pathogenesis

1.3.1.1 The 2-hit model of leukaemogenesis

AML is a genetic disorder, resulting in the uncontrolled proliferation of myeloblasts that are arrested at an immature stage of differentiation. In 2002 Gilliland and Griffin hypothesised a multi-step 2-hit model for the pathogenesis of AML. This was based on the observation that *FLT3* mutations (resulting in the constitutive activation of FLT3 tyrosine kinase) could cause a myeloproliferative neoplasm (MPN) but was not sufficient to generate AML in murine models. Similarly, translocations resulting in oncogenes such as *PML-RARA* and *AML1-ETO* (*A1E*) were also not sufficient to cause AML but resulted in impaired differentiation of haemopoietic cells. They also observed that *FLT3* mutations often occurred in conjunction with gene rearrangements. Thus, the authors hypothesised that 2 types of mutations were required for the development of AML. Type I mutations activate signal transduction pathways and confer a proliferation advantage on hematopoietic cells. Examples of type I mutations include activating mutations in tyrosine kinase and Ras signalling pathways, such as *FLT3*, *NMP1* and *KIT* mutations. Type II mutations result in a maturation block and enhanced self-renewal. Examples of type II mutations include cytogenetic abnormalities resulting in the fusion oncogenes *PML-RARA*, *A1E* and *NUP98-HOXA9* (*NH9*), and mutations in transcription factors such as *CEBPA* and *RUNX1*. (Gilliland and Griffin, 2002) More recently, a third type of mutation, type III mutations have been described. These mutations affect epigenetic regulators such as *DNMT3A*, *IDH1/2* and *TET2*, and result in epigenetic dysregulation.

1.3.1.2 Leukaemia stem cells and clonal evolution

Similar to the concept of normal haemopoiesis in which differentiated cells arise from common HSCs, studies show that leukaemia is also hierarchically organised. At the apex of the hierarchy is the leukaemia stem cell (LSC), a quiescent, self-renewing cell from which the leukaemia bulk cells differentiate. (Dick, 2008) Experimentally, the LSC is the cell that can initiate AML in serial transplanted recipients. (Dick, 1996) Evidence for a stem cell origin for haematological malignancy arose from work in the 1960s and 1970s, which demonstrated that a small subset of malignant cells gave rise to clonally derived colonies *in vitro* and

in vivo. (Bruce and Van Der Gaag, 1963, Park et al., 1971) Seminal work by Bonnet and Dick showed that the LSC, able to initiate leukaemia in NOD/SCID recipient mice, arose from the $CD34^+CD38^-$ compartment of leukaemic blasts, regardless of the maturation status of the disease. These LSCs exhibit self-renewal capability, demonstrated by the ability to generate AML in secondary and tertiary recipients. Furthermore, the AML generated was identical to the donor disease, comprising of $CD34^+CD38^+$ and $CD34^-$ bulk leukaemic cells. Thus, similar to normal HSCs, LSCs demonstrate self-renewal, proliferative and differentiative properties. (Bonnet and Dick, 1997) At the same time, the Sutherland group demonstrated that human AML cells lacking CD90 could form leukaemic colonies *in vitro* after 8 weeks in suspension culture and engraft in NOD/SCID recipients. While most leukaemic populations with leukaemia maintenance properties *in vitro* and *in vivo* had a $CD34^+CD90^-$ phenotype, in one sample LSC activity was demonstrated in the $CD34^-CD90^-$ sub-fraction too, suggesting that LSCs are not limited to the $CD34^-$ fraction. (Blair et al., 1997) The same group also identified CD71 and CD117 (or cKit) expression as markers of functional LSCs. $CD34^+CD71^-$ populations sorted from human AML could engraft in NOD-SCID recipients while the $CD34^+CD71^+$ population did not. (Blair et al., 1998) Similarly, $CD34^+CD117^-$ compartment could also engraft in NOD/SCID recipients. In contrast, only the $CD34^+CD117^+$ compartment of normal bone marrow could engraft NOD/SCID recipients, showing that the LSC could be discriminated from normal HSCs immunophenotypically. (Blair and Sutherland, 2000) Jordon *et al* demonstrated aberrant expression of CD123 on $CD34^+CD38^-$ AML blasts but was lacking on normal $CD34^+CD38^-$ HSCs. Furthermore, $CD34^+CD123^+$ leukaemic blasts could initiate and maintain AML in NOD/SCID recipients. (Jordan et al., 2000) Abnormal $CD123^+$ LSCs displayed constitutive activation of the NFκB pathway at the transcriptional and protein level whereas normal CD123+ HSCs did not. This provides a molecular basis for the functional differences in $CD123^+$ LSC and HSC and is a potential therapeutic target. (Guzman et al., 2001)

Hope *et al* demonstrated hierarchical organisation within the LSC compartment. Human AML was serially transplanted into NOD/SCID mice and clonal analysis was performed by Southern hybridisation of DNA on the resultant AML. A single

patient sample could generate multiple clones. However, some clones only appeared in primary recipients, some were present in primary, secondary and tertiary recipients and others only emerged in later recipients. The authors concluded that LSCs, like normal HSCs, are hierarchically organised. Some LSCs have limited self-renewal capacity and clones generated from them are only evident in primary recipients. Others have long-term self-renewal capacity and are evident in secondary and tertiary recipients. (Hope et al., 2004) As such, it has been hypothesised that the cell of origin in AML is the HSC with inherent self-renewal and differentiative properties. As well as functional similarities with normal HSCs, LSCs also share transcriptional overlap with normal HSCs. Microarray analysis comparing the $CD34^{+}CD38^{-}$ (LSC) and $CD34^{+}CD38^{+}$ (bulk) population of 15 AML samples identified an LSC transcriptional signature. This transcriptional signature was shared with normal HSCs with an enrichment of self-renewal pathways and repression of pathways related to proliferation, cell cycle, and differentiation. Furthermore, expression of this LSC signature in AML samples in publicly available databases was associated with adverse clinical outcomes. (Gentles et al., 2010)

More recently, LSCs have been found in the $CD34^{+}CD38^{+}$, and $CD34^{-}$ compartment in some human AMLs, suggesting that the LSC is more heterogenous than previously presumed. (Taussig et al., 2008, Taussig et al., 2010) Furthermore, in experimental mouse models, retroviral transduction of oncogenes into committed progenitor cells including CMP and GMPs can generate a transplantable AML in recipient mice, suggesting that committed progenitors can be imbued with leukaemia initiating properties. (Cozzio et al., 2003, Huntly et al., 2004, Krivtsov et al., 2006) These studies have challenged the concept that LSCs originate only from normal HSCs. In a large cohort of AML samples (n=100) Goardon *et al* identified subsets of AML blasts, which shared immunophenotypic similarity with the normal LMPP and GMP. Both subsets demonstrated LSC activity by generating AML in serial transplantation studies. In addition, leukaemic LMPPs (L-LMPP) gave rise to both L-LMPP and leukaemic GMPs (L-GMP) but L-GMPs could not give rise to L-LMPPs, mirroring the hierarchy observed in normal haemopoiesis. Global gene expression showed that L-LMPP and L-GMPs were molecularly distinct from each other, and shared molecular similarity with

their normal progenitor counterpart. Interestingly however, compared to their normal progenitor population, L-LMPP and L-GMP subsets expressed self-renewal pathways, suggesting that attainment of abnormal self-renewal programmes is indicative of LSC capability. (Goardon et al., 2011)

Thus, AML is organised in a hierarchical fashion with LSCs at the apex, able to maintain and differentiate into bulk leukaemic cells. The LSC is not necessarily derived from the normal HSC. However, LSCs share HSC-like qualities, namely self-renewal. There is growing evidence that eradication of the LSC pool is critical for long-term cure from AML.

Related to the concept of the LSC is the concept of clonal evolution. Clonal evolution describes how the genetic landscape and phenotype of a cancer can change over time. Peter Nowell first proposed this concept in 1976. He postulated that genetically unstable cancer cells undergo step-wise mutations and selection, resulting in the emergence of new subclones. Therefore, at different points over the course of the same disease, different cancer clones may predominate, as the cancer mutates in a linear fashion. (Nowell, 1976) A similar theory suggests that at any time multiple malignant subclones exist, but environmental stresses (such as chemotherapy) may eradicate 1 major clone but subsequently allow a minor clone to expand.

This concept is true of haematological malignancies and was first described in paediatric ALL. DNA copy number abnormalities of paired ALL samples at diagnosis and relapse showed that ALL at relapse were not genetically identical to disease at diagnosis. Backtracking studies revealed that cells corresponding to the relapsed clone were present at diagnosis at low level. (Mullighan et al., 2008) AML also displays clonal evolution. Ding *et al* performed WGS on 8 paired diagnostic and relapse AML samples. They discovered 2 patterns of clonal evaluation at relapse. In the first, the dominant clone that predominated at diagnosis acquired additional mutations. In the second, a minor subclone that was present at diagnosis gained additional mutations and dominated at relapse. Interestingly, in all cases the subclones in a particular patient were derived from

the same ancestral founding clone that was not eradicated by chemotherapy. (Ding et al., 2012)

1.3.2 Classification

In 1976, the French-American-British (FAB) group developed a classification system to provide a consistent morphological and cytochemical framework for the diagnosis of acute leukaemia. (Bennett et al., 1976) Diagnosis was based on at least a 500 cell count performed on PB and BM smears. The FAB classification for AML is shown in Table 1.1. However, with the exception of acute promyelocytic leukaemia (APL, FAB classification M3), the FAB classification did not correlate with clinical outcome. The World Health Organization (WHO) in 2008 revised the classification of AML to take into account the accumulating knowledge of cytogenetic and molecular characteristics of AML that had prognostic implications. (Vardiman et al., 2009) In addition, the presence of certain genetic abnormalities, namely t(8;21)(q22;q22), inv(16)(p13.1q22), t(16;16)(p13.1;q22) and t(15;17)(q22;q12), were pathognomonic of AML regardless of blast count. In 2016 the WHO further revised the classification criteria to incorporate APL with cryptic PML-RARA translocations, biallelic *CEBPA* mutations and AML with *BCR-ABL* as a provisional entry. While the revised 2016 WHO classification acknowledges rare genetic abnormalities that occur primarily in the paediatric population, these do not represent new disease categories. (Arber et al., 2016) The 2016 WHO classification of AML is shown in Table 1.2.

Table 1.1 FAB classification of AML

FAB subtype	Morphology/name
M0	Undifferentiated acute myeloblastic leukaemia
M1	Acute myeloblastic leukaemia with minimal maturation
M2	Acute myeloblastic leukaemia with maturation
M3	Acute promyelocytic leukaemia (APL)
M4	Acute myelomonocytic leukaemia
M4Eo	Acute myelomonocytic leukaemia with eosinophilia
M5	Acute monocytic leukaemia
M6	Acute erythroid leukaemia
M7	Acute megakaryoblastic leukaemia (AMKL)

Table 1.2 2016 WHO classification of AML

AML with recurrent genetic abnormalities
AML with t(8;21)(q22;q22.1);*RUNX1-RUNX1T1*
AML with inv(16)(p13.1q22) or t(16;16)(p13.1;q22);*CBFB-MYH11*
APL with *PML-RARA*
AML with t(9;11)(p21.3;q23.3);*MLLT3-KMT2A*
AML with t(6;9)(p23;q34.1);*DEK-NUP214*
AML with inv(3)(q21.3q26.2) or t(3;3)(q21.3;q26.2); *GATA2*, *MECOM*
AML (megakaryoblastic) with t(1;22)(p13.3;q13.3);*RBM15-MKL1*
Provisional entity: AML with BCR-ABL1
AML with mutated *NPM1*
AML with biallelic mutations of *CEBPA*
Provisional entity: AML with mutated RUNX1
AML with myelodysplasia-related changes
Therapy-related myeloid neoplasms
AML, not otherwise specified (NOS)
AML with minimal differentiation
AML without maturation
AML with maturation
Acute myelomonocytic leukaemia
Acute monoblastic/monocytic leukaemia
Pure erythroid leukaemia
Acute megakaryoblastic leukaemia
Acute basophilic leukaemia
Acute panmyelosis with myelofibrosis
Myeloid sarcoma
Myeloid proliferations related to Down syndrome
Transient abnormal myelopoiesis (TAM)
Myeloid leukaemia associated with Down syndrome

1.3.3 Prognostic factors

Risk stratification is an essential component of clinical AML workup as it guides therapy decisions. Many factors influence disease response to therapy and risk of relapse. Patient defined prognostic factors include age and performance status. Disease defined prognostic factors include presenting WCC, cytogenetic and molecular aberrations, achievement of complete remission (CR) after induction chemotherapy and antecedent myelodysplasia. By far, the most important prognostic factors are genetic risk group and response to induction chemotherapy. (Grimwade et al., 2010, Grimwade et al., 1998) Genetic risk groups in paediatric and adult AML categorise AML into good, intermediate and poor risk disease at diagnosis. In addition, use of specific molecular markers of AML are being used to detect minimal residual disease (MRD) after therapy to further prognosticate disease. (Ivey et al., 2016) However, age remains an important independent prognostic factor for disease outcome with superior clinical outcomes in childhood and adults <30 year (y) old, compared to adults

>50y old. (Juliusson et al., 2009, Creutzig et al., 2013) The impact of patient age on AML characteristics will be further discussed in Section 1.3.6.

Despite models of risk-stratification, the majority of patients fall within the heterogeneous intermediate risk group, often without any identifiable genetic aberrations based on cytogenetic and molecular diagnostics. GEP of AML patients has attempted to further sub-classify patients based on gene expression. Valk *et al* investigated GEP in 285 patient samples (aged 15-78y) and found 16 molecularly defined clusters that were predictive of clinical outcome. While some clusters were discriminated based on established chromosomal and molecular abnormalities, including t(15;17), t(8;21) and inv(16), 6 clusters did not fall into a pre-defined classification. (Valk et al., 2004) However, there is marked heterogeneity between gene expression studies. A meta-analysis of 25 GEP studies including 2744 patient samples found concordant gene dysregulation in only 9.6% of genes. (Miller and Stamatoyannopoulos, 2010) Targeted DNA sequencing of 111 genes known to drive cancer was performed in 1540 adult patients with AML. Established cytogenetic risk groups, as defined by the WHO, could also be discriminated based on mutation pattern. In addition, new subtypes of AML, defined by the pattern of co-mutations that were predictive of clinical outcome were also identified. (Papaemmanuil et al., 2016) Thus, in the future GEP and targeted gene sequencing may also guide treatment decisions. Studies of GEP and next generation sequencing (NGS) in AML are discussed in more detail in Section 5.1.3.

1.3.4 Cytogenetic and molecular subtypes in AML

1.3.4.1 PML-RARA

The *PML-RARA* fusion oncogene results from the translocation t(15;17)(q22;q12). (Goddard et al., 1991) The retinoic acid receptor alpha (*RARA*) gene on chromosome 15 encodes the RARA protein, which regulates retinoic acid mediated transcription. Downstream targets of RARA include *CEBPA*, the homeobox (*HOX*) family of genes, *c-MYC* and *p21*, and play a role in differentiation and granulopoiesis. (Park et al., 1999, Conlon, 1995, Grosso and Pitot, 1985, Jiang et al., 1994) It is a type II mutation resulting in a

differentiation block at the promyelocytic stage of myeloid maturation. The fusion oncoprotein PML-RARA binds DNA via RARA DNA binding sites but acts as a transcriptional repressor by the recruitment of co-repressors. It causes the distinct entity APL. APL accounts for 10% of paediatric and 6% of adult AML and has the best prognosis of all AML subtypes, with OS of >85%. APL is very sensitive to the differentiation agents ATRA and arsenic trioxide (ATO), which lifts the maturation block in APL, resulting in the differentiation of APL blasts into terminally differentiated granulocytes. ATRA in combination ATO (chemotherapy free regimen) is highly successful in inducing CR and has been shown to be non-inferior to chemotherapy based induction regimens, with lower toxicity. (Efficace et al., 2014, Lo-Coco et al., 2013)

1.3.4.2 AML1-ETO

A1E is the fusion gene produced by the balanced translocation t(8;21)(q22;q22). The oncoprotein produced disrupts the functions of core binding factor (CBF), an essential transcription factor in haemopoiesis. *AML1* (also known as *RUNX1* and *CBFa*) located on chromosome 21 forms the DNA binding unit of the CBF transcription factor. CBF is essential for embryonic haemopoietic cell development. Furthermore, CBF mediates myelopoiesis by transcription of gene targets important in myeloid differentiation. (Goyama and Mulloy, 2011) *ETO*, located on chromosome 8, is a co-repressor involved in epigenetic changes. The A1E fusion results in ETO mediated inhibition of AML1 transcription leading to impaired cell cycle progression and immortalisation of HSCs and progenitors. Furthermore, A1E inhibits genes critical for haemopoiesis including *PU.1* (myeloid differentiation), *CEBPA* (granulopoiesis) and *GATA1* (erythroid transcription factor) leading to differentiation blockade. (Vangala et al., 2003, Pabst et al., 2001a, Choi et al., 2006) It is one of the most common cytogenetic aberrations in AML, occurring in 10-15% of paediatric AML and 8% of adult AML. (Chaudhury et al., 2015) It confers good risk disease, with >90% of patients achieving CR after induction chemotherapy.(Grimwade et al., 2010)

1.3.4.3 CBFB-MYH11

CBFB-MYH11 is the fusion oncogene resulting from the cytogenetic aberrations inv(16)(p13.1q22) or t(16;16)(p13.1;q22). Like *A1E*, it is a CBF leukaemia and confers good risk. (Grimwade et al., 2010) The CBFB-MYH11 oncoprotein retains the AML1 binding domain in CBFß-subunit and contains additional AML1 binding domains in MYH11, resulting in a higher binding affinity for AML1 than WT CBFß-subunit. (Lukasik et al., 2002) Therefore, WT AML1 is sequestered onto the CBFB-MYH11 oncoprotein and prevented from associating with its DNA targets. *CBFB-MYH11* is a common cytogenetic aberration in AML, occurring in 10% of paediatric AML and 5% of adult AML. (Chaudhury et al., 2015) It is almost exclusively associated with FAB subtype M4Eo (AML with eosinophilia) and confers good risk disease. (Grimwade et al., 2010)

1.3.4.4 MLL rearrangement

The mixed lineage leukaemia (*MLL*) gene (recently renamed *KMT2A*, lysine (K)-specific methyltransfersase 2A) located on chromosome 11 is one of the most frequently disrupted genes in acute leukaemia. The encoded MLL protein contains several domains. At the C-terminus a highly conserved SET domain is the site of methyltransferase activity that specifically methylates histone H3 at lysine 4. To allow for efficient chromatin remodelling and transcriptional activation, other proteins including MOF, WDR5, RBBP5 and ASH2L, are recruited to form the MLL complex. At the MLL N-terminus AT hooks and a minor groove DNA binding motif ensures correct targeting of the MLL complex. The resultant H3K4me3 marks MLL target genes for transcriptional activation. In particular, *HOX* gene expression is dependent on MLL chromatin modification. (Slany, 2009)

Rearrangements of the MLL gene (*MLLr*) are very common in acute leukaemia and occur in both ALL and AML. In particular, *MLLr* are present in 77% of infant AML. In *MLLr* the breakpoint occurs between the CXXC domain and PHD fingers, resulting in a loss of the C-terminus transactivation and SET domain. This leads to uncontrolled activation of both MLL and novel gene targets. (Armstrong et al., 2002) In particular, dysregulation of *HOX* genes, especially *HOXA9* and its co-factor *MEIS1*, is the most important factor in MLL mediated leukaemogenesis.

(Milne et al., 2005) Over 80 partner genes have been identified in *MLLr* but the most common are *ENL*, *AF9*, *AF4*, *ELL*, and *AF10*. *MLL-AF4* is the most common rearrangement seen in ALL, while *MLL-AF9* (*MA9*) is the most common rearrangement seen in AML. (Meyer et al., 2013) *MLLr* occurs at a higher incidence in paediatric than in adult AML (38% versus 2%, respectively) with the highest incidence occurring in infant AML at 77%. (Chaudhury et al., 2015) In adult AML, all *MLLr* expect *MA9* confers poor risk disease. In contrast in paediatric AML, only certain *MLLr* confer poor risk (*MLL-A*F4, *MLL-AF6*, *MLL-AF10*) while *MLL-MLLT11* may confer good risk. (Balgobind et al., 2009)

1.3.4.5 NUP98 rearrangements

Rearrangement of the Nucleoporin 98 (*NUP98*) gene, located on chromosome 11p15.4, has been observed in haematological malignancies. It was first reported in 1996 by Nakamura *et al* and Borrow *et al* in a study of patients harbouring the rare t(7;11)(p15;p15) translocation in AML. (Nakamura et al., 1996, Borrow et al., 1996) Since then, *NUP98* rearrangements have also been observed in blast crisis chronic myeloid leukaemia (CML), MDS and T-acute lymphoblastic leukaemia (T-ALL), albeit rarely. (Romana et al., 2006) Over 28 partners have been identified. (Gough et al., 2011) *NUP98* encodes a component of the nuclear pore complex on the nuclear membrane, which facilitates nuclear export of protein and mRNA. (Nakielny and Dreyfuss, 1999) Studies in Drosophila show that NUP98 protein is also freely located in the nucleus, where it plays a role in transcription activation of genes involved in cell cycle progression and development. (Kalverda et al., 2010, Capelson et al., 2010) Partner genes can be divided into those encoding homeobox proteins and those encoding non-homeobox proteins. The most frequent partner gene is the transcription factor *HOXA9* located on chromosome 7p15 and corresponds to the translocation t(7;11)(p15;p15), resulting in the fusion oncogene *NH9*. This is a type II mutation, resulting in impaired differentiation and enhanced self-renewal. Fusion of the phenylalanine and glycine (FG) repeat rich C-terminus of NUP98 protein to the transcription regulatory region of HOXA9 leaves the DNA binding and PBX transcription factor interaction domains on HOXA9 intact. This results in NUP98 mediated activation of HOXA9 and collaboration with the oncoprotein MEIS1. (Kasper et al., 1999, Calvo et al., 2002) Considering all published data

overall incidence of NUP98 rearrangements in AML is approximately 1-2% in unselected patients and the incidence of NH9 in AML is 1.4-2.23%. (Gough et al., 2011, Kwong and Pang, 1999, Chou et al., 2009) Patients harbouring this translocation tend to be younger adults, with a median age of 31-41years; it is rarely seen in the elderly. Interestingly, it is seen predominantly in patients from Asian countries. NH9 AML presents as FAB subtype M2 in the majority of cases, M4 has also been reported and in 50% of cases cells have dysplastic features. Patient with NH9 have worse outcome, with high induction failure and RR. (Chou et al., 2009, Huang et al., 1997, Kwong and Pang, 1999) NH9 is rare in paediatric AML with a frequency of <0.5%, and tends to occur in therapy related AML rather than *de novo* AML. (Romana et al., 2006, Bisio et al., 2014) In paediatric AML, *NUP98* rearrangements occur in 6.6% of patients. (Bisio et al., 2014) The most frequent partner gene is the nuclear receptor binding SET domain protein 1 (*NSD1*) located on chromosome 5, resulting in the fusion oncogene *NUP98-NSD1*. A study screening >1000 patients for this abnormality found that *NUP98-NSD1* was present in 16% of paediatric patients with cytogenetically normal (CN) disease, compared to only 2% of adult patient with CN disease. Patients with *NUP98-NSD1* presented with high WCC, FAB subtype M4/M5 disease and in 91% of cases had a co-occurring *FLT3-ITD* mutation. Like NH9, *NUP98-NSD1* was associated with high RR and poor OS. (Hollink et al., 2011)

1.3.4.6 FLT3-ITD

The *FLT3* gene located on chromosome 13q12 encodes the membrane bound Fms-like tyrosine kinase receptor. It is found on HSCs and early progenitor cells, as well as AML blasts. (Rosnet et al., 1996) Binding of the FLT3 ligand to its receptor results in receptor dimerisation and autophosphorylation. The complex is rapidly internalised and activates downstream signalling pathways including STAT5 activation. (Zhang et al., 2000, Gilliland and Griffin, 2002) Internal tandem duplications (ITD) of the juxtamembrane (JM) domain coding sequence of the *FLT3* gene (*FLT3-ITD*) results in elongation of the JM domain leading to disrupted autoinhibitory function and constitutive activation. *FTL3-ITD* is a type I mutation resulting in increased proliferation and reduced apoptosis. (Kiyoi et al., 1998) *FLT3-ITD* is more prevalent in adult AML occurring in 20-40% of adult AML and in only 10% of paediatric AML. (Meshinchi et al., 2001, Schneider et al.,

2012, Chaudhury et al., 2015) In both paediatric and adult AML, *FLT3-ITD* without co-expression of a mutation in nucleophosmin 1 (*NPM1*) is associated with adverse outcomes with increased RR following CR. (Kottaridis et al., 2001) Therefore, *FLT3-ITD* is now included in the prognostic risk stratification of AML. (Dohner et al., 2010)

1.3.4.7 NPM1 mutations

The *NMP1* gene on chromosome 5 encodes the NPM1 protein that acts as a nuclear chaperone. (Frehlick et al., 2007) Nuclear-cytoplasmic shuttling of NPM1 is critical to its functions including ribosome biosynthesis, maintenance of genomic stability and regulation of DNA transcription. (Grisendi et al., 2006) Mutations in *NPM1* result in aberrant cytoplasmic localisation of NPM1 protein, resulting in the destabilisation of p53 and ARF mediated tumour suppressor pathways. (den Besten et al., 2005) In the absence of *FLT3-ITD*, *NPM1* mutations confer good risk disease with superior CR rates compared to patients with WT *NPM1*. (Thiede et al., 2006, Becker et al., 2010) NPM1 mutations are more common in adult AML occurring in 35% of adult cases. (Thiede et al., 2006, Schneider et al., 2012) NPM1 mutations are not seen in paediatric AML presenting at <3y of age. In older children it occurs at a frequency of 5-10%. (Hollink et al., 2009)

1.3.4.8 CEBPA mutations

The *CEBPA* gene on chromosome 19 encodes the transcription factor C/EBPα. C/EBPα plays a critical role in proliferation and myeloid differentiation. C/EBPα levels increase as HSC and progenitors differentiate, with highest expression in GMPs and loss of C/EBPα blocks transition from the CMP to the GMP stage. (Zhang et al., 1997b) Mutations of *CEBPA* are type II mutations, causing a differentiation block. Two types of mutations of the *CEBPA* gene occur in AML. N-terminal frame-shift mutations result in the translation of a short isoform, which inhibits the function of the full-length protein by a dominant negative mechanism. C-terminal mutations in the DNA-binding domains disrupt binding to DNA leading to impaired target gene transcription. (Pabst et al., 2001b) Biallelic mutations of *CEBPA* confers good risk to AML patients with CN disease with

reduced RR. (Green et al., 2010) *CEBPA* mutations do not occur in infant AML but are observed in 5% of paediatric and 15% of adult AML. (Ho et al., 2009, Taskesen et al., 2011)

1.3.4.9 HOX deregulation

The homeobox (*HOX*) family of transcription factors are important regulators of development. In mammals, the *HOX* genes are clustered in 4 clusters (*HOXA*, *HOXB*, *HOXC* and *HOXD*). (Duboule and Dolle, 1989) Individual *HOX* genes are expressed in precise temporal and spatial patterns and disruption of expression during embryogensis results in dramatic morphogenic abnormalities. (Mallo et al., 2010) *HOX* genes are also expressed in adult haemopoietic tissue with highest expression in HSCs and progressive downregulation with differentiation. (Pineault et al., 2002) Targeted disruption of *HoxA9* in murine models results in decreased myeloid, erythroid and lymphoid haemopoiesis, while overexpression of *Hox* genes results in enhanced self-renewal of HSCs and leukaemogenesis. (Lawrence et al., 1997, Thorsteinsdottir et al., 2001, Antonchuk et al., 2002) *HOX* deregulation is observed in the majority of AML. *HOX* deregulation can occur by various mechanisms. Firstly, specific *HOX* genes can be disrupted by chromosomal translocations, as seen in *NUP98* rearrangements involving *HOXA9*, *HOXA10*, *HOXC10* and *HOXD13*. Secondly, overexpression of *HOXA6*, *HOXA7*, *HOXA9* and its co-factor *MEIS1* has been correlated with MLLr disease, which is a regulator of *HOX* expression. Finally, other mechanisms upstream of *HOX* expression, such as *CDX2* overexpression, result in HOX overexpression in AML. (Scholl et al., 2007) *HOX* deregulation has prognostic value; *HOX* overexpression is associated with intermediate and adverse risk cytogenetic groups. Furthermore, among 6187 genes investigated in AML, *HOXA9* correlated with inferior OS and RR. (Golub et al., 1999) Conversely, low *HOXA9* expression correlated with superior OS and response to therapy. (Andreeff et al., 2008)

1.3.4.10 DNMT3A mutations

The *DNMT3A* gene, located on chromosome 2 encodes the enzyme DNMT3A and belongs to the family of methyltransferases including DNMT1 and DNMT3B. They catalyse the addition of methyl groups to the cytosine residue of CpG

dinucleotides and thus play an important role in epigenetic gene silencing. (Mizuno et al., 2001) Mutations in *DNMT3A* are type III mutations resulting in epigenetic dysregulation and deregulated methylation status. DNMT3A mutations are common within the ageing population, occurring in up to 10% of people >65y of age. (Genovese et al., 2014) DNMT3A mutations occur in 15-25% of adult AML. They are enriched in CN disease and are associated with co-expression of mutations in *FLT3*, *NPM1* and *IDH1*. (Ley et al., 2010) The presence of *DNMT3A* mutations is associated with poorer clinical outcomes, primarily due to disease recurrence. (Thol et al., 2011a, Tie et al., 2014) *DNMT3A* mutations result in the development of pre-leukaemic clones that precede AML development and evade chemotherapy. (Jaiswal et al., 2014, Shlush et al., 2014) In contrast, *DNMT3A* mutations are a rare event in paediatric AML, occurring in <1% of cases. (Ho et al., 2011, Hollink et al., 2012)

1.3.5 Mixed phenotype acute leukaemia

While most acute leukaemias can be defined as either myeloid or lymphoid, approximately 2-5% show expression of more than one lineage. (Rubnitz et al., 2009, Mejstrikova et al., 2010, Weinberg and Arber, 2010, Yan et al., 2012) These are termed the mixed phenotype acute leukaemia (MPAL). Leukaemic cells can express features of both lineages (biphenotypic) or 2 populations can be present (bilineal). Sometimes it is difficult to distinguish between biphenotypic and bilineal leukaemia as both may arise from the same ancestral clone. MPAL also includes leukaemias that switch lineage during therapy or show undifferentiated features. The 2016 revised diagnostic criteria for mixed lineage leukaemia is shown in Table 1.3. The St Jude's group investigated the outcomes (n=35) and gene expression (n=13) in paediatric patients with MPAL as defined by the WHO diagnostic criteria. Gene expression using a 100 probe set to define AML, B-acute lymphoblastic leukaemia (B-ALL) and T-ALL showed that the majority (8 out of 13) of MPAL did not cluster with single lineage disease. Patients were treated with either ALL or AML treatment. A proportion of disease refractory to induction therapy responded to treatment directed to the other lineage. Overall, MPAL had similar outcomes to AML but were significantly inferior to ALL. (Rubnitz et al., 2009) In another series, 100 paediatric and adult patients (63% adult) with MPAL were assessed for disease characteristics and

outcomes. Only 13% had CN disease. Median survival (MS) was poor at 18m, but the paediatric population did fare better with a MS of 139m in children versus 11m in adults. There was no consensus on best treatment, some receiving a mixture of AML and ALL therapy while others starting with therapy directed to one lineage and then switched to treatment directed against the other lineage on treatment failure. (Matutes et al., 2011)

Table 1.3 2016 WHO diagnostic criteria for MPAL

Myeloid lineage
MPO (flow cytometry, immunohistochemistry, or cytochemistry) or Monocytic differentiation (at least 2 of the following: nonspecific esterase cytochemistry, CD11c, CD14, CD64
T-lineage
Strong† cytoplasmic CD3 (with antibodies to CD3 ε chain) or Surface CD3
B-lineage
Strong CD19 with at least 1 of the following strongly expressed: CD79a, cytoplasmic CD22, or CD10 or Weak CD19 with at least 2 of the following strongly expressed: CD79a, cytoplasmic CD22, or CD10

1.3.6 Clinical and biological differences in AML with age

As discussed in Section 1.3.3, age is an important independent prognostic factor in AML, with superior clinical outcomes at younger age. Younger patients have less co-morbidity and are therefore better able to tolerate intensive therapy. However, there is growing evidence that AML pathogenesis and biology may be different in paediatric and adult populations. Table 1.4, adapted from Chaudhury *et al* (Chaudhury et al., 2015) summarises key clinical and genetic differences in paediatric and adult AML.

Table 1.4 Clinical and genetic differences in AML with age

Table showing key differences in paediatric and adult AML. CN = cytogenetically normal. ND = not detected. *CR in patients ≥60y eligible for intensive therapy. Risks groups as per (Dohner et al., 2010, Creutzig et al., 2012)

Age Group		0-1y	>1-<10y	10-<18y	18-<60y	≥60y
Incidence	(/100000/y)	1.5	0.75	0.8	2	17
Prognosis (%)	CR	92	93	90	72	51*
	RR (5y)	35	30	32	54	>99
	OS (5y)	68	66	57	45-50	7
Risk group (%)	Good	4	23	28	22	4
	Intermediate	71	63	64	65	77
	Poor	25	13	8	13	19
Cytogenetic aberrations (%)	t(8;21)	-	28	11	8	1
	inv(16)	7	11	6	5	<1
	t(15;17)	2	14	13	10	2
	MLLr	77	31	7	2	<1
	Complex	-	-	5	6	14
Molecular aberration (%)	FLT3-ITD	1	8-17	17-27	20-40	21
	NPM1	-	8	13	35-50	37
	CEBPα		10 (CN)	17 (CN)	10-15	11 (CN)
	DNMT3A	ND	ND	Rare	20	24
	TET2	1.7			2 - 23	
	ASXL1	<1			5 – 30	
	IDH1/2	0.5 - 1			15 - 30	

1.3.6.1 Incidence and survival

Rates of AML incidence and survival are shown in Figure 1.5. AML is rare in childhood, with an incidence of 1/100,000 per annum in children aged <18y. The incidence rises to 2/100,000 per annum in adult aged 18-60y, with an exponential rise in incidence after the age to 60y to 17/100,000 per annum. (Howlader N, 2014, Chaudhury et al., 2015) The increase in AML incidence observed in the elderly is like due to an increase in clonal haemopoiesis and the emergence of pre-leukaemic clones (see Section 1.3.6.4). Within the paediatric population, AML is most common in infants up to the age of 1y, with an incidence of 1.5/100,000 per annum, compared to an incidence of 0.8/100,000 per annum in children aged 1-18y. Infant leukaemia is associated with distinct genetic abnormalities and is often considered a separate biological entity. Infant AML will be discussed in Section 1.3.6.3.

In contrast, younger age is associated with superior survival. For patients treated with intensive therapy with curative intent, 5 year OS is 65-70% in people aged <18y versus 45-50% in people aged 18-60y. In accordance with this, RR is lower in people aged <18y at 30-35% versus 54% in people aged 18-60y. The superior OS

and RR in childhood is party due to the fact that children with less co-morbidity are better able to tolerate intensive chemotherapy. However, the paediatric AML cohort may contain more chemoresponsive disease than AML in adults. For adult AML current guidelines recommend upfront consolidation with allogeneic haemopoietic stem cell transplant (HSCT) in first CR in all patients with intermediate or adverse risk disease. (Dohner et al., 2010) However, paediatric AML is more responsive to both induction and salvage (post relapse) chemotherapy. As such, for paediatric AML, HSCT in first CR is reserved for patients with adverse risk disease only. (B. E. Gibson, personal communication)

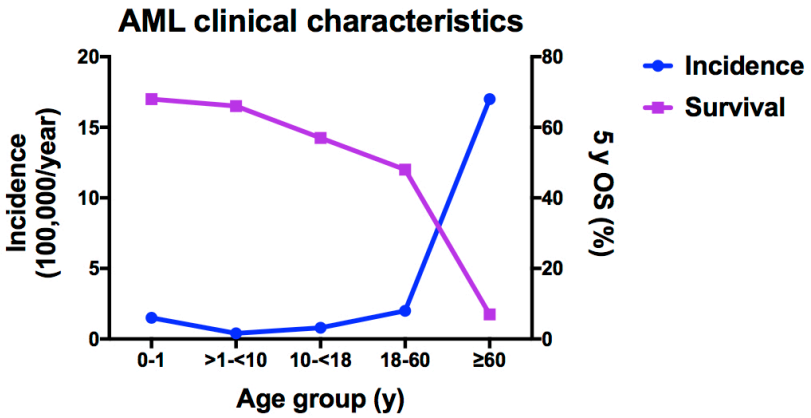

Figure 1.5 Differences in clinical characteristic of AML with age

Graph of incidence rates (blue) and 5Y OS (purple) for different age groups.

1.3.6.2 Genetic aberrations

The genetic profile of paediatric and adult AML is very different. Paediatric AML is characterised by gross cytogenetic anomalies whereas adult AML is characterised by CN disease. (Table 1.4) 75% of paediatric patients with AML have a cytogenetic aberration, compared to only 50% of adults with AML. (Grimwade et al., 1998) The pattern of cytogenetic aberration also varies with patient age. Some cytogenetic aberrations occur almost exclusively in paediatric AML such as t(5;11)(*NUP98-NSD1*), inv(16)(*CBFA2T3-GLIS2*) and t(7;12)(*MNX1-ETV6*). In infant AML, 80% of patients have a cytogenetic abnormality, 77% of which are *MLLr*. Beyond infancy good risk cytogenetic aberrations (APL and CBF leukaemias) are more prevalent in the paediatric population (25% in paediatric versus 13% in adult AML). In contrast, poor risk cytogenetics are more common in adult AML (13% in paediatric versus 16% in adult AML). While the t(15;17),

t(8;21) and inv(16) carry the same favourable risk in both paediatric and adult AML, some cytogenetic categories that are deemed high risk in an adult population are not necessarily so in paediatric AML. (Grimwade et al., 1998, Harrison et al., 2010) Complex karyotype (≥3 cytogenetic abnormalities) is increasingly common with increasing age and is associated with a very poor outcome in adult AML. However, complex karyotype is not consistently associated with inferior outcome in paediatric studies and as such does not necessarily warrant consolidation with HSCT in first CR as it would in adult AML. (Niewerth et al., 2010) It is unclear if the difference in outcome in patients with complex cytogenetics is due to better tolerance of chemotherapy at younger age, or a difference in downstream cellular consequences in young cells, making AML with complex cytogenetics in paediatric AML more chemosensitive.

With increasing age, CN disease is more prevalent. In both paediatric and adult AML, the presence of molecular aberrations, including *FLT3-ITD*, *NMP1* and biallelic *CEBPA* mutations can further risk stratify patients with CN disease. However, in all cases the incidence of molecular aberrations is higher in adult AML. (Table 1.4 and Section 1.3.4) Mutations in epigenetic regulators, including *DNMT3A*, *TET2* and *IDH1/2* are common in adult AML, occurring in 25-30% of cases. (Papaemmanuil et al., 2016) These mutations are implicated in creating a pre-leukaemic clone that precedes clinically evident AML and evades chemotherapy, leading to relapse. Such mutations are extremely rare in paediatric AML. (Thol et al., 2011b, Liang et al., 2013) Clonal haemopoiesis is discussed in more detail in Section 1.3.6.4. Thus, the genetic composition of paediatric and adult AML are different. Furthermore, clinical outcomes suggest that for some genetic subtypes, biological consequences of the same genetic insult may be different depending on the age of the patient.

1.3.6.3 Infant leukaemia

In paediatric AML, the highest incidence occurs in infants <1y of age. In infant AML, there is usually evidence of a founding mutation occurring *in utero*. Certain AML associated genetic and molecular aberrations occur exclusively in this age group and not in childhood and adolescence, suggesting a reliance on the foetal environment and HSC. As such, infant AML is often considered a distinct

biological entity. Infant AML can be subdivided into AML occurring in Down Syndrome (DS trisomy 21) (ML-DS) in association with *GATA1* mutations and non-DS AML. (Swerdlow et al., 2008)

Haematological disorders associated with DS include transient abnormal myelopoiesis (TAM), which presents in infancy and ML-DS, an acute megakaryoblastic leukaemia (AMKL, FAB subtype M7) that presents in the first 4 years of life. (Al-Kasim et al., 2002, Ahmed et al., 2004) In both, the pathological driver is a mutation of the *GATA1* gene on the X chromosome that leads to the translation of a truncated protein. (Gurbuxani et al., 2004) Analysis of 585 newborn blood spots showed that 4% of children with DS have a *GATA1* mutation at birth. (Pine et al., 2007) In addition, there are case reports of *GATA1* positive TAM/ML-DS presenting prenatally as hydrops fetallis. (Heald et al., 2007) Both prove that the *GATA1* mutation occurs *in utero,* in the foetal HSC.

TAM occurs in 5-10% of DS children and is characterised by leucocytosis, thrombocytopenia and circulating blasts. (Al-Kasim et al., 2002) In the majority of cases, TAM regresses spontaneously by the age of 4y. In 19% of cases, TAM progresses to ML-DS. (Massey et al., 2006, Klusmann et al., 2008, Gamis et al., 2011) Paired samples from patients with TAM preceding ML-DS show the same *GATA1* mutation detectable at both stages. In addition, retrospective analysis of newborn blood spots from patients with ML-DS without preceding TAM shows GATA1 mutations at birth. This suggests that *GATA1* mutations cause a pre-leukaemic clone that predisposes to TAM and ML-DS.

Non-DS infant AML is also considered a distinct biological entity. Infant AML is usually FAB subtype M4/M5 disease and often presents with adverse features such as high WCC and central nervous system involvement.(Chessells, 1992, Pui et al., 1995) *MLLr* is very common in this age group, accounting for 77% of the chromosomal abnormalities. In addition, some cytogenetic abnormalities such as t(7;12)(*MNX1-ETV6*), t(1;22)(*RBM15(OTT)-MKL1(MAL)*) and inv(16)(*CBFA2T3-GLIS2*) are almost exclusively seen in the infant AML group. (Arber et al., 2016) Unlike older children and adolescents, the good risk cytogenetic subtypes (APL

and CBF factor AML) are rare. Similar to ML-DS, there is evidence of founding mutations occurring *in utero*. Studies in monozygous twins with *MLLr* infant acute leukaemia show that each twin pair express the same unique breakpoint, which was distinct to other twin pairs and other patients with MLLr leukaemia. Furthermore the *MLLr* is not expressed in the patient's non-haematological tissue or parental DNA, proving that the mutations are acquired rather than inherited in the germline. The authors conclude that the mutation must have arisen as a single clonal event *in utero*, which gave rise to a pre-leukaemic clone in both twins. (Ford et al., 1993) Retrospective analysis of newborn blood spots in patients with *MLL-AF4* acute leukaemia presenting in patients aged 5m-2y show that the *MLL-AF4* rearrangement was present at birth, suggesting the mutation occurred *in utero*. (Gale et al., 1997)

Thus, the evidence suggests that infant AML is derived from mutations occurring prenatally in foetal cells resulting in a pre-leukaemic clone and a second mutational hit occurring early in the post-natal period results in clinically evident leukaemia in infancy. As discussed in Section 1.2 the foetal HSC is behaviourally and transcriptionally distinct from older post-natal HSCs. The fact that foetal derived pre-leukaemic clones regress spontaneously and the presence of genetic aberrations that are exclusive to an infant age group suggest foetal clones are dependent on the foetal HSC and microenvironment and the mature BM environment is not sustainable for foetal derived clones to fully transform without additional mutations.

1.3.6.4 Clonal haemopoiesis

Mutations in epigenetic regulators such as *DNMT3A*, *TET2*, *ASXL1* and *IDH1/2* are increasingly prevalent in aged HSCs. (Liang et al., 2013, Genovese et al., 2014, Jaiswal et al., 2014) Mutations in epigenetic regulators cause alterations in the epigenetic landscape, which give an HSC competitive survival advantage resulting in clonal expansion (clonal haemopoiesis). Clonal haemopoiesis is a recognised precursor to AML development. (Busque et al., 2012, Xie et al., 2014, Genovese et al., 2014, Jaiswal et al., 2014) Whole exome sequencing (WES) of PB in a large dataset (>12,000) of people unselected for disease, shows that clonal haemopoiesis occurs in 10% of people aged >65y, increasing to 18% in

people aged >90y. In contrast, clonal haemopoiesis occurs in only <1% of people <50y old. Mutations most associated with clonal haemopoiesis are *DNMT3A*, *TET2* and *ASXL1*. Furthermore, there is an enrichment of haematological disorders in people with clonal haemopoiesis, such as AML and MDS. (Genovese et al., 2014, Jaiswal et al., 2014) Studies of clonal evolution in AML samples show that mutations occur in a step-wise fashion and that mutations in epigenetic regulators are initiating events, resulting in pre-leukaemic clones that require further genetic insult to drive leukaemia. Furthermore, pre-leukaemic clones harbouring epigenetic mutations often evade chemotherapy and act as a reservoir for relapse even after CR. (Jan et al., 2012, Shlush et al., 2014, Corces-Zimmerman et al., 2014) Therefore, the adverse outcomes of patients with *DNMT3A*, *TET2*, *ASXL1* and *IDH1/2* mutations are due to increased RR, arising from pre-leukaemic clones that evade chemotherapy. While mutations in epigenetic regulators are increasingly common in adult and elderly AML, they are rarely present in paediatric AML (Table 1.4). A study of co-operating mutations in 206 paediatric AML patients found mutations in epigenetic regulators in only 5.6% of cases and did not necessarily correlate with adverse clinical outcome. (Liang et al., 2013) The low incidence of these mutations in paediatric AML suggests that clonal haemopoiesis is not a driver of AML in the paediatric age group and highlights that the pathogenic process of leukaemia development and relapse are different in paediatric and adult AML.

1.3.7 Treatment

For the majority of patients with AML, treatment is delivered as part of a clinical trial. Due to the low incidence of AML in childhood, in the UK children have been included in predominantly adult trials and treatment strategies extrapolated from adult data. The mainstay of treatment for both paediatric and adult AML is chemotherapy consisting of anthracycline and cytarabine to induce remission (induction therapy). After achieving CR, remission is consolidated to remove any residual LSCs that may be a reservoir for relapse. Consolidation therapy consists of chemotherapy alone, or with high dose therapy and HSCT in disease with a high risk of relapse. Purine analogues and etoposide are often incorporated into induction and consolidation therapy but treatment regimens are inconsistent. In essence, treatment has remained the same for 30y and

improvement in outcomes has been largely due to better supportive care reducing treatment and transplant related mortality. (Stevens et al., 1998, Perel et al., 2005, Gibson et al., 2011, Burnett et al., 2013, Creutzig et al., 2013, Kaspers et al., 2013) However, RR remains high at 35% in paediatric AML and 54% in adult AML. New drugs under investigation include small molecule inhibitors, epigenetic modifiers and immunotherapy. Midostaurin and sorafenib are both multi-kinase inhibitors with potent anti-FLT3 action. In a phase III study of newly diagnosed adults with *FLT3* mutated AML the addition of midostaurin to standard chemotherapy resulted in improved OS and event free survival (EFS). (Stone et al., 2017) In phase I and II studies of relapsed and refractory disease, addition of sorafenib to re-induction chemotherapy resulted in improved CR rates, in both paediatric and adult AML patients. (Ravandi et al., 2010, Inaba et al., 2011) In the current COG AAML1031 phase III trial of paediatric AML (age up to 30y) patients with high risk *FLT3-ITD* disease receive sorafenib with HSCT in first CR. The cell surface molecule CD33 is found on >80% of AML myeloblasts. (Griffin et al., 1984) Gemtuzumab ozogamicin (GO) is an immunoconjugate in which CD33 antibody is conjugated to the potent cytotoxic antibiotic calachemicin. A meta-analysis of 5 trials (MRC/NCRI AML 15 and 16, ALFA-0701, SWOG-0106 and GOELAMS AML 20061R) of predominantly adult patients showed improved OS and RR with the addition of GO in induction therapy in good and intermediate risk disease but no benefit in poor risk disease. (Hills et al., 2014) Furthermore, the COG AAML 0531 study of predominantly paediatric patients found a trend towards improved RR following HSCT in high risk patients. (Gamis et al., 2014) On the basis of these studies, the current international phase III trial MyeChild001, exclusively for paediatric AML, is investigating the use of GO in induction therapy for all children with AML and high risk MDS.

1.4 BM microenvironment

The BM is a complex structure comprising of HSCs that ultimately produce terminally differentiated erythroid, myeloid and lymphoid cells, and mesenchymal stem cells (MSCs), which give rise to components of the BM stroma including osteoblasts, chondrocytes and adipocytes. The close proximity of haemopoietic and stromal cells suggest a reciprocal relationship between the

two. In 1978, Schofield proposed the idea that HSCs reside in association with other cells within a BM niche, when he observed that the spleen was unable to support HSCs the way the BM could. (Schofield, 1978) The niche protects HSCs from environmental stress and helps regulate a balance between HSC self-renewal and maintenance and differentiation. It does so by providing a physical anchor for HSCs and by the secretion of extrinsic factors. Together, the HSCs and the niche maintain homeostasis while responding to stress and disease. Two distinct niches are present in the BM. The endosteal (osteoblastic) niche is located by bone, and the perivascular niche located at the sinusoids. In general LT-HSCs tend to reside in the endosteal niche while ST-HSCs and progenitors reside near the vascular niche. However, this is a dynamic situation and both niches are located in close proximity to each other and secrete cytokines, chemokines and ligands that promote HSC propagation, quiescence, maintenance and survival.

1.4.1 The endosteal niche

The endosteal niche is located at the trabecular or cortical bone and consists of bone forming osteoblasts, bone resorbing osteoclasts, glial non-myelinated Schwann cells and T regulatory cells (Tregs). Imaging of HSPCs within the niche shows that HSCs with the greatest repopulating ability (LT-HSCs) localise to the endosteal surface while ST-HSCs and progenitors localise further away. (Nilsson et al., 2001, Haylock et al., 2007, Xie et al., 2009, Lo Celso et al., 2009) Overall, the endosteal niche sustains HSCs and maintains their quiescent state.

1.4.1.1 Osteoblasts

Osteoblasts synthesise mineralised bone. However, by the release of cytokines and direct cell-to-cell contact, osteoblasts also play a key role in HSC maintenance, number and quiescence. Osteoblasts sustain the growth of human HSCs *in vitro* by production of G-CSF and presenting the protein in a membrane bound fashion to the HSC. (Taichman and Emerson, 1994) Studies in which osteoblast number is increased either by bone morphogenetic protein receptor 1a (BMPR1A) inactivation (leading to increased spindle-shaped N-cadherin^{+} CD45^{-} osteoblasts and a resultant ß-catenin expression in HSCs) or PTH over-expression

(causing Notch1 activation in HSCs) results in a parallel increase in functional HSCs. (Zhang et al., 2003, Calvi et al., 2003) HSCs expressing the tyrosine kinase TIE2 are quiescent, adhere to the bone surface and evade myelosuppressive therapy. Their quiescence is dependent on TIE2 binding to its ligand Angiopoietic-1 (ANGPT1), which is produced and expressed on osteoblasts. (Arai et al., 2004) Osteopontin, a glycoprotein synthesised by osteoblasts and located on the endosteal surface, aids HSC localisation to the endosteal surface via CD44 and integrins. It also inhibits HSC proliferation and regulates HSC number. (Nilsson et al., 2005, Stier et al., 2005) Finally, osteoblasts produce CXCL12, a major HSPC chemoattractant. The CXCL12/CXCR4 axis is crucial in HSC homing, quiescence and repopulating ability. (Peled et al., 1999, Bonig et al., 2004, Nie et al., 2008, Tzeng et al., 2011) Thus osteoblasts produce and express various components that regulate and maintain the HSC.

1.4.1.2 Osteoclasts

Osteoclasts are multinucleated cells derived from macrophages; their development relies on the expression of receptor activator of nuclear factor κß ligand (RANKL) and M-CSF from neighbouring stroma. Osteoclasts resorb bone, allowing for remodelling and healing as well as calcium haemostasis. Release of calcium may play a role in localising HSCs to the osteoblastic niche, via the calcium sensing receptors expressed on the surface of HSCs. During development haemopoiesis moves from FL to the BM niche. HSCs from antenatal mice deficient in calcium sensing receptors successfully migrate to the BM but fail to localise to the endosteal surface. (Adams et al., 2006) In contrast to this, stimulation of osteoclasts by RANKL (seen physiologically in stress conditions) results in reduced CXCL12, SCF and osteopontin, all important HSPC chemoattractants. This causes mobilisation of HSPCs into the circulation. (Kollet et al., 2006) Treatment of mice with the bisphosphonate alendronate, which inhibits osteoclast activity, stimulates HSC cycling resulting in a reduced HSC number with an increase in HPCs. This suggests that inhibition of osteoclasts results in the proliferation and differentiation of HSCs. (Lymperi et al., 2011)

1.4.2 The perivascular niche

The perivascular niche is located at the sinusoidal vascular endothelium. It consists of CXCL12 abundant reticular (CAR) cells, endothelial cells, nestin-positive MSCs, and leptin receptor positive perivascular stromal cells. The perivascular niche is the primary site of HSC homing post BMT. It plays a role in HSC proliferation, differentiation and mobilisation. It is likely that ST-HSCs reside in the perivascular niche and are primed for differentiation and mobilisation. (Passegue et al., 2005)

1.4.2.1 The CXCL12/CXCR4 axis and CAR cells

As discussed above, the CXCL12/CXCR4 axis is crucial in HSC homing and function. CXCL12 (also called SDF-1) is a chemokine protein produced by osteoblasts. CXCL12 is expressed on osteoblasts and nestin positive MSCs but it is expressed at highest levels on CAR cells. Its receptor CXCR4 is expressed on the surface of HSCs. CAR cells surround the sinusoidal endothelium in the perivascular niche. Under normal conditions, HSCs co-localise with CAR cells. Induced Cre-mediated deletion of *CXCR4* by pIC in adult mice results in significant reduction in HSC number (defined as LSK-CD34$^-$) and LTC-ICs due to enhanced exit from quiescence. (Sugiyama et al., 2006) Deletion of *CXCL12* in selected stromal cells reveal different effects on haemostasis. Deletion in osterix-expressing stromal cells, which include CAR cells and osteoblasts, results in HSC mobilisation but normal HSC function. Deletion in endothelial cells results in a modest reduction in HSC number. Deletion in nestin negative mesenchymal progenitors results in marked HSC reduction and loss of repopulating ability. (Greenbaum et al., 2013)

1.4.2.2 The sympathetic nervous system and nestin positive MSCs

Components of the sympathetic nervous system are located in both the endosteal and perivascular niche. HSC mobilisation from the osteoblastic niche into the bloodstream is regulated by circadian release of noradrenaline by sympathetic nerves. Nestin positive MSCs normally express high levels of HSC maintenance genes, including, *Cxcl12*, *Scf*, *Angpt1* and *Vcam1*. Nestin positive MSCs are in direct contact with sympathetic nerves. In response to

noradrenaline, there is downregulation of HSC maintenance genes, resulting in the mobilisation of HSCs. Similarly, exogenous administration of $ß_2$ adrenergic agonists results in HSC mobilisation. (Mendez-Ferrer et al., 2008, Katayama et al., 2006) Glial non-myelinated Schwann cells are located with the sympathetic nerves and are in direct contact with HSCs. Glial cells release transforming growth factor ß (TGFß) activating molecules. TGFß/SMAD signalling is active in HSCs and results in HSC quiescence and maintains function; HSCs deficient in TGFß type II receptor TGFRB2 have impaired long term repopulating capacity. Autonomic denervation results in a rapid loss of HSCs. (Yamazaki et al., 2011)

1.4.3 Niche derived HSC regulators

1.4.3.1 Secreted ligands

As discussed above, the ligand CXCL12, secreted from osteoblasts and CAR cells, and its receptor CXCR4 on HSCs, is crucial for HSC homing and localisation. Other ligands secreted by the niche include SCF, TPO and ANGPT1 and are implicated in HSC quiescence, maintenance and survival. The interaction of the ligand SCF and its receptor cKit on HSCs is implicated in HSC function. *Sl/Sl* mice (discussed in Section 1.2.2.4) do not produce SCF in the BM microenvironment and by 16w of age produce only 10% of the number HSCs produced by WT controls. HSCs from *Sl/Sl* mice also display reduced repopulating ability compared to WT controls. However, early transplant of HSCs from *Sl/Sl* mice into a normal BM microenvironment rescues HSC function, and 8m post primary transplant, *Sl/Sl* HSC show no deficiency in repopulating secondary recipients. (Barker, 1997) Interaction of TPO, secreted by osteoblasts, and the thrombopoietin receptor (MPL) on HSCs regulates HSC quiescence. Quiescent LT-HSCs express MPL and localise to TPO producing osteoblastic cells. Disruption of the TPO/MPL axis by the MPL neutralising antibody, directed against the AMM2 antigen on MPL, results in a loss of quiescence and an upregulation of cell cycle regulators in HSCs. (Yoshihara et al., 2007) ANGPT1 is produced and secreted by osteoblasts. Binding to it receptor TIE2 on HSCs maintains the repopulating ability of HSCs cultured *in vitro*, and regulates HSC quiescence *in vivo*. Furthermore, stimulation of the ANGPT1/TIE2 axis *in vivo* can protect mice from the myelosuppressive effects of 5-FU. (Arai et al., 2004)

1.4.3.2 Wnt signalling

The Wnt family of glycoproteins are a family of growth factors that are highly expressed in the BM microenvironment. The canonical Wnt pathway is the best characterised. Transduction of Wnt signalling is via cytoplasmic ß-catenin, which is normally marked for proteosomal degradation by glycogen synthase kinase 3 beta (GSK3ß). Binding of Wnt to its receptor frizzled (Fz) and co-receptors low density lipoprotein receptor related protein (LRP5 and LRP6) inactivates GSK3ß and lifts the degradation of ß-catenin. The accumulated ß-catenin translocates to the nucleus where it displaces co-repressors, resulting in the transcription of target genes, including *c-M*yc, *c-Jun* and *Ccnd1*. (Figure 1.6) (Staal and Clevers, 2005) Wnt signalling has been implicated in HSC self-renewal and proliferation. Overexpression of ß-catenin in HSCs expands HSC number in *in vitro* culture and inhibition of Wnt signalling by Fz antagonism inhibits HSC growth *in vitro* and repopulating ability *in vivo*. (Reya et al., 2003) Overexpression of the Wnt inhibitor dickkopf1 (*Dkk1*) in osteoblasts results in reduced Wnt signalling in HSCs. Reduced Wnt signalling results in increased HSC cycling and loss of reconstitution ability on serial transplantation. Transplantation of Wnt deficient HSCs into a normal microenvironment rescues HSC function. This suggests that Wnt pathway activation from the niche is required to limit HSC proliferation and maintain HSC repopulating ability. (Fleming et al., 2008)

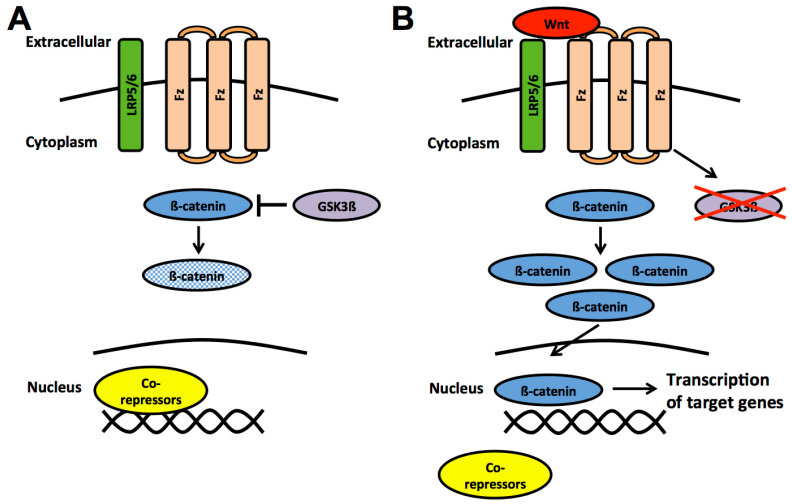

Figure 1.6 Wnt signalling pathway

(A) Schematic showing that in the absence of Wnt, ß-catenin is degraded by GSK3ß and unable to translocate to the nucleus.
(B) Schematic of the canonical Wnt signalling pathway. Binding of Wnt to its receptors LRP5/6 and Fz inactivates GSK3ß resulting in an accumulation of ß-catenin. Translocation of ß-catenin into the nucleus displaces co-repressors resulting in target gene transcription.

1.4.3.3 Notch signalling

The Notch1 receptor is a large transmembrane receptor and is found on HSCs and HPCs. The membrane bound Notch ligands, including Jagged 1 and 2 (JAG1, JAG2) and Delta-like 1/3/4 (DLL1, DLL3, DLL4), are expressed on BM stroma. Binding of ligand to Notch1 results in proteolytic cleavage of the Notch1 receptor, releasing intracellular Notch (ICN). ICN translocates to the nucleus where it activates the transcription of Notch target genes, including hairy-enhancer of split (*Hes*) 1, *Hes5*, Hes related repressor protein (*Herp*) and *Notch1*. (Figure 1.7A) (Jarriault et al., 1995) Notch signalling has been implicated in HSC function and self-renewal. Exogenous JAG1 expands HSCs in *in vitro* co-culture. (Varnum-Finney et al., 1998) Studies using transgenic Notch reporter mice show that Notch1 signalling is active in HSCs *in vivo* and is downregulated upon differentiation. Furthermore, active Notch1 signalling is required for Wnt mediated maintenance of HSCs, suggesting cross-talk between niche signalling pathways. (Duncan et al., 2005)

1.4.3.4 Hedgehog signalling

Hedgehog (Hh) ligands Sonic, Desert and Indian are produced by the BM microenvironment. Binding of Hh ligands to their receptors patched (PTCH) 1

and 2 on HSCs releases PTCH mediated inhibition of the membrane protein smoothened (SMO). Activated SMO enhances nuclear translocation of the transcription factors GLI1 and GLI2. This results in the transcription of pro-survival genes including ABC transporters, *Mdr1*, *Bcrp* and the anti-apoptotic gene *Bcl-2*. (Figure 1.7B) (Regl et al., 2004, Sims-Mourtada et al., 2007) *In vitro* stimulation of the Hh pathway by exogenous Sonic Hh results in the expansion of human HSCs by upregulation of bone morphogenetic protein (BMP) 4. (Bhardwaj et al., 2001) However, loss of Hh signalling through conditional deletion of *Smo* in the adult hematopoietic compartment or pharmacologic inhibition of Hh has no effect on adult hematopoiesis, suggests that Hh signalling is dispensable in the adult murine haemopoietic system. (Hofmann et al., 2009)

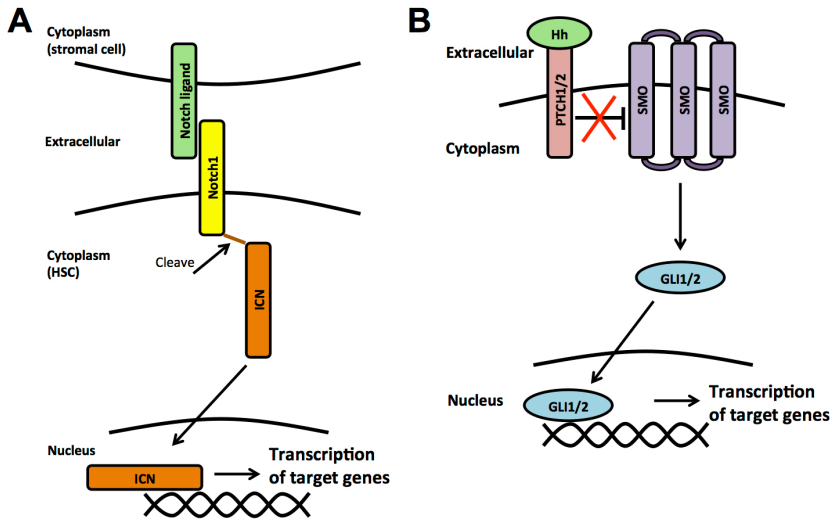

Figure 1.7 Notch and Hh signalling

(A) Schematic of the Notch signalling pathway. Binding of membrane bound Notch ligands to Notch1 on the surface of HSCs results in cleavage of the Notch1 receptor, releasing ICN. ICN translocates to the nucleus where it activates the transcription of Notch target genes.
(B) Schematic of the Hh signalling pathway. Binding of Hh ligand to its receptor PTCH1/2 released PTCH mediated inhibition of SMO. Activated SMO enhances nuclear translocation of GLI1/2 resulting in target gene transcription.

1.4.3.5 TGFß and BMP signalling

This family of ligands, including TGFß, activin and BMP, regulate gene expression via SMAD signalling. Ligand binding to type II receptors on the HSC surface results in phosphorylation of adjacent type I receptors, which in turn activate the responsive SMADs (R-SMAD). TGFß and activin activate R-SMADs 2 and 3 while BMP activates R-SMADs 1, 5 and 8. R-SMADs associate with the common SMAD4

and the complex translocates to the nucleus where it facilitates target gene expression. (Figure 1.8) (Blank et al., 2008) Mx1-Cre mediated conditional deletion of the TGFß receptor *Tgfbr2* on murine HSCs results in increased cycling and reduced long-term repopulating ability, implicating TGFß signalling in HSC maintenance and quiescence. While many cells secrete TGFß, TGFß secreted from glial cells of the sympathetic nervous system in particular activate TGFß signalling in HSCs. (Yamazaki et al., 2011) BMP signalling is crucial for haemopoietic development and the majority of embryonic HSCs display BMP pathway activation. (Crisan et al., 2015) Mx1-Cre mediated conditional inactivation of the BMP receptor, *Bmpr1a*, in mice results in an increase in niche size and thereby HSC number. (Zhang et al., 2003) Singbrant *et al* used a conditional model to delete *Smad1* and *Smad5* in murine haemopoietic cells. *Smad1/5* deletion in foetal (at E14.5) and adult mice had no effect on HSC and progenitor number, quiescence or *in vitro* proliferation. Furthermore, HSCs from *Smad1/5* deficient mice did not display perturbed self-renewal and reconstitution *in vivo* compared to WT controls, suggesting that BMP signalling is dispensable in foetal and adult haemopoiesis beyond E14.5. (Singbrant et al., 2010)

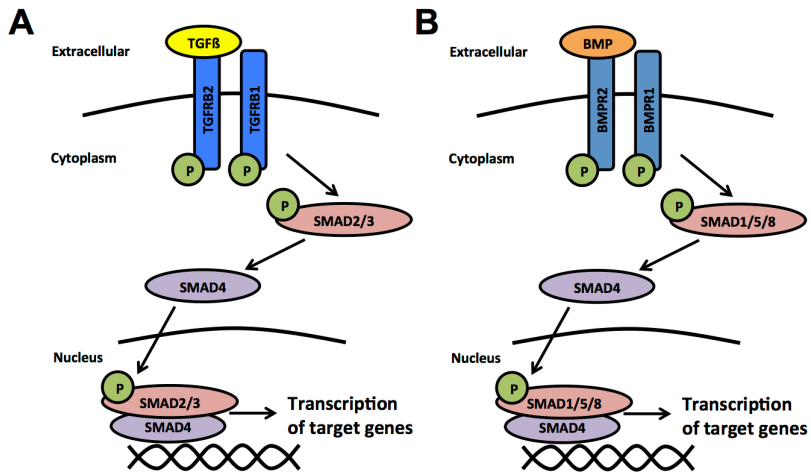

Figure 1.8 TGFß and BMP signalling

(A) Schematic of the TGFß signalling pathway. Binding of TGFß ligand to TGFRB2 receptor causes phosphorylation of TGFRB1 receptor, resulting in activation of the R-SMADs SMAD2/3. R-SMADs associate with SMAD4 and the complex translocates to the nucleus where it activates target gene transcription.
(B) Schematic of the BMP signalling pathway. Binding of BMP ligand to BMPR2 receptor causes phosphorylation of BMPR1 receptor, resulting in the activation of the R-SMADs SMAD1/5/8. R-SMADs associate with SMAD4 and the complex translocates to the nucleus where it activates target gene transcription.

1.4.3.6 Adhesion molecules

Adhesion molecules serve to adhere and retain HSCs in the niche. The ß-integrins VLA4, VLA1 and VLA5 mediate retention and homing of HSCs to the endosteal niche. (Nilsson et al., 2005, Priestley et al., 2007) This may in part be by mediating CXCL12/CXCR4 homing. (Peled et al., 1999)

1.4.4 The BM microenvironment in leukaemia

With increasing knowledge of the role of the BM microenvironment in the maintenance of HSCs, so too is the understanding of the importance of the microenvironment in the propagation and survival of leukaemic cells. Location of leukaemic cells within the BM niche protects them from external stress and may even play a role in chemotherapy resistance and relapse. (Ishikawa et al., 2007) Culture of primary AML is difficult in media, with a requirement of cytokines, normally secreted from niche cells, to help survival *in vitro*. (van Gosliga et al., 2007, Ito et al., 2015) Physical contact between primary leukaemic cells and stromal cells is often required to successfully culture AML cells, showing that signals from the niche, both secreted and direct cell-to-cell interaction is important in LSC maintenance and propagation.

Dysregulation of niche derived signalling in malignant cells suggest a role for niche signalling in leukaemia propagation and survival. The Wnt pathway is active in HOXA9/MEIS1 and MA9 murine AML. Treatment with indomethacin, which blocks Wnt signalling, results in reduced LSC frequency. (Wang et al., 2010) Dysregulation of the BMP pathway in APL results in suppression of ATRA mediated differentiation via the upregulation of the inhibitor of DNA binding (*ID*) family of genes, suggesting an oncogenic role for the BMP pathway. (Topic et al., 2013) In contrast, while Notch receptors are expressed on leukaemic cells, Notch signalling is downregulated in human AML cell lines and primary samples. Activation of the Notch pathway results in growth arrest and apoptosis *in vitro*. (Kannan et al., 2013)

There is evidence that leukaemic cells may alter the BM microenvironment in their favour, at the expense of normal haemopoietic cells. Elegant imaging

studies have shown that malignant cells home to sites of normal HSC residence within the niche. In a xenotransplantation model human AML LSCs ($CD34^+CD38^-$) home to and engraft in the endosteal niche of recipient NOD/SCID/IL2rγ^{null} mice. Compared to bulk leukaemic cells residing in the marrow space, $CD34^+CD38^-$ cells localising to the endosteal niche are quiescent and resistant to cytarabine chemotherapy. (Ishikawa et al., 2007) In another xenotransplantation model, normal human $CD34^+$ HSCs, progenitors and the ALL cell line Nalm-6 all home to the same microdomains in the perivascular niche that are characterised by CXCL12 expression. Engrafted Nalm-6 cells directly downregulated CXCL12 in the niche, impeding the initial homing of normal HSPCs to these sites. Nalm-6 cells also secreted SCF resulting in sequestration of normal HSPCs into inhabitable leukaemic microenvironments where their numbers and function declined. (Sipkins et al., 2005, Colmone et al., 2008) In an *in vitro* model, culture of normal human $CD34^+$ HSCs on AML derived MSCs results in reduced CD34 number and LTC-IC frequency, suggesting that in the context of AML, stromal cells are altered so that they do not support normal HSCs. (Geyh et al., 2016) (Discussed in detail in Section 4.1.3).

Intriguingly, there is evidence that mutations occurring in the BM niche may drive abnormal haemopoiesis and malignancy in normal haemopoietic cells. Deletion of the retinoic acid receptor gamma (*RARγ*) in mice leads to an MPN-like disorder. However, BMT of *RARγ* KO haemopoietic cells into WT recipients does not result in disease, while BMT of WT haemopoietic cells into *RARγ* KO recipients does result in disease. Therefore, the *RARγ* mediated MPN is not intrinsic to haemopoietic cells but rather due to environmental loss of *RARγ*. (Walkley et al., 2007a) KO of the retinoblastoma gene (*Rb*) in mice results in a profound MPN. Transplantation studies reveal that MPN development requires KO in both myeloid and BM niche cells, suggesting an interplay between haemopoietic and stromal cells to drive disease. (Walkley et al., 2007b) Raaijmakers *et al* deleted the microRNA-processing gene *Dicer1* in murine osteolineage cells. Deletion of *Dicer1* in osteoprogenitors (but not osteoblasts) resulted in myelodysplasia. In some cases, further mutations in the dysplastic haemopoietic cells resulted in AML. However, these leukaemic cells had intact *Dicer1*. (Raaijmakers et al., 2010) Kode *et al* introduced an activating mutation

of *ß-catenin* specifically in murine osteoblasts but not haemopoietic cells. Activated ß-catenin stimulated the expression of *Jag1* in osteoblasts. Subsequent activation of Notch signalling in HSPCs induced myelodysplasia and AML. (Kode et al., 2014) These studies show that an initiating mutation in a non-haemopoietic cell can result in haemopoietic malignancy.

As the importance of the BM microenvironment in leukaemia survival is understood, drugs targeting the microenvironment have been trialled in AML. Targets under investigation include CD44 blockade to prevent AML homing to the BM (Jin et al., 2006) and CXCR4 antagonists to release LSC from their protective location in the niche, rendering them susceptible to cytotoxic killing. (Zeng et al., 2009, Nervi et al., 2009) Pharmacological inhibition of CXCR4 in AML cell lines and primary AML samples by BL-8040 *in vitro* results in reduced propagation and increased cell death. *In vivo* treatment of NOD/SCID gamma (NSG) mice engrafted with human AML with BL-8040 resulted in rapid mobilisation of AML cells into the periphery and subsequent AML cell apoptosis. (Tavor et al., 2004) BL-8040 in combination with cytarabine is being investigated in the National Institute of Health (NIH) NCT01838395 phase II trial. Initial monotherapy with BL-8040 resulted in rapid mobilisation of AML blasts into the periphery coupled with a median 78.65% reduction of AML blasts within the BM from baseline, while normal progenitor number was unchanged. Additionally, AML blasts showed elevated cleaved caspase 3 suggesting apoptosis. (Borthakur et al., 2015)

1.4.5 The ageing BM microenvironment

Emerging evidence suggests that the ageing BM microenvironment contributes to haemopoietic decline and is more permissive to malignant propagation. With age, BM adipose tissue increases. While MSCs can be derived from both BM and adipose tissue, only BM derived MSCs can form a BM niche that sustains HSCs. (Tuljapurkar et al., 2011, Reinisch et al., 2015) Moreover, aged (18-20m) HSCs localise further from the endosteal niche than their young (2-4m) counterparts do. (Kohler et al., 2009) Leukaemia, and indeed cancer in general, occurs due to an accumulation of genetic mutations suggesting it is driven by an intrinsic breakdown of normal cellular control. However, oncogenic mutations can occur decades before cancer development. In addition, increasing age is associated

with an exponential rise in cancer incidence, without an exponential rise in the number of occurring mutations. These observations suggest that extrinsic factors from the microenvironment contribute to cancer suppression and these factors change with age. An evolutionary model of cancer hypothesises that the young microenvironment (during the reproductive stage of the organism) actively supresses oncogenic transformation to ensure genomic integrity. The aged microenvironment, in contrast, is more permissive to mutational aberration. (Rozhok and DeGregori, 2015) Vas *et al* investigated the contribution of the ageing microenvironment on haemopoietic disease in transplantation studies using young (2m) and aged (18-23m) murine recipients. Donor Lin^- BM from young (2-4m) mice was transduced with the replication incompetent SF91 retrovirus. The SF91 virus behaves similar to an insertional mutation screen, causing activation of proto-oncogene. This technique generates HSPCs with an intrinsic potential for clonal expansion but low frequency of malignant transformation. Clonality was assessed 26w post BMT. Within the young microenvironment, donor HSPCs displayed oligo-clonality whereas within the aged microenvironment donor HSPCs displayed mono-clonality. Donor cells transplanted into the aged microenvironment were also myeloid skewed. (Vas et al., 2012a) In a similar experiment, young donor BM transduced with A1E retrovirus was transplanted into young and aged recipients. After normalising for different levels of engraftment, aged recipients displayed more $A1E^+$ LSKs, myeloid precursors and terminally differentiated myeloid cells than young recipients. (Vas et al., 2012b) These 2 studies show that the aged BM microenvironment supports haemopoietic clonality, myeloid skewing and pre-leukaemic expansion and thus likely contributes to the increased incidence of haematological malignancy seen with increasing age.

1.5 Summary and Aims

This chapter has described the impact of cellular age on haemopoiesis. Foetal and neonatal HSCs display high self-renewal and proliferation as they populate the developing haemopoietic system. In contrast, adult HSCs must preserve the haemopoietic system for life. As such, adult HSCs are quiescent and proliferate rarely to safeguard against proliferative stress. (Rebel et al., 1996, Bowie et al.,

2007b, Holyoake et al., 1999) Ageing of the haemopoietic system is associated with an expansion of the HSCs pool, but functional decline. Compared to young adult HSCs, aged HSCs display inferior self-renewal, increased proliferation, myeloid skewed lineage output. (Morrison et al., 1996b, Rossi et al., 2005) An accumulation of DNA damage and the emergence of clonal haemopoiesis result in an increased incidence of malignancy. (Rossi et al., 2007a, Beerman et al., 2014, Jaiswal et al., 2014, Shlush et al., 2014) Furthermore, the ageing BM microenvironment may impact on HSC function and malignant transformation.

Clinically, patient age has an impact on AML biology and clinical outcomes. Paediatric AML is rare and associated with superior survival compared to AML in adults and the elderly. Paediatric AML is characterised by gross cytogenetic abnormalities, some of which occur almost exclusive in the paediatric population. Adult AML is characterised by molecular aberrations, often of epigenetic regulators, that are associated with a prodrome of clonal haemopoiesis. (Chaudhury et al., 2015) This suggests that the pathogenesis of paediatric and adult AML may be different. Furthermore, differences in the molecular landscape may mean that potential therapeutic targets may be different in paediatric and adult AML.

Therefore, HSC age has a profound impact on HSC biology. Furthermore, clinical and biological features of AML change with patient age. However, there is a paucity of data directly investigating the impact of cellular age on leukaemia biology. This thesis aims to examine the hypothesis that cellular age will impact cellular transformation, leukaemia biology and transcriptional landscape.

2 Materials and methods

2.1 Plasmids and cell lines

2.1.1 Plasmids

Plasmids were used in this thesis to overexpress oncogenes of interest. All plasmids were constructed in the MigR1 backbone, for the production of retrovirus. MigR1 is a murine stem cell virus (MSCV) based vector containing the internal ribosome entry site (IRES) for translation initiation, and expressing the enhanced green fluorescent protein (GPF) allowing for plasmid detection by flow cytometry. (Pear et al., 1998)

The NUP98HOXA9-MSVC-IRES-GFP and FLT3-ITD(N51)-MSVC-IRES-GFP vectors were a kind gift from Brian Huntly (Cambridge Institute for Medical Research, University of Cambridge, UK). The AML1ETO-MSVC-IRES-GFP vector was a kind gift from James Mulloy (Cincinnati Children's Hospital Medical Center, University of Cincinnati College of Medicine, USA). The human NUP98HOXA9 sequence was first extracted from patients with AML harbouring the t(7;11)(p15;p15) translocation. (Borrow et al., 1996) The NUP98HOXA9 sequence was cloned into the EcoRI site of the MigR1 vector to construct the NUP98HOXA9-MSVC-IRES-GFP vector. (Kroon et al., 2001) The FLT3-ITD(N51)-MSVC-IRES-GFP was constructed by ligating ITD sequences to human FLT3 complementary DNA (cDNA) and the resulting FLT3-ITD mutant cloned into the MigR1 vector. (Kelly et al., 2002) The AML1ETO-MSVC-IRES-GFP was constructed by cloning the human AML1-ETO cDNA into the MigR1 vector. (Mulloy et al., 2002)

All plasmids were purified from transformed chemically competent DH5α E.coli cells using the PureYield™ Plasmid Midiprep System (Promega) according to the manufacturer's protocol. In brief, 2µl of DNA glycerol stock was added to 250mL of Luria Broth (Sigma-Aldrich) and incubated at 37°C overnight. Cells were pelleted at 300 x g for 10 minutes (min) and resuspended in 6mL Resuspension Solution. Cells were lysed at room temperature (RT) by incubation for 3min in 6mL Lysis Buffer. Lysis was stopped by the addition of 10mL Neutralisation Buffer and the lysate centrifuged at 9,000 x g for 15min. The lysate was

transferred to the PureYield™ Clearing Column and plasmid was bound to the PureYield™ Binding Column and eluted by vacuum application. Plasmid concentration and purity were determined using a NanoDrop spectrophotometer ND-1000 (Labtech International).

2.1.2 Cell lines

All cell lines were internally sourced. Cell lines were maintained in a humidified incubator at 37°C with 5% CO_2 and routinely tested for mycoplasma contamination using the MycoAlert Mycloplasma Detection Kit (Lonza) as per manufacturer's protocol. A summary of cells lines used in this thesis is shown in Table 2.1.

2.1.2.1 HEK293T

The HEK293T cell line was used for the production of retrovirus. The HEK293 cell line was generated in 1973 by the transformation of human embryonic kidney cells with sheared adenovirus 5 DNA in the van der Eb lab. (Graham et al., 1977) They have been utilised in laboratory practice due to their ease of culture and transfection. The 293T variant contains the SV40 Large T-antigen, which allows more efficient replication of plasmids containing the SV40 origin of replication and thus higher titre virus. (DuBridge et al., 1987) The HEK293T cell line was cultured in Dulbecco's Modified Eagle medium (DMEM) (Life Technologies) supplemented with 10% foetal bovine serum (FBS), 1mg/mL Penicillin/Streptomycin (PS) (Invitrogen) and 2mM L-glutamine (L-glut) (Invitrogen). When cells reached a confluency of 80% they were sub-cultured in fresh media at a density of 2-4x10^4 cells/cm^2.

2.1.2.2 NIH/3T3

The NIH/3T3 cell line was generated in 1962 from murine fibroblasts and immortalised after 20-30 rounds of culture. (Todaro and Green, 1963) Due of its ease of transduction, the NIH/3T3 cell line was used to quantify the efficiency of viral transduction. The NIH/3T3 cell line was cultured in DMEM supplemented with 10% FBS, 1mg/mL PS and 2mM L-glut. When cells reached a confluency of 60% they were sub-cultured in fresh media at a density of 3-5x10^3 cells/cm^2.

2.1.2.3 OP9 cells

The OP9 cell line is a stromal murine cell line, established from newborn osteopetrotic (*op*/*op)* mutated mouse calvaria. Due to the osteopetrotic mutation, OP9 cells do not produce functional M-CSF. (Nakano et al., 1994) As it is a stromal cell line, co-culture of cells on OP9 cell is used as an *in vitro* surrogate for the BM niche. Co-culture of haemopoietic cells with OP9 cells has been utilised to study erythroid, myeloid, and lymphoid differentiation. OP9 cells were cultured in α-Minimum Essential medium (αMEM) (Invitrogen) supplemented with 20% FBS, 1mg/mL PS, 2mM L-Glut, 1% 100mM sodium pyruvate (Invitrogen), 1% 1M 4-(2-hydroxyethyl)-1-piperazineethanesulfonic acid (HEPES) (Invitrogen) and 0.1% 2-mercaptoethanol (BME) (Sigma-Aldrich). When cells reached a confluency of 60% they were sub-cultured in fresh media at a density of $4x10^3$ cells/cm^2.

2.1.2.4 WEHI-3B

The WEHI-3B cell line is a myelomonocytic leukemia cell line generated from the Balb/c mouse, which had undergone paraffin injections, intended to induce plasma cell tumour development. (Warner et al., 1969) WEHI-3B cells secrete high levels of IL3 into the media which can be collected as a source of IL3. WEHI-3B cells were maintained in Roswell Park Memorial Institute medium 1640 (RPMI1640) (Invitrogen), 10% FBS, 1mg/mL PS and 2mM L-Glut. When cells reached a density of $2x10^6$ cells/mL they were sub-cultured in fresh media at a density of $1\text{-}2x10^5$ cells/mL.

2.1.2.5 Production of WEHI conditioned media

The WEHI-3B cell line was used to produce IL3 containing conditioned media. WEHI-3B cells were seeded in T175 flasks at a density of 10^5 cells/mL. Flasks were incubated for 3-5d, at which point the media turns yellow due to a pH change from cell expansion. The conditioned media was removed, centrifuged at 300 x g for 10min and passed through a vacuum filter to remove cell debris. The conditioned media was stored at -20°C in aliquots of 20 or 50mL.

Table 2.1 Cell lines used

Cell line	Origin	Culture media
HEK293T	Human embryonic kidney	DMEM, 10% FBS, PS 1mg/mL, L-Glut 2mM
NIH/3T3	Mouse fibroblast	DMEM, 10% FBS, PS 1mg/mL, L-Glut 2mM
OP9	Mouse mesenchymal stem cell	αMEM, 20% FBS, PS 1mg/mL, L-Glut 2mM, 1% 100mM sodium pyruvate, 1% 1M HEPES, 0.1% BME
WEHI-3B	Mouse myelomonocytic leukaemia	RPMI1640, 10% FBS, PS 1mg/mL, L-Glut 2mM

2.2 Tissue culture

Tissue culture was performed in a laminar air-flow hood (Biosafety Class II). Strict aseptic technique was adhered to, to ensure sterile working procedures.

2.2.1 Cell line passage

Cell lines were sub-cultured at the appropriate dilution for up to 2m. For adherent cell lines (HEK293T, HIN/3T3 and OP9 cells) media was aspirated and cells washed with phosphate buffered saline (PBS) (Table 2.2). Trypsin-EDTA (Sigma-Aldrich) was used to detach cells from the culture plate. Excess media was then added to stop the reaction and cells pelleted at 300 x g at RT for 5min. Cells were resuspended and sub-cultured in fresh warmed media at an appropriate dilution. For suspension cell lines (WEHI-3B) the desired number of cells was pelleted at 300 x g at RT for 5min resuspended at the appropriate density in fresh media.

Table 2.2 Components of PBS

ddH_2O = double distilled water

Components	Final concentration
Diluent ddH_2O	
NaCl	137 mM
KCl	2.7 mM
Na_2HPO_4	10 mM
KH_2PO_4	2 mM

2.2.2 Thawing and cryopreservation of cells

To thaw cryopreserved cells, cells were thawed quickly at 37°C in a waterbath and suspended in 15mL pre-warmed complete media. Cells were centrifuged at 300 x g at RT for 5min, resuspended in 15mL media and centrifuged again to remove dimethysulfoxide (DMSO) (Sigma-Aldrich). The cell pellet was

resuspended in 10mL complete media and transferred to a culture flask/plate. For cryopreservation, cells were centrifuged at 300 x g at RT for 5min and the supernatant discarded. Cell pellets were resuspended in freezing media and 1mL aliquots transferred to cryotubes. Cells were stored at -80°C for short-term storage, or in liquid nitrogen for long-term storage. For cell lines, cells were resuspended at a concentration of up to 10^6 cells/mL. Freezing media was 50% complete media, 40% FBS and 10% DMSO. For primary murine cells, cells were resuspended at a concentration of up to $50x10^6$ cells/mL. Freezing media was FBS with 10% DMSO.

2.2.3 Manual cell count

Dye exclusion by trypan blue (Sigman-Aldrich) was used to determine live cell counts, based on the principle that live cells have an intact cell membrane to exclude dyes. Cells were prepared in media/PBS and added to 0.04% trypan blue. 10uL of the mixture was loaded on a counting chamber. At least 100 cells were counted in a whole number of large squares. (Figure 2.1) Total cell number in solution was determined using the following calculation:
Total cells ($x10^4$) = cells counted/number squares x dilution factor x volume

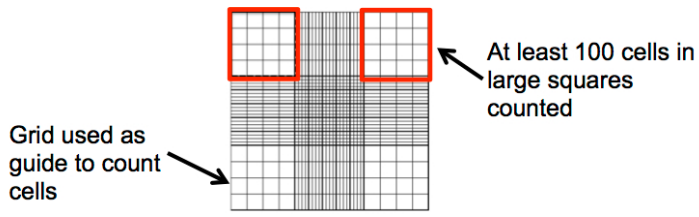

Figure 2.1 Cell counting

2.2.4 Retroviral production

Retrovirus was produced utilising the calcium phosphate method of transfection, in order to introduce DNA material into mammalian cells. The HEK293T cell line was used to package MigR1 based expression vectors using the packaging plasmid pCGP (which encodes the *pol* precursor protein and *gag* reverse transcriptase) and envelope plasmid pHIT123.

At least 6 hours (h) before transfection $5x10^6$ HEK293T cells were plated in 10cm dishes. Fresh 2X transfection buffer (Table 2.3) and 500µL of DNA cocktail (Table 2.4 and Table 2.5) were prepared in 15mL falcon tubes. Just prior to transfection, the media was removed from the cells and 3mL fresh warm media added to the plates. 500µL of 2X transfection buffer was added drop-wise to 500µL of DNA cocktail and bubbles gently introduced into the mixture using a 1mL sterile pipette. The mixture was added drop by drop to the culture dish, the plates gently tilted to aid even distribution of the mixture and returned to the incubator. After 6h, the media was removed and 4.5mL of fresh media added to the plates. Retrovirus containing supernatants were harvested at 24, 36 and 48h post transfection. The supernatant was centrifuged at 300 x g at RT for 5min to remove cellular debris. Aliquots of 1mL were snap frozen on dry ice and stored at -80°C.

Table 2.3 Transfection buffer for retrovirus production

Components	Final concentration
Diluent ddH_2O	
HEPES (pH 7.1)	0.05 M
NaCl	0.28 M
Na_2HPO_4	2 mM

Table 2.4 10X NaCl-Tris-EDTA (NTE) buffer

Components	Final concentration
NaCl	1.5 M
Tris-HCl (pH 7.4)	0.1 M
EDTA (pH 8.0)	10 mM

Table 2.5 DNA cocktail for retroviral transduction

Components	Final concentration
$CaCl_2$	0.25 M
10X NTE buffer	1X
MigR1 (control) DNA	15 µg
pCGP	10 µg
pHIT13	6 µg
Diluent ddH_2O	To make up to 500µL

Components	Final concentration
$CaCl_2$	0.25 M
10X NTE buffer	1X
NH9, A1E or FLT3-ITD DNA	30 µg
pCGP	20 µg
pHIT13	12 µg
Diluent ddH_2O	To make up to 500µL

2.2.5 Titration of retrovirus using NIH/3T3 cells

For retroviral constructs expressing GFP, retroviral titre was determined by transduction into NIH/3T3s. The day before transduction $2x10^5$ NIH/3T3 cells were plated onto 6cm culture dishes and incubated overnight. Two plates were prepared for each viral harvest. After 24h the media was removed and replaced with 1mL of media supplemented with 4µg/mL polybrene (Sigma-Aldrich). Polybrene, or hexadimethrine bromide, is a cationic polymer used to increase the efficiency of viral transduction. It does so by neutralising the charge repulsion between viral particles and sialic acid on the cell surface. Either 10µL or 100µL of virus was added to each plate and incubated overnight. After 24h, 2mL of fresh media was added to each plate so that the total volume was 3mL. After a further 24h, transduced cells were harvested and GFP expression determined by flow cytometry on a FACSCanto II (BD Biosciences) using the FITC channel. The percentage of GFP positive cells equated to the viral titre. Untransduced NIH/3T3 cells were used as a negative control. (Figure 2.2) To calculate the volume of virus required in subsequent experiments the following formula was used:

(X / % titre) x (tested volume in µL / 100) = volume of virus (in mL) required in a total volume of 4mL, where X is the desired % titre.

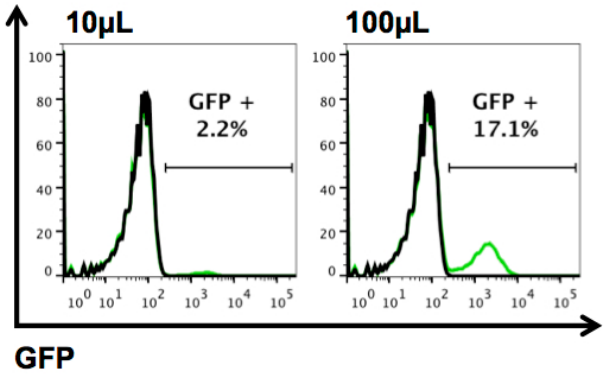

Figure 2.2 Retrovirus titration

Representative flow cytometry plots of virus titre, measured by GFP% in NIH/3T3s transduced with 10µL (left) and 100µL (right) of retrovirus. Black line represents untransduced control and green line represents transduced sample.

2.2.6 Retroviral transduction of primary cells

Murine BM and FL cells were retrovirally transduced to express GFP tagged oncogenes. Single cell suspension of BM or FL was obtained as described in Section 2.4.1. Cells were cKit enriched as described in Section 2.2.10. cKit enriched BM or FL cells were pre-stimulated overnight in pre-stimulation cocktail supplemented with recombinant murine (rm) IL3, rmIL6 and rmSCF (all Peprotech) (Table 2.6). Cells were pre-stimulated in a final concentration of 1-5x10^6 cells/mL. The following day cells were washed from the plates and counted; 40-60% recovery was expected. Cells were centrifuged at 350 x g at 4°C for 10min and resuspended in activation cocktail (Table 2.7) without virus and 3mL transferred to 6 well plates. At this point, virus was quickly thawed and added to the appropriate well. If the volume of virus was less than 1mL, DMEM was added to make up the volume to 4mL. The final cell concentration was 0.5-2x10^6 cells/mL. Plates were centrifuged at 1290 x g at RT for 90min and then incubated at 37°C. After 6-12h a second spinoculation was done. 1mL of cell suspension was removed from each well into a 1.5mL Eppendorf tube and centrifuged at 350 x g at 4°C for 10min. The supernatant was removed and the cell pellet dislodged by flicking. The pellet was resuspended in 1mL virus (made up to volume with DMEM if required) and fresh cytokines and polybrene (for 4mL) and returned to the corresponding well. The plates were centrifuged at 1290 x g at 4°C for 90min and then returned to the incubator until they were required.

For transduction of progenitor cells (LSK, CMP and GMP) the above method was used with the following adjustments for low cell number. Cells were pre-stimulated in a volume of 0.3-1mL at a final concentration of 1-4x10^6 cells/mL. The following day cells were counted, but to minimise cell loss, cells were not washed from the plate. An equal volume of virus was added directly to the well, as well as cytokines and polybrene at a final concentration as per Table 2.7. Progenitor cells were transduced in a volume of 0.6-2mL at a cell density of 0.5-2x10^6 cells/mL. Plates were centrifuged at 1290 x g at 4°C for 90min and returned to the incubator. After 3h cells were removed, washed and centrifuged at 350 x g at RT for 5min, ready for downstream culture experiments.

Table 2.6 Pre-stimulation cocktail for retroviral transduction

Components	Final concentration
DMEM	Quantity sufficient to desired volume
FBS	15%
PS	1% (100 mg/mL)
L-Glut	1% (2mM)
rmIL3	10 ng/mL
rmIL6	10 ng/mL
rmSCF	100 ng/mL

Table 2.7 Activation cocktail for retroviral transduction

Components	Final concentration
DMEM	Quantity sufficient to desired volume
FBS	15%
PS	1 mg/mL
L-Glut	2mM
rmIL3	10 ng/mL
rmIL6	10 ng/mL
rmSCF	10 ng/mL
Polybrene	4 µg/mL
Viral supernatant	Volume for desired final titre

2.2.7 Colony forming cell assay

The CFC assay is utilised to determine the proliferative and differentiative ability of stem and progenitor cells *in vitro*. Culturing HSPCs in cytokine supplemented semi solid media such as methylcellulose results in the formation of colonies. The number of colonies produced relates to the proliferative potential of the HSPC and the morphology and surface marker expression of the colony relates to the differentiative potential. Furthermore, cells harvested from primary platings (CFC1) can be reseeded in serial replatings (CFC2, CFC3 etc.) as an indication of *in vitro* self-renewal capacity. Normal HSPCs differentiate and exhaust after the second plating (CFC2) while oncogene transformed cells serially replate for at least 3 rounds. Methocult GF M3434 (Stemcell Technologies) has been optimised for the growth and enumeration of murine HSPCs from BM, PB, spleen and FL. It is supplemented with the cytokines 50ng/mL rmSCF, 10ng/mL rmIL3, 10ng/mL recombinant human (rh) IL6 and 3U/mL rhEPO. M3434 was supplemented with 1mg/mL PS and stored in aliquots of 3mL or 4mL (for duplicate and triplicate cultures, respectively) at -20°C. Before use, M3434 was thawed at 4°C overnight. Cells were prepared in culture media at 10X of the final concentration required per mL. For example, for a final concentration of $5x10^2$ cells/mL in methylcellulose, cells were prepared at

a concentration of $5x10^3$ cells/mL in media. Cells were injected into M3434 using a 16 gauge blunt end needle (Stem Cell Technologies) fitted with a 3 mL luer slip syringe (Terumo) and vortexed to mix. For duplicate cultures 300µL of cells were added to 3mL of M3434 and for triplicate cultures 400µL of cells were added to 4mL of M3434. The mixture was left to stand for 10min to allow bubbles to dissipate. The mixture was drawn up into the needle and syringe and 1.1mL of mixture was carefully dispensed to 35mm culture dishes, avoiding the creation of air bubbles. Up to 4 35mm dishes were placed in a 150mm petri dish. Two additional uncovered 35mm dishes containing 3mL ddH_2O were also added to the petri dish to help maintain humidity during the culture. Plates were incubated at 37°C. After 7-10d, resulting colonies were counted, identified and images taken on an EVOS XL Core Imaging System (Fisher Scientific). Cells were harvested for flow cytometry analysis, cytospin and to reseed in serial replating cultures. To harvest the cells M3434 was liquefied by the addition of 3mL PBS to each plate. Plates were washed and total cell number per plate quantified by trypan blue counts. For replating, cells were prepared and added to fresh M3434 as described above. Figure 2.3A shows a diagrammatic representation of the process, seeded cell number and interval between platings.

M3434 allows the detection of myeloid colony forming units. These include granulocyte erythroid macrophage megakaryocyte (GEMM), granulocyte macrophage (GM), granulocyte, macrophage and erythroid colonies. Representative images of colony types are shown in Figure 2.3B and a description of the colonies that can be produced are shown in Table 2.8.

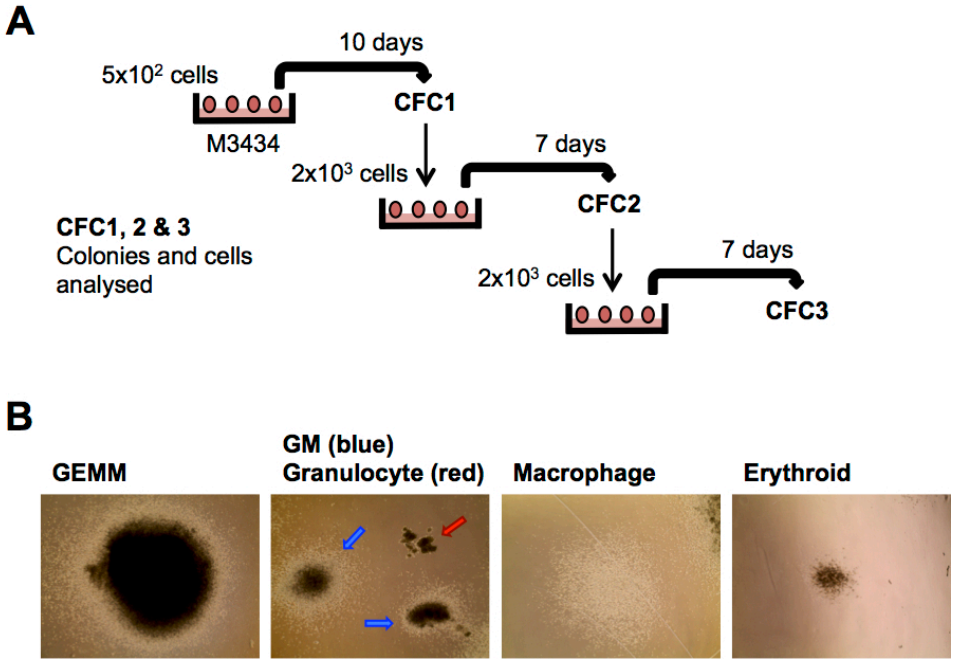

Figure 2.3 CFC assay

(A) Overview of CFC assay
(B) Representative photographs of GEMM, GM, granulocyte, macrophage and erythroid colonies (taken at x4 magnification)

Table 2.8 Identification of colony type

Colony defined as a collection of >50 cells. Table modified from Mouse Colony Forming Assay by Methocult® Technical Manual version 3.1.1 (Stemcell Technologies).

Colony type	Description
GEMM	Large colony containing >500 cells with a highly dense core and indistinct boarder between the core and peripheral cells. Erythroblast clusters visible along the periphery of the colony. Monocytic/macrophage and granulocytic cells identifiable. Large megakaryocytic cells usually present.
GM	Usually smaller that GEMM colonies. Often contain multiple cell clusters (dense core surrounded by cells). The monocytic/macrophage lineage cells are large cells with an oval to round shape with a grainy or grey centre. The granulocytic lineage cells are round, bright, and are much smaller and more uniform in size than macrophage cells.
Granulocyte	Tight cluster of cells with distinct boarder. Granulocytic lineage cells are round and bright.
Macrophage	Loose, spread out cluster of cells with indistinct boarder. Monocytic/macrophage lineage cells are large, oval/round shaped.
Erythroid	Made up of erythroid clusters, which are scattered and lack a dense core. Cells are small and irregular in shape. Cells contain red pigmentation due to haemoglobin.

2.2.8 Liquid culture

Cells were cultured in cytokine supplemented media as an *in vitro* assessment of intrinsic transformation ability. Normal cells do not continually grow in liquid culture. Therefore, prolonged growth in liquid culture suggests the attainment

of self-renewal properties. Retrovirally transduced FL HSCPs (LSK, CMP and GMP) were seeded in 24 well plates at a density of $1x10^5$ cells/mL in DMEM supplemented with 15% FBS, 1mg/mL PS, 2mM L-Glut and either cytokine mix 1 or 2 (Table 2.9). Once cells could expand without cytokine supplementation, they were cultured in DMEM supplemented with 10% FBS, 15% WEHI conditioned media, 1mg/mL PS and 2mM L-Glut. Cells were counted every 3-4 days. When cells had expanded to a density of $\geq 1x10^6$ cells/mL, they were diluted 1:10 to $1x10^5$ cells/mL. Excess cells were used for flow cytometry analysis to ascertain GFP percentage. All cell counts were normalised to GFP percentage. To assess cumulative cell growth, the following calculation was used:
Cumulative cell number = counted cell number x cumulative dilution factor

Table 2.9 Cytokine mixture for liquid culture

Components	Final concentration
Mix 1	
rmIL3	10 ng/mL
rmIL6	10 ng/mL
rmSCF	100 ng/mL

Mix 2	
rmIL3	5 ng/mL
rmIL11	40 ng/mL
rmSCF	600 ng/mL

2.2.9 OP9 co-culture

The OP9 co-culture system has been used to differentiate cells into myeloid, B and T-lymphoid cells. As OP9 cells are a stromal cell line, sharing the immunophenotype of normal murine MSCs, OP9 cells can be used as an *in vitro* model for the BM niche. The day before co-culture (D-1), 1mL of OP9 cells were seeded in 24 well plates at a density of $5x10^5$ cells/mL. After 24h (D0) transduced FL HSPCs (LSK, CMP and GMP) were prepared in OP9 media (Table 2.1) supplemented with either cytokine 1 or 2 (Table 2.9) at a density of $1x10^5$ cells/mL. Media was removed from the OP9 plates and 1mL of cells added to the empty wells with an OP9 layer. After 2d (D2), the media was aspirated from each well. The media was centrifuged at 350 x g at RT for 5min to recover any suspension cells that had also been aspirated. The supernatant was discarded and the cell pellet resuspended in fresh media with cytokines and returned to the corresponding OP9 layer containing well. After 24h (D3), fresh OP9 cells

were plated in 24 plates at a density of $5x10^5$ cells/mL (as for D-1). After 24 hours (D4) cells from each well were removed and transferred to 1.5mL Eppendorf tubes. Each well was washed with 500µL of PBS to remove any remaining cells but not OP9s and added to the Eppendorf. Cells were enumerated by trypan blue counts. The cells were centrifuged at 350 x g at RT for 5min and the supernatant discarded. The cells were resupended in 1mL of fresh OP9 media supplemented with cytokines. If cells had expanded to a density of $\geq 1x10^6$ cells/mL a 1:10 dilution was carried out. The media was removed from the OP9 layer plated 24h previously and media containing cells added to the empty well with the OP9 layer. Excess cells were used for flow cytometry analysis to determine GFP percentage. Complete media (without cytokines) was added to the old OP9 plates and incubated for 1-2 days to recover cells that had burrowed beneath the OP9 layer and emerged on later days. These cells were also used for flow cytometry analysis.

2.2.10 Magnetic activated cell sorting

Magnetic activated cell sorting (MACS) allows cells to be separated based on surface antigen expression by incubating with magnetic nanoparticles coated with antibodies against a particular surface antigen. Cells are separated by passing through a magnetic column. Cells attached to the nanoparticles (expressing antigen) bind to the column (positive selection) while the remaining cells (not expressing antigen) flow through (negative selection). MACS was used to enrich murine BM and FL for HSPCs by positively selecting for cKit expressing cells. MACS buffer (Table 2.10) was used throughout the procedure. Cells were kept on ice to minimise non-specific antibody binding.

BM and FL cells were harvested and red blood cells (RBC) lysed as per Section 2.4.1. Cells were counted and centrifuged at 350 x g at 4°C for 5min. The supernatant was aspirated completely. Up to $8x10^7$ cells were resuspended in buffer and 20µL cKit (CD117) microbeads (Miltenyi Biotec) in a total volume of 400µL. Cells were mixed well and incubated at 4°C for 15min. Cells were washed by adding 1mL of buffer to 10^7 cells and centrifuged at 350 x g at 4°C for 5min. The supernatant was aspirated completely. Up to 10^8 cells were resuspended in 500µL buffer before proceeding with magnetic separation.

MS columns (Miltenyi Biotec) can bind up to 10^7 magnetically labelled cells and were used when the sample cell number did not exceed $2x10^8$. LS columns (Miltenyi Biotec) can bind up to 10^8 magnetically labelled cells and were used when the sample cell number did not exceed $2x10^9$. An MS or LS column was placed in the magnetic field of a MACS Separator (Miltenyi Biotec) and prepared by rinsing with 500µL (MS column) or 3mL (LS column) of buffer. Cells were passed through a 40µm strainer (Fisher Scientific) to remove clumps and applied to the prepared column. The flow through was collected. The column was washed 3 times with 500µL (MS column) or 3mL (LS column) and the flow through collected. The total effluent was the unlabelled ($cKit^-$) cell fraction. To collect the labelled ($cKit^+$) fraction, the column was removed from the separator and placed in a 15mL falcon. Either 1mL (MS column) or 5mL (LS column) was added to the column and the magnetically labelled cells flushed out by firmly pushing the plunger into the column.

Table 2.10 MACS buffer

Components	Final concentration
Diluent PBS	
EDTA	2 mM
FBS	2 %

2.3 Flow cytometry

Flow cytometry technology is used to analyse the physical and chemical characteristics of cells in a fluid as it passes through a laser. Cell components are fluorescently labelled and then excited by the laser to emit light at varying wavelengths. Samples were stained, washed and analysed in PBS/2% FBS, kept on ice and protected from light. To pellet cells, cells were centrifuged at 350 x g at 4°C for 5min. Compensation was done using unstained controls and single colour stained UltraComp Beads (Affymetrix eBioscience). Flow cytometry data were acquired using a FACSCanto II (BD Biosciences). Flow cytometry data were analysed using FlowJo software v7 (Treestar Inc). Data were analysed on single cells gated through forward scatter-area (FSC-A) versus forward scatter-height (FSC-H). Viable cells were gated through FSC-A versus side scatter-area (SSC-A). Where possible, dead cells were also excluded using either a 4',6-diamidino-2-phenylindole (DAPI) (Sigma-Aldrich) or 7-aminoactinomycin-D (7-AAD) dye.

(Figure 2.4) Unstained or fluorescence-minus-one (FMO) controls were used to determine placement of gates.

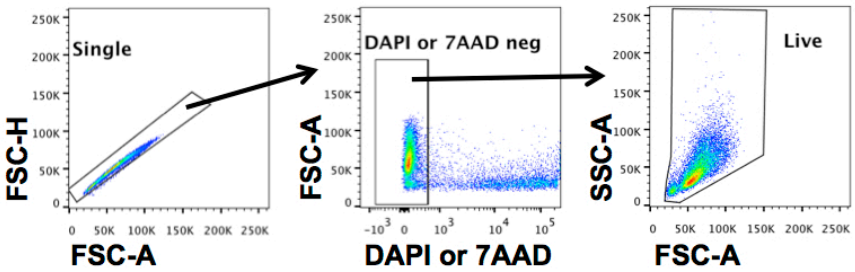

Figure 2.4 Initial gating strategy for flow cytometry analysis

2.3.1 Determining surface marker expression

Samples were harvested and washed. Cell pellets were resuspended in 50µL of PBS contained antibody cocktail. For antibody cocktails see Table 2.11. Samples were mixed and incubated for 20min on ice, protected from light. For biotinylated antibodies, after incubation with primary antibody, cells were washed and incubated with fluorochrome-conjugated streptavidin (SV) for 20min on ice, protected from light. Cells were washed again and resuspended in 200µL buffer containing DAPI (1:1000 dilution of 1mg/mL stock) and flow cytometry analysis was performed.

2.3.2 Cell trace violet staining

CellTrace™ Violet (CTV) (Invitrogen) is a stable, non-toxic membrane permeable dye. Upon entry into the cell, the non-fluorescent molecule is converted to a fluorescent derivative by cellular esterases. The active succinimydyl ester covalently binds to amine groups in proteins, resulting in long-term dye retention within the cell. Through subsequent cell divisions, daughter cells receive approximately half of the fluorescent label of their parent cells. CTV can be detected by flow cytometry in the Pacific Blue channel. CTV staining was used to label donor cells prior to BMT homing experiments. Recipients were sacrificed 18h post BMT, when donor cells would not have undergone cell cycle and thus would retain 100% of CTV staining. A 5mM stock of CTV was made by adding 20µL of DMSO to 1 vial of CTV reagent and stored at 4°C. Samples were

washed and pelleted. Up to 10^6 cells were resuspended in 1mL buffer. To this, 1µL of CTV was added for a final working concentration of 5µM. Cells were incubated for 20min at 37°C, protected from light. The reaction was quenched by adding 4mL PBS/20% FBS and incubated for 5min at RT, protected from light. Cells were pelleted and washed once more with buffer. Cells were resuspended in PBS/2% FBS in the desired concentration for BMT.

2.3.3 Fluorescence activated cell sorting

Fluorescence activated cell sorting (FACS) uses the principles of flow cytometry to sort cells based on their fluorescently labelled components. MACS cKit enriched BM or FL (either prior to or after transduction with GFP expressing retrovirus) was sorted for LSK, CMP and GMP populations. Samples were washed and incubated with antibody as described in Section 2.3.1. For antibody cocktail see Table 2.11. Cells were washed and resuspended in 300-1000µL of buffer and passed though a 40µm cell strainer prior to sorting. FACS was performed by Jennifer Cassels using a BD FACSAria III (BD Biosciences). Representative plots demonstrating FACS are shown in Figure 2.5. Cells were collected in buffer, or for RNA extraction, directly into RNA lysis buffer.

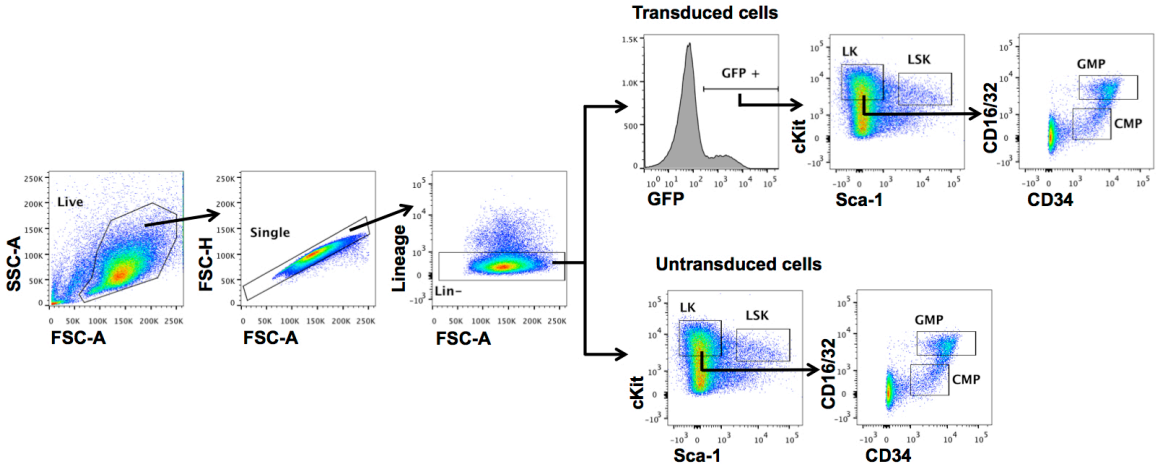

Figure 2.5 FSCs for HSPCs

Strategy for sorting transduced (top) and untransduced (bottom) LSK, CMP and GMP populations

Table 2.11 Antibody cocktails for flow cytometry

Stain	Antibody	Clone	Dilution	Flurochrome	Supplier
Lineage (CD11b omitted for FL)	CD3	145-2C11	1:200	eFlur®450	eBioscience
	CD4	RAM4-5	1:200	eFlur®450	eBioscience
	CD8a	53-6.7	1:200	eFlur®450	eBioscience
	CD11b	M1/70	1:200	eFlur®450	eBioscience
	GR1	RB6.8C5	1:200	eFlur®450	eBioscience
	B220	RA3-6B2	1:200	eFlur®450	eBioscience
	Ter119	Ter-119	1:200	eFlur®450	eBioscience
HSPC sort	Lineage				
	cKit	2B8	1:200	APC	eBioscience
	Sca-1	D7	1:250	PE-Cy7	eBioscience
	CD34	RAM34	1:200	Biotin	eBioscience
			1:200	→ SV PE	eBioscience
	CD16/32	2.4 G2	1:200	APC-Cy7	BD Pharmigen
	+/- GFP				
Myeloid	CD11b	M1/70	1:200	PE	eBioscience
	GR1	RB6.8C5	1:250	PerCP-Cy5.5	eBioscience
	F4/80	BM8	1:200	APC	eBioscience
	cKit	2B8	1:200	APC-Cy7	Biolegend
	CD34	RAM34	1:200	Biotin	eBioscience
			1:200	→ SV PE-Cy7	eBioscience
	DAPI		1:1000		Sigma-Aldrich
	GFP				
Lymphoid	CD3	17A2	1:250	Biotin	eBioscience
			1:200	→ SV PE Cy7	eBioscience
	CD4	RAM4-5	1:250	APC	eBioscience
	CD8a	53-6.7	1:250	PE	eBioscience
	B220	RA3-6B2	1:250	PerCP-Cy5.5	eBioscience
	CD19	eBio ID3	1:150	APC-Cy7	eBioscience
	DAPI		1:1000		Sigma-Aldrich
	GFP				

2.4 Animal work

Animal work was carried out in accordance with the Animals (Scientific Procedures) Act 1986 and UK Home Office regulations. All experiments were performed under the author's personal license (I2E19129B) and Dr Karen Keeshan's project licence (60/4512). Animals were housed either at the Veterinary Research Facility or the Beatson Institute for Cancer Research at the University of Glasgow. WT C57Bl/6 mice, used for *in vitro* studies and as donors for BMT experiments were bred in house. WT C57Bl/6 mice used as BMT recipients were purchased from Charles River Laboratories. Injection of donor cells into recipients and assistance in monitoring and harvesting of experimental animals was done by Karen Dunn, University of Glasgow.

2.4.1 Harvesting tissue

Mice were sacrificed by authorised Schedule 1 methods. After confirming death blood was obtained for analysis by cardiac puncture. Sternum, legs, pelvic girdle, spleen, thymus and liver were dissected out. Sterna were stored in 10% buffered formalin. Tibiae, femurs and hips were clean and dipped in 70% ethanol (EtOH) followed by sterile PBS. Bones were crushed by mortar and pestle in 10ml PBS/2% FBS 3 times and the solution passed through a 40μM strainer to obtain BM cells. To obtain a single cell solution from spleen, thymus and liver a 40μM cell strainer was placed on a 50mL falcon and moistened with 10mL PBS/2% FBS. The organ was homogenised through the cell strainer using the plunger from a sterile 5ml syringe (Terumo) and the strainer washed with 10mL PBS/2% FBS and cells collected in the 50mL falcon. This was repeated 2 times. To harvest FL at E14.5, pregnant females were sacrificed 14.5d after observation of a vaginal plug and the foetuses excised. Whole foetal liver was dissected out and a single cell suspension obtained using the same method as for adult spleen, thymus and liver. For all tissues, single cell suspensions were centrifuged at 350 x g at 4°C for 5min. To lyse RBCs, the cell pellet was incubated in 2ml RBC lysis buffer (Table 2.12). After 7min 10mL of PBS/2% FBS was added to quench the reaction. The mixture was centrifuged at 350 x g at 4°C for 5min, the supernatant discarded and cells used in downstream experiments.

Table 2.12 RBC lysis buffer

Components	Final concentration
Diluent ddH_2O	
NH_4AC	150 mM
$KHCO_3$	10 mM
EDTA	0.1 mM

2.4.2 BMT for leukaemogenesis

The murine BM reconstitution assay allows the study of primitive HSCs that can repopulate the haemopoietic system of lethally irradiated recipients. BMT of oncogene expressing cells results in leukaemia in recipient mice and is a powerful model of leukaemogenesis. Pre-transplant transformation and expansion of oncogene expressing cells *in vitro* increases donor cell number,

thereby improving engraftment efficiency. As such, recipients can receive a sub-lethal dose of irradiation, thereby decreasing irradiation related toxicity.

LSK, CMP and GMPs, transduced with GFP tagged NH9 retrovirus, were expanded in methylcellulose and donor cells harvested at CFC2, as described in Section 2.2.7. The final donor cell dose per mouse was resuspended in 200µL of sterile PBS/2% FBS. 0.1-1x10^6 cells were transplanted per recipient. Four hours prior to transplantation recipient mice received a sub-lethal dose of X-ray irradiation of 5.5 grays (Gy) using a RS225 Cabinet GS032 irradiator (Xstrahl). Donor cells were injected into the tail veil after heat lamp vasodilation. Animals were housed in individually ventilated cages for the duration of the experiment. Enrofloxacin 80mg/L (Baytril® injectable solution) was supplemented into the drinking water for 10-14d post transplant to minimise risk of sepsis. Animals were monitored for clinical signs of disease and by regular PB sampling every 2-4 weeks. Donor cells were identified as GFP^+. Animals were sacrificed when they displayed clinical signs of leukaemia, had a WCC of >20x10^6/mL or a rising GFP% in PB. Clinical signs of leukaemia included weight loss, reduced activity, hunched posture, piloerection and increased respiratory rate. Mice that did not succumb to disease were sacrificed at the end of the experiment (12m post BMT as per animal license). Organs were harvested as described in Section 2.4.1. Spleen and thymus were photographed and weighed before single cell suspensions were made. Cytospins of BM and spleen were made as described in Section 2.4.5. Flow cytometry analysis was performed on the critical organs.

2.4.3 BMT for homing

LSKs, transduced with GFP tagged NH9 retrovirus, were expanded in methylcellulose and donor cells harvested at CFC2, as described in Section 2.2.7. To aid *in vivo* detection, GFP-tagged NH9 transduced donor cells were dyed with CTV (Section 2.3.2). 0.2-1x10^6 cells were transplanted into each recipient. The final donor cell dose per mouse was resuspended in 200µL of sterile PBS/2% FBS. Four hours prior to transplantation recipient mice received X-ray irradiation at a sub-lethal dose of 5.5Gy. Donor cells were injected into the tail veil after heat lamp vasodilation. Animals were housed in individually ventilated cages for the duration of the experiment. Mice were sacrificed 18h post tail vein injection. BM

and PB were harvested as described in 2.4.1. Percentage of donor cells in BM and PB was assessed by flow cytometry and total cellularity of BM and PB was calculated by trypan blue counts. Absolute donor cell number in BM and PB was calculated as a percentage of donor cells (determined by flow) of the total cell count in BM or PB. The number of injected cells was not uniform. To allow for comparison between the 2 groups, the percentage of donor cells homing to BM or PB was calculated. (Figure 2.6)

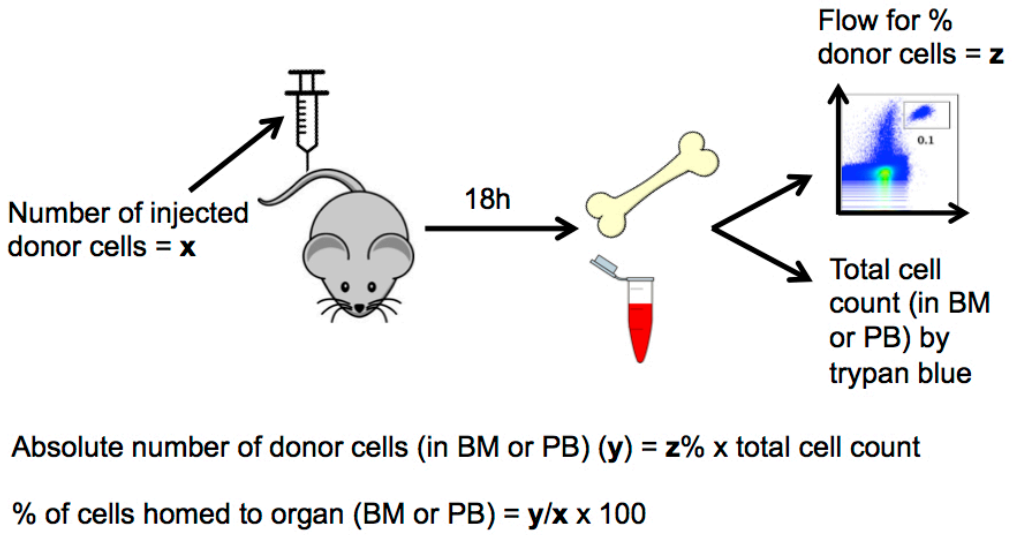

Figure 2.6 Overview of homing experiment

Schematic of homing experiment and calculations to determine absolute number of donor cells in BM or PB, and percentage of donor cells homed to BM or PB.

2.4.4 Peripheral blood sampling

PB was obtained from the tail vein after vasodilation by heat lamp. The vein was lanced using a 25 gauge needle (BD Pharmaceuticals) and 10-30µL blood was collected by capillary action into an EDTA lined Microvette® capillary blood tube (Sarstedt). 5µL of blood was added to 95µL of 3% acetic acid (1:20 dilution) and a manual cell count performed. Blood smears were made by dropping 3µL of blood on a microscopy slide (VWR International). The edge of another slide was used to smear the blood on the slide, making a thin film. Slides were air dried and stained as described in Section 2.4.6. The remaining blood was lysed in 500µL RBC lysis buffer for 5min and quenched with 4mL PBS and then prepared for flow cytometry as per Section 2.3.1 to assess donor engraftment and expression of myeloid surface antigens.

2.4.5 Cytospin

Cytospins were made of BM and spleen harvested from BMT recipients and from total cells harvested from CFC assays. A microscopy slide and chamber was loaded on a Cytospin™ clip (Thermo Scientific). 50µL of single cell suspension containing 5-10x10^4 cells was loaded into the chamber and deposited onto the microscopy slide using the Shandon™ Cytospin™ 4 Cytocentrifuge (Fisher Scientific). The cells were centrifuged at 23 x g at RT for 4min with medium acceleration rate. The slide was air dried and fixed and stained as described in 2.4.6. Slides were viewed on an Olympus CKX41 inverted microscope (Olympus) and images taken using a Colorview U-CMAD3 camera (Olympus) and Cell B Imaging Software (Olympus).

2.4.6 Kwik- Diff™ stain

The Shandon™ Kwik-Diff™ stain (Thermo Scientific) is a quick method for differential staining. PB smears and cytospins were stained using this method. Dried slides were inserted 10 times each into reagent 1 (methanol-fixative), followed by reagent 2 (eosin), followed by reagent 3 (methylene blue) and then dipped in water to clean excess reagent. Slides were air dried and visualised using a standard light microscope.

2.4.7 Histochemistry

Sternal sections were prepared by Lynn Stevenson at the Veterinary Diagnostic Services, University of Glasgow. Sterna were decalcified with 5.5% EDTA solution containing 10% formaldehyde for 7-8d. Decalcified sterna were embedded in paraffin and sections cut at 2.5µm and fixed onto microscopy slides. Slides were stained with Gills haematoxylin (Fischer Scientific) and Potts eosin (Merck) (H&E), or submitted for immunohistochemistry (IHC) with antibodies directed against markers for myeloid/granulocytic cells (myeloperoxidase, MPO) and T-lymphocytes (CD3). Details of the antibodies used are shown in Table 2.13. Tissue sections were dewaxed in xylene and descending alcohols and rehydrated in ddH_2O; endogenous peroxidase was quenched by immersion in 3% hydrogen peroxide in PBS for 5min. The IHC procedure was completed with the Dako Autostainer (Agilent). The Dako Envision (Agilent) visualisation system was used

to detect antibody binding followed by 3,3'-diaminobenzidine chromogen. Following completion of the chromogen reaction, slides were rinsed in ddH_2O, counterstained in Harris' haematoxylin for 30 seconds, rinsed in water, dehydrated in ascending alcohols and xylene, and coverslipped. Slides were independently reviewed by Francesco Marchesi and Pamela Johnston from the Veterinary Diagnostic Services, University of Glasgow and correlated with the author's findings.

Table 2.13 Antibodies used for IHC

Antibody	Species	Raised in	Dilution	Supplier
MPO	Mouse	Rabbit (polyclonal)	1:3000	Dako Agilent
CD3	Mouse	Rabbit (polyclonal	1:100	Dako Agilent

2.5 Gene expression

2.5.1 Primer design

Primers were designed for use with Fludigm™ quantitative polymerase chain reaction (qPCR) using Primer-BLAST software on the NCBI website (http://www.ncbi.nlm.nih.gov/tools/primerblast) using the following specifications. Forward and reverse primers were approximately 20 base pairs (bp) in length with a melting temperature of ~60°C and GC content of 40-60%. Primers were designed to span an exon-exon gap, to ensure amplification of cDNA and not residual genomic DNA. Primer pairs were selected to amplify a product sequence of 50-150bp and checked for the absence of self-complementary binding using OligoCalc software (http://biotools.nubic.northwestern.edu/OligoCalc.html), to prevent the formation of hairpin structures and primer dimerisation. Primer pair specificity was confirmed using Nucleotide-BLAST software on the NCBI website (https://blast.ncbi.nlm.nih.gov/Blast.cgi?PAGE_TYPE=BlastSearch). Primer pairs that displayed >80% overlap with unintended sequences were not used. Primers were synthesised commercially from Integrated DNA Technologies. Lyophilised primers were reconstituted with nuclease free water (Qiagen) to make up a 100mM stock solution. Primers were stored at -20°C. A list of primers used can be found in Appendix 2. Primers were designed by the author and Joana Campos, University of Glasgow.

2.5.2 RNA extraction

Total RNA was extracted using the RNeasy Mini kit (Qiagen) for 0.5-5x10^6 cells. For cell numbers <0.5x10^6, the Arcutus PicoPure kit (Fisher Scientific) was used. For RNA that was to be used for sequencing, an additional DNAse treatment was performed. RNA extraction and centrifuges were performed at RT. Eluted samples were quantified on a Nanodrop ND1000 spectrophotometer (Labtech International). RNA was stored at -80°C until required.

2.5.2.1 RNA extraction by the RNeasy Mini kit

Up to 5x10^6 cells were washed in PBS and centrifuged at 300 x g for 5min and the supernatant removed. The cell pellet was loosened and 350µL of Buffer RLT was added to lyse the cells. The lysate was transferred to a QIAshredder spin column (Qiagen) placed in a 2mL collection tube and centrifuged at full speed for 2min. 350µL of 70% EtOH was added to the homogenised lysate and mixed well by pipetting. 700µL of sample was transferred to an RNeasy spin column (Qiagen) placed in a 2mL collection tube and centrifuged at 8000 x g for 15seconds (s). The flow through was discarded. If required, a DNase digestion was performed at this point. Otherwise, 700µL of Buffer RW1 was added to the spin column and centrifuged at 8000 x g for 15s to wash the spin column membrane. The flow through was discarded. 500µL of Buffer RPE was added to the spin column and centrifuged at 8000 x g for 15s to wash the spin column membrane. The flow through was discarded. Another 500µL of Buffer RPE was added to the spin column and centrifuged at 8000 x g for 2min, to ensure no carry over of EtOH. The spin column was placed on a new 2mL collection tube and centrifuged at full speed for 1min. The spin column was placed on a new 1.5mL collection tube and 30µL of nuclease free water was added directly to the spin column membrane. The spin column was centrifuged at 8000 x g for 1min to elute the RNA.

2.5.2.2 RNA extraction by the Arcutus PicoPure kit

Either, cells were washed and pelleted at 300 x g for 5min and resuspended in 100µL extraction buffer, or cells were collected directly into 100µL of extraction buffer. The sample was incubated for 1h at 42°C and then centrifuged at 3000 x g for 2min and supernatant containing RNA pipetted into a new microcentrifuge

tube. RNA was either extracted immediately or stored at -80°C. To extract RNA, first an RNA purification column (Fisher Scientific) was pre-conditioned by adding 250µL of Conditioning Buffer to the column and incubating for 5min at RT. The column was centrifuged at 16,000 x g for 1min. 100µL of EtOH was pipetted into the cell extract, mixed by pipetting up and down and transferred to the pre-conditioned column. To bind the RNA, the column was centrifuged at 100 x g for 2min, then immediately at 16,000 x g for 30s to remove the flow through. 100µL of Wash Buffer (WB) 1 was added to the column and centrifuged at 8,000 x g for 1min. If required, a DNase digestion was performed at this point. 100µL of WB2 was added to the column and centrifuged at 8,000 x g for 1min. Another 100µL of Wash Buffer 2 was added to the column and centrifuged at 16,000 x g for 2min. If any residual WB2 remained, a second centrifugation at 16,000 x g for 1min was done. To elute the RNA, the column was transferred to a 0.5mL microcentrifuge tube. 12µL of Elution Buffer was added directly to the column membrane and incubated for 1min at RT. The column was centrifuged at 1,000 x g for 1min and then at 16,000 x g for 1min to elute the RNA.

2.5.2.3 DNase digestion

DNase digestion was performed on samples to remove any genomic DNA using the RNase-Free DNase Set (Qiagen). DNase I stock solution was prepared by dissolving lyophilised DNase I (1500 Kunitz units) in 550µL of nuclease free water. To avoid loss of DNase I nuclease, free water was injected directly into the vial and mixed by inverting the vial. Stocks were stored at -20°C.
DNase I solution was added to Buffer RDD to make an incubation mix at a 1:8 dilution. For use with the RNeasy Mini kit, 350µL Buffer RW1 was added to the RNeasy spin column, centrifuged at 8000 x g for 15s and the flow through discarded. 80µL of DNase incubation mix was pipetted onto the spin column membrane and incubated for 15min at RT. 350µL Buffer RW1 was added to the RNeasy spin column, centrifuged at 8000 x g for 15s and the flow through discarded. Thereafter, RNA extraction continued from the first Buffer RPE wash, as described in Section 2.5.2.1. For use with the Arcutus PicoPure kit, 40µL of DNase I incubation mix was pipetted onto the column membrane and incubated for 15min at RT. Then, 40µL of WB1 was added to the column and centrifuged at

8000 x g for 15s. Thereafter, RNA extraction continued from the first WB2 wash, as described in Section 2.5.2.2.

2.5.3 Complementary DNA synthesis

cDNA was synthesised using the High Capacity cDNA Reverse Transcription Kit (Invitrogen). Up to 0.5µg of RNA was converted to cDNA in a 20µL reaction. For low RNA yields, the maximum volume of RNA was added to the reaction. A 2X Master Mix (Table 2.14) was prepared comprising of 10x RT buffer, dNTP mix, 10x RT random primers, RNase Inhibitor and MultiScribe Reverse Transcriptase (all Applied Biosystems). 6.8µL of Master Mix was deposited into PCR tubes on ice. RNA was prepared in a volume of 13.2µL nuclease free water and added to the Master Mix. PCR tubes were vortexed and centrifuged briefly, before being loaded into a Mastercycler™ PCR machine (Eppendorf UK). The thermal cycling conditions are shown in Table 2.15. All cDNA samples were stored at -20°C until used in quantitative polymerase chain reaction (qPCR) reactions.

Table 2.14 Master Mix for cDNA synthesis

Component	Volume per reaction (µL)	Final concentration in 20µL
10X RT Buffer	2	1X
25X dNTP mix (100 mM)	0.8	4 mM
10X RT Random Primers	2	1X
Multiscribe Reverse Transcriptase (50 U/µL)	1	2.5 U/µL
RNase Inhibitor (20 U/µL)	1	1 U/µL

Table 2.15 Thermal cycling conditions for cDNA synthesis

Step	Temperature (°C)	Duration (min)
1	25	10
2	37	120
3	85	5
4	4	Indefinite

2.5.4 Fluidigm™ high-throughput qPCR

Fludigm™ is a high-throughput qPCR system that utilises integrated fluidic circuit (IFC) technology to analyse many samples across many genes. Pre-amplified cDNA and assays (primer or probes of interest) are loaded into individual inlets on a 48.48 or 96.96 microfluidics chip. The IFC controllers push samples and reagents into individual compartments in which individual qPCR

reactions take place. Therefore, the 48.48 and 96.96 chips can simultaneously analyse up to 2,304 or 9,216 reactions, respectively.

2.5.4.1 Pre-amplification and exonuclease treatment

In the Fluidigm™ system individual reactions occur in nanolitre volumes. As such, cDNA was pre-amplified for target genes of interest. A primer pool was made by combining 2µL of each 100µM primer pair. Tris-EDTA (TE) buffer (Promega) was added to make the final volume 400µL; the final concentration of each primer was 500nM. Pre-amplification samples were prepared in PCR tubes, combining 1µL Qiagen Multiplex PCR Kit (Qiagen), 0.5µL pooled primer mix, 2.25µL nuclease free water and 1.25µL cDNA, to a final volume of 5µL. PCR tubes were vortexed and centrifuged briefly, before being loaded into a thermal cycler. The thermal cycling conditions are shown in table Table 2.16. To remove unincorporated primers pre-amplified samples were treated with Exonuclease I (Exo I) (New England BioLabs). Exo I was diluted to 4U/µL in water and Exo I Reaction Buffer (New England BioLabs) and 2µL added to the 5µL reaction. PCR tubes were vortexed, centrifuged, and placed into a thermal cycler and incubated with the program in Table 2.17. The final product was diluted in 18µL TE buffer (1:5 dilution) and stored at -20°C.

Table 2.16 Thermal cycling conditions for pre-amplification

Step	Temperature (°C)	Duration	Condition	
1	95	15 min	Hold	
2	94	30 s	Denature	14 cycles
3	60	1 min 30 s	Anneal	
4	72	1 min 30 s	Extend	
5	4	Indefinite	Hold	

Table 2.17 Program for Exo I treatment

Step	Temperature (°C)	Duration	Condition
1	37	30 min	Enzyme digestion
2	80	15 min	Enzyme inactivation

2.5.4.2 Sample and assay preparation

Samples and primers (assays) were prepared in a 96 well plate. Individual samples were prepared by combining 3µL 2X TaqMan Gene Expression Master Mix (Applied Biosystems), 0.3µL 20X DNA Binding Dye Sample Loading Reagent

(Fluidigm™), 0.3µL 20X EvaGreen DNA bindin dye (Biotium) and 2.4µL pre-amplified Exo I treated sample (total volume 6µL). To prepare the assays forward and reverse primer pairs were diluted to a final concentration of 20µM. Next, 2.7µL of each primer pair mix was combined with 3µL 2X Assay Loading Reagent (Fluidigm™) and 0.3µL TE buffer (total volume 6µL). Plates were vortexed for 30s and centrifuged for 30s.

2.5.4.3 Loading the chip, data acquisition and analysis

A 48.48 Dynamic Array IFC (Fluidigm™) chip was used to analyse 44 assays (with 4 housekeeping genes) and 47 samples (with 1 water control). Control line fluid was injected into each accumulator. The chip was placed into an IFC Controller MX (Fluidigm™) and the chip primed to prevent premature mixing of samples and assays. 5µL of each assay mixture was loaded into the appropriate inlet to the left of the chip and 5µL of each sample mixture was loaded into the appropriate inlet to the right of the chip. The chip was returned to the IFC Controller MX and the assays and samples were loaded into the reaction chambers. The chip was transferred to the BioMark HD system (Fluidigm™) for thermal cycling and fluorescence detection. The thermal cycling conditions are shown in Table 2.18. Fluidigm Real-Time PCR Analysis software (Fluidigm™) was used to perform data analysis and raw data were exported to Microsoft Excel. Gene expression in each sample was normalised to the average expression of the 4 housekeeping genes to generate the ΔCT. For a list of the housekeeping genes used, see Appendix 2. Relative gene expression was calculated using the $2^{-\Delta\Delta CT}$ method to generate the fold change (FC).

Table 2.18 Thermal cycling program for Fluidigm™ qPCR

Step	Temperature (°C)	Duration (s)	
1	50	120	
2	95	600	
3	95	15	40 cycles
4	60	60	
5	4	Indefinite	

2.5.5 RNA sequencing

RNA for sequencing was prepared with DNase treatment as described in Section 2.5.2. RNA sequencing (RNA-seq) was performed by Glasgow Polyomics at the University of Glasgow. Samples were assessed for quality and purity on a 2100 Bioanalyser (Agilent) to produce an RNA integrity number (RIN). A RIN of ≥8 was adequate for RNA-seq. RNA libraries were prepared by polyA selection using the TruSeq stranded mRNA kit (Illumina). RNA-seq was performed on a NextSeq™ 500 platform (Illumina). Paired end sequencing was performed (ie, each RNA fragment was sequenced from both ends) with a read length of 75bp and fragment length of 150bp. RNA was sequenced to a depth of 33 million reads per sample. Raw sequencing data was analysed by Graham Hamilton from Glasgow Polyomics, University of Glasgow. Raw fastq files were pseudo-aligned to the Mus Muscularis transcriptome and transcription reads quantified using the high-speed transcript quantification tool Kallisto. (Bray et al., 2016) Transcripts were annotated and differential transcript and gene expression analysis was performed using DEseq2 software. Transcript data were collapsed to corresponding genes to obtain differentially expressed genes (DEGs). Pairwise comparisons generated FC, standard error and p-value. A Benjamini-Hochberg correction for false discovery rate (FDR) due to multiple testing was applied to generate the q-value (adjusted p-value). Further analysis was performed by the author.

2.5.5.1 Pathway analysis of RNA-seq data

Unless otherwise stated, significant DEGs were defined as having a q-value <0.05 and FC≥±1.5. Gene lists of DEGs were interrogated for pathway analysis using the Molecular Signatures Database (MSigDB) (Broad Institute) and the Database for Annotation, Visualization and Integrated Discovery (DAVID) (Laboratory of Immunopathogenesis and Bioinformatics). MSigDB is a collection of curated gene sets. A test gene list can be investigated for overlap with reference gene sets. A p-value was generated using the hypergeometric distribution and the Benjamini-Hochberg correction was applied to generate the q-value. A q-value of <0.05 was used to identify significantly enriched gene sets. (Subramanian et al., 2005) DAVID is on online bioinformatics resource that allows functional clustering data

to be extracted from a gene list. A significant enrichment score was defined as >1.3. (Huang da et al., 2009a, Huang da et al., 2009b)

Assessment of DEGs can miss small differences in gene expression, which may cumulatively result in significant differences in pathway expression. Therefore, gene expression data was interrogated for gene set enrichment using Gene Set Enrichment Analysis (GSEA) from the Broad Institute. (Subramanian et al., 2005) Gene sets were downloaded from MSigDB. Pairwise comparisons were performed using 1000 permutations for enriched gene sets. A normalised enrichment score (NES) of $\geq \pm 1.3$ and a q-value (FDR) of less than 5% ($q<0.05$) was taken as significant. Where stated, a leading edge analysis of gene sets of interest was performed. The leading edge of a gene subset are the gene members in the investigated dataset that contribute most to the enrichment score. For a positive enrichment score, these are the member genes that occur just prior to the peak score. (Figure 2.7A) For a negative enrichment score, these the member genes that occur just after the peak score. (Figure 2.7B) Investigation of the leading edge subset across several gene sets can identify the most differentially expressed and biological significantly genes.

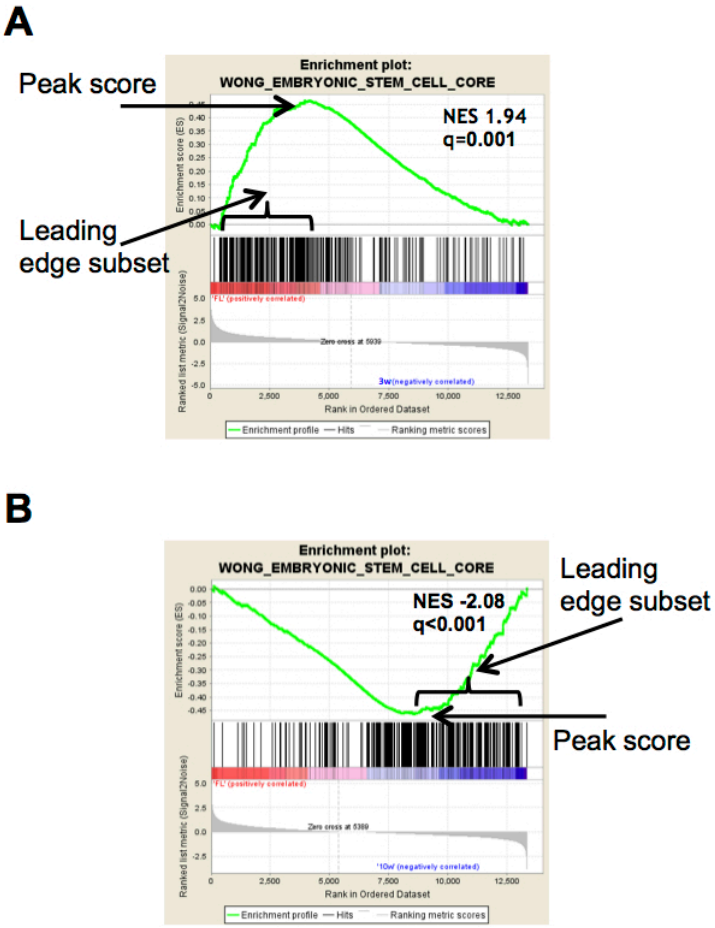

Figure 2.7 Example GSEA plots

(A) Example GSEA enrichment plot with positive enrichment score. Plot depicts peak score and leading edge gene subset prior to peak score.
(B) Example GSEA enrichment plot with negative enrichment score. Plot depicts peak score and leading edge gene subset after peak score.

2.5.6 Statistical analysis

GraphPad Prism v7 (GraphPad Software Inc.) was used for statistical analysis and production of graphs. All results are shown as mean values with standard deviation (SD) unless otherwise stated. When 2 groups were compared, an unpaired, 2-tailed Student's t-test was used to determine significance. When more than 2 groups with 1 variable were compared, a 1-way ANOVA with Bonferroni post-test for FDR was used to determine significance. When more than 2 groups with 2 variables were compared, a 2-way ANOVA with Bonferroni post-test for FDR was used to determine significance. For comparison of survival curves the Log-rank test was used. Significance was attained with a p-value (or adjusted p-value for FDR) of <0.5 (*), <0.01 (**), <0.001 (***) and <0.0001 (****).

3 An examination of the transformability of HSPCs of different ages *in vitro*

3.1 Introduction

Studies of ageing and haemopoiesis have shown that HSC characteristics alter as the haemopoietic system ages. Differences in cellular behaviour, including cell cycle status and lineage potential, DRR and repair mechanisms and transcriptional and mutational profile are observed in foetal, young adult and aged HSCs. Foetal and neonatal HSCs display high self-renewal, cycle frequently and have myeloerythroid biased lineage output as they populate the developing haemopoietic system. Adult HSCs, in contrast, are quiescent and display balanced myeloid and lymphoid output, as they maintain the haemopoietic system for life. (Rebel et al., 1996, Bowie et al., 2007b) With increasing age HSC function declines, associated with an increase in HSC number and cell cycle activity and myeloid skewing. An accumulation of DNA damage and emergence of clonal haemopoiesis results in an increased risk of haematological malignancy. (Morrison et al., 1996b, Sudo et al., 2000, Rossi et al., 2007a, Jaiswal et al., 2014) The hypothesis is that intrinsic age defined differences in normal cellular biology will impact oncogene mediated transformation and resultant leukaemia phenotype. In Chapter 1, clinical and molecular differences in paediatric and adult AML were discussed. However, there is a paucity of investigation into the impact of cellular age on the transformability of HSPCs.

3.1.1 Correlating murine age with human age

Mice exhibit similarities in physiology, genome and disease pathogenesis with humans. The lifespan of laboratory mice is approximately 24m, after which there is a sharp decline in survival. Due to their short life span and biological similarities with humans, the murine model is an excellent model to study the effects of ageing. To do so, however, murine ages must be correlated with human age as accurately as possible. Representative ages for murine development and maturity and comparison with human ages are shown in Figure 3.1. Correlating the average lifespan of laboratory mice to humans (24m versus 80y, respectively) 9 mouse days have been correlated with 1 human year.

However, as developmental stages between mice and human are not uniform, other markers of ageing need to be taken in to consideration. (Dutta and Sengupta, 2016) Methods to determine stages of ageing can be sub-categorised into the immature phase and mature phase. In the immature phase, the mouse is not yet fully developed. Markers to help correlate age to the human counterpart include increase in body weight, closure of epiphyseal plates and completion of puberty. In the mature phase, adult mice have fully developed. Markers of completion of development include full reproductive ability and completion of bone growth. (Dutta and Sengupta, 2016, Kilborn et al., 2002) As mice age, biomarkers of senescence, or biological ageing, become positive. Senescence is the gradual deterioration of cellular function with increasing age. Cellular senescence is characterised by irreversible growth arrest and altered cellular function. Biomarkers of senescence include loss of reproductive potential, glucose intolerance and an accumulation of memory T-lymphoid cells. Molecular biomarkers of senescence include permanent cell cycle arrest, persistent DNA damage response, senescence associated secretory phenotype and altered metabolism. (Miller et al., 1997, Campisi, 2005)

3.1.1.1 Foetal age

Gestation in mice is 19-21d and in humans 40w. In both mice and humans, the foetal stage is any stage before birth.

3.1.1.2 Neonatal/infant age

In mice, the neonatal stage is from birth up to 21d. Pups are born naked, with their eyes closed and in females, a closed vagina. During this stage, pups nurse on their mother's milk and wean at 3-4w of age. This is also the age at which an abrupt change in HSC phenotype is observed from highly cycling to quiescent. Humans wean from 6-12m of age. In humans, a switch in HSC proliferative phenotype, based on telomere shortening, is suggested to occur at around 3y of age (although this can occur later, up to 13y of age). (Rufer et al., 1999, Sidorov et al., 2009) Therefore, the neonatal period in a mouse correlates to a human age from birth to early childhood.

3.1.1.3 Juvenile age

The juvenile stage in murine development is considered to be between 3-6w of age and is characterised by puberty. Markers of puberty in mice include vaginal opening and commencement of the oestrus cycle in females and balanopreputial separation in males. (Pinter et al., 2007) In humans, puberty generally occurs between the age of 10-16y. Therefore, the juvenile age in mice correlates to a human age of 10-16y.

3.1.1.4 Young adult age

In mice, young adult age is considered to be between 2-6m of age, when the mouse is no longer developing. Biologically, adulthood is defined by the attainment of sexual maturity. Mice gain sexual maturity at 8-12w. In addition, sexual maturity is associated with the fusion of epiphyseal growth plates. In humans, this occurs at around 20y. Furthermore, in young adulthood biomarkers of ageing are not positive. Young adult age in mice corresponds to a human age of 20-30y. (Flurkey et al., 2007)

3.1.1.5 Adult middle aged

In mice, adult middle age is considered to be between 10-15m, when some senescent changes can be identified. It is associated with a decline in reproductive function. An equivalent decline in reproductive activity in humans is female menopause, which occurs between 45-55y. Thus, middle age in mice corresponds to a human age of 40-50y. (Flurkey et al., 2007)

3.1.1.6 Old/aged adult

In mice, old age is considered to be 18-24m, although any mouse exceeding the lifespan of 24m can be considered old aged. It refers to an age at which senescent changes can be detected in almost all biomarkers. Old age in mice corresponds to a human age of 60-70y and older. (Flurkey et al., 2007)

3.1.1.7 Rational for murine ages investigated

After the age of 60y, the incidence of AML rises sharply with an increase in adverse risk cytogenetics and an association with preceding clonal haemopoiesis. As such, AML of the elderly is often considered biologically distinct from AML occurring in childhood and young to middle aged adults. In addition, AML in the elderly is treated with palliative intent. In contrast, both childhood and young to middle aged adult AML is usually treated with intensive therapy with curative intent, often within the same clinical trial. Therefore, this study aimed to model AML occurring in childhood and young to middle aged adults. The 4 murine ages investigated were FL, 3w, 10w and >52w (52-67w). The rational for choosing these ages are as follows. In human infant AML, founder mutations have been identified to occur *in utero*. (Ford et al., 1993, Gale et al., 1997, Pine et al., 2007) By assessing the transformation of FL HSCs, disease occurring in infancy was modelled, in which the oncogenic aberrations occurred before birth. In mice, an abrupt switch in HSC phenotype from high proliferation to quiescence occurs between 3 and 4w. (Rebel et al., 1996, Bowie et al., 2007b) In humans, investigation of telomere length in leukocytes suggests that this phenotypic switch occurs approximately at 3-13y of age. (Rufer et al., 1999, Sidorov et al., 2009) Therefore, by choosing to investigate mice aged 3w, disease occurring in childhood was modelled, before the HSC phenotypic switch has occurred. At 10w of age, mice are considered young adults with full sexual maturity and no evidence of ageing related senescence. Therefore, 10w mice were chosen to represent young adults, with an age range of 20-30y. At 52-67w, mice are considered middle aged, with minor senescent changes in some but not all biomarkers of ageing. Therefore, >52w mice were used to represent the middle aged group, with an human equivalent age range of 40-50y.

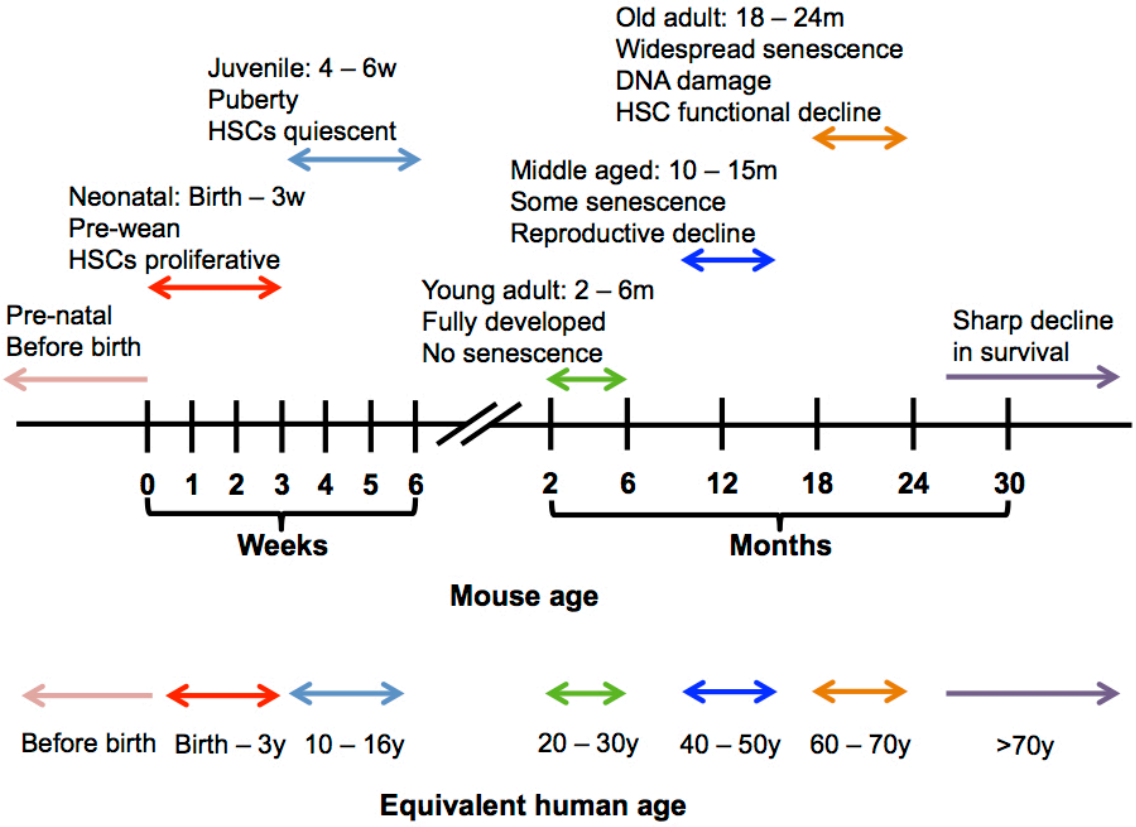

Figure 3.1 Correlating murine and human age

Schematic showing the characteristics of different stages of murine ageing. Equivalent human ages are shown below.

3.1.2 The impact of the cell of origin

AML is considered a disorder of HSCs, in which genetic altercations imbue primitive self-renewing cells properties of uncontrolled proliferation and inability to differentiate. This implies that for AML, the cell of origin is the LT-HSC. However, studies have shown that progenitor populations, without inherent self-renewal properties, can also undergo oncogene mediated leukaemic transformation and act as the leukaemia initiating cell (LIC). (Cozzio et al., 2003, Huntly et al., 2004, Krivtsov et al., 2006, Kvinlaug et al., 2011) This was first investigated by Cozzio *et al*, using an MLL-ENL model of AML. HSCs (defined as LSK-Thy1.1^{lo}) and the committed myeloid progenitors CMP, GMP and MEPs were retrovirally transduced with MLL-ENL and assessed for *in vitro* and *in vivo* transformation. Transduced MEPs did not transform *in vitro* nor give rise to leukaemia *in vivo*. Transduced HSC, CMP and GMPs serially replated in methylcellulose and subsequently grew in liquid culture to form immortalised cell lines. In addition, all 3 populations gave rise to similar immature colonies

morphologically and immunophenotypic profile. BMT of transduced HSC, CMP and GMPs gave rise to AML in primary recipients with a latency of 90-100d in all groups. Disease characteristics including infiltration of immature myeloblasts in the spleen and liver and CD11b/GR1 expression by flow cytometry was also similar in HSC, CMP and GMP derived AML. Therefore, in addition to HSCs, myeloid committed progenitors could initiate MLL-ENL AML *in vivo*, with no difference in the resultant leukaemic phenotype. However, titration studies showed that more primitive cells exhibited greater transformation efficiency. (Cozzio et al., 2003) Since this seminal study, other oncogenes have been shown to transform committed myeloid progenitors, *in vitro* and result in *in vivo* AML. These include MOZ-TIF2, MA9 and NH9. (Huntly et al., 2004, Krivtsov et al., 2006, Kvinlaug et al., 2011) This suggests that oncogenes can reactivate self-renewal pathways as part of the transformation process. The ability to transform committed progenitors appears to be oncogene specific to a degree. Huntly *et al* compared MOZ-TIF2 and BCR-ABL mediated transformation of CMP and GMPs. Both are known to transform HSCs. Retroviral expression of MOZ-TIF2 imbued CMP and GMPs with self-renewal properties, evidenced by serial replating ability and development of AML in primary recipients. In contrast, BCR-ABL expressing CMP and GMPs did not serially replate and did not drive leukaemia *in vivo*. (Huntly et al., 2004)

This poses an interesting question. If both HSCs and committed progenitors can act as the LIC, are intrinsic cellular differences that define HSC and progenitor cells retained after transformation and impact the biology of the resultant leukaemia? The study by Cozzio *et al* suggests that for MLL-ENL, leukaemic phenotype is similar irrespective of cell of origin. This hypothesis was investigated by Krivtsov *et al*. The authors compared MA9 mediated transformation in HSCs (defined as $CD34^-$ LSK cells), and GMPs. Retrovirally transduced HSC and GMPs serially replated in single cell serial CFC assays showing that both populations had similar transformation potential *in vitro*. However, BMT of freshly transduced populations or single cell derived clones showed a difference in latency to disease in primary recipients, with a shorter latency to disease for HSC derived AML (AML^{HSC}) compared to GMP derived AML (AML^{GMP}). Furthermore, LIC frequency was higher in single cell clones from MA9

expressing HSCs compared to GMPs (1/29,388 versus 1/16,847, respectively). Thus, oncogene expression in stem cells was a more potent driver for leukaemia development. However, both AML^{HSC} and AML^{GMP} displayed similar morphological and immunophenotypic features. Furthermore, the LSC frequency to generate AML in secondary recipients was the same for AML^{HSC} and AML^{GMP} at 1/93 and 1/86, respectively. However, despite phenotypic similarity, cell of origin had significant impact on molecular characteristics. GEP by microarray analysis showed that both AML^{HSC} and AML^{GMP} clustered with normal GMPs transcriptionally. However, AML^{HSC} showed an enrichment of stem cell signatures while AML^{GMP} displayed an enrichment of myeloid differentiated signatures. In addition, the AML^{HSC} transcriptional signature correlated with adverse clinical outcomes, including increased RR in 3 independent datasets of human MA9 AML. The epigenome of AML^{HSC} and AML^{GMP} was assessed by enhanced reduced representation bisulfite sequencing assay, to assess for global 5'-mC methylation. Higher 5'-mC methylation in MA9 AML is associated with high *EVI1* expression and poorer clinical outcomes in human studies, compared to lower *EVI1* expression. (Lugthart et al., 2008) AML^{GMP} exhibited relative 5'-mC hypomethylation compared to AML^{HSC}. Finally, AML^{HSC} was more resistant to *in vitro* treatment with doxorubicin and *in vivo* treatment with combination doxorubicin and cytarabine. Therefore, despite similar morphological features, AML^{HSC} and AML^{GMP} displayed differences in GEP, epigenetic state and drug response. (Krivtsov et al., 2006, Krivtsov et al., 2013) This study highlights that while leukaemic phenotype, as defined by morphological assessment and immunophenotype may be the same, the cellular properties that define the maturity of the cell of origin can impact leukaemic susceptibility to transformation, molecular characteristics and response to therapy. Therefore, cellular properties, defined by the age of the cell may also impact transformation susceptibility and resultant leukaemia biology, as hypothesised.

3.1.3 Experimental *in vitro* models of AML

The HSC is a cell with self-renewal properties and the ability to differentiate into all lineages. Experimentally, this is defined as a cell that results in long-term, multilineage engraftment *in vivo* in serial transplantation. (Morrison and Weissman, 1994) Similarly, the definition of an LSC is a cell that can result in

leukaemia *in vivo* in serial transplantation. (Hope et al., 2004) However *in vivo* transplantation studies can be laborious and expensive. Therefore, *in vitro* techniques have been developed that can investigate normal and leukaemic stem properties. Growth of cells in liquid culture investigates intrinsic cellular properties of cellular proliferation and self-renewal. Usually, media is supplemented with cytokines to promote cell growth and survival. However, *in vivo*, cells do not exist in suspension but thrive in conjunction with the stromal cells of the microenvironment. Therefore, other *in vitro* techniques that mimic the microenvironment have been developed. The simplest is the co-culture of cells of interest on a stromal layer. Adherent stromal cells are seeded prior to culture of cells of interest. Proliferation and survival of cells is enhanced compared to liquid culture due to the secretion of soluble factors from the stromal cells and direct cell-to-cell contact. (Kohler and Milstein, 1975) The differentiative properties of a cell can be investigated by the CFC assay. (See Section 2.2.7). Cells of interest are seeded in cytokine supplemented semi solid media, such as methylcellulose. Progenitor cells produce colonies of cells that can be lineage defined based on morphological features. Colonies can be harvested and replated. Normal haemopoietic cells will differentiate into non-self-renewing cells and eventually die out. The ability for cells to serially replate denotes the acquisition of self-renewal properties and immortalisation. (Ogawa and Livingston, 2002) HSC and progenitor functional assessment can by assessed using the cobblestone-area forming cell (CAFC) assay. In this assay primitive cells migrate through a stromal layer and proliferate, resulting in the formation of cobblestone areas that can be viewed microscopically. For murine cells, committed progenitors produce cobble-stone areas after 7d while HSCs produce cobble-stone areas up to 5w in culture. LDA for CAFC can be used as a surrogate to quantify the *in vivo* LT-HSC. (de Haan and Ploemacher, 2002) A method to isolate and quantify the most primitive LT- HSC is the LTC-IC assay. That is, a cell that can generate differentiated progeny after several weeks of *in vitro* culture. Cells of interest are cultured long-term (usually >5w) on a stromal feeder layer. After the culture period, mature cells have died out, leaving only LTI-ICs, that can be functionally demonstrated using the CFC assay. Similar to the CAFC assay, by using LDA, the LTC-IC assay can be used as a surrogate to enumerate the *in vivo* long-term engrafting HSC. (Miller and Eaves, 2002) The

study of leukaemia has relied on the identification and isolation of AML associated genetic aberrations that can be investigated experimentally. Examples of *in vitro* models of AML that have been utilised to investigate leukaemogenesis are discussed in the following sections. *In vivo* AML models will be discussed in the following Chapter 4.

3.1.3.1 NH9

Studies of human AML harbouring the t(7;11)(15p;15p) translocation revealed the genomic fusion of the *HOXA9* gene on chromosome 7p15 to the *NUP98* gene on chromosome 11p15, resulting in the in frame fusion transcript *NH9*. (Borrow et al., 1996, Nakamura et al., 1996) (See Section 1.3.4.5) Experimentally, expression of NH9 in haemopoietic cells results in a proliferative advantage and self-renewal properties *in vitro* and differentiation blockade. (Calvo et al., 2002, Kroon et al., 2001, Iwasaki et al., 2005, Takeda et al., 2006, Chung et al., 2006) Transgenic mice expressing human *NH9* under the control of the murine cathepsin G promoter express the oncogene specifically in myeloid cells from the promyelocyte stage of maturation. Chimeric mice develop a MPN with subsequent AML at an incidence of 10% at 12m. Total BM harvested from chimeric mice, before the onset of leukaemia, serially replate in methylcellulose for up to 5 platings. WT littermate controls stop producing colonies by 2-3 platings, showing that the expression of NH9 in myeloid progenitors imbues the cell with abnormal self-renewal properties. (Iwasaki et al., 2005)

Retroviral transduction of NH9 into total murine BM confers self-renewal *in vitro* demonstrated by the ability to serial replate in methylcellulose. NH9 expressing cells also produce very large colonies compared to empty vector (EV) controls. (Kroon et al., 2001) Retroviral expression of NH9 in Lin^- cells (as a method to isolate stem and progenitor cells) immortalises myeloid progenitors and confers a proliferative advantage over EV controls. NH9 expressing cells proliferate in cytokine supplemented liquid culture, outgrowing EV controls. In addition, EV controls differentiate into mast cells (with IL3) or neutrophils and monocytes (with GM-CSF) depending on cytokine supplementation. NH9 cells, in contrast, produce myelomonocytic blasts in either culture conditions, indicative of maturation blockade. (Calvo et al., 2002) Retroviral transduction of NH9 into

myeloid committed progenitors (CMP, GMP and MEP) also results in the acquisition of self-renewal properties. NH9 expressing CMP, GMP and MEPs serially replate in methylcellulose and grow in liquid culture for up to 6w. (Kvinlaug et al., 2011) Retroviral expression of NH9 in human $CD34^+$ CB cells results in a proliferative advantage compared to MigR1 EV controls. NH9 CB cells proliferate in liquid culture and stromal co-culture, displaying an increase in total cell number over 5w, while for EV controls cell number remains constant. NH9 CB serially replate in methylcellulose while EV controls do not replate beyond CFC2, suggesting the acquisition of self-renewal properties in NH9 expressing cells. HSC and progenitor functional assessment using the CAFC assay show that NH9 CB produce more CAFCs at week 5 compared to EV controls, suggesting an expansion of the HSC and progenitor cells in NH9 expressing cells. Morphological assessment of CB cultured in suspension, stroma and CAFC show that NH9 CB exhibits a maturation block at the myeloblast and promyelocyte stage, while control cells fully differentiate into terminally differentiated neutrophils. (Chung et al., 2006) Similarly, retroviral expression of NH9 in adult human $CD34^+$ cells results in a proliferative advantage, maturation block and enrichment of the LTC-IC, compared to EV controls. (Takeda et al., 2006) In CFC assays, NH9 cells produce large colonies (similar to murine NH9 studies) and produce more cells per plate than controls. Morphological assessment from cells recovered from CFC assays show a predominance of immature blasts and early erythroid cells in NH9, while control cells show a predominance of differentiated myeloid cells. LTC-IC assays show a dramatic 40-fold increase in LTC-IC generation in NH9 expressing cells, suggesting that NH9 promotes proliferation of long-term self-renewing cells. Comparing growth in liquid culture with control, NH9 cells are initially slower than control. However, after 9d in culture, NH9 cells outgrow EV controls. GEP by microarray shows an early induction of IFN inducible genes and cell cycle inhibitors at day 3 of culture, which may account for the early growth suppression. However, from day 8 and beyond, NH9 cells express genes associated with cell proliferation and leukaemogenesis, including *HOXA9*, *HOXA7*, *MEIS1*, *FLT3*, *KIT*, *WT1* and *ANGPT1*. In addition, there is down regulation of genes associated with myelomonocytic terminal differentiation, including, *TCN1*, *LTF* and *ABP1*, in keeping with the maturation block observed morphologically. (Takeda et al., 2006)

3.1.3.2 A1E

Human AML harbouring the translocation t(8;21)(q21;q22) results in the fusion gene *A1E*. Fusion of the co-repressor *ETO* to the *AML1* subunit of the CBF transcription factor prevents CBF mediated transcription of key targets in haemopoietic and granulocytic differentiation. (See Section 1.3.4.2). Knockin mouse models of human A1E result in death *in utero* due to abnormal foetal haemopoiesis. (Yergeau et al., 1997, Okuda et al., 1998) Therefore, inducible transgenic and retroviral models have allowed the study of this oncogene. (Rhoades et al., 2000, Yuan et al., 2001, Higuchi et al., 2002, de Guzman et al., 2002, Schwieger et al., 2002, Mulloy et al., 2003) In a transgenic A1E model, a tetracyline responsive *A1E* construct was cloned into mice containing the murine mammary tumour virus–tet-controlled transcriptional activator (*MMTV-tTA*). Transgenic *MMTV-tTA*/*A1E* mice continually expressed A1E in BM cells while *A1E* expression was switched off in the presence of tetracycline. *A1E* expressing mice had normal haemopoiesis and survival (to 24m). However, *A1E* expressing total BM serially replated in methylcellulose while total BM from *MMTV-tTA* controls exhausted after 3-4 platings. Cellular morphological examination showed immature blasts and early myeloid cells in the A1E group, while control plates produced fully differentiated neutrophils and monocytes. Therefore, A1E expression resulted in self-renewal properties and differentiation block *in vitro*. (Rhoades et al., 2000) In another transgenic model, an *A1E* knockin allele was constructed by fusion of the lox bracketed human *A1E* sequence at the site of the murine *Aml1* gene. Using the *Mx-Cre* model expression of *A1E* was achieved on exposure to pIC. Similar to the study by Rhoades *et al*, transgenic mice did not develop AML *in vivo*. However, *A1E* expressing total BM serially replated in methylcellulose while non-A1E expressing controls did not, indicating that A1E expression results in *in vitro* self-renewal. (Higuchi et al., 2002) Retroviral transduction and transplantation (T&T) of A1E expressing LSKs results in engraftment and altered myelopoiesis *in vivo*, with a differentiation block. BM harvested from engrafted recipients produce more colonies in methylcellulose than EV control BM, suggesting an increase in myeloid progenitors *in vivo*. (de Guzman et al., 2002) Retroviral transduction of A1E into murine myeloid progenitor populations (CMP, GMPs and MEPs) results in immortalisation *in vitro*. A1E expressing CMP, GMP and MEPs serially replate in methylcellulose and grow

in liquid culture, indicating the acquisition of self-renewal properties. (Kvinlaug et al., 2011) This suggests that both primitive LSKs and committed myeloid progenitor cells acquire self-renewal properties *in vitro*, on expression of A1E. Retroviral transduction of A1E also immortalises human $CD34^+$ cells isolated from either CB or adult derived PB, resulting in long-term growth in cytokine supplemented liquid culture. Both $CD34^+$ HSCs and terminally differentiated cells (based on morphological and flow cytometric assessment) are present in liquid culture. However, only the $CD34^+$ cells are proliferative, suggesting that in culture A1E expressing $CD34^+$ cells proliferate and differentiate in liquid culture. In addition, A1E expressing $CD34^+$ grown in culture and transferred to lineage specific conditions can differentiate into granulocytes, megakaryocytes and B-lymphoid cells, showing A1E expressing $CD34^+$ cells retain multilineage potential. Thus, retroviral expression of A1E in human CD34+ cells enriches for HSCs with self-renewal and multipotency. (Mulloy et al., 2003)

3.1.3.3 FLT3-ITD

The *FLT3* gene located on chromosome 13q12 encodes the membrane bound Fms-like tyrosine kinase receptor. (Rosnet et al., 1996) The mutation *FLT3-ITD* results in an elongated JM domain leading to disrupted autoinhibitory function and constitutive activation. (Kiyoi et al., 1998) (See Section 1.3.4.6). Cloning of the human FLT3-ITD cDNA into the MSCV vector has allowed investigation of this oncogene. Retroviral transduction on FLT3-ITD into the IL3 dependent murine cell lines, Ba/F3 and 32D, results in IL3 independent growth, while transduction of WT FLT3 does not. (Hayakawa et al., 2000) Retrovirally expressed FLT3-ITD in total murine BM results in a lethal MPN after transplantation into recipient mice at a median latency of 40-50d. (Kelly et al., 2002) However, progenitor cells (CMP, GMP, MEP) transduced with FLT3-ITD fail to serially replate in CFC assays or to grow in liquid culture, suggesting that FLT3-ITD does not imbue self-renewal properties to committed progenitors *in vitro*. (Kvinlaug et al.) Lentiviral expression of FLT3-ITD in human $CD34^+$ CB results in increased expansion in serum free cultures, compared to EV controls. Cell cycle analysis at day 7 of culture show that 46.4% of FLT3-ITD expressing cells are in active cell cycle, compared to 22.5% of EV controls. In addition, there is an enrichment of the primitive $CD34^+CD38^{dim}$ cells at day 7 in FLT3-ITD cells compare to EV controls

(22% versus 1.8%, respectively). Furthermore, FLT3-ITD cells continued to grow in liquid culture for over 30w whereas EV controls exhaust after 12-14w. Therefore, expression of FLT3-ITD in human $CD34^+$ cells results in increased proliferation, enrichment of primitive HSCs and *in vitro* immortalisation. (Li et al., 2007) Several transgenic models of FLT3-ITD exist. In all cases, chimeric mice develop a MPN *in vivo*. (Lee et al., 2007, Lee et al., 2005, Li et al., 2008) Total BM harvested from chimeras produce more colonies than WT controls in CFC assays, but do not serially replate, suggesting that FLT3-ITD does not imbue self-renewal properties *in vitro*. (Lee et al., 2007, Li et al., 2008) However, FLT3-ITD BM can expand in cytokine supplemented liquid culture for over 10w (while WT control BM exhausted after 3-4w). Withdrawal of cytokines results in cell death, showing that continued survival *in vitro* is cytokine dependent. (Li et al., 2008) BMT of total BM, Lin^- and LSKs results in reduced engraftment in FLT3-ITD expressing populations compared to control. However, LT-HSCs sorted according to SLAM staining ($Lin^-CD150^+CD48^-$) showed similar engraftment in FLT3-ITD and WT controls, with FLT3-ITD recipients developing MPN. This suggests the LIC in FLT3-ITD MPN is the SLAM defined LT-HSC. Interestingly, the FLT3-ITD groups show a depletion of LT-HSCs, with increased proliferation within this normally quiescent compartment.

3.1.3.4 MLLr

MLLr are one of the most common chromosomal abnormalities found in AML and ALL and, as such, have been widely investigated in experimental models. MLL is associated with over 80 partner genes, the commonest being *AF4*, *AF9*, *ENL*, *AF10* and *ELL* and can result in either myeloid or lymphoid leukaemia. Major MLL fusion partners in AML include *AF9* and *ENL*. (Meyer et al., 2013) Pathogenesis is due to the uncontrolled activation of target genes and thus downstream activation of oncogenic pathways including those mediated by HOXA9 and its cofactor MEIS1. (Yip and So, 2013) (See Section 1.3.4.4). Retroviral expression of MLL-ENL in murine HSPCs (either cKit enriched Lin^- progenitors or Thy-1^{lo}Sca-1^-H-$2K^{hi}$ cells) results in their immortalisation *in vitro*. MLL-ENL expressing cells serially replate in methylcellulose, producing large colonies of immature cells while EV controls exhaust after secondary platings. After serially replating, MLL-ENL cells grow in liquid culture to make a cytokine dependent cell line, which

produces a highly penetrant AML in primary recipients with a latency of 12-20w. Therefore, MLL-ENL expressing cells also have LIC properties. (Lavau et al., 1997) Retroviral expression of mutant MLL-ENL vectors into cKit enriched Lin^- HSPCs identify that the DNA binding domains of MLL and the carboxy-terminal transactivation domain of ENL are crucial for MLL-ENL mediated immortalisation of HSPCs *in vitro*. (Slany et al., 1998) Similarly, $cKit^+$ BM (as a source of HSPCs) retrovirally transduced with MA9 also serially replate in methylcellulose and thereafter grow in liquid culture, indicating *in vitro* immortalisation. BMT of *in vitro* MA9 immortalised cells results in AML in 100% of recipients, with a latency of 80d, showing that MA9 expressing cells have LIC properties. (Somervaille and Cleary, 2006) Retroviral expression of MLL-ENL or MA9 into Lin^- human CB cells also results in *in vitro* immortalisation. MLL-ENL or MA9 expressing cells grow in liquid culture supplemented with myeloid cytokine whereas EV controls died. Transplantation of *in vitro* expanded MLLr (either MLL-ENL or MA9) expanded CB results in AML or ALL in recipient mice. (Barabe et al., 2007)

3.2 Aims

Studies of normal ageing and haemopoiesis have highlighted differences in the foetal, young adult and the aged haemopoietic system. Foetal HSCs are highly cycling with greater differentiative potential compared to adult HSCs that are quiescent and have a myeloid bias. There is evidence that paediatric and adult AML differ both clinically and genetically. However, there is a paucity of investigation into the impact of cellular age on the transformability of HSPCs. The hypothesis is that cellular age will impact the transformability of HSPCs. Young HSPCs may be more resistant to leukaemic transformation, accounting for the lower incidence of leukaemia in childhood. Therefore, this chapter aims to examine the transformability of normal HSPCs of different cellular age. Specifically,

i) To examine the impact of cellular age on *in vitro* transformation of HSPCs LSKs, CMPs and GMPs isolated from FL, 3w, 10w and >52w mice were transduced with NH9 and underwent serial CFC assay.

ii) To examine the intrinsic transformability of foetal HSPCs irrespective of oncogene insult, FL-LSK, CMP and GMPs were transduced with the oncogenes NH9, AE1 and FLT3-ITD and transformation assessed by:
   a. Growth in liquid culture (cell intrinsic transformation)
   b. Co-culture on the stromal OP9 cell line (cell intrinsic plus microenvironment)

3.3 Results

3.3.1 LSKs from all ages transform with NH9 *in vitro*

To investigate if the cellular age of the HSC will impact oncogene mediated HSC transformation, LSKs, which contain LT-HSCs, ST-HSCs and MPPs were isolated from FL, 3w, 10w and >52w old C57Bl/6 mice. LSKs were retrovirally transduced with NH9 oncogene or MigR1 EV control and assessed for *in vitro* transformation by CFC assay. The ability of cells to serially replate in methylcellulose denotes *in vitro* transformation, with acquisition of self-renewal properties. Absolute number and morphological assessment of colonies and cells was assessed at each plating. In addition, surface expression by flow cytometry for immature (cKit and CD34) and myeloid markers (CD11b, GR1 and F4/80) was performed at each plating. (Figure 3.2A) GFP expression measured by the median fluorescent intensity (MFI) as a surrogate for protein expression was similar across all samples. (Figure 3.2B) MigR1 controls from all ages failed to produce colonies beyond the second plate (CFC2). (Figure 3.3A) Irrespective of cellular age, LSKs transduced with NH9 produced multiple colonies and cells at CFC3, indicating *in vitro* transformation and acquisition of self-renewal properties. However, at each plating (CFC1, CFC2 or CFC3), there was no difference in the number of colonies or cells produced with cellular age. (Figure 3.3B) Cellular morphology showed that the majority of cells produced were blasts, with high nuclear to cytoplasmic ratio, basophilic cytoplasm and open chromatin nuclear pattern. Mature myeloid cells, including neutrophils with segmented nuclei, and macrophages with abundant slate grey cytoplasm and vacuolation, were also seen in smaller numbers. This morphological pattern was observed at each plating, regardless of LSK cellular age. (Figure 3.4) Colonies were identified as GEMM, GM, granulocyte, macrophage or erythroid by morphological assessment

shown in Table 2.8 and Figure 2.3B. Representative pictures of colonies produced at CFC1, CFC2 and CFC3 are shown in Figure 3.5A. At CFC1, CFC2 and CFC3, for all ages of LSK, the majority of colonies produced were of GM type. At CFC1, post-foetal LSKs (3w, 10w and >52w) transduced LSKs produced very large GEMM colonies, while transduced FL-LSKs produced smaller colonies. However, there was no significant difference in the proportion of GEMM, GM, granulocyte or macrophage colonies produced at CFC1 from the 4 ages investigated. (Figure 3.5B left) At CFC2, FL-LSKs produced more granulocyte colonies compared to 3w, 10w and >52w LSK, suggesting that FL colonies were more differentiated. (Figure 3.5B middle) At CFC3 this difference was lost. However, >52w LSKs produced proportionally more macrophage colonies than the FL or 10w group. (Figure 3.5B right)

The phenotype of cells produced at each plating was further assessed by flow cytometry. Initial gating strategy and negative controls are shown in Figure 3.6. The expression of immature markers cKit and CD34 and myeloid markers CD11b, GR1 and F4/80 are shown in Figure 3.7. Surface marker and GFP expression are summarised in Figure 3.8. At CFC1, >52w-LSKs displayed increased expression of cKit (Figure 3.7A and Figure 3.8A left). However, at CFC2 and CFC3, there was no difference in the expression of the immature markers cKit and CD34, or myeloid markers CD11b, GR1 or F4/80, with cellular age (Figure 3.7). In addition, at each plating, there was no difference in the MFI of GFP with cellular age, suggesting similar expression of GFP protein as a surrogate marker of NH9 protein level. (Figure 3.8B) Therefore, regardless of age, NH9 transformed LSKs *in vitro* with no difference in resultant proliferative potential, morphology or immunophenotype with cellular age.

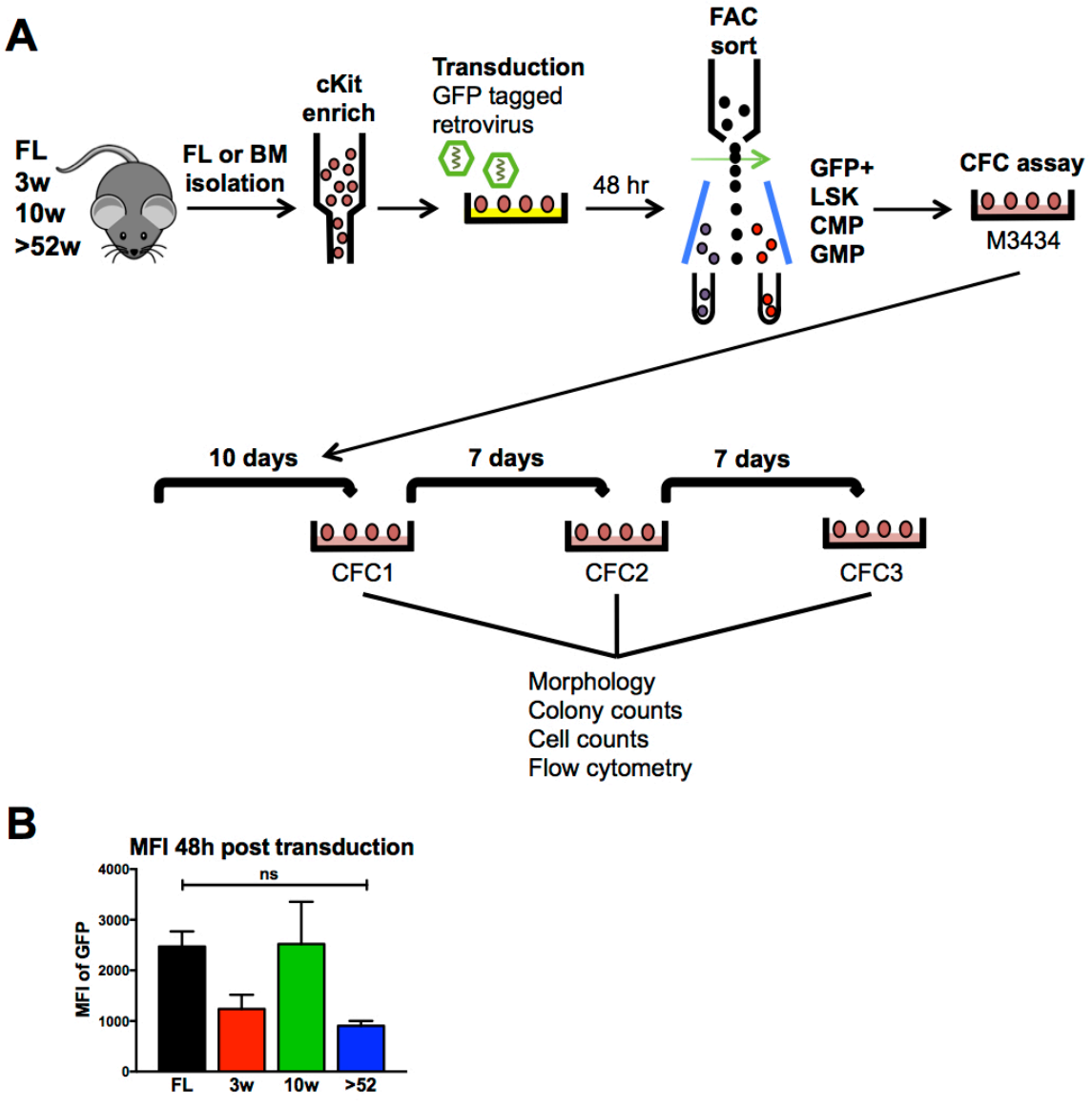

Figure 3.2 Method for cell isolation, retroviral transduction and CFC assay

(A) Schematic showing transduction and isolation of LSK, CMP and GMP populations from FL and BM. GFP^+ populations were serially plated on methylcellulose. Plates were assessed for colony and cell counts, morphology and flow cytometry for surface marker expression.
(B) Graph of difference in MFI of GFP between GFP^+ and GFP^- populations 48h post transduction. Graphs depict mean +SD. Significance determined by 1-way ANOVA and Bonferroni post-test, FL n=3, 3w n=3, 10w n=3, >52w n=2.

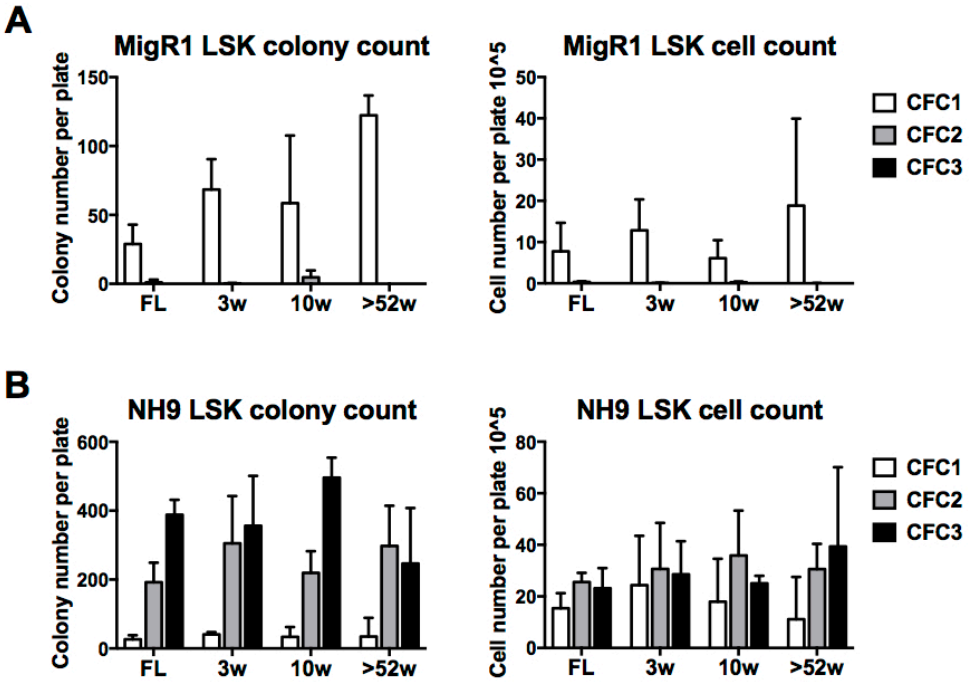

Figure 3.3 NH9 transduced LSKs serially produce CFCs, irrespective of cellular age

(A) Graph of number of colonies (left) and cells produced (right) per plate from CFC assay from LSKs transduced with MigR1 EV control. Irrespective of age, MigR1 expressing LSKs do not serially replate in methylcellulose.
(B) Graph of number of colonies (left) and cells produced (right) per plate from CFC assay from LSKs transduced with NH9. Irrespective of age, NH9 expressing LSKs serially replate in methylcellulose.
Graphs depict mean +SD, n=3 for groups except FL in which n=4. Significance determined by 2-way ANOVA and Bonferroni post-test.

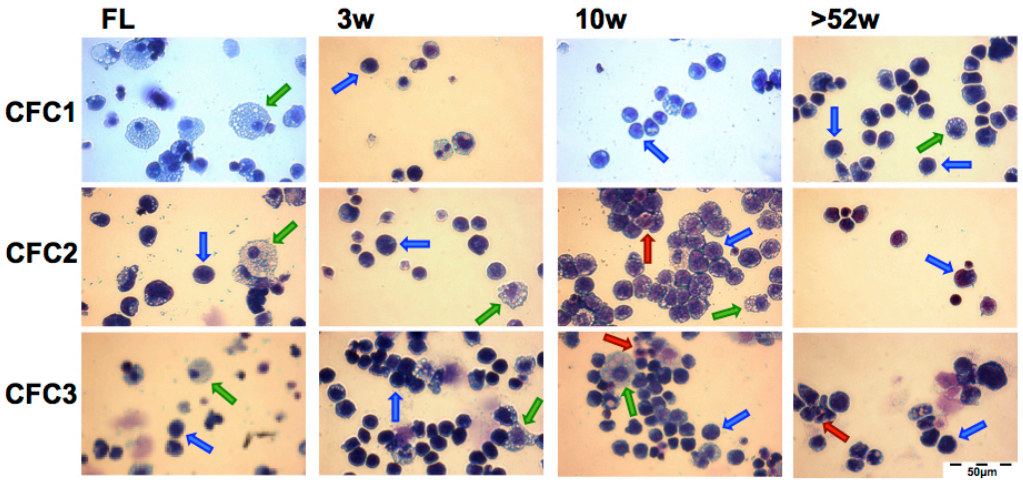

Figure 3.4 Cellular morphology from CFC assay of NH9 transduced LSKs from FL, 3w, 10w and >52w mice

Representative photographs from cytospins taken from cells harvested at CFC1 (top), CFC2 (middle) and CFC3 (bottom), pictured at x40 magnification. The majority of cells are blasts (blue arrows). Some differentiated myeloid cells are also present including neutrophils (red arrows) and macrophages (green arrows).

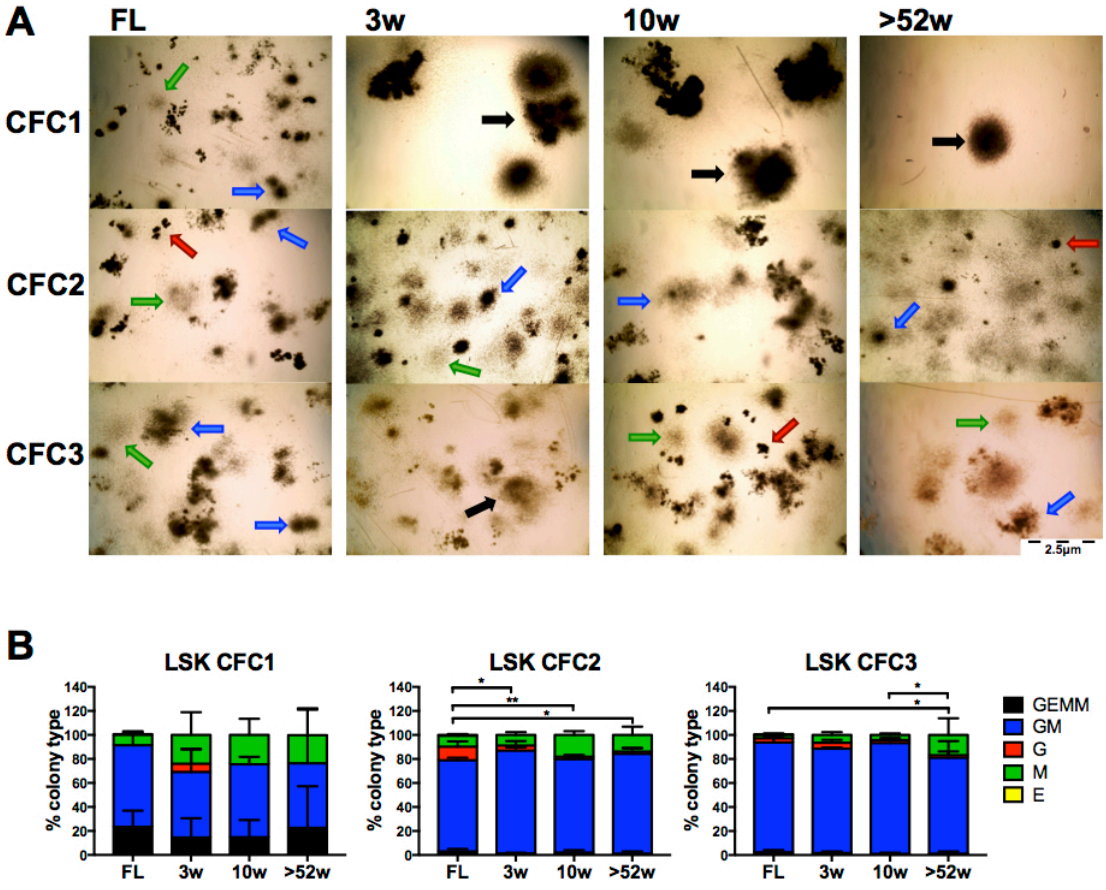

Figure 3.5 Colony morphology from CFC assay of NH9 transduced LSKs from FL, 3w, 10w and 52w mice

(A) Representative morphology of colonies at x2 magnification from CFC1 (top), CFC2 (middle) and CFC3 (bottom). Arrows indicate colony type, GEMM=black, GM=blue, granulocyte=red, macrophage=green.
(B) Graph of percentage colony type produced at CFC1 (left), CFC2 (middle) and CFC3 (right) from NH9 transduced LSKs. G=granulocyte M=macrophage and E=erythroid. Graphs depict mean percentage +SD. Significance determined by 2-way ANOVA and Bonferroni post-test, *p<0.05, **p<0.01, ***p<0.001. FL n=4, 3w n=3, 10w n=3, >52w n=3.

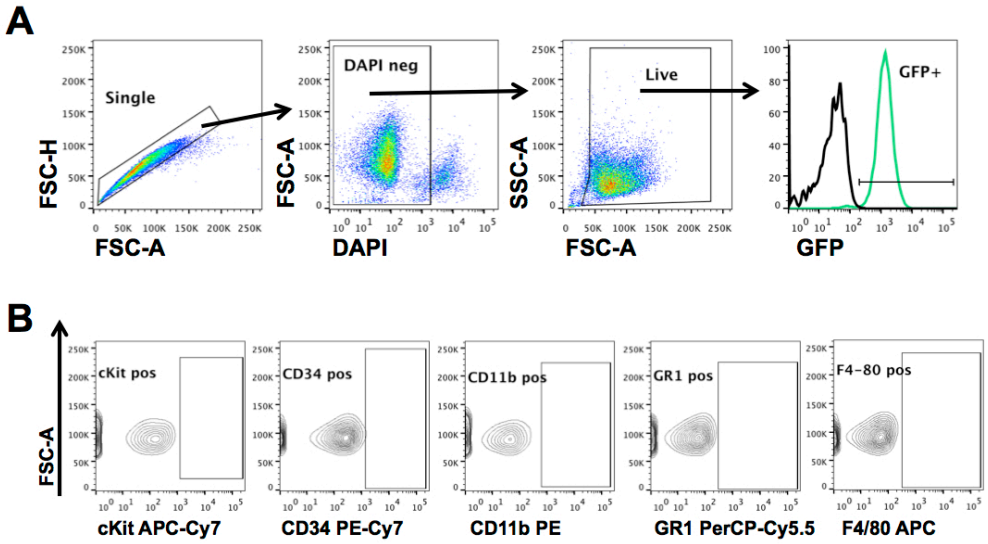

Figure 3.6 Flow cytometry method to assess immunophenotype from CFC analysis

(A) Initial gating strategy. In GFP plot (right), black line indicates untransduced GFP^- control and green line indicates transduced GFP^+ sample.
(B) Control samples to illustrate gating placement for positive surface marker expression. Gates applied based on FMO.

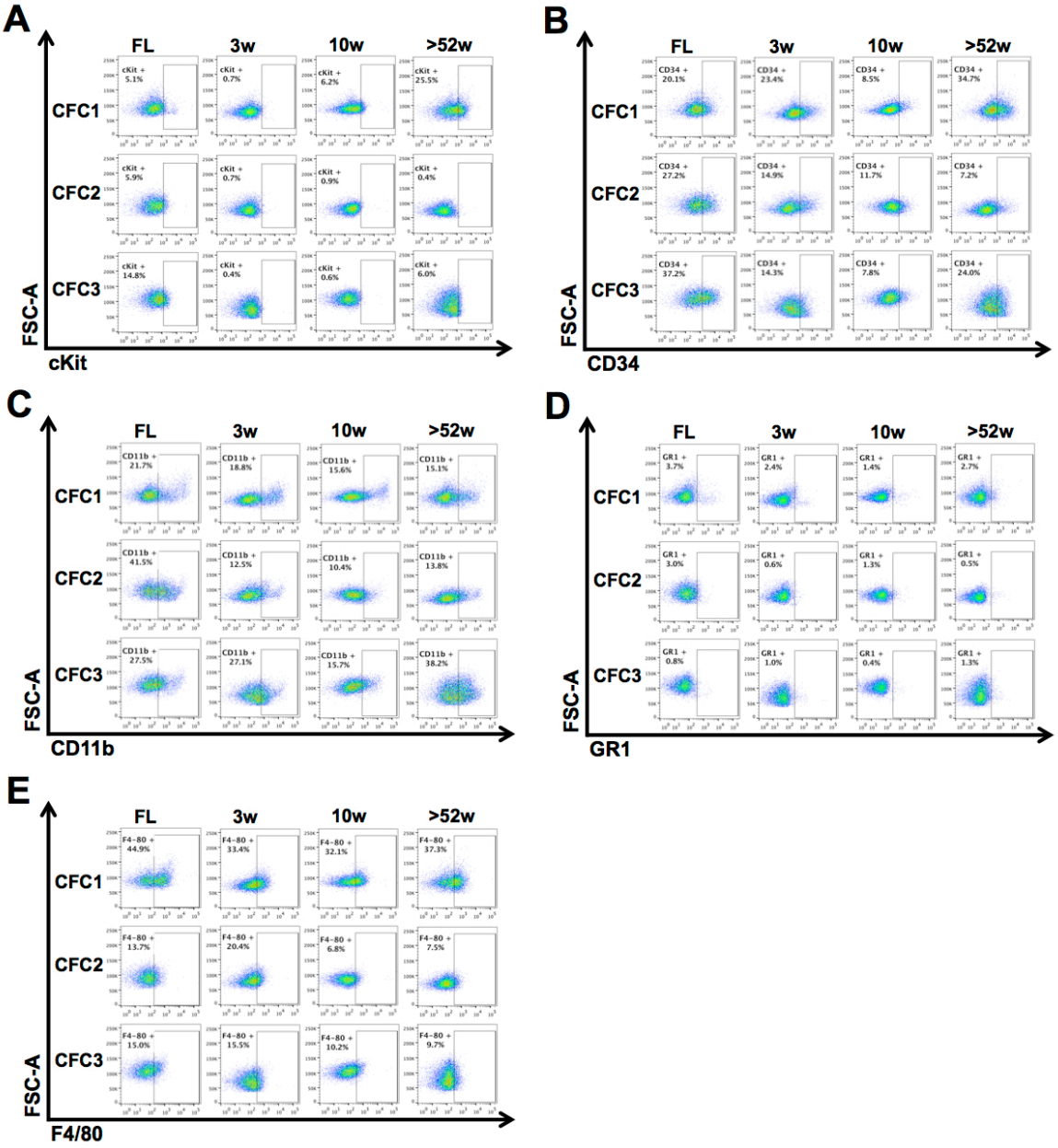

Figure 3.7 Expression of surface markers on NH9 transduced LSKs

(A) Representative flow cytometry plots of cKit surface expression on NH9 transduced FL, 3w, 10w and >52w LSKs from CFC1, CFC2 and CFC3.
(B) Representative flow cytometry plots of CD34 surface expression on NH9 transduced FL, 3w, 10w and >52w LSKs from CFC1, CFC2 and CFC3.
(C) Representative flow cytometry plots of CD11b surface expression on NH9 transduced FL, 3w, 10w and >52w LSKs from CFC1, CFC2 and CFC3.
(D) Representative flow cytometry plots of GR1 surface expression on NH9 transduced FL, 3w, 10w and >52w LSKs from CFC1, CFC2 and CFC3.
(E) Representative plots flow cytometry of F4/80 surface expression on NH9 transduced FL, 3w, 10w and >52w LSKs from CFC1, CFC2 and CFC3.
For initial gating strategy and control samples see Figure 3.6.

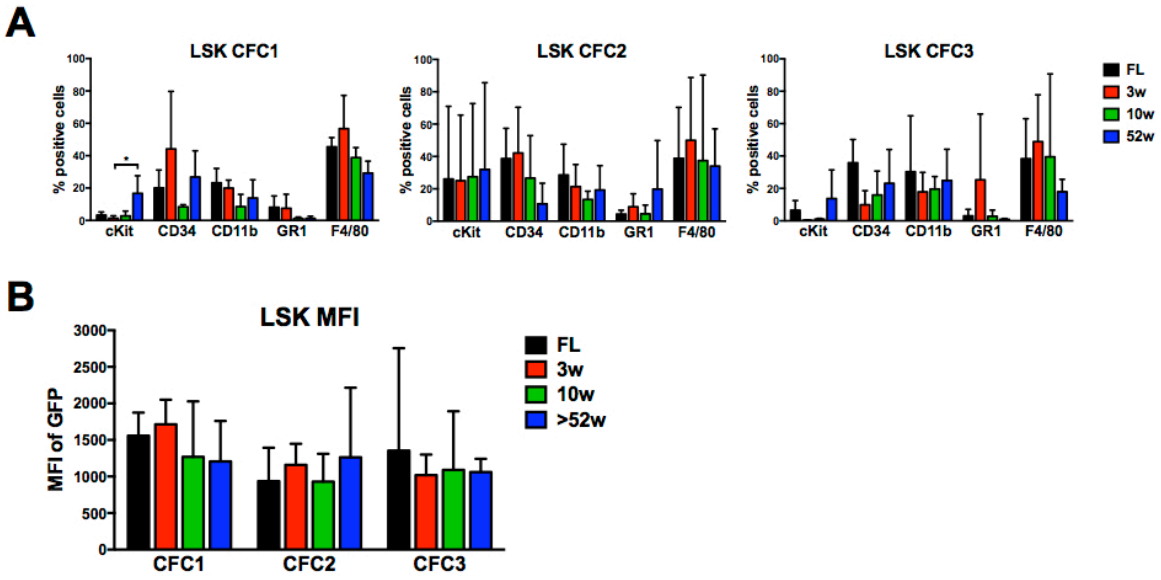

Figure 3.8 Immunophenotype from serial CFC assay of NH9 transduced LSKs

(A) Graph of surface marker expression at CFC1 (left), CFC2 (middle) and CFC3 (right).
(B) Graph of MFI of GFP at CFC1, CFC2 and CFC3 showing no difference in MFI with cellular age. Graphs depict mean +SD. Significance determined by 1-way ANOVA and Bonferroni post-test, *p<0.05. FL n=4, 3w n=3, 10w n=3, >52w n=3.

3.3.2 Post-foetal CMPs transform *in vivo* but FL-CMPs do not

To investigate age related differences in leukaemogenesis of myeloid progenitor populations, CMPs from FL, 3w, 10w and >52w old C57Bl/6 mice were transduced with NH9 or MigR1 EV control and assessed for *in vitro* transformation potential by serial replating in methylcellulose. (Figure 3.2) No MigR1 controls produced colonies past CFC2. (Figure 3.9A) CMPs from post-foetal (3w, 10w and >52w) mice transduced with NH9 produced multiple colonies and cells at CFC3, indicating transformation and acquisition of self-renewal properties. However, CMPs from FL mice transduced with NH9 showed a trend towards fewer colonies or cells per plate at CFC3 and one FL-CMP replicate did not produce colonies post CFC2. (Figure 3.9B) Cellular morphology at each plating of 3w, 10w and >52w NH9 transduced CMPs showed blasts with some differentiation into neutrophils and macrophages and at CFC1, occasional megakaryocytes. In contrast, at each plating, the predominant cells produced in FL-CMPs were mature macrophages. (Figure 3.10) Colonies were identified by morphology at each plating and representative pictures are shown in Figure 3.11A. Similar to LSKs, NH9 expressing CMPs from 3w, 10w and >52w mice produced large colonies at CFC1. In contrast, FL-CMPs at CFC1 produced small

colonies. However, at CFC1 there was no difference in the type of colonies produces; irrespective of cellular age the predominant colony produced was of GM type. (Figure 3.11A top and B left) At CFC2 and CFC3, the predominant colony produced in 3w, 10w and >52w-CMPs was GM colonies. In contrast, FL-CMPs produced proportionally more diffuse M colonies. (Figure 3.11B middle and left) This is in keeping which the cellular morphological appearances from cytospins taken from FL-CMP and suggests that FL-CMPs produce terminally differentiated cells.

The phenotype of cells produced at each plating was further assessed by flow cytometry. Initial gating strategy and negative controls are shown in Figure 3.6. The expression of immature markers and myeloid markers are shown in Figure 3.12. Surface marker and GFP expression are summarised in Figure 3.13. At CFC1, >52w-CMPs displayed increased expression of the myeloid marker CD11b, while at CFC2 there was a trend towards increased CD11b expression with increasing age. (Figure 3.12C and Figure 3.13A left and middle). This suggests that transforming adult CMPs are more myeloid skewed, than their younger counterparts. At CFC3, no difference in surface marker expression was observed between *in vitro* transformed 3w, 10w and >52w CMPs. In contrast, FL CMPs showed very high cKit expression with low expression of the myeloid markers, specifically CD11b, mirroring the expression seen in MigR1 controls. (Figure 3.12A and C and Figure 3.13A) Like the LKS groups, at each plating, there was no difference in the MFI of GFP with cellular age, suggesting similar expression of GFP protein as a surrogate marker of NH9 protein level. (Figure 3.13B) Therefore, NH9 transformed post-foetal (3w, 10w and >52w) CMPs *in vitro* with no difference in resultant proliferative potential, morphology or immunophenotype. However, NH9 expressing FL-CMPs produced fewer colonies at CFC3 and showed mature macrophage morphology. This suggests that using this AML model, FL-CMP are more resistant to *in vitro* transformation compared to post-foetal-CMPs.

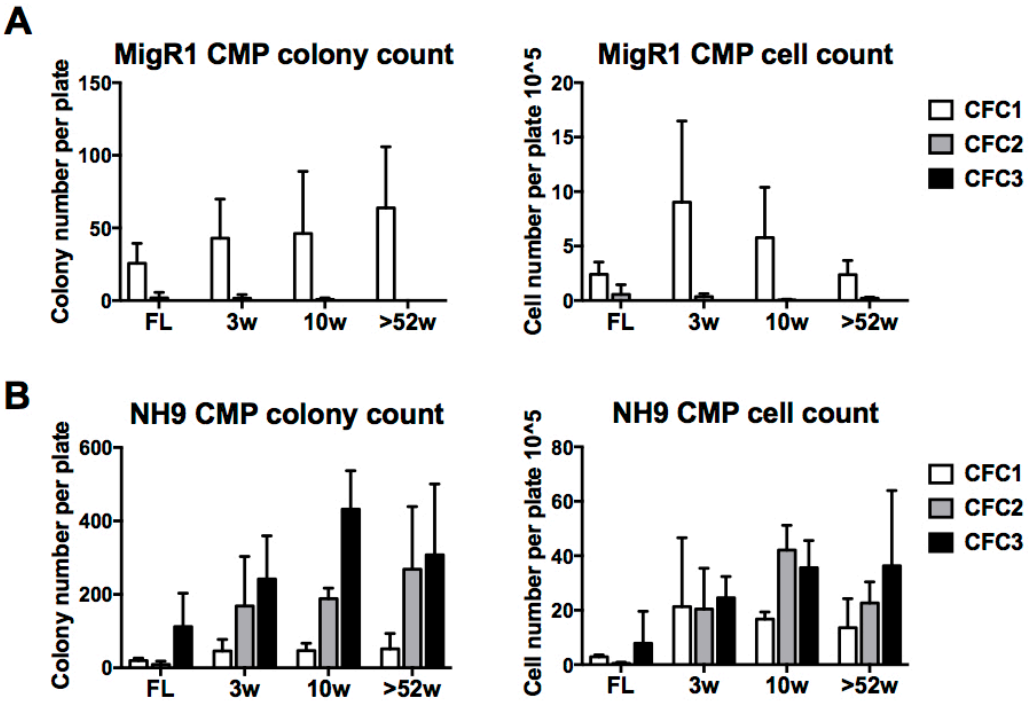

Figure 3.9 Post-foetal CMPs transduced with NH9 serially produce CFCs, FL-CMP produce fewer colonies and cells at CFC3

(A) Graph of number of colonies (left) and cells produced (right) per plate from CFC assay in CMPs transduced with MigR1 EV control. Irrespective of age, MigR1 expressing CMPs do not serially replate in methylcellulose.
(B) Graph of number of colonies (left) and cells produced (right) per plate from CFC assay in CMPs transduced with NH9. Post-foetal, NH9 expressing CMPs from 3w, 10w and >52w serially replate in methylcellulose, while there is a trend towards fewer colonies and cells in FL-CMPs at CFC3. Graphs depict mean +SD, FL n=4, 3w n=3, 10w n=3, >52w n=3. Significance determined by 2-way ANOVA and Bonferroni post-test.

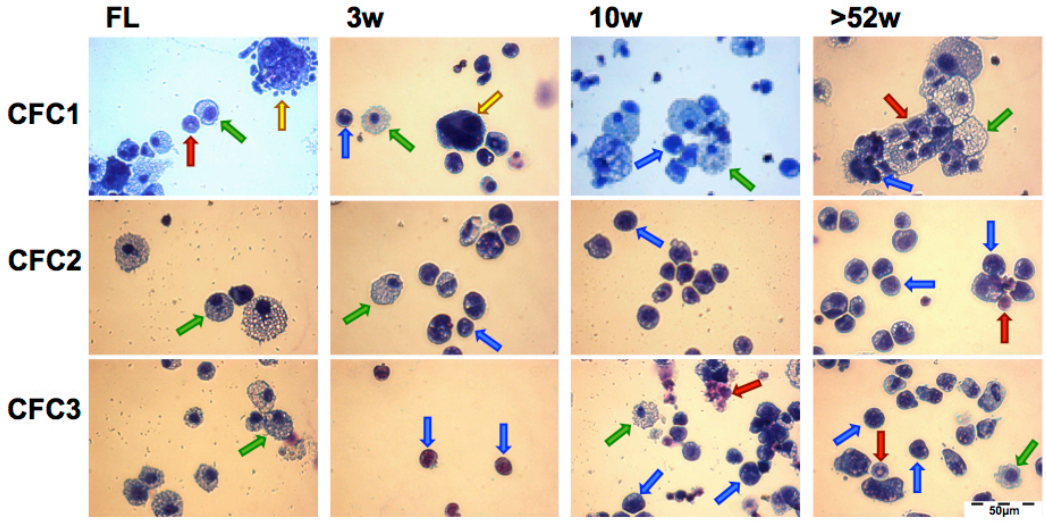

Figure 3.10 Cellular morphology from CFC assay of NH9 transduced CMPs from FL, 3w, 10w and >52w mice

Representative photographs from cytospins taken from cells harvested at CFC1 (top), CFC2 (middle) and CFC3 (bottom), pictured at x40 magnification. The majority of cells in 3w, 10w and >52w groups are blasts (blue arrows). Some differentiated myeloid cells are also present including neutrophils (red arrows) and macrophages (green arrows). In FL, the predominant cells are macrophages (green arrows). Occasional megakaryocytes (yellow arrows) are seen at CFC1 in FL and 3w CMP groups.

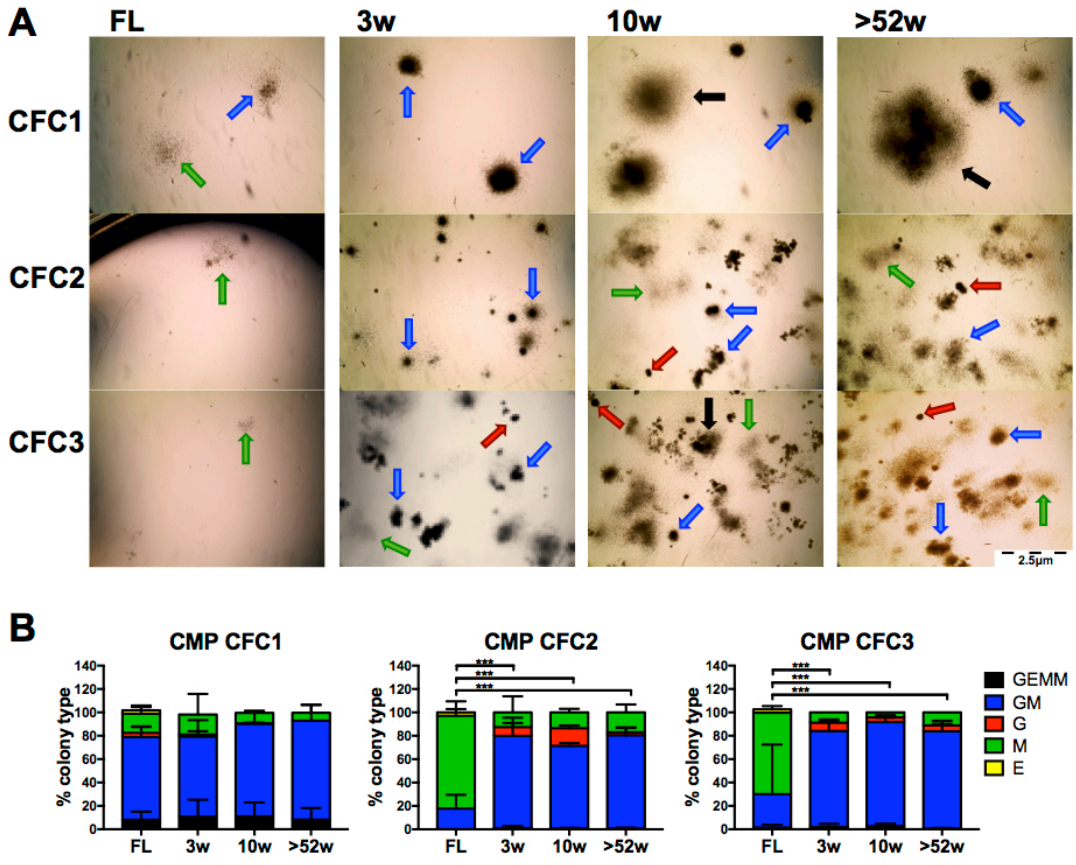

Figure 3.11 Colony morphology from CFC assay of NH9 transduced CMPs from FL, 3w, 10w and >52w mice

(A) Representative morphology of colonies at x2 magnification from each plating. Arrows indicate colony type, GEMM=black, GM=blue, granulocyte=red, macrophage=green.
(B) Graphs of percentage colony type produced at CFC1 (left), CFC2 (middle) and CFC3 (right) from NH9 transduced LSKs. G=granulocyte, M=macrophage and E=erythroid. Graphs depict mean percentage +SD. FL n=4, 3w n=3, 10w n=3, >52w n=3. Significance determined by 2-way ANOVA and Bonferroni post-test, *p<0.05, **p<0.01, ***p<0.001.

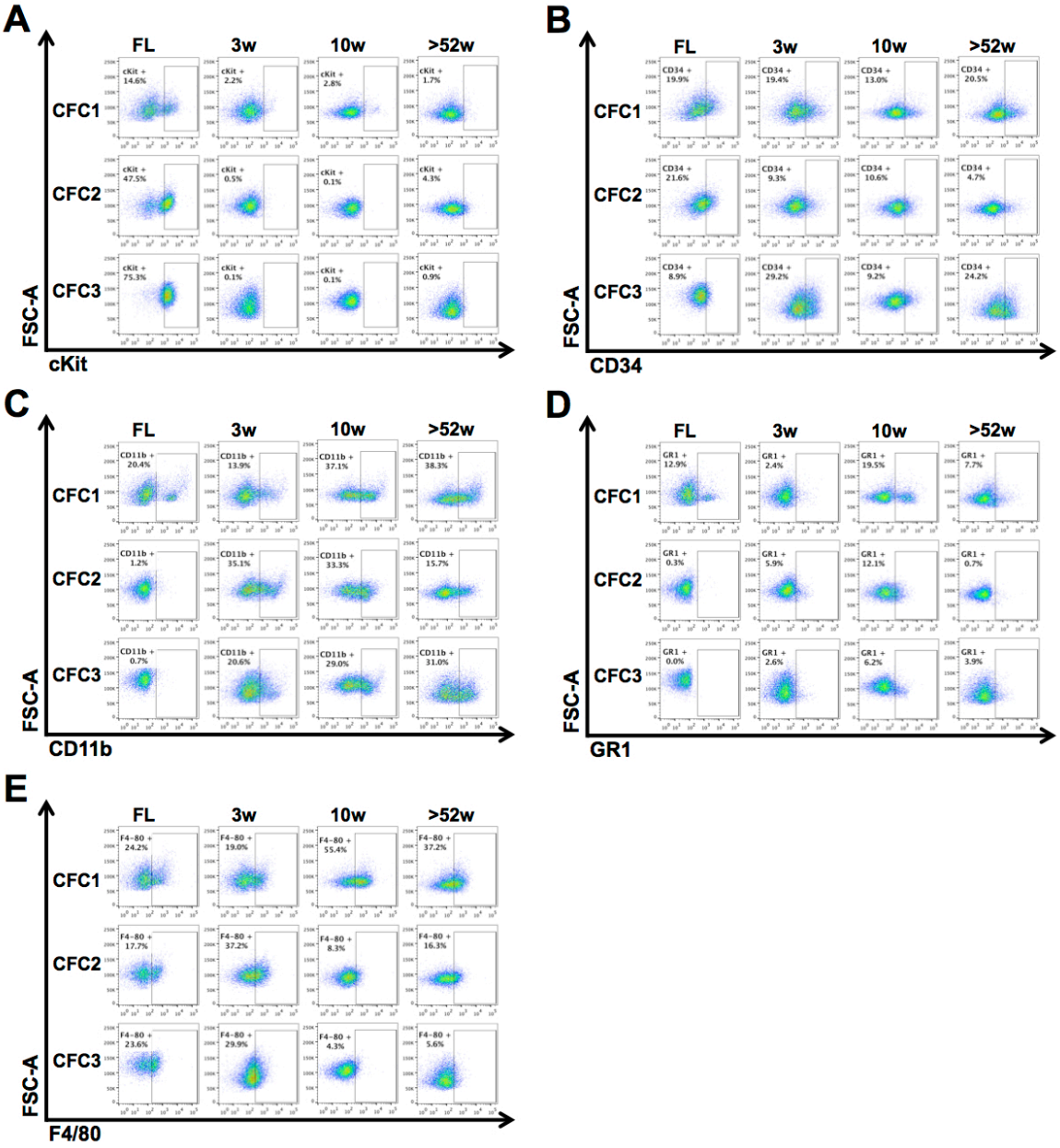

Figure 3.12 Expression of surface markers on NH9 transduced CMPs

(A) Representative flow cytometry plots of cKit surface expression on NH9 transduced FL, 3w, 10w and >52w CMPs from CFC1, CFC2 and CFC3.
(B) Representative flow cytometry plots of CD34 surface expression on NH9 transduced FL, 3w, 10w and >52w CMPs from CFC1, CFC2 and CFC3.
(C) Representative flow cytometry plots of CD11b surface expression on NH9 transduced FL, 3w, 10w and >52w CMPs from CFC1, CFC2 and CFC3.
(D) Representative flow cytometry plots of GR1 surface expression on NH9 transduced FL, 3w, 10w and >52w CMPs from CFC1, CFC2 and CFC3.
(E) Representative flow cytometry plots of F4/80 surface expression on NH9 transduced FL, 3w, 10w and >52w CMPs from CFC1, CFC2 and CFC3.
For initial gating strategy and control samples see Figure 3.6.

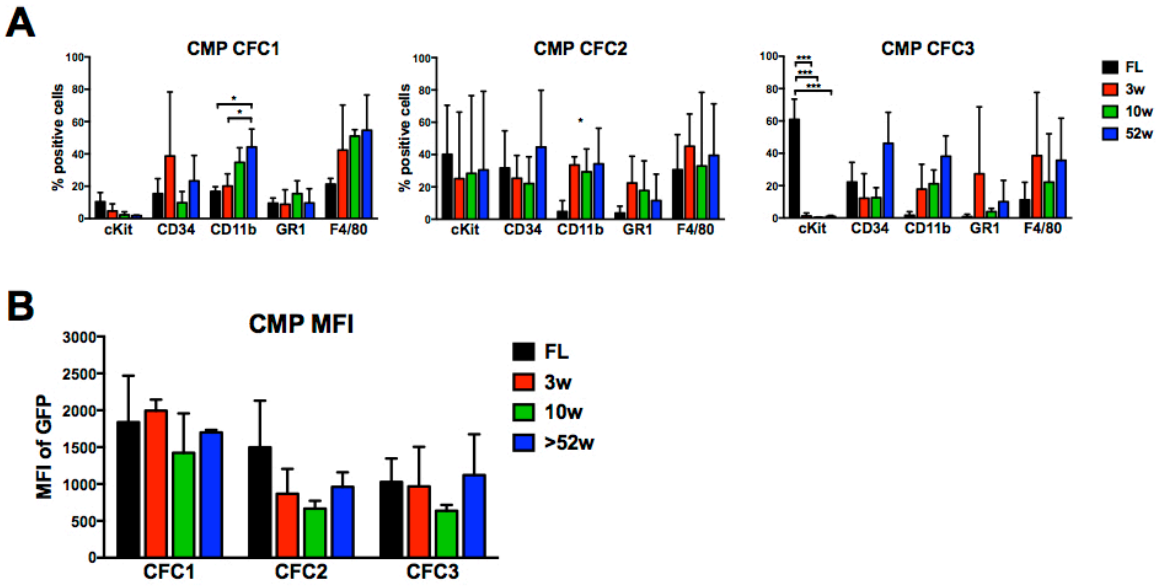

Figure 3.13 Immunophenotype from serial CFC assay of NH9 transduced CMPs

(A) Graphs of surface marker expression at CFC1 (left), CFC2 (middle) and CFC3 (right).
(B) Graph of MFI of GFP at CFC1, CFC2 and CFC3 showing no difference in MFI with cellular age.
Graph depicts mean +SD. Significance determined by 1-way ANOVA and Bonferroni post-test.
FL n=4, 3w n=3, 10w n=3, >52w n=3, *p<0.05, **p<0.01, ***p<0.001.

3.3.3 Post-foetal GMPs transform *in vivo* but FL-GMPs do not

To further investigate age related differences in leukaemogenesis of myeloid progenitor populations, GMPs from FL, 3w, 10w and >52w old C57Bl/6 mice were transduced with NH9 or MigR1 EV control and assessed for *in vitro* transformation potential by serial replating in methylcellulose. (Figure 3.6) No MigR1 controls produced colonies beyond CFC2. (Figure 3.14A) GMPs from post-foetal (3w, 10w and >52w) mice transduced with NH9 produced multiple colonies at CFC3 indicating *in vitro* transformation and acquisition of self-renewal properties. In contrast, no FL-GMPs produced colonies or cells beyond CFC2, similar to MigR1 controls. (Figure 3.14B) Cellular morphology at each plating showed that 3w, 10w and >52w NH9 transduced GMPs predominantly produced blasts with some differentiation into neutrophils and macrophages. In contrast, at CFC1 and CFC2 FL-GMPs produced mature macrophages but no blasts. (Figure 3.15) Colonies were identified by morphology at each plating and representative pictures are shown in Figure 3.16A. NH9 expressing GMPs from post-foetal (3w, 10w and >52w) mice produced large colonies at CFC1. In contrast, FL-GMPs at CFC1 produced small macrophage colonies. (Figure 3.16A

top) While the predominant colony type at CFC1 was GM in post-foetal GMPs, FL-GMPs produced proportionally more macrophage colonies. (Figure 3.16B left) At CFC2 and CFC3, the predominant colony produced in 3w, 10w and >52w-GMPs was GM colonies. In contrast, of the FL-replicates that produced any colonies at CFC2, these were exclusively macrophage type, and did not replate to CFC3. (Figure 3.16B middle and right) This suggests that FL-GMPs progressively differentiate on serial replating and do not acquire self-renewal properties.

The phenotype of cells produced at each plating was further assessed by flow cytometry. Initial gating strategy and negative controls are shown in Figure 3.6. The expression of immature markers and myeloid markers are shown in Figure 3.17. Surface marker and GFP expression are summarised in Figure 3.18. At CFC1, FL-GMPs displayed a trend towards increased expression of cKit (Figure 3.17A and Figure 3.18A left). However, at CFC2, there was no difference in the expression of immature markers cKit and CD34, or myeloid markers CD11b, GR1 or F4/80, with cellular age. (Figure 3.18A middle) At CFC3, transformed 3w-GMPs displayed increased expression of the myeloid marker GR1 compared to 10w and >52w transformed GMPs, suggesting transformed 3w-GMPs have a more differentiated immunophenotype. (Figure 3.17D and Figure 3.18A right) At each plating, there was no difference in the MFI of GFP with cellular age, suggesting similar expression of GFP protein as a surrogate marker of NH9 protein level. (Figure 3.18B) Thus, NH9 can transform post-foetal GMPs but FL-GMPs are resistant to *in vitro* transformation by NH9. In summary, NH9 can transform FL-LSKs but not the myeloid committed CMPs and GMPs. In contrast, NH9 can transform post foetal LSKs, CMPs and GMPs. This suggests that age defined characteristics in foetal CMPs and GMPs inhibit leukemic transformation, but that these intrinsic features are lost with increasing age.

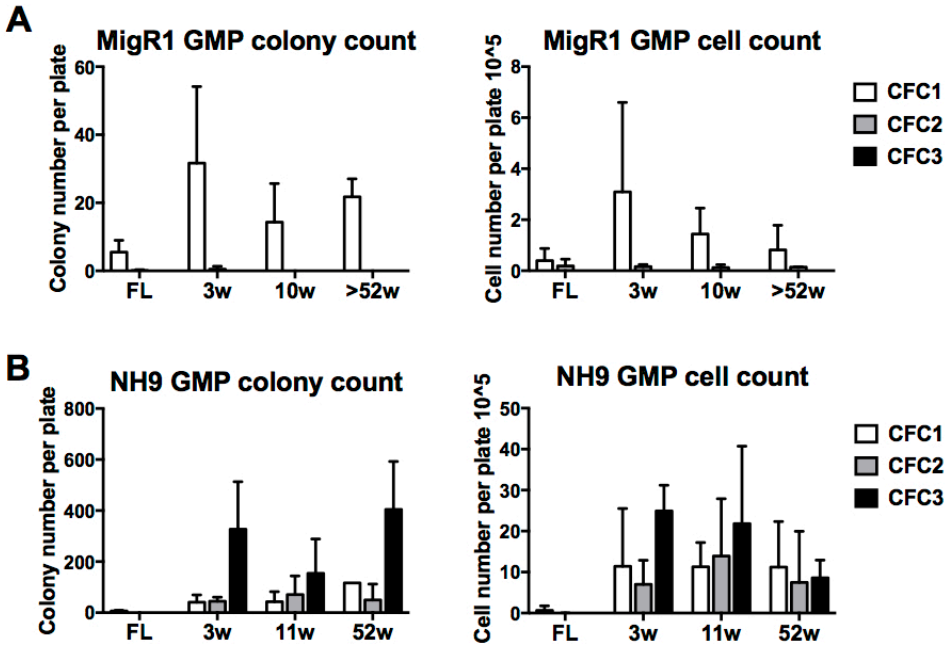

Figure 3.14 Post-foetal GMPs transduced with NH9 serially produce CFCs, FL-GMP do not replate beyond CFC2

(A) Graph of number of colonies (left) and cells produced (right) per plate from CFC assay in GMPs transduced with MigR1 EV control. Irrespective of age, MigR1 expressing GMPs do not serially replate in methylcellulose.
(B) Graph of number of colonies (left) and cells produced (right) per plate from CFC assay in GMPs transduced with NH9. Post-foetal NH9 expressing GMPs from 3w, 10w and >52w serially replate in methylcellulose. FL-GMPs do not produced colonies or cells beyond CFC2.
Graphs depict mean +SD, FL n=4, 3w n=3, 10w n=3, >52w n=3.

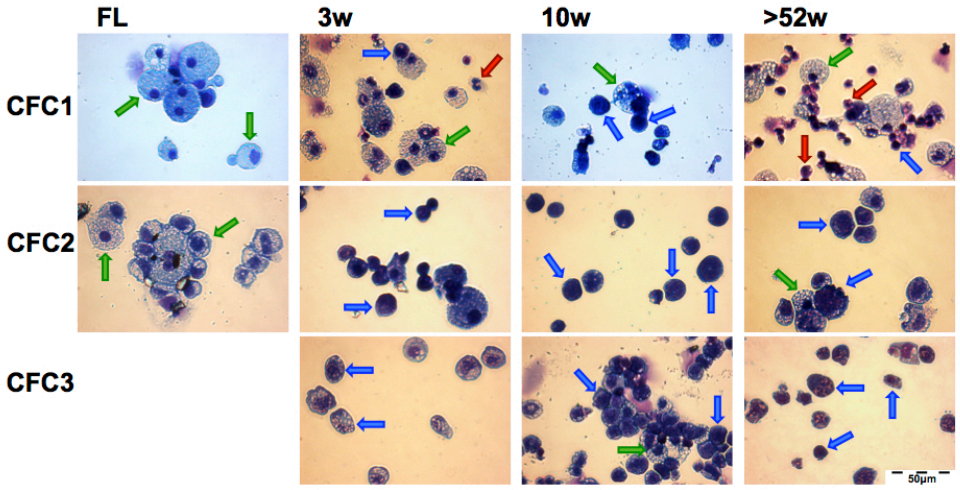

Figure 3.15 Cellular morphology from CFC assay of NH9 transduced GMPs from FL, 3w, 10w and >52w mice

Representative photographs from cytospins taken from cells harvested at CFC1 (top), CFC2 (middle) and CFC3 (bottom), pictured at x40 magnification. The majority of cells in 3w, 10w and >52w groups are blasts (blue arrows). Some differentiated myeloid cells are also present including neutrophils (red arrows) and macrophages (green arrows). In FL, the predominant cells are macrophages (green arrows). No FL GMP cells survived beyond CFC2.

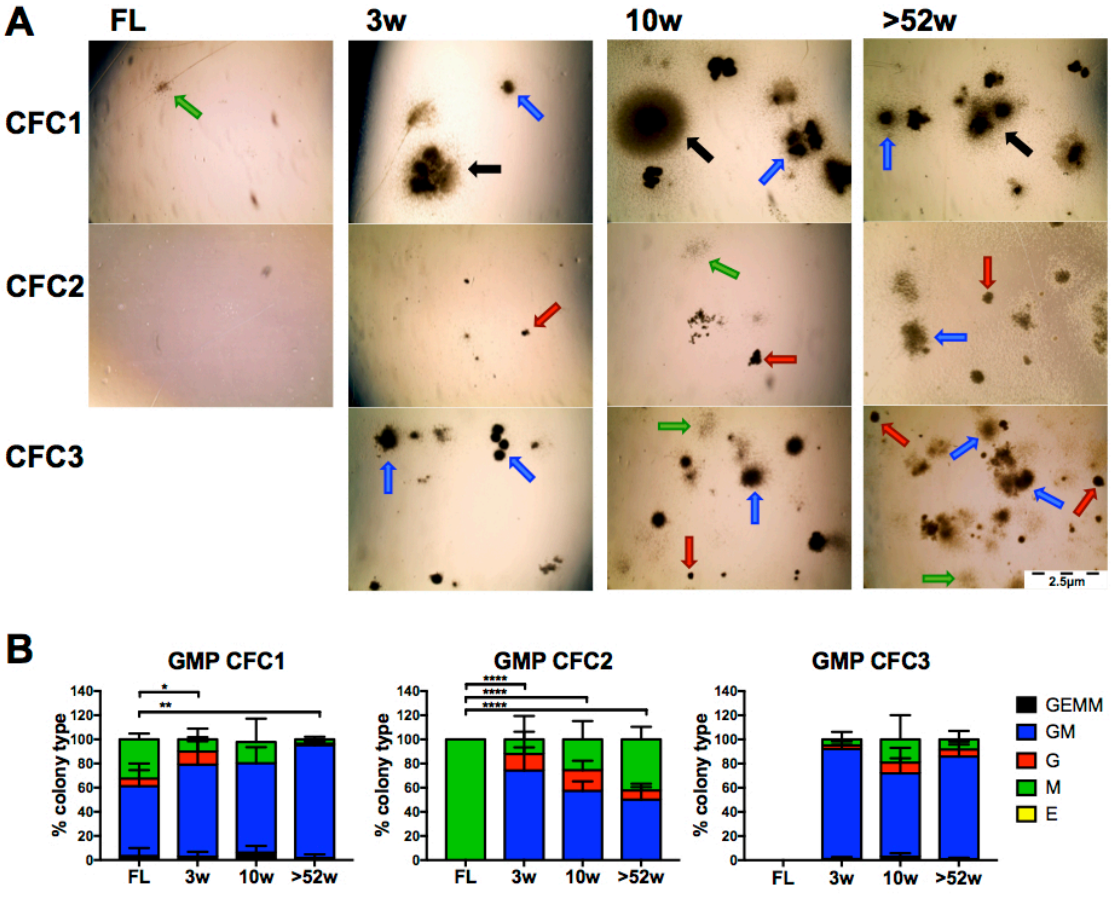

Figure 3.16 Colony morphology from CFC assay of NH9 transduced GMPs from FL, 3w, 10w and >52w mice

(A) Representative morphology of colonies at x2 magnification from each plating. Arrows indicate colony type, GEMM=black, GM=blue, granulocyte=red, macrophage=green.
(B) Graphical depiction of percentage colony type produced at CFC1 (left), CFC2 (middle) and CFC3 (right) from NH9 transduced GMPs. FL-GMPs produce proportionally more macrophage colonies at CFC1, only macrophage colonies at CFC2 and no colonies at CFC3. G=granulocyte, M=macrophage and E=erythroid. Graphs depict mean percentage +SD. Significance determined by 2-way ANOVA and Bonferroni post-test, *p<0.05, **p<0.01, ***p<0.001, ****p<0.0001. FL n=4, 3w n=3, 10w n=3, >52w n=3.

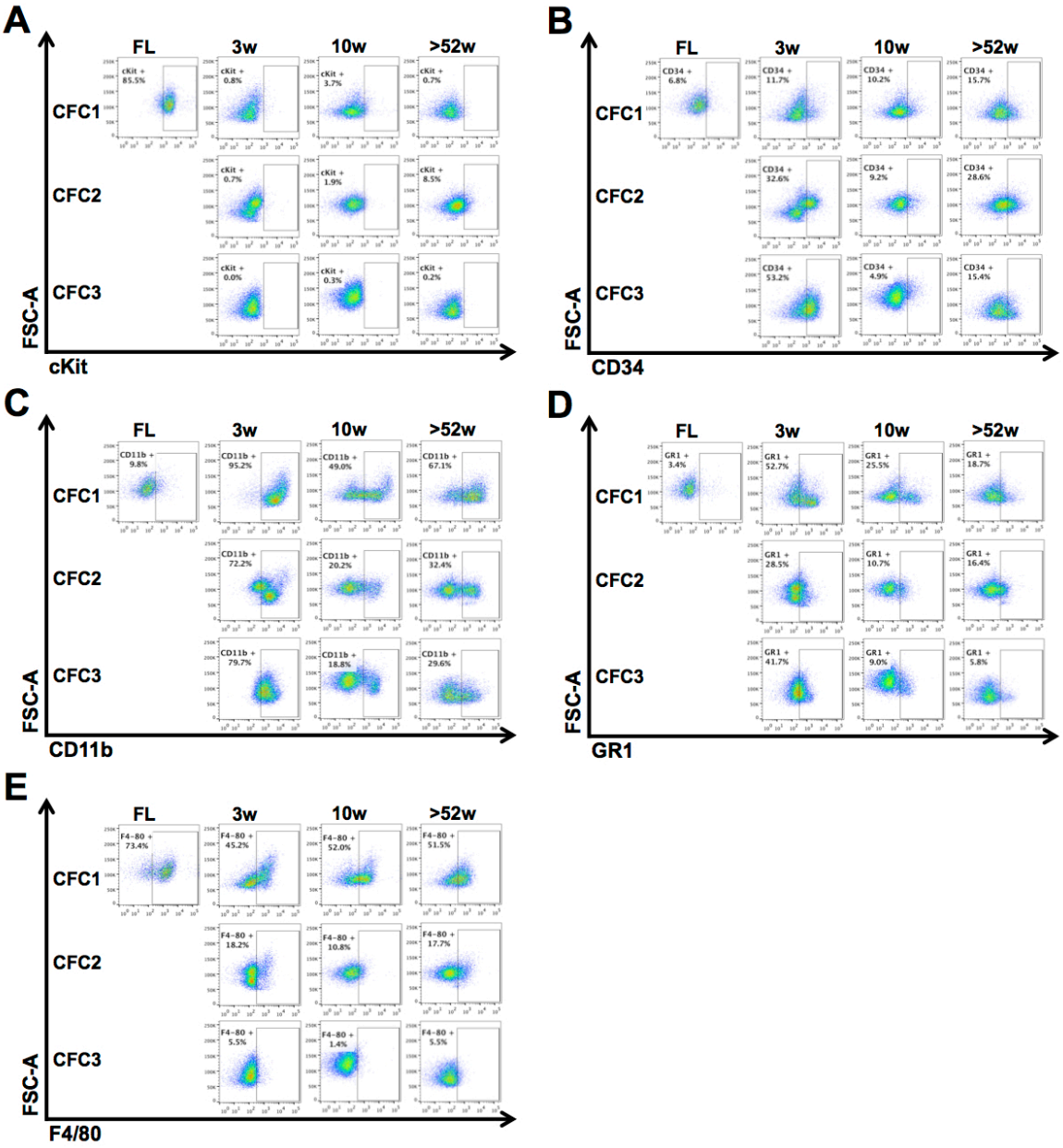

Figure 3.17 Expression of surface markers on NH9 transduced GMPs

(A) Representative flow cytometry plots of cKit surface expression on NH9 transduced FL, 3w, 10w and >52w GMPs from CFC1, CFC2 and CFC3.
(B) Representative flow cytometry plots of CD34 surface expression on NH9 transduced FL, 3w, 10w and >52w GMPs from CFC1, CFC2 and CFC3.
(C) Representative flow cytometry plots of CD11b surface expression on NH9 transduced FL, 3w, 10w and >52w GMPs from CFC1, CFC2 and CFC3.
(D) Representative flow cytometry plots of GR1 surface expression on NH9 transduced FL, 3w, 10w and >52w GMPs from CFC1, CFC2 and CFC3.
(E) Representative flow cytometry plots of F4/80 surface expression on NH9 transduced FL, 3w, 10w and >52w GMPs from CFC1, CFC2 and CFC3.
For initial gating strategy and control samples see Figure 3.6. No FL-GMPs replated to CFC3.

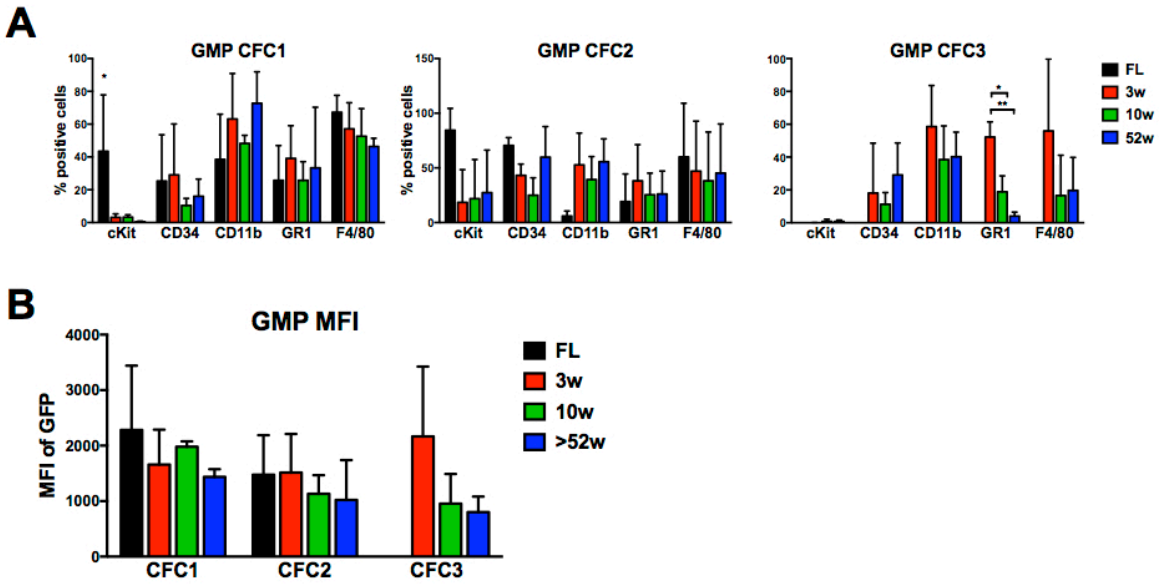

Figure 3.18 Immunophenotype from serial CFC assay of NH9 transduced GMPs

(A) Graph of surface marker expression at CFC1 (left), CFC2 (middle) and CFC3 (right).
(B) Graph of MFI of GFP at CFC1, CFC2 and CFC3 showing no difference in MFI with cellular age. Graph depicts mean +SD. Significance determined by 1-way ANOVA and Bonferroni post-test, *p<0.05, **p<0.01. FL n=4, 3w n=3, 10w n=3, >52w n=3.

3.3.4 Adult transduced HSPCs display transformed characteristics compared to young HSPCs at CFC1

Transformed progenitor populations showed no difference between age groups at CFC3 in terms of absolute colony or cell number. With the exception of GR1 expression in transformed GMPs, surface marker expression in transformed populations also showed no difference with cellular age. However, the inability of FL-CMPs and GMPs to transform indicates that age dependent factors may play a role in leukaemic susceptibility that may be present in transforming populations. To investigate age dependent differences in transformation kinetics, colony and cell number was assessed at an early time point. For each sample, colony and cell number was normalised to its respective MigR1 control at CFC1. While FL-LSKs showed similar colony numbers to control at CFC1, LSKs from post-foetal mice (3w, 10w and >52w) showed a trend towards fewer colonies than control, with >52w-LSKs showing significantly fewer colonies at CFC1 compared to MigR1 controls. (Figure 3.19A) However, there was no difference in cell number in LSKs of any age at CFC1. (Figure 3.19B) At CFC1 the colonies in the post-foetal groups were larger than their controls or NH9

expressing FL-LSKs. (Figure 3.5A top) NH9 overexpression characteristically produces large colonies in CFC assay. (Kroon et al., 2001) Therefore, post-foetal LSKs showed more transformed characteristics at CFC1 than FL-LSKs. There was no significant age related difference in normalised colony or cell count at CFC1 for transduced CMPs. (Figure 3.20) Transduced GMPs from FL and 3w mice showed no difference in colony or cell number compared to control. In contrast, 10w and >52w GMPs produced significantly more colonies and cells showing they were already outgrowing age matched controls and NH9 expressing FL and 3w GMPs by CFC1. (Figure 3.21) The data suggest that adult HSPCs (10w and >52w) are more susceptible to transformation by NH9 *in vitro* than young HSPCs (FL and 3w). Specifically, FL CMPs and GMPs cannot transform, unlike their older counterparts. FL-LSKs do transform *in vitro*, but do not produce large NH9-like colonies at CFC1. Furthermore, while all post-foetal GMPs transform *in vitro*, at CFC1 10w and 52w display increased proliferation compared to 3w. This indicates there is a difference in transformation kinetics with age, with adult cells showing faster transformation at an early time point.

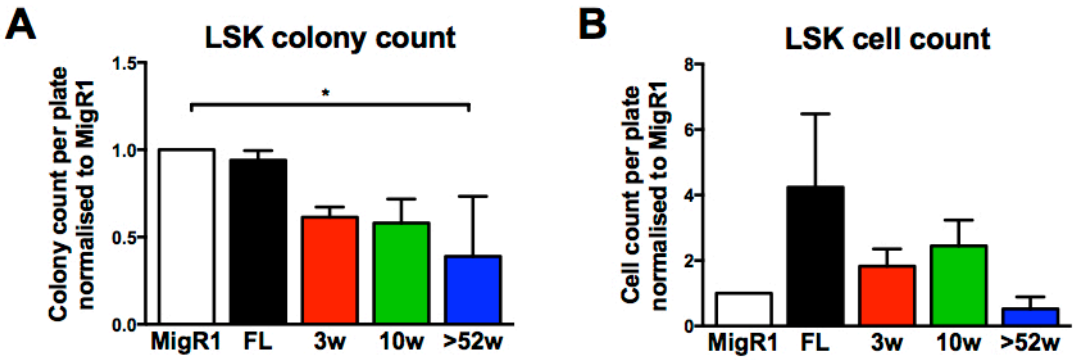

Figure 3.19 Adult LSKs transduced with NH9 produce relatively fewer colonies at CFC1

(A) Graph of normalised colony count at CFC1. Colony count normalised against age matched MigR1 control at CFC1.
(B) Graph of normalised cell count at CFC1. Cell count normalised against age matched MigR1 control at CFC1, showing no difference in cell count compared to MigR1 control, irrespective of cellular age of LSK.
Graphs depict mean +SD. Significance determined by 1-way ANOVA and Bonferroni post-test, *p<0.05. FL n=4, 3w n=3, 10w n=3, >52w n=3.

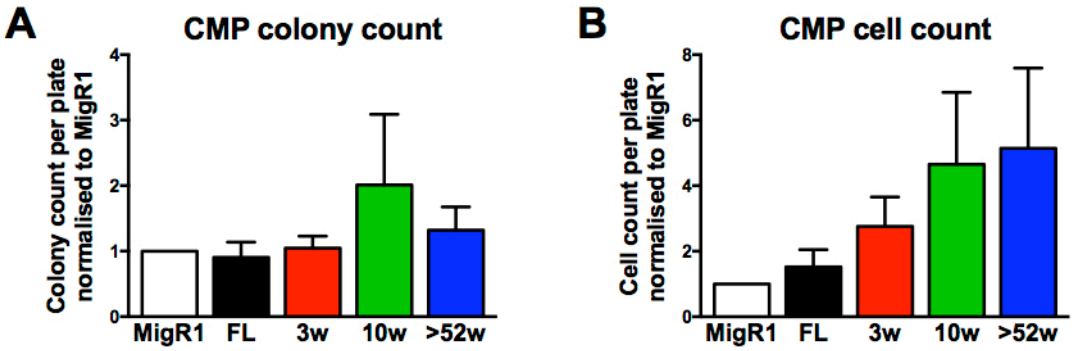

Figure 3.20 CMPs transduced with NH9 show no difference in relative colony number and cells produced at CFC1 with cellular age

(A) Graph of normalised colony count at CFC1. Colony count normalised against age matched MigR1 control at CFC1, showing no difference in colony count compared to MigR1 control, irrespective of cellular age of LSK.
(B) Graph of normalised cell count at CFC1. Cell count normalised against age matched MigR1 control at CFC1, showing no difference in cell count compared to MigR1 control, irrespective of cellular age of CMP.
Graphs depict mean +SD. Significance determined by 1-way ANOVA and Bonferroni post-test. FL n=4, 3w n=3, 10w n=3, >52w n=3.

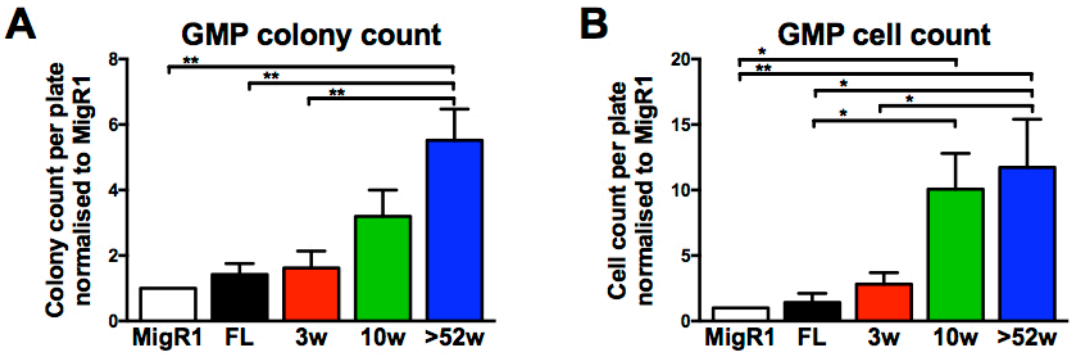

Figure 3.21 Adult GMPs transduced with NH9 produce relatively more colonies and cells at CFC1 compared to young GMPs

(A) Graph of normalised colony count at CFC1. Colony count normalised against age matched MigR1 control at CFC1.
(B) Graph of normalised cell count at CFC1. Cell count normalised against age matched MigR1 control at CFC1.
Graphs depict mean +SD. Significance determined by 1-way ANOVA and Bonferroni post-test, *p<0.05, **p<0.01. FL n=4, 3w n=3, 10w n=3, >52w n=3.

3.3.5 Common AML oncogenes transform FL-LSKs but fail to transform FL-CMP and FL-GMPs

Investigating the age dependent transformability of LSK, CMP and GMP populations showed that while LSKs from all ages transform *in vitro* with NH9, FL-CMP and GMPs do not, whereas post-foetal committed progenitors do. To

investigate if the failure of FL committed progenitors to transform was specific to NH9 or an intrinsic property of foetal cells, FL-LSK, CMP and GMPs were transduced with the common AML driving mutations, A1E and FLT3-ITD as well as NH9. Transformation was assessed by growth in liquid culture to assess intrinsic cellular transformability and on OP9 co-culture as an *in vitro* model for the BM niche. (Figure 3.22) Regardless of oncogene, FL-LSKs grew in liquid culture while FL-CMP and GMPs exhausted after 50-75 days, (Figure 3.23A) supporting that this is an intrinsic feature of foetal committed myeloid progenitors rather than due to the specific oncogenic insult. Similarly, FL-LSKs grew on stroma while FL-CMP and GMPs exhausted, albeit quicker than liquid culture after 25-50 days suggesting that signals from the microenvironment further impede transformation of foetal committed progenitors. (Figure 3.23B)

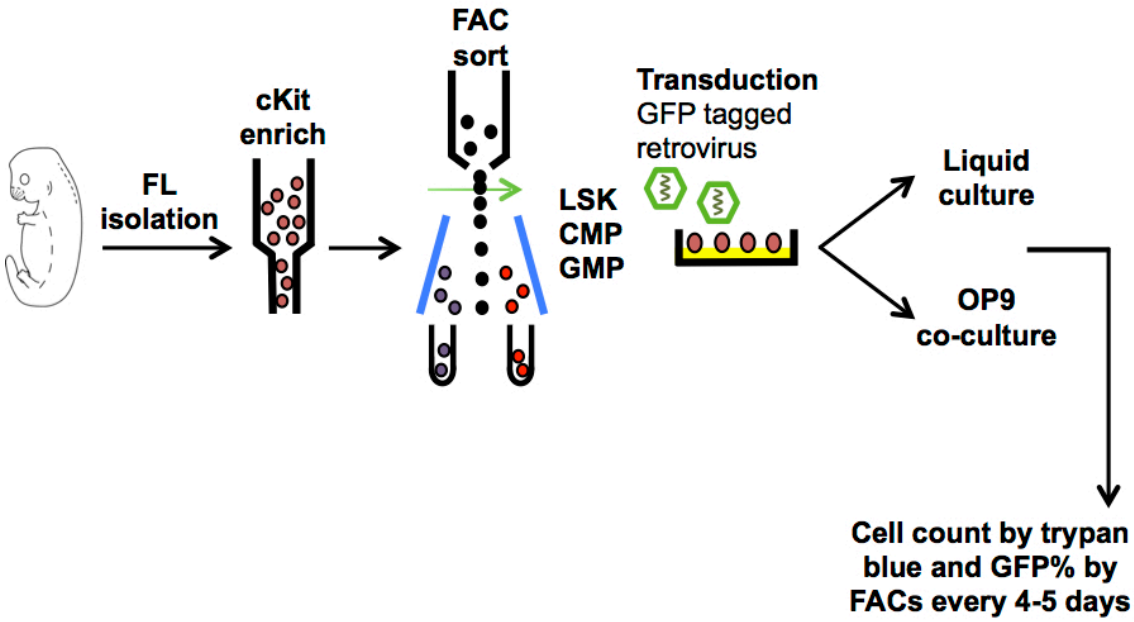

Figure 3.22 Method for cell isolation, retroviral transduction and culture of FL HSPCs

Schematic showing isolation and transduction of LSK, CMP and GMP populations from FL. Populations unsorted for GFP were grown in liquid culture and OP9 co-culture. Cells were counted by trypan blue and GFP% measured by flow cytometry every 4-5 days.

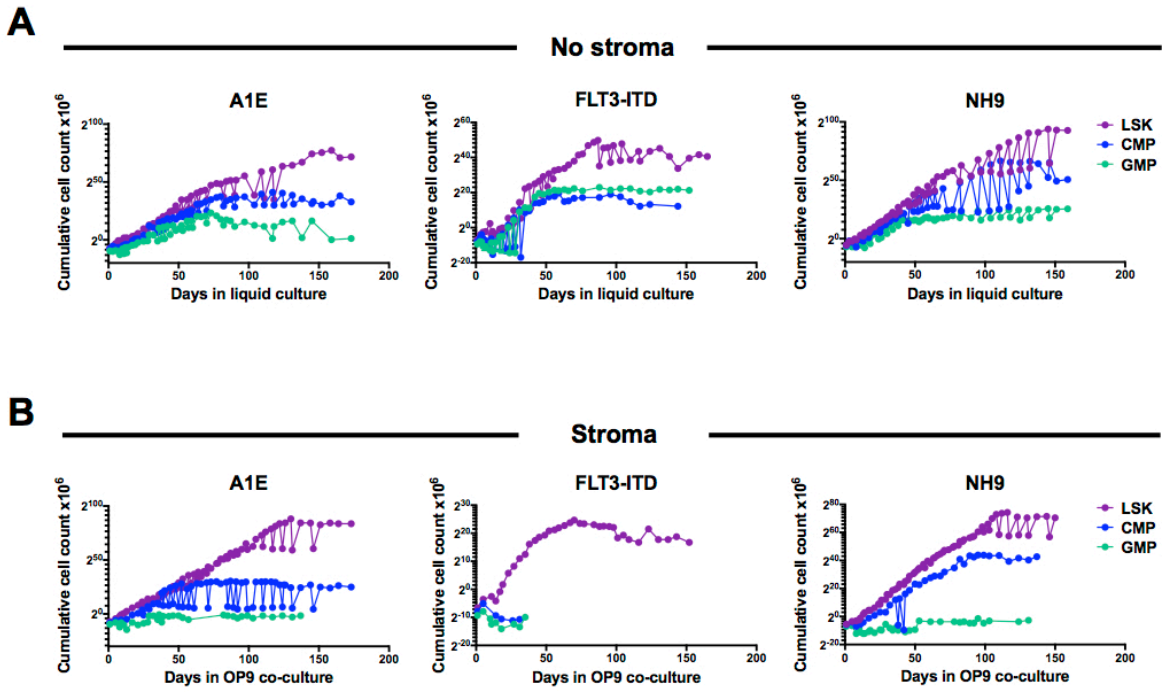

Figure 3.23 AML associated oncogenes transform FL-LSKs, but fail to transform FL-CMP and GMPs *in vitro*

(A) Growth of oncogene transduced FL-LSKs, CMPs and GMPs grown in liquid culture (without stroma).
(B) Growth of oncogene transduced FL-LSKs, CMPs and GMPs grown on stromal OP9 co-culture. Graphs shown log2 mean cumulative cell number normalised to GFP%, n=2 for all groups except A1E grown on OP9 co-culture in which n=3.

3.4 Discussion

To assess age dependent differences in leukaemogenesis, HSPCs (LSK, CMP and GMPs) from mice representing infancy (FL), childhood (3w), young adult (10w) and middle age (>52w) were transduced with NH9 and *in vitro* immortalisation assessed by serial CFC assay. In all age groups, LSKs were readily transformed *in vitro*, evidenced by the presence of multiple colonies at CFC3. At CFC3, there was no difference in colony and cell number, cellular morphology or immunophenotype with cellular age. Therefore, after NH9 mediated transformation, the resulting phenotype of the transformed LSK was the same, irrespective of cellular age. However, we observed a trend towards delayed transformation in FL-LSKs. At CFC1 NH9 transduced FL-LSKs produced multiple small to medium sized colonies. In contrast, post-foetal (3w, 10w and >52w) transduced LSKs produced very large colonies, typical of NH9 expressing cells. (Kroon et al., 2001) This was quantified by calculating the colony and cell count, normalised to age matched MigR1 control. Post-foetal LSKs showed a trend

towards relatively fewer colonies at CFC1. However, as the colonies were large, there was no difference in relative cell number at CFC1. This suggests that while FL-LSKs did transform with NH9, transformation was slower than in post-foetal LSKs.

In both adult BM and FL, the LSK compartment contains the HSC, capable of long term, multi-lineage reconstitution in adult recipients. However, some phenotypic differences exist between BM and FL derived LSKs. FL-LSK contain more long-term repopulating clones (67% of total LSK population) and are highly cycling (40% in cycle based on Hoechst 33342 uptake). In contrast, only 25% of adult LSKs result in long-term repopulation and only 4% are actively in cycle. (Morrison and Weissman, 1994, Morrison et al., 1995) As such, FL-LSKs are more efficient in reconstituting the BM of lethally irradiated recipients than adult LSKs. (Rebel et al., 1996) The difference in the phenotype of FL-LSKs may impart cellular protective properties onto FL-LSK. Cells in active cell cycle upregulate DNA repair mechanisms and this may delay oncogenic insults in the FL-LSK cells. (Beerman et al., 2014)

The foetal properties of increased cycling and more efficient repopulating ability persist until 3w, after which there is an abrupt switch to an adult phenotype of quiescence and relatively less efficient repopulating ability. (Bowie et al., 2007b) In the data presented, 3w LSKs also displayed characteristic NH9 colony morphology at CFC1 (as seen for 10w and >52w), rather than sharing morphological features with FL-LSKs. Therefore, a delay in transformation in 3w-LSK was not observed *in vitro*. This is surprising, as normal 3w-LSKs share phenotypic similarities with FL-LSKs. One hypothesis is that foetal-like characteristics in LSKs may subtly attenuate progressively from FL to 3w of age, to a critical point at which *in vitro* transformation is more permissible in 3w LSKs. While foetal cycling and repopulation ability persist up to 3w of age, B-differentiation potential attenuates within the first week. Both FL and adult (8w) LSKs are able to produce all classes of B-cells in adult recipients post transplantation. FL-LSK from *IL-7Rα*$^{-/-}$ mice can also produce all classes of B-cells in recipient mice, while adult LSKs from *IL-7Rα*$^{-/-}$ mice do not differentiate into B-cells. Therefore, IL-7Rα is dispensable for FL, but not adult B-cell

differentiation. IL-7Rα independent B-cell production is observed in BM from 1w old donors, but after 2w of age, IL-7Rα is essential. (Kikuchi and Kondo, 2006) Therefore, foetal B-cell differentiative properties switch to an adult phenotype between 1 and 2w. Other pathways important for genetic fidelity may attenuate before 3w of age, resulting in 3w-LSKs being more permissible to oncogenic insult. Another hypothesis is that 3w LSKs originate from the BM (as do 10w and >52w LSKs), and the originating microenvironment may also contribute to 3w-LSKs being more permissive to *in vitro* transformation by NH9. This could by further investigated by assessing NH9 mediated transformation by CFC assay at multiple foetal and neonatal stages, for example, in E16.5, E18.5, 1w, and 2w-LSKs and from cells derived from the embryonic BM as well as FL. In addition, transcriptional and proteomic analysis of FL and 3w-LSKs at baseline (before oncogene) and at CFC1 may identify molecular pathways to account for the differences observed.

There are few examples in the literature comparing FL with neonatal and adult transformation *in vitro*. Johnson *et al* investigated the effect of oncogene in perinatal cells by introducing the MA9 fusion into embryonic stem (ES) cells. *MA9*$^{+/-}$ heterozygous mice were obtained by cross breeding chimeric males with WT females. *MA9*$^{+/-}$ mice express MA9 prenatally, and develop AML after a latency of 6m. *In vitro* myeloid potential and self-renewal properties were assessed by serial CFC assay of total FL and 6d neonatal BM. Both FL and 6d BM displayed expanded myeloid potential with an increase in immature colony types and cKit^{+} myeloid cells compared to WT controls. However, significant differences were observed in the self-renewal capacity of FL and 6d BM. FL did not serially replate, while 6d BM serially replated. In addition, assessment of CD11b^{+} myeloid cells by IHC in *MA9*$^{+/-}$ FL showed no expansion of myeloid cells compared to WT FL controls. Conversely, *MA9*$^{+/-}$ 6d BM showed marked expansion of myeloid cells compared to *MA9*$^{+/-}$ FL and WT 6d BM. Therefore, in perinatal *MA9*$^{+/-}$ expressing cells, myeloid expansion *in vivo* and increased self-renewal capacity was only observed postnatally. (Johnson et al., 2003) While the ages and populations investigated do not exactly correspond to the data presented (LSKs and 3w BM was investigated rather than total FL or BM and 6d

old BM) this study shows that FL cells exhibit attenuated oncogenic phenotypes compared to early postnatal cells and is consistent with the data presented.

A striking difference between the ages was that FL-CMP and GMPs did not serially replate while post-foetal committed progenitors did. The ability of FL HSPCs to transform *in vitro* was further investigated using 2 common AML driving oncogenes, A1E and FLT3-ITD in addition to NH9. Regardless of oncogene used, FL-LSKs grew in culture, while FL-CMP and GMPs did not continue to proliferate beyond 75 days, whether cultured in isolation or on stroma. This is not so surprising for FLT3-ITD meditated transformation as adult (10w) murine CMP and GMPs also fail to display self-renewal in vitro after overexpression of FLT3-ITD. (Kvinlaug et al., 2011) However, transduction of NH9 and A1E into adult CMP and GMPs does result in vitro immortalisation, as demonstrated in this chapter and described in Kvinlaug et al. (Kvinlaug et al., 2011) This suggests that foetal transformation may be restricted to the immature LSK compartment. In adult BM, haemopoiesis occurs through a hierarchy of progressively lineage restricted progenitors. Myeloid differentiation occurs via the CMP which gives rise to all myeloerythroid cells. CMPs differentiate into GMPs, which give rise to granulocytes and monocytes, and MEPs, which give rise to megakaryocytes and erythrocytes. CMP, GMP and MEP populations can be isolated based on surface markers expression of CD34 and CD16/32. (Akashi et al., 2000) In all 4 ages investigated, CD34 and CD16/32 expression was used to isolate CMP and GMP populations by FACS (See Section 1.1.2.1 and 2.3.3). However, one could postulate that the CMP and GMP compartment of FL cells may not be defined by the same surface marker expression as adult BM cells. Indeed, the LSK population in FL is largely the same immunophenotypically as it is in adult. However, FL LSKs express CD11b, which is absent on adult LSKs. (Morrison et al., 1995) The characterisation of FL myeloid progenitors has been investigated experimentally by Traver *et al*. FL-CMP, GMP and MEPs were isolated using surface expression of CD34 and CD16/32, (as for the isolation of adult myeloid progenitors). *In vitro* characterisation was assessed by CFC assay for lineage output. FL-CMPs produced all types of myeloid colonies. FL-GMPs only produced GM, granulocyte and macrophage colonies, while MEPs only produced megakaryocyte and erythroid colonies. In addition, FL-CMP cultured on OP9

stromal layer could differentiate into GMP and MEPs (based on surface marker expression and colony production in CFC), while GMPs or MEPs did not give rise to the other myeloid progenitor populations. Therefore, FL-CMP, GMP and MEPs, defined by surface marker expression, showed characteristic lineage output similar to adult progenitors defined by the same method. Furthermore, FL progenitors displayed hierarchical differentiation, with FL-CMPs as the precursor to FL-GMP and MEPs. The *in vivo* reconstitution and differentiation of FL progenitors was also assessed. Transplantation of FL-CMP resulted in donor derived CD11b/GR1$^+$ myelomonocytes and Ter119$^+$ erythroid cells in recipients. Transplantation of FL-GMP transiently reconstituted CD11b$^+$ granulocytes only, while transplantation of FL-MEP transiently reconstituted Ter119$^+$ erythroid cells only. In addition, FL progenitors had a similar transcriptional profile to adult progenitors. For example, the expression of *Cebpa*, a master regulator of granulocytes, was highest in FL-GMPs while *GATA1* and *EpoR* expression, both important in erythrocytosis, was strongly expressed in FL-MEPs. (Traver et al., 2001) CMP, GMP and MEP populations isolated based on immunophenotype show near identical lineage output and expression of lineage associated genes, whether originating from FL or adult BM. This confirms that the definition used in this thesis to isolate CMP and GMPs applies to FL as well as post-foetal age groups. Therefore, the failure of FL-CMP and GMPs to transform *in vitro* is an intrinsic property of FL progenitors. In contrast, beyond the foetal stage, LSK, CMP and GMP populations were transformed by NH9 while in foetal cells transformation capacity is restricted to the LSK.

The self-renewal and proliferative potential of FL progenitors was investigated in competitive reconstitution assays in which 200 HSCs were co-transplanted with 10000 FL-CMP, GMP or MEPs. Interestingly, transplantation of FL progenitors (CMP, GMP or MEP) only resulted in transient reconstitution (up to 3 weeks) in recipients, suggesting that normal FL progenitors have limited or no self-renewal capacity *in vivo*. (Traver et al., 2001) This supports the finding that the failure of FL-CMP and GMP to immortalise in the context of oncogene overexpression, is a lack of self-renewal ability that is intrinsic to FL progenitors. Similar competitive reconstitution studies, transplanting CMP, GMP and MEPs isolated from adult BM also show that reconstitution in recipients is transient, with donor

cells detectable only up to 4w post transplant. Therefore, normal adult myeloid progenitors also show limited self-renewal properties *in vivo*. (Akashi et al., 2000) Therefore, in the absence of oncogene, both FL and adult myeloid progenitors display limited self-renewal properties. However, in the presence of oncogene, post-foetal CMP and GMPs acquire self-renewal properties while FL-CMP and GMPs do not. Hitherto unidentified mechanisms present in FL-CMP and GMPs may prevent oncogene mediated immortalisation. Cell protective programmes may be employed in foetal committed progenitors to protect the developing haemopoietic system from oncogenic insult. To investigate this further, transcriptional and proteomic analysis of FL-LSK, CMP and GMPs before and just after oncogene transduction could identify pathways upregulated in FL committed progenitors in response to oncogenic insult as candidate protective pathways.

Investigation of several AML models have shown that for adult BM (6-8w), the LIC is not restricted to the HSC compartment. In the NH9 model, overexpression in CMP, GMP and MEPs results in *in vitro* immortalisation and *in vivo* AML, while overexpression of A1E in the same progenitor populations results in immortalisation *in vitro* and *in vivo*, but not progression to AML. (Kvinlaug et al., 2011) Similarly, overexpression of MLLr, including MA9 and MLL-ENL in CMP and GMPs also results in *in vitro* immortalisation and AML *in vivo*. (Cozzio et al., 2003, Krivtsov et al., 2013) However, there is a paucity of data investigating the transformability of FL progenitors. The data presented would suggest that for FL HSPCs, only the LSK compartment contains LIC activity, while CMP and GMPs do not. To our knowledge, this is the first time the transformability of FL-CMP and GMP has been investigated.

In transforming populations that acquired self-renewal properties the impact of cellular age on proliferative capacity and lineage output was assessed. For all ages the LSK compartment readily transformed. At each plating (CFC1, CFC2 and CFC3) no difference was observed in absolute colony or cell number, suggesting that transforming LSKs had similar proliferative capacity regardless of cellular age. No difference with age was observed in the colony output at CFC1, but >52w did show higher expression of the immature marker, cKit, suggesting more

stem cell like properties. At CFC2 FL-LSKs produced relatively more granulocyte colonies. However, this was not associated with granulocytic (CD11b and GR1) expression by immunophenotype. At CFC3 >52w-LSKs produced relatively more macrophage colonies but this was not associated with higher monocyte/macrophage (CD11b and F4/80) expression by immunophenotype. Therefore, there is a trend towards skewed lineage output from young (FL) versus adult (>52w) transformed LSKs.

Only post-foetal (3w, 10w and >52w) CMPs transformed *in vitro* with NH9. At CFC1, >52w-CMP exhibited more CD11b expression by flow cytometry compared to 3w-CMPs. However, by CFC2 and CFC3 no difference was observed in colony and cell number, colony and cell morphology or immunophenotype in transformed CMPs. Similarly, only post-foetal (3w, 10w and <52w) GMPs transformed *in vitro* with NH9. However, unlike transformed CMPs, at CFC3 transformed 3w-GMPs exhibited significantly more expression of the granulocyte marker GR1 compared to transformed 10w and <52w-GMPs. Therefore, while all post-foetal GMPs acquired self-renewal properties, 3w-GMPs also displayed some granulocytic differentiation. Furthermore, investigation of transformation kinetics at CFC1 showed that adult GMPs (10w and >52w) were outgrowing MigR1 controls and 3w-GMPs, suggesting faster oncogenic transformation in adult GMPs.

Overall, the data support a trend towards faster *in vitro* transformation of adult (10w and >52w) HSPCs, compared to young (FL and 3w). This suggests that adult HSPCs are more susceptible to leukaemic transformation and would be consistent with the higher incidence of AML in adult versus paediatric populations. (Howlader N, 2014, Cancer Research UK, 2014) In addition, transforming young HSPCs express markers associated with myeloid differentiation, while adult HSPCs express immature markers suggesting more stem cell like properties. The expression of stem cell transcriptional pathways in human leukaemia and solid tumours is associated with adverse clinical outcomes, including inferior OS and chemotherapy refractory disease. (Wong et al., 2008, Gentles et al., 2010, Ng et al., 2016) Assessment of immunophentype in 209 human AML showed that expression of immature markers, CD34 and HLA-DR, was associated with increased RR. In contrast, the expression of the myeloid

markers CD15 and CD33 was associated with continued complete remission. (Webber et al., 2008) Therefore, there is a suggestion that transformed adult HPSCs may result in an aggressive leukaemia that is chemoresistant, while transformed young HSPCs may be more chemosensitive. One method to accentuate these subtle differences in young and adult transformed HSPCs would be to assess transformation in an *in vivo* experiment. This will be addressed in the following chapter. In addition, investigation of sensitivity to chemotherapy agents on young and adult transformed HSPCs (either in an *in vitro* or *in vivo* setting) would functionally test if young transformed cells are chemosensitive and adult transformed cells are chemoresistant.

4 An examination of the transformability of HSPCs of different ages *in vivo*

4.1 Introduction

In the previous chapter, the impact of HSPC age on oncogene mediated transformation was investigated using *in vitro* techniques. LSKs from all ages transformed *in vitro*, as evidenced by their ability to serially replate in methylcellulose. However, the gold standard for the assessment of leukaemogenesis is the ability to generate and transplant leukaemia *in vivo*. This may exaggerate subtle differences in transformation that are not evident from *in vitro* techniques. In this chapter, impact of cellular age on leukaemic transformation *in vivo* will be in investigated.

4.1.1 Experimental *in vivo* models of AML

4.1.1.1 NH9

The NH9 oncogene has been utilised as a model of AML to study leukaemia development. Transgenic and T&T models are established experimental models. (Kroon et al., 2001, Iwasaki et al., 2005, Chung et al., 2006) Transgenic mice expressing *NH9* under the control of the cathepsin G promoter express the oncogene specifically in myeloid cells. Chimeric mice develop an MPN with subsequent AML at an incidence of 10% at 12 m. The long latency to disease suggests further genetic mutations are required for leukaemia development. Transferring the *NH9* transgene into the *BXH2* genetic background and performing retroviral insertion mutagenesis analysis identified *Meis1* as the most frequent co-operating gene. Other co-operating genes include *Dnalc4*, *Fcgr2b*, *Fcrl*, and *Con1*. (Iwasaki et al., 2005)

Retroviral T&T of NH9 expressing total adult murine BM into primary recipients initially results in myeloid differentiation but little B and T-lymphoid differentiation in PB, BM and spleen at 2m. BM and splenic cells give rise to myeloid CFCs that can serially replate in methylcellulose. Thereafter, 100% of primary recipients develop an MPN characterised by neutrophilia, monocytosis and splenomegaly. After a median latency of 9m from transplantation, there is

transformation to AML, characterised by infiltration of immature blasts in the BM, PB, spleen, liver, thymus, lungs and kidney, with an incidence of 80%. AML blasts are predominantly positive for the myeloid antigen CD11b. BMT of AML blasts from primary animals into secondary recipients results in AML with a much shorter latency of 1-2m. Viral integration studies show that NH9 induced AML is a monoclonal disease. Interestingly, overexpression of *Meis1* with NH9 leads to accelerated AML development. (Kroon et al., 2001) In another study co-expression of NH9 with BCR-ABL also results in faster AML development with a latency of only 21d. (Mayotte et al., 2002) Similar to the transgenic model, a shorter latency to disease with the overexpression of additional oncogenes suggests that NH9 requires additional mutations for leukaemia development. T&T of NH9 expressing purified murine progenitor populations such as CMP, GMP or MEPs all result in AML in primary recipients, with an incidence of 40-50% at 1 year, showing committed progenitors can act as the LIC for NH9 AML. (Kvinlaug et al., 2011) Interestingly, T&T of NH9 expressing human $CD34^+$ CB into NOD/SCID primary recipients does not lead to leukaemia development. However, NH9 expressing cells display a proliferative advantage, with a 3.3 fold increase in donor cells at 5-7w relative to initial cell input, compared to a 1.9 fold increase in EV controls. In addition, NH9 results in extramedullary engraftment of $CD14^+$ myelomonocytic cells in the liver and spleen, which is not observed in EV controls. While leukaemia does not develop (with no increase in organ size nor raised WCC), uncontrolled proliferation and extramedullary infiltration of mature myeloid cells is characteristic of MPNs. (Chung et al., 2006) Thus, overexpression of NH9 results in increased proliferation and myeloid lineage output. Although the latency to disease and identification of co-operating genes suggests secondary oncogenic hits are required for AML development, overexpression of NH9 alone leads to AML with up to 80% penetrance.

4.1.1.2 A1E

As discussed in Section 1.3.4.2, A1E is one of commonest fusion oncogenes observed in human AML, observed in 15% of paediatric and 8% of adult AML. (Chaudhury et al., 2015) As such, many experimental models of A1E disease exist. Most transgenic models of A1E result in increased proliferation of haemopoietic progenitors but not leukaemia, suggesting that additional

mutations are required for AML development. (Buchholz et al., 2000, Rhoades et al., 2000) Indeed, transgenic *A1E* models do require further mutagenic events for overt leukaemia, such as injection with the alkylating agent *N*-ethyl-*N*-nitrosurea to induce mutations. (Yuan et al., 2001, Higuchi et al., 2002) Cabezas-Wallscheid *et al* describe a conditional doxycycline inducible model for A1E in which mosaic *A1E* expression is induced specifically in haemopoietic cells. BMT of *A1E* expressing BM into primary recipients resulted in an indolent MPN with a long latency of 16-18m, characterised by high WCC, circulating blasts and infiltration into the spleen, thymus, liver, lungs and kidney. However, while there was evidence of leukaemic cells, mice survived despite prolonged exposure to doxycycline. (Cabezas-Wallscheid et al., 2013) Retroviral expression of A1E in murine total BM and LSKs results in HSC and myeloid expansion but does not lead to AML in BMT and T&T models. (Schwieger et al., 2002, de Guzman et al., 2002) A1E expression in progenitor populations (CMP, GMP and MEPs) does not result in long term engraftment in primary recipients, suggesting that A1E cannot imbue self-renewal properties to committed progenitors. (Kvinlaug et al., 2011) A1E expressing human $CD34^+$ cells (from CB or cytokine mobilised adult PB progenitors) expand *in vitro* but transplanted into NOD/SCID mice do not cause leukaemia. (Mulloy et al., 2003) Leukaemia development requires either transduction of abnormal A1E variants that result in expression of a truncated fusion protein (Yan et al., 2004, Yan et al., 2006), additional genetic factors, such as transduction into recipients lacking the tumour suppressor IFN regulatory factor (Schwieger et al., 2002) or co-expression of oncogenic drivers such as the activated receptor tyrosine kinase, TEL/PDGFBR (Grisolano et al., 2003). Therefore, although A1E is the product of one of the commonest AML subtypes, experimental murine models of AML utilising the A1E oncogene have limitations, as overexpression of A1E alone does not result in AML development.

4.1.1.3 FLT3-ITD

As discussed in Section 1.3.4.6, activating mutations of the *FLT3* receptor are observed in human disease and are an adverse prognostic factor, associated with an increase in relapse rates. The most common mutation is *FLT3-ITD* in which internal tandem duplications of the gene results in a constitutively activated receptor. Transgenic models of *FLT3-ITD* result in MPN. (Lee et al., 2007, Lee et

al., 2005, Li et al., 2008) Lee *et al* describe a transgenic model in which *FLT3-ITD* is conditionally expressed in haemopoietic cells under the control of the *Vav* haemopoietic promoter. With a latency of 6-12m, mice develop a non-lethal MPN reminiscent of essential thrombocythaemia, characterised by splenomegaly, thrombocytosis and megakaryocyte hyperplasia. (Lee et al., 2005) Knockin of the human *ITD* mutation into the endogenous *Flt3* locus results in a fully penetrant MPN in chimeric mice characterised by neutrophilia, monocytosis and infiltration of mature myeloid cells in the BM and spleen. BMT of BM from chimeric donors results in MPN in secondary recipients with a latency of 4m. (Lee et al., 2007) In an inducible model, administration of pIC induces *Mx1-Cre* mediated expression of *FLT3-ITD*, resulting in MPN with a latency of 6-12m, characterised by high WCC, increased BM granulocyte and monocytes and splenomegaly. BMT of total BM from MPN affected chimeric mice causes MPN in primary recipients with a latency of 12m. (Li et al., 2008) Retroviral expression of FLT3-ITD in the BM from 5FU treated donors (as a source of HSPCs) results in a lethal MPN in primary recipients with a latency of 3m but not in secondary recipients. Similar to transgenic models, there is no progression to AML. (Kelly et al., 2002) The absence of AML suggests that while overexpression of *FLT3-ITD* can result in increased proliferation, in isolation it is not able to drive acute leukaemia. Deletions of *RUNX1* or *DNMT3A* can cooperate with *FLT3-ITD* overexpression to cause a rapidly fatal, fully penetrant AML with a latency of 5 and 7w, respectively. (Mead et al., 2013, Meyer et al., 2016) Interestingly, progenitor cells (CMP, GMP and MEPs) transduced with FLT3-ITD fail to transform *in vitro* and do not cause leukaemia *in vivo* suggesting that, unlike NH9, the LIC is not within the CMP, GMP or MEP compartment. (Kvinlaug et al., 2011) Therefore, models of FLT3-ITD can cause MPN *in vivo*, but do not recapitulate human AML and as such, similar to A1E models, have limitations as an experimental model of AML.

4.1.1.4 MLLr

As discussed in Section 1.3.4.4 MLLr are one of the commonest chromosomal abnormalities found in acute leukaemia. The partner gene AF9 resulting in the fusion oncogene MA9 is most frequently see in AML, accounting for 29% of MLLr cases across all age groups. (Meyer et al., 2013) Knockin of the human *AF9*

sequence to the *Mll* locus in murine ES cells leads to *MA9* expression under the control of the *Mll* promoter. Injection of ES clones into blastocytes and subsequent transfer into pregnant female recipients results in chimeric mice in which MA9 is expressed at physiological levels from the prenatal period and throughout life. Chimeric mice show myeloid expansion and transformation to AML with a latency of 4-6m. (Corral et al., 1996) BMT of LSKs and CLPs from chimeric donors results in AML in 90% of primary recipients, with a latency of 6m. BMT of CMP results in AML in only 40% of recipients while BMT of GMPs does not results in AML, suggesting that for this MA9 model, the LIC is not found in the GMP compartment and is present at low frequency in the CMP compartment. (Chen et al., 2008) Retroviral overexpression of MA9 in LSK and GMPs results in a rapid AML in primary recipients in T&T models. However, with equal donor cell doses, latency to disease is faster in LSKs compared and GMPs (1.5m and 3m, respectively). (Krivtsov et al., 2013) The leukaemic potential of MA9 expressing cells can be augmented by pre-transplant expansion in methylcellulose. Retroviral expression of MA9 immortalises cKit$^+$ HSPCs, evidenced by serial replating in methylcellulose and growth in liquid culture. Transplantation of *in vitro* immortalised HSPCs results in AML in primary recipients with a latency of 2-3m that is phenotypically similar to recipients transplanted with freshly transduced HSPCs. (Somervaille and Cleary, 2006) This useful feature of MA9 AML models has been utilised to increase LIC number *in vitro* before transplantation into recipient mice.

4.1.2 Experimental models of ageing

4.1.2.1 Models of normal ageing

As discussed in the Chapters 1 and 3, HSC number, phenotype, function and gene profile differ as the haemopoietic system ages. Three stages of haemopoietic ageing have been described. At the foetal and neonatal stage, the haemopoietic system is developing and as such foetal and young HSCs (in mice, up to 3w old) are highly proliferative and display myeloerythoid biased lineage output. Adult HSCs in contrast (in mice >8w old), are required to maintain the established haemopoietic system. As such they are quiescent, replicating rarely in order to maintain genomic integrity and display balanced lineage output. (Rebel et al.,

1996, Bowie et al., 2007b) The aged haemopoietic system (in mice, >24m) is associated with an accumulation of DNA damage, myeloid lineage skewing and clonal haemopoiesis. (Rossi et al., 2007a, Pang et al., 2011, Jaiswal et al., 2014, Xie et al., 2014) Aged HSCs show increased self-renewal and proliferation as they increase in number to compensate for functional decline. (Morrison et al., 1996b, Sudo et al., 2000) *In vivo* models have been used to investigate the characteristics of HSCs at different ontological stages and elucidate mechanisms of ageing.

Experimental models have attempted to characterise the phenotype of foetal and neonatal HSCs in comparison with adult HSCs. BMT of normal HSCs from FL and BM from E14.5d up to 3w old results in superior repopulating ability and myeloid biased engraftment in recipients, compared to adult HSCs. After the age of 3w, transplanted HSCs behave similar to adult HSCs (defined as >8w) with fewer repopulating units per recipient and balanced myelolymphoid output. This is associated with a change in gene expression profile. FL and neonatal HSCs have higher expression of cell cycle and self-renewal regulating genes (e.g. *Ccnd2*, *Ikaros*, *Mef*, *Rae-28*) in keeping with enhanced proliferation in order to populate the developing haemopoietic system. In contrast, adult HSCs have higher expression of genes associated with HSC maintenance (e.g. *Atm*, *Ezh2*, *Gata2*, *Mel-18*) in keeping with their role in maintaining the established haemopoietic system. (Bowie et al., 2007b) Several mechanisms to explain this switch from a highly cycling foetal HSC to quiescent adult HSC phenotype have been postulated and will be discussed in detail in Section 1.2.3.4, 1.2.3.4 and 5.1.2.2. In brief, developmentally determined changes in the expression of *Cebpa*, *Sox17* and *Lin28b*/*Hmga2* have been implicated in a foetal to adult switch in HSC phenotype. (Ye et al., 2013, Kim et al., 2007, Copley et al., 2013) C/EBPα is a transcription factor essential for granulopoiesis but in HSCs is a negative regulator of cell cycle and promotes quiescence. There is a sharp rise in *Cebpa* expression in murine HSCs from 2w to 4w, coinciding with reduced proliferation. (Ye et al., 2013) In contrast, *Sox17* is expressed in 86% of LT-HSCs in foetal and 2w old mice and is essential for their maintenance. However, by 4w only 50% of LT-HSCs express *Sox17*, while expression is undetectable in adult 8w old LT-HSCs. (Kim et al., 2007) *Lin28b* exhibits high expression in FL LSKs and

FL HSCs and regulates self-renewal in foetal cells, via inhibition of the *Let-7* family of microRNAs and thereby high levels of *Hmga2*, resulting in enhanced self-renewal. After the age of 3w, *Lin28b* and thereby *Hmga2* expression falls dramatically resulting in reduced self-renewal and increased quiescence. (Copley et al., 2013) In all the mechanisms of ageing described, the mechanisms by which gene expression changes between foetal and adult HSCs are largely unknown.

Experimental models have also investigated changes in phenotype between young adult HSCs (in mice, 2-4m) and old adult HSCs (in mice >24m). (See Section 1.2.5) As adult HSCs age, absolute numbers of LSKs and LT-HSC increases resulting in a 2-10 fold increase in the number of immunophenotypic HSCs. (Morrison et al., 1996b, de Haan and Van Zant, 1999) 4m post BMT of total BM from old (24m) mice results in a greater number of donor derived LT-HSCs in recipients aged 2-3m, compared to recipients transplanted with total BM from young 2-3m old mice. Therefore the expanded LT-HSC population seen in aged mice retain self-renewal and repopulating ability. (Rossi et al., 2005) Despite an increase in total LT-HSC number, compared to young adult (2-3m) donors, engraftment and donor derived B-lymphoid reconstitution post BMT is significantly reduced from old HSCs with a myeloid bias and increased GMP population. (Morrison et al., 1996b, Rossi et al., 2005) Impairment of the B-lymphoid reconstitution is not observed when young HSC are transplanted into old recipients, suggesting that the attenuated B-lymphoid potential observed in old HSCs is cell intrinsic and independent of the BM microenvironment. (Rossi et al., 2005) Furthermore, old HSCs are highly cycling, unlike their younger counterparts (from 2-3m) that are largely quiescent. (Morrison et al., 1996b) Thus, aged stem cells have exaggerated self-renewal and cycling, in order to compensate in number for a functionally impaired population.

A phenomenon of ageing is the acquisition of DNA damage. In murine models of haemopoietic ageing there is an accumulation of DNA damage with increasing age, as evidenced by an increase in γH2AX staining and increased alkaline comet tail moments, both markers of DNA double strand breaks. (Rossi et al., 2007a, Beerman et al., 2014) Additionally, the stem cell repopulating ability in aged

HSCs from different murine models of impaired DNA repair (including nucleotide excision repair (NER), NHEJ and telomerase maintenance) is significantly diminished compared to WT controls, suggesting that the accumulation of DNA damage contributes to the functional decline observed in aged HSCs. (Rossi et al., 2007a) Likewise, at baseline, human $CD34^+$ HSCs and $CD34^-$ progenitors from CB have less γH2AX staining compared to adult BM up to the age of 50y, which in turn have less γH2AX staining than from adults older than 50y. After inducing further DNA damage with ionising radiation, $CD34^+$ from CB are able to repair their DNA resulting in fewer γH2AX foci compared to adult (either <50y or >50y) after 24h. (Rube et al., 2011) Thus, not only is there an accumulation of DNA damage with increasing age, DNA repair mechanisms may be less efficient. However, models of impaired DNA repair are not associated with a change in HSC number, suggesting that DNA damage alone does not cause the aged HSC phenotype. (Rossi et al., 2007a) In addition to gross strand breaks, aged HSCs acquire mutations in epigenetic modifiers such as *DNMT3A*, *TET2* and *IDH1/2*, which can alter the epigenetic landscape and drive clonal haemopoiesis, a recognised precursor to AML development. (Busque et al., 2012, Xie et al., 2014, Genovese et al., 2014, Jaiswal et al., 2014)

The transcriptional landscape of different aged HSCs reflects the change in their phenotype. Compared to FL HSCs, young adult (3-4m) and old adult (23-24m) HSCs show downregulation of DDR and repair genes. (Beerman et al., 2014) Compared to young adult HSCs, old HSCs have increased expression of genes involved in cell signalling and self-renewal, myeloid specification and downregulation of genes involved in lymphoid determination. Many of these genes are implicated in the development of leukaemia. (Rossi et al., 2005) Thus, adult HSCs have phenotypic and molecular features that may render them more susceptible to oncogenic mutation.

4.1.2.2 Age and leukaemia models

We hypothesise that intrinsic characteristics of HSCs defined by cellular age persist when a cell undergoes leukaemic transformation. Therefore, the same oncogenic insult can result in different disease biology in young and old HSCs. Furthermore, this would imply that paediatric and adult leukaemia have

differences in cell biology due to the oncogenic insult occurring in a young or adult HSC. This has been explored experimentally in two AML models using MA9. The first utilised the knockin mouse model described in Section 4.1.1.4 in which *MA9* is expressed under the control of the *Mll* promoter. Transfer of blastocytes into female recipients results in chimeric mice that express MA9 *in utero* and after birth, with the development of AML after 6m. (Corral et al., 1996) BMT of HSCs from FL chimeras at E14.5 into WT primary recipients resulted in a longer latency to leukaemia compared to BMT of HSCs from 8w old adult chimeras (latency to disease 12m and 6m, respectively). Lineage assessment by IHC showed that FL HSCs could develop either MPO positive myeloid or B220 positive lymphoid leukaemia whereas only myeloid leukaemia developed from adult HSCs. This suggests that FL cells are more resistant to oncogenic transformation and retain multilineage potential. However, the longer latency to disease observed with foetal cells in this model may be due to the duration of oncogene mediated cellular modification rather than age of transplanted cell per se, as FL donor cells had less exposure to the oncogene prior to BMT than adult donor HSCs. (Chen et al., 2011) In a T&T model, human $CD34^+$ cells from CB or adult BM lentivirally transduced with MA9 was investigated by transplantation into NOD/SCID or NSG recipients. All mice transplanted with CB expressing MA9 developed a fatal leukaemia. The majority of CB recipients developed ALL, but a proportion developed AML or MPAL with expression of both myeloid and lymphoid markers by flow cytometry. In contrast, transplantation of adult BM expressing MA9 resulted in myeloid biased engraftment in recipient mice, without progression to leukaemia. GSEA of CB derived ALL and AML showed an enrichment of embryonic transcriptional signatures, which were not expressed in adult BM derived engraftment, suggesting that after oncogenic insult, CB retains a transcriptional profiles pertaining to its embryonic origin. (Horton et al., 2013)

4.1.3 The role of the BM microenvironment in leukaemogenesis

In the Section 1.4, the role of the BM microenvironment in normal haemopoiesis and the importance of the BM microenvironment in leukaemogenesis is described. Similar to normal HSCs, LSCs reside in specialised niches within the bone marrow. (Nilsson et al., 2001, Colmone et al., 2008) Hijacking of the microenvironment, often at the expense of normal HSPCs, can protect LSCs from

chemotherapy and result in relapse. (Colmone et al., 2008, Civini et al., 2013) The localisation of normal and leukaemia cells has been investigated in *in vivo* mouse models using real time *in vivo* microscopy imaging. (Sipkins et al., 2005, Colmone et al., 2008) Following transplantation into SCID mice, ALL cell lines home to and engraft in specialised areas of the perivascular niche that express the adhesion molecule E-cadherin and chemoattractant CXCL12 (also known as SDF-1). Normal murine HSPCs also home to the same perivascular niche. (Sipkins et al., 2005)

To assess homing in the normal and leukaemic microenvironment, normal human $CD34^+$ donor cells were transplanted into normal WT recipient mice or SCID mice that had been engrafted with the Nalm-6 ALL human cell line. In a normal microenvironment, $CD34^+$ cells initially homed to the CXCL12 expressing perivascular niche with later engraftment in the perivascular, osteoblastic and vascular niche. In the leukaemic microenvironment, Nalm-6 leukaemic cells occupied the sites of normal homing. Therefore, $CD34^+$ cells homed to atypical sites lateral to the specialised perivascular niche. Interestingly, ALL cells downregulated the expression of CXCL12 and the authors hypothesise that reduced CXCL12 expression prevented the homing of normal $CD34^+$ cells to these sites. To determine if leukaemic cells could disrupt the engraftment of normal $CD34^+$ cells, Nalm-6 cells were transplanted into recipients following engraftment with normal $CD34^+$ cells. After 1 month, normal $CD34^+$ cells were found in leukaemic niches. Furthermore, fewer $CD34^+$ cells were recovered from leukaemic mice compared to control, suggesting that leukaemic cells could localise to sites normally occupied by normal HSCs, but also make it less sustainable for normal HSCs. (Colmone et al., 2008) The BM microenvironment can also determine leukaemic lineage. Retroviral expression of MA9 in human $CD34^+$ CB can result in myeloid, lymphoid or mixed phenotype disease when transplanted into NOD/SCID or NOD/SCID-ß2M null mice. However, transplantation into transgenic NOD/SCID mice that express human SCF, GM-CSF, and IL3 results in AML, in all recipients, irrespective of pre-transplant expansion in myeloid or lymphoid permissive conditions. (Wei et al., 2008) Not only do microenvironmental cues aid leukaemic development and propagation, there is a growing body of evidence that leukaemia cells themselves may modify the

microenvironment, making it more permissive to leukaemia maintenance rather than supporting normal HSCs. Human AML derived MSCs exhibit disordered fibroid morphology and decreased osteogenic differentiation. Normal $CD34^+$ cells co-cultured on abnormal AML derived MSCs exhibit alteration in the expression of haemopoiesis regulating factors, including downregulation of KIT and upregulation of the Notch ligand, *JAG1*. This is accompanied by a 5-fold reduced self-renewal capacity (as evidenced by reduced LTC-IC frequency) compared to $CD34^+$ cells co-cultured on normal MSCs. Interestingly, culture of normal MSCs in conditioned media harvested from AML cell lines also results in morphological abnormalities observed in AML derived MSCs. (Geyh et al., 2016) With growing understanding about the relationship between leukaemia and the microenvironment, groups are investigating pharmacological targeting of the microenvironment to eradicate leukaemia stem cells.

4.2 Aims

Studies assessing normal stem cell function *in vivo* have highlighted differences with age. Foetal HSCs having greater proliferative potential than young adult HSCs and are more efficient at repopulating the BM compartment in transplantation studies, compared to adult HSCs. *In vivo* studies of ageing and leukaemic transformation using the MLLr model suggest that age of the transforming cell may impact leukaemic susceptibility. In addition, foetal HSCs retain both myeloid and lymphoid potential while adult HSCs are myeloid restricted. Results from the previous chapter showed that foetal progenitors did not transform *in vitro*. While LSKs from all ages did transform *in vitro* there was a trend towards delayed transformation in foetal LSKs. To further investigate the transformation capacity of different aged HSPCs, *in vivo* development of leukaemia of HSPCs transformed *in vitro* by NH9 was assessed. Specifically:

i) Using the NH9 T&T model for AML, determine the impact of cellular age on *in vivo* leukaemia development of HSPC populations (LSK, CMP, GMP) from FL, 3w, 10w and >52w aged donors, by assessing latency to disease, incidence and leukaemic burden.

ii) Using the NH9 T&T model for AML, determine the impact of cellular age on lineage output of *in vivo* generated leukaemia from HSPCs (LSK, CMP and GMP) from FL, 3w, 10w and >52w aged donors.

iii) Using the NH9 T&T model for AML, determine the homing of young and adult pre-leukaemic donor cells to BM.

4.3 Results

4.3.1 NH9 transduced CMPs and GMPs from any age fail to transform *in vivo*

To investigate the impact of cellular age on leukaemic transformability *in vivo*, up to $1x10^6$ NH9 transduced LSK, CMP and GMPs from CFC2 were transplanted into sub-lethally irradiated WT adult (6-8w) C57Bl/6 recipients. Mice were monitored for engraftment by measurement of the percentage of GFP^+ cells in PB by flow cytometry. Long-term engraftment was determined by the presence of GFP^+ cells in PB at 16w post transplant. (See Section 2.4.2) Regardless of age, CMP and GMPs did not result in long-term engraftment. CMPs from 3w and >52w donors did exhibit short-term engraftment up to 8w post transplant and CMPs from 10w donors showed evidence of low level GFP^+ cells in PB at 18w. However, FL-CMPs did not exhibit any discernable engraftment. Only transplantation of 3w and 10w GMPs was performed. Neither GMP groups exhibited engraftment at any time point. (Figure 4.1A) The CMP and GMP recipients were therefore culled after 16 weeks. Assessment of the bone marrow also showed no GFP^+ cells. (Figure 4.1B) The exception was the 10w CMP group that showed little GFP^+ cells in PB, but showed evidence of GFP^+ cells in the BM. (Figure 4.1) However, in general, NH9 transduced CMPs and GMPs harvested from methylcellulose did not engraft *in vivo*. CMPs from 3w, 10w and >52w did exhibit short-term engraftment, but FL-CMPs and GMPs from 3w and 10w donors did not engraft at all.

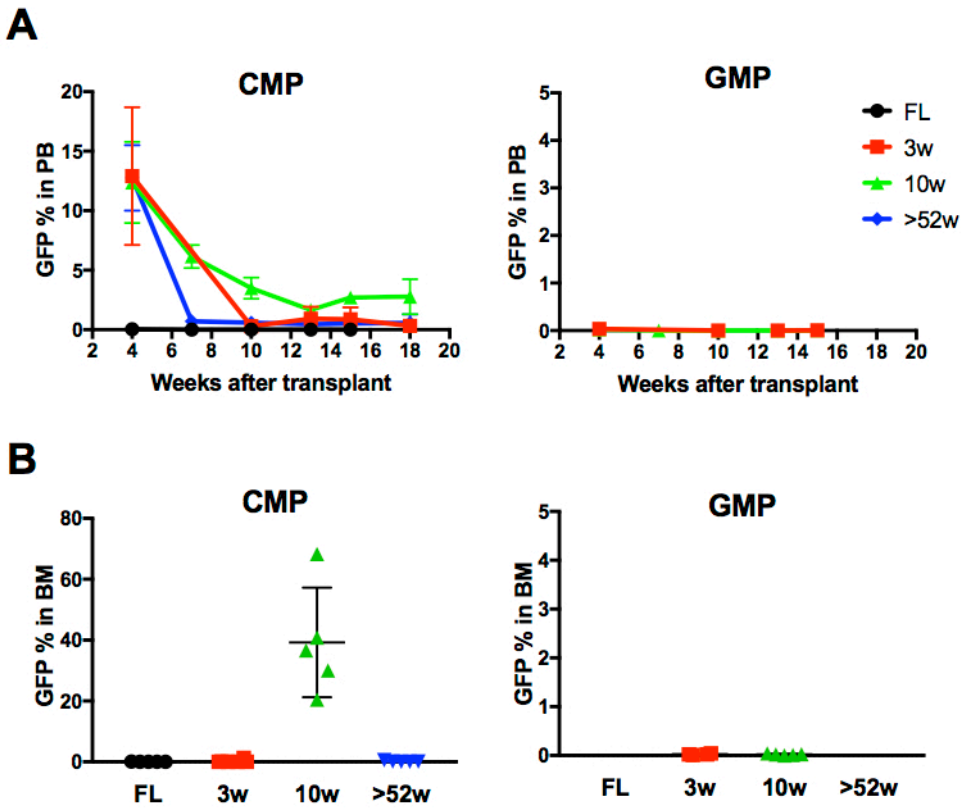

Figure 4.1 NH9 expressing CMP and GMPs do not result in leukaemia *in vivo*

(A) Graph of sequential PB monitoring for donor cell engraftment by GFP% in recipients transplanted with CMP (left) and GMP (right). Graphs depict mean +/-SD.
(B) Graph of GFP% in BM 16w from recipients transplanted with CMP (left) and GMP (right). Graphs depict individual values and mean +/-SD.
$1x10^5$ FL CMP were transplanted, for all other groups $1x10^6$ cells were transplanted. FL-GMP did not replate to CFC2 and >52w GMP cells at CFC2 were lost pre-transplant so were not performed. N=5 for all groups, except 3w-CMP n=6 and 3w-GMP n=4.

4.3.2 Young LSKs are less susceptible to leukaemia *in vivo* compared to adult LSKs, as evidenced by longer latency and reduced penetrance

NH9 transduced LSKs from all ages resulted in early engraftment with presence of GFP^+ cells in PB at 16w with no significant difference across the 4 age groups. (Figure 4.2)

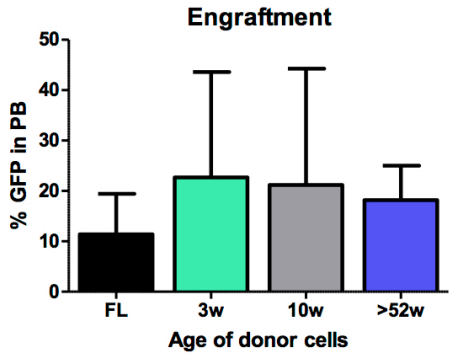

Figure 4.2 Engraftment of GFP+ cells is similar across donor age groups transplanted with NH9 expressing LSKs

Percentage of GPF^{+} cells in PB at 16w as a measure of long term engraftment. Graph depicts mean +SD from 2 independent experiments, n=10 for FL, 3w and >52w, n=5 for 10w. Significance determined by 1-way ANOVA and Bonferroni post-test (p=0.44).

Recipients were monitored for clinical signs of leukaemia and sacrificed on leukaemia development or after 12m if no leukaemia developed. The overall median latency to donor derived leukaemia in the whole experiment was 320d. However, there was a clear difference in latency to disease with age. NH9 transduced donor LSKs from the FL and 3w groups had a significantly longer latency to disease compared to LSKs from the 10w and >52w groups. Pooling the results into young (FL and 3w) and adult (10w and >52w) showed an almost 100 day increase in median survival (MS) in the young group compared to adult (MS 315 days vs 245 days, respectively). (Figure 4.3) Furthermore, while 10w and >52w transduced LSK donors generated leukaemia in all recipients (100% penetrance), FL and 3w donors generated leukaemia in only 50-75% of recipients. The remainder survived to the end of the experiment or died of non-donor cell causes such as irradiation related thymoma. Table 4.1 shows the outcome of each recipient. Pooling the data into young and adult groups revealed that young LSKs had a significantly lower penetrance of leukaemia compared to 100% penetrance in adult LSKs. (Figure 4.4) As engraftment at 16w was similar across the age groups, engraftment efficiency cannot account for differences observed. Therefore, the longer latency to disease and lower penetrance indicate that young LSKs are less susceptible to leukaemic transformation. This suggests the presence of protective mechanisms in young cells that delays or prevents leukaemia, or pro-leukaemic mechanisms in adult cells that are required for leukaemogenesis.

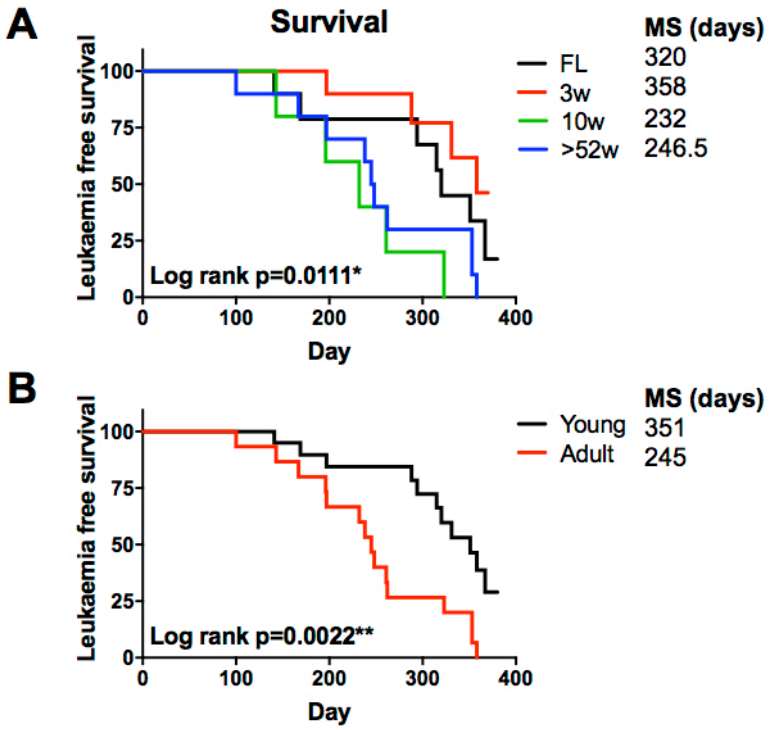

Figure 4.3 Young LSKs have a longer latency to leukaemia compared to adult LSKs

(A) Kaplan-Meier survival curve of recipients transplanted with NH9 transduced LSKs from CFC2 showing results from 4 age groups. FL n=10, 3w n=10, 10w n=5, >52w n=10.
(B) Kaplan-Meier survival curve of recipients pooled into young (FL and 3w) and adult (10w and >52w). Young n=20, adult n=15.
Recipients censored at death. Results from 2 independent experiments. Significance determined by overall log rank, *p<0.05 **p<0.01. MS=median survival.

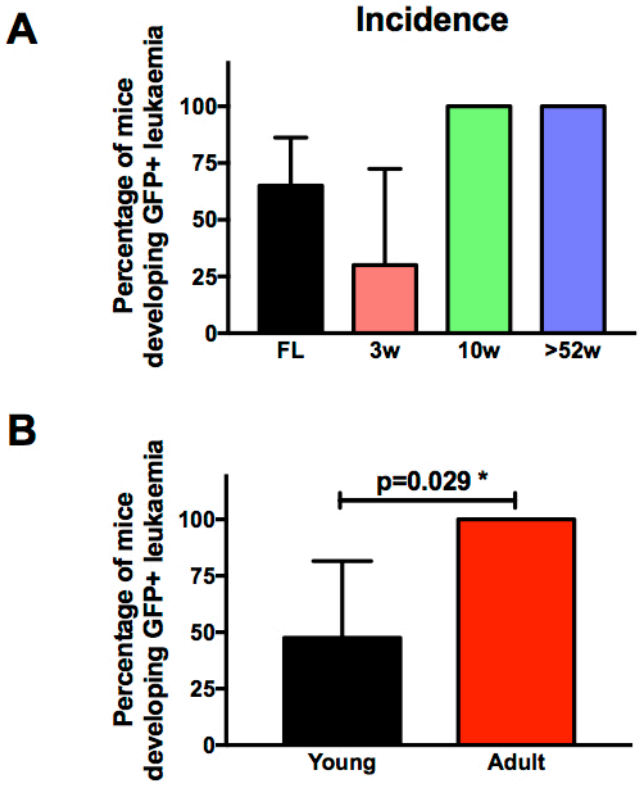

Figure 4.4 Young LSKs have lower incidence of leukaemia

(A) Graph of incidence of all donor derived leukaemia in recipients transplanted with NH9 transduced LSKs from CFC2 showing results from 4 age groups. FL n=10, 3w n=10, 10w n=5, >52w n=10.
(B) Graph of incidence of all donor derived leukaemia showing data pooled into young (FL and 3w) and adult (10w and >52w). Young n=20, adult n=15.
Graphs depict mean +SD from 2 independent experiments. For 4 way comparisons, significance determined by 1-way ANOVA and Bonferroni post-test. For pairwise comparisons, significance determined by Student's t-test, *$p<0.05$.

Table 4.1 Summary of outcomes from LSK transplantation

Table of outcome for each recipient and lineage characteristics determined by flow cytometry and IHC. Donor derived AML highlighted in grey, ALL in blue and MPAL in red.
IHC staining for the lineage markers in neoplastic cells is reported according to the following semi-quantitative grading system:
- = neoplastic cells are negative for the marker
+ = up to 20% of neoplastic cells positive for the marker
++ = 20-40% of neoplastic cells positive for the marker
+++ = 40-60% of neoplastic cells positive for the marker
++++ = >60% of neoplastic cells positive for the marker

Age	Flow (of GFP^+ cells)		IHC		Disease
	Myeloid	Lymphoid	MPO	CD3	
FL	n/a	n/a	n/a	n/a	AML
FL	Pos	Neg	+	-	AML
FL	Pos	Neg	n/a	n/a	AML
FL	Neg	Pos CD19	-	++++	ALL
FL	Pos	Neg	++	++/+++	MPAL
FL	Pos	Neg	+/++	++	MPAL
FL	Pos (low)	Neg	++	+++	MPAL
FL	n/a	n/a	n/a	n/a	Non donor thymoma
FL	n/a	n/a	n/a	n/a	Non donor leukaemia
FL	n/a	n/a	n/a	n/a	Lost engraftment
3w	Pos	B220 (low)	++++	-	AML
3w	Pos	Neg	++++	-	AML
3w	Pos (low)	B220	-	++++	ALL
3w	Pos	B220 (low)	++++	++/+++	MPAL
3w	Pos	Neg	n/a	n/a	End of experiment
3w	Pos	Neg	n/a	n/a	End of experiment
3w	Pos	B220 (low)	n/a	n/a	End of experiment
3w	n/a	n/a	n/a	n/a	Non donor thymoma
3w	n/a	n/a	n/a	n/a	Non donor leukaemia
3w	n/a	n/a	n/a	n/a	Lost engraftment
10w	Pos	Neg	++++	-	AML
10w	Pos	Neg	++/+++	-	AML
10w	Pos	Neg	++++	-	AML
10w	Pos	Neg	++/+++	-/+	AML
10w	Pos	Neg	++++	-	AML
>52w	Pos	Neg	++	-	AML
>52w	Pos	Neg	+++	-	AML
>52w	Pos	Neg	++	-	AML
>52w	Pos	Neg	n/a	n/a	AML
>52w	Pos	Neg	n/a	n/a	AML
>52w	Pos	Neg	++	-	AML
>52w	Pos	Neg	n/a	n/a	AML (+thymoma)
>52w	Pos	Neg	+++	-	AML
>52w	Pos	Neg	++	+	AML
>52w	Pos	Neg	n/a	n/a	AML (+thymoma)

4.3.3 NH9 transduced LSKs result in leukaemia *in vivo* with no age related difference in leukaemic phenotype

The characteristics of leukaemia derived from NH9 transduced LSKs were investigated to assess if the age of the transforming cells impacted leukaemia phenotype. In all age groups, leukaemia development was indicated by clinical deterioration including reduced movement, hunched posture, piloerection, weight loss and rapid breathing. This was associated with an increase in GFP^+ and total WCC in PB. (Figure 4.5) On vivisection, affected recipients had pale bones, splenomegaly and hepatomegaly. (Figure 4.6A) The range of measured spleen weights in all recipients that succumbed to donor derived leukaemia are shown in Table 4.2. Morphological assessment of PB, BM and spleen showed large blasts with high nuclear to cytoplasmic ratio, open chromatin and nucleolus. Most affected mice also displayed myeloid differentiation to terminally differentiated neutrophils identified as granulated cells with condensed chromatin and a segmented nucleus. (Figure 4.6B) All mice had leukocytosis, anaemia and thrombocytopenia with no difference in these parameters between mice transplanted with FL, 3w, 10 or >52w LSKs. (Figure 4.6C) Similarly, there was no age related difference in leukaemic burden as assessed by marrow and splenic cellularity and splenic weight. (Figure 4.6D)

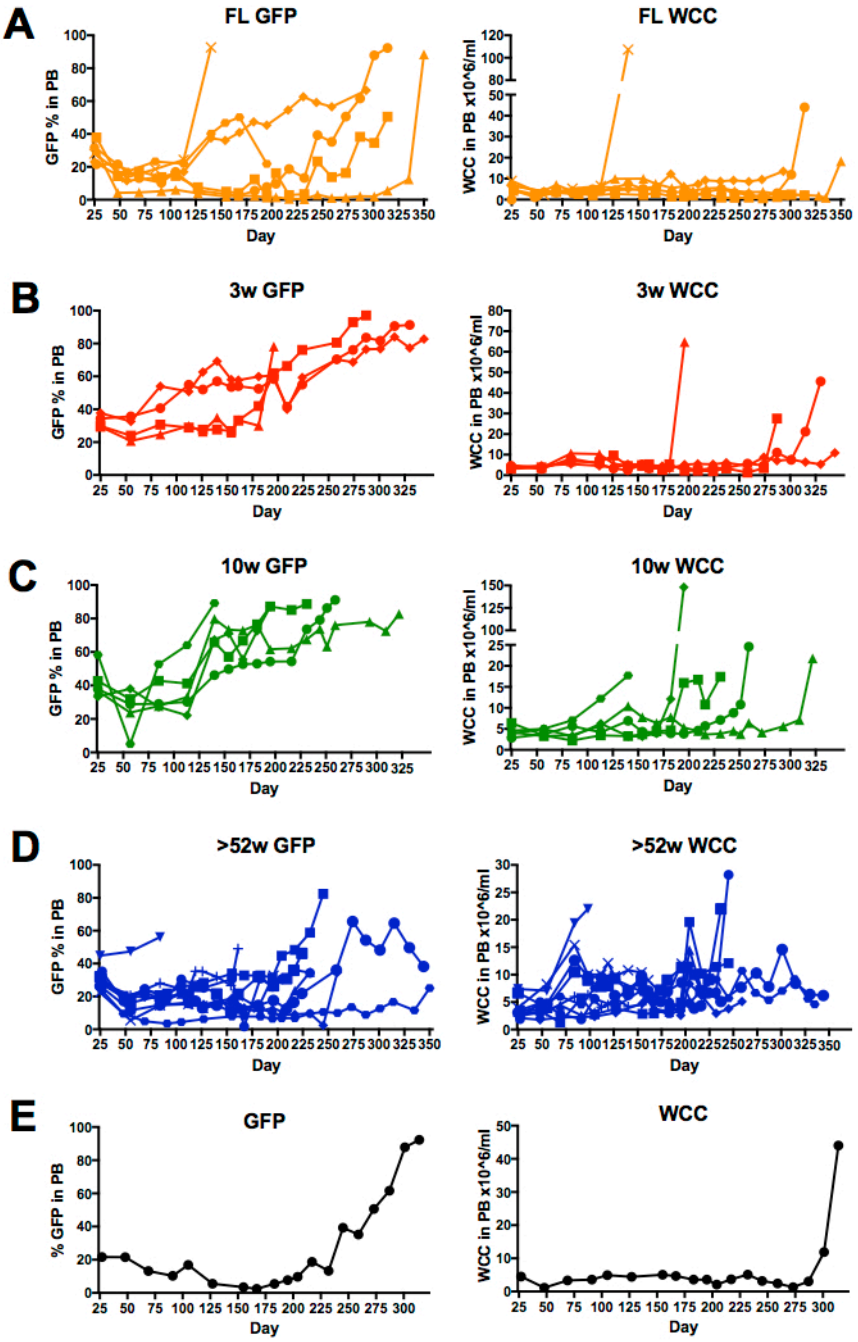

Figure 4.5 Sequential peripheral bleedings show a rise in GFP% and WCC on the development of NH9 leukaemia

(A) PB monitoring of recipients that developed donor derived leukaemia from NH9 transduced FL-LSKs, showing GPF% (left) and total WCC (right), n=6.
(B) PB monitoring of recipients that developed donor derived leukaemia from NH9 transduced 3w-LSKs, showing GPF% (left) and total WCC (right), n=4.
(C) PB monitoring of recipients that developed donor derived leukaemia from NH9 transduced 10w-LSKs, showing GPF% (left) and total WCC (right), n=5.
(D) PB monitoring of recipients that developed donor derived leukaemia from NH9 transduced >52w-LSKs, showing GPF% (left) and total WCC (right), n=10.
(E) Representative graph of sequential PB monitoring from a recipient of FL LSK donor cells. Graphs show an increase in GFP% (left) and WCC (right) with time indicating donor derived leukaemia detectable in PB.

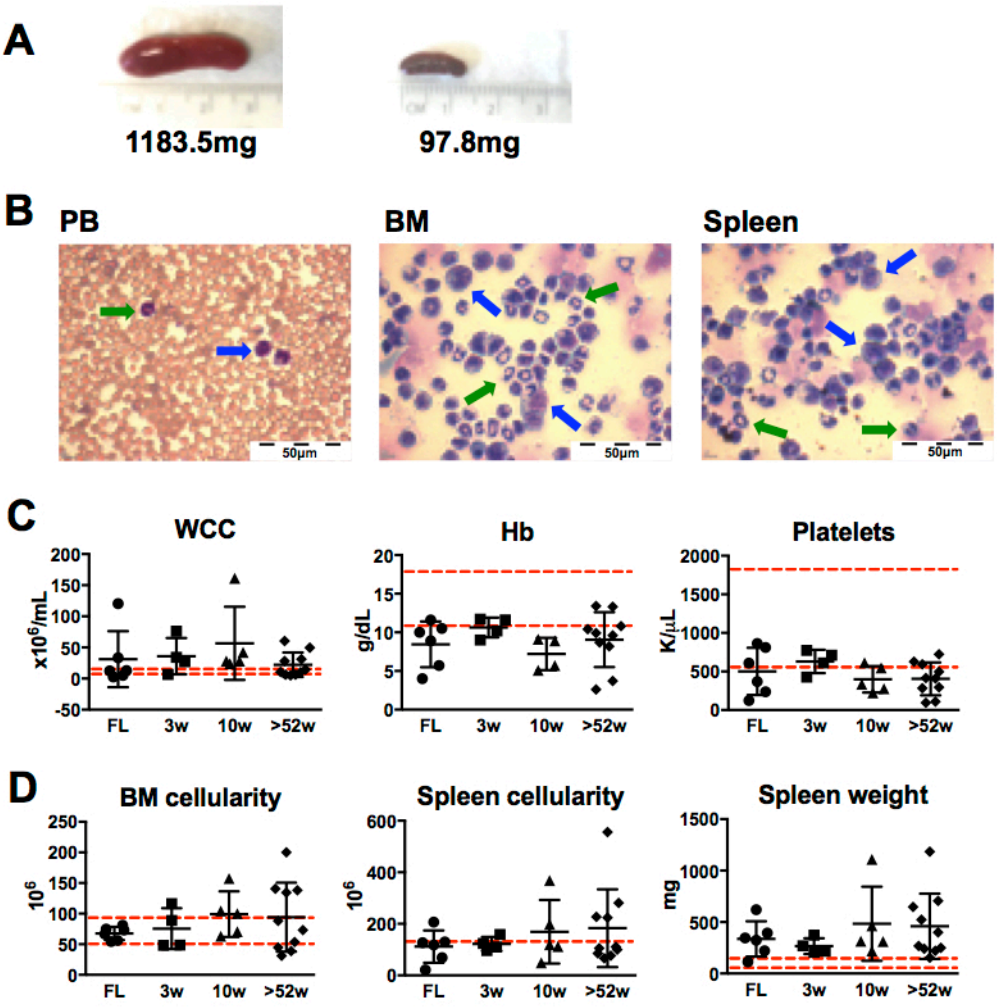

Figure 4.6 Characteristics of NH9 leukaemia *in vivo*

(A) Photograph of representative leukaemic spleen (left) with normal spleen (right) for comparison.
(B) Representative morphology of NH9 AML from PB, BM and spleen showing myeloblasts (blue arrows) and terminally differentiated neutrophils (green).
(C) PB parameters at terminal bleed of recipients with donor derived leukaemia were analysed on a HemaVet 950 (Drew Scientific). Graphs show individual results and mean +/-SD. Red dotted lines depict normal ranged. FL n=6, 3w n=4, 10w n=5, >52w n=10.
(D) Leukaemic burden assessed by BM and spleen cellularity and spleen weight. Graphs show individual results and mean +/-SD. Dotted red lines depict normal values. FL n=6, 3w n=4, 10w n=5, >52w n=10.

Table 4.2 NH9 leukaemia results in splenomegaly

Table of spleen weights for all recipients that developed donor derived leukaemia. Normal range for spleen weight 80-124mg.

Age	Spleen weight (mg)
FL	345.45
FL	620.3
FL	393.8
FL	323.46
FL	112.5
FL	221.2
3w	372.3
3w	206.07
3w	269.75
3w	217
10w	313.52
10w	1109.05
10w	311.67
10w	464.55
10w	220.2
>52w	706.4
>52w	250
>52w	1183.5
>52w	268
>52w	220.61
>52w	646.89
>52w	154.4
>52w	241.3
>52w	522.68
>52w	400

4.3.4 NH9 transduced LSKs from all ages causes an MPN-like disorder *in vivo* that progresses to acute leukaemia

To monitor leukaemia development *in vivo*, sequential PB was assessed for the expression of myeloid markers (CD11b and GR1) and immature marker cKit by flow cytometry. Once recipients succumbed to donor derived leukaemia, in addition to the aforementioned markers, PB, BM and spleen was assessed for B-lymphoid (B220 and CD19) and T-lymphoid (CD3, CD4 and CD8) markers and an additional immature marker, CD34. Post BMT, after engraftment *in vivo* but before leukaemia development, GFP^+ donor cells were present in the PB of recipient mice. These cells expressed dual surface CD11b/GR1 markers but low expression of the immature marker cKit. (Figure 4.7B top) This is the typical immunophenotype of an MPN-like disorder in which there is an overproduction of mature granulocytes. However, as these mice were clinically well and did not have a raised WCC, they did not have MPN *per se*. Irrespective of donor age, with disease progression the immunophenotype of GFP^+ donor cells changed with a loss of myeloid expression, in particular GR1 expression, and an emergence of

a cKit$^+$ population, in keeping with acute leukaemia with immature blasts with a differentiation block. (Figure 4.7B bottom) Therefore, NH9 transduced LSKs from all age groups showed a progression in immunophenotype early post BMT compared to later stages. Our observations are in keeping with published data for NH9 causing an MPN early post BMT with later transformation to an aggressive acute leukaemia.

Recipients that developed NH9 leukaemia displayed leukaemia infiltration with a high percentage of GFP$^+$ cells in PB, BM and spleen. In PB, a higher percentage of GFP$^+$ cells were present in the 3w group compared to the >52w group. Otherwise, the percentage of GFP$^+$ cells in PB, BM and spleen was comparable across all age groups. (Figure 4.8A) Similarly, when data were pooled into young (FL and 3w) and adult (10w and >52w) groups, there was no difference with age in infiltration in PB, BM and spleen. (Figure 4.8B) Flow cytometry analyses of GFP$^+$ leukaemia cells in PB, BM and spleen are shown in figure Figure 4.9. All NH9 leukaemia from 10w and >52w and majority of NH9 leukaemia from FL and 3w showed expression of the mature myeloid marker CD11b and were thus defined as AML, with a proportion also expressing GR1. The exception was 2 mice (1 from FL and 1 from the 3w group) that did not express myeloid markers and will be discussed in Section 4.3.5. However, age of the transforming cell did not result in a difference in CD11b nor CD11b/GR1 expression in donor derived AML, whether analysed in 4 groups or pooled into young and adult. (Figure 4.10A) In all age groups and in all mice, a proportion of leukaemic cell expressed the immature markers, cKit and CD34, in keeping with the differentiation block seen in acute leukaemia. However, there was no difference in the percentage of cKit or CD34 expressing cells with donor cell age, whether the data were analysed in 4 groups or pooled into young and adult. (Figure 4.10B) Across all groups, in the majority of cases, 2 leukaemic populations were present, which could be defined by cKit expression. Considering the entire dataset (irrespective of donor age) in the majority of cases 2 leukaemic populations were present, defined by cKit expression. The expression of CD11b and CD11b/Gr1 was significantly higher in cKit$^-$ cells, while the expression of CD34 was significantly higher in cKit$^+$ cells. (Figure 4.11A and B) This suggests that 2 populations of leukaemic cells were present, an MPN-like population (cKit$^-$) that retain

expression of mature myeloid markers and a transformed, immature AML population (cKit$^+$) that displays a differentiation block. This again is in keeping with NH9 resulting in an MPN early post BMT with later transformation into an aggressive AML. When comparing 4 donor ages, only the >52w groups displayed significantly more expression on CD11b or CD11b/GR1 cells in the cKit$^-$ population. (Figure 4.11C) When the data were pooled into young and adult, the adult group showed significantly higher expression of CD11b and GR1 in the cKit$^-$ population and significantly higher expression of CD34 in the cKit$^+$ population, while this was only a trend in the young group. (Figure 4.11D) Overall, irrespective of the age of the donor cell transduced, LSKs from all 4 ages developed leukaemia *in vivo* with no difference in the immunophenotype of the resultant AML.

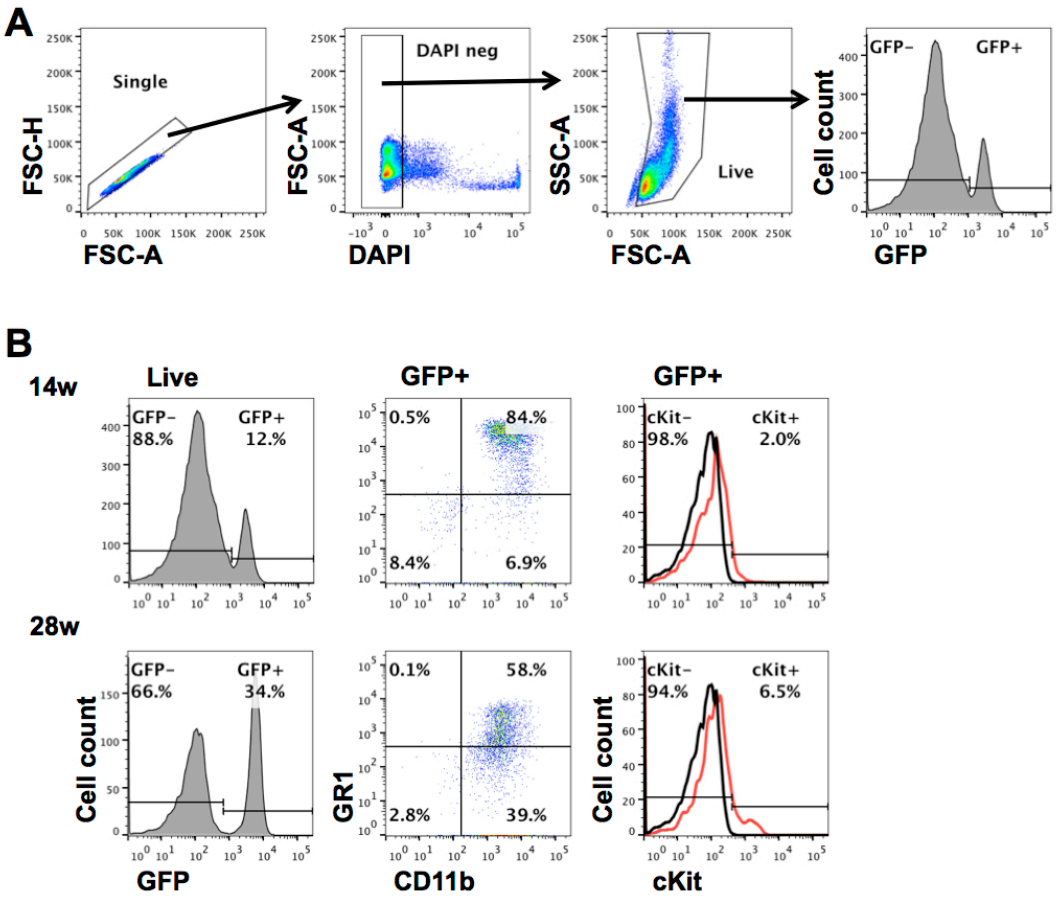

Figure 4.7 NH9 expressing cells results in an MPN early post transplant with progression to acute leukaemia

(A) Gating strategy for flow cytometry analysis.
(B) Representative flow cytometry plots of sequential PB bleeds taken in 1 recipient at 14w (top) and 28w (bottom) post BMT. Plots show an increase in GFP% (left), loss of GR1 expression (middle) and emergence of cKit$^+$ cells (right) at 28w. In cKit histogram, red line denotes GFP$^+$ cells stained with anti-cKit antibody and black line denotes unstained control.

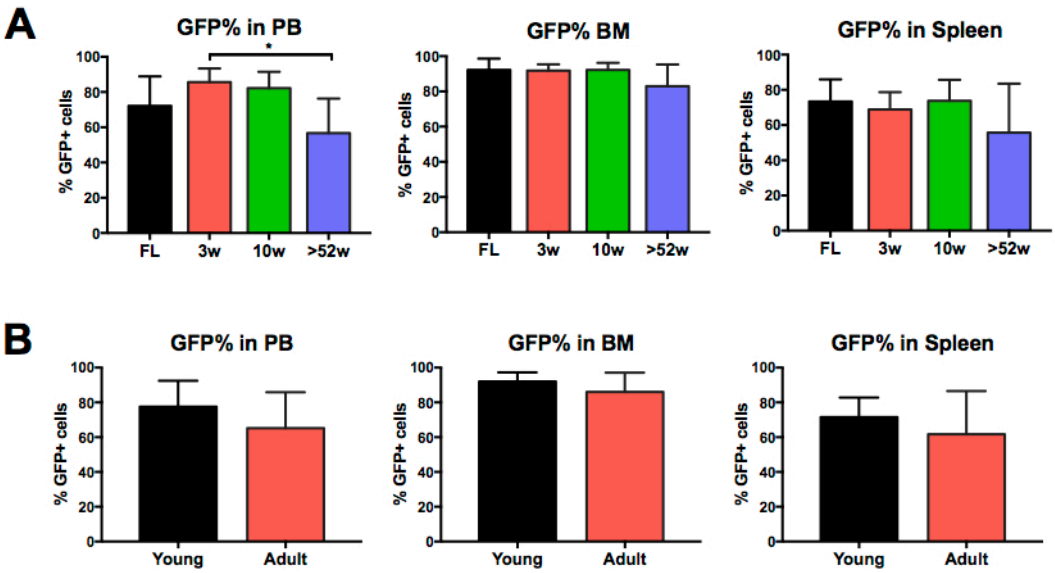

Figure 4.8 Percentage of GFP+ cells in recipients is comparable across all donor age groups on onset of acute leukaemia

(A) Assessment of leukaemic infiltration as GFP% in PB (left), BM (middle) and spleen (right) after recipient mice developed donor derived leukaemia, from 4 ages groups. FL n=6, 3w n=4, 10w n=5, >52w n=10.
(B) Assessment of leukaemic infiltration as GFP% in PB (left), BM (middle) and spleen (right) after recipient mice developed donor derived leukaemia, from pooled young (FL and 3w) and adult (10w and >52w) groups. Young n=10, adult n=15.
Graphs depict mean GFP% +SD. For 4 way comparisons, significance determined by 1-way ANOVA and Bonferroni post-test. For pairwise comparisons, significance determined by Student's t-test, *p<0.05.

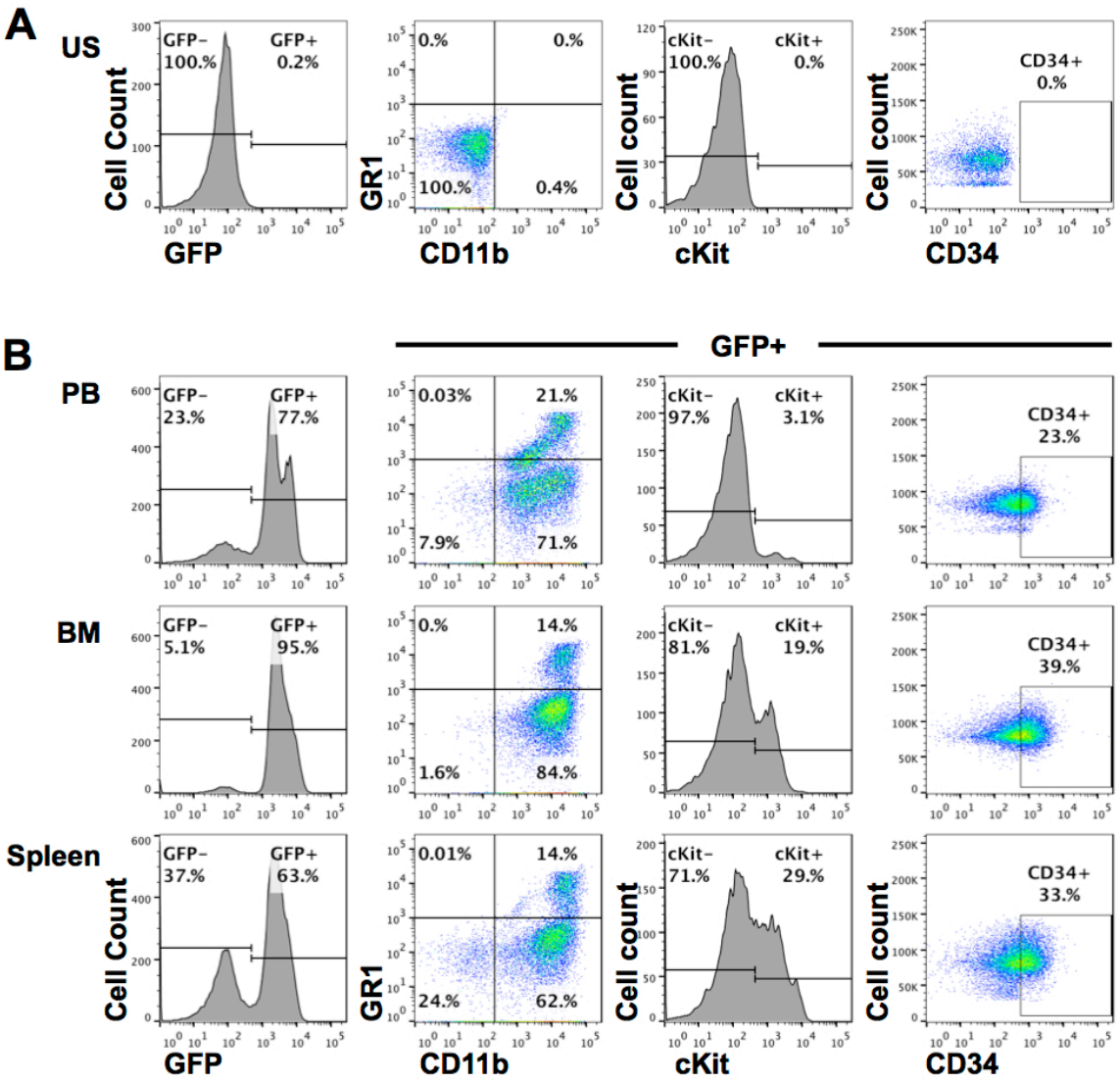

Figure 4.9 Immunophenotypic features of NH9 AML *in vivo*

(A) Unstained control to show the placement of gates for flow cytometry analysis.
(B) Representative flow cytometry plots of PB (top), BM (middle) and spleen (bottom) from recipients that succumbed to NH9 AML. Recipients showed high GFP organ burden, myeloid expression, dual cKit expression and CD34 expression.
US=unstained control. For initial gating strategy, see Figure 4.7A.

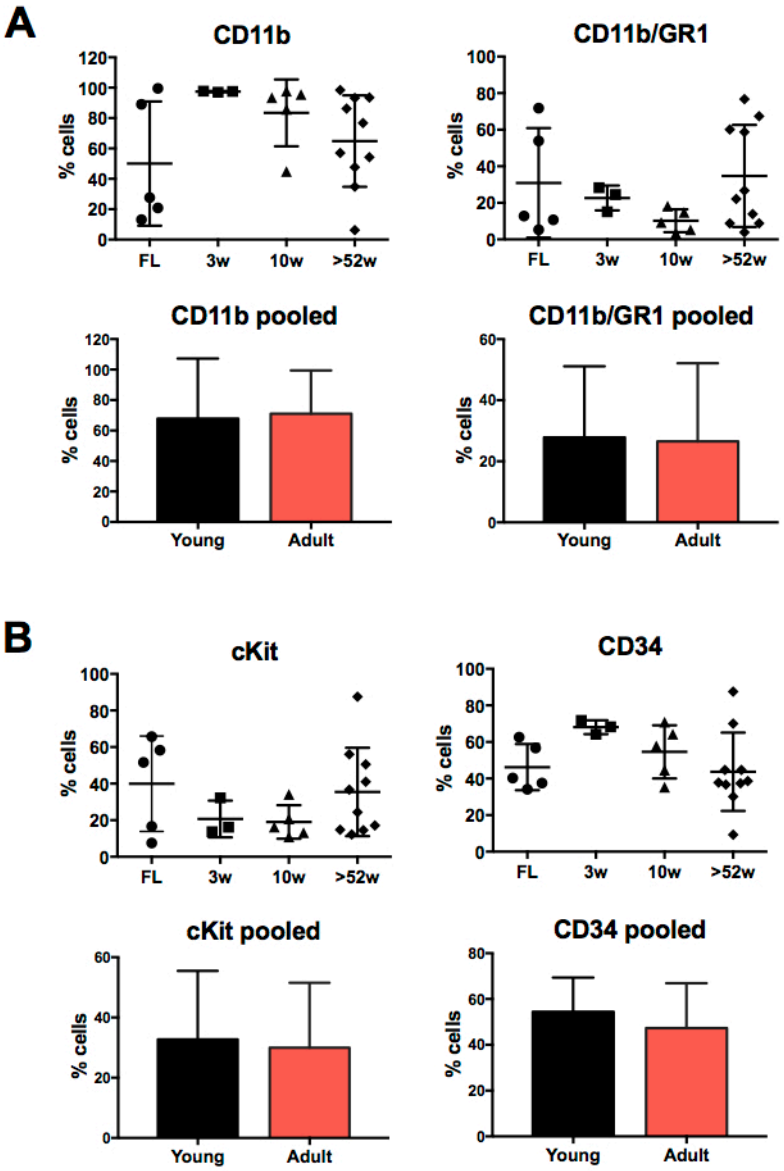

Figure 4.10 Immunophenotype of NH9 derived AML is not affected by age of the donor cells

(A) Myeloid expression of GFP$^+$ cells from BM of recipients that succumbed to NH9 AML. Graphs above show individual result and mean +/-SD from 4 age groups. Graphs below show mean +SD of results pooled into young (FL and 3w) and adult (10w and >52w).
(B) Expression of immature surface markers on GFP+ cells from BM of recipients that succumbed to NH9 AML. Graphs above show individual result and mean +/-SD from 4 age groups. Graphs below show mean +SD of results pooled into young (FL and 3w) and adult (10w and >52w).
For 4 way comparisons, significance determined by 1-way ANOVA and Bonferroni post-test. For pairwise comparisons, significance determined by Student's t-test. FL n=5, 3w n=3, 10w n=5, >52w n=10, young n=8, adult n=15.

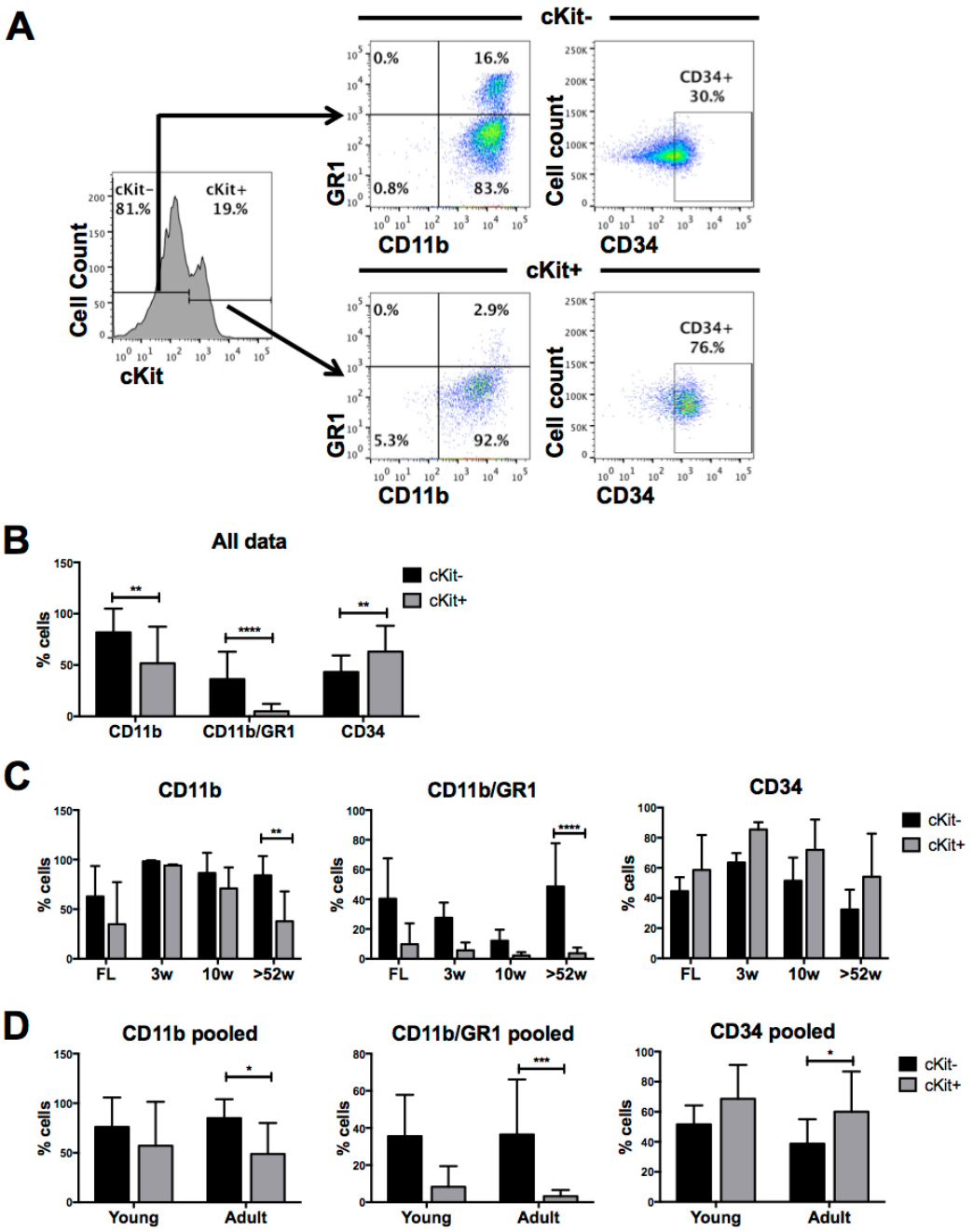

Figure 4.11 NH9 AML has 2 populations defined by cKit expression

(A) Representative FACs plots of cKit$^-$ and cKit$^+$ populations from NH9 AML. cKit$^-$ cells show higher expression of myeloid markers (CD11b and GR1), cKit$^+$ cells show higher expression of immature markers (CD34). For initial gating strategy, see Figure 4.7A.
(B) Expression of CD11b, CD11b/GR1 and CD34 in cKit- and cKit+ cells from recipients succumbing to NH9 AML across all donor age groups. Graph depicts mean +SD, n=23. Significance determined by Student's t-test.
(C) Expression of CD11b (left), CD11b/GR1 (middle) and CD34 (right) in cKit$^-$ and cKit$^+$ cells from recipients succumbing to NH9 AML. Graphs depict mean +SD. FL n=5, 3w n=3, 10w n=5, >52w n=10. Significance determined by 2-way ANOVA and Bonferroni post-test.
(D) Expression of CD11b (left), CD11b/GR1 (middle) and CD34 (right) in cKit$^-$ and cKit$^+$ cells from recipients succumbing to NH9 AML, pooled into young and adult. Graphs depict mean +SD. Young n=8, adult n=15. Significance determined by 2-way ANOVA and Bonferroni post-test.
*p<0.05, **p<0.01, ***p<0.001, ****p<0.0001.

4.3.5 Adult LSKs exclusively develop AML while young LSKs can develop AML, ALL or MPAL

The NH9 oncogene has been exclusively associated with myeloid leukaemia both clinically and in experimental models. In our *in vitro* analysis, donor cells at CFC2 from all ages also expressed myeloid surface markers. (Figure 4.12) All mice in the adult group (10w and >52w) succumbed to myeloid leukaemia, with myeloblasts seen by morphology and expression of the myeloid markers CD11b and GR1 by flow cytometry. Additionally, they did not express the lymphoid markers, B220, CD19 (B-lymphoid) CD3, CD4 or CD8 (T-lymphoid). (Figure 4.13) Of the mice in the young group (FL and 3w) that succumbed to NH9 leukaemia, the majority also developed myeloid leukaemia, as determined by the expression of myeloid markers CD11b and GR1 by flow cytometry. (Figure 4.14A and B, black panels) However, 1 mouse from FL and 1 mouse from the 3w group developed acute leukaemia that did not express myeloid markers by flow cytometry. Instead, 100% of GFP^+ leukaemia cells expressed B-lymphoid markers (CD19 or B220) and were thus diagnosed as ALL. (Figure 4.14A and B, blue panels) Furthermore, in the 3w group, a proportion of recipients that developed AML (indicated as a high percentage by flow of $CD11b^+$ cells) also expressed the lymphoid marker B220, albeit not in 100% of cells. (Figure 4.14B, red panel) ALL and leukaemia with dual expression of myeloid and lymphoid markers was not observed in 10w or >52w recipients.

To further assess the lineage of the leukaemia that developed, available sternal sections were assessed for the myeloid marker MPO and lymphoid marker CD3 by IHC. Positive expression of a marker was defined as expression on more than 20% of leukaemia cells. The results are summarised in Table 4.1. AML generated from 10w and >52w LSKs displayed strong expression of MPO (>40% expression) with little (<20%) or no expression of CD3 (grey in table). AML generated from the FL and 3w LSKs also expressed MPO, as expected. However, unlike adult generated AML, a proportion of AML generated from FL and 3w LSKs also expressed intracellular CD3, indicating they were of mixed phenotype (red in table). (Figure 4.15) Dual expression of MPO and CD3 is one of the diagnostic criteria MPAL according to the WHO. (Section 1.3.5) Interestingly, samples that were positive for CD3 staining by IHC were not detected as $CD3^+$ by flow cytometry, as

only surface marker expression was assessed by flow cytometry. Therefore, despite being phenotypically myeloid by morphology and flow cytometry, in young-AML the population of leukaemic cells can exhibit dual expression of myeloid and lymphoid markers, while adult-AML is myeloid restricted.

Co-expression of myeloid and lymphoid markers at the single cell level was not assesed, either by flow cytometry or IHC. Therefore, in the acute leukaemias in which both lineages were expressed, we cannot conclude if this was due to 2 populations of leukaemic blasts (myeloid and lymphoid - bilineal) or 1 population of leukaemic blasts co-expressing myeloid and lymphoid markers on the same cell (biphenotypic), or a mixture of the 2. (Figure 4.16A) However, both would be termed MPAL. Table 4.1 and Figure 4.16B summarise the lineage features of the leukaemia that developed in each group. When the data were pooled into young and adult, age was a significant factor determining leukaemia lineage. Upon transplantation young LSKs could develop either AML, ALL or MPAL. This is despite young donor LSKs expressing CD11b and GR1 prior to engraftment. In contrast, adult LSKs only gave rise to AML. This suggests that young LSKs have strong intrinsic lymphoid programmes that can override a myeloid oncogene.

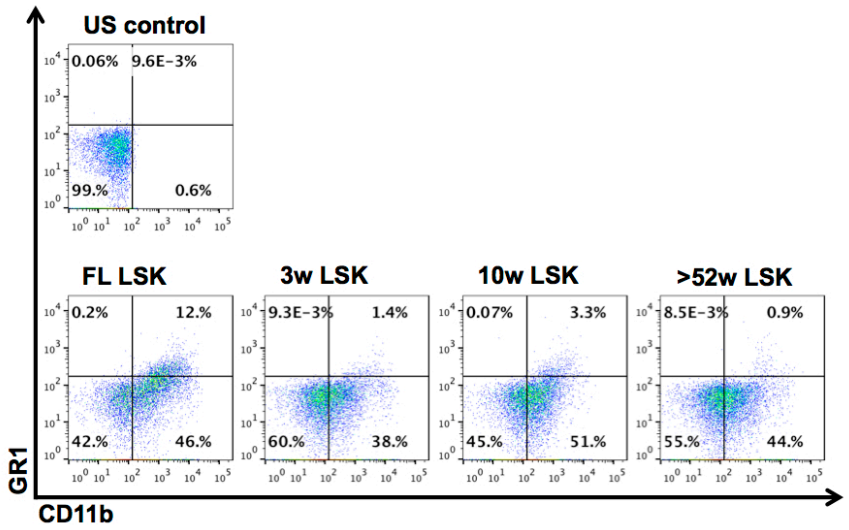

Figure 4.12 Donor cells from NH9 transduced LSKs at CFC2 express myeloid surface markers

Representative FACs plots of unstained control (above) and donor cells from FL, 3w, 10w and >52w (below) NH9 transduced LSKs at CFC2. Donor cells express the myeloid marker CD11b with some expression of GR1.
All plots are gated through GFP+ cells, US=unstained. For initial gating strategy see Figure 4.7A.

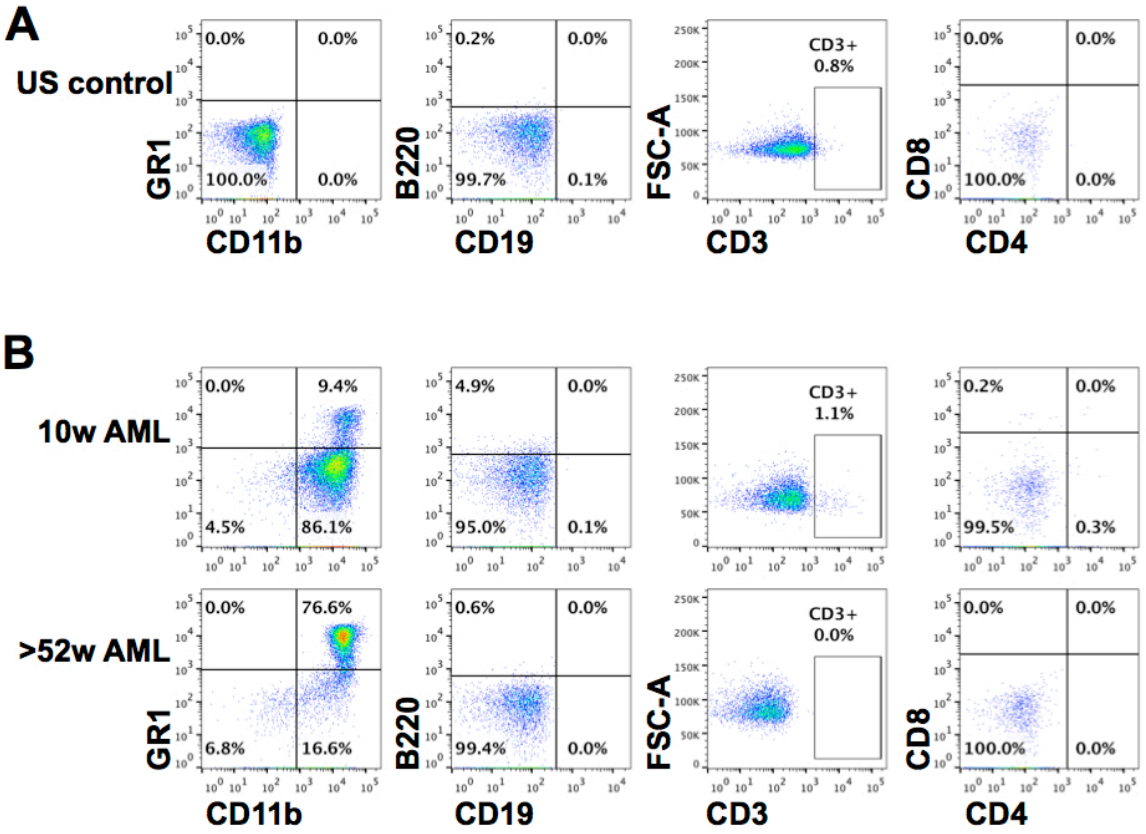

Figure 4.13 NH9 AML generated from adult LSKs express myeloid markers but do not express lymphoid markers

(A) Representative flow cytometry plots of unstained control showing gating strategy for myeloid (CD11b/GR1 left), B-lymphoid (CD19/B220, middle left) and T-lymphoid (CD3, middle right and CD4/CD8, right). US=unstained.
(B) Representative flow cytometry plots from BM of recipients that developed NH9 AML after transplantation with 10w LSKs (top) and >52w LSKs (bottom). 10w and >52w generated AML expresses myeloid markers (left) but not B-lymphoid (CD19/B220, middle left) or T-lymphoid (CD3, middle right and CD4/CD8, right) markers.
All plots are gated through GFP^+ leukaemia cells. For initial gating strategy see Figure 4.7A.

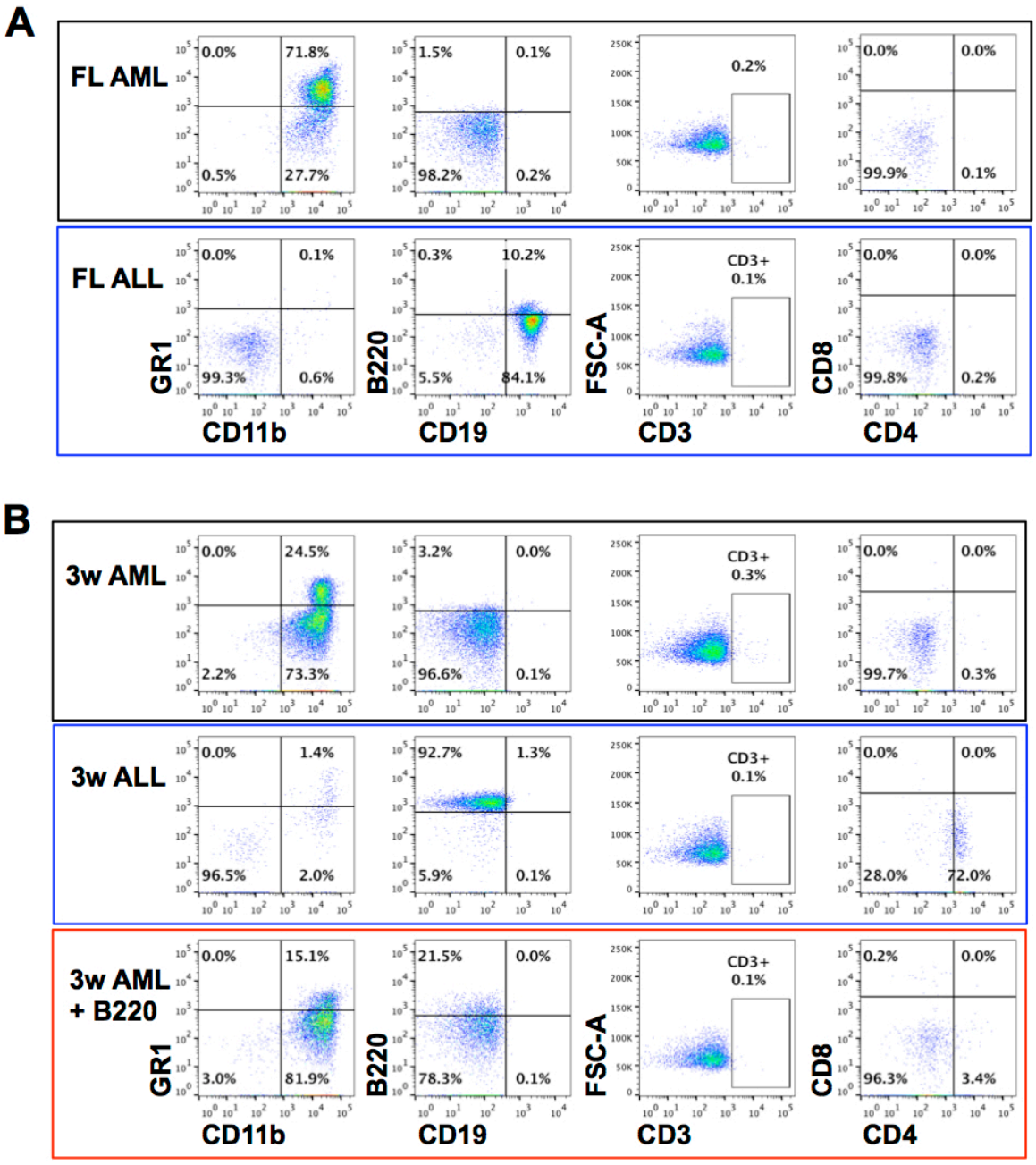

Figure 4.14 NH9 transduced LSKs from FL and 3w donors can express myeloid and lymphoid markers

(A) Representative flow cytometry plots of the BM of recipients that developed NH9 leukaemia from FL LSKs. Top panel (black) shows FL-AML, which expresses myeloid markers CD11b and GR1 but does not express lymphoid markers. Bottom panel (blue) shows FL-ALL, which does not express myeloid markers but does express the B-lymphoid marker CD19.
(B) Representative flow cytometry plots of the BM of recipients that developed NH9 leukaemia from 3w LSKs. Top panel (black) shows 3w-AML, expressing myeloid markers CD11b and GR1 but not expressing lymphoid markers. Middle panel (blue) shows 3w-ALL, which does not express myeloid markers but expresses the B-lymphoid marker B220. Bottom panel (red) shows 3w-AML with lymphoid expression, which shows strong expression of myeloid markers, but also expresses the B-lymphoid marker B220 on 21.5% of cells.
All plots are gated through GFP^+ leukaemia cells. For initial gating strategy see Figure 4.7A.

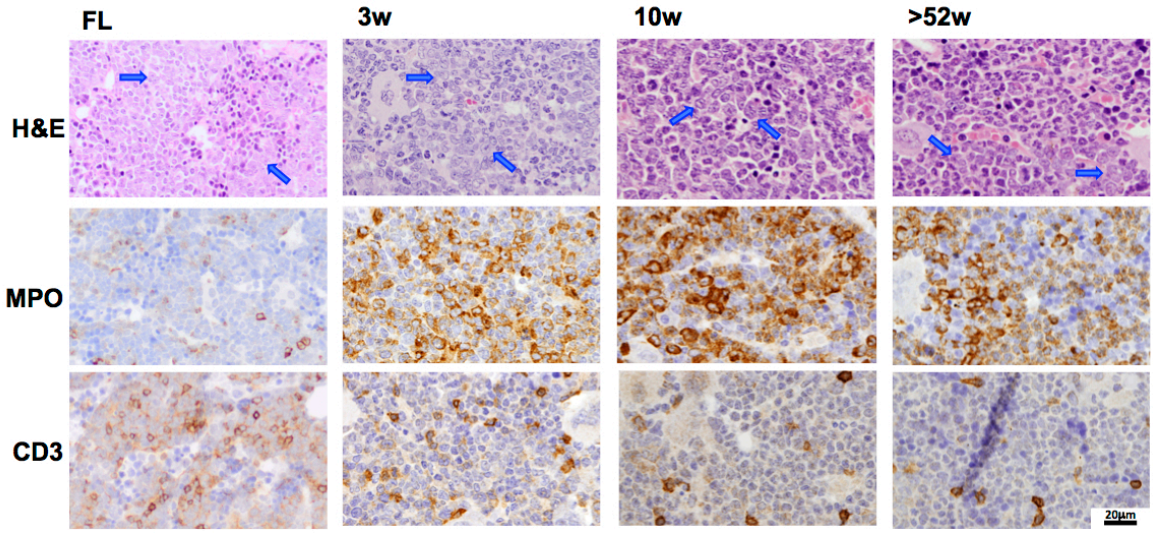

Figure 4.15 Immunohistochemistry from BM of NH9 AML

Representative sternal sections from recipients that developed NH9 AML from FL (left), 3w (middle left), 10w (middle right) and >52w (right) LSKs. Top panel shows H&E stain, in which leukaemic blasts are identified by blue arrows. Middle panel shows MPO stain, positive cells exhibit brown cytoplasmic staining. AML from all ages shows high percentages of cells are positive from MPO. Bottom panel shows CD3 staining, positive cells exhibit brown cytoplasmic staining. AML from FL and 3w LSKs exhibit more CD3 staining than AML from 10w and >52w LSKs.

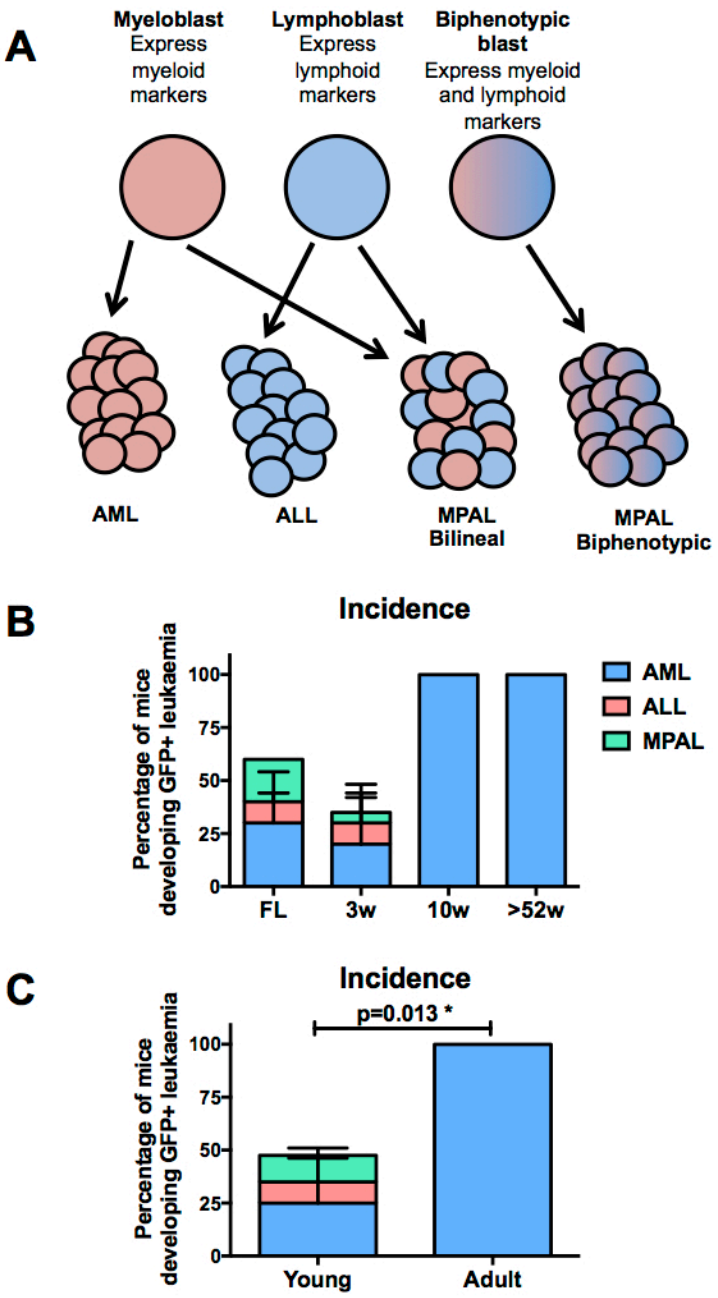

Figure 4.16 Adult LSKs result in AML, young LSKs result in AML, ALL or MPAL

(A) Schematic of AML, ALL and MPAL showing AML consists of myeloblasts and ALL consists of lymphoblasts. MPAL can result from a mixture of myeloblasts and lymphoblasts (bilineal) or biphenotypic blasts (biphenotypic).
(B) Bar chart of lineage of all donor derived leukaemia in recipients transplanted with NH9 transduced LSKs from CFC2 showing results from 4 age groups. FL n=6, 3w n=4, 10w n=5, >52w n=10.
(C) Bar chart of lineage of all donor derived leukaemia showing data pooled into young (FL and 3w) and adult (10w and >52w). Age is a significant factor in determining resultant leukaemic lineage. Young n=10, adult n=15.
Graphs depict mean +SD from 2 independent experiments. Significance determined by 2-way ANOVA, *p<0.05.

4.3.6 Adult LSKs home to the BM at an early time point

In the BMT experiment, donor cells from 4 ages were transplanted into young adult recipients aged 6-8w. Intrinsic cellular factors, determined by the age of the transplanted cell, could effect homing to the recipient BM. To assess if there were differences in homing of NH9 transduced LSKs from different ages to the BM, 3w (young) and >52w (adult) NH9 expressing LSKs expanded in methylcellulose were harvested at CFC2 and transplanted into sub-lethally irradiated mice aged 6-8w. To aid *in vivo* detection, GFP-tagged NH9 transduced donor cells were dyed with CTV. Mice were sacrificed 18h post tail vein injection. Percentage of donor cells in BM and PB was enumerated, relative to donor cell dose as described in section 2.4.3 and Figure 2.6.

More donor cells were detected in the BM in recipients transplanted with >52w transduced LSKs than 3w transduced LSKs by flow cytometry. (Figure 4.17 top) After normalisation to adjust for the difference in number of donor cells injected, significantly more >52w LSKs had homed to the BM of recipient mice at 18h compared to 3w LSKs (4.73% vs 0.59%, respectively). (Figure 4.17B) Very few donor cells were detected in the PB of recipients transplanted with either 3w or >52w LSKs by flow cytometry. (Figure 4.17A bottom) When normalised for injected cell number, there was no difference in the percentage of donor cells circulating the in the PB recipients transplanted with 3w or >52w transduced LSKs. (Figure 4.17C) These results show that >52w transduced LSKs are more efficient at homing to the BM compared to 3w transduced LSKs. In both age groups, very few donor cells remained in the PB 18h post transplantation, suggesting that 3w LSKs may have homed to sites other than the BM. Flow cytometry was not performed on other organs. However, these results suggest that adult LSKs are more efficient at homing to the BM. In addition, different aged cells may home to different sites, which may impact leukaemogenesis and account for the difference in latency, penetrance and phenotype that we observed. In human disease, homing to different sites may account for the higher rates of extramedullary disease observed in human infant AML. (Chessells, 1992)

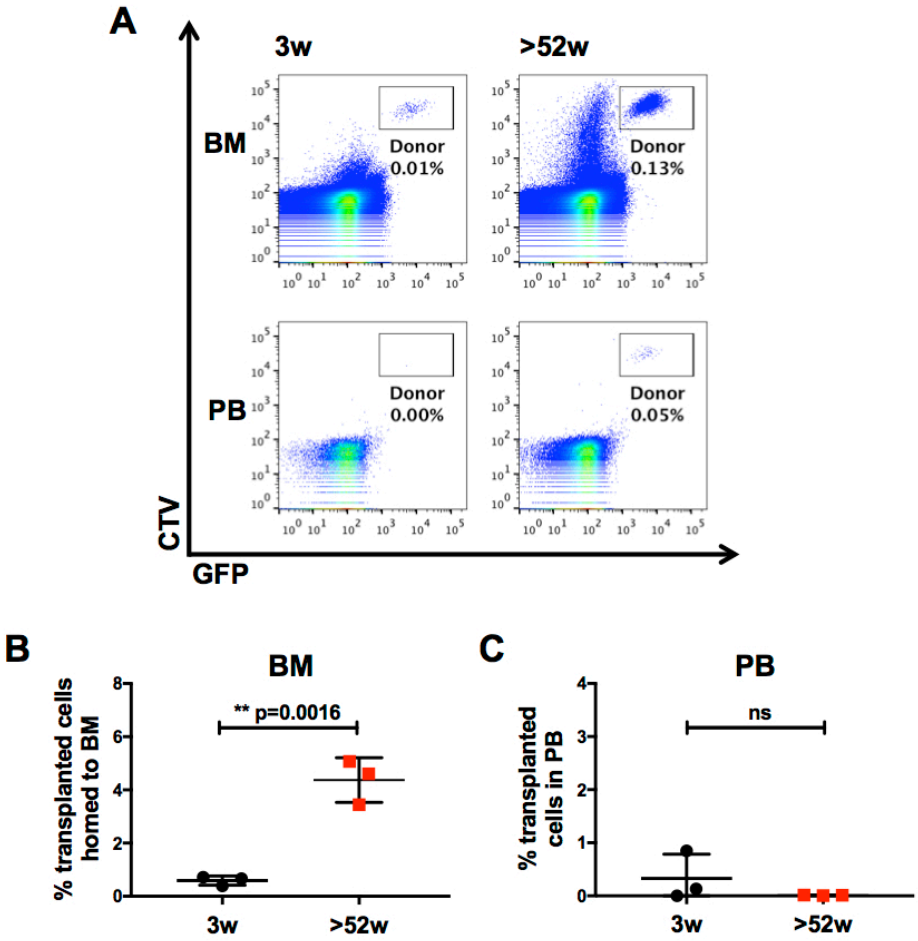

Figure 4.17 Homing of NH9 transduced LSKs

(A) Representative flow cytometry plots of BM (top) and PB (bottom) from adult recipients transplanted with 3w (left) and >52w (right) LSKs transduced with NH9 and stained with CTV. Donor cells are dual positive for GFP and CTV.
(B) Graph of donor cells homed to BM 18h post tail vein injection, expressed as % injected donor cells to control for differences in donor cell number. Significantly more >52w NH9 transduced LSKs home to the BM.
(C) Graph of donor cells in PB 18h post tail vein injection, expressed as % injected donor cells to control for differences in donor cell number.
Graphs depict individual values and mean +/-SD. Significance determined by Student's t-test, n=3 for all groups.

4.4 Discussion

In this chapter leukaemia development and phenotype *in vivo* was investigated using the NH9 AML model in young and adult HSPCs. The NH9 model was utilised as, unlike other AML oncogenes such as A1E, it drives a potent leukaemia *in vivo* without the overexpression of additional mutations. Retroviral transfer of NH9 to total BM, CMP, GMP and MEPs imbues these populations with leukaemia initiating properties. (Kroon et al., 2001, Kvinlaug et al., 2011) Contrary to published data, CMPs and GMPs from all ages transduced with NH9 and following replating

in CFC did not engraft in recipient mice. As FL-CMPs and GMPs did not exhibit self-renewal properties *in vitro*, it was not surprising that they did not engraft *in vivo*. However, 3w-CMP and GMPs, 10w-GMPs and >52w-CMPs did acquire self-renewal properties *in vitro* so the failure of these cells to establish long-term engraftment was unexpected. Interestingly, the only progenitor population that did show BM engraftment at 16w was 10w CMP, which corresponds to the age investigated in Kvinlaug *et al*. One possible explanation for this observation is that CMPs and GMPs are not the transforming cell of origin for 3w or >52w aged cells. Another theory is that while NH9 confers self-renewal properties to post-natal CMPs and GMPs *in vitro*, unlike the MA9 model, it does not result in an expansion of the engrafting cell. Omission of pre-transplant expansion in methylcellulose would clarify this.

The LSK compartment was the common transforming population in all 4 ages using *in vitro* techniques. In keeping with this, LSKs from all 4 ages developed acute leukaemia *in vivo*. However, the age of the LSKs had significant impact on susceptibility to disease and disease lineage. Mice transplanted with young (FL and 3w) LSKs developed leukaemia after a longer latency compared to those transplanted with adult LSKs (10w and >52w). Furthermore, leukaemia from young donors was not 100% penetrant, in contrast to the adult groups. This strongly implies that young LSKs are less susceptible to leukaemic transformation and is line with clinical data showing a lower incidence of AML in childhood compared to adults. (Howlader N, 2014) As hypothesised, this may be due to cell intrinsic factors. Young LSKs may employ cell protective mechanisms that ensure the development of a healthy haematopoietic system. Furthermore, different protective mechanisms may be important at different developmental ages. McGee *et al* investigated the role of the tumour suppressor phosphatase and tensin homolog (*Pten*) in leukaemogenesis. PTEN maintains HSC quiescence by suppression of the PI3 kinase pathway. Deletion of *Pten* in adult (2m) mice resulted in PI3 kinase mediated HSC proliferation and leukaemia. However, *Pten* deletion in E14.5 and neonatal (14d) mice did not lead to PI3 kinase activation or leukaemia. Tumour suppression programmes that are critical in adults may be unnecessary in foetal or neonatal HSCs, resulting in differences in leukaemic susceptibility in young and old HSCs. (Magee et al., 2012)

As detailed earlier, the long latency to disease suggests that NH9 expressing cells must acquire further mutations in order to develop AML. Many studies, both in the murine and human system, show there is an accumulation of DNA damage with increasing age, as well as an attenuation of DDR and repair mechanisms. (Rossi et al., 2007a, Rube et al., 2011, Beerman et al., 2014, Walter et al., 2015, Moehrle et al., 2015) Additionally, aged HSCs exhibit increased expression of self-renewal genes that have been implicated in driving leukaemia such as *AML1*, *ETO* and *PML*. (Rossi et al., 2005) Thus, there is the potential acquisition of leukaemia driver mutations in older cells. Adult HSCs are typically quiescent, proliferating only occasionally in order to maintain genetic integrity. (Allsopp et al., 2003, Wilson et al., 2008, Flach et al., 2014) Aged HSCs (>24m), in contrast, proliferate more than young adult HSCs to make up for functional decline. At the other extreme, foetal and neonatal HSCs are rapidly proliferating. It is perhaps surprising that these pre-adult HSCs are not also prone to DNA damage as their older quiescent counterparts are. Quiescent cells attenuate DDR mechanisms, employing the error prone NHEJ mechanism. On entering cell cycle, aged stem cells upregulate DDR and repair mechanisms. (Beerman et al., 2014) Thus, while the state of quiescence may protect adult HSCs from proliferative stress, their response to other genotoxic stresses is relatively impaired and may result in the accumulation of DNA mutations that prime the cell for cancerous transformation. Conversely, the cycling nature of FL and 3w HSCs may in fact protect young HSCs from DNA damage due to more efficient DDR and repair mechanisms. Thus, both explicit differences in cellular protective mechanisms and the mutational background of the cells may explain the differences observed in leukaemic susceptibility.

An interesting observation was the progression of surface marker expression during leukaemia development *in vivo*. After engraftment but before acute leukaemia development, flow cytometry of GFP^+ cells in PB showed a typical myeloproliferative phenotype with high CD11b/GR1 expression. However, with the onset of AML, differentiation markers were lost and there was an increase in the expression of the immature cell surface marker, cKit. This is in line with published data in which NH9 results in MPN with later development of AML. (Kroon et al., 2001) The SCF receptor, cKit, is normally highly expressed on stem

and progenitor cells. The emergence of cKit expression in NH9 acute leukaemia suggests that there is an acquisition of stem cell signatures that may drive the transformation from an indolent MPN to acute leuakemia. This supports the theory that NH9 alone cannot drive acute leukaemia and further mutations are required for transition to AML. Older LSKs, with presumably more background mutational load, may need fewer further mutations in addition to NH9 to completely develop acute leukaemia. Additionally, the acquisition of stem cell features is thought to be a characteristic of LSCs. As discussed in section 1.3.1.2 there is evidence that, like haemopoiesis, leukaemia cells follow a hierarchical system in which leukaemia is propagated by LSCs. LSCs share biological properties and transcriptional signatures with normal HSCs, implying stem cell qualities such as self-renewal and longevity. (Dick, 2008) The expression of stem cell signatures in cancers, including acute leukaemia, is associated with aggressive disease and poor prognosis. (Gentles et al., 2010, Eppert et al., 2011, Ng et al., 2016) At the point of leukaemia development when recipients were sacrificed, there was no difference in cKit expression by flow cytometry between young and adult groups. However, adult donors generated AML more rapidly and with 100% penetrance, suggesting a more aggressive phenotype. Investigation of stem cell transcriptional profiles in young and adult generated AML would elucidate if the expression of stem cell programmes in adult AML could explain the shorter latency to disease observed in this group.

A proportion of mice in the FL and 3w group developed lymphoid leukaemia determined by flow cytometry, defined by the absence of myeloid markers CD11b and GR1 and the presence of B-lymphoid markers, either CD19 or B220. Furthermore, a proportion of FL and 3w mice that developed AML, determined by the expression of CD11b/GR1 by flow cytometry, also showed either aberrant expression of B-lymphoid markers by flow or dual expression of the myeloid marker MPO and T-lymphoid marker CD3 by IHC. This is despite evidence of myeloid surface marker expression in the donor cells prior to transplantation and in the sequential PB bleeds. Clinically, NH9 has only been implicated in myeloid leukaemias, making the development of a lymphoid disease more unexpected. (Romana et al., 2006) The ability of young stem cells to produce a mixed lineage disease has been shown in experimental models using MA9 (discussed in section

4.1.2.2). In a knockin mouse model all leukaemias from adult HSCs gave rise to myeloid leukaemia (defined as MPO positive) whereas leukaemia from foetal HSCs or unsorted cells could give rise to myeloid, lymphoid or mixed phenotype disease, evidenced by MPO (myeloid) and/or B220 (lymphoid) staining by IHC. (Chen et al., 2011) In a T&T model, human $CD34^+$ cells from CB gave rise to either myeloid or lymphoid leukaemia *in vivo* while adult BM resulted in myeloid biased engraftment without leukaemia development. (Horton et al., 2013) However, both examples use MA9 disease, which is known to drive both myeloid and lymphoid leukaemia and as such, the authors conclude that their results recapitulate human disease. In the model presented in this thesis, the NH9 oncogene known to drive only myeloid disease is utilised. The ability of cells to develop lymphoid disease in this context suggests that lymphoid bias is an intrinsic characteristic of young cells rather than dependent on the specific oncogenic driver, while adult cells are lineage restricted. Two scenarios may occur to explain these findings. First, a dual population model in FL and 3w LSKs, in which NH9 transduced 2 populations of cells, one with myeloid and one with lymphoid potential and either could develop into leukaemia. Or, a lineage plasticity model in which NH9 transduced one population of cells but young LSKs are able to switch from myeloid to lymphoid lineage. The experimental design does not specifically address this question and lymphoid markers were not investigated on the donor cells or PB bleeds. However, all donor cells did express myeloid markers before transplantation. Of the mice that did succumb to ALL, early bleeds showed that the GFP^+ cells were positive for myeloid markers. Therefore, the data would suggest a lineage plasticity model. In clinical practice, infant ALL (occurring <1y of age) is associated with a high incidence of MLLr, $CD10^-$ blasts and the co-expression of myeloid antigens, suggesting an immature, mixed lineage phenotype. (Basso et al., 1994) As such, treatment regimens for infant ALL incorporate both lymphoid and myeloid directed therapy. (Pieters et al., 2007) As intracellular CD3 by flow is not part of standard testing clinically, MPAL may be missed. Interestingly, lineage switching is observed in human disease in which the leukaemia at relapse is different to when diagnosed. (Arber et al., 2016) In line with the presented data, lineage switching is more common in infant and congenital leukaemia than adult leukaemia. (Dorantes-Acosta and Pelayo, 2012) If young acute leukaemias are

indeed lineage plastic, this has therapeutic implications, as these leukaemias may benefit from a mixture of chemotherapy regimens that are effective against both myeloid and lymphoid leukaemia.

In addition to cell intrinsic factors, the microenvironment may provide cues for leukaemia development. The BM microenvironment is a highly specialised organ with major importance in protecting and maintaining the HSC compartment. Additionally, the microenvironment plays a role in leukaemia propagation, maintenance and lineage determination. Moreover, leukaemia cells can manipulate the microenvironment making it more permissive to sustaining malignant growth at the expense of normal HSCs. (Matsunaga et al., 2003, Colmone et al., 2008, Wei et al., 2008, Geyh et al., 2016) There is a theory that the young microenvironment is evolutionary selected to suppress oncogenic insult, while the aged unselected microenvironment is more permissive to mutational aberration. (Rozhok and DeGregori, 2015) While the role of the ageing microenvironment *in vivo* was not tested *per se* (all recipients were adult mice aged 6-8w), one hypothesis is that the adult BM niche is less supportive of foetal/young stem cell transformation. The data presented would support impaired or delayed homing of young LSKs to the BM compared to adult LSKs. FL LSKs normally reside in the vascular foetal liver while BM derived 3w HSCs have just migrated from the foetal liver. On transplantation of these foetal-like cells into an adult recipient, these cells may respond to the microenvironmental cues differently to the 10w and >52w adult LSKs. Therefore, the adult microenvironment may also play a role in promoting or suppressing leukaemia development, depending on stem cell age. This phenomenon is already seen in human myeloid proliferation. TAM with *GATA1* mutation is seen in 10% of newborns with DS. (See Section 1.3.6.3). TAM spontaneously regresses in the majority of cases with only 20% progressing to AML, suggesting that the maturing BM compartment may not be supportive of leukaemogenesis. (Gamis et al., 2011)

There is evidence that different aged HSPCs localise differently within the BM microenvironment. Kohler *et al* transplanted LSKs from young (2-4m) and aged (18-20m) mice and performed time-lapsed intravital imaging in the tibia of

recipient mice. Young LSKs localised near to and directly attached to the endosteum and were completely immobile. However, these cells did present with active cell protrusion movements, associated with a dynamic change in individual cell volumes, suggesting recognition and response to cues from the microenvironment. While aged LSKs were also generally immobile, they resided further away from the endosteum and displayed more cellular protrusion compared to young LSKs. *Ex vivo* cobblestone-adhesion-forming cell assays showed aged LSKs had significantly less adhesion to the FBMD-1 stromal cell line compared to young LSKs. Furthermore, aged LSKs showed impaired ability to polarise in response to adhesion to fibronectin. The authors postulate that impaired polarisation and adhesion leads to the aged HSC residing in a BM niche that is distinct from the young HSCs and this may impact HSC function. (Kohler et al., 2009) It is important to note that in this study, young HSCs were 2-4m old and would have been defined as 'adult' in the data presented in the thesis. However, it raises the possibility that with age, the normal localisation and behaviour of the HSC in relation to the microenvironment changes and may impact not only function but also susceptibility to oncogenic insult. Aurora *et al* investigated the engraftment of embryonic and adult HSCs in neonatal and adult recipient mice. They found that early embryonic HSCs (E9.5-11.5) robustly engrafted in neonatal hosts but did not engraft into adult recipients. Conversely, E14.5 and adult HSCs better engrafted in adult compared to neonatal recipients. Therefore, microenvironment age does affect the engraftment potential of transplanted cells. (Arora et al., 2014) It is interesting to note that in this study, E14.5 HSCs, which was the youngest cell age investigated in this thesis, showed similar reconstituting cell frequency as adult HSCs. The authors also compared homing of adult LT-HSCs in neonatal and adult recipients 15h post injection. They found that adult LT-HSCs would preferentially home to the liver when transplanted into neonatal recipients (88% of injected cells), compared to balanced homing to liver and spleen when injected into adult recipients. Unlike the homing experiment described in this thesis, the authors did not investigate homing of both young and adult HSCs into adult recipients. Liang *et al* investigated homing of young adult (2-4m) and old adult (22-25m) HSCs into young and old adult recipients. They found that with increasing age of donor and recipient, homing to BM declined. This is in contrast to the presented findings in

which older transformed LSKs displayed more efficient homing to the adult BM. However, the adult LSKs investigated in this thesis were much younger than the authors' 'old' group at >52w and the young group was much younger at 3w. In addition, increasing donor or recipient age was also associated with myeloid-skewed engraftment. (Liang et al., 2005) While neither study can be directly compared with the data presented here, both highlight that recipient age also has a role in efficient homing, engraftment and lineage output post transplant. To date, there are no studies investigating leukaemia development generated from foetal-like and adult HSCs in different aged microenvironments. This would further clarify the interplay between stem cell age and environmental age in leukaemia development and phenotype.

In summary, using the same oncogenic model, the data show that stem cell age has significant impact on leukaemogenesis. Specifically, young, foetal-like LSKs display delayed or impaired leukaemia development, with a longer latency to disease and reduced disease penetrance compared to adult LSKs. Additionally, foetal-like LSKs retain lymphoid potential and can develop myeloid, lymphoid and mixed phenotype acute leukaemia while leukaemia from adult LSKs is myeloid restricted. Several possible cell intrinsic and extrinsic factors that may explain the phenomenon observed have been postulated. In the following chapter, the potential underlying mechanisms will be investigated by transcriptional analysis.

5 An examination of the age discriminating transcriptional profiles of transformed LSKs

5.1 Introduction

In the previous 2 chapters differences in oncogene mediated transformation *in vitro* and *in vivo* due to the age of the transforming cell were presented. Specifically, NH9 expressing FL and 3w LSKs are less susceptible to leukaemic transformation *in vivo* compared to 10w and >52w LSKs and retain lymphoid potential while adult transformed LSKs are myeloid restricted. In this chapter the underlying transcriptional programmes that may underpin these observations will be investigated.

5.1.1 Gene expression techniques

Modern gene expression techniques, including high throughput PCR, microarray technology and RNA-seq, have made it possible to screen the expression of 1000s of genes quickly and simultaneously in the same sample. GEP can confirm cellular behaviour and characteristics at the transcriptional level as well as highlight novel pathways important for cellular function. In disease biology, GEP can identify molecular signatures that are clinically relevant for diagnosis, risk stratification and therapeutic targeting.

5.1.1.1 DNA Microarray

In DNA microarrays, DNA sequences (termed probes) are deposited on the surface of a 2D or 3D chip and 'probe' a sample for target nucleic acids of interest. Labelled target nucleic acid is hybridised to the attached probes. The relative concentration of bound targets is then detected by various methods, including fluorescence, radioactive signal and chemoilluminescent detection. Because 1000s of probes can be bound on a chip, a microarray can effectively detect almost all genes in a genome. Increasing knowledge of the DNA sequence in species has allowed shorter, more specific probes to be developed. Development of automated robotic systems, progress in chip production and improvements in fluorescent detection techniques have made DNA microarray an affordable method to detect a vast number of nucleotides rapidly.

Microarrays are primarily used to assess gene expression. For this, RNA is extracted from cells of interest, converted into its complementary cDNA, labelled and run on the microarray chip to give a comprehensive measurement of transcript levels in a sample. (Richter et al., 2002) Microarrays have also been combined with chromatin immunoprecipitation to assess DNA binding sites of transcription factors or epigenetic marks. (Solomon et al., 1988, Horak and Snyder, 2002) Microarrays can also be used in genotyping to screen for single nucleotide polymorphisms (SNP) in a genome. (Matsuzaki et al., 2004) The limitation of microarray technology is that it is an indirect method of quantifying nucleotide concentration. Hybridisation kinetics and efficacy of detection methods may lead to false readings. Background signal noise and saturation mean that this method is poor at detecting low level and highly expressed transcripts. Furthermore, a microarray can only detect what it is designed to. Direct sequencing techniques of the nucleic acids of interest are fast superseding microarray technology. However, many seminal studies have used microarray to generate publicly available datasets and examination of microarray data is well validated. As such, microarray data has an important place in understanding normal and disease biology. (Bumgarner, 2013)

5.1.1.2 RNA-seq

Sanger sequencing or the chain termination method, is based upon the irreversible incorporation of chain terminating dideoxynucleotides (ddNTPs) in a PCR reaction. A sample is run in 4 parallel reactions, with all 4 normal dNTPs (adenine, guanine, cytosine and thymine) and 1 type of ddNTP. This results in different lengths of product DNA with a particular base at the chain-terminating end. These products can be run on a gel and the sequence computed thereafter. Sanger sequencing is highly accurate and generates long sequence reads that can be mapped onto a reference genome. (Sanger and Coulson, 1975) However, it is time consuming, low throughput and expensive. In NGS, DNA fragments are anchored to a solid surface and sequenced *in situ*. Fluorescently labelled ddNTPs are incorporated reversibly, 1 nucleotide at a time, the signal read and the process repeated in an automated process. NGS is a high throughput sequencing technique that allows the entire genome, exome, transcriptome or epigenome to be sequenced and quantified rapidly. (Mortazavi et al., 2008)

RNA-seq specifically generates data on global gene expression of an organism or tissue. RNA is extracted from cells of interest and converted into a library of cDNA fragments, 200-500bp in length. cDNA is fragmented as elongation of the PCR reaction leads to errors in sequencing. Adaptors are attached to one or both ends of the cDNA to allow initiation of the sequencing reaction. Each fragment is then sequenced from one end (single end read) or both ends (paired end reads) to obtain short sequences or reads, 100-150bp in length. These reads are either aligned to a reference genome or transcriptome, or assembled *de novo* to produce a transcription map.

RNA-seq has advantages over other high throughput gene expression methods, such as microarray based methods. First and foremost, RNA-seq allows the measurement of the entire transcriptome, without the need for the underlying genomic sequence to be known. Additionally, transcript and splice variants can also be detected. RNA-seq is a direct measure of the transcript level and as such, does not have background signal noise nor is it saturated at high transcript levels, unlike hybridisation techniques. Therefore RNA-seq has a large range of transcript detection, estimated as 5 orders of magnitude in a study of murine transcriptomes. (Mortazavi et al., 2008) Thus it is superior to microarray in detecting low and highly expressed genes. Direct measurement of the transcriptome also means that RNA-seq data from different experiments, tissue and platforms should, in theory, be easier to compare without complex normalisation processes. As such, RNA-seq is superseding microarray in the research setting.

RNA-seq has its challenges. To be compatible with deep sequencing techniques, mRNA must be converted into cDNA fragments 200-500bp in length. Fragmenting techniques can bias outcome. Furthermore, as short transcript reads are sequenced, a transcript can map onto multiple sites of the reference genome. Paired end reads, in which a DNA fragment is sequenced from both ends, can minimise these errors. A consideration in an RNA-seq experiment is read depth and coverage. Coverage is the percentage of the transcriptome that is surveyed and is proportional to the read depth. That is, the number of times a transcript

is sequenced. In general, coverage of 80% is achieved by reading a transcript 30-40 times. More sequencing depth will increase coverage and detect rare transcripts, but this needs to be balanced with increased cost. RNA-seq has data storage implications. RNA-seq produces a large quantity of data that must be stored, processed and analysed efficiently and accurately. Such analysis is still expensive and time consuming, although costs are decreasing and developments in pipe-lines and software are making analysis easier. (Wang et al., 2009) Clinical application of GEP does not necessarily require sequencing of the entire transcriptome, but rather key pathways that have clinical relevance. GEP needs to be rapid and cost effective in order to be adopted as part of standard work-up in disease diagnosis. In this context, microarray and limited high throughput technology targeting specific genes or pathways may be more appropriate than global RNA-seq techniques.

5.1.2 Transcriptional analysis in normal HSCs

In stem cell biology, GEP has given insight into the molecular programmes defining stem and progenitor cells, biological processes important in stem cell function and mechanisms of normal stem cell ageing.

5.1.2.1 Defining the HSC molecularly

The HSC is defined as a pluripotent primitive cell, capable of self-renewal and production of multilineage progenitor daughter cells. Functionally, the HSC is capable of long term engraftment (>16w) of all lineages in primary and secondary transplant recipients. Immunophenotypic characterisation of the HSC suggests that, in general, LT-HSCs reside in the $Lin^{-}Sca\text{-}1^{+}cKit^{+}CD150^{+}CD48^{-}$ (SLAM) population in mice (Kiel et al., 2005) and the $CD34^{+}CD38^{-}$ compartment in humans (Bonnet and Dick, 1997). (Section 1.3.1.2) Transcriptome analysis has attempted to define HSCs further by their gene expression profile.

Several studies have investigated stem cell populations at different stages of development and from different tissues to identify a universal stem cell signature. Using microarray technology, Ivanova *et al* investigated the gene expression in primary murine FL-HSCs, BM-HSCs, cultured murine neural crest

and ES cells and human FL-HSCs, to find a 238 stem cell signature that was conserved over tissue type and species. These included genes involved in stem cell maintenance such as *Edr1*, *Tcf3* and cell cycle regulators including *Efnb2* and *Hes1*. (Ivanova et al., 2002) Ramalho-Santos *et al* performed similar experiments comparing murine HSCs neural stem and ES cells with corresponding differentiated tissue and overlapped differentially expressed genes from each tissue type to derive a 230 gene stem cell signature. Assessment of functional clustering showed that many of these genes were involved in signalling pathways, including signals from the microenvironment, such as integrinα6/β1, *Adam9* and *Smad1/2*. Other enriched clusters were the ubiquitin pathway and transcriptional regulatory pathways. (Ramalho-Santos et al., 2002)

Other investigators have looked at defining the molecular signature of HSCs in comparison to more differentiated haemopoietic cells. Transcriptional data from HSCs has been compared with data from committed progenitors including MPP, CMP, GMP, MEP, CLP, pro-B and pro-T progenitor populations. HSCs express self-renewal pathways, while progenitors downregulated these pathways. Instead, progenitors express genes related to haemopoietic differentiation, immune regulation and metabolism. In addition, as progenitors become more differentiated, their gene expression is progressively lineage restricted. (Akashi et al., 2000, Terskikh et al., 2003) Venezia *et al* investigated the molecular profile by microarray of murine HSCs (defined as SP based on Hoechst 33342 efflux) at steady state and HSCs stimulated to proliferate after *in vivo* treatment with 5-FU at multiple time-points up to 30d post injection. DEGs upregulated in 5-FU treated HSCs were hypothesised to denote a 'proliferation signature'. Gene ontology analysis showed that 5-FU treated HSCs upregulated genes pertaining to DNA replication, ATP synthesis and nucleotide and protein biosynthesis. DEGs downregulated in 5-FU treated HSCs were hypothesised to denote a 'quiescence signature'. Gene ontology also demonstrated that downregulated DEGs were enriched for inhibitors of cell cycle and stem cell maintenance genes including *c-fos*, *Gata2*, *Nfatc*, *Hdac5*, *Tie1* and *Igflr*. (Venezia et al., 2004) Kent *et al* found that the $CD45^{+}EPCR^{+}CD48^{-}CD150^{+}$ ESLAM defined HSC in murine FL and adult (8-12w) BM was highly enriched for LT-HSCs, while the $CD45^{+}EPCR^{+}CD48^{-}CD150^{-}$ compartment was enriched for ST-HSCs with short term repopulating ability.

RNA sequencing of the ESLAM, $CD45^{+}EPCR^{+}CD48^{-}CD150^{+}$ and Lin^{-} cells in FL and adult found that ESLAM cells (enriched for LT-HSCs) expressed significantly elevated levels of *Vwf*, *Rhob*, *Pld3*, suggesting these genes gave rise to high self-renewal in stem cells. (Kent et al., 2007) Using microarrays, Forsberg *et al* compared the gene expression of quiescent HSCs with MPPs, mobilised HSCs and LSCs from a murine MPN model. A 93 gene signature characterising normal quiescent HSCs was identified. This signature displayed enrichment of components of the extracellular matrix (ECM) and cell-to-cell interactions, including biglycan, *Angpt1* and *Jam1*, implicating the BM microenvironment's role in maintaining quiescence in HSCs. (Forsberg et al., 2010) Cabezas-Wallscheid *et al* performed comprehensive integrated analysis of the proteome, transcriptiome and methylome of adult (8-12w) murine HSCs and MPP populations (MPP1-4). At the protein and transcriptional level, HSCs expressed pathways related to stem cell maintenance and preservation, including immune defence, detoxification against cellular stress and anaerobic metabolic programmes, which are employed by quiescent stem cells. In addition, self-renewal pathways including the Wnt and BMP signalling pathway were also enriched in HSCs. In contrast, MPPs expressed pathways and genes related to DNA metabolism, proliferation and DDR and repair mechanism. Furthermore, with differentiation to MPP4 there was a progressive difference in differentially methylated regions. This was anti-correlated to gene expression, with methylated regions in progenitors populations corresponding to the regulatory domains of stem cell associated genes, including *Hoxb*2, *Rorc* and *Cd34*. (Cabezas-Wallscheid et al., 2014) Overall, studies like the examples above have enhanced the understanding of genes important for stem cell maintenance, quiescence and self-renewal.

5.1.2.2 Molecular characterisation of HSCs throughout ontogeny

In murine haemopoietic development, FL HSC are highly cycling up to 3w of age with enhanced repopulating ability in transplantation studies. (Rebel et al., 1996, Bowie et al., 2007b) Adult HSCs in both the murine and human system are quiescent, cycling rarely. (Leemhuis et al., 1996, Gothot et al., 1997) As the haemopoietic system ages, there is an increase in HSC number but functional decline, with reduced serial repopulating ability and myeloid predominance at

the expense of lymphoid output. (Morrison et al., 1996b) Transcriptome analysis has provided insight on the molecular signatures that distinguish HSCs at different stages of ontogeny. In addition, changes in gene expression have identified pathways critical in changing HSC phenotype in foetal, adult and aged HSCs.

Comparison of transcription of HSCs at different developmental ages has aided understanding of the molecular basis for differences in HSC phenotype with age. In the developing haemopoietic system, HSCs and related tissue derived at various stages of embryonic development (yolk sac, placenta, AGM, E12.5, E13.5 and E14.5) and adult BM (6-8w) cluster into 3 transcriptional states. These are characteristic of the definitive yolk sac (yolk sac derived HSCs), HSCs undergoing specification (placenta, AGM and a subset of E12.5), and definitive HSCs (E13.5, E14.5, BM and a subset of E12.5). It is interesting that FL cells beyond E12.5 cluster with adult HSCs when they are phenotypically so different. This suggests that the transcriptional landscape of FL cells beyond E12.5 is very different to HSCs at a very early embryonic developmental stage (earlier than E12.5). These primitive HSCs do not share the same transcriptional programmes as FL HSCs ≥E12.5 and definitive HSCs from the BM, and may reflect the endothelial origin of primitive HSCs. (McKinney-Freeman et al., 2012) The adult ageing haemopoietic system has also been investigated. In one study, GEP in LT-HSCs from young adult (2-3m) and old adult (22-24m) mice was investigated using microarray. Functionally, old HSCs have enhanced self-renewal and restricted B-lymphoid potential with a trend towards increased myeloid lineage (as demonstrated in primary BMT recipients). Transcriptionally, old HSCs exhibit upregulation of cell signalling pathways, genes related to leukaemia (many of which play a role in normal haemopoietic homeostasis) and myeloid specification, while pathways relating to lymphoid specification were downregulated. (Rossi et al., 2005) Comprehensive integrated genomic analysis of HSCs from young adult (4m) and old adult (24m) mice show changes in the transcriptome, DNA methylation and histone modification that contribute to increasing DNA instability with increasing age. Genes involved in cell adhesion, proliferation and protein synthesis are upregulated in old adult HSCs while there is a downregulation of genes related to DNA replication, DNA repair and cell

cycle (eg. *Smad3*, *Sp1*, *Erg1*, *Cebpa* and *Nr4a1*). Epigenetic modifiers, which have been implicated in the pathogenesis of leukaemia and other cancers, also show differing expression with age. These include members of the polycomb group: *Ezh1* increases with age while *Ezh2* and *Cbx2* decrease with age. The Tet family of DNA dioxygenases and the DNMT family of methyltransferases also decrease with increasing age. Histone and methylation status were also investigated. In both young and old HSCs, some genes had both activating H3K4me3 and repressive H3K27me3 histone marks. These bi-valent genes likely represent master transcriptional regulators that are poised for activation. These included genes important for haemopoietic differentiation (*Cebpa*, *Ebf1*, *Pax5*, and *Gata3*) and signalling pathways (*Wnt*, *Hh*, *Bmp*, and *Tgfß*). However, old adult HSCs exhibit broader H3K4me3 peaks across HSC identity and self-renewal genes, suggesting activation of these pathways. In addition, old adult HSCs showed hypomethylation at binding site of transcription factors important in self-renewal and in oncogenesis, including *Myc* and *Bcl2* and hypermethylation at transcription factor binding sites associated with differentiation-promoting genes combined with a reduction at genes associated with HSC maintenance. (Sun et al., 2014)

Transcriptional studies have also highlighted key genes and pathways that are critical for HSC function and survival at a particular developmental age, while redundant at other ages. Temporal changes in the expression of these key regulators drive developmental changes in HSC phenotype. Many of these genes have been identified by comparison of stem cell populations at different developmental stages or with progenitor populations.

In adult HSCs, *Bmi1* and *Etv6* are essential for HSC maintenance and self-renewal but are not required for HSC function in the foetal HSCs (Park et al., 2003, Hock et al., 2004b), while *Cebpa* and *Gfi1* regulate adult HSC quiescence (Ye et al., 2013, Hock et al., 2004a). BMI1 is a component of the polycomb repressor complex 1. *Bmi1*$^{-/-}$ mice aged 4-5w had a 10-fold reduction in absolute HSC number compared to WT and heterozygous controls. In BMT studies, total BM from 5w old *Bmi1*$^{-/-}$ mice show significantly reduced short-term engraftment compared to WT and heterozygous controls, and no long-term engraftment in

primary recipients. In contrast, total FL cells from *Bmi1*$^{-/-}$ mice have no reduction in HSC number compared to WT controls and BMT of FL from *Bmi1*$^{-/-}$ mice results in short-term engraftment in primary recipients, although long-term engraftment is impaired. This indicates that *Bmi1* is essential for HSC maintenance and self-renewal in adult HSCs but is not crucial for foetal haemopoiesis. GEP using microarray shows that, relative to aged matched WT controls, FL-HSCs from *Bmi1*$^{-/-}$ mice exhibit significantly fewer DEGs compared to adult BM from *Bmi1*$^{-/-}$ mice. In particular, the inhibitors of cell cycle progression, p16 and p19, are upregulated in adult *Bmi1*$^{-/-}$ HSCs but not FL *Bmi1*$^{-/-}$ HSCs. (Park et al., 2003) C/EBPα is a transcription factor that regulates granulopoiesis. In FL HSCs it also has a role in the negative regulation of self-renewal, and *Cebpa*$^{-/-}$ mice have enhanced repopulation activity despite no increase in HSC number. (Zhang et al., 2004) Using the *Mx1-Cre*$^{+}$*Cebpa*$^{fl/fl}$ mouse model, *Cebpa* gene deletion is induced by administration of pIC. Adult *Cebpa* KO HSCs show an increase in phenotypic and functional HSCs demonstrated by flow cytometry and LDA, respectively. *Cebpa* KO adult HSCs display increased proliferation compared to WT controls, which was maintained in donor derived HSCs from *Cebpa* KO mice in secondary transplant recipients, suggesting that C/EBPα regulates quiescence. Interestingly, GEP of *Cebpa* KO and WT adult HSCs and WT FL HSC showed that KO *Cebpa* HSC clusters with FL HSCs. Furthermore, GSEA showed an enrichment of foetal transcriptional programmes in *Cebpa* KO adult HSCs. Conversely, overexpression of *Cebpa* in foetal HSC induces quiescence. *Cebpa* gene expression increases with increasing age with a 2-fold increase in 4w HSCs compared to 2w HSCs. Thus, the authors hypothesise that the increase in C/EBPα levels may mediate the foetal to adult switch in HSC phenotype. (Ye et al., 2013)

Genes critical for foetal HSC generation, maintenance and self-renewal include *Sox17*, *Ezh2*, *Lin28b* and *Hmga2*. *Sox17* is highly expressed in foetal HSCs but expression falls rapidly after 4w of age. *Sox17*$^{-/-}$ embryos fail to develop HSCs and conditional deletion of *Sox17* in E14.5 and neonates results in a marked reduction in HSC number, showing that *Sox17* is required for HSC generation and maintenance of foetal HSCs. However, conditional deletion of *Sox17* in mice >4w old has no effect on HSC number or function. (Kim et al., 2007) Furthermore,

retroviral expression of *Sox17* in adult (8w) HSCs increases their multilineage reconstituting potential in primary recipients with a slight myeloid predominance, akin to transplantation with FL HSCs. (He et al., 2011) EZH2, a component of the polycomb repressive complex 2, is required for FL HSC maintenance. Tamoxifen mediated conditional deletion of *Ezh2* in haemopoietic and endothelial cells, using the *Tie2-Cre;Ezh2*$^{fl/fl}$ mouse model, results in embryonic death in mid-gestation due to anaemia, and significantly reduced numbers of HSCs in the FL at E14.5, despite similar HSC numbers in the yolk sac of *Tie2-Cre;Ezh2*$^{fl/fl}$ and *Tie2-Cre;Ezh2*$^{+/+}$ controls. Deletion of *Ezh2* in adult BM does not affect the reconstitution potential of adult HSCs, although lymphoid differentiation is impaired. Interestingly, transplantation of *Tie2-Cre;Ezh2*$^{fl/fl}$ FL cells results in long-term reconstitution in 50% of primary recipients, albeit with severe lymphopoiesis, indicating that *Ezh2* is required for foetal HSC maintenance but not self-renewal. (Mochizuki-Kashio et al., 2011) Transcriptional analysis by microarray comparing FL and adult BM (8-12w) derived WT LSKs reveal that FL-LSKs have enhanced expression of *Lin28b*. LIN28B is an inhibitor of the *Let-7* family of inhibitory microRNAs that inhibit gene expression, including *Hmga2*. Further investigation of the *Lin28b* pathway by RT-PCR shows upregulation *Lin28b* and its downstream target *Hmga2* in FL LSKs and HSCs compared to adult LSKs and HSCs, whereas the *Let-7* family is downregulated in FL populations. In addition, *Lin28b* and *Hmga2* expression fall abruptly after 3w of age. Overexpression of *Lins28b* or *Hmga2* in adult HSCs confers enhanced self-renewal akin to normal FL HSCs, demonstrated as increased repopulating ability in primary and secondary recipients post BMT. Conversely, *Hmga2*$^{-/-}$ KO mice can generate HSCs but FL-HSCs displayed a 10-fold reduction in self-renewal capacity (by transplantation assay) compared to WT FL HSC controls. The authors hypothesise that the *Lin28b-Let-7-Hmga2* axis may control the switch from a foetal to an adult HSCs phenotype.(Copley et al., 2013)

5.1.3 Transcriptional and genomic analysis in human AML

In human leukaemia, transcriptome analysis, genome sequencing for gene mutations, and epigenetic profiling have aided the understanding of leukaemia biology. These techniques have identified prognostically significant AML

subtypes, provided insight into understanding important biological processes explaining treatment resistance, and identified potential therapeutic targets.

5.1.3.1 Transcriptional analysis in human AML

Many studies have investigated GEP of human AML using microarray technology to understand the biological processes underlying the disease. These studies have shown that cytogenetically defined AML subtypes, such as t(15;17), t(8;21) and inv(16) have a distinctive molecular signature. (Schoch et al., 2002, Valk et al., 2004, Ross et al., 2004, Haferlach et al., 2010, Balgobind et al., 2011a) Assessment of molecular signatures has provided insight into the biology of AML subtypes. Ross *et al* investigated a molecular signature to define acute leukaemia (AML or ALL) with abnormalities of the MLL gene. They found that MLLr acute leukaemia had a distinct molecular signature, regardless of lineage, which included expression of *MBNL1*, *MEIS1*, *HOXA4*, *HOXA5*, *HOXA9 HOXA10* and *MYH9*. However, leukaemia in which there was partial tandem duplication of the MLL gene (*MLL-PTD*) did not cluster with MLL rearranged disease, suggesting it is a distinct entity. (Ross et al., 2004) In addition, GEP has identified new AML subtypes with prognostic predictive significance that can only be defined by their gene expression profile. In particular, GEP helps predict outcomes in the heterogeneous cytogenetically normal group of patients with intermediate risk. (Bullinger et al., 2004, Valk et al., 2004) One of the largest studies by Valk *et al* investigated GEP in 285 patient samples (aged 15-78y). Sixteen molecularly defined clusters were discovered. Some were discriminated based on established chromosomal abnormalities, including t(15;17), t(8;21), inv(16) and MLLr, and genetic mutations including *CEBPA*. However, previously undefined groups were identified, based solely on GEP. One cluster in particular (cluster 10) was predictive of inferior OS and EFS due to an increased RR. The molecular profile of normal $CD34^+$ HSCs overlapped with cluster 10 AML, suggesting that the molecular profile of treatment resistance may transcriptionally resemble stem cell programmes. (Valk et al., 2004)

Paediatric AML has also been investigated specifically in some studies. Yagi *et al* investigated 54 paediatric AML samples (age 6d-14y, APL excluded) to identify a molecular signature that could predict outcome. They found a 35 gene

expression signature predictive of good prognosis and poor prognosis, measured by EFS. Expression of cell cycle progression regulators and anti-apoptotic genes were upregulated in poor prognosis disease. (Yagi et al., 2003) Ross *et al* performed GEP by microarray in 130 paediatric AML samples (age up to 15y). Similar to adult studies, t(15;17), t(8;21) and inv(16) expressed distinctive molecular signatures which could predict their respective chromosomal abnormality in both paediatric and adult cohorts. In addition, AMKL (FAB subtype M7), which is common in paediatric AML, also exhibited a distinctive molecular profile. Interestingly, the 35 gene signature for poor prognosis devised by Yagi *et al* was not predictive of adverse outcome in this cohort. (Ross et al., 2004) Balgobind *et al* investigated GEP in 237 paediatric AML samples for diagnostic molecular signatures. As previously demonstrated, t(15;17), t(8;21) and inv(16) had molecular signatures with high predictive value in a validation cohort. In addition, the authors found discriminating signatures for MLLr and t(7;12). In contrast, while gene mutations including, *NPM1* and *KIT* mutations, *FLT3-ITD* and *MLL-PTD* had molecular signatures discriminating them from other AML subtypes, these were not predictive in the validation cohort. (Balgobind et al., 2011b)

Groups have investigated if GEP could replace standard diagnostic techniques for risk stratification in AML. However, there is marked heterogeneity between studies. A meta-analysis of 25 gene expression profiling studies including 2744 patient samples looked to identify unifying genes expression profiles that were predictive of favourable and poor risk disease. While paediatric cohorts were included, the majority of patients were adults. Surprisingly, only 9.6% of genes were deregulated in the same direction according to clinical outcome across the studies. However, the authors did identify functional gene ontology categories that were up- or down- regulated in favourable and poor risk disease. The top differentially expressed processes in favourable risk disease included upregulation of the protein kinase cascade and RNA metabolic processes and downregulation of cell division, cell cycle regulation and mitosis. Poor risk disease was associated with the opposite expression pattern. (Miller and Stamatoyannopoulos, 2010) In addition, while GEP can predict t(15;17), t(8;21), inv(16), *NPM1* mutations and *CEBPA* mutations with a high positive and negative predictive value, other prognostically significant anomalies such as *FLT3*

mutations and MLLr cannot be accurately predicted using GEP alone. (Verhaak et al., 2009) Therefore, GEP will complement rather than replace standard diagnostic techniques.

5.1.3.2 Genome sequencing in AML

NGS has been utilised to gain insight into the mutational landscape of AML and enabled better understanding of the evolution of disease. Ley *et al* first described whole genome sequencing of a patient with FAB subtype M1 AML in which 10 acquired mutations were identified. (Ley et al., 2008) Since then, studies using whole genome, whole exome and targeted gene sequencing have resulted in better understanding of the genetic landscape of AML. This includes the discovery of novel driver mutations such as *IDH1* and *DNMT3A* and patterns of mutational co-operation and mutual exclusivity. (Mardis et al., 2009, Ley et al., 2010, Cancer Genome Atlas Research et al., 2013) Furthermore, sequencing data paralleled with clinical outcome has identified mutations that can predict disease outcomes including treatment failure and relapse risk. (Kihara et al., 2014, Papaemmanuil et al., 2016)

The largest study investigating genome sequencing in AML was undertaken by Papaemmanuil *et al*. Targeted DNA sequencing of 111 genes, known to drive cancer, was performed in 1540 adult patients with AML. At least 1 driver mutation was identified in 96% of patients and 86% of patients had 2 or more driver mutations. With correlation to clinical outcome, groups of mutually exclusive co-mutated genes were identified. Established cytogenetic risk groups, as defined by the WHO, such as t(15;17), t(8;21), inv(16)-t(16;16), t(6;9), inv(3)/t(3;3) and MLL fusion genes could also be discriminated based on mutation pattern. AML with *NPM1* mutations was also a genetically defined category. In addition, new subtypes of AML, defined by the pattern of co-mutations that were predictive of clinical outcome were also identified. These included AML with *TP53* mutations and/or chromosomal aneuploidy, AML with mutated chromatin and/or RNA splicing genes and AML with $IDH2^{R172}$ mutation. These subtypes would have been designated intermediate risk in standard classification systems. Furthermore, the authors found that clinical outcome depended not only on a mutation, but its co-occurrence with other mutations.

NPM1 mutations in general are considered a favourable molecular subtype. However, co-expression with both *FLT3-ITD* and *DNMT3A* mutations was associated with very poor outcome. Conversely, co-expression of NPM1 mutation with mutations in both NRAS and DNMT3A was associated with a favourable outcome. (Papaemmanuil et al., 2016) While this study was performed on an adult cohort, it highlights the genetic complexity of AML and targeted gene sequencing can have prognostic benefit.

Genome sequencing in paediatric AML (up to 18y) was investigated by Shiba *et al*. WES of 22 AML samples revealed on average 5 mutations per sample. In addition to known mutational drivers of paediatric AML, WES identified mutations in the components of the cohesion complex and epigenetic regulators. These, along with more common drivers of AML, were investigated by targeted gene sequencing in an additional 182 samples (total n=204). Mutations in the components of the cohesion complex (*RAD21*, *SMC3*, *STAG2*) were present in 8.3% of samples. Patients with these mutations had a similar outcome to patients without cohesin complex mutations (OS of 76% versus 71% in non-mutated patients). This is in contrast to the results from adult data in which mutations in the chromatin-cohesin complex results in inferior outcome. (Papaemmanuil et al.) Mutations in the epigenetic regulators *ASXL1/2* were identified in 8.8% of patients and was associated with t(8;21) in 61% of cases. In this context *ASXL1/2* mutations did not impede the favourable outcome normally observed in t(8;21) disease. When not co-expressed with t(8;21), AML with *ASXL1/2* mutations had an increased RR, but patient were salvageable with HSCT. Therefore, unlike in adult AML, *ASXL1/2* mutations were not associated with worse clinical outcomes. Other mutations in epigenetic regulators identified at low frequency included *BCOR*/*BCORL1* (3.4%) and *EZH2* (<1%) and *IDH2* (<1%). Commonly mutated epigenetic regulators in adult AML, *DNMT3A* and *IDH1*, were not mutated in any of the paediatric samples investigated. In contrast, up to 40% of paediatric samples contained activating kinase mutations, including mutations in *NRAS*, *KRAS*, *KIT*, *MPL* and *FLT3-ITD*. Another interesting observation was that MLLr AML and AMKL (both of which was more prevalent in infant AML) had no or few additional somatic mutations, compared to other AML subtypes. (Shiba et al., 2016) This study highlights that mutations found in

paediatric AML may be different to adult AML and may not have the same clinical implications. (Section 1.3.6)

To date, only one study has directly compared genomic mutations in paediatric and adult AML. Marjanovic *et al* performed targeted exome sequencing of 48 cancer-related genes in 20 paediatric (1-16y) and 20 adult (25-73y) AML samples. The samples were not matched for cytogenetic anomaly. While both paediatric and adult AML had on average 3 mutations per patient, the genes and type of mutations were different. Paediatric AML almost exclusively contained missense mutations, while adult AML had a higher proportion of frame-shift mutations. In addition, mutations in *JAK3*, *ABL1*, *GNAQ* and *EGFR* (tyrosine kinases or related genes) were exclusively found in paediatric AML while mutations in *IDH1*, *APC*, *HNF1A*, *GNAS*, and *SMARCB1* (methylation and histone modifiers) were found exclusively in adult AML. (Marjanovic et al., 2016) This is further evidence that the pathogenesis and driver mutations in paediatric and adult AML are different and as such, may result in differences in phenotype and response to therapy.

The diagnostic work-up for AML includes morphology of BM smears, cytogenetic analysis including fluorescence *in situ* hybridisation, immunophenotyping by flow cytometry and qPCR for common gene mutations and fusion transcripts. However, with growing evidence for clinically significant AML subtypes characterised by unique gene expression profiles and the emergence of new mutations in leukaemia drivers, there is a move to incorporate GEP and NGS in the standard work up of AML in the clinic.

5.2 Aims

In chapter 4 the NH9 oncogenic model was used to show that young LSKs from FL and 3w are less susceptible to leukaemic transformation *in vivo* than adult LSKs from 10w and >52w. Several mechanisms have been postulated to explain this including; differences in the response to microenvironmental cues; acquisition of stem cell programmes; age dependent differences in DDR and repair; and mutational load. Additionally, young transformed LSKs could develop myeloid, lymphoid and mixed phenotype leukaemia while adult transformed LSKs were

myeloid restricted, suggesting differences in the expression of lineage determining programmes. To further investigate the mechanisms governing the aforementioned observations the transcriptional landscape of NH9 transforming cells from different ages was investigated. Specifically:

i) Utilising Fluidigm™ technology, the expression of genes important in mediating cues from the microenvironment was examined in untransduced WT LSKs and LSKs transformed *in vitro* and *in vivo* by NH9 from FL, 3w, 10w and >52w old mice.

ii) Utilising Fluidigm™ technology, the expression of genes crucial for stem cell properties and lineage determination was examined in untransduced WT LSKs and LSKs transformed *in vitro* and *in vivo* by NH9 from FL, 3w, 10w and >52w mice.

iii) Using global transcriptional sequencing (RNA-seq), age dependent transcriptional pathways discriminating *in vivo* generated AMLs from FL, 3w, 10w and >52w LSKs was examined.

5.3 Results - Fluidigm™

Untransduced WT LSKs and LSKs transformed *in vitro* at CFC2 (donor cells) and *in vivo* generated AMLs from 4 ages (FL, 3w, 10w and >52w) and *in vivo* generated ALL (FL and 3w) were assessed for gene expression using high output Fluidigm™ technology based qPCR. As lymphoid leukaemia developed *in vivo* from FL and 3w LSKs, genes important in lineage commitment and determination were investigated. As we hypothesise that differences in the response to microenvironmental cues may account for the findings, samples were assessed for the expression of genes related to microenvironmental signalling. Fold change values generated from the $2^{-\Delta\Delta CT}$ method from each pairwise comparison were assessed for data skew. (Figure 5.1) For a summary of genes investigated and primers used, see Appendix 2.

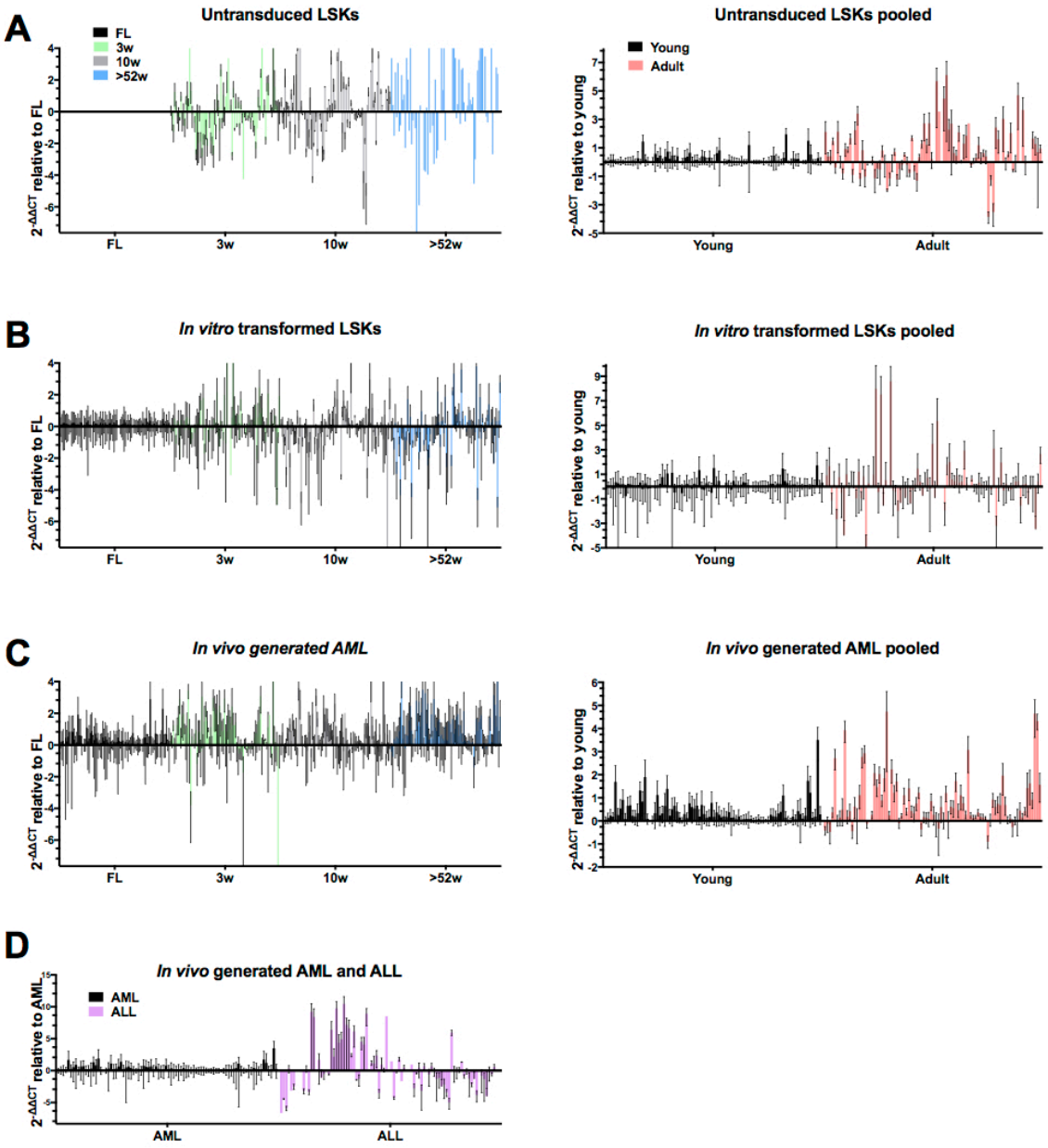

Figure 5.1 Pairwise comparisons from entire Fluidigm™ experiment showing distribution of change in gene expression

(A) Graphical representation of all $2^{-\Delta\Delta CT}$ values from untransduced LSKs. Left shows data from 4 ages relative to FL and right shows data pooled into young (FL and 3w) and adult (10w and >52w) relative to young. FL n=1, 3w n=3, 10w n=2, 52w n=1, young n=4, adult n=3.
(B) Graphical representation of all $2^{-\Delta\Delta CT}$ values from LSKs transformed *in vitro* by NH9 at CFC2. Left shows data from 4 ages relative to FL and right shows data pooled into young and adult relative to young. FL n=4, 3w n=3, 10w n=3, >52w n=4, young n=7, adult n=7.
(C) Graphical representation of all $2^{-\Delta\Delta CT}$ values from *in vivo* AML generated from NH9 transformed LSKs. Left shows data from 4 ages relative to FL and right shows data pooled into young and adult relative to young. FL n=4, 3w n=3, 10w n=4, >52w n=8, young n=7, adult n=12.
(D) Graphical representation of all $2^{-\Delta\Delta CT}$ values in AML and ALL generate *in vivo* from young (FL and 3w) LSKs transformed with NH9 relative to AML.
Graphs depict mean $2^{-\Delta\Delta CT}$ generated FC +/-SD

5.3.1 Young transformed cells express multiple lineage associated genes; adult transformed cells express stem cell associated genes

To investigate if the mixed lineage phenotype observed in young LSKs could be explained by the expression of multiple lineage transcription programmes, the expression of lineage commitment transcription factors and lineage defining genes was measured. In untransduced LSKs there was upregulation of *Csf3r*, a myeloid receptor and *Gata3*, a regulator for T-cell development, in 10w LSKs compared to 3w LSKs. When samples were pooled into young (FL and 3w) and adult (10w and >52w) *Gata3* remained upregulated in adult cells. Additionally, the myeloid associated genes, *Runx1* and *Tlr4* were also upregulated in adult LSKs, while another myeloid associated gene, *Irf8* was downregulated in adult LSKs. (Figure 5.2A) In FL and 3w LSKs transformed *in vitro* at CFC2 compared to adult LSKs transformed *in vitro* at CFC2 there was upregulation of genes of multiple lineages. These included *Gata1*, *Mpo* and *Irf8* (myeloid), *Klf1* and *Fcgr3* (erythroid) and *Il7ra* and *Bcl11b* (lymphoid). When age groups were pooled into young and adult, *Gata1*, *Mpo*, *Klf1*, *Il7ra* and *Bcl11b* remained upregulated in the young group. (Figure 5.2B) However, when these genes were investigated in *in vivo* transformed LSK, there was no difference in the expression of lineage genes. This was true when comparing 4 ages or pooling into young and adult. (Figure 5.2C) The results from a limited gene set suggests that at baseline there is increased expression of myeloid associated genes in adult LSKs compared to young LSKs. When an oncogene is introduced into the cell, but before the development of AML *in vivo,* FL and 3w cells retain lineage plasticity with the expression of both myeloid and lymphoid associated genes. However, this difference is less apparent at the transcriptional level when phenotypically defined myeloid leukaemia has developed from young and adult cells.

In contrast, genes associated with stem cell function and maintenance were upregulated in 10w and >52w LSKs transformed by NH9 *in vitro*. This included *Tal1* and *Epcr*, which were upregulated in adult cells, whether the age groups were analysed individually or pooled. The exception was the expression of *Mpl* which was downregulated in 10w and >52w or pooled adult cells. (Figure 5.3B) In *in vivo* transformed cells, *Mpl* was upregulated in 10w and 52w leukaemic cells.

Additionally, there was a trend toward upregulation of *cKit* and *Flt3* in 10w and >52w cells. (Figure 5.3C left) Only *Mpl* expression was significantly upregulated when age groups were pooled into young and adult. (Figure 5.3C right) Considering *Mpl* showed the opposite expression pattern in *in vitro* transformed cells, this suggests that adult cells continue to exhibit upregulated stem cell gene expression in the transformed cell. There was no difference between young and adult untransduced LSKs in the expression of stem cell associated genes. (Figure 5.3A) These results show that at early transformation adult LSKs upregulate stem cell genes in response to the oncogene. With progression to AML adult cells acquire more stem cell gene expression compared to young cells. As expression of stem cell signatures has been associated with more aggressive leukaemia, the higher expression of stem cell genes in adult cells relative to young cells may contribute to the shorter latency and 100% penetrance observed in the 10w and >52w groups.

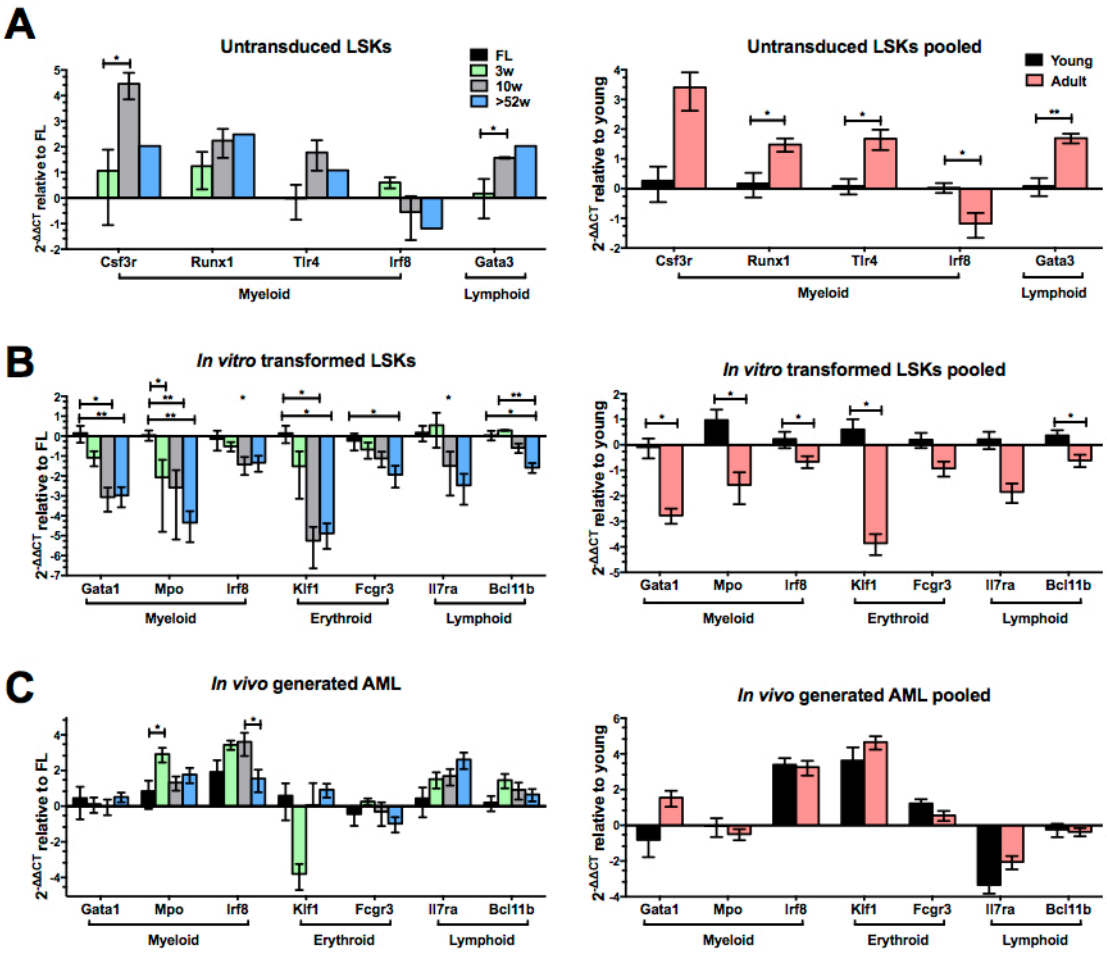

Figure 5.2 Expression of lineage associated genes in untransduced and transformed LSKs

(A) Relative gene expression of lineage genes in untransduced LSKs, comparing FL, 3w, 10w and >52w (left, FL comparator) and pooled young and adult (right, young comparator). FL n=1, 3w n=3, 10w n=2, 52w n=1, young n=4, adult n=3.
(B) Relative gene expression of lineage genes in LSKs transformed *in vitro* by NH9 at CFC2, comparing FL, 3w, 10w and >52w (left, FL comparator) and pooled young and adult (right, young comparator). FL n=4, 3w n=3, 10w n=3, >52w n=4, young n=7, adult n=7.
(C) Relative gene expression of lineage genes in *in vivo* AML generated from NH9 transformed LSKs, comparing FL, 3w, 10w and >52w (left, FL comparator) and pooled young and adult (right, young comparator). FL n=4, 3w n=3, 10w n=4, >52w n=8, young n=7, adult n=12.
Graphs depict mean $2^{-\Delta\Delta CT}$ generated FC +/-SD. For 4 way comparisons, significance determined by 1-way ANOVA and Bonferroni post-test. For pairwise comparisons, significance determined by Student's t-test, *p<0.05, **p<001, ***p<0.001.

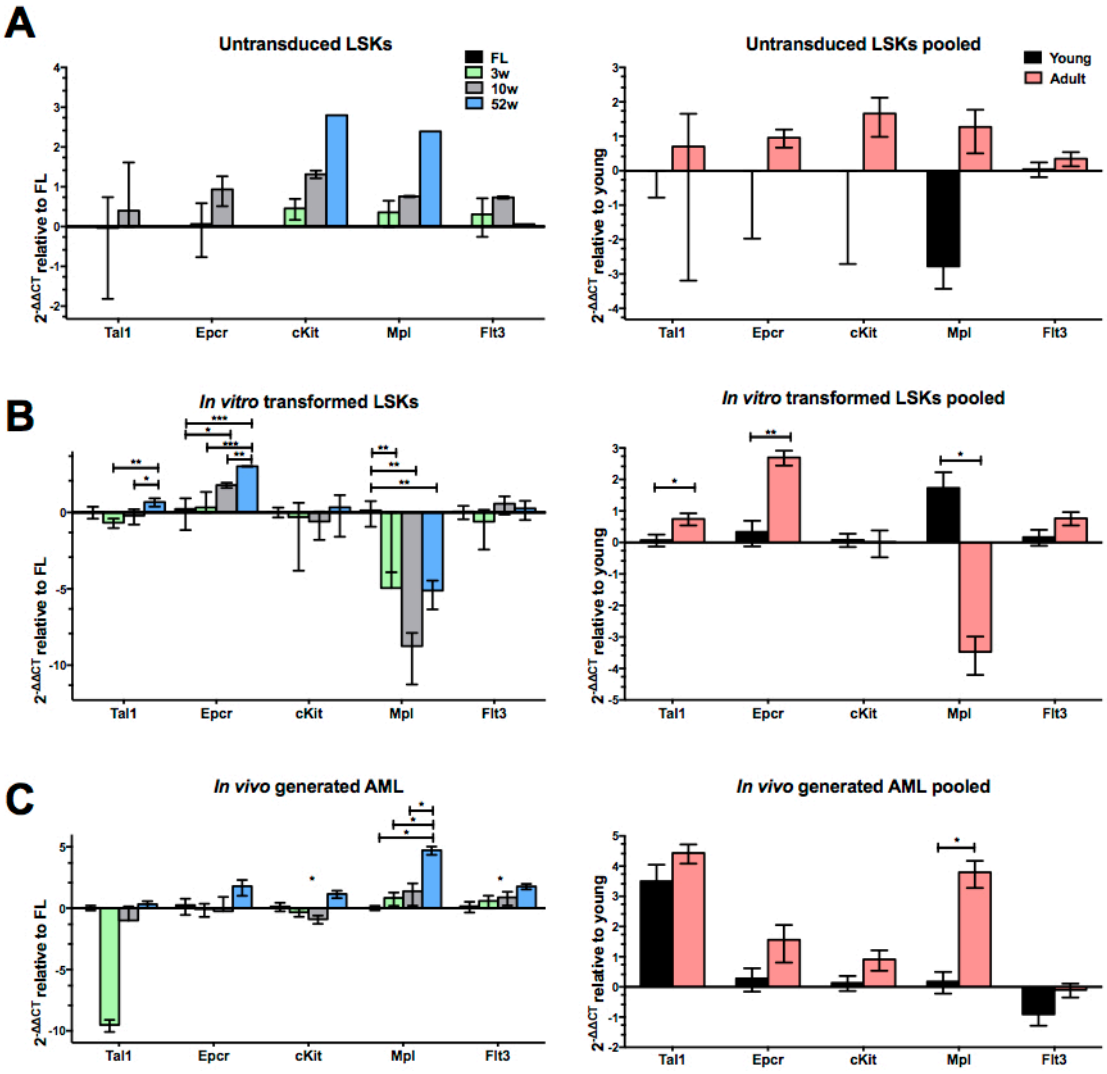

Figure 5.3 Expression of stem cell associated genes in transformed LSKs

(A) Relative gene expression of stem genes in untransduced LSKs, comparing FL, 3w, 10w and >52w (left, FL comparator) and pooled young and adult (right, young comparator). FL n=1, 3w n=3, 10w n=2, 52w n=1, young n=4, adult n=3.
(B) Relative gene expression of stem cell genes in LSKs transformed *in vitro* by NH9 at CFC2, comparing FL, 3w, 10w and >52w (left, FL comparator) and pooled young and adult (right, young comparator). FL n=4, 3w n=3, 10w n=3, >52w n=4, young n=7, adult n=7.
(C) Relative gene expression of stem cell genes in AML generated from NH9 transformed LSKs, comparing FL, 3w, 10w and >52w (left, FL comparator) and pooled young and adult (right, young comparator). FL n=4, 3w n=3, 10w n=4, >52w n=8, young n=7, adult n=12.
Graphs depict mean $2^{-\Delta\Delta CT}$ generated FC +/-SD. For 4 way comparisons, significance determined by 1-way ANOVA and Bonferroni post test. For pairwise comparisons, significance determined by Student's t-test, *p<0.05, **p<001, ***p<0.001.

5.3.2 ALL cells express lymphoid transcriptional programmes compared to AML cells, matched for age of donor cell

One recipient from each of the FL and 3w groups developed ALL (n=2 in total). The expression of lineage associated genes was investigated in these 2 cases of ALL generated *in vivo*. Compared to AML generated from young transformed

LSKs, ALL had lower expression of the myeloid genes *Cebpb*, *Cebpe* and *Fcgr3*. (Figure 5.4A) However, the B-lymphoid genes *CD79a*, *B220*, *Pou2af1*, *Foxo1* and *Vpreb1* were upregulated in ALL. (Figure 5.4B) In addition, the T-lymphoid associated genes *Rag1*, *Rag2*, *Ilr7a* and *Flt3* were also upregulated in ALL. (Figure 5.4C) This suggests that the transcriptional landscape of ALL is characterised by the expression of both B and T-lymphoid programmes, reflecting the lymphoid phenotype determined by flow cytometry and IHC.

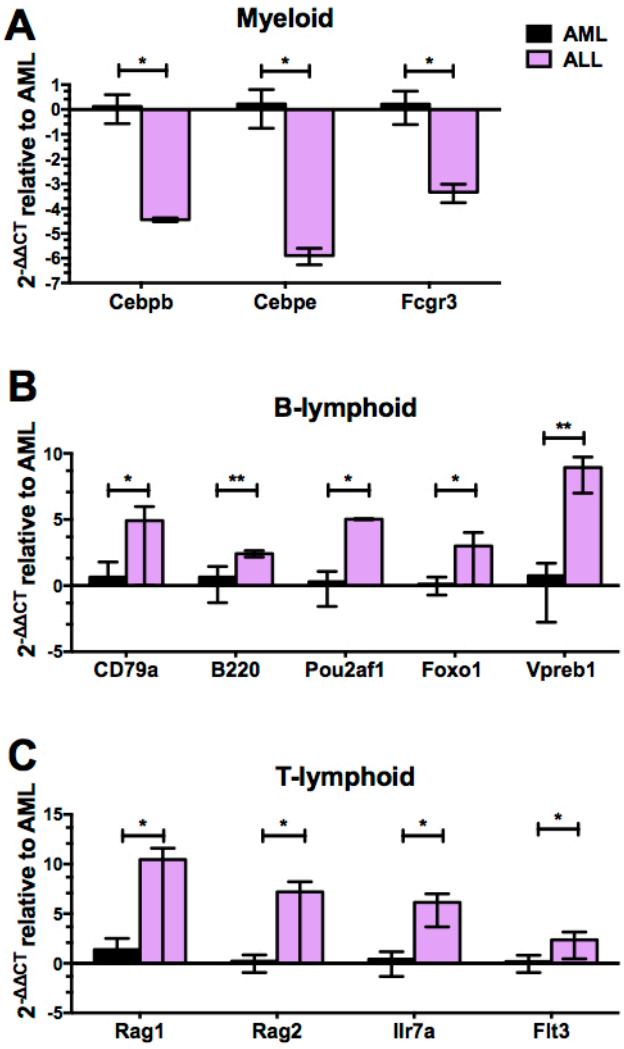

Figure 5.4 ALL generated for young LSKs expresses lymphoid associated genes while AML expresses myeloid associated genes

(A) Relative gene expression of myeloid genes in AML and ALL generated *in vivo* from young LSKs transformed with NH9.
(B) Relative gene expression of B-lymphoid genes in AML and ALL generated *in vivo* from young (FL and 3w) LSKs transformed with NH9.
(C) Relative gene expression of T-lymphoid genes in AML and ALL generated *in vivo* from young (FL and 3w) LSKs transformed with NH9.
Graphs depict mean $2^{-\Delta\Delta CT}$ generated FC +/-SD (compared to young AML as comparator). Significance determined by Student's t-test, *p<0.05, **p<001, AML n=7, ALL n=2.

5.3.3 The BMP pathway is upregulated in adult transformed cells

We hypothesise that differences in the response to extrinsic cues from the adult microenvironment could explain the longer latency to disease, incomplete penetrance and mixed lineage phenotype observed in young LSKs. Therefore, we assessed the expression of genes important in transducing signals from the microenvironment in untransduced WT, *in vitro* transformed and *in vivo* generated leukaemia from FL, 3w, 10w and >52w LSKs. Untransduced LSKs showed no difference in the expression of the BMP pathway with cellular age. (Figure 5.5A) In the presence of oncogene *in vitro*, CFC2 donor cells showed upregulation of type 1 and type 2 BMP receptors and the transducer *Smad1* in adult LSKs, while *Nog*, the inhibitor of the pathways was downregulated in adult *in vitro* transformed LSKs. This was observed both when the 4 ages were analysed individually or pooled into young and adult, suggesting that adult cells specifically upregulate the BMP pathway in response to oncogene whereas young cells do not. Further investigation of the BMP pathway in CFC2 donor cells revealed an upregulation of the gene target *Id3* in adult cells, which behaves as an oncogene when overexpressed. (Man et al., 2016, Perk et al., 2005) Interestingly, another gene target of the BMP pathway, *Creb3l1*, was upregulated in young LSKs; this gene has been implicated in having a tumour suppressor role in solid tumours. (Rose et al., 2014) This was observed whether the data were analysed in 4 separate groups or pooled into young and adult. (Figure 5.5B) Investigation of the BMP pathway in *in vivo* generated AML showed a trend towards an upregulation of the BMP pathway in adult cells with higher expression of *Bmpr2* in >52w cells. This trend was also seen when samples were pooled in to young and adult, but did not reach statistical significance. (Figure 5.5C) The upregulation of the BMP pathway in transformed adult cells may provide a mechanism by which to explain the shorter latency and 100% penetrance observed in the adult groups. Interestingly, as the pathway was not upregulated at baseline, the BMP pathway may be activated specifically in adult LSKs in response to oncogene resulting in more aggressive disease. Despite lower expression of BMP receptors and transducer, the target *Creb3l1* was upregulated in young cells in the presence of oncogene, suggesting that it is not simply upregulation but deregulation of this pathway that may explain the difference in latency and penetrance in young and adult transformed LSKs.

The BMP pathway was also investigated in recipients that developed ALL *in vivo* (both from FL and 3w group). Compared to AML from FL and 3w donors, there was downregulation of the BMP pathway in ALL with reduced expression of the receptor *Bmpr2* and transducer *Smad1*. In addition, the downstream targets of the BMP pathway, *Id1* and *Id2* were also downregulated in ALL. (Figure 5.6) Therefore, in acute leukaemia generated from young LSKs, upregulation of the BMP pathway and its targets is associated with myeloid disease while downregulation of the BMP pathway is associated with lymphoid disease. Therefore, in addition to driving more aggressive disease, the BMP pathway may also steer transforming cells down myeloid lineage programmes.

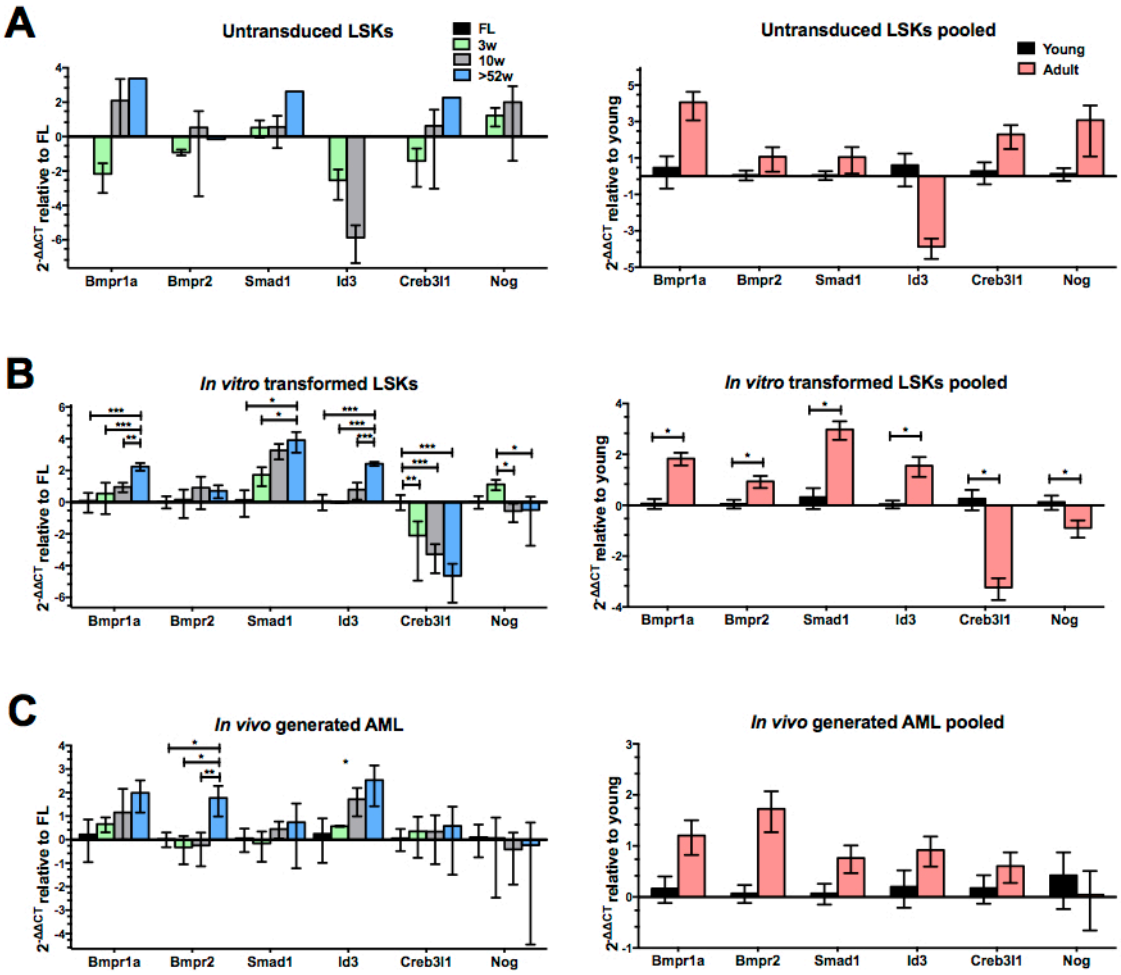

Figure 5.5 The BMP pathway is upregulated in adult cells transformed by NH9

(A) Relative gene expression of the BMP pathway in untransduced LSKs, comparing FL, 3w, 10w and >52w (left, FL comparator) and pooled young and adult (right, young comparator). FL n=1, 3w n=3, 10w n=2, 52w n=1, young n=4, adult n=3.
(B) Relative gene expression of the BMP pathway in LSKs transformed *in vitro* by NH9 at CFC2, comparing FL, 3w, 10w and >52w (left, FL comparator) and pooled young and adult (right, young comparator). FL n=4, 3w n=3, 10w n=3, >52w n=4, young n=7, adult n=7.
(C) Relative gene expression of the BMP pathway in AML generated from NH9 transformed LSKs, comparing FL, 3w, 10w and >52w (left, FL comparator) and pooled young and adult (right, young comparator). FL n=4, 3w n=3, 10w n=4, >52w n=8, young n=7, adult n=12.
Graphs depict mean $2^{-\Delta\Delta CT}$ generated FC +/-SD. For 4 way comparisons, significance determined by 1-way ANOVA and Bonferroni post test. For pairwise comparisons, significance determined by Student's t-test, *p<0.05, **p<001, ***p<0.001.

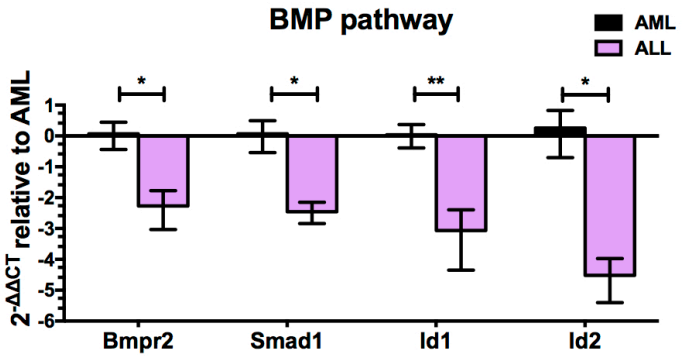

Figure 5.6 The BMP pathway is downregulated in ALL generated from young LSKs

Relative gene expression of the BMP pathway in AML and ALL generated *in vivo* from young LSKs. Graphs depict mean $2^{-\Delta\Delta CT}$ generated FC +/-SD (compared to young AML). Significance determined by Student's t-test, *p<0.05, **p<001, n=7 for AML, n=2 for ALL.

5.4 Results – Global RNA sequencing

RNA-seq was performed on *in vivo* generated AML from FL, 3w, 10w and >52w LSKs transduced with NH9. On average, 33 million reads were measured per sample. (Table 5.1) Read quality was assessed by Graham Hamilton (Glasgow Polyomics, University of Glasgow) and was satisfactory (personal communication, data not shown). Principal component analysis (PCA) is a statistical method to cluster samples based on the main sources of variability, taking into account the entire transcriptional profile. The first principal component (PC1) relates to the greatest source of variability between samples. The second principal component (PC2) is the second greatest source of variability once PC1 is removed. PCA revealed that the samples separated according to age, with the greatest discrimination between 3w and >52w. (Figure 5.7A) The data were analysed in 2 ways. First, significant DEGs were identified in pairwise comparisons between age groups, producing FC, p-value and q-value (adjusted p-value calculated with the Benjamini-Hochberg correction for FDR. Unless otherwise stated, DEGs were defined as having a q value of <0.05 and FC≥±1.5. Figure 5.7B summarises the up and downregulated DEGs returned from each pairwise comparison. A full table of DEGs can be found in Appendix 3. These gene lists were interrogated for pathway membership using the MSigDB and the DAVID. (Section 2.5.5.1) However, this method can miss small differences in gene expression, which may cumulatively result in significant differences in pathway expression. Therefore, the second method of analysis focussed on cumulative pathway deregulation.

The raw expression data was interrogated for gene set enrichment using GSEA from the Broad Institute. Pairwise comparisons were performed using 1000 permutations for enriched gene sets. A NES of ≥±1.3 and a q-value (FDR) of less than 5% (q<0.05) was taken as significant. (Section 2.5.5.1)

Table 5.1 Sequencing depth

Table showing the number of 75bp reads sequenced per sample. On average 33 million reads were performed per sample.

Sample	Reads
FL-AML1	43355956
FL-AML2	39277564
FL-AML3	38039377
3w-AML1	30479030
3w-AML2	38034687
3w-AML3	38386658

Sample	Reads
10w-AML1	40148368
10w-AML2	39006084
10w-AML3	35764220
>52w-AML1	32399907
>52w-AML2	34821633
>52w-AML3	33108873

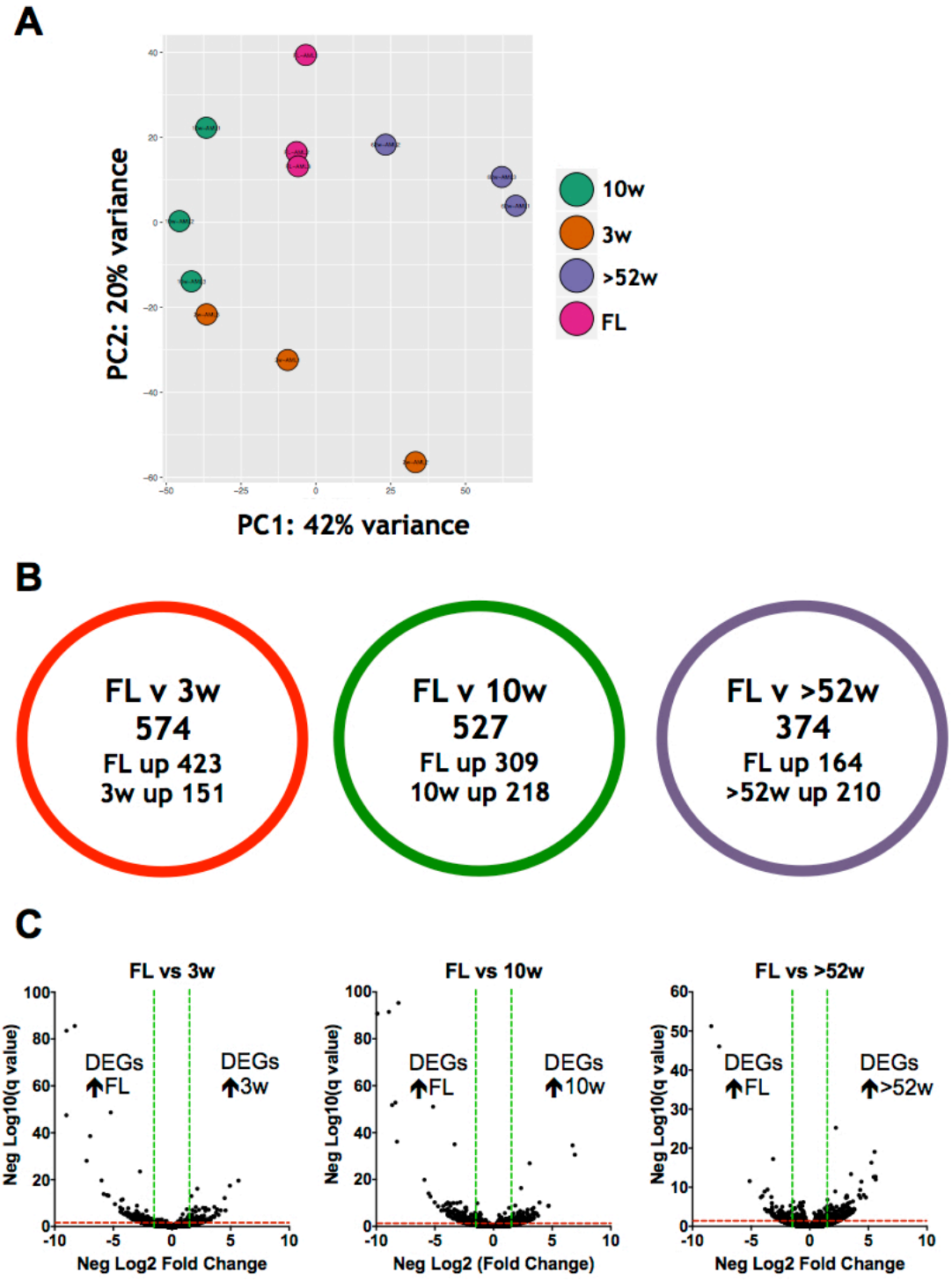

Figure 5.7 Age dependent differential gene expression in AML

(A) PCA plot of gene expression in AML generated from FL, 3w, 10w and >52w LSKs.
(B) DEGs returned from pairwise comparisons. FL used as comparator.
(C) Volcano plots of statistical significance against fold change between FL-AML and 3w-AML (left), 10w-AML (middle) and >52w-AML (right). Green dotted line at FC of ±1.5 and red dotted line at q-value of 0.05.
Results from 1 RNA sequencing experiment, n=3 for each group. Significant DEGs q<0.05 and FC≥1.5. Significance determined by t-test and Benjamini-Hochberg post-test.

5.4.1 FL-AML expresses erythroid programmes, 3w-AML expresses tumour suppressive and cell-membrane programmes

The first question asked was how the cell of origin residing in the FL rather than the BM niche would influence leukaemia cells generated from a highly cycling foetal type HSC that has not yet undergone the switch at 3w of age but now resided in a BM niche. To do this, significant DEGs were identified between FL and 3w-AML. Both AMLs originated from HSCs at an age when they would retain a foetal like phenotype. (Bowie et al., 2007b) 574 DEGs were identified, 423 upregulated in FL-AML and 151 upregulated in 3w-AML. (Figure 5.7B left) The top 10 enriched pathways determined by MSigDB of pathways upregulated in FL and 3w are shown in Figure 5.8. Of pathways enriched in FL-AML, 7 were involved in haemoglobin metabolism and erythrocytosis. Another enriched gene set was AML bearing the expression profile seen in cluster 7 in the Valk database. AMLs in this cluster tend to have normal karyotype and be FAB subtype M1 or M2. Of pathways enriched in 3w-AML, 2 were associated with a granulocyte/macrophage signature. ECM and associated proteins were also enriched in 3w-AML, in keeping with 3w HSCs residing in the bone marrow. Interestingly, pathways upregulated in response to TP53 and TP63, both tumour suppressors, were also enriched in 3w-AML as well as DNA repair pathways. Interrogating the gene list with DAVID for functional annotation clustering produced similar results. Pathways involved in erythrocytosis, erythrocytes cytoskeletal structure and haem or porphyrin biosynthesis were enriched in FL-AML. (Figure 5.9A) Pathways involved in innate immunity, membrane or transmembrane peptides were enriched in 3w-AML. (Figure 5.9B) Therefore, FL-AML retains foetal transcriptional programmes with strong enrichment of erythroid programmes, in keeping with the high red cell production seen in normal foetal HSCs. 3w-AML have an enrichment of programmes pertaining to the bone marrow microenvironment. Additionally, 3w-AMLs have an enrichment of tumour suppressive and DNA repair programmes, suggesting that as foetal-like stem cells move from the FL to the BM, protective mechanisms are switched on to ensure DNA integrity.

A

Gene Set Name	q-value	
CHYLA_CBFA2T3_TARGETS_DN	5.49E-73	Erythrocytosis
IVANOVA_HEMATOPOIESIS_MATURE_CELL	3.50E-22	
PILON_KLF1_TARGETS_UP	8.19E-22	
WELCH_GATA1_TARGETS	1.56E-15	
BIOCARTA_AHSP_PATHWAY	2.76E-14	
STEINER_ERYTHROCYTE_MEMBRANE_GENES	1.59E-13	
REACTOME_METABOLISM_OF_PORPHYRINS	8.25E-12	
VALK_AML_CLUSTER_7	2.01E-12	
DIAZ_CHRONIC_MEYLOGENOUS_LEUKEMIA_UP	8.20E-12	
MEISSNER_BRAIN_HCP_WITH_H3K4ME3_AND_H3K27ME3	2.01E-12	

B

Gene Set Name	q-value	
CHYLA_CBFA2T3_TARGETS_UP	6.65E-07	Granulocyte
CHEN_METABOLIC_SYNDROM_NETWORK	1.32E-03	
NABA_MATRISOME	1.47E-03	ECM
PEREZ_TP53_TARGETS	2.43E-04	Apoptosis, DNA repair
PEREZ_TP53_AND_TP63_TARGETS	1.32E-03	
DODD_NASOPHARYNGEAL_CARCINOMA_UP	9.52E-06	
BENPORATH_SUZ12_TARGETS	9.52E-06	
LIU_PROSTATE_CANCER_DN	2.43E-04	
OSADA_ASCL1_TARGETS_UP	1.26E-03	
MEISSNER_BRAIN_HCP_WITH_H3K4ME3_AND_H3K27ME3	1.81E-03	

Figure 5.8 Enriched pathways by MSigDB comparing FL and 3w-AML

(A) Top 10 enriched pathways in FL-AML compared to 3w-AML.
(B) Top 10 enriched pathways in 3w-AML compared to FL-AML.
Significant pathway enrichment determined by $q<0.05$, n=3 for each group.

A

Cluster	Gene sets	Genes	Enrichment
Haem, porphyrin biosynthesis	15	22	7.1
Erythrocyte development	9	33	5.64
Cortical cytoskeleton	3	10	3.77
Iron, ion, cation biosynthesis	12	26	2.25
Magnesium biosynthesis	3	18	2.24

B

Cluster	Gene sets	Genes	Enrichment
Peptidase, protienase, protease inhibitor	13	5	2.91
Lectin binding	14	20	2.66
Membrane, transmembrane proteins	13	58	2.58
Membrane anchor	3	8	1.62
Innate immunity	4	7	1.42

Figure 5.9 Functional annotation clustering by DAVID in FL and 3w-AML

(A) Functional clusters enriched in FL-AML.
(B) Functional clusters enriched in 3w-AML.
Significant enrichment denoted by enrichment score >1.3, n=3 for each group.

5.4.2 Compared to FL-AML, adult-AMLs express pathways related to the BM niche, oncogenic pathways and myeloid differentiation

To assess the impact of increasing age of the cell of origin on the transcriptional profile of resultant leukaemic cells, FL-AML was compared with adult generated AML. First, FL-AML was compared to 10w-AML, 10w-LSKs being young adult HSCs that normally reside in the BM. 527 DEGs were identified, 309 up-regulated in FL-AML and 218 up-regulated in 10w-AML. (Figure 5.7B middle) Pathway analysis by MSigDB is shown in Figure 5.10. Enriched pathways in FL-AML (Figure 5.10A) included 2 pathways by Benporath *et al*, relating to ES cells, showing FL-AML retains embryonic transcriptional programmes. Three gene sets of genes downregulated in breast and prostate cancer were also enriched in FL-AML. These pathways are characterised by reduced Wnt signalling. Another pathway enriched in FL-AML was characterised by reduced E-cadherin signalling. Both Wnt and E-cadherin signalling are important in signal transduction from the BM niche and aberrant signalling has been implicated in leukaemia pathogenesis. Reduced niche signalling in FL-AML further supports the BM microenvironment's importance in suppressing in young, or promoting in adult, leukaemia

development. In contrast, enriched pathways in 10w-AML (Figure 5.10B) included signal transduction and cell adhesion, supporting the role of the BM microenvironment in promoting leukaemia in 10w-AML. Additionally, pathways defined by macrophage and granulocyte signatures were also enriched in 10-AML, consistent with the fully penetrant myeloid phenotype of the adult AMLs. Downregulation of apoptotic pathways was seen in 1 pathway enriched in 10w-AML suggesting a role for increased cell survival in adult leukaemia. Interestingly, a pathway defined as genes upregulated due to NH9 transduction was also enriched in 10w-AML cells. It is surprising that genes defined by the oncogene used to transform both FL and 10w cells would be differentially expressed in young versus adult derived leukaemia from the same oncogene. This suggests that in response to the same oncogenic stimulus, adult HSCs activate different downstream programmes to young HSCs, resulting in an oncogenic phenotype similar to published data for NH9 in leukaemia that is generated from adult HSCs. Investigating for pathway enrichment, comparing FL-AML with 10w-AML using DAVID showed enrichment clustered around membrane proteins, signal transduction and immunoglobulins in both FL-AML and 10w-AML groups. (Figure 5.11A and B) However, the enriched genes were different in FL-AML versus 10w-AML. Investigating for specific Kyoto Encyclopedia of Genes and Genomes (KEGG) pathways revealed that FL-AML had an enrichment of multiple haemopoietic lineage genes and purine metabolism while 10w-AML had an enrichment of chemokine receptors and ligands. (Figure 5.11C)

To further investigate the impact of increasing age of the cell of origin on resultant leukaemia, FL-AML was compared with >52w-AML. >52w HSCs, which reside in the BM niche, are middle-aged and hypothesised to exhibit some senescent changes. (See Section 3.1.1) 374 DEGs were identified, 164 upregulated in FL-AML and 210 upregulated in >52w-AML. (Figure 5.7B right) Pathway analysis by MSigDB revealed pathways relating to haemoglobin synthesis and erythrocytosis were upregulated in FL-AML similar to FL versus 3w comparison. In addition, pathways involved in solid tumour invasion and metastasis were also upregulated in FL-AML suggesting FL-AML express fewer genes involved in localising to the BM niche compared to >52w-AML. While one pathway involved in the ECM was enriched in FL-AML upregulated genes (Naba

Matrisome), the enriched genes within this pathway were associated with the vascular niche rather than the osteoblastic niche, such as *Vcan* and *Hpse*. (Figure 5.12A) In keeping with the hypothesis that the BM niche is important in leukaemogenesis of adult cells, 2 of the enriched pathways upregulated in >52w-AML related to genes important in the ECM and cell-to-cell contact. This is similar to niche pathways upregulated in the 10w AMLs when comparing FL and 10-AML, but was not identified when FL and 3w-AML were compared. Pathways with a granulocyte or macrophage signature were also enriched in >52w-AML, consistent with the myeloid bias seen in aged HSCs. Interestingly, another pathway enriched in >52w-AML is characterised by removal of p53 suppression and solid tumour oncogenesis. This suggests that >52w-AML has more pro-oncogenic pathways and is consistent with the shorter latency to disease observed in our *in vivo* experiments. (Figure 5.12B) Assessing pathway enrichment by DAVID, comparing FL-AML and >52w-AML showed peptide/disulfide and early growth factor signalling were enriched in both FL and >52w-AML. As these are large pathways, components of the pathway may be expressed differently in FL and >52w cells resulting in different downstream effects. Also upregulated in FL-AML were pathways involving fibronectin, a component of the ECM. (Figure 5.13)

A

Gene Set Name	q-value	
BENPORATH_ES_WITH_H3K27ME3	3.37E-09	Embryonic stem cell
BENPORATH_SUZ12_TARGETS	1.98E-06	
SMID_BREAST_CANCER_LUMINAL_B_DN	4.35E-11	Wnt down
SMID_BREAST_CANCER_BASAL_DN	6.10E-07	
ACEVEDO_FGFR1_TARGETS_IN_PROSTATE_CANCER_MODEL_DN	1.47E-06	
ONDER_CDH1_TARGETS_2_DN	5.96E-07	E-cadherin down
PEDERSEN_METASTASIS_BY_ERBB2_ISOFORM_7	6.10E-07	
MEISSNER_BRAIN_HCP_WITH_H3K4ME3_AND_H3K27ME3	1.11E-11	
DURAND_STROMA_S_UP	1.11E-11	
KUMAR_TARGETS_OF_MLL_AF9_FUSION	1.11E-11	

B

Gene Set Name	q-value	
CHEN_METABOLIC_SYNDROM_NETWORK	5.12E-17	Granulocyte, macrophage
TONKS_TARGETS_OF_RUNX1_RUNX1T1_FUSION_MONOCYTE_UP	4.55E-12	
BOQUEST_STEM_CELL_CULTURED_VS_FRESH_UP	5.12E-17	Adhesion, migration
HECKER_IFNB1_TARGETS	3.16E-13	
GRAESSMANN_RESPONSE_TO_MC_AND_SERUM_DEPRIVATION_UP	6.06E-12	Anti-apoptotic
TAKEDA_TARGETS_OF_NUP98_HOXA9_FUSION_3D_UP	1.47E-11	NH9 up
BROWNE_INTERFERON_RESPONSIVE_GENES	6.03E-15	
WONG_ADULT_TISSUE_STEM_MODULE	1.10E-11	Adult stem cell
HELLER_SILENCED_BY_METHYLATION_UP	1.25E-11	
SEITZ_NEOPLASTIC_TRANSFORMATION_BY_8P_DELETION_UP	1.77E-11	

Figure 5.10 Enriched pathways by MSigDB comparing FL with 10w-AML

(A) Top 10 enriched pathways in FL-AML compared to 10w-AML.
(B) Top 10 enriched pathways in 10w-AML compared to FL-AML.
Significant pathway enrichment determined by $q<0.05$, $n=3$ for each group.

A

Cluster	Gene sets	Genes	Enrichment
Membrane, signal transduction	11	126	3.14
Membrane glycoprotein	8	84	2.03
Cell junction, adhesion	13	39	1.8
Immunoglobulin	20	22	1.79
Tetraspanin	4	3	1.48

B

Cluster	Gene sets	Genes	Enrichment
Lectin binding	9	17	4.05
Chemokine, chemotaxis	23	26	2.7
Membrane, signal transduction	19	94	2.65
Immunoglobulin	8	15	2.23
GPCR proteins	7	10	1.57
Cell migration	5	8	1.44

C

Enriched in FL	Enriched in 10w
Hematopoietic cell lineage	Cytokine-cytokine receptor interaction
Nicotinate & nicotinamide metabolism	Chemokine signaling pathway
Purine metabolism	Cytosolic DNA-sensing pathway
Pathways in cancer	
Calcium signaling pathway	
Gap junction	

Figure 5.11 Functional annotation clustering by DAVID in FL and 10w-AML

(A) Functional clusters enriched in FL-AML.
(B) Functional clusters enriched in 10w-AML.
(C) KEGG pathways enriched in FL and 10w-AML.
Significant enrichment denoted by enrichment score >1.3, n=3 for each group.

A

Gene Set Name	q-value	
DIAZ_CHRONIC_MEYLOGENOUS_LEUKEMIA_DN	2.12E-08	Haem and erythrocytosis
CHYLA_CBFA2T3_TARGETS_UP	3.15E-07	
SCHUETZ_BREAST_CANCER_DUCTAL_INVASIVE_UP	5.09E-12	Invasive cancer
POOLA_INVASIVE_BREAST_CANCER_UP	1.78E-08	
NABA_MATRISOME	2.40E-08	ECM
IVANOVA_HEMATOPOIESIS_LATE_PROGENITOR	2.09E-09	Progenitor
CHEN_METABOLIC_SYNDROM_NETWORK	2.25E-20	
MCLACHLAN_DENTAL_CARIES_UP	3.73E-10	
MEISSNER_BRAIN_HCP_WITH_H3K4ME3_AND_H3K27ME3	8.98E-09	
VERHAAK_GLIOBLASTOMA_MESENCHYMAL	2.12E-07	

B

Gene Set Name	q-value	
WANG_SMARCE1_TARGETS_UP	1.41E-06	Cell contact
NABA_MATRISOME	3.81E-04	ECM
CHYLA_CBFA2T3_TARGETS_UP	9.74E-05	Granulocyte/ macrophage
ZWANG_TRANSIENTLY_UP_BY_2ND_EGF_PULSE_ONLY	1.54E-05	Pro-oncogenic (p53 supression)
SERVITJA_ISLET_HNF1A_TARGETS_UP	1.84E-04	Oncogensis
BENPORATH_EED_TARGETS	4.38E-05	
BENPORATH_ES_WITH_H3K27ME3	6.64E-05	
BENPORATH_SUZ12_TARGETS	1.05E-04	
MEISSNER_NPC_HCP_WITH_H3_UNMETHYLATED	1.58E-04	
PEDRIOLI_MIR31_TARGETS_DN	9.76E-04	

Figure 5.12 Enriched pathways by MSigDB comparing FL with >52w-AML

(A) Top 10 enriched pathways in FL-AML.
(B) Top 10 enriched pathways in >52w-AML.
Significant pathway enrichment determined by $q<0.05$, $n=3$ for each group.

A

Cluster	Gene sets	Genes	Enrichment
Peptide, disulfide signalling	6	52	3.21
Phagocytosis, invagination	6	8	2.33
EGF, EGF calcium binding	26	17	2.26
Fibronectin	11	11	1.95
GTPase	24	18	1.87

B

Cluster	Gene sets	Genes	Enrichment
Proteinase, pepdidase inhibition	13	8	5.11
Pedtide, disulfide, membrane	14	81	3.69
EGF domains	11	8	1.85

Figure 5.13 Functional annotation clustering in FL and >52w-AML

(A) Functional clusters enriched in FL-AML.
(B) Functional clusters enriched in >52w-AML.
Significant enrichment denoted by enrichment score >1.3, n=3 for each group.

5.4.3 Lineage, BM localising, tumour suppressive and pro-oncogenic transcriptional programmes are differentially expressed with age

A summary of the transcriptional programmes identified is shown in Figure 5.14. Common signatures in FL-AML in all comparisons were those relating to erythrocytosis. This is in keeping with the extreme red cell expansion that occurs prenatally. However, it also suggests that cells retain transcription programmes pertaining to their origin age even after leukaemic transformation. AML generated from post-foetal LSKs (3w, 10w and >52w) expressed granulocytic and macrophage programmes. FL-AML expressed transcriptional programmes relating to cell migration rather than localisation to the BM. In contrast, 10w and >52w-AML expressed transcriptional programmes for cell contact and adhesion, in keeping with increased marrow niche localisation. In addition, adult AMLs also expressed pro-oncogenic programmes, in line with the faster onset to disease and 100% penetrance observed *in vivo*. While 3w-AMLs also expressed genes relating to the marrow, this was less marked than when FL was compared with 10w or >52w-AML. In addition, 3w-AML expressed apoptotic and tumour suppressive programmes, in keeping with a shorter latency to disease and incomplete penetrance.

FL	3w	10w	>52w
Erythrocytosis	Membrane	Granulocyte, macrophage	Granulocyte, macrophage
Cell migration	Apoptosis	Anti-apoptosis	Anti-apoptosis
Reduced localisation to marrow niche	Tumour suppression	NH9 signature	Pro-oncogenic
	ECM	Marrow niche, adhesion	Marrow niche, adhesion

Figure 5.14 Summary of age dependent enriched pathways in NH9 AML

Summary of enriched pathways of DEGs identified by pairwise comparisons, using FL-AML as comparator.

5.4.4 Compared to 3w-AML, >52w-AML express pro-oncogenic and microenvironmental programmes, while 3w-AML express multilineage and tumour suppressive programmes

To further investigate the role of age in the transcriptional profile of leukaemias, we compared the transcriptional profile of 3w-AMLs, generated from a foetal type cell originating from the BM, and >52w-AML, generated from adult aged cells also originating from the BM. Using the same criteria above we identified 1079 DEGs, 435 genes upregulated in 3w-AML and 644 upregulated in >52w-AML. (Figure 5.15A) A full list of DEGs can be found in Appendix 3. Pathway analysis using MSigDB is shown in Figure 5.15 and using DAVID in Figure 5.16. Investigating genes upregulated in 3w-AML by MSigDB showed 4 pathways involved in the immune process, lymphoid and myeloid lineage. The dual expression of genes involved in myeloid and lymphoid lineage is consistent with a proportion of young-AMLs developing lymphoid leukaemia *in vivo*. Three of the pathways related to a transcriptional signature associated with cellular migration, 2 associated with reduced cell migration and 1 with increased migration. Interestingly, 2 pathways were associated with reduced proliferation and increased apoptosis, further supporting that AML arising from young cells express more tumour suppressive pathways and is keeping with the increased latency and lower penetrance observed in our *in vivo* experiment. (Figure 5.15B) Investigation of functional clustering using DAVID revealed several significantly enriched pathways. These included lysosomal pathways (enrichment = 5.54), lectin pathways (enrichment = 3.65), pyrin (enrichment 2.82), immunoglobulin (enrichment = 2.74) and phagocytosis/endocytosis (enrichment = 1.94). (Figure 5.16A) What is interesting about these pathways is that the component genes

relate to both myeloid and lymphoid associated function. This further suggests that young LSCs retain both myeloid and lymphoid programmes. 644 DEGs upregulated in >52w-AML were found. Interrogating this gene list in MSigDB (Figure 5.15C) revealed 2 pathways relating to a stem cell signature and 3 pathways relating to a leukaemic or oncogenic signature. Interestingly, one of these cancer pathways is associated with HoxA9 targets in response to MA9. This suggests that the oncogenic pathway response to NH9 is different in adult cells compared to foetal cells, leading to a stronger HoxA9 signature and therefore, potency. Two pathways were involved in DNA repair, consistent with an accrual of DNA damage with increasing age. (Rossi et al., 2007a, Rube et al., 2011, Beerman et al., 2014) One pathway was involved in ECM metabolism, further implicating the importance of the role of the microenvironment in adult derived AML. Interrogation of this gene list in DAVID further supported the role of the BM niche in adult-AML. This included functional clustering of cell adhesion pathways (enrichment 3.3) and membrane components (enrichment 3.23), which includes *Bmpr2*, previously hypothesised to play a role in the pro-oncogenic processes in adult derived AML. In addition, a cluster involved in haemopoiesis (enrichment 3.85) contained stem cell associated genes including *Klf1*, *Tal1* and *Meis1*. (Figure 5.16B) Therefore, even when normalising for the cell of origin originating from the BM, leukaemia derived from young foetal-like 3w HSCs expresses multiple lineage (myeloid and lymphoid) and tumour suppressive programmes while adult derived leukaemia expresses stem cell and pro-oncogenic programmes. Additionally, adult derived AML expresses transcriptional programmes relating to the BM niche, suggesting the BM microenvironment plays a role in the increased leukaemic potency seen in adult derived leukaemia.

A

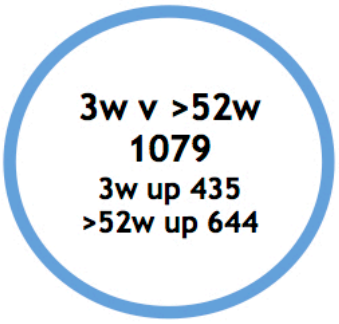

B

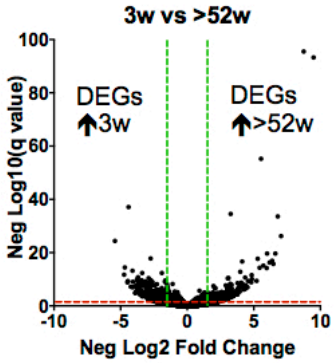

C

Gene Set Name	q-value	
CHEN_METABOLIC_SYNDROM_NETWORK	1.69E-46	Macrophoage
REACTOME_IMMUNE_SYSTEM	1.31E-13	Myeloid/ lymphoid
DELYS_THYROID_CANCER_UP	1.31E-13	Lymphoid
CHYLA_CBFA2T3_TARGETS_UP	1.80E-29	Macrophage Proliferation ↓
GRAESSMANN_APOPTOSIS_BY_DOXORUBICIN_UP	1.67E-14	Apoptosis
SMID_BREAST_CANCER_NORMAL_LIKE_UP	1.06E-13	Migration ↓
FULCHER_INFLAMMATORY_RESPONSE_LECTIN_VS_LPS_ DN	8.17E-15	Migration ↓
SCHUETZ_BREAST_CANCER_DUCTAL_INVASIVE_UP	6.24E-13	Migration ↑
MEISSNER_BRAIN_HCP_WITH_H3K4ME3_AND_H3K27ME3	9.38E-18	
SWEET_LUNG_CANCER_KRAS_UP	1.03E-11	

D

Gene Set Name	q-value	
WONG_ADULT_TISSUE_STEM_MODULE	5.94E-25	Stem cell
LIM_MAMMARY_STEM_CELL_UP	2.06E-14	
TORCHIA_TARGETS_OF_EWSR1_FLI1_FUSION_UP	2.06E-14	Cancer
KUMAR_TARGETS_OF_MLL_AF9_FUSION	1.40E-16	
DODD_NASOPHARYNGEAL_CARCINOMA_UP	9.17E-14	Cancer
PEREZ_TP53_TARGETS	1.10E-14	DNA repair
YOSHIMURA_MAPK8_TARGETS_UP	8.59E-15	ECM
CHYLA_CBFA2T3_TARGETS_DN	8.79E-66	Proliferation ↑
PILON_KLF1_TARGETS_UP	2.48E-17	Erythrocytosis ↓
MEISSNER_BRAIN_HCP_WITH_H3K4ME3_AND_H3K27ME3	9.25E-20	

Figure 5.15 Enriched pathways by MSigDB comparing 3w with >52w-AML

(A) Differentially expressed genes, defined as q<0.05 and FC≥±1.5 in pairwise comparison.
(B) Volcano plot of statistical significance against fold change between 3w-AML and >52w-AML. Green dotted line at FC of ±1.5 and red dotted line at q-value of 0.05.
(B) Top 10 enriched in 3w-AML.
(C) Top 10 enriched pathways in >52w-AML.
Significant pathway enrichment determined by q<0.05, n=3 for each group.

A

Cluster	Gene sets	Genes	Enrichment
Transmembrane proteins	14	206	7.99
Lysosome	5	17	5.54
Lectin	9	19	3.65
Pleckstrin	6	17	2.82
Pyrin	5	6	2.74
Immunoglobulin	16	32	2.7
Phagocytosis	6	16	1.95

B

Cluster	Gene sets	Genes	Enrichment
Haemopoiesis	8	21	3.85
Cell adhesion	4	31	3.30
Membrane, transmembrane	9	228	3.23
Porphyrin	15	18	3.08
Membrane, sulfide, disulfide proteins	8	157	2.62

Figure 5.16 Functional annotation clustering by DAVID in 3w and >52w-AML

(A) Functional clusters enriched in 3w-AML.
(B) Functional clusters enriched in >52w-AML.
Significant enrichment denoted by enrichment score >1.3, n=3 for each group.

5.4.5 Investigating overlapping DEGs to find pathways related to bone marrow cell of origin and adult cell of origin

In order to identify the key genes/pathways that change due to the cell of origin arising from the BM rather than FL, DEGs generated from pairwise comparisons with FL-AML as the comparator were overlapped to identify the common DEGs seen in all comparisons. (Figure 5.17) Compared to FL-AML, 38 common genes were differentially expressed in 3w, 10w and >52w-AML, denoting a BM derived cell of origin signature. Pathway analysis using MSigDB of this gene set revealed 10 enriched pathways. (Figure 5.18A) Three of these pathways were involved in cell localisation, adhesion and migration. The Matrisome pathway is an ensemble of genes encoding ECM and associated proteins. The Syndecan-1 mediated signalling pathway mediates cell binding, signalling, cytoskeletal organisation, proliferation, migration and call matrix interactions. The PDEF pathway was developed from the knock down to PDEF in prostate cancer, leading to increased migration by activation of the TGFß, intergrin, VEGF and Wnt pathways. These pathways enriched in the AMLs generated from cells with a BM origin are consistent with the different niche origins of the cell prior to transformation.

These genes were also investigated in DAVID. (Figure 5.18B) This returned 4 functional clusters with significant enrichment scores of >1.3. Three of these clusters were involved in the ECM, cell motility and localisation. The fourth cluster was involved in the immunoglobulin domain.

Finally, the key genes that were differentially expressed in leukaemia arising from adult HSCs, regardless of the microenvironment of the cell of origin, were investigated. These genes should contain the key players that led to the longer latency and retained lymphoid potential observed *in vivo* in the FL and 3w derived leukaemias. Using FL-AML as the comparator, 23 genes were found that were differentially expressed in 10 and >52w-AML but not in 3w-AML, that denote an adult derived signature. (Figure 5.17) Functional annotation clustering using DAVID revealed 2 clusters. While both clusters had low enrichment scores (0.67 and 0.4) they highlight mechanisms that may be important in distinguishing leukaemia arising from a young versus an adult cell of origin. The first was involved in membrane binding and signalling, suggesting that with increasing age, pathways involved in localising to the BM niche are increasingly important. The second cluster related to pathways in nucleotide binding. (Figure 5.19A) Using MSigDB, only 16 out of 23 genes mapped onto entrez genes resulting in only 2 enriched pathways. The first, a pathway related to dental caries and the second, a pathway enriched in ageing kidneys. (Figure 5.19B) Genes associated with inflammation characterise both pathways (eg. *IGVK*, *IRF8*, *CD209*, *CX3CR1*) suggesting increased inflammation or immune surveillance with AML from adult stem cells.

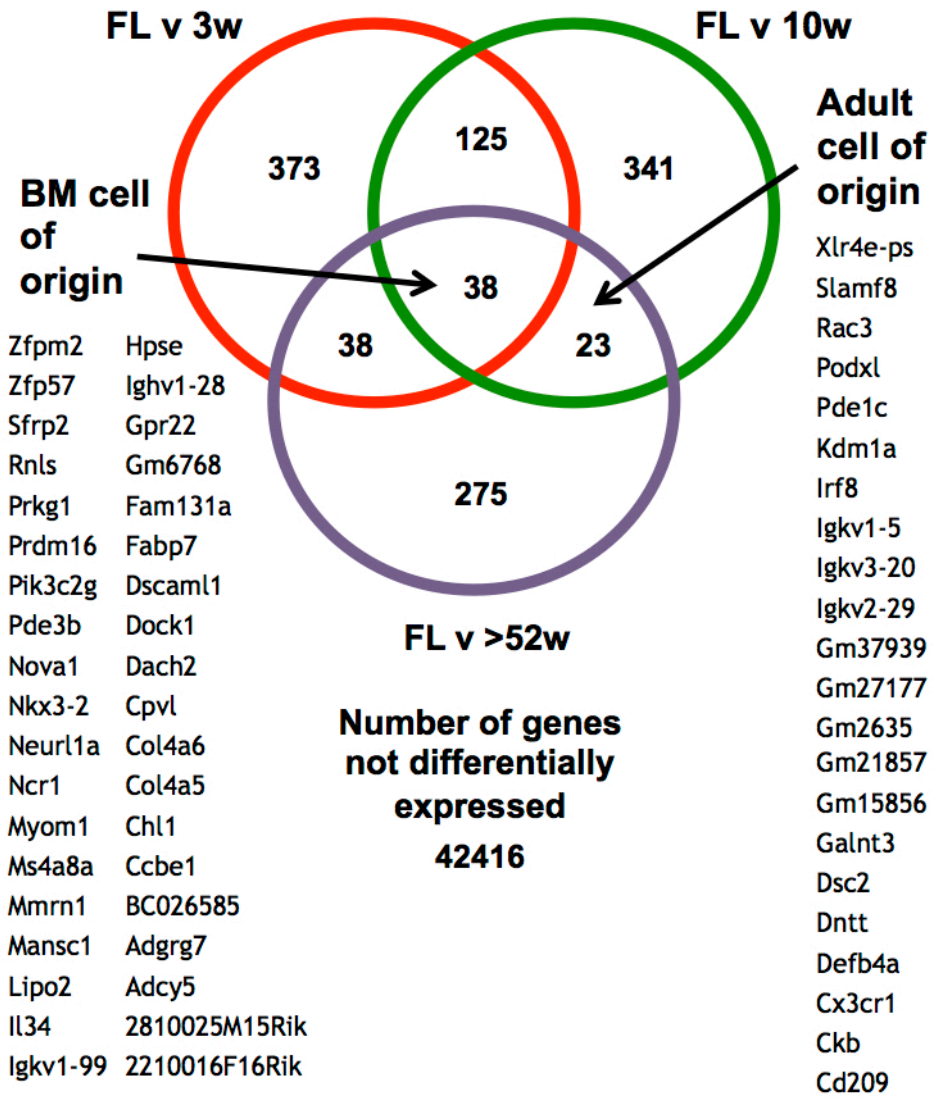

Figure 5.17 Overlapping DEGs

All DEGs (regardless of direction of change) from each pairwise comparison were overlapped to find a common signature relating to a BM derived cell of origin and an adult derived cell of origin.

A

Gene Set Name	q-value	
NABA_MATRISOME	4.17E-03	Localisation, adhesion, migration
PID_SYNDECAN_1_PATHWAY	4.17E-03	
GU_PDEF_TARGETS_UP	8.23E-03	
BENPORATH_PRC2_TARGETS	4.17E-03	Stem cell and oncogenic
BENPORATH_SUZ12_TARGETS	4.17E-03	
BENPORATH_EED_TARGETS	4.17E-03	
BENPORATH_ES_WITH_H3K27ME3	4.87E-03	
REACTOME_HEMOSTASIS	8.20E-03	
BIOCARTA_VITCB_PATHWAY	1.19E-02	
BIOCARTA_ACE2_PATHWAY	1.51E-02	

B

Cluster	Gene sets	Genes	Enrichment
Extracellular matrix	3	5	1.55
Cell motility, localisation, migration	5	4	1.54
Immunoglobulin, fibronectin	12	4	1.39
Peptide signal, ECM, cytoplasmic	8	15	1.32

Figure 5.18 Enriched pathways by MSigDB and DAVID of common DEGs in 3w, 10w and >52w when compared with FL-AML (BM derived cell of origin)

(A) Pathway analysis by MSigDB of common DEGs, significant q<0.05.
(B) Functional clustering by DAVID of common DEGs, significant enrichment >1.3.
N=3 for all groups.

A

Cluster	Gene sets	Genes	Enrichment
Membrane binding and signalling	22	10	0.67
Nucleotide binding	5	3	0.4

B

Gene Set Name	q-value	
MCLACHLAN_DENTAL_CARIES_UP	9.75E-05	Immune, inflammation
RODWELL_AGING_KIDNEY_UP	4.85E-02	

Figure 5.19 Enriched pathways by MSigDB and DAVID of DEGs in 10w and >52w but not 3w, when compared to FL-AML (adult derived cell of origin)

(A) Functional clustering by DAVID of common DEGs, significant enrichment <1.3.
(B) Pathway analysis my MSigDB of common DEGs, significant q<0.05, n=3 for all groups.

5.4.6 Programmes related to nucleotide transcription and cell adhesion/membrane signal transduction are differentially expressed in AML, depending on age of the transforming cell

To find the keys genes that distinguished leukaemia arising from a young cell versus an adult cell, the data from FL and 3w-AML (young) and 10w and >52w-AML (adult) were pooled and compared and significant DEGs between the young and adult groups identified. Using a value of q<0.05, (without specifying a FC difference) 15 DEGs were found. When these genes were investigated for functional clustering by DAVID, the only significant cluster (enrichment score of 1.74) was involved in transcription and RNA/nucleotide metabolism. The enriched genes were *Glis3*, *Prdm16*, *Neo1*, *Satb2* and *Tacc2*. Of these genes, *Glis3*, *Prdm16* and *Tacc2* were upregulated in young-AML with *Glis3* and *Prdm16* being significant (FC>1.5) while *Neo1* was upregulated in adult-AML (FC<-1.5). GLIS3, PRDM16 and TACC2 act to regulate and repress transcription while NEO1 has been implicated in transition from cell proliferation to differentiation as well as cell adhesion and migration. Using a value of q<0.1 37 DEGs were found. Again, the only significant cluster (enrichment score 1.43) was involved in transcription and RNA/nucleotide metabolism. In addition to the genes identified above, *Hes1*, *Zfp69*, *Zfp558*, *GstT2* and *Srp54* were also enriched. Of these, *Zfp69* was significantly upregulated in adult (FC<-1.5). ZFP69 is a zinc finger protein and plays a role in gene expression and transcription factor activity. This analysis suggests that pathways repressing transcription are upregulated in young-AML while pathways promoting transcription are upregulated in adult-AML. Another cluster that was identified using a q<0.1 related to cell adhesion and membrane signal transduction. The enriched genes were *Gria2*, *Mfap3l*, *Klk1b27*, *Slc4a5*, *Parvb*, *Mpp7*, *Axl*, *Hes1*, *Fcna*, *Cd5l*, *Col5a1*, *Ncam1* and *Neo1*. Of these, the first 4 were significantly upregulated in young-AML. The genes upregulated in young-AML, *Gria1*, *Mfap3l*, *Klk1b27* and *Slc4a5* tend to compose of ligand receptor and membrane channels not specific to the BM niche. GRIA1 forms part of the glutamine receptor; MFAP3L is a component of elastin associated microfibrils; KLK1B27 is a serine protease and tends to be expressed in testes and submaxillary glands and SLC4A5 codes a membrane protein that regulates intracellular pH. In contrast, *Fnca*, *Col5a1*, *Ncam1* and *Neo1* were upregulated in adult-AML (FC<-1.5) and were either collagen related genes or

involved in cell adhesion. In addition, CD5L plays a role in immunity and macrophage survival and is consistent with both the 100% myeloid lineage observed in the adult-AML groups *in vivo*. While the enrichment score was not significant (1.21), it highlights a trend towards the BM niche being particularly important in adult-AML.

Cluster	Enrichment	Enriched genes
Transcription (q<0.05)	1.73	**Glis3**, **Prdm16**, Satb2, Tacc2, **Neo1**
Transcription (q<0.01)	1.43	**Glis3**, **Prdm16**, Satb2, Tacc2, Hes1, Zfp558, GstT2, Srp54, **Neo1**, **Zfp69**
Adhesion, membrane signal transduction (q<0.01)	1.21	**Gria2**, **Mfap3l**, **Klk1b27**, **Slc4a5**, Parvb, Mpp7, Axl, Hes1, Cd5l, **Fcna**, **Col5a1**, **Ncam1**, **Neo1**

Figure 5.20 Functional clustering by DAVID of DEGs comparing young and adult AML

Functional clustering by DAVID of common DEGs including overlapping genes. Genes in bold expressed with a FC >±1.5. Significant enrichment >1.3, n=6 for both groups.

5.4.7 GSEA analysis – specific pathway analyses

Results from the targeted gene expression investigation and DEGs based analysis of RNA-seq data identified pathways that may be pertinent in determining differences in leukaemic phenotype based on the age of the transforming cell. Next, the entire dataset was analysed for gene set enrichment of specific pathways using GSEA from the Broad Institute. Gene sets from MSigDB were chosen for the following classifications:

BMP pathway

Haemopoietic differentiation

Differentiation

Stem cell

DDR and DNA repair

NH9 signature

Adhesion

Inflammation and immune

This method returned some irrelevant or small pathways that were excluded from analysis. Pairwise comparisons were performed using FL as the comparator, against 3w, 10w and >52w (n=3 in each group). 3w and >52w were also compared

to assess the effect of cellular age on the transcriptional landscape, from cells originating from the same (BM) microenvironment. The data were also pooled into young (FL and 3w, n=6) and adult (10w and >52w, n=6) for pairwise comparison. The number of enriched pathways is summarised in Table 5.2.

Table 5.2 Enriched gene set pathways from pairwise comparisons for specific pathways

Results from pairwise comparisons for gene set enrichment of specific pathways. Enrichment compared to younger age group for each comparison. Number of gene sets investigated in each pathway classification indicated in parentheses. Significantly enriched pathways defined as a NES≥±1.3 and q<0.05.

Comparison	BMP pathway (13)		Haemopoiesis (52)		Differentiation (190)		Stem cell (57)	
	Young	Older	Young	Older	Young	Older	Young	Older
FL v 3w	0	0	1	0	1	0	3	0
FL v 10w	0	0	0	1	0	2	0	2
FL v >52w	0	0	0	1	0	0	4	3
3w v >52w	0	0	0	0	0	0	1	0
Young v adult	0	0	0	0	0	0	0	2

Comparison	DNA response (35)		NH9 (10)		Adhesion (42)		Immune (93)	
	Young	Older	Young	Older	Young	Older	Young	Older
FL v 3w	6	0	1	0	0	0	0	0
FL v 10w	0	0	0	0	2	0	0	32
FL v >52w	0	0	0	0	0	0	7	0
3w v >52w	0	0	3	1	0	0	24	0
Young v adult	0	8	1	1	0	0	0	0

5.4.7.1 BMP Pathway

Gene sets relating to BMP pathway control, activation and regulation were analysed in pairwise comparisons. (Table 5.2) Comparing FL-AML with 3w-AML or 10w-AML, showed no enrichment of BMP pathways in either group. Comparing FL-AML with >52w-AML, and 3w-AML and >52-AML showed a trend towards enrichment of the BMP pathway in adult groups but did not reach significance (q>0.05). (Figure 5.21A and B) When young-AML (FL and 3w) and adult-AML (10w and >52w) were pooled, there was a trend towards enrichment of the BMP pathway in adult AML but did not reach significance. (Figure 5.21C)

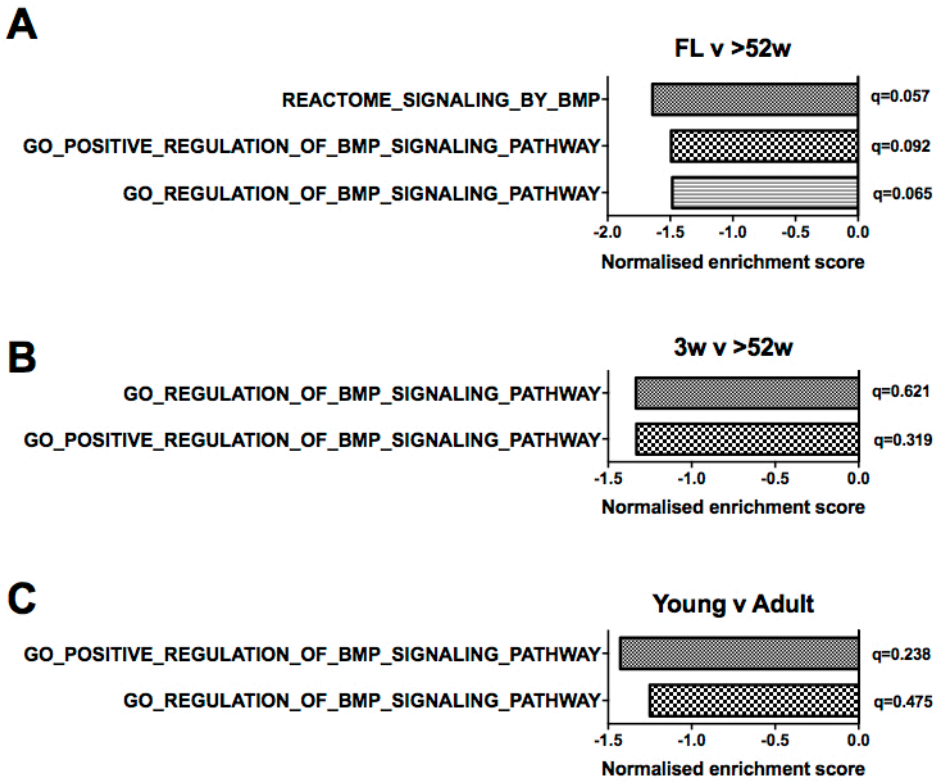

Figure 5.21 GSEA analysis of BMP pathways shows a trend towards enrichment of the BMP pathway in adult AML

(A) Graph of BMP pathways comparing FL-AML and >52w-AML. Negative NES indicates enrichment in >52w-AML, n=3 for each group.
(B) Graph of BMP pathways comparing 3w-AML and >52w-AML. Negative NES indicates enrichment in >52w-AML, n=3 for each group.
(C) Graph of BMP pathways comparing young-AML and adult-AML. Negative NES indicates enrichment in adult-AML, n=6 for each group.
Significant enrichment defined as NES≥±1.3 and q<0.05.

5.4.7.2 Haemopoietic differentiation

Gene sets relating to haemopoietic differentiation of progenitors and terminally differentiated lineages were analysed. These included erythroid, myeloid, B and T-lymphoid, dendritic cell and natural killer cell differentiation. Comparing FL-AML and 3w-AML revealed enrichment of erythroid differentiation in FL-AML. (Figure 5.22A) Comparing FL-AML with 10w-AML showed enrichment of 1 myeloid pathway in FL-AML. (Figure 5.22B) However, comparing FL-AML with >52w-AML, 3w-AML with >52w-AML or young-AML with adult-AML did not reveal enrichment for haemopoietic differentiation pathways.

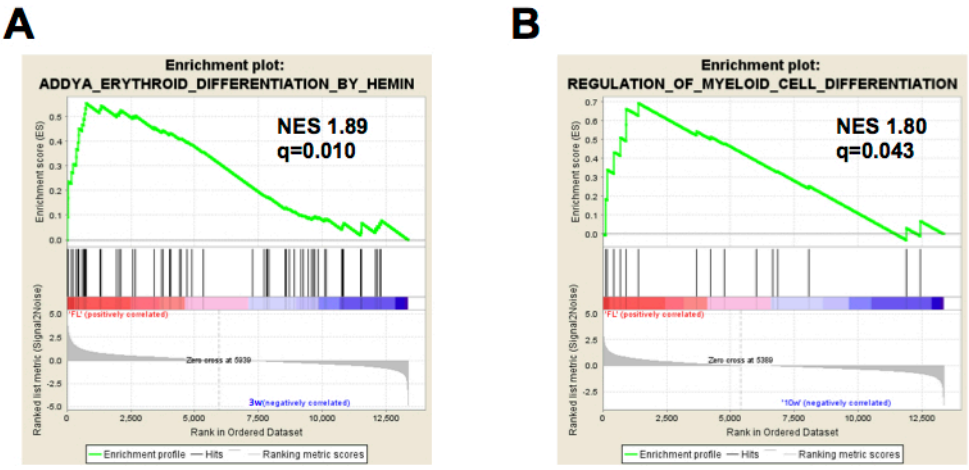

Figure 5.22 GSEA analysis of haemopoietic differentiation pathways

(A) Enrichment plot showing enrichment of the erythroid differentiation pathway in FL-AML compared to 3w-AML.
(B) Enrichment plot showing enrichment of the myeloid cell differentiation pathway in FL-AML compared to 10w-AML.
Significant enrichment defined as NES≥±1.3 and q<0.05, n=3 for each group.

5.4.7.3 Differentiation

Gene sets relating to differentiation to any tissue were analysed in pairwise comparisons. Comparing FL-AML with 3w-AML showed enrichment of the same erythroid differentiation pathway in FL-AML as seen when investigating for haemopoietic differentiation pathways. Comparing FL-AML with 10w-AML revealed enrichment of 2 pathways in 10w-AML. (Table 5.2 and Figure 5.23) One pertained to dendritic cell differentiation and another to osteoclast differentiation. Osteoclasts are an important component of the BM endosteal niche and signalling from the niche may play an important role in leukaemic propagation and survival. Enrichment of this pathway in 10w-AML not only implicates the BM microenvironment in leukaemogenesis in adult AML specifically, but also suggests that adult derived AML may modify the BM to create a pro-leukaemic environment.

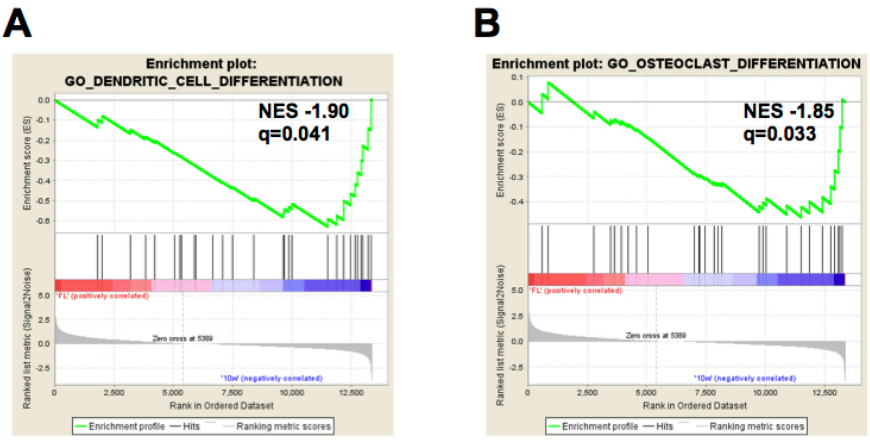

Figure 5.23 GSEA analysis of differentiation pathways comparing FL-AML with 10w-AML

(A) Enrichment plot showing enrichment of a dendritic differentiation pathway in 10w-AML compared to FL-AML.
(B) Enrichment plot showing enrichment an osteoclast differentiation pathway in 10w-AML compared to FL-AML.
Significant enrichment defined as NES>±1.3 and q<0.05, n=3 for each group.

5.4.7.4 Stem cell

Transcriptional signatures relating to stem cell pathways were interrogated in our samples. Comparing FL-AML with 3w-AML showed an enrichment of an ES cell signature in FL-AML. However, comparison of FL-AML and 10w-AML showed this same pathway was highly enriched in 10w-AML. (Figure 5.24A and B) This suggests that FL-AMLs retain embryonic signatures due to the cell of origin being embryonic in nature. However, re-expression of these same pathways in adult AML may result in pathological self-renewal. Comparing FL-AML and >52w-AML another 3 stem cell pathways, characterised by high self-renewal, were enriched in >52w-AML showing that a stem cell like signature is a common transcriptional profile in adult AML. In contrast, enriched pathways in FL-AML included a pathway of genes downregulated in stem cells and interestingly, a pathway pertaining to pro-B cell lymphoid progenitors. (Figure 5.24C) The same pro-B cell pathway was also enriched in 3w-AML when compared to >52w-AML, in keeping with the hypothesis that young cells retain lymphoid programmes. When comparing young and adult AML, the ES cell signature was enriched in adult AML, further supporting the hypothesis that embryonic signatures are re-expressed in adult HSCs when are transformed. (Figure 5.24D) Interestingly, another stem cell signature that was enriched in adult AML was of genes that were up-regulated in human $CD34^{+}$ stem cells cultured on collagen, as an *in vitro* model of the

microenvironment, compared to CD34$^+$ cells cultured in media. (Figure 5.24E) This further suggests that signalling from the microenvironment is crucial for adult AML but less important in young AML.

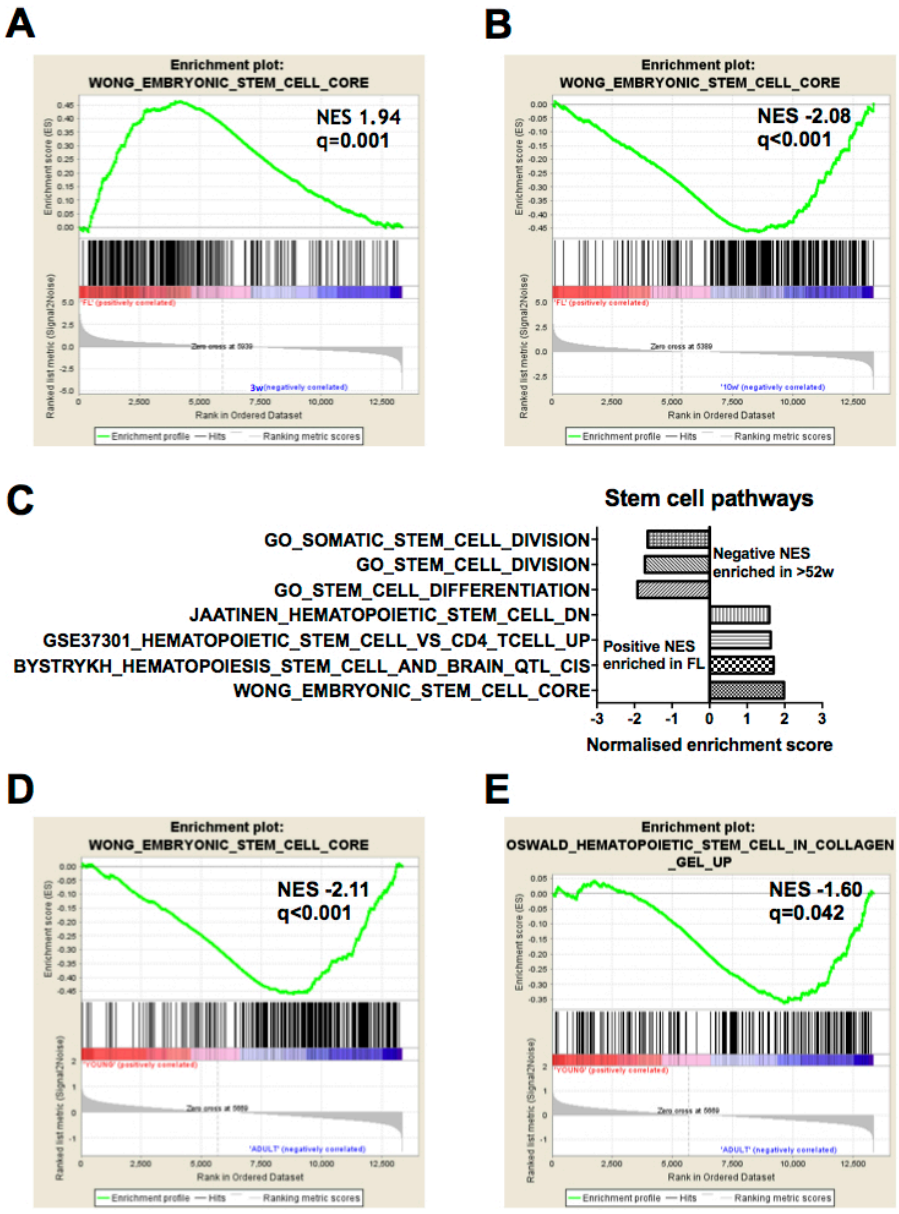

Figure 5.24 GSEA analysis of stem cell pathways

(A) Enrichment plot showing enrichment of the embryonic stem cell signature in FL-AML compared to 3w-AML, n=3 for each group.
(B) Enrichment plot showing enrichment of the embryonic stem cell signature in 10w-AML, compared to FL-AML, n=3 for each group.
(C) Graph of enriched stem cell pathways comparing FL-AML with >52-AML. N=3 for each group, q<0.05 for all enriched pathways.
(D) Enrichment plot showing enrichment of the embryonic stem cell signature in adult AML compared to young AML, n=6 for each group.
(E) Enrichment plot showing enrichment of genetic signature of CD34$^+$ cells cultured on collagen in adult AML compared to young AML, n=6 for each group.

5.4.7.5 DDR and DNA repair

Pathways relating to DDR and repair were investigated in our dataset. Comparing FL-AML with 3w-AML revealed 6 DNA repair pathways enriched in FL-AML. Comparing FL-AML with 10w and >52w-AML showed no enrichment of DNA repair pathways in FL-AML. However, there was an enrichment of p53 dependent and independent damage response and apoptosis in 10w-AML. Conversely, 2 DDR pathways were enriched in FL-AML when compared to >52w-AML. (Table 5.2) When DDR and repair pathways were investigated in young and adult AML, 1 DDR and 7 DNA repair pathways were enriched in adult AML, with no enrichment of these pathways in young AML. (Figure 5.25) This may reflect the accumulation of DNA damage that occurs with increasing age, and is carried through when an aged HSC undergoes leukaemic transformation, or an inappropriate activation of these pathways that leads to leukaemia cell survival in adult-AML.

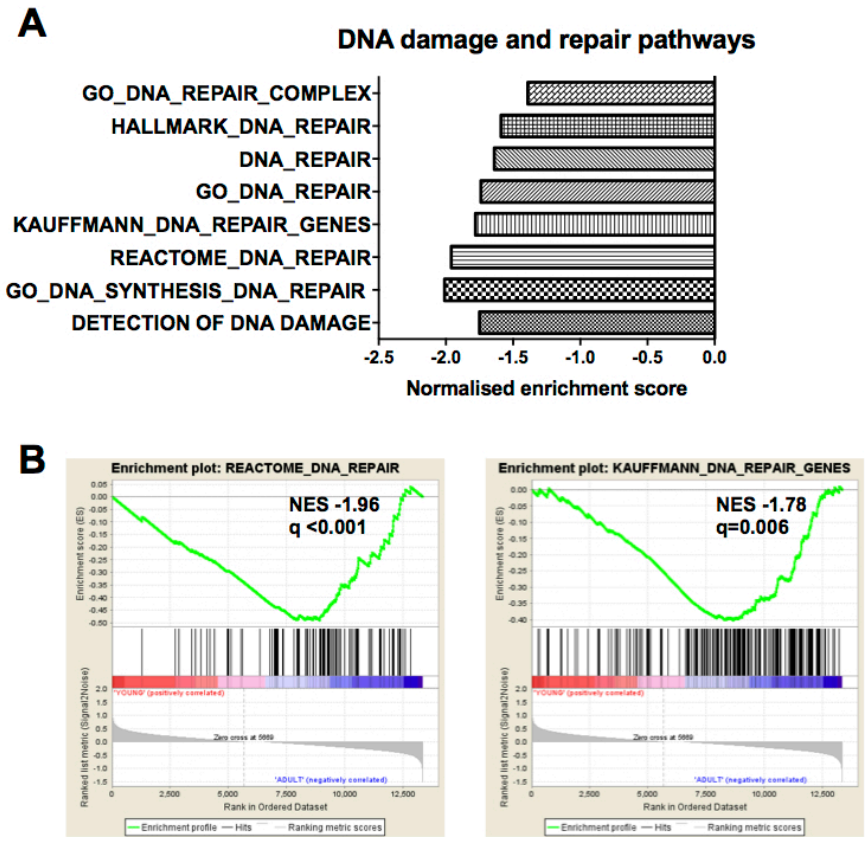

Figure 5.25 GSEA analysis of DDR and repair pathways in young and adult AML

(A) Graph of enriched DDR and repair pathways, comparing young and adult AML. Negative NES indicates enrichment in adult AML, q<0.05 for all enriched pathways, n=6.
(B) Representative enrichment plots of 2 DNA repair pathways, enriched in adult-AML, n=6 for each group.

5.4.7.6 NH9 Signatures

Pathways relating to changes in gene expression in response to ectopic expression of NH9 were investigated. As this was the oncogenic model used in all 4 four cellular ages investigated, enrichment of these pathways was not expected. However, age dependent enrichment was observed. (Table 5.2) Comparing FL-AML to 3w-AML there was an enrichment of downregulated NH9 targets in FL-AML. Comparing 3w-AML and >52w-AML showed an enrichment of NH9 targets in >52w-AML, while 3 gene sets of genes downregulated in response to NH9 were enriched in 3w-AML, suggesting that with increasing cellular age, the transcriptional response to NH9 is stronger. Comparing young and adult AML showed the same pattern: enrichment of NH9 downregulated genes in young and enrichment of NH9 upregulated genes in adult. (Figure 5.26).

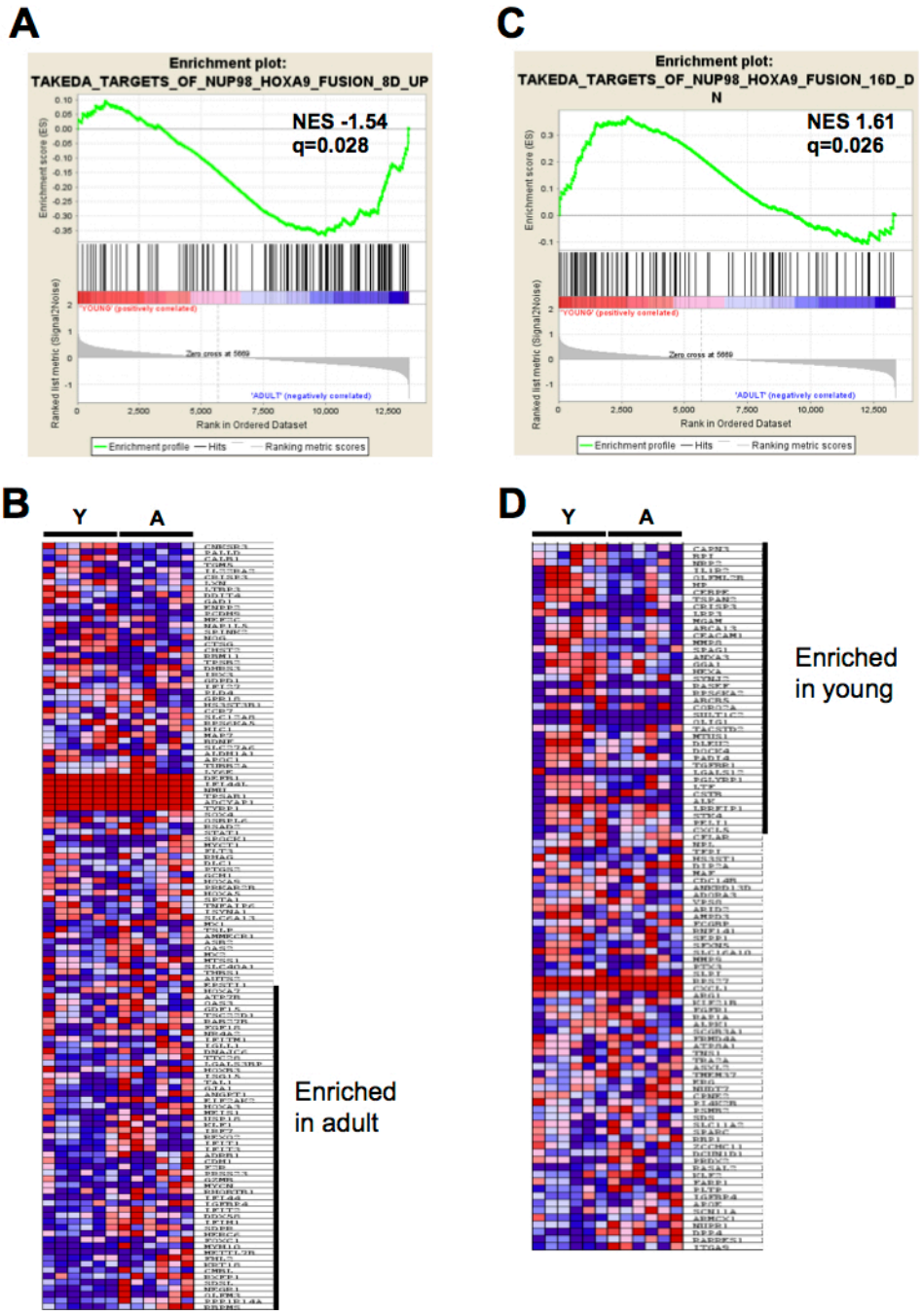

Figure 5.26 GSEA analysis of NH9 pathways in young versus adult AML

(A) Enrichment plot showing enrichment of genes upregulated in NH9 disease in adult AML. (B) Heat map of expression of genes upregulated in NH9. Relative expression values represented as colours in which red=high, pink=moderate, light blue=low and dark blue=lowest expression in young-AML compared to adult-AML. Vertical line depicts core enriched genes in adult group. (C) Enrichment plot showing enrichment of genes downregulated in NH9 disease in young AML. (D) Heat map of expression genes downregulated in NH9. Relative expression values represented as colours in which red=high, pink=moderate, light blue=low and dark blue=lowest expression in young-AML compared to adult-AML. Vertical line depicts core enriched genes in young group. Y = young, A = adult. Positive NES enriched in young, negative NES enriched in adult, significant enrichment defined as NES≥±1.3 and $q<0.05$, n=6.

5.4.7.7 Adhesion

Pathways relating to cell adhesion and cell contact were interrogated in our dataset. The only enriched pathways were found when FL-AML and 10w-AML were compared. Two pathways relating to cell adhesion via the plasma membrane were enriched in FL-AML. (Figure 5.27) In both pathways, there was an enrichment of the cadherin family of transmembrane proteins (cadherins, desmosomal and protocadherins). Cadherins play an important role in foetal development, ensuring correct tissue separation and migration.

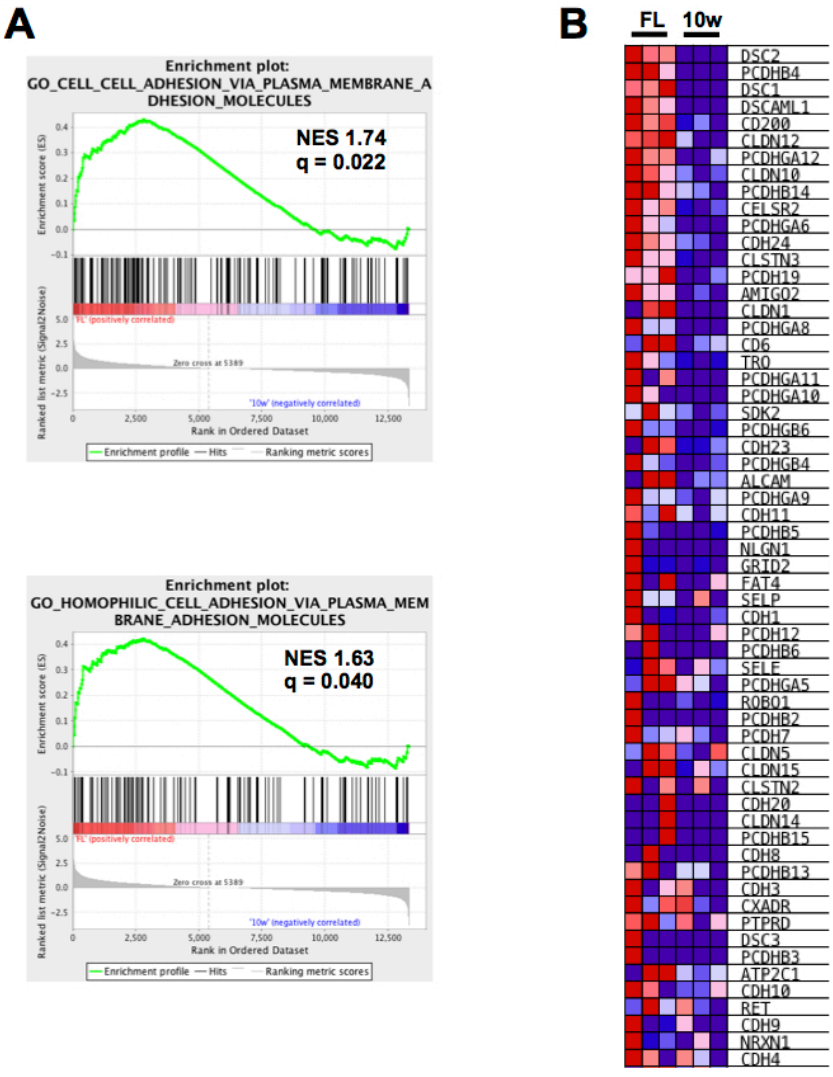

Figure 5.27 GSEA analysis of adhesion pathways in FL-AML versus 10w-AML

(A) Enrichment plots of 2 pathways characterised by adhesion via plasma membrane molecules. Both show enrichment in FL-AML. Significant enrichment NES≥±1.3 and q<0.05, n=3.
(B) Heat map of enriched genes in FL-AML in both adhesion pathways, showing enrichment of the cadherin family of proteins. Relative expression values represented as colours in which red=high, pink=moderate, light blue=low and dark blue=lowest expression in FL-AML compared to 10w-AML.

5.4.7.8 Inflammation and Immunity

In Section 5.4.5 we found a trend towards inflammation and immune response enrichment as a common feature of adult AML. Our data was therefore investigated for inflammatory and immune related pathways. There was no enrichment of these pathways when we compared FL-AML with 3w-AML. However, comparing FL-AML with 10w-AML showed 32 enriched pathways in 10w-AML but none in FL-AML. Leading edge analysis showed that the top enriched pathways related to the innate immune response. (Figure 5.28A) Conversely, when FL-AML or 3w-AML was compared to >52w-AML the opposite was seen. There was enrichment of immune and inflammatory pathways in young cells; 7 in FL-AML and 24 in 3w-AML. These pathways also related to the innate immune response. (Figure 5.28B and C and Table 5.2) Comparing pooled data from young and adult AML showed no enrichment in either population. These contradictory results may suggest that immune responses increase in early adult life, as immune pathways were enriched in 10w-AML compared to FL-AML. However, with increasing age the same immune responses are suppressed or reduced with ageing as immune pathways were enriched in FL and 3w-AML compared to >52w-AML.

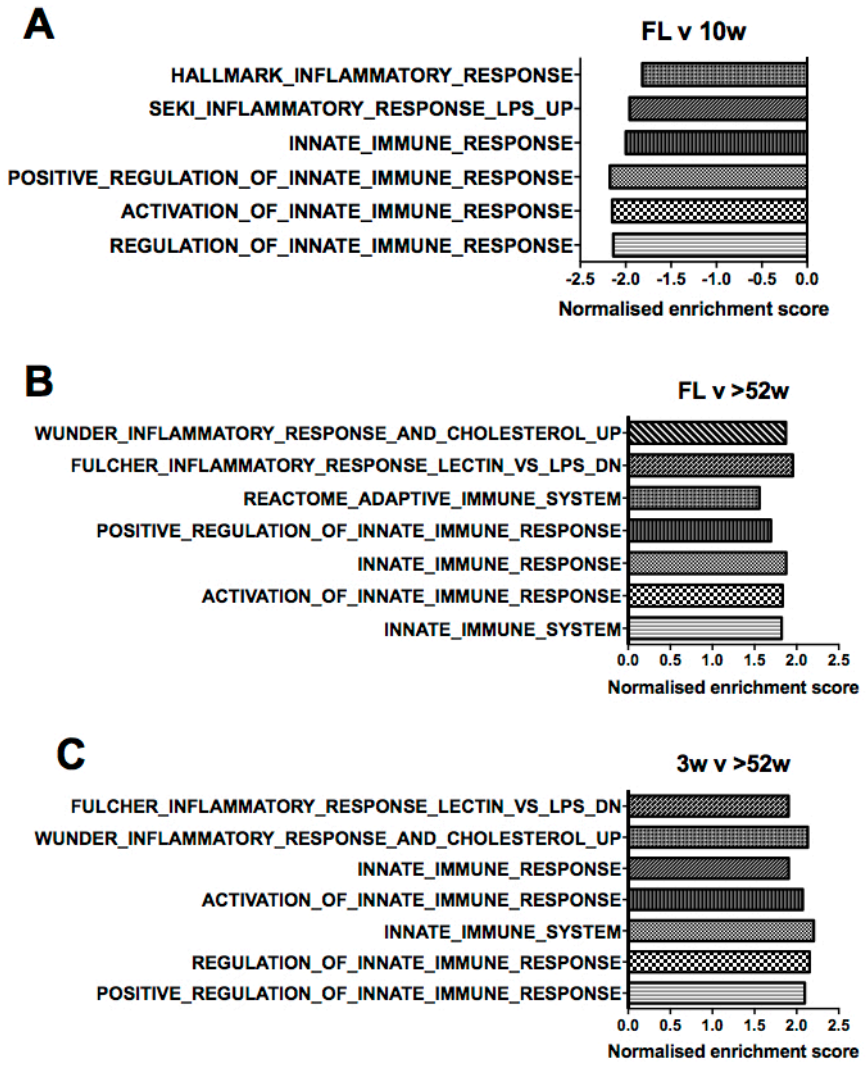

Figure 5.28 GSEA analysis of immune and inflammation pathways

(A) Graph of top enriched pathways comparing FL-AML with 10w-AML. Negative NES indicates enrichment in 10w-AML.
(B) Graph of top enriched pathways comparing FL-AML with >52w-AML. Positive NES indicates enrichment in FL-AML.
(C) Graph of top enriched pathways comparing 3w-AML with >52w-AML. Positive NES indicates enrichment in 3w-AML.
Significant enrichment defined as NES≥±1.3, q<0.05; n=3 for all groups, q<0.05 for all pathways.

5.4.8 GSEA analysis – unbiased pathway analysis

Previously, the dataset was interrogated for specific gene sets of interest. Next, the dataset was investigated for enrichment of any pathway in an unbiased approach. The raw expression data was interrogated for gene set enrichment using GSEA from the Broad Institute. Pairwise comparisons between FL and all other ages were performed using 1000 permutations for enriched gene sets. Curated MSigDB gene sets for pathways (C2) were used. An NES of >±1.3 with an FDR of less than 5% (q<0.05) was taken as significant. Table 5.3 shows the

number of enriched pathways from each comparison. The highest number of enriched pathways resulted from the comparison FL-AML with adult generated AML (either 10w-AML or >52w-AML), while comparing FL-AML with 3w-AML yielded the fewest number of enriched pathways, suggesting that transcriptional differences between AMLs are correlated with the cellular age of the transforming cell.

Table 5.3 Enriched gene set pathways from pairwise comparisons from unbiased GSEA analysis

Results from pairwise comparisons for gene set enrichment of all 4738 curated gene sets for pathways (C2) from MSigDB. Enrichment compared to younger age group for each comparison. Significantly enriched pathways defined as NES≥±1.3 and q<0.05.

Comparison	Enriched pathways		
	Young	Older	Total
FL v 3w	85	8	93
FL v 10w	3	226	229
FL v >52w	270	2	272
3w v >52w	111	5	116
Young v adult	6	149	155

5.4.8.1 FL-AML express erythroid, cell cycle and embryonic programmes while 3w-AML express programmes related to the BM niche

To investigate the impact of a foetal type cell originating from the FL rather than the BM, pairwise comparison was performed between FL-AML and 3w-AML. Using the MSigDB for C2, 85 gene sets were enriched in FL-AML. The top enriched pathways are shown in Figure 5.29A. Similar to the results in Section 5.4.1, which showed enrichment of erythroid programmes in FL-AML using the DEG method, 4 pathways were associated with erythropoiesis. Interestingly, 3 pathways related to AML subtypes characterised by distinct transcriptional programmes were also enriched in FL-AML. The genes from our dataset enriched in these pathways were also associated with the erythroid membrane and cytoskeleton. Four pathways were associated with cell cycle. One pathway was associated with embryonic haemopoietic differentiation from the hemangioblast, while 2 other pathways related to genetic signatures in mature progenitor or blood cells compared to stem cells. Assessing all enriched pathways in FL-AML showed that erythroid programmes and cell cycling programmes were highly enriched with 7 erythroid and 15 cell cycle related programmes. Embryonic

signatures and cell differentiation pathways were also enriched in FL-AML. (Figure 5.29B) Therefore, AML derived from FL retains a genetic signature from an early prenatal cell with an enrichment of erythroid and embryonic transcriptional pathways. While both FL and neonatal cells are highly proliferative, FL-AML displays greater cell cycling programmes. Eight pathways were enriched in 3w-AML. (Figure 5.29C) Five of these pathways related to granulocyte, macrophage or lymphoid programmes. The relative enrichment of multiple lineage programmes in 3w-AML is likely a reflection of the strong erythroid signature seen in FL-AML. Interestingly, 1 enriched pathway in 3w-AML was the CXCR4 pathway, an important pathway in the interaction of the HSC to the BM microenvironment. The sympathetic nervous system is also an important component of the BM microenvironment. The adrenergic pathway and the G alpha q subunit pathway, which is involved in adrenergic signalling, were also enriched in 3w-AML. Therefore, while FL-AML retains a prenatal, erythrocyte-biased signature, 3w-AML retains genetic signatures pertaining to its origin from the BM rather than the FL.

A

Gene Set Name	NES	q	
CHYLA_CBFA2T3_TARGETS_DN	3.18	<0.001	Erythropoiesis
WELCH_GATA1_TARGETS	2.42	<0.001	
KEGG_PORPHYRIN_AND_CHLOROPHYLL_METABOLISM	2.18	<0.001	
PILON_KLF1_TARGETS_UP	2.09	0.001	
VALK_AML_CLUSTER_7	2.20	<0.001	AML subtypes
VALK_AML_CLUSTER_8	2.19	<0.001	
ROSS_AML_OF_FAB_M7_TYPE	1.99	0.006	
GUO_HEX_TARGETS_DN	2.24	<0.001	Embryonic
GRAHAM_CML_QUIESCENT_VS_NORMAL_QUIESCENT_UP	2.17	0.003	Cell cycle
GRAHAM_CML_DIVIDING_VS_NORMAL_QUIESCENT_UP	2.13	0.003	
GRAHAM_NORMAL_QUIESCENT_VS_NORMAL_DIVIDING_DN	2.09	0.001	
REACTOME_MRNA_PROCESSING	2.00	0.005	
IVANOVA_HEMATOPOIESIS_MATURE_CELL	2.58	<0.001	Mature cell
EPPERT_PROGENITOR	2.27	<0.001	

B

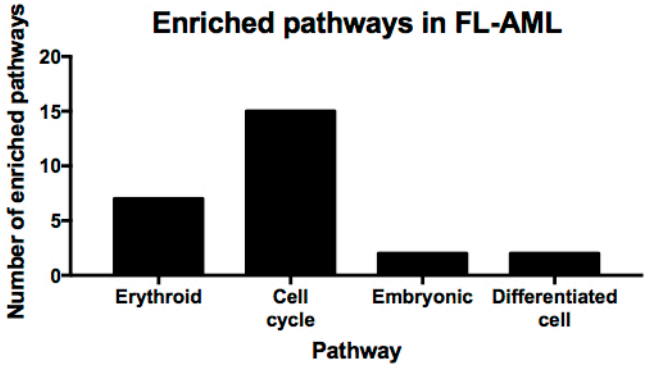

C

Gene Set Name	NES	q	
CHYLA_CBFA2T3_TARGETS_UP	-2.46	<0.001	Multiple haemopoietic lineage programs
REACTOME_TOLL_RECEPTOR_CASCADES	-2.09	0.028	
KEGG_NK_CELL_MEDIATED_CYTOTOXICITY	-2.04	0.041	
LEE_DIFFERENTIATING_T_LYMPHOCYTE	-1.98	0.047	
PID_IL12_2PATHWAY	-2.02	0.037	
PID_CXCR4_PATHWAY	-1.97	0.042	Bone marrow microenvironment
ST_ADRENERGIC	-2.04	0.035	
ST_GAQ_PATHWAY	-1.97	0.045	

Figure 5.29 GSEA analysis comparing FL-AML with 3w-AML

(A) Top enriched pathways in FL-AML.
(B) Graph of number of enriched pathways in FL-AML related to erythroid, cell cycle, embryonic and differentiated cell programmes.
(C) Enriched pathways in 3w-AML.
Significant enriched pathway defined as NES>1.3 and q<0.05, n=3 for each group.

5.4.8.2 FL-AMLs express multi-lineage haemopoietic and tumour suppressive programmes while adult-AMLs express stem cell programmes and BM microenvironment cues

To further investigate the impact of increasing cellular age of the transforming cell on the transcriptional profile of resultant leukaemia, pairwise comparisons were performed between FL-AML and 10w-AML and FL-AML and >52w-AML. Comparing FL-AML with 10w-AML, only 3 pathways were enriched in FL-AML. (Figure 5.30A) These were a pathway associated with plasma cell dyscrasia, head and neck tumours, both of which had enrichment of B-lymphoid and myeloid associated genes, and female fertility. However, 226 pathways were enriched in 10w-AML and are summarised in Figure 5.30B. The majority of these pathways were related to RNA and DNA metabolism, transcription and translation, and cell cycle regulation. In addition, stem cell signatures were also enriched in 10w-AML. This included an ES cell signature (Wong et al., 2008) characterised by self-renewal. Adult cancerous cells acquired the embryonic transcriptional signature via expression of *Myc*. It is interesting that this signature would be enriched in adult derived AML rather than FL derived AML. This suggests that adult AML acquire foetal-like transcriptional profiles but without normal control mechanisms, resulting in uncontrolled proliferation and self-renewal. Signalling pathways from HSC microenvironment interactions were also enriched in 10w-AML, including Wnt, Notch1 and cytokine signalling, further supporting the role of the BM microenvironment in the pathogenesis of adult AML.

When FL-AML and >52w-AML were compared 270 pathways were enriched in FL-AML. In addition to myeloid and erythroid programmes, many of these pathways related to B-cell signalling and differentiation, T-cell development and immune response, providing further support that AML derived from young HSCs retain lymphoid transcriptional programmes and have multilineage potential. In addition, pathways relating to late progenitors rather than stem cells were enriched in FL-AML suggesting they have a more mature transcriptional signature. (Figure 5.31A) The pathways with the highest NES related to oxidative metabolism and respiratory electron transport. Normal foetal HSC, which are highly cycling, utilise oxidative metabolic mechanisms rather than the anaerobic glycolytic metabolism utilised in adult HSCs. (Manesia et al., 2015) In addition, pathways related to tumour migration and increased cellular mobility were also

enriched in FL-AML suggesting FL derived AML does not localise to the BM. (Figure 5.31B) Proliferative pathways and protein synthesis pathways were enriched in FL-AML. With this, tumour suppressor programmes including p53 related pathways, cell cycle checkpoints, the DDR and apoptotic pathways were also enriched in FL-AML. (Figure 5.31B) This suggests that while FL-AML is highly proliferative, AML derived from young HSCs have tumour suppressive programmes that may delay or prevent leukaemogenesis and is in keeping with the longer latency to disease and incomplete penetrance we observed in our *in vivo* model. Interestingly, one tumour suppressive pathway resulted in degradation of Cdh1 or E-cadherin, which is important in cell-to-cell interactions, suggesting that some of the tumour suppressive pathways may be related to altered localisation of young AML cells in the BM niche. Only 2 pathways were enriched in >52w-AML. Both of these pathways belonged to cell populations characterised by self-renewal. The first pathway was a subset of genes found in induced pluripotent stem (IPS) cells, identified as bearing the tri-methylation mark at H3K27. (Figure 5.31C) These IPS cells are lineage-committed cells that are reprogrammed to become pluripotent. In doing so, they express genes and have epigenetic states similar to ES cells. The second pathway contains genes important in the embryonic germ cell. (Figure 5.31D) Interestingly, enriched genes found in this pathway and >52w-AML samples include members of the BMP pathway, *BMP4*, *BMP8b* and *SMAD5*. The enrichment of stem cell programmes with embryonic features supports the hypothesis that abnormal stem cell transcriptional programmes are expressed in adult-AML and may contribute to the aggressive phenotype observed in adult derived AML.

A

Gene Set Name	NES	q
BOYLAN_MULTIPLE_MYELOMA_PCA1_UP	1.95	0.048
MATZUK_CENTRAL_FOR_FEMALE_FERTILITY	1.92	0.049
RICKMAN_HEAD_AND_NECK_CANCER_D	1.91	0.049

B

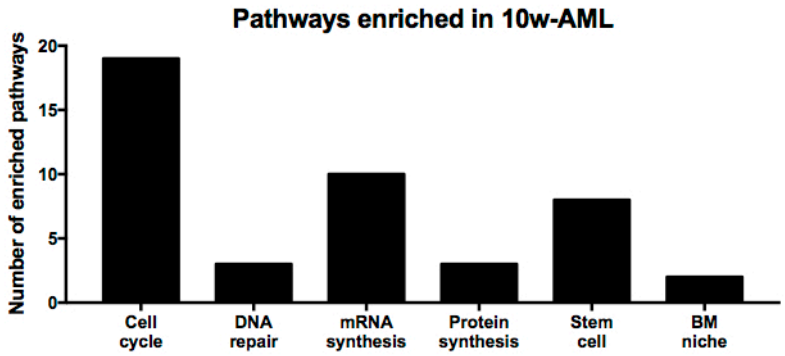

Figure 5.30 GSEA analysis comparing FL-AML and 10w-AML

(A) Significantly enriched pathways in FL-AML.
(B) Graph of significantly enriched pathways in 10w-AML compared to FL-AML showing enrichment of cell cycle associated pathways, stem cell programmes and BM niche signalling. Significant enrichment defined as NES≥±1.3 and $q<0.05$, n=3 for each group.

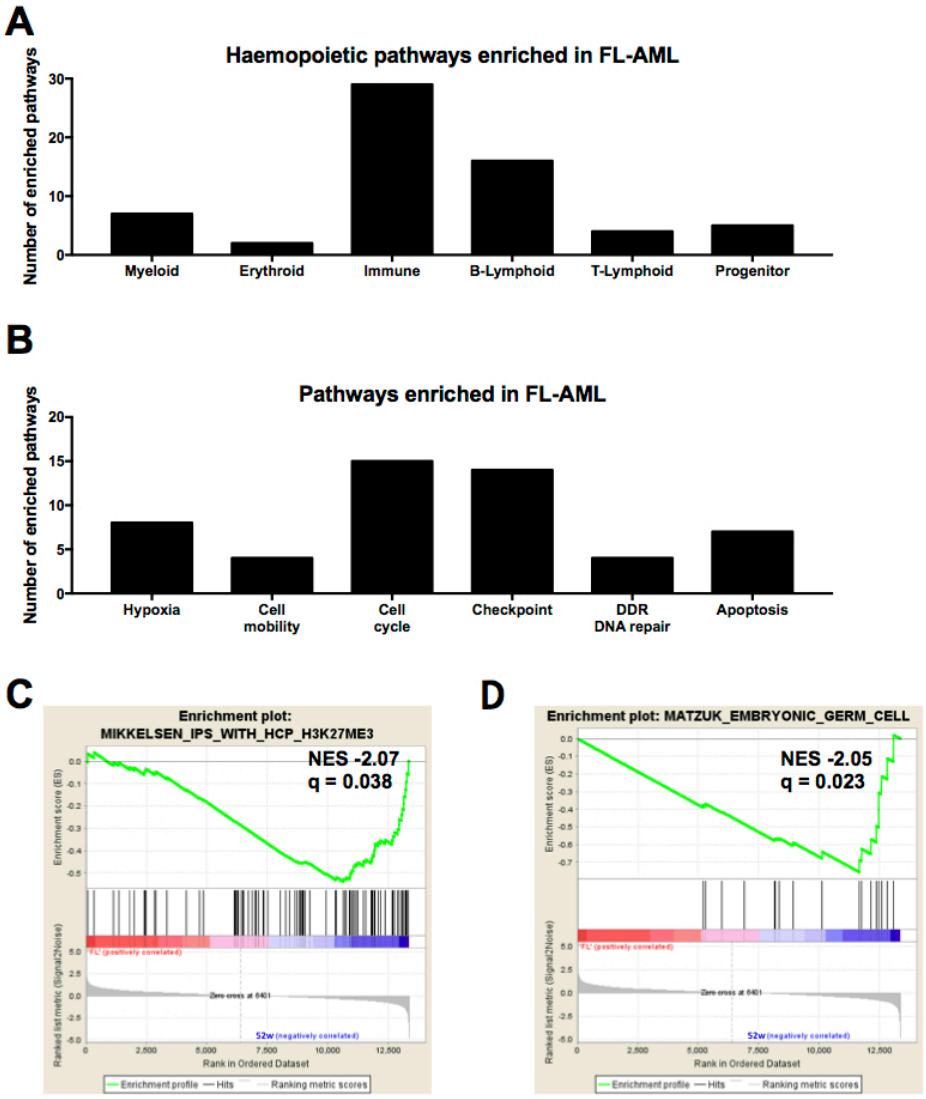

Figure 5.31 GSEA analysis shows FL-AML expresses multilineage and cell cycle programmes while >52w-AML expresses stem cell programmes

(A) Graph of significantly enriched haemopoietic pathways by GSEA analysis in FL-AML compared to >52w-AML.
(B) Graph of significantly enriched pathways by GSEA analysis in FL-AML compared to >52w-AML.
(C) Enrichment plot of IPS stem cell transcriptional program comparing FL-AML with >52w-AML. Negative NES denotes enrichment in >52w-AML.
(D) Enrichment plot of embryonic germ cell transcriptional program comparing FL-AML with >52w-AML. Negative NES denotes enrichment in >52w-AML.
Significant enrichment defined as NES>±1.3 and q<0.05, n=3 for each group.

5.4.8.3 3w-AMLs express programmes for multiple lineages while >52w-AMLs express myeloid associated programmes

To further investigate the effect of age, without the confounding factor of different originating environments, GSEA analysis was performed comparing 3w-AML with >52w-AML, using the above statistical methods. This showed 110 enriched pathways in 3w-AML. The majority of enriched pathways in 3w-AML

were involved in inflammation and immunity. In addition, specific B and T-lymphoid, natural killer, dendritic cell and myeloid pathways were also enriched in 3w-AML. Seven transcriptional signatures of cytogenetically defined AML were enriched in 3w, including MLLr, inv(16), APL and FAB subtype M4/M5 (acute myelomonocytic and acute monocytic leukaemia). A common feature of these AML gene sets is the expression of myeloid associated genes. Conversely, genes downregulated in stem cells were also enriched in 3w-AML. (Figure 5.32A) The results further support that AML from young LSKs retain multilineage haemopoietic programmes. In addition, they have a less primitive genetic signature, which may contribute to a delay in leukaemia development. Leukaemic cells often acquire transcriptional programmes normally found in stem cells and these programmes can lead to a more aggressive disease. Interestingly, Ras and MAP kinase pathways are also enriched in 3w-AML. Only 5 pathways were enriched in >52-AML. (Figure 5.32B) Three of these pathways related to AML subsets defined by specific transcriptional profiling. The first is a cluster identified in paediatric AMKL (FAB subtype M7). (Ross et al., 2004) The other 2 clusters, were identified in adult AML samples and are characterised by FAB subtype M1 (AML with minimal differentiation) and M2 (AML with differentiation). (Valk et al., 2004) Leading edge analysis was performed on these 3 AML associated pathways to investigate the subset of genes that contribute most to the enrichment results. Figure 5.32C shows the overlapping enriched genes in >52w-AML. These include the oncogene *Tal1*, genes associated with contractile function and motility (*Ank1*, *Tpm1*, *Myl4*, *Kel*, *Dnajc6* and *Rhag*) and the integrin *Itga2b*. Furthermore, compared to the FAB subtypes enriched in 3w-AML, M1 and M2 subtype are morphologically less differentiated, in keeping with adult derived AML expressing immature/stem cell transcriptional programmes. (Figure 5.32C) The other 2 enriched pathways in >52w-AML related to GATA1 targets, important in erythropoiesis, and targets of CBFA2T3, which is important in granulocyte differentiation. Thus, while 3w-AML express transcriptional programmes relating to multiple lineages, >52w-AML express strong myeloid profiles, in keeping with myeloid skewing observed in ageing and in the 100% myeloid leukaemias we observed *in vivo*.

A

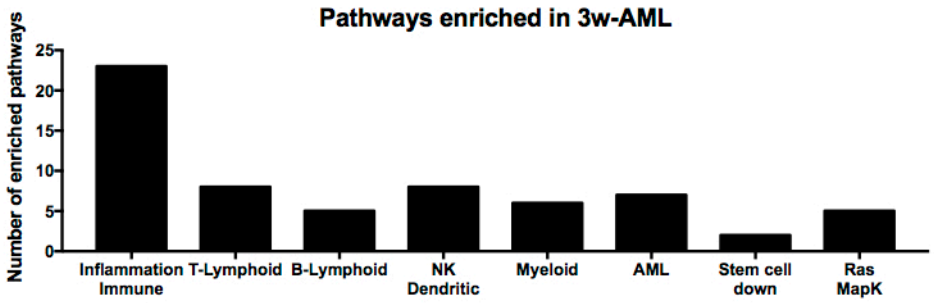

B

Gene Set Name	NES	q	
ROSS_AML_OF_FAB_M7_TYPE	-2.40	<0.001	AML subtypes
VALK_AML_CLUSTER_7	-2.13	<0.001	
VALK_AML_CLUSTER_8	-2.07	0.003	
CHYLA_CBFA2T3_TARGETS_DN	-2.92	<0.001	Erythroid
WELCH_GATA1_TARGETS	-2.21	<0.001	

C

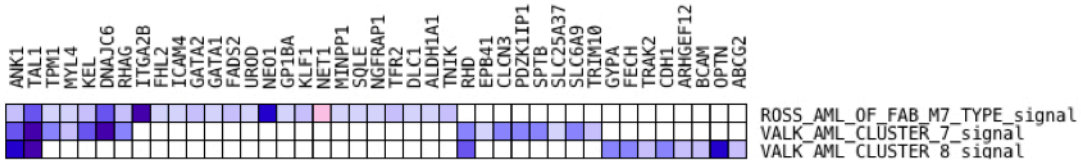

Figure 5.32 Lineage determining pathways are enriched in 3w-AML while myeloid programmes are enriched in >52w-AML

(A) Graph of number of significantly enriched pathways by GSEA analysis in 3w-AML compared to >52w-AML. Gene sets related to immunity and lineage determination are enriched in 3w-AML Significant enriched pathway defined by NES≥±1.3 and q<0.05, n=3 for each group.
(B) Enriched pathways in >52w-AML compared to 3w-AML showing gene set name, NES and q-value. Significant enriched pathway defined by NES≥±1.3 and q<0.05, n=3 for each group.
(C) Heat map from leading edge analysis of AML subtype gene sets enriched in >52w-AML showing myeloid genes are overlapping common enriched genes. Relative expression values represented as colours in which red=high, pink=moderate, light blue=low and dark blue=lowest expression in 3w-AML compared to >52w-AML.

5.4.8.4 Young-AMLs express programmes for myeloid and lymphoid lineage determination while adult-AMLs express stem cell and Myc related programmes

Young-AML (FL and 3w, n=6) and adult-AML (10w and >52w, n=6) were interrogated to find the transcriptional programmes discriminating AML generated from young and adult LSKs, using the same statistical conditions as above. Using the C2 curated MSigDB pathways, 6 pathways were enriched in

young-AML. Five of these pathways were related to lineage specification. (Figure 5.33A) Two related to myeloid associated genes; 1 to the C/EBPα related network of myeloid genes and another to granulocytic genes upregulated in mycobacterium infection. Two pathways related to B-cell signalling; 1 to plasma cells and another to B-cell receptor signalling. Interestingly, another pathway enriched in young AMLs related to a gene signature in progenitors immortalised by both HoxA9 and Meis1. (Wang et al., 2005) These cells acquire self-renewal and have multilineage potential, with expression of both myeloid and lymphoid related genes. Thus, there is an enrichment of both myeloid and lymphoid programmes in young-AML. Despite a myeloid phenotype, young-AML also expresses lymphoid programmes suggesting lineage plasticity and lymphoid potential. This is in keeping with the small percentage of FL and 3w recipients developing lymphoid leukaemia *in vivo*. In contrast, adult AML expressed stem cell pathways. (Figure 5.33A) This included the ES cell core (Wong et al., 2008) which was also upregulated in 10w, >52w and adult AML when we performed GSEA analysis specifically for stem cell programmes in Section 5.4.7.4. This ES cell transcriptional program is characterised by self-renewal. Abnormal activation of this pathway in adult solid tumours is associated with metastasis and death. The second stem cell related pathway enriched in adult-AML comprised of a common stem cell signature detected in murine embryonic, neural and haemopoietic stem cells (described in Section 5.1.2.1). (Ramalho-Santos et al., 2002) Leading edge analysis was performed to investigate the subset of genes that contribute most to the enrichment results. Figure 5.33B shows the overlapping genes enriched in both pathways in adult-AML. These include cell cycle regulators (*Ccnd1*, *Xpo1*, *Dtymk*, *Yap1*), DNA repair genes (*Xrcc5*, *Msh2*) and genes involved in transcription and translation (*Rpl22*, *Tmrps2*, *Gars*, *Iars*). Thus, while young-AML expresses multilineage transcription programmes, adult AML expresses abnormal, often embryonic, stem cell programmes. When expressed in human cancer, these programmes are associated with adverse disease and clinical features. Therefore the shorter latency to disease and complete penetrance, suggesting aggressive disease, which we observed in adult-AML may occur as a result of stem cell transcriptional programmes.

In total, 148 pathways were enriched in adult-AML. Eight of these pathways were Myc related pathways. Myc is a transcription factor that drives proliferation and cell growth, downregulates apoptosis and promotes self-renewal in stem cells. The majority of the remaining enriched pathways in adult AML were related to proliferation and cell cycle regulation, RNA or DNA metabolism, DNA repair and translation, in keeping with Myc related functions. (Figure 5.34A) To further investigate this, GSEA analysis was repeated on young and adult-AML, looking specifically for enrichment of Myc related pathways. Of 71 Myc pathways found in MSigDB, none were enriched in young AML. In contrast, 18 Myc related pathways were enriched in adult AML. (Figure 5.34B) Myc is an oncogene and overexpression of Myc is observed in many human cancers. The enrichment of Myc related pathways in adult AML suggests a mechanistic role for Myc to account for the shorter latency and 100% penetrance of adult AML observed *in vivo*. The expression of c-Myc from our targeted screen was evaluated in *in vitro* transformed LSKs. Regardless of whether the samples were analysed in 4 age groups, or pooled into young and adult, there was no difference in the expression of c-Myc at the transcriptional level. (Figure 5.35)

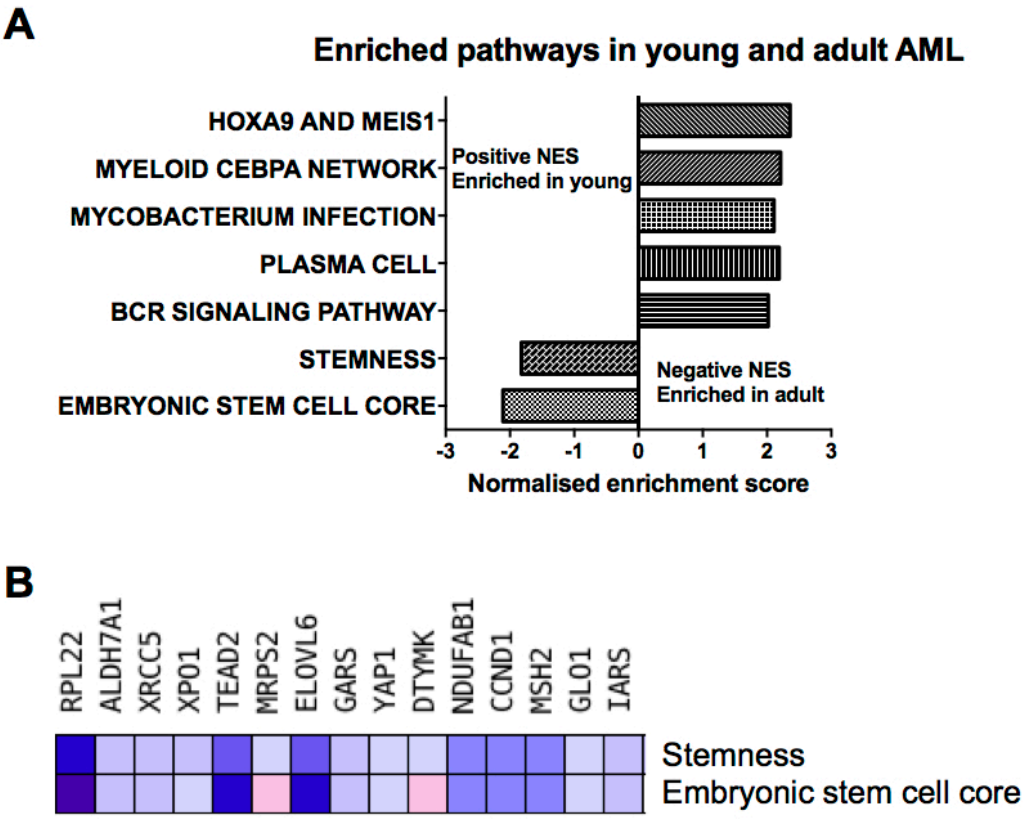

Figure 5.33 Lineage determining pathways are enriched in young AML while stem cell programmes are enriched in adult AML

(A) Graph of significantly enriched pathways by GSEA analysis in young and adult AML. Significant enrichment defined by NES≥±1.3 and q<0.05, n=6 for each group. Positive NES denotes enrichment in young AML, negative NES denotes enrichment in adult AML.
(B) Heat map from leading edge analysis of stem cell pathways enriched in adult AML showing genes enriched in both stem cell pathways. Relative expression values represented as colours in which red=high, pink=moderate, light blue=low and dark blue=lowest expression in young-AML compared to adult-AML.

A

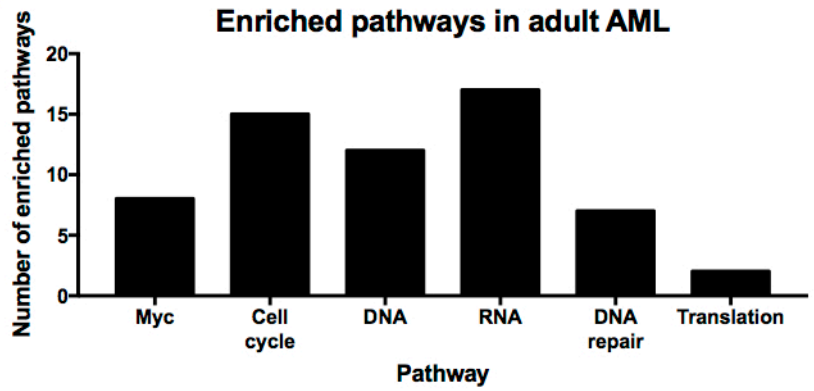

B

Gene Set Name	NES	q
HALLMARK_MYC_TARGETS_V1	-2.61	<0.001
HALLMARK_MYC_TARGETS_V2	-2.29	<0.001
SCHLOSSER_MYC_TARGETS_REPRESSED_BY_SERUM	-2.03	<0.001
SCHUHMACHER_MYC_TARGETS_UP	-2.04	<0.001
SCHLOSSER_MYC_TARGETS_AND_SERUM_RESPONSE_DN	-1.88	0.002
COLLER_MYC_TARGETS_UP	-1.79	0.006
DANG_MYC_TARGETS_UP	-1.74	0.009
SANSOM_APC_TARGETS_REQUIRE_MYC	-1.74	0.010
MENSSEN_MYC_TARGETS	-1.70	0.010
MORI_EMU_MYC_LYMPHOMA_BY_ONSET_TIME_UP	-1.69	0.013
YU_MYC_TARGETS_UP	-1.61	0.026
PID_MYC_ACTIV_PATHWAY	-1.59	0.029
BILD_MYC_ONCOGENIC_SIGNATURE	-1.55	0.038
DANG_REGULATED_BY_MYC_UP	-1.52	0.041
GCM_MYCL1	-1.52	0.043
KIM_MYC_AMPLIFICATION_TARGETS_UP	-1.53	0.046
MYC_UP.V1_UP	-1.49	0.045
CAIRO_PML_TARGETS_BOUND_BY_MYC_UP	-1.49	0.048

Figure 5.34 GSEA analysis shows enrichment of Myc related pathways in adult AML compared to young AML

(A) Graph of significantly enriched pathways in adult AML compared to young AML, using the whole C2 pathway database from MSigDB, showing enrichment of Myc pathways and pathways related to Myc function.
(B) All enriched pathways comparing young and adult AML specifically for Myc pathways. All pathways were enriched in adult AML, with no enrichment in young-AML.
Significant enriched pathway defined by NES>±1.3 and q<0.05, n=6 for each group. Positive NES denoted enrichment in young-AML, negative NES denotes enrichment in adult-AML.

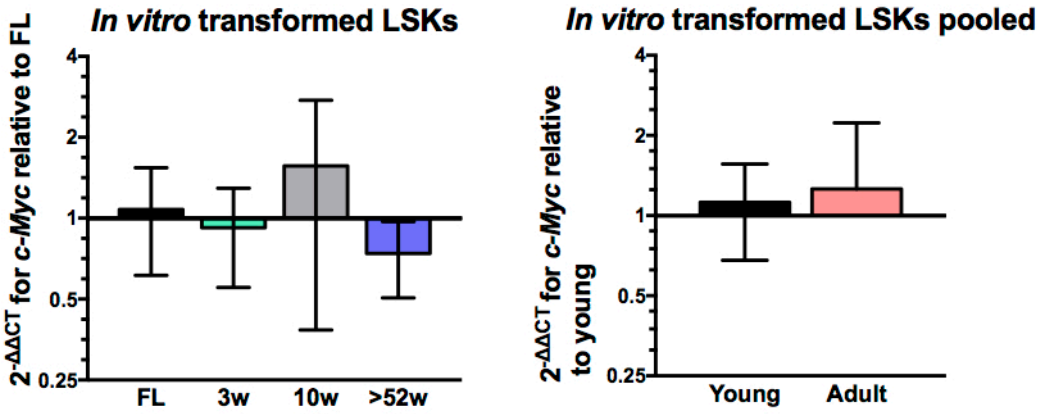

Figure 5.35 *c-Myc* expression is similar across age groups in *in vitro* transformed LSKs

Relative *c-Myc* expression in LSKs transformed *in vitro* by NH9 at CFC2, comparing FL, 3w, 10w and >52w (left, FL comparator) and pooled young and adult (right, young comparator). FL n=4, 3w n=2, 10w n=3, >52w n=3, young n=6, adult n=6. Graphs depict mean $2^{-\Delta\Delta CT}$ generated FC +/-SD. For 4 way comparisons, significance determined by 1-way ANOVA and Bonferroni post-test. For pairwise comparisons, significance determined by Student's t-test.

5.5 Discussion

In the previous chapter impact of cellular age on the propagation of NH9 driven leukaemia *in vivo* was discussed. Specifically, young LSKs were more resistant to leukaemia and retained lymphoid potential while adult LSKs developed leukaemia more rapidly, with 100% penetrance, and were myeloid restricted. Both cell intrinsic and cell extrinsic (from the microenvironment) factors were postulated to account for these differences. In this chapter, potential mechanisms to explain the observed findings were investigated at a transcriptional level. A targeted screen was performed, investigating the expression of lineage and stem cell determining genes and cues from the microenvironment in untransduced WT LSKs, *in vitro* transformed and *in vivo* generated leukaemia from 4 ages. Furthermore, global RNA-seq was performed on AML generated from 4 ages to investigate the transcriptional programmes that discriminate leukaemia generated from young versus adult LSKs.

5.5.1 Lineage discrimination

In vivo, FL and 3w transformed LSKs could develop either myeloid, lymphoid or mixed phenotypic leukaemia, while 10w and >52w exclusively developed AML. Using a targeted screen for lineage markers, young LSKs transformed by NH9 *in*

vitro (before leukaemia development), exhibited higher relative expression of genes associated with both myeloid and lymphoid lineages, compared to adult. This suggests that immediately after oncogene induction, both myeloid and lymphoid programmes are active in young HSCs, giving them the potential to develop either lineage. The NH9 model was used, which results in pathological overexpression of *HOXA9*. HOXA9 is a critical regulator of haemopoiesis in the embryo and plays a role in HSC proliferation and differentiation postnatally and HoxA9$^{-/-}$ mice have impaired myeloid, erythroid and lymphoid development. (Kessel and Gruss, 1990, Lawrence et al., 1997) Both NH9 and HOXA9 overexpression have been implicated in myeloid lineage restriction and malignancies but not in lymphoid malignancies. (Gough et al., 2011, Wang et al., 2005) The upregulation of both programmes in young LSKs suggests that retention of lymphoid programmes is an intrinsic feature of young HSCs rather than dependent on the specific oncogene. This finding would be in keeping with a proportion of recipient mice from the FL and 3w group developing ALL as well as the higher incidence of lymphoid malignancies occurring in childhood compared to adulthood.

Investigation of the lineage genes in AML generated *in vivo*, showed that the difference in the expression of myeloid and lymphoid markers detected in *in vitro* transformed LSKs between young and adult diminished once AML developed. Also, comparing AML and ALL generated from young LSKs showed that AML expressed myeloid genes while ALL expressed lymphoid genes, despite both originating from cells that expressed both programmes *in vitro*. This suggests that the transcriptional landscape reflects the lineage of the resultant leukaemia as defined by flow cytometry and IHC.

Interestingly, global transcriptional analysis of *in vivo* AML generated from 4 ages showed that lineage programmes were differentially expressed in young and adult AML. Whether using the DEG or GSEA method of investigation, erythroid programmes were enriched in FL-AML. This enrichment most likely relates to the high rate of red cell development in the FL. The continued enrichment of these programmes in FL derived AML suggests that intrinsic transcriptional programmes that predominate in a particular age of cell are carried through once that cell

transforms. Using either the DEG or GSEA method showed that FL and 3w-AML expressed lineage programmes relating to both myeloid and lymphoid differentiation. This is in line with some FL and 3w AML expressing aberrant B and T-lymphoid markers by flow cytometry and IHC. The dual expression of myeloid and lymphoid transcriptional programmes in young AML suggests that young LSKs have potential for both myeloid and lymphoid lineage that is retained even after oncogenic transformation. It also suggests that young AML retains lymphoid programmes while being phenotypically myeloid, and thus one could hypothesise that it has the potential to lineage switch. Experimentally, forced expression of lineage determining transcription factors can alter the differentiation of lineage-committed progenitors. Overexpression of C/EBPα can convert T-cell progenitors to macrophages while overexpression of C/EBPα or GATA2 in CLPs causes differentiation down granulocyte/macrophage or megakaryocyte/erythroid lineages, respectively. (Laiosa et al., 2006, Iwasaki et al., 2006)

The mechanisms for lineage switching in acute leukaemia are not well understood and both intrinsic and extrinsic factors may play a part. Two clones of differing lineage may be present at diagnosis with 1 clone dominating. Eradication of the dominant clone by chemotherapy could select for the other clone. Alternatively, transcriptional and epigenetic changes in the leukaemic stem cell may lift lineage silencing, allowing the original clone to switch phenotype. Examining the leukaemic bulk population, both myeloid and lymphoid programmes were expressed in young AML. From the data presented, it cannot be concluded if this comprised of dual populations of lymphoid and myeloid expressing cells, or if multiple lineage programmes were expressed in the same cell. Single cell analysis could elucidate this. What is clear is that lymphoid transcriptional programmes are expressed in young AML transformed with NH9. This is in contrast to 10w and >52w AML in which myeloid differentiation programmes were expressed. In keeping with the myeloid skewing in normal aged HSCs, adults are also likely to develop myeloid, rather than lymphoid disease. (Howlader N, 2014) Extrinsic cues can also determine lineage fate. There is evidence that inflammatory signals, including Notch and TLR signalling can promote myeloid differentiation and activation. (Welner et

al., 2008, Shang et al., 2016) Many of the myeloid associated programmes enriched in adult AML related to innate immunity and TLR signalling. Therefore cues from the BM niche may also promote myeloid disease development in adult LSKs, while these signalling pathways may not dominate in young AML.

5.5.2 Stem cell programmes

The expression of lineage programmes in young-AML could suggest that AML from young cells have a more mature, differentiated transcriptional profile. In contrast, adult-AML expressed more immature, stem cell related programmes, which could contribute to adult LSKs being more permissive to leukaemic transformation. The cancer stem cell model suggests that a small population of LSCs propagate leukaemia and eradication of this population is required to cure disease. In addition, expression of LSC transcriptional signatures is associated with adverse disease characteristics and outcomes. LSCs share biological characteristics with normal HSCs such as self-renewal and the ability to differentiate into non stem cell bulk leukaemic cells. (Dick, 2008) In human AML, the LSC is thought to reside primarily in the $CD34^{+}CD38^{-}$ fraction. (Bonnet and Dick, 1997) (See Section 1.3.1.2). Gentles *et al* characterised the transcriptional properties of the LSC in AML. Using microarray analysis to compare AML LSCs and leukaemia progenitor cells ($CD34^{+}CD38^{+}$), the authors identified a leukaemic stem cell signature of genes enriched in LSCs. This gene signature shared a transcriptional profile with normal human HSCs. Interrogation of the LSC signature in public datasets showed that expression of this signature in bulk AML was associated with adverse clinical outcomes (reduced OS, refractory disease and disease relapse) and was an independent predictor of inferior OS. (Gentles et al., 2010) As some LSCs may reside outwith the $CD34^{+}CD38^{-}$ compartment, Eppert *et al* assessed the transcriptional profile of functionally defined LSCs. LSCs from human AML that resulted in AML in primary and secondary NOD/SCID recipients were subjected to microarray analysis and compared to the bulk AML fraction to generate a 48 gene LSC signature. Comparison with a normal HSC signature (generated by comparison of normal $CD34^{+}CD38^{-}$ cells with more differentiated progenitors) revealed that the LSC signature was enriched in normal HSCs. Comparing their dataset with previously generated datasets for immature, progenitor and mature populations showed that the LSC signature was

positively correlated with primitive cell gene sets and negatively correlated with progenitor and mature cell gene sets. Similar to Gentles *at al*, the LSC signature was positively correlated with adverse prognostic groups and poorer clinical outcome in AML datasets. (Eppert et al., 2011) Ng *et al* identified differentially expressed genes comparing human AML with and without LSCs properties and this with patient survival. The resultant 17 gene LSC score was highly predictive of induction failure in 5 independent cohorts. (Ng et al., 2016) In the presented dataset, genes related to stem cell maintenance and function were upregulated in adult *in vitro* transformed LSKs and *in vivo* generated AML, such as *Tal1*, *Epcr* and *Mpl*. Furthermore, global transcriptional analysis showed enrichment of primitive stem cell programmes in adult AML while transcriptional profiles relating to progenitor populations and differentiated cells were enriched in young AML. One pathway in particular, identified by Wong *et al*, was enriched in 10w, >52w or adult AML in several pairwise comparisons with young AML. This ES cell signature was identified by comparison of the transcriptional profile of murine ES cells with that of adult tissue stem cells. Interestingly, activation of this signature was found in various human cancers, including leukaemia, lymphoma and solid tumours. Furthermore, expression of the ES signature in cancer cells was associated with adverse outcomes including metastasis of solid tumours, poorly differentiated subtypes and death. (Wong et al., 2008) In the transcriptional analysis performed in this thesis, stem cell genes were expressed early after oncogenic insult in adult LSKs and an enrichment of stem cell programmes was retained in adult AML. Furthermore, adult AML expressed an embryonic signature that is known to be associated with adverse disease and clinical outcomes in cancer. This suggests that in adult LSKs, stem cell programmes drive more aggressive disease, which manifests as shorter latency and complete penetrance of leukaemia. Conversely, the relative lack of active stem cell programmes in FL and 3w LSKs immediately after oncogene introduction may protect against leukaemia development. In addition, the reduced expression of stem cell programmes in established AML generated from young LSKs may make them more sensitive to treatment compared to adult AML. This was not investigated, but an interesting line of investigation would be to assess whether the generated young AML is more sensitive to chemotherapeutic agents than adult AML.

5.5.3 Oxidative metabolism

An interesting finding from the unbiased GSEA analysis comparing FL-AML with >52w-AML was the enrichment of oxidative metabolism pathways in FL-AML. Normal adult HSCs tend to utilise the anaerobic glycolytic metabolic pathway to generate energy, with oxidative mechanisms being employed in more differentiated progenitors. (Simsek et al., 2010, Klimmeck et al., 2012) However, FL HSCs, which are highly proliferative, use oxidative metabolism. RNA-seq comparing FL-derived LT-HSCs and LSKs with LT-HSCs from 8w mice showed enrichment of oxidative metabolic pathways in primitive FL cells. (Manesia et al., 2015) Similar to the enrichment of erythroid pathways, the enrichment of oxidative pathways in transformed FL-AML in the presented dataset likely represents retention of foetal programmes in the transformed cells. While this may not explain the reduced susceptibility to leukaemia and lymphoid potential observed in the FL groups, it is further evidence that transcriptional programmes defined by cellular age are retained when the cell undergoes leukaemic transformation.

5.5.4 DDR and DNA repair

As detailed in the previous chapter, increasing HSC age is associated with an accumulation of DNA damage, which is thought to contribute to the ageing phenotype of old HSCs and a prelude to cancerous transformation. (Rossi et al., 2007b, Rube et al., 2011, Beerman et al., 2014) Even in foetal HSCs, impaired DNA repair mechanisms leads to a decline in absolute numbers of ST and LT-HSCs and functional decline with reduced competitive repopulating ability compared to controls with intact repair mechanisms. (Suzuki et al., 2017) Drivers of DNA damage include daily genotoxic stress when HSCs are quiescent and replicative stress when they enter cell cycle. Beerman *et al* analysed the expression of 190 DDR genes in HSCs from FL at E14.5, young adult mice (3-4m) and old mice (24-26m). There was no difference comparing young and old adult HSCs, bar reduced NER related genes in old HSCs. However, compared to FL there was reduced expression of all DDR mechanisms in adult HSCs. This appeared to be dependent on cell cycle status, as adult HSCs that entered cell cycle upregulated DDR genes to levels similar to FL and resulted in a reduction in cellular DNA damage as

measured by comet tail assays. (Beerman et al., 2014) Impaired DDR and repair mechanisms play an important role in leukaemia pathogenesis. Inherited disorders of DNA repair pathways (eg. Fanconi Anaemia due to mutations in the *FANC* genes) can lead to BM failure, AML and solid tumours in childhood and early adulthood. Ionizing radiation and cytotoxic chemotherapy causing DNA damage, if ineffectively repaired, may lead to therapy related AML. Therefore, young foetal HSCs that are highly cycling have activation of DDR and repair mechanisms, which may be protective against oncogenic insult and would explain the delayed incidence and incomplete penetrance observed *in vivo*.

Conversely, upregulation of DDR and repair mechanisms in leukaemic cells may contribute to their survival and chemoresistance, as they attempt to repair damaged DNA rather than undergoing apoptosis. (Seedhouse et al., 2006, Hahnel et al., 2014) When DDR and repair pathways were investigated in the presented dataset, DRR and repair pathways were not correlated with age when individual age groups were compared. However, when samples were pooled into young and adult AMLs and GSEA analysis performed, there was an enrichment of 1 DDR and 7 DNA repair pathways in adult AML. In addition, comparing FL-AML with >52w-AML showed an enrichment of anti-apoptotic pathways in >52w, while comparing 3w-AML with >52w-AML showed an enrichment of tumour suppressor and apoptotic pathways in 3w. The enrichment of DDR and repair pathways in adult-AML could be interpreted in 2 ways. Either, in response to oncogene, appropriate DDR and repair pathways were initiated to ensure genetic fidelity, which ultimately failed. Or, as hypothesised, that the continued activation of DDR and repair mechanisms in adult AML cells is an inappropriate response to oncogenic stress allowing for cell survival rather than apoptosis. Additionally, activation of these pathways may also indicate a greater background mutational burden in adult LSKs prior to oncogenic insertion. This was not measured directly. Direct measurement for DNA damage (for example, by γH2AX levels or comet tail assays) in untransduced LSKs from the 4 ages would verify if adult LSKs harbour more DNA damage prior to oncogenic insult. Assessment of DNA damage in leukaemic cells, in comparison to background levels, would determine if leukaemia development in adult AML is associated with more additional DNA damage compared to young AML. DNA sequencing (either of the whole genome

or whole exome) could provide further information on site and type of mutations that occur in normal LSKs and leukaemia from different ages.

5.5.5 NH9 transcriptional programmes

In our experiment the NH9 model was used to transform different aged LSKs. It was therefore unexpected that transcriptional profiling showed enrichment of NH9 upregulated pathways in DEGs upregulated in 10w-AML compared to FL-AML. Interrogation of the entire dataset by GSEA analysis corroborated this finding; adult-AML displayed an enrichment of genes upregulated in response to NH9 while young-AML displayed an enrichment of genes downregulated in response to NH9. The gene sets used in the NH9 investigation came from a study that investigated the outcome of adult human $CD34^+$ cells after retroviral transduction with NH9. Using a variety of culture assays (growth in liquid culture, CFC assay and LTC-IC assay) the authors showed that compared to EV control, NH9 transduced $CD34^+$ cells displayed increased proliferation, impaired erythroid and myeloid differentiation and enhanced self-renewal with an enrichment of LTC-IC cells. Microarray analysis performed from day 3 to day 16 in culture revealed extensive transcriptional changes in NH9 positive cells. At day 3 there was an early upregulation of IFN inducible genes. From day 8 onwards, there was an upregulation of haemopoietic growth factors, *HOX* genes including *HOXA9* and *MEIS1*, and genes associated with oncogenesis and AML such as *KIT*, *FLT3*, *MYC*, *WT1* and *SOX4*. Conversely, genes associated with cell cycle inhibition, myelomonocytic differentiation and tumour suppression were downregulated. (Takeda et al., 2006) Similarly, the enrichment of NH9 downregulated genes in young AML is in line with the observed delay in leukaemia generation in FL and 3w LSKs. It is surprising that depending on the age of the transforming cell, there is such a polarised difference in the expression of genes associated with the same oncogenic driver. This does raise the question as to whether levels of NH9 gene and protein expression were similar across the different aged cell populations transduced in our experiment. Protein and mRNA expression levels were not confirmed post transduction. However, virus titre was controlled to ensure uniform transduction across samples and GFP expression, measured by MFI, was similar 48 hours post transduction and in CFC2 donor cells between all samples. (Figure 3.2B and

Figure 3.8B) Assuming that NH9 expression levels were similar in all investigated age groups, the difference in NH9 responsive genes in young and adult AML suggests a differential response to NH9 that is determined by the age of the transforming cell. Specifically, adult cells upregulate proliferation, self-renewal and oncogenic genes, with an increase in stem cell programmes. Young cells, on the other hand, employ mechanisms to prevent or delay leukaemia onset, either due to increased baseline expression of tumour suppressive programmes or upregulation in response to oncogene attack. The enrichment of tumour suppressive programmes was seen in young AML, while potential inappropriate DDR and repair mechanisms were enriched in adult AML. Therefore, young LSKs may inhibit an oncogenic signal while adult LSKs may be more permissive, resulting in different downstream NH9 targets in young and adult AML. The authors only investigated adult $CD34^+$ cells in this study. It would be interesting to compare the transcription profile of adult CD34+ with paediatric or CB $CD34^+$ transduced with NH9 to determine if there is, in humans, a difference in transcriptional profile with age of transforming cell, as was seen in our murine model.

5.5.6 BMP pathway

In the previous chapter in addition to cell intrinsic factors, an interplay with the BM microenvironment was postulated to also affect leukaemia development and account for the difference in latency, penetrance and lineage output in young and adult groups. Screening for microenvironmental cues, the BMP pathway was upregulated in adult cells in the presence of oncogene but before the development of AML. However, the upregulation of the BMP pathway in adult leukaemia diminished at the transcriptional level measured either by qPCR or gene set enrichment.

The importance of the BMP pathway in foetal haemopoietic development is well established. HSCs emerge from the embryonic AGM at E10.5-11.5 in mice and at E19 in human. Mammalian models show that BMP4 is highly expressed specifically at the ventral wall of the dorsal aorta (where HSCs emerge) and that early HSCs are universally BMP activated. (Marshall et al., 2000, Crisan et al., 2015) Furthermore, models of deletion of *BMP4*, *BMP2*, *Bmpr1a* or *Bmpr2* result

in early embryonic death and abnormal development of the mesoderm. (Winnier et al., 1995, Zhang and Bradley, 1996, Mishina et al., 1995, Beppu et al., 2000) However, the canonical BMP pathway is dispensable for stem cell function in E14.5 FL and adult BM HSCs. Singbrant *et al* used the pIC inducible MxCre;Smad1$^{fl/fl}$/Smad5$^{fl/fl}$ conditional double knock out mouse model for *Smad1* and *Smad5*. Deletion of *Smad1*, *Smad5* or both in adult HSCs did not affect the repopulation, differentiation or self-renewal capacity in primary and secondary recipients post BMT compared to WT controls. Similarly, transplantation of FL HSCs with deletion of *Smad5* or both *Smad1* and *Smad5* resulted in short and long-term multilineage engraftment in lethally irradiated primary recipients, comparable to WT controls. (Singbrant et al., 2010) Crisan *et al* used a BMP responsive element (*BRE*) GFP transgenic mouse model to investigate the activation of the BMP pathway in embryonic and adult HSCs. In this model GFP is expressed when BMP4 ligand binds to receptor and signals through phosphorylation of SMAD1/5 to activate transcription from the *BRE* sequence. While total percentage of BMP activated cells was similar for FL E14.5 and adult BM (3.7% and 5.5%, respectively), the percentage of phenotypic HSCs that were BMP activated (defined as LSK-SLAM) was significantly higher in FL (73%) than in adult (9%). Therefore, with increasing age activation of the BMP pathway in HSCs decreases and after the early embryonic stage BMP signalling becomes dispensable for stem cell function. (Crisan et al., 2015) However, BMP signalling can modulate stem cell function. Culture of human CD34^{+}CD38^{-}Lin^{-} HSCs in the presence of high concentrations of BMP2 and BMP7 (50ng/mL) resulted in increased proliferation, reduced CFC capacity but no difference in differentiation. Culture with BMP4 at low dose (5ng/mL) resulted in reduced HSC proliferation while culture at moderate dose (25ng/mL) resulted in increased proliferation and CFC capacity. Furthermore, low dose BMP4 treatment caused differentiation of HSCs with gain of CD38 expression, while prolonged moderate dose of BMP4 maintained HSCs in a primitive state. (Bhatia et al., 1999) Therefore, the BMP pathway can result in contrasting outcomes depending on ligand and dose. In addition, Sonic Hh induced proliferation of human CD34^{+}CD38^{-}Lin^{-} HSCs is mediated via BMP signalling. (Bhardwaj et al., 2001) Therefore, while the BMP pathway may not be essential for stem cell function,

re-expression and overexpression of the pathway may lead to pathological self-renewal, proliferation and differentiation programmes.

Crisan *et al* also performed transcriptional profiling of BMP activated and non-activated HSCs by RNA sequencing. BMP activated HSCs showed upregulation of Bmpr2 and its downstream targets confirming activation of the pathway. In addition, Myc and Stat5b target genes were upregulated in BMP activated cells. Deregulation of both pathways has been implicated in oncogenesis, leading to uncontrolled proliferation and self-renewal. (Crisan et al., 2015) Accounting for differences in initial populations (the bulk LSK population rather than LSK-SLAM was investigated in the thesis) no difference with age of cell was observed in the expression of BMP receptors, downstream signalling elements or targets in untransduced LSKs. However, with oncogene, adult LSKs showed higher expression of the BMP receptors, *Smads* and targets than in young LSKs, suggesting a pathological activation of the BMP pathway specifically in adult cells. Interestingly, while there was only a trend towards an increase in BMP activation in adult leukaemia cells, these cells showed an enrichment of Myc and stem cell programmes, which may have been activated as a result of initial BMP stimulation to drive more aggressive disease.

Crisan *et al* also investigated the lineage output 4m post BMT of BMP activated and non-activated HSCs from FL and adult donors. In adult HSCs, BMP activation was associated with balanced lineage output while non-BMP activation was associated with myeloid predominance. In addition, there was higher expression of lymphoid determining genes including *Ikaros*, *E2a* and *Flt3* in BMP activated adult HSCs. In FL HSCs there was no difference in lineage output with BMP activation. This goes against the observations in this thesis, in which BMP activation in adult LSKs transformed *in vitro* was associated with myeloid predominance in *in vivo* leukaemia. However, here a leukaemic model is investigated rather than normal HSCs. It is interesting to note that the BMP pathway could discriminate between lineage output of HSCs in adult but not in FL, further suggesting that the same signalling pathway may have different outcomes depending on intrinsic cellular factors that are determined by cellular age. (Crisan et al., 2015)

The role of the BMP pathway in haematological malignancy has not been well defined. High expression of BMP ligands and receptors has been observed in APL with levels returning to normal after response to therapy. (Grcevic et al., 2003) In vitro treatment of APL cell lines with BMP ligands inhibited the differentiation effect of ATRA. (Topic et al., 2013) Interestingly, a novel cryptic translocation has been identified in paediatric non-Downs syndrome AMKL. The translocation inv(16)(p13.3q24.3) results in the fusion product CBFA2T3-GLIS2. Gene expression studies comparing this subtype of AMKL with other AMLs shows marked overexpression of *BMP2* and *BMP4*. Retroviral expression of the fusion protein results in enhanced self-renewal of murine haemopoietic progenitors *in vitro*. This phenomenon is inhibited by the BMP antagonist dorsomorphin, suggesting downstream effects of the fusion protein are dependent on BMP signalling. (Gruber et al., 2012) Thus, deregulation of the BMP pathway can contribute to the propagation of leukaemia and BMP related genes in adult preleukaemic cells transformed *in vitro* suggesting a mechanistic role for the BMP pathway in driving more aggressive disease in adult AML.

5.5.7 Expression of microenvironmental cues

Differences in response to microenvironmental signalling were hypothesised to contribute to the differences in lineage and leukaemic susceptibility between leukaemia generated from young and adult LSKs. In the targeted screen, only the BMP pathway was differentially expressed in *in vitro* transformed LSKs but not in *in vivo* generated AML. Adhesion and membrane signalling pathways were investigated in AML samples generated from the 4 ages. While GSEA analysis for adhesion pathways did not yield enrichment in pairwise comparisons, age related differential expression of membrane, adhesion, cell contact and ECM related genes was identified. Compared to FL, genes associated with cell adhesion and the ECM were significantly upregulated in 3w, 10w, >52w. Furthermore, DEGs common to 3w, 10w, and >52w-AML (when compared to FL-AML) were also associated with cell adhesion, suggesting that transformed post foetal LSKs retain transcriptional programmes pertaining to their BM origin. However, comparison between 3w and >52w-AML as well as young and adult AML, showed genes associated with membrane signalling and the ECM were upregulated in

adult transformed cells. Thus, in addition to originating from the BM, adult LSKs have expression of adhesion associated pathways, suggesting the BM microenvironment may contribute to leukaemogenesis particularly in adult LSKs. Assessment of tissue differentiation pathways also revealed enrichment of osteoclastic differentiation in 10w-AML compared to FL-AML, suggesting that in adult AML, leukaemic cells may directly alter the niche to promote a pro-leukaemic environment.

There is evidence that adhesion molecules on the surface of leukaemic blasts are important in homing and engraftment of leukaemic cells in transplant experiments, such as VLA4, CXCR4 and CD44. VLA4 has been implicated in adhesion of leukaemic cells to the endothelial membrane in the vessel wall. (Stucki et al., 2001) CXCR4 and its stromal receptor CXCL12 are important in AML homing and leukaemia development. Despite variable surface expression of CXCR4 by flow cytometry, all AML blasts express internal CXCR4 and CXCL12. Exogenous CXCL12 enhances the survival of primary AML samples and cell lines *in vitro*, while CXCR4 or CXCL12 antagonists inhibit proliferation and survival. Similarly, pre-transplant treatment of AML cells with anti-CXCR4 antibody reduces AML homing to the BM and spleen of NOD/SCID recipients. (Tavor et al., 2004) CD44 is also required for homing of AML cells to the BM and administration of anti-CD44 antibody inhibits engraftment of primary human AML in NOD/SCID mice. (Jin et al., 2006) In addition to initial homing, adhesion molecules may also be important in leukaemia maintenance and progression. *In vivo* treatment of recipient mice with anti-CXCR4 antibody 2 days post BMT with primary human AML (to allow for initial engraftment) results in reduced engraftment. (Tavor et al., 2004) Administration of anti-CD44 antibody *in vivo* to NOD/SCID recipients 3-4w after transplantation with primary human AML cells results in reduced leukaemic burden. (Jin et al., 2006) In an inducible mouse model of AML, overexpression of *HOXA10* by administration of doxycycline, in addition to retroviral overexpression of Meis1 leads to AML development. Continued expression of *HOXA10* was required for leukaemia maintenance in the majority of secondary recipients. However, the 20% of recipients that did not require continued *HOXA10* expression for leukaemia maintenance exhibited increased protein expression of cell-to-cell and cell matrix proteins, including MMP, CD177

and CD44. High expression of CD44 on LICs was sufficient to generate AML in the absence of HOXA10 expression, while administration of an anti-CD44 antibody prior to transplantation prevented leukaemia development. (Quere et al., 2011) Expression of adhesion molecules may have prognostic implications. High expression of CXCR4 by flow cytometry on $CD34^+$ AML blasts in adult patients correlates with reduced OS and relapse free survival (RFS) of 11m and 8.7m, respectively, while OS and RFS is greater than 90m for patients with low expression of CXCR4. (Rombouts et al., 2004) Conversely, expression of VLA4 on AML blasts, a protein that promotes adhesion to the vascular wall via VCAM1, correlates with improved OS. In 175 adult AML samples, increased binding of VCAM1 to VLA4 on leukaemic blasts by functional assay correlated with an estimated 5y OS of 31%, compared to 10% in patients without increased VCAM1/VLA4 binding. (Becker et al., 2009) VLA4 expression assessed by flow cytometry in 216 paediatric patients with AML identifies low VLA4 expression as an independent prognostic factor for RR and lower disease free survival by multivariate analysis. (Walter et al., 2010) The exact mechanism by which the expression of adhesion molecules effect disease prognosis is unclear, but may include dislodging of leukaemic blasts and stem cells from the protective niche, rendering them sensitive for cytotoxic eradication. Therefore, the expression of adhesion molecules is not only crucial for initial engraftment of the AML cells but also for AML maintenance, suggesting that contact with the BM niche is essential for AML progression and maintenance. Furthermore, expression of adhesion molecules has prognostic implications. The enrichment of adhesion and membrane pathways in adult AML suggests that localisation to the protective BM niche contributes to the accelerated leukaemogenesis seen in the 10w and >52w group while in the FL and 3w, pro-oncogenic cues from the microenvironment are not transmitted. Furthermore, adhesion to the BM niche may render adult-AML less chemoresponsive. To further investigate this, intra-vital visualisation of young and adult leukaemic cells would determine if they localised differently in relation to the BM stroma.

5.5.8 Myc related pathways

An enrichment of Myc-related pathways in adult-AML was observed. The role of MYC in cancer has been well established. The *Myc* gene encodes a protein

transcription factor that through direct DNA binding and recruitment of histone acetyltransferases causes chromatin conformational changes, leading to the expression of genes involved in a multitude of cellular functions. These include proliferation, apoptosis, stem cell function and differentiation. (Dang, 2012) Activating mutations of *MYC* resulting in constitutive expression are present in a wide variety of cancers, including lymphoma, multiple myeloma, colon and breast cancer. (Beroukhim et al., 2010, Chesi et al., 2008, Sikora et al., 1987, Kozbor and Croce, 1984) Interestingly, reduced Myc expression has been associated with longevity and increased survival. Myc haploinsufficient *(Myc*$^{+/-}$) C57BL/6 mice were left to die of natural causes. Both male and females had longer life expectancy than their *Myc*$^{+/+}$ controls. This was not due to a reduction in tumour incidence in *Myc*$^{+/-}$ mice, although in mice that did die of cancer, tumour burden was lower in the *Myc*$^{+/-}$ group. Microarray analysis revealed an increase in immune mediators such as IFNs, interleukins, colony stimulating factors and NF-κB with age in *Myc*$^{+/+}$ controls, which was counteracted by *Myc* haploinsufficieny. (Hofmann et al., 2015) Myeloid skewing and reduced immune surveillance is a hallmark of aged HSCs and Myc expression may contribute to this ageing phenotype. In a tamoxifen inducible murine model, the effect of *Myc* overexpression on the BM microenvironment was assessed. *Myc* overexpression in donor BM resulted in a rapid lethal MPN in recipient mice. *Myc* overexpression was triggered once donor BM had successfully engrafted in the host. Four days of *Myc* overexpression in haemopoietic cells resulted in a decrease in CD31^{+} endothelial cells. These endothelial cells expressed upregulation of hypoxia and glucose related pathways and downregulation of VEGFR, calcium clearance, small GTPase and RhoB signalling pathways. These changes were not coupled with a change in haemopoietic cells. Therefore, alterations in the BM microenvironment are an early effect of *Myc* overexpression, preceding changes in the haemopoietic cells. (Franke et al., 2015) The results presented in this thesis show that Myc related pathways are enriched in adult AML, suggesting that Myc activation may account for the shorter latency and 100% penetrance observed in 10w and >52w groups in our *in vivo* experiment. Additionally, in adult AML, Myc may exert its pro-leukaemia effects by altering the BM microenvironment, resulting in abnormal tumour surveillance and an environment that promotes leukaemogenesis. An

enrichment of an ES cell pathway in adult AMLs was also observed. (Wong et al., 2008) Expression of this pathway in epithelial tumours is associated with increased metastasis and death in patients. Interestingly, reactivation of this pathway in normal and cancerous cells is *Myc* dependent. Therefore, the expression of stem cell programmes in adult AML may be in part due to *Myc* overexpression. No difference in *c-Myc* gene expression was detected in pre-leukaemic cells at CFC2 with cellular age. This may be because *c-Myc* transcriptional upregulation in adult LSKs does not occur early after oncogenic insult. Alternatively, c-Myc protein expression may display differential expression due to protein stabilisation in adult, or degradation in young cells. Investigation of Myc protein levels in pre-leukaemic cells would clarify this. However, upregulation of the BMP pathway as an early response to NH9 specifically in adult LSKs was demonstrated. As BMP activation is associated with *Myc* activation at the transcriptional level, one can hypothesise that early upregulation of the BMP pathway in adult cells leads to activation of Myc pathways that is retained once the cell is leukaemic. Furthermore, Myc activation may drive a more aggressive disease, both by cell intrinsic mechanisms and effect on the BM microenvironment. Knock-down, KO and overexpression in young and adult LSKs with subsequent assessment of NH9 mediated leukaemogenesis would answer if the differences observed in leukaemic susceptibility in young and adult LSKs could be explained by activation of these pathways.

5.5.9 Conclusions

The presented data have highlighted several transcriptional pathways that discriminate young and adult generated AML. In general, young AMLs express transcription programmes pertaining to multiple lineages. In contrast, adult generated AMLs express stem cell and Myc related pathways, which are associated with aggressive and poor risk disease in human cancer. In addition, adult AMLs have enrichment of the BMP pathway and membrane signalling pathways, suggesting interplay with the BM microenvironment contributes to leukaemogenesis specifically in adult AML. To further explore how cellular age affects leukaemia initiation it would be interesting to perform global RNA-seq on normal LSKs from the 4 ages investigated to compare directly if age dependent

transcriptional programmes present at baseline are retained through to malignancy. We have focused on the age dependent differences in transcriptional profiles. However, there is evidence for an accrual of DNA damage and mutational burden with increasing age, which may impact susceptibility to disease. WGS or WES would provide further information regarding the quantity and type of mutations that are required for AML generation in young and adult LSKs.

Thus far, the expression of age dependent pro-oncogenic pathways and their affect on leukaemic transformation has been discussed in a murine model. Investigation of these pathways in human leukaemia from paediatric and adult patients would translate if the changes found in the murine model could discriminate AML based on age of patient. In addition, identification of these pathways may provide potential therapeutic targets. Inhibitors of the Myc (BET inhibitors) and BMP (dorsomorphin) pathway inhibitors are already available and have shown promise in pre-clinical studies. (Owens et al., 2015) In the era of small molecule inhibitors and targeted therapy, the results presented also highlights that pathways that are upregulated in adult AML may not be relevant in paediatric disease and as such, specific oncogenic pathways must be sought in a paediatric population. This further emphasises the need for trials dedicated to paediatric patients.

6 Main discussion

The changes in HSPC biology with age have been extensively studied and we now have an appreciation of the biological, transcriptional and epigenetic changes that occur as an HSC ages from the foetal to the young and aged adult. However, the effect of cellular age on leukaemic transformation and its implication on human paediatric and adult AML has not been investigated. Using a murine model, leukaemogenesis at different ages has been successfully modelled and showed that cellular age has a direct impact on leukaemia susceptibility and resultant leukaemia lineage. Furthermore, the transcriptional landscapes in AML generated from young and adult LSKs are different. Young generated AML expresses transcriptional programmes pertaining to multiple lineages whereas adult generated AML expresses stem cell and Myc-related programmes and pathways related to BM microenvironmental signalling.

The striking result from the investigations is that cellular age influences susceptibility to leukaemia transformation and lineage determination. *In vitro* data showed that for FL cells, transformation is restricted to the LSK compartment, while the FL-CMP and GMPs are not transformed. This was observed using 3 different AML models, suggesting that the failure of FL committed progenitors to transform is a cell intrinsic property. *In vivo* data showed that young LSKs were less susceptible to leukaemic transformation, exhibiting longer latency to disease and incomplete disease penetrance, compared to adult LSKs. In addition, a small but significant proportion of young LSKs developed ALL and young AML expressed lymphoid markers by IHC, suggesting retention of strong lymphoid programmes in young LSKs. This was also evident at the transcriptional level. Young AML expressed transcriptional programmes for multiple lineages whereas adult AML expressed myeloid programmes. These 2 results are in line with clinical data, showing that the incidence of acute leukaemia is lower in childhood than in adults, and that in the paediatric context, lymphoid leukaemias are more prevalent. First, this gives validity to this ageing model in that it faithfully recapitulates human patterns of leukaemia development. Secondly, the data suggest that young LSKs are resistant to leukaemia development and have strong lymphoid potential. Further experiments assessing transformation using different oncogene models for AML

would confirm that our observations are due to intrinsic properties of young LSKs and irrespective of the specific oncogenic insult.

Overall, the data presented strongly suggest that young foetal-like LSKs express or upregulate cell protective mechanisms that can delay or even prevent leukaemia development. Alternatively, adult LSKs express or upregulate pro-oncogenic programmes that are necessary for leukaemic transformation. These programmes may be due to cell intrinsic factors, cell extrinsic cues from the microenvironment, or an interplay of both. In Chapter 5 mechanisms that may promote oncogenesis in adult LSKs were discussed. These included the expression of stem cell and Myc-related pathways. In addition, the inappropriate expression of DDR and repair pathways in transforming adult LSKs could result in the survival of oncogene expressing cells rather than inducing apoptosis.

Cells do not develop cancer in isolation but rather within a microenvironment in which complex cell signalling interactions occur. As discussed in Chapter 4 the importance of the microenvironment in supporting leukaemic maintenance, propagation and lineage determination have come to light. There is a theory that the young microenvironment is evolutionary selected to suppress oncogenic insult, while the aged unselected microenvironment is more permissive to mutational aberrations. In the data presented, adult pre-leukaemic and AML cells displayed an enrichment of BMP and membrane signalling pathways, suggesting interplay with the BM microenvironment contributed to leukaemogenesis specifically in adult-AML. In contrast, *in vitro*, oncogene mediated transformation in FL committed progenitors was impeded when grown on stroma. While the role of the ageing microenvironment was not tested *in vivo* per se (all recipients were adult mice aged 6-8w), one can hypothesise that the adult BM niche is less supportive of foetal/young stem cell transformation. This phenomenon is already seen in human malignancy, in the context of neonatal disease. TAM with GATA1 mutation (discussed in Section 1.3.6.3) is an abnormal proliferation of myeloid cells and precursors, seen in 10% of newborns with DS. TAM spontaneously regresses in the majority of patients with only 20% of cases progressing to AML. (Gamis et al., 2011, Massey et al., 2006) Outwith the haemopoietic system, neuroblastoma is a malignancy of the neural crest cells

and presents in children up to the age of 5y. A particular subtype of the disease, stage 4S neuroblastoma, is seen in children ≤1y of age. Despite presenting with disseminated disease, it often regresses spontaneously and patients with 4S neuroblastoma have a good overall prognosis. (Schleiermacher et al., 2003) In both of these examples, founding mutations occur *in utero* in the foetal cell. The spontaneous regression of these neonatal disorders suggests that the mature microenvironment is not suited to sustaining malignant cells of foetally derived pre-cancerous clones. Therefore, the data presented would support the hypothesis that in addition to cell intrinsic protective mechanisms, pro-oncogenic signals from the recipient adult BM microenvironment were not transferred to young NH9 expressing donor LSKs. As discussed in Section 4.4, investigation of the age of the recipient microenvironment alongside the age of the transforming donor cell would clarify the interplay between cell intrinsic and extrinsic factors in promoting leukaemia development. Furthermore, it would be interesting to elucidate if the transcriptional differences we observed in young and adult AML persisted if the age of the microenvironment was accounted for.

A question regarding genetic aberrations in AML is whether the same genetic mutation has the same downstream transcriptional and biological consequences if it occurs in a young versus adult cell. Transcriptional profiling from paediatric and adult patients with APL and CBF leukaemias suggests that for these cytogenetic aberrations the downstream transcriptional pathways and biological consequence hold true in both paediatric and adult disease. However, disparity in clinical outcome is also observed, such as for patients with complex cytogenetics. This is associated with very poor risk in adult AML but this is not necessarily true for paediatric AML. Recently, the differential role of ID1 in MA9 leukaemia initiation and maintenance has been highlighted. Deletion of *Id1* in FL cells transduced with MA9 increased the latency of *in vivo* MA9 leukaemia in primary and secondary recipients, compared to *Id1* expressing FL controls. In contrast, loss of *Id1* in adult BM decreased the latency of MA9 leukaemia in primary and secondary recipients, suggesting that the same pathway may have different oncogenic roles depending on cell ontogeny. (Man et al., 2016) In this thesis differing biological consequences of NH9 expression in young and adult LSKs were observed. Specifically, in young LSKs leukaemic potency was

diminished and lymphoid potential was retained. Furthermore, NH9 transcriptional targets were differentially expressed in young and adult AML. The data support that the downstream molecular and biological sequelae is dependent on cell ontogeny. Therefore it is not only the genetic insult but also the cellular context of that genetic insult that determines leukaemia development and behaviour. To further characterise the ontogeny dependent molecular effects of NH9 expression, it would be interesting to compare the transcriptional profile of FL, 3w, 10w and >52 LSKs at baseline (before transduction), immediately after transduction and in established AML.

Despite differences in leukaemia initiation, gross phenotypic differences were not observed in the *in vivo* generated AMLs from the 4 ages investigated. Some may reason that if the resultant leukaemias are phenotypically similar it makes little difference if latency or pathogenesis is different. We would argue that age dependent cell intrinsic factors that impact transformability are retained even after the cell is transformed. While the impact of this may not be evident on gross observations such as morphology or leukaemic burden, differences at the molecular level may exist. This is indeed what was observed in the transcriptional profile of *in vivo* generated AML. For example, FL-AML expressed erythroid and oxidative metabolism pathways. This is similar to other studies investigating leukaemia generated from young and adult HSCs, in which leukaemia generated from young HSCs (from CB) retained foetal transcriptional programmes. (Horton et al., 2013) In contrast, adult AML expressed stem cell and Myc related pathways, both of which are associated with aggressive and chemoresistant disease in human cancer. The next step in the investigation would be to assess if the pathways enriched in young and adult generated AML from the murine data translated to enriched pathways in human paediatric and adult AML.

Fundamentally, these differences in transcriptional profile between young and adult generated AML could have major implications on disease therapy. Stem cell and Myc related pathways have been associated with aggressive and chemoresistant disease in human cancer. (Wong et al., 2008, Gentles et al., 2010, Eppert et al., 2011, Ng et al., 2016) The enrichment of these pathways in

adult AML suggests that adult AML may be intrinsically more chemoresistant than paediatric AML, which conversely may be inherently more amenable to therapy. Pertinent follow-up experiments to this work would be to treat young and adult generated AML (either *in vitro* or *in vivo*) to standard chemotherapeutic agents and ascertain if young AML is more chemoresponsive than adult AML. If so, this has important clinical implications. Better outcomes from paediatric AML is thought to be due to children being fitter and able to withstand intensive therapy and also that in general children present with good risk cytogenetics. However, the results presented in the thesis show that even with the same oncogenic driver, young transformed cells display better risk features, such as the absence of stem cell transcriptional profiles. The aim of therapy is to cure disease but also to minimise long-term complications of treatment. This is even more pertinent in the paediatric setting where the patient could survive for many decades. As such, minimising toxicity is as important as disease control. Proof that paediatric AML is inherently chemosensitive raises the possibility of reducing upfront therapy in order to minimise long-term toxicity.

The treatment for AML has been static for the last 30y, with improved survival being achieved by better supportive care. New agents are desperately needed to improve AML outcomes. In the era of small molecule inhibitors and targeted therapy, finding potential drug targets is crucial. This thesis highlights that potential therapeutic targets in paediatric AML may be different to those in adult AML. Myc and BMP related pathways were enriched in adult AML. The investigation of inhibitors of these pathways, including BET inhibitors and dorsomorphin, in adult AML is warranted. The BET inhibitor OTX015 is currently being investigated in haematological malignancies in the phase 1 NCT01713582 clinical trial. (Berthon et al., 2016, Amorim et al., 2016) In contrast, oxidative phosphorylation and electron transport chain function were highly enriched in young AML, suggesting a reliance on oxidative metabolism in young AML. If so, targeting mitochondrial ATP production may be a therapeutic option in paediatric AML. One such drug is the biguanide metformin, which is currently used for the treatment of type 2 diabetes mellitus. Epidemiological studies have shown that diabetic patients on metformin have a lower incidence of cancer and *in vitro* studies show that metformin has anti-proliferative effects on breast

cancer cells. (Evans et al., 2005, Janzer et al., 2014) The anti-tumour mechanisms of metformin include inhibition of mitochondrial ETC complex I, and reducing insulin levels, thereby reducing insulin mediated stimulation of the pro-oncogenic PI3K signaling pathway. (El-Mir et al., 2000, Pollak, 2012) The advantage of metformin is that it is an established drug with a known side effect profile. Furthermore, it is not a cytotoxic agent, thereby minimising toxicity to normal cells. If the enrichment of oxidative pathways is confirmed in human paediatric AML, the use of metformin would be an attractive, low-toxic adjunct to standard chemotherapy to trial in the paediatric setting.

Recent studies using NGS and GEP have highlighted the complexity of AML, from the importance of mutational co-expression, to the expression of clinically relevant transcriptional programmes. As these techniques become less labour intensive and more cost effective, results for NGS and GEP will guide therapeutic decision making in AML. Congruent to this, the development of targeted therapies, including small molecule inhibitors such as sorafenib (anti FLT3) and immunoconjugates such as GO (anti CD33) will complement established chemotherapy regimens. In the future, clinicians aim to deliver personalised medicine, in which the mutational, transcriptional and epigenetic profile of a patient's disease is taken into account when deciding on treatment strategies. In addition to this, the cellular context that these aberrations occur, specifically, the cell ontogeny also must be considered. The results from this thesis demonstrate that cellular age does indeed influence oncogene mediated transformability and leukaemia phenotype. We hypothesise that cellular age may also directly influence therapeutic targets and response to therapy. This highlights the need for continued pre-clinical investigation into leukaemic transformation in young cells. Furthermore, these results suggest that clinical data cannot be extrapolated onto a paediatric cohort, thus emphasising the necessity for dedicated trials in paediatric AML.

Appendices

Appendix 1 – List of suppliers

Table 6.1 List of suppliers

Company	Address
Accord Healthcare Limited	Durham, NC 27703, USA
Active Motif	Carlsbad, CA 92008, USA
affymetrix eBioscience	Hatfield AL10 9NA, UK
Agilent	Edinburgh, EH12 9DJ, UK
Applied Biosystems	Warrington, WA3 7QH, UK
BD Biosciences	Oxford UK Oxford, OX4 4DQ, UK
BD Medical	Oxford UK Oxford, OX4 4DQ, UK
BioRad	West Sussex, HP2 7DX, UK
Biotium	Hayward, CA 94545, USA
Charles River UK	Tranet, EH33 2NE, UK
Drew Scientific	Dallas, TX 75237, USA
Dutscher Scientific	Essex, CM13 3FR, UK
Eppendorf UK	Stevenage, SG1 2FP, UK
Fisher Scientific	Leicestershire, LE1 5RG, UK
Fluidigm™	San Francisco, CA 94080, USA
GraphPad Software Inc.	La Jolla, CA 92037, USA
Integrated DNA Technologies	B-3001 Leuven, Belgium
Invitrogen	Paisley, PA4 9RF, UK
Labtech International Ltd.	Milton Keynes, MK5 8LB, UK
Life Technologies	Ghent 9050, Belgium
Lonza	Basel, Switzerland
Merck	Nottingham, NG9 2JR, UK
Millipore	West Lothian, EH54 7BN, UK
Miltenyi Biotec	Surrey, GU24 9DR, UK
New England BioLabs	Ipswich, MA 01938, USA
PeproTech Ltd	London, W6 8LL, UK
Promega	Madison, WI 53711, USA
Qiagen	West Sussex, RH10 9NQ, UK
Sarstedt	51588 Numbrecht, Germany
Sigma-Aldrich	Dorset, SP8 4XT, UK
Stemcell Technologies	38000 Grenoble, France
Stuart	Staffordshire, ST15 0SA, UK
Terumo	Lakewood, CO 80215, USA
Tree Star, Inc.	Ashland, OR 97520, USA
VWR	Wayne, PA 19087, USA
Xstrahl	Camberley, GU15 3YL, UK

Appendix 2 – Primers

Table 6.2 House keeping genes

Gene	Forward	Reverse
B2m	TGCTATCCAGAAAACCCCTCA	TTTCAATGTGAGGCGGGTGG
Gusb	GGGACAAAAATCACCCTGCG	GCGTTGCTCACAAAGGTCAC
Rnf20	ACCATCAATGCCCGGAAGTT	GCAGCGATACTCTGGGGTTT
ABL	TGGAGATAACACTCTAAGCATAACTAAAGGT	GATGTAGTTGCTTGGGACCCA

Table 6.3 Stem cell genes

Gene	Forward	Reverse
Bmi1	ATACCTGGAGAAGAAATGGCCC	CAGCTCTCCAGCATTCGTCA
Tpr53	ATCCTGGCTGTAGGTAGCGA	ATCCGACTGTGACTCCTCCA
Ink4 (p16)	GCCGTGTGCATGACGTG	GCCCATCATCATCACCTGAATC
Arf (p19)	GGTGAAGTTCGTGCGATCC	CGTGAACGTTGCCCATCATC
cKit	AATTCACCCTCAAAGTGCGG	CTATGTGCTGAGGCTGAGGG
Mpl*	AACAAGACCGCACTAGCTCC	GCGGTTCCTCCTCTTCACAT
Tal1	TCTGATGGTCCTCACACCAA	TACTTCATGGCAAGGCGGAG
Epcr	GCTCAATGCCTACAACCGGA	CCTGTTTGGCTCCCTTTCAT

Table 6.4 Myeloid and erythroid genes

Gene	Forward	Reverse
Myeloid		
Cebpa	CAAGAACAGCAACGAGTACCG	GTCACTGGTCAACTCCAGCAC
Cebpb	CCGGATCAAACGTGGCTGAG	CACGTGTGTTGCGTCAGTC
Cebpe	GAGGCAGCTACAATCCCCTG	CACAGGGGCCTTGAGGACA
Runx1	AGGCAGGACGAATCACACTG	CTCGTGCTGGCATCTCTCAT
Gata1	CTCCCCAGTCTTTCAGGTGT	CAGGGTAGAGTGCCGTCTTG
Pu.1	CCCGGATGTGCTTCCCTTAT	TCAAGCCATCAGCTTGCC
Gfi1	GCTCCGAGTTCGAGGACTTT	TGCATAGGGCTTGAAAGGCA
Mpo	CTGCAACAGACGAAGCC	AGCCATTGCGATTGACTCCA
Gata2	TCACCCCTAAGCAGAGAAGC	CATTGCACAGGTAGTGGCCC
Tlr2	GAGCATCCGAATTGCATCACC	AGATTTGACGCTTTGTCTGAGGT
Tlr4	GCTTGAATCCCTGCATAGAGGTAG	TGTCATCAGGGACTTTGCTGAG
Fcgr3	TCTGCTGCTGTTTGCTTTTGC	CCAGTTTCACCACAGCCTTC
Csf1r	TTCCTCTGTTCCCTTTCAGGC	CACGTTCCTGTCTGTTGCAC
Csf3r	GACGGGGCTAGAAAGAGAAGTT	GTCTCAGCAATGACTGGGGCTA
Irf8	ACGTGGAAGACGAGGTTACG	GCCCAGCTTGCATTTTTGTTC
E2f1	GCAACTGCTTTCGGAGGACT	GTCTCAGGAGGGGCCTTGAT
Erythroid		
Klf1	CTAAGAGGCAGGCGGCACAT	CTGAGCGAGCGAACCTCC
Fli-1	ATCTGAAGGGGCTACGAGGT	ACCACAGACAGAGCCTCCTTA

Table 6.5 Lymphoid genes

* Also involved in microenvironmental signalling

Gene	Forward	Reverse
B-Lymphoid		
Ikaros	AGGGTCAAGACATGTCCCAAG	GCTGTGCTCCAGAGGTAGTG
Pax5	TCACAGCATAGTGTCTACAGGC	TCCCTCTTGCGTTTGTTGGT
Tcf3	GCCTGGATACTCAGCCGAAG	TAGAAGGGGGAGGGGTAAGC
Ebf1	AAGCCAACAGCGAAAAGACC	TTCTGTCCGTATCCCATTGCTG
Blnk	GACTACGCATTAGACAGCCCT	CTCGGCAGGCATCACATACA
Cd79a	GTCATACGCCTGTTTGGGTCC	AAGGCTGAACCACCATGTGA
Rag1	GTTGCTATCTCTGTGGCATCG	TAAGCTACCTTGCTCCACAGG
Rag2	AGTGACTCTTCCCCAAGTGC	TTCTTATTTTGGCACTGAAGGC
Cd19	AAACCTGACCATCGAGAGGC	GGGTCAGTCATTCGCTTCCTT
Ptprc	GTCACAGGGCAAACACCTACA	AGGGCATTCTCTGTTGTGCTC
Il7ra	GGCCTAGTCTCCCCGATCA	TTCAGACTCGTTTTTGGCTTCT
Pou2af1	CCTCGGTGTTGACCTATGCT	CAGTGCTTCTTGGCGTGACA
Foxo1	GAGTTAGTGAGCAGGCTACATTT	TTGGACTGCTCCTCAGTTCC
Vpreb1	CTGGACGTCTGTCCTGCTCA	AGGGCCACAACCTGTGAGATAG
Cxc4	TGCAGCAGGTAGCAGTGAAA	TGTATATACTCACACTGATCGGTTC
Stat5	CAGCATTTCCCCATCGAGGT	GAGCTGGGTGGCCTTAATGT
T-Lymphoid		
Gata3	CCCATTACCACCTATCCGCC	GTTCACACACTCCCTGCCTT
Notch1*	ATCAAGCGCTCTACAGTGGG	ACATTGCCGGTTGTCGATCT
Tcf1/7	AACCCCCGCTGCATAACAA	TTGCTTCTGGCTGATGTCCG
Flt3	TTGGCCTTTGTGTCTTCCGT	TTGCGAGCTGGTAGCGTTTA
Cd3g	TCTCATTGCGGGACAGGATG	TATTCCCGGTCCTTGAGGGG
Bcl11b	CTGAGTACCTGAACCGGCAT	AGAATCCACTCACACCCCAAC
Tcf12	TCTAGGGGCAGAACAAGCAGTA	CGCTCTCTGGCATTGTTAGC
Ptcra	ACTGGGTCATGCTTCTCCAC	GCGATGCCTGATGGTAGAGC
Cd7	CACCTGGATTTGGGCGTCAT	ACTGGTGTACGTCTTGGGC

Table 6.6 Microenvionmental signalling genes

* Also stem cell associated gene
** Also involved in T-lymphoid differentiation

	Gene	Forward	Reverse
Homing	Itgb1	TGGCCAAACAGATAAAAATAGATGT	ACATCGTGCAGAAGTAGGCA
	Itga4	GCACTCCTACAACCTGGACC	GATGAGCCAGCGCTTCGAC
	Psgl-1	GGCAGATTGGGACCACAAGT	ATGGTACCGTGCCCAACAGA
	Icam1	CTCCGGACTTTCGATCTTCCA	TTCAGAGGCAGGAAACAGGC
	Cxcr4	TGCAGCAGGTAGCAGTGAAA	TGTATATACTCACACTGATCGGTTC
	Cd44	TTAGCTGGACACTCAAGTGCG	AGACGGCAAGAATCAGAGCC
	CD26	TTTCCAAGCAATGTGGTACACG	GTAAGGAGAAGCACTGCTGGA
Other integrins	Itgal	CATTACAGACGGGGAGGCAA	TGCTTGCCAATCCCGATGAT
	Itgb7	ACCGGCTCTCTGTGGAAATC	GGATTGTTGTCCTGCTTCCAG
	Itga6	TTACTGTGGAAGTGTGGCTTC	CAGCCTTGTGATAGGTGGCAT
	Itgb4	GAGTACTGCTCCTTCCGGGAT	GGGAGGGCAGTCTTTCTTTTTG
	Itga7	TAACTGGAAGGGGTTGCTTTTTG	TATTCAAGGTCAAGTCTCCGGC
	Itga3	CCAGCCGTCAGAGACAGAAA	GGCTTAAAGAAGTCACACCGGG
	Itga5	GAAGGCAGGCACCAGTCTCT	AGGAGACCACGTTGCTTTGT
	Itgav	TGTTCACACTTTGGGCTGTG	TCATGAACGTCTCGGTCCAC
	Itga1	AGCCTCGGTACAATCACACC	ATCCGATCTGCTCTCCACTGA
	Itga2	TGGTAGTTGTGACCGATGGC	ACCCAAGAACTGCTATGCCG
Calcium	Cdh2	TTGCTTCAGGCGTCTGTGGAG	TTCGTGCACATCCTTCGGTAA
	CasR	ATCTTCCCAGACCAACAGCAG	CCCGAGATGTTTTCTGAGAGAC
	Gja1	GCCCGAACTCTCCTTTTCCT	CTGGGCACCTCTCTTTCACTT
Vascular niche	Angpt1	CTTCCAGAACACGACGGGAA	TCTCAAGTTTTTGCAGCCACTG
	Mpl*	AACAAGACCGCACTAGCTCC	GCGGTTCCTCCTCTTCACAT
Tgfß	Tgfbr1	GGGGCGAAGGCATTACAGTG	GGTGCACATACAAATGGCCT
	Tgfbr2	GGTCTATGACGAGCGACGG	GCTTCCATTTCCACATCCGAC
Notch	Notch1**	CAACTGCCAGAACCTTGTGC	TGGTACTGCGTGTTGGTCTG
	Hes1	GAAAAATTCCTCCTCCCCGGT	GGCTTTGATGACTTTCTGTGCT
Hh	Ptch1	AATTCTCGACTCACTCGTCCA	CTCCTCATATTTGGGGCCTT
	Ptch2	CCTTGCAGAGCACCTTCCT	CCTGGGCTAGCTGCACAAAG
	Gli1	CTACTCGGGGTTCAATGATGC	TGTGGAGTTGGGGCTAGACAT
	Gli2	AAACTTTTGTCTCCTCGGGTCC	CTGCTGTCCTCCAAGAGACC
Wnt	Lrp5	TGCTCCCACATCTGTATCGC	AGGTAGGAGGCTCACCACAA
	Lrp6	TTTATTTTGGCAAGAGTTGGATCA	GTCCAGTACATGAACCCACTTGA
	Fzd4	AGAACCTCGGCTACAACGTG	ACCGAACAAAGGAAGAACTGC
	Fzd5	TCGTTAAACTTTCCCAGCTCT	CTCCAAGGACAGAACTCTCG
	Gsk3b	TTGGACAAAGGTCTTCCGGC	AGCTTCCAGTGGTGTTAGCC
	Ctnnb1	TGAGGACCAGGTGGTAGTTAAT	TGCGTACAATGGCAGACACC
Egr1	Egr1	CCTGACCACAGAGTCCTTTTC	AGCGGCCAGTATAGGTGATG
	c-Myc	GTTGGAAACCCCGCAGACAG	ATAGGGCTGTACGGAGTCGT
	Cdk6	AGAAGTCCTGCTCCAGTCCA	CACGTCTGAACTTCCACGAA
	Chk1	ATGACGCAAGCAGGTTTTGG	ACAGCGACAAGCAGTCCTTT

Table 6.7 BMP pathway genes

	Gene	Forward	Reverse
Ligands	Bmp2	CTGCGGTCTCCTAAAGGTCG	CTGGGGAAGCAGCAACACTA
	Bmp4	AGCTAGGTGAGTTCGGCATC	GCAGGCTCCAAGACGGTTTA
	Bmp7	AGCCAGAATCGCTCCAAGAC	CACTGCTGCTGTTTTCTGCC
	Bmp6	CAGGAGCATCAGCACAGAGAC	GTCACCACCCACAGATTGCT
	Bmp5	GCCTGCAAGAAGCACGAAC	GGTGCTATGATCCAGTCCTGC
Receptors	Bmpr1a	TCATGTTCAAGGGCAGAATCTAGA	GGCAAGGTATCCTCTGGTGCTA
	Bmpr1b	TTGGCGCTGAGCTATGACAA	AACTTCTCTCTTCACTTATGGCCG
	Bmpr1b	GTTACGGCCTTCATTCCCCA	CCATCTGCCTGAGACACTCAT
	Acvr1	TCGAATCTACAGGGATGAATGG	ATGGCTCCTTGGACGACTAC
	Acvr1	AGCCGGTTATACAATGGTCG	TGGGCTTCTCATCTTCCACAC
	Bmpr2	GAGCACAGAGGCCCAATTCT	TTGTGTTGACTCACCTATCTGT
	Acvr2a	CTACTCAAGACCCAGGACCAC	GGGCTTTCCAGACACAACCA
	Acvr2b	TGCCCACAGGGACTTCAAAA	CTTCCCTGGCTCAAACCGAA
Canonical	Smad1	GCTTCACCCACACGGTTGTT	TCCAAGCGGAGACAGATCAAC
	Smad5	GCAGAGCCATCACGAGCTAA	GAGGTAAGACTGGACTCTCCAC
	Smad8/9	ATCAACACTCAGACTTCCGGC	ATTGGAAGGGTCGGTGAAGC
	Smad4	TCCAATCATCCTGCTCCTGA	AAAGCGATCTCCTCCCGAAG
Non-Canonical	Xiap	TGCTTTAGGTGAAGGCGATAA	GGGTCTTCACTTGGCTTCCA
	Map3k7	TTCCTGCCACAAACGACACT	AAGCTCAGGCGTCCAGATTC
	Mapk8	AGGAGAACGTTGACATTTGGTC	GACAAGGTGTTCCGAGCTGT
	Map2k3	TAGATTAGTGCTCTCCGCCG	GATTTTCCTTTGGTCTGAGGCA
	Map2k4	GCGGAGTAGTGATTGCCCAT	GATCCAACAGTCGCCCTCTC
	Mapk14	TGAGCTGTTGACCGGAAGAA	TTTCTTGCCTCATGGCTTGGC
Targets	Id1	ACCCTGAACGGCGAGATCA	GGAACACATGCCGCCTCG
	Id2	CTCGCATCCCACTATCGTCA	ATTCAGATGCCTGCAAGGACAG
	Id3	GCATCTCCCGATCCAGACAG	TCAGTGGCAAAAGCTCCTCT
	Creb3l1	CTAGAGACTGCCAACAGGACC	GCTGCCATCTTGTACGGTCT
	Snai1	CCACACTGGTGAGAAGCCAT	CACATCCGAGTGGGTTTGGA
	Snai2	AGAACTCACACTGGGGAAAAGC	TGATCTGTCTGCAAAAGCCCT
	Klf4	AGAACAGCCACCCACACTTG	GTGGTAAGGTTTCTCGCCTGT
	Klf2	CCAAGAGCTCGCACCTAAAG	GTGGCACTGAAAGGGTCTGT
Inhibitors	Smurf1	TCCCCAGAGACCTTAACAGTG	GATGTGGTGAAGCCGTGGAT
	Smurf2	ATAGGCACGGGAGGACAAGT	CGCCTTTCTTCCCAACCATCT
	Smad6	CCACTGGATCTGTCCGATTCT	TCTGAGAATTCACCCGGAGC
	Smad7	CCTCGGAAGTCAAGAGGCTG	CAGCCTGCAGTTGGTTTGAG
Ant-agonists	Nog	TCCCATCCAGTACCCCATCA	ATCCATCAAGTGTCTGGGCG
	Chrd	GTGAGAAGGTGCAGTGTCCT	TAGTCCCTGACCCTACTGGAC

Appendix 3 – Significant DEGs from RNA-seq

Table 6.8 FL vs 3w-AML, up in FL

Gene	FC	q-value		Gene	FC	q-value
Ddx3y	8.295	2.84E-86		Hbb-bs	2.851	3.54E-03
Eif2s3y	8.996	2.96E-84		Apol8	2.711	3.56E-03
Uty	5.223	2.02E-49		Rab3il1	2.523	3.61E-03
Zfpm2	9.005	3.22E-48		Nova1	2.876	3.76E-03
Gm6768	6.979	2.65E-39		1700071M16Rik	2.874	3.92E-03
BC018473	7.281	8.55E-29		Rassf10	2.985	3.92E-03
Kdm5d	2.730	3.37E-24		Hcn3	1.975	3.94E-03
St6galnac1	6.010	2.12E-20		Aqp11	2.420	4.02E-03
Nkx3-2	5.827	1.34E-14		Tmem56	2.822	4.17E-03
Pgm5	5.552	3.83E-14		Trib3	2.587	4.17E-03
Gm11735	5.407	6.48E-14		Gucy1a3	2.042	4.28E-03
Rims2	4.204	2.59E-12		A930038B10Rik	2.434	4.32E-03
Cr2	4.318	5.30E-12		Blvrb	2.328	4.46E-03
Pcdh7	4.864	2.74E-10		Dmtn	2.655	4.47E-03
Ighd	2.986	1.25E-09		Cox6b2	2.765	4.54E-03
Tmem252	4.412	7.80E-09		Trim58	2.696	4.58E-03
Ccbe1	3.730	1.47E-08		Orm1	2.630	4.90E-03
Chl1	4.228	3.34E-08		Med12l	2.164	4.90E-03
Dock7	2.184	1.79E-07		Jag1	2.717	4.97E-03
Arrdc4	3.021	2.22E-07		Fam210b	2.112	5.03E-03
Rcvrn	4.367	4.06E-07		Ypel4	2.760	5.47E-03
Col4a5	4.373	4.41E-07		Igkv4-50	2.389	5.47E-03
B230118H07Rik	3.812	7.75E-07		Tgm5	2.788	5.52E-03
Mab21l2	3.937	1.07E-06		Hba-a2	2.704	5.52E-03
Ppm1l	2.860	1.50E-06		Zfpm1	2.347	5.59E-03
Col4a6	3.737	2.01E-06		Reep6	2.622	5.70E-03
Myct1	3.658	2.51E-06		Gm25193	2.753	5.76E-03
Ighv1-28	4.147	3.38E-06		Sh3yl1	1.925	5.93E-03
Dscaml1	3.955	4.16E-06		Slc4a1	2.703	6.04E-03
Gm37915	3.166	4.32E-06		Camsap2	1.854	6.44E-03
1700017G19Rik	4.023	5.66E-06		Gja6	2.863	6.44E-03
Pde3b	2.497	7.11E-06		Nhlrc4	2.674	6.71E-03
Gm29650	3.795	7.87E-06		Dach2	2.607	6.74E-03
Abat	3.310	7.91E-06		Cgn	2.504	6.78E-03
Gm37527	3.539	7.91E-06		Chst3	2.081	7.12E-03
Atoh8	3.382	1.03E-05		Fam46c	2.423	7.44E-03
Neurl1a	2.967	1.93E-05		Nxpe2	2.479	7.56E-03
Tspan15	2.707	2.31E-05		Exoc3l2	1.805	7.79E-03
Tspo2	3.389	3.13E-05		Trdv5	2.752	7.79E-03
Tie1	2.641	3.74E-05		Cygb	2.343	7.86E-03
Phyhip	3.582	4.15E-05		Ptdss2	1.928	7.86E-03
Sphk1	3.558	4.15E-05		Dnah12	2.077	7.90E-03

Gene	FC	q-value		Gene	FC	q-value
Abca4	2.108	4.67E-05		Cela1	2.269	7.90E-03
F930017D23Rik	3.280	4.67E-05		Urod	1.816	8.55E-03
Eya4	3.513	4.72E-05		Rnf212	2.638	8.72E-03
Gpr22	3.755	4.74E-05		Nt5c3	1.628	8.96E-03
Cachd1	2.875	5.77E-05		Hbb-bt	2.614	8.96E-03
Ebf1	2.765	5.84E-05		Abcb10	1.922	8.98E-03
Mei4	2.059	6.01E-05		Bcl2l15	2.032	8.98E-03
Spire1	3.471	6.29E-05		Xpo7	1.583	9.02E-03
Hemgn	3.167	6.77E-05		Traf4	2.087	9.07E-03
Myom1	2.388	7.52E-05		Tmem9	2.087	9.08E-03
A730036I17Rik	3.116	7.52E-05		Clcn3	1.589	9.23E-03
Snx31	3.431	7.81E-05		Fgfrl1	2.281	9.43E-03
Samd11	3.317	8.38E-05		Adcy6	2.428	9.74E-03
Cd79a	2.825	1.08E-04		Iqcd	2.356	9.74E-03
Rbm11	2.411	1.09E-04		E130215H24Rik	2.194	9.74E-03
Rhd	3.245	1.13E-04		Jsrp1	2.601	9.74E-03
Popdc2	3.215	1.16E-04		Gabrg1	2.694	9.78E-03
Aqp1	3.272	1.17E-04		Gstm5	2.544	9.80E-03
Bpgm	2.676	1.21E-04		Calml4	2.364	9.80E-03
Fam234b	2.382	1.23E-04		Steap3	1.992	1.05E-02
Nuggc	2.218	1.43E-04		Dip2c	2.309	1.05E-02
Epor	3.206	1.50E-04		C130012C08Rik	1.982	1.08E-02
37681	3.009	1.56E-04		Cpvl	2.674	1.14E-02
Hpn	3.378	1.72E-04		Cd36	2.133	1.15E-02
Igkv12-46	2.317	1.74E-04		Igkv4-59	1.919	1.15E-02
Spon2	3.527	1.86E-04		Stac2	2.172	1.20E-02
Gm9522	3.243	1.86E-04		Stard10	2.130	1.22E-02
Scd1	3.465	1.89E-04		Cth	2.615	1.23E-02
Rhag	3.277	1.95E-04		Prdx2	1.892	1.23E-02
Adcy5	2.732	2.06E-04		Gm12999	2.465	1.23E-02
Mgst3	2.687	2.06E-04		Cdr2	2.242	1.23E-02
Igkv1-99	3.275	2.11E-04		Id3	1.770	1.32E-02
Slc43a1	2.952	2.16E-04		Soat2	1.913	1.32E-02
A730089K16Rik	3.249	2.17E-04		Gng11	1.503	1.33E-02
Dock1	3.198	2.20E-04		4930426D05Rik	2.600	1.36E-02
Fabp7	3.306	2.51E-04		Exoc3l	1.563	1.38E-02
Mylk3	3.272	2.54E-04		Cyp4b1	2.558	1.39E-02
1700063D05Rik	1.939	2.54E-04		Pigq	1.598	1.39E-02
Car2	3.154	2.61E-04		Gm38326	2.539	1.40E-02
Epdr1	3.200	2.96E-04		Redrum	2.586	1.41E-02
Abcb4	3.071	2.98E-04		Sema3a	2.584	1.41E-02
Mapk12	2.024	3.17E-04		Igkv5-43	2.299	1.41E-02
Aldh1a1	3.201	3.34E-04		Itsn1	1.731	1.43E-02
Pxdc1	2.830	3.48E-04		Asb17os	2.568	1.43E-02
Cenpv	2.118	3.77E-04		Armc9	1.689	1.50E-02
St6galnac2	3.447	3.83E-04		Gm26513	2.083	1.50E-02

Gene	FC	q-value		Gene	FC	q-value
Btnl10	3.131	3.94E-04		Gm15816	2.570	1.50E-02
Fhdc1	3.088	3.97E-04		Ngfr	2.632	1.51E-02
Dpf3	3.007	3.97E-04		E130309D14Rik	2.552	1.51E-02
Otub2	2.843	4.03E-04		Shank3	2.501	1.55E-02
Ermap	3.132	4.48E-04		Atp1b2	2.417	1.58E-02
Cldn12	2.298	4.57E-04		Gm33280	1.953	1.68E-02
Tmcc2	2.876	4.65E-04		Chchd10	1.847	1.69E-02
Cdkl1	3.156	4.91E-04		Pla2g12a	2.191	1.70E-02
Gm867	3.217	4.91E-04		Ttll12	1.710	1.75E-02
Entpd3	3.363	4.95E-04		Rab4a	2.269	1.76E-02
Acss2	1.924	5.09E-04		Tfrc	2.086	1.76E-02
Tspan33	3.013	5.14E-04		Bcar3	1.602	1.77E-02
Aknad1	2.940	5.37E-04		Btbd3	2.299	1.77E-02
Klf1	3.048	5.37E-04		Ms4a8a	2.573	1.82E-02
Tfdp2	1.701	6.17E-04		Tshz3	2.605	1.84E-02
Nags	3.389	6.27E-04		Gm12649	2.509	1.84E-02
Prkg1	2.815	6.56E-04		Pcolce2	2.588	1.85E-02
Sec14l2	3.029	7.14E-04		Pik3c2g	2.429	1.85E-02
Acp5	1.772	7.57E-04		Arhgef12	1.665	1.85E-02
Gypa	3.095	7.57E-04		Tfpi	2.410	1.93E-02
Icam4	2.766	8.07E-04		Sfrp2	2.545	1.93E-02
Tfr2	2.973	8.10E-04		Nudt9	1.531	1.96E-02
Dapk1	2.305	8.16E-04		Adam33	2.248	1.97E-02
Endod1	1.796	8.16E-04		Klhdc8b	1.782	1.97E-02
1300017J02Rik	3.065	8.21E-04		Nudt12	2.077	1.98E-02
BC021767	3.098	8.33E-04		Hif3a	2.279	2.00E-02
Il34	3.149	8.52E-04		Zbtb46	2.148	2.00E-02
Pdia2	3.153	8.69E-04		Rgs12	1.581	2.00E-02
39692	2.989	8.80E-04		Rnf217	2.499	2.00E-02
Pkhd1l1	3.098	8.96E-04		Slc2a4	2.462	2.02E-02
Mt2	2.802	9.18E-04		Slc14a1	1.954	2.04E-02
Prokr1	2.814	9.64E-04		Snap47	1.581	2.04E-02
Plpp1	2.990	9.94E-04		Gm28857	2.343	2.06E-02
Crip2	2.917	1.01E-03		Arhgap6	1.990	2.06E-02
Cldn13	3.017	1.01E-03		Eya2	2.145	2.14E-02
Lmna	2.813	1.01E-03		Scrn3	1.510	2.16E-02
Pla2g4c	2.690	1.01E-03		Asb11	2.532	2.17E-02
Mycn	2.606	1.01E-03		Ifrd2	1.714	2.20E-02
Slc22a23	2.936	1.01E-03		Kcnc1	2.539	2.20E-02
Snx22	2.391	1.01E-03		Arl4a	1.882	2.21E-02
E330017A01Rik	3.112	1.01E-03		4932441J04Rik	2.554	2.21E-02
Gm15491	2.737	1.01E-03		Mns1	1.867	2.22E-02
Scarf1	2.215	1.04E-03		Alad	1.902	2.26E-02
Smim1	3.013	1.07E-03		Dhrs11	1.688	2.26E-02
Ighv1-31	3.258	1.09E-03		Fam228b	2.214	2.27E-02
Kel	2.987	1.09E-03		Sowaha	2.474	2.28E-02

Gene	FC	q-value		Gene	FC	q-value
S1pr1	2.450	1.09E-03		Ccdc27	2.504	2.29E-02
Ctse	2.767	1.12E-03		Ripply3	1.722	2.29E-02
Art4	2.932	1.12E-03		Ak1	1.893	2.35E-02
Mfsd2b	2.890	1.12E-03		1700063H04Rik	2.508	2.35E-02
Pkd1l1	3.242	1.12E-03		Cnn3	1.920	2.35E-02
Gm30414	2.597	1.12E-03		Abcb6	1.742	2.37E-02
Abcg4	2.920	1.14E-03		Cecr2	2.098	2.40E-02
Spta1	2.982	1.18E-03		Rab40b	2.494	2.42E-02
Gm14490	3.020	1.21E-03		Minpp1	1.666	2.42E-02
Cpox	2.483	1.21E-03		Ctla2a	1.867	2.54E-02
St3gal5	2.089	1.21E-03		Abi3bp	1.883	2.55E-02
Tal1	2.874	1.23E-03		Gm29554	2.469	2.58E-02
Epb42	2.936	1.29E-03		4933431E20Rik	2.263	2.58E-02
Fech	2.289	1.29E-03		Sorbs1	2.044	2.62E-02
Gdpd1	2.577	1.36E-03		Mboat2	2.411	2.66E-02
Ube2o	2.305	1.40E-03		Gcsam	1.732	2.67E-02
Sptb	2.903	1.44E-03		Vsig2	2.390	2.71E-02
Acmsd	2.662	1.44E-03		Tgif2	1.933	2.73E-02
Ube2l6	2.277	1.47E-03		Tro	2.449	2.75E-02
Hmbs	2.379	1.47E-03		Dmwd	2.123	2.76E-02
Slc38a5	2.929	1.47E-03		Fam220a	1.638	2.76E-02
Clcn2	2.128	1.53E-03		Meiob	2.473	2.76E-02
AI427809	2.829	1.53E-03		Ubac1	1.763	2.78E-02
Smo	2.350	1.53E-03		Mill2	2.422	2.93E-02
Uros	2.251	1.53E-03		Lgr4	1.923	3.08E-02
Atp8b1	2.561	1.53E-03		Clic5	1.826	3.08E-02
Galm	2.145	1.56E-03		Fer1l6	2.373	3.12E-02
Scin	3.033	1.58E-03		Fads3	1.969	3.14E-02
Nrgn	2.509	1.58E-03		Ttc39a	2.321	3.14E-02
Gm37192	3.016	1.58E-03		Dnajb2	2.087	3.17E-02
Ces2g	2.920	1.59E-03		Ighv1-72	2.212	3.21E-02
Pklr	2.956	1.59E-03		Hmgb3	1.779	3.21E-02
Map9	2.765	1.61E-03		6030468B19Rik	2.175	3.21E-02
Cd59a	3.008	1.64E-03		Rab30	1.971	3.21E-02
Dhcr24	1.942	1.71E-03		Rarb	1.601	3.22E-02
Atp7b	2.861	1.75E-03		1700086O06Rik	1.890	3.22E-02
Tmod1	2.721	1.76E-03		Myl4	1.516	3.27E-02
Ank1	2.857	1.76E-03		Plekha5	1.852	3.35E-02
Ccdc74a	2.787	1.87E-03		Tom1l1	2.020	3.37E-02
Slc26a1	2.619	1.88E-03		Gm6634	2.307	3.37E-02
Gypc	1.875	1.96E-03		Rnf180	2.066	3.38E-02
Golm1	2.320	1.96E-03		Xrcc5	1.971	3.47E-02
Gfi1b	2.762	1.96E-03		Bfsp2	1.966	3.51E-02
Pdzk1ip1	2.887	1.96E-03		Glipr1l1	2.429	3.62E-02
Limch1	2.420	2.07E-03		D330045A20Rik	2.213	3.62E-02
Ighv1-12	2.394	2.13E-03		Slc30a10	2.234	3.63E-02

Gene	FC	q-value		Gene	FC	q-value
Clec11a	2.728	2.19E-03		Gm11827	2.015	3.63E-02
Samd14	2.777	2.31E-03		Klhl14	2.395	3.67E-02
Dyrk3	2.130	2.32E-03		NA	1.725	3.68E-02
Abca1	1.586	2.40E-03		Bag2	1.793	3.68E-02
Cited4	2.597	2.50E-03		Isg20	1.803	3.69E-02
Sox6	2.865	2.51E-03		Olfr248	2.367	3.69E-02
Trim10	2.849	2.51E-03		Hist3h2ba	1.880	3.73E-02
Slfn14	2.940	2.51E-03		Zfp354c	1.887	3.79E-02
Paqr9	2.839	2.53E-03		Cd55	1.873	3.83E-02
Add2	2.864	2.57E-03		Slc6a20a	2.368	3.89E-02
Gata1	2.765	2.57E-03		Me1	2.095	3.94E-02
Gpsm2	2.098	2.62E-03		Zfp57	2.184	3.95E-02
Csgalnact1	2.013	2.73E-03		2010109A12Rik	2.131	3.95E-02
Crisp3	3.040	2.74E-03		Syngr1	1.687	4.05E-02
Rasgef1b	2.129	2.74E-03		Gm28230	2.396	4.05E-02
C530008M17Rik	2.573	2.82E-03		Stap2	1.963	4.09E-02
Pla2g7	2.855	2.90E-03		Ninl	2.107	4.15E-02
Mrap	1.881	2.92E-03		Zfp820	2.074	4.18E-02
Ache	2.648	2.99E-03		Nme9	2.315	4.24E-02
Alas2	2.835	3.01E-03		Gab1	1.839	4.25E-02
Wdr60	2.306	3.04E-03		Optn	1.786	4.26E-02
Hba-a1	2.793	3.05E-03		Isca1	1.528	4.52E-02
A230056P14Rik	1.916	3.09E-03		Gm26669	1.938	4.56E-02
Arvcf	2.156	3.13E-03		Adamtsl5	2.129	4.58E-02
Clstn3	2.318	3.13E-03		Odf3b	2.225	4.60E-02
Pfkm	1.799	3.13E-03		Vopp1	1.885	4.61E-02
Nipa1	2.394	3.13E-03		Kif7	2.051	4.77E-02
Sp7	2.811	3.13E-03		Rhbdf1	1.745	4.89E-02
Dusp8	2.737	3.13E-03		B4galnt3	2.131	4.91E-02
Cyth3	2.336	3.29E-03		Gsta4	1.942	4.93E-02
Il1rl1	2.361	3.29E-03		Kcns1	2.303	4.99E-02
Tmem120b	2.457	3.39E-03				

Table 6.9 FL vs 3w-AML, up in 3w

Gene	FC	q-value		Gene	FC	q-value
Adgrg7	-5.672	2.5E-20		B3gnt8	-1.821	7.6E-03
Hpgd	-4.936	3.8E-18		Xcl1	-2.262	7.8E-03
Zfp62	-2.159	7.4E-17		Plekhh3	-2.234	7.9E-03
Eps8l1	-1.653	1.0E-13		Kmo	-1.537	8.5E-03
Gm8494	-4.496	6.9E-13		Cav2	-2.086	9.0E-03
Mfsd7a	-3.612	4.7E-09		Stfa1	-1.908	9.0E-03
Camk1	-2.030	5.1E-09		Hspd1-ps4	-2.745	9.0E-03
Pvrl4	-2.643	1.1E-08		Nxpe5	-1.991	9.4E-03
Rnls	-2.863	1.3E-08		Ccdc136	-2.417	9.5E-03
Mansc1	-3.858	4.8E-08		Gm21370	-1.798	9.8E-03
BC026585	-3.128	5.9E-08		Asgr2	-2.391	9.8E-03
2210016F16Rik	-2.294	7.1E-08		Arsi	-2.324	9.8E-03
G530011O06Rik	-1.760	8.9E-08		Sash1	-1.609	1.0E-02
Ncr1	-4.158	1.2E-07		Notumos	-2.701	1.1E-02
Raet1e	-4.569	1.3E-07		Ldhb	-1.742	1.1E-02
Lipo2	-2.854	1.9E-07		Arhgap32	-2.070	1.1E-02
Il17rb	-1.995	4.7E-07		Gm28403	-2.482	1.1E-02
Klk1b27	-3.772	1.1E-06		Tlr12	-1.827	1.1E-02
Arhgap27os3	-1.723	6.1E-06		Btnl7-ps	-2.037	1.2E-02
Gm16531	-3.981	1.2E-05		Gm15701	-2.650	1.3E-02
Bace1	-1.678	1.6E-05		Gm15433	-1.788	1.3E-02
Xist	-2.733	1.9E-05		Eomes	-2.081	1.5E-02
Gm26581	-3.608	2.7E-05		Atf3	-2.288	1.6E-02
Gm37820	-2.525	3.0E-05		Vmn1r65	-1.794	1.7E-02
H60c	-3.490	4.2E-05		Tnfsf12	-1.574	1.7E-02
Serpinf1	-2.111	4.7E-05		NA	-2.233	1.7E-02
Skint3	-3.597	9.1E-05		Gm15575	-2.361	1.8E-02
Prdm16	-2.151	1.2E-04		Tppp3	-2.321	2.0E-02
Otogl	-2.364	1.4E-04		Rgs8	-2.331	2.0E-02
Upb1	-1.805	1.8E-04		1700097N02Rik	-2.540	2.0E-02
Rasal2	-3.281	1.8E-04		BC100530	-1.809	2.2E-02
5730409E04Rik	-1.548	3.3E-04		Ak8	-1.685	2.2E-02
Gm15503	-2.027	3.7E-04		Hs3st3b1	-1.829	2.2E-02
Sema4c	-1.812	5.6E-04		Igkv14-126	-2.335	2.3E-02
2810025M15Rik	-2.716	6.2E-04		4933408N05Rik	-1.758	2.4E-02
Cd300c	-2.612	6.2E-04		2410004P03Rik	-1.586	2.4E-02
Rasa4	-1.760	6.3E-04		Rassf4	-1.642	2.4E-02
Chst14	-1.541	6.6E-04		Cxcl14	-2.001	2.6E-02
Rap1gap	-2.748	8.1E-04		Adamts14	-2.288	2.6E-02
Klk1	-2.981	8.1E-04		Gm37909	-1.723	2.7E-02
Kcnt1	-2.916	9.6E-04		Arl14epl	-2.348	2.8E-02
Pcdh17	-3.231	1.1E-03		Gm15280	-1.902	2.8E-02
Upk1b	-3.093	1.1E-03		Fam131a	-1.866	2.8E-02
Plekhh2	-2.732	1.1E-03		Hpse	-1.923	2.9E-02
Raet1d	-3.295	1.1E-03		Gm26804	-1.639	3.0E-02

Gene	FC	q-value		Gene	FC	q-value
Igkv1-122	-3.206	1.2E-03		Gm23306	-1.972	3.0E-02
Mmrn1	-3.110	1.4E-03		Gm15845	-1.664	3.0E-02
Gm12057	-2.522	1.5E-03		Tnfsf15	-2.043	3.1E-02
Pcp4l1	-2.211	1.8E-03		Mx1	-2.061	3.2E-02
Slmapos2	-1.633	1.8E-03		NA	-1.608	3.2E-02
Cp	-2.104	1.8E-03		Krt7	-1.509	3.2E-02
Stox2	-2.638	1.9E-03		Gm16238	-2.224	3.2E-02
Gm7582	-2.153	1.9E-03		Dbx2	-2.430	3.5E-02
Klrb1a	-2.816	2.2E-03		Dnah8	-2.369	3.5E-02
Sdk1	-2.556	2.6E-03		Myadml2	-2.014	3.6E-02
Alpk1	-1.789	2.7E-03		Gtsf1	-1.541	3.6E-02
Ighv11-2	-2.726	2.8E-03		Gm1972	-2.360	3.7E-02
Pdzd4	-1.804	2.9E-03		Rasd2	-2.322	3.8E-02
Trbv29	-2.790	3.3E-03		Fmnl2	-1.731	3.8E-02
Gm12505	-1.620	3.4E-03		Stfa2	-1.708	3.8E-02
Cd160	-2.050	3.4E-03		C1ra	-1.595	3.9E-02
Myadml2os	-2.737	3.8E-03		Stfa2l1	-1.695	4.0E-02
Hlf	-2.550	3.8E-03		Cgnl1	-2.312	4.0E-02
Ier5l	-1.777	4.0E-03		Trav13-4-dv7	-2.089	4.0E-02
Lpar5	-1.721	4.1E-03		Klra8	-2.120	4.1E-02
Gm12709	-2.720	4.6E-03		D430040D24Rik	-1.901	4.2E-02
Sec16b	-1.861	4.9E-03		Scarf2	-1.723	4.3E-02
Dync2li1	-1.543	4.9E-03		Tcrg-C4	-1.814	4.4E-02
Pdlim4	-1.822	5.1E-03		Nostrin	-1.618	4.4E-02
Gm13564	-2.302	5.5E-03		Ablim2	-1.837	4.5E-02
Klra3	-2.182	5.9E-03		Ptpn5	-2.257	4.6E-02
Hoxc9	-2.365	6.4E-03		Stfa3	-1.711	4.6E-02
Tmem173	-1.559	6.5E-03		Ntn1	-2.337	4.8E-02
Klk1b11	-2.858	6.8E-03		Dio2	-2.038	4.9E-02
Clec9a	-1.934	7.4E-03		Klra7	-1.882	4.9E-02
Gm5380	-2.189	7.6E-03				

Table 6.10 FL vs 10w-AML, up in FL

Gene	FC	q-value		Gene	FC	q-value
Gm10184	9.905	1.8E-91		Gm11639	2.330	3.3E-02
Eif2s3y	8.926	3.0E-92		BC016579	2.327	4.8E-02
Zfpm2	8.648	1.8E-52		Sspn	2.321	2.2E-02
Gm6768	8.370	1.6E-53		Dtx1	2.319	9.7E-03
BC018473	8.235	7.5E-37		Ffar2	2.318	1.2E-07
Ddx3y	8.112	5.2E-96		A930038B10Rik	2.317	7.1E-03
St6galnac1	5.892	1.4E-20		Zfp354c	2.310	5.5E-03
Gm11735	5.527	8.4E-15		Perp	2.307	1.8E-02
Nkx3-2	5.385	1.8E-13		Rhbdf1	2.303	3.1E-03
Uty	5.157	9.5E-52		5830411N06Rik	2.303	3.5E-02
Chl1	5.018	5.7E-11		Gm20506	2.296	2.9E-02
Igkv1-99	4.731	2.7E-09		Pknox2	2.294	2.2E-02
Col4a5	4.450	1.8E-07		Phldb2	2.289	1.7E-02
Pgm5	4.300	2.2E-09		P2rx6	2.277	4.4E-02
Orm1	4.216	1.4E-07		Rhcg	2.275	3.9E-02
Ccbe1	4.056	3.3E-10		Spock2	2.275	2.5E-02
Xlr4e-ps	3.992	1.2E-07		Cpvl	2.275	4.5E-02
Ighv1-28	3.911	1.1E-05		Jag1	2.268	2.9E-02
Tex15	3.907	3.0E-08		Ddx25	2.254	2.2E-02
Dapk1	3.904	7.0E-11		Gm37347	2.253	9.9E-03
Gm29650	3.903	2.4E-06		Rasgef1a	2.253	3.9E-03
1700017G19Rik	3.880	9.3E-06		Ggt5	2.252	1.2E-02
Nova1	3.879	2.1E-05		Tmem17	2.246	4.7E-03
1700071M16Rik	3.837	2.2E-05		Fabp7	2.244	2.8E-02
Dock1	3.754	4.4E-06		Fam71b	2.241	3.9E-03
Prdm16	3.735	1.9E-10		Clec11a	2.234	2.1E-02
Rcvrn	3.733	2.4E-05		Map10	2.232	4.9E-02
Gm14085	3.715	2.8E-07		H2afy2	2.227	3.5E-02
Dsc2	3.692	6.4E-05		Fcer2a	2.227	3.0E-03
Cr2	3.687	2.0E-09		G0s2	2.223	2.0E-02
C230014O12Rik	3.654	3.4E-06		Bst1	2.222	3.8E-02
Tmem252	3.563	8.9E-07		Adamtsl3	2.218	4.9E-02
St6galnac2	3.478	3.1E-04		Tmem121	2.211	3.7E-02
Ehbp1	3.469	6.8E-07		Me1	2.208	2.3E-02
Dhcr24	3.430	1.1E-10		Maged2	2.196	3.1E-04
Pcolce2	3.427	5.0E-04		2010007H06Rik	2.195	2.3E-02
Ak4	3.341	5.4E-08		Gm38259	2.186	3.5E-02
Kdm5d	3.318	1.0E-35		Scrg1	2.186	1.6E-02
Col4a6	3.316	1.7E-05		Sall2	2.171	2.5E-03
Scin	3.253	5.5E-04		AA467197	2.171	4.2E-02
Crtac1	3.214	7.9E-05		Cdk18	2.149	9.9E-03
Atoh8	3.214	2.1E-05		Hist1h2br	2.146	4.0E-04
Myct1	3.210	5.4E-05		Cyp11a1	2.134	4.6E-02
Cygb	3.154	1.3E-04		Stap2	2.128	2.0E-02
Ncam1	3.152	2.2E-07		Armc12	2.128	2.8E-02

Gene	FC	q-value		Gene	FC	q-value
Il34	3.132	8.1E-04		Mmp8	2.128	3.1E-02
Smo	3.119	5.7E-06		Xlr4c	2.125	1.2E-02
Ighd	3.116	1.2E-10		Gm16548	2.125	3.9E-02
Gm21857	3.091	5.0E-04		Vsig10	2.122	1.2E-03
Dscaml1	3.073	4.6E-04		1500009L16Rik	2.118	3.7E-02
Gm9522	3.071	3.6E-04		Gm16170	2.115	4.8E-03
Gm11827	3.039	1.8E-04		Gm26649	2.114	4.9E-02
Rassf10	3.029	3.4E-03		Prom1	2.112	2.1E-02
Crisp3	3.027	3.1E-03		Gm38158	2.109	1.9E-02
Chrm3	3.011	8.8E-05		Il9r	2.096	2.5E-02
Tie1	3.011	7.9E-07		Ica1	2.095	3.4E-04
Pik3c2g	2.968	2.0E-03		Adtrp	2.093	3.3E-02
Btbd3	2.968	8.4E-04		Grm1	2.092	3.2E-03
4930426D05Rik	2.967	3.1E-03		4930516B21Rik	2.091	3.2E-02
Pde1c	2.952	1.9E-03		Mapk12	2.081	1.4E-04
Cd79a	2.944	3.3E-05		Ispd	2.069	2.6E-02
Ighg3	2.932	5.4E-04		Inhba	2.066	3.6E-02
Dach2	2.904	1.9E-03		Mreg	2.050	1.6E-02
Rbm11	2.896	1.1E-06		Rufy4	2.046	8.4E-03
Gm37199	2.863	3.0E-03		Gucy1a3	2.037	4.3E-03
Ebf1	2.847	2.2E-05		Gm14703	2.036	3.3E-02
Gm29264	2.844	1.0E-03		B3gnt5	2.035	1.1E-02
Pxdc1	2.837	2.6E-04		Echdc3	2.031	3.7E-02
Scml2	2.831	8.4E-03		Gm17619	2.029	3.0E-02
Gabrg1	2.827	5.7E-03		2310047D07Rik	2.021	4.9E-02
Pik3c2b	2.826	5.0E-11		Adam33	2.019	4.4E-02
Serpina11	2.805	3.2E-03		Slc34a1	2.016	4.8E-02
Igkv4-62	2.801	9.5E-03		Arrdc4	2.006	2.3E-03
Fcmr	2.786	3.6E-03		Rgs9bp	2.005	1.3E-04
Gm10401	2.770	6.2E-03		A330023F24Rik	1.997	1.2E-02
Snx31	2.768	1.6E-03		Abca5	1.983	2.3E-02
Gm11992	2.767	3.3E-04		Obscn	1.982	3.4E-02
Mill2	2.759	8.4E-03		Myom1	1.971	1.9E-03
Neurl1a	2.759	3.7E-05		2810410L24Rik	1.970	4.9E-03
Ankrd66	2.756	3.0E-03		Lgr4	1.968	2.3E-02
Krt86	2.756	2.3E-03		C130060C02Rik	1.960	2.5E-02
Kcnc1	2.753	9.9E-03		Filip1	1.940	1.3E-02
Rhobtb3	2.742	3.0E-03		Slc22a15	1.933	5.6E-03
Prps1l1	2.739	2.7E-03		Mrap	1.929	1.8E-03
Mycn	2.726	4.7E-04		Sept4	1.925	3.6E-02
Il1r2	2.700	3.4E-03		Gm16556	1.923	3.1E-02
Med12l	2.700	1.5E-04		BC051142	1.913	3.9E-02
Gja6	2.685	1.3E-02		Cmtm4	1.908	7.6E-06
Klhl14	2.668	1.4E-02		Pde3b	1.905	1.8E-03
B230118H07Rik	2.659	1.9E-03		Pou2af1	1.895	2.6E-02
Ccdc91	2.648	8.6E-07		Tgfb3	1.887	3.9E-02

Gene	FC	q-value		Gene	FC	q-value
Adgrf3	2.648	6.8E-03		Mdfi	1.886	4.9E-02
Igkv6-32	2.647	1.4E-02		Stk36	1.879	2.8E-02
D130043K22Rik	2.644	4.5E-03		Tnnt1	1.877	4.4E-03
Gm10451	2.642	1.2E-03		Chrnb1	1.865	1.6E-02
Ccdc149	2.641	8.3E-03		Ighv1-12	1.862	3.2E-02
Bend5	2.633	4.2E-03		Psd3	1.859	1.8E-02
Gjb3	2.632	1.8E-02		Exoc3l2	1.852	5.6E-03
Scd1	2.608	1.1E-02		Zfp93	1.851	1.2E-02
Gm13073	2.608	1.2E-02		Tert	1.851	4.1E-02
Tctex1d1	2.596	1.6E-02		Aox1	1.849	2.7E-02
Entpd3	2.590	1.4E-02		H2-Ob	1.846	1.9E-02
Zfp57	2.590	8.4E-03		Rarb	1.833	8.9E-03
Gm37192	2.583	8.9E-03		Aldh5a1	1.811	2.3E-02
Pax8	2.574	2.3E-03		Sorbs3	1.810	4.2E-02
Ighv7-1	2.565	1.0E-02		Klhl8	1.797	3.3E-03
Clstn3	2.556	8.1E-04		Apbb2	1.790	2.4E-02
Igkv4-61	2.542	1.6E-02		5830444B04Rik	1.788	2.3E-02
Cyp2j6	2.527	8.4E-03		Cideb	1.778	2.6E-02
Gpr22	2.524	1.7E-02		Galnt3	1.776	5.9E-03
Bfsp2	2.524	2.8E-03		Lrrc46	1.775	2.3E-02
Igkv3-10	2.520	1.6E-03		Oosp1	1.774	3.6E-02
Tspan2	2.515	1.3E-05		4933406C10Rik	1.774	5.9E-03
Pla2g7	2.515	1.3E-02		S1pr1	1.764	3.9E-02
Upp1	2.510	1.7E-02		Cpm	1.762	2.4E-02
Gm29554	2.503	2.2E-02		Zfp30	1.752	1.1E-02
Prkg1	2.495	3.3E-03		Rac3	1.738	1.6E-02
Ighv1-61	2.489	1.7E-02		H2-DMb2	1.724	1.5E-02
Sfrp2	2.484	2.2E-02		Mmp23	1.718	9.9E-03
Ms4a8a	2.479	2.4E-02		2610037D02Rik	1.715	3.4E-05
Shroom4	2.479	3.0E-03		Adgrd1	1.712	1.3E-02
Scarna3a	2.473	1.9E-02		Zdhhc2	1.707	2.1E-05
Eya2	2.473	4.6E-03		Cldn12	1.706	1.7E-02
Glipr1l1	2.466	3.1E-02		Ltbp3	1.697	7.2E-03
Lrrc23	2.465	2.3E-02		Pdzd3	1.696	4.0E-02
Sprn	2.459	3.1E-02		Epm2a	1.684	3.3E-02
Ighv6-6	2.448	8.4E-03		Zfp558	1.661	1.8E-02
Olfr248	2.448	2.6E-02		Il18r1	1.647	3.0E-03
Defb40	2.444	1.8E-02		Marveld1	1.646	1.2E-03
Slc4a5	2.443	8.4E-03		Btnl9	1.641	5.2E-05
Plekha5	2.442	1.6E-03		Afp	1.641	4.6E-02
Limch1	2.433	2.0E-03		Gm5577	1.639	4.6E-02
Rasl11b	2.428	7.9E-03		Zfp938	1.635	9.0E-03
Abca4	2.417	8.9E-07		Map4k3	1.624	8.5E-03
Serpina12	2.412	3.2E-02		Cd38	1.623	4.4E-02
Fam69b	2.411	1.2E-08		Dab2ip	1.621	5.1E-04
Pard3b	2.410	7.2E-03		F730311O21Rik	1.619	6.4E-03

Gene	FC	q-value		Gene	FC	q-value
Mirt2	2.403	2.5E-03		Plin3	1.617	1.6E-02
Bcar3	2.401	3.7E-05		Cd9	1.613	5.4E-03
Map9	2.389	9.4E-03		Hoxc8	1.609	2.7E-02
Kcns1	2.383	3.6E-02		Cd63	1.608	6.7E-04
Cyp26a1	2.366	1.7E-02		Fbxo10	1.607	2.6E-03
Chst3	2.365	1.4E-03		Rimbp3	1.604	3.2E-02
Fmn2	2.354	4.4E-02		Scarf1	1.584	3.8E-02
Cuedc1	2.354	7.2E-03		Gm37939	1.580	1.5E-06
Ffar1	2.354	2.6E-02		Hook1	1.566	5.3E-04
Abi3bp	2.348	2.5E-03		Marveld2	1.562	3.1E-02
Cldn1	2.345	4.2E-02		Stox1	1.560	3.7E-02
Spatc1	2.343	1.6E-03		Mroh6	1.552	4.4E-04
Tmie	2.341	2.5E-02		Gm15856	1.539	3.2E-02
Zfp2	2.339	1.6E-02		Rab17	1.535	1.9E-02
Ighv5-6	2.339	3.5E-02		Gm37759	1.529	2.2E-02
Gm28230	2.337	4.6E-02		Clic3	1.520	5.1E-04
Dock7	2.336	8.8E-09		5830415G21Rik	1.509	1.4E-02
Adcy5	2.335	2.0E-03				

Table 6.11 FL vs 10w-AML, up in 10w

Gene	FC	q-value		Gene	FC	q-value
Adgrg7	-6.9283	2.7E-31		Gm6377	-2.1389	1.3E-02
Hpgd	-6.7436	2.9E-35		Gpr4	-2.1239	8.1E-03
Podxl	-4.7019	1.5E-09		Olfr56	-2.1223	2.1E-03
Rasal2	-4.6796	1.9E-09		Gm5544	-2.1033	4.1E-02
Mfsd7a	-3.9288	6.1E-11		Gm21370	-2.1029	1.4E-03
Ifi44	-3.8045	2.8E-05		Hlf	-2.1020	2.9E-02
Atf3	-3.6754	3.5E-06		Ifit1bl1	-2.0983	1.2E-02
Plekhh2	-3.6045	2.2E-06		2210016F16Rik	-2.0922	1.4E-06
Gm15726	-3.5854	3.6E-06		Ckb	-2.0867	1.4E-04
Gm16867	-3.4372	1.2E-04		Ppm1e	-2.0849	1.4E-02
Gm27177	-3.4172	1.1E-08		Mnda	-2.0783	4.5E-02
Gm21860	-3.4016	4.4E-04		Gm2635	-2.0495	1.8E-02
Gm21748	-3.4016	4.4E-04		Adgre4	-2.0448	1.2E-02
Cd300c	-3.3882	9.5E-07		Kpna2	-2.0439	1.3E-04
2810025M15Rik	-3.3436	4.7E-06		Slamf8	-2.0385	3.4E-03
Clec9a	-3.2555	5.8E-08		Rasa4	-2.0346	2.7E-05
Cda	-3.2352	1.0E-03		Trim30c	-2.0321	4.2E-02
Cxcl10	-3.1133	2.4E-05		Pcdhgc3	-2.0307	4.8E-02
Mansc1	-3.0919	3.7E-05		Lipo2	-2.0285	1.3E-03
Ccl12	-3.0908	3.0E-03		Sh2d6	-2.0245	3.2E-02
G530011O06Rik	-3.0742	1.2E-27		Slamf9	-2.0159	2.9E-03
Myh10	-3.0464	2.3E-03		Adgra2	-2.0057	5.5E-04
Phf11d	-2.9789	5.7E-05		Gm17024	-1.9983	7.3E-03
Pdlim4	-2.9031	7.5E-08		Fcna	-1.9943	1.4E-02
Mmrn1	-2.8741	4.3E-03		Pcp4l1	-1.9934	7.2E-03
Xist	-2.8652	3.9E-06		Cd300lg	-1.9890	4.6E-02
BC026585	-2.8561	1.2E-06		1700012B09Rik	-1.9880	4.7E-02
Tppp3	-2.8420	1.9E-03		Cd40	-1.9809	3.0E-03
Ifi205	-2.8273	1.5E-03		Pydc3	-1.9788	9.6E-03
Ifit3	-2.8226	1.8E-03		Kmo	-1.9769	1.9E-04
Apod	-2.8105	4.2E-03		Tnfsf9	-1.9723	3.6E-04
Gm12551	-2.8007	7.4E-03		Irf7	-1.9627	2.0E-02
Frmd5	-2.7535	1.1E-03		Gm7592	-1.9521	2.6E-02
Mlana	-2.7500	7.0E-03		Gbp2b	-1.9505	1.2E-02
Pla2g5	-2.7253	1.2E-02		Xcl1	-1.9471	3.2E-02
Phf11a	-2.7205	2.0E-04		Scarf2	-1.9384	1.4E-02
Cttn	-2.7023	8.7E-03		Bst2	-1.9346	6.0E-04
Tmem171	-2.6886	1.6E-03		BC147527	-1.9345	1.1E-02
Tlr11	-2.6682	9.4E-03		Pigz	-1.9341	3.4E-03
Cfb	-2.6535	2.1E-03		Klf4	-1.9298	3.0E-02
Mx1	-2.6452	2.1E-03		Gm7609	-1.9297	5.4E-03
Folr1	-2.6451	5.2E-03		Klri2	-1.9241	2.1E-02
Arhgap32	-2.6398	3.3E-04		Pir	-1.9216	1.3E-03
Ccl7	-2.6045	1.8E-02		C4b	-1.9197	3.7E-02
Gm7582	-2.5725	7.4E-05		Alpk1	-1.9159	1.1E-03

Gene	FC	q-value		Gene	FC	q-value
Rnls	-2.5471	8.9E-07		Dntt	-1.9057	5.3E-03
Ccl8	-2.5130	3.4E-03		Gm37665	-1.9025	4.7E-03
Ncr1	-2.5118	7.5E-03		Pltp	-1.9009	1.2E-02
Zfp69	-2.4937	2.9E-05		Serpinf1	-1.9006	3.9E-04
Wnt6	-2.4935	2.7E-03		Stk32c	-1.8980	2.2E-02
Gm21762	-2.4923	1.9E-02		Cx3cr1	-1.8916	3.7E-02
Ifit3b	-2.4890	1.4E-02		Inppl1	-1.8770	9.9E-04
Tubb3	-2.4697	7.8E-04		Pkd1l3	-1.8765	8.4E-03
NA	-2.4614	2.0E-02		Trem2	-1.8607	4.3E-02
Gm12187	-2.4510	2.2E-02		Aif1	-1.8576	2.7E-02
Pros1	-2.4466	3.7E-03		Zbp1	-1.8564	2.3E-02
Ip6k3	-2.4383	5.1E-03		Cd300lh	-1.8551	4.5E-02
Cp	-2.4293	1.5E-04		Phlda3	-1.8546	3.3E-03
Hist1h4m	-2.4258	3.5E-02		Aox2	-1.8512	4.7E-02
Pid1	-2.4173	3.3E-02		Nr1h3	-1.8487	2.1E-02
Ighv7-3	-2.4150	2.0E-03		Cdk5rap1	-1.8479	1.2E-09
Cav2	-2.4111	1.5E-03		Usp18	-1.8359	4.1E-02
Fam131a	-2.4071	1.5E-03		Pmaip1	-1.8225	4.5E-03
Cd5l	-2.4035	1.2E-02		Amotl1	-1.8161	3.3E-02
Xcr1	-2.3876	4.7E-03		Pvrl4	-1.8101	5.1E-04
Ccdc92	-2.3840	1.9E-02		Klra3	-1.8044	3.7E-02
Gm15701	-2.3805	3.3E-02		Cd34	-1.8003	1.3E-02
Ifit2	-2.3685	2.1E-05		Pde8b	-1.7916	1.9E-02
Arsi	-2.3591	8.5E-03		Gm37614	-1.7900	1.1E-02
Nav1	-2.3527	2.5E-03		Kank2	-1.7680	1.9E-03
Ednrb	-2.3520	3.4E-03		Igf1	-1.7539	1.1E-02
Rilp	-2.3515	3.1E-05		Fam26f	-1.7515	5.5E-04
Fmo1	-2.3510	4.7E-17		Frmd4b	-1.7508	9.6E-03
Cd209a	-2.3452	1.5E-02		Pdzd4	-1.7493	4.5E-03
Klri1	-2.3449	2.6E-02		Prdx4	-1.7437	3.7E-03
Igkv3-9	-2.3306	4.7E-02		Cd180	-1.7287	4.6E-04
Cyp27a1	-2.3300	1.4E-02		Oasl1	-1.7067	4.3E-02
Gm15503	-2.3279	1.1E-05		Camk1	-1.6994	2.6E-06
Prr5l	-2.3265	4.7E-03		Cd69	-1.6923	4.0E-02
Mycl	-2.3252	1.3E-03		Hs3st3b1	-1.6914	4.1E-02
Mrc2	-2.3244	2.0E-03		Gm12250	-1.6873	4.5E-02
Gm5602	-2.3203	4.3E-02		Ivd	-1.6858	1.9E-02
Six1	-2.3165	4.9E-02		Hfe	-1.6853	2.3E-02
Klrg2	-2.3096	4.4E-02		Tubb6	-1.6822	2.4E-03
Cd300e	-2.3060	1.7E-02		Nxpe5	-1.6568	4.7E-02
Ass1	-2.2997	7.0E-05		Ifi47	-1.6562	3.1E-03
Hpse	-2.2933	4.6E-03		Ms4a7	-1.6503	3.9E-02
Aloxe3	-2.2848	5.4E-03		AA414768	-1.6483	3.2E-02
Batf2	-2.2698	2.2E-02		Sema4c	-1.6447	2.5E-03
Upb1	-2.2671	2.8E-07		Rnf157	-1.6416	7.2E-03
Gm9396	-2.2410	3.9E-02		Dusp5	-1.6314	3.4E-05

Gene	FC	q-value		Gene	FC	q-value
Sdc3	-2.2271	3.2E-03		Tlr12	-1.6314	3.1E-02
3300005D01Rik	-2.2187	3.6E-03		Tex14	-1.6070	4.2E-02
D13Ertd608e	-2.2160	4.9E-02		Sgcb	-1.6027	1.3E-04
Mx2	-2.2157	1.4E-02		Plxdc1	-1.6005	4.1E-02
Ccr9	-2.2137	1.2E-02		Gm26885	-1.5986	1.8E-03
Ifit1	-2.2094	8.5E-03		Kdm6bos	-1.5953	3.1E-02
Phf11b	-2.2021	6.8E-03		Dynlt1b	-1.5886	2.8E-03
Gm4955	-2.1929	4.8E-03		Gbp3	-1.5828	2.0E-02
Stox2	-2.1866	1.8E-02		Rassf4	-1.5748	3.3E-02
Nr4a1	-2.1864	6.0E-04		Rgl1	-1.5743	2.4E-02
Kcng1	-2.1827	1.6E-02		Irf8	-1.5579	3.5E-02
Cacnb3	-2.1680	4.9E-02		Gm37472	-1.5565	5.9E-03
Ank2	-2.1670	3.1E-02		Pnp2	-1.5412	4.6E-02
Tgtp1	-2.1596	1.2E-02		Ciart	-1.5393	1.8E-02
Gm15433	-2.1555	1.4E-03		A530040E14Rik	-1.5363	5.4E-03
Eps8	-2.1477	2.1E-02		Trex1	-1.5292	7.1E-03
Gm16238	-2.1476	3.9E-02		Gm9864	-1.5200	3.6E-02
Cdkn1a	-2.1462	6.4E-03		L1cam	-1.5141	2.5E-02

Table 6.12 FL vs >52w-AML, up in FL

Gene	FC	q-value		Gene	FC	q-value
Zfpm2	8.397	5.6E-52		Gm27252	2.276	2.2E-02
Gm6768	7.724	8.9E-47		Smkr-ps	2.275	2.4E-02
Nkx3-2	5.125	2.6E-12		Pkdcc	2.274	1.7E-02
Chl1	4.178	3.9E-08		Tmem158	2.272	6.9E-03
Kctd4	4.034	1.6E-08		Pld4	2.272	2.7E-04
Camkv	3.860	1.3E-09		Adgre1	2.259	2.2E-03
Gpr22	3.812	3.8E-05		Gm5960	2.259	3.8E-02
Ms4a8a	3.645	1.5E-04		Ifi27l2a	2.253	3.5E-02
Slc15a2	3.596	3.9E-10		Nucb2	2.251	1.3E-03
Ighv1-28	3.587	1.0E-04		Anxa8	2.231	4.4E-02
Vcan	3.575	1.5E-04		Klhl30	2.226	2.9E-02
Fabp7	3.523	8.2E-05		Gm2635	2.224	2.6E-02
Penk	3.395	1.2E-04		Tns4	2.221	2.0E-02
Il34	3.284	4.8E-04		Cx3cr1	2.220	1.1E-02
Prdm16	3.275	3.1E-08		Stab1	2.213	1.3E-02
Ccbe1	3.239	1.1E-06		Lgmn	2.208	3.1E-03
Gm21857	3.225	2.7E-04		Dscaml1	2.206	2.8E-02
Lmo1	3.217	1.2E-05		Fcgr1	2.197	4.9E-02
Abca9	3.212	7.8E-05		Dnah12	2.183	5.7E-03
Cysltr1	3.206	3.6E-05		Gm13147	2.183	1.3E-02
Igkv6-32	3.193	1.8E-03		Pyhin1	2.180	6.8E-03
Rasgrf2	3.119	6.0E-18		Ifi204	2.171	4.4E-02
Lifr	3.021	6.0E-04		Ptpro	2.146	3.5E-02
Gm20431	2.977	4.9E-03		Hpse	2.143	1.3E-02
Sfrp2	2.960	4.9E-03		Dmrtb1	2.142	3.2E-02
Gpnmb	2.911	4.0E-03		Slamf8	2.129	5.3E-03
Dntt	2.854	1.0E-05		Myom1	2.127	7.1E-04
Col4a5	2.833	3.5E-03		Gm5431	2.124	2.8E-02
F13a1	2.790	4.5E-03		Tlr7	2.120	1.1E-02
Trdv5	2.785	8.9E-03		Cd302	2.119	3.4E-02
Igkv4-62	2.784	1.3E-02		Clec4a3	2.118	3.2E-02
Ms4a4a	2.748	9.1E-03		Mpeg1	2.118	2.8E-02
Nova1	2.734	9.2E-03		Gm17767	2.100	2.9E-02
AI607873	2.722	3.3E-03		Lrp1	2.095	3.1E-02
Tifab	2.693	2.1E-04		Tlr9	2.085	8.3E-04
Xkr7	2.678	1.5E-02		Gdf9	2.067	1.0E-02
Arhgef37	2.670	6.1E-03		Rnd3	2.062	2.0E-02
Glis3	2.662	4.4E-03		Ifi30	2.052	5.9E-04
Ppfia4	2.656	1.6E-03		A730036I17Rik	2.026	3.3E-02
Chit1	2.622	1.9E-02		Tmem106a	2.010	3.6E-03
Tgm5	2.612	1.3E-02		8430408G22Rik	1.990	1.3E-02
Cds1	2.607	1.7E-03		Gm30414	1.989	3.2E-02
Rspo1	2.596	1.6E-03		Xlr4e-ps	1.985	3.5E-02
Col4a6	2.588	1.6E-03		Zeb2os	1.975	5.2E-03
Fam84a	2.583	1.9E-02		Slc4a8	1.965	1.8E-02

Gene	FC	q-value		Gene	FC	q-value
Dpep2	2.578	6.8E-03		Aldh1b1	1.952	3.3E-02
Fam78b	2.554	1.2E-02		Kalrn	1.936	5.3E-03
Afap1	2.551	6.0E-03		Hopx	1.931	5.0E-02
Siglech	2.545	2.9E-03		Tmem51	1.916	1.2E-02
C130046K22Rik	2.542	3.9E-03		Cryba4	1.915	3.4E-02
Nr0b2	2.541	1.4E-02		Igkv12-46	1.906	4.9E-03
Plxnb2	2.532	2.5E-04		Mst1r	1.903	3.8E-02
Dsc2	2.531	1.8E-02		Matn2	1.892	4.7E-02
Ctss	2.530	3.4E-04		Neurl1a	1.887	1.1E-02
Dach2	2.520	1.2E-02		4933424M12Rik	1.879	3.8E-02
Gm12161	2.516	1.7E-02		Trio	1.873	3.3E-03
Irf8	2.503	6.5E-05		Hip1	1.863	1.2E-02
Apba1	2.499	3.6E-03		Arhgef10l	1.827	1.1E-02
Igkv1-99	2.499	1.3E-02		Scpep1	1.821	2.5E-04
Efemp2	2.480	2.4E-04		Adap2	1.810	4.3E-02
Gm10698	2.460	3.9E-02		Nid2	1.808	3.8E-02
Slc27a2	2.445	3.6E-02		Rhbdl3	1.799	3.0E-02
Depdc7	2.435	1.0E-03		Nostrin	1.795	2.9E-02
Cd209a	2.433	1.3E-02		1700063D05Rik	1.794	1.1E-03
Ms4a4c	2.428	5.0E-03		Mafb	1.791	4.4E-02
Npy	2.419	4.6E-02		Ctsh	1.777	2.2E-02
Gm10645	2.408	7.4E-03		Dab2	1.771	4.5E-02
Cyp2ab1	2.394	8.2E-03		Tacc2	1.761	3.9E-04
Pik3c2a	2.394	1.2E-04		Ccr2	1.723	5.0E-02
Aox3	2.393	4.9E-02		Oas1a	1.721	4.6E-02
Gm15899	2.390	4.9E-02		Stard9	1.721	4.5E-02
Adcy5	2.371	2.0E-03		Irf5	1.667	4.7E-02
Dock1	2.363	1.7E-02		Zcchc24	1.649	2.3E-02
P2ry6	2.356	1.0E-02		Fam49a	1.645	5.1E-06
Pde1c	2.352	2.4E-02		Rac3	1.623	3.6E-02
Drc7	2.343	9.1E-06		AW011738	1.609	4.6E-02
Il31ra	2.335	4.5E-02		Ckb	1.583	1.3E-02
Trib3	2.325	1.8E-02		Dusp3	1.581	8.0E-03
Galnt9	2.321	2.8E-02		Rwdd2a	1.571	1.1E-02
Nlrp1a	2.321	6.8E-03		Slc7a7	1.549	9.7E-05
Ddx4	2.306	2.3E-02		Ctsc	1.545	3.4E-02
Ly86	2.306	6.1E-04		Sh2d1b1	1.538	5.0E-02

Table 6.13 FL vs >52w-AML, up in >52w

Gene	FC	q-value		Gene	FC	q-value
Adcyap1r1	-5.623	1.1E-12		Eid2	-2.394	2.8E-02
Slc4a10	-5.606	2.0E-13		Rec8	-2.383	2.8E-02
Neo1	-5.530	8.6E-20		Ighv9-1	-2.377	3.7E-02
Hnmt	-5.451	2.3E-13		Gm371	-2.376	3.9E-02
Adgrg7	-5.257	5.1E-17		Samd13	-2.367	1.0E-02
Chga	-4.784	4.0E-08		Stfa2l1	-2.366	1.1E-03
Tmem108	-4.604	9.3E-09		1700020N18Rik	-2.363	4.5E-02
Gm8494	-4.400	3.7E-12		Slc36a4	-2.353	4.9E-03
Mmp15	-4.336	5.1E-08		Gm14542	-2.351	3.6E-02
Mansc1	-4.304	4.8E-10		Ncr1	-2.336	2.0E-02
Ncam2	-4.200	1.1E-08		Hoxc9	-2.320	1.1E-02
Epx	-3.822	4.9E-05		Fbn1	-2.320	1.2E-04
Cib3	-3.766	3.2E-05		Ighv14-3	-2.307	1.3E-02
Procr	-3.686	4.1E-07		Hdac9	-2.282	5.6E-03
Gm17641	-3.670	2.0E-04		Gm28187	-2.280	8.7E-06
Gpha2	-3.636	2.4E-04		4931431F19Rik	-2.249	4.2E-02
Vill	-3.564	9.7E-05		Pnma1	-2.247	7.5E-03
1110032F04Rik	-3.563	1.8E-04		Cacng8	-2.244	2.2E-02
Pik3c2g	-3.537	4.9E-05		Gm5483	-2.237	4.6E-03
Ighv1-9	-3.517	4.4E-14		Eps8l1	-2.230	6.2E-26
Gpc4	-3.514	3.9E-04		Kcnq3	-2.227	3.5E-02
Prg2	-3.472	7.6E-05		Zscan18	-2.225	2.6E-02
Gm16252	-3.431	7.2E-04		Jsrp1	-2.209	2.2E-02
Lpar4	-3.426	1.3E-04		Arhgef9	-2.201	1.6E-02
Msrb3	-3.420	7.9E-07		Spry4	-2.190	4.5E-02
Frmpd4	-3.359	9.7E-04		NA	-2.186	1.1E-02
Clec2f	-3.354	1.8E-05		Lipo2	-2.184	3.9E-04
Adam11	-3.259	1.3E-06		Arhgap27os3	-2.175	1.1E-09
Adgrg6	-3.236	1.5E-04		Erc2	-2.153	4.7E-02
D930020B18Rik	-3.192	2.7E-04		4933406I18Rik	-2.153	4.2E-02
Ighv5-4	-3.176	9.3E-05		Rnls	-2.149	1.3E-04
1700048O20Rik	-3.171	3.9E-08		Flywch2	-2.145	4.0E-03
Cxx1b	-3.165	3.5E-06		Gm27177	-2.145	2.9E-03
Sema3e	-3.163	1.3E-08		Adgrl1	-2.143	5.6E-03
Ppp4r4	-3.160	2.5E-03		Ptgdr	-2.140	1.1E-02
H60c	-3.157	3.7E-04		Pcdhb17	-2.132	5.0E-02
Podxl	-3.143	4.4E-04		Mmp14	-2.126	3.0E-02
Gm5416	-3.108	1.1E-05		Ighg1	-2.120	9.5E-03
Lhx2	-3.108	2.6E-03		Epb41l1	-2.105	1.2E-02
Sec16b	-3.085	4.7E-08		Ighg2b	-2.090	4.9E-02
Ramp2	-3.001	2.5E-04		Zfp57	-2.089	4.9E-02
Nxf2	-2.966	5.6E-03		Zfp114	-2.070	7.7E-05
Spin4	-2.962	2.4E-04		Arntl2	-2.060	5.0E-02
Raet1e	-2.956	4.0E-03		Gm26668	-2.058	2.4E-02
Alox12e	-2.933	6.1E-03		D930048G16Rik	-2.055	1.2E-02

Gene	FC	q-value		Gene	FC	q-value
Dkk3	-2.927	3.0E-03		Gm996	-2.029	8.1E-04
Dleu7	-2.924	4.9E-03		Prkg1	-2.025	3.1E-02
Gm15845	-2.913	3.4E-06		Gm37034	-2.022	4.4E-02
Gja5	-2.897	7.9E-03		4930555F03Rik	-2.020	4.6E-02
Stfa2	-2.887	2.1E-05		2810025M15Rik	-2.017	3.0E-02
Ighv1-5	-2.863	2.3E-03		Pld6	-2.016	1.2E-02
Atp8b5	-2.862	2.5E-04		Igkv6-15	-1.991	5.4E-03
NA	-2.861	9.3E-04		Bahcc1	-1.982	1.6E-02
Gm23306	-2.852	2.4E-04		Cntd1	-1.969	2.7E-03
Defb40	-2.846	2.0E-03		Gm13051	-1.961	3.5E-02
Tek	-2.833	2.4E-03		2210016F16Rik	-1.955	1.6E-05
Gm10913	-2.826	3.4E-03		Nlgn2	-1.953	2.1E-02
Dio2	-2.814	1.9E-03		Galnt3	-1.945	1.1E-03
Acot6	-2.805	5.1E-06		Faah	-1.928	1.1E-03
BC100530	-2.802	3.4E-05		Hgfac	-1.924	8.4E-04
Ybx2	-2.789	7.3E-03		Igkv5-45	-1.922	1.3E-02
Tmem45a2	-2.784	5.7E-03		Cacnb2	-1.919	6.6E-03
Foxc1	-2.783	1.0E-02		Gm10134	-1.916	4.9E-02
Tnip3	-2.768	1.4E-03		Slc7a8	-1.889	3.3E-05
Stfa3	-2.754	1.0E-04		Acvr1	-1.886	3.4E-02
Zan	-2.735	8.3E-03		Fam131a	-1.874	3.3E-02
Htr1b	-2.719	4.5E-03		Gm5380	-1.866	4.4E-02
Gm17771	-2.708	1.2E-02		Sema4f	-1.860	1.2E-02
Cxx1a	-2.700	8.5E-05		Antxr1	-1.857	3.2E-02
Epb41l4a	-2.687	1.2E-02		Tnfrsf25	-1.835	2.3E-02
Mab21l2	-2.680	3.8E-03		Fhl2	-1.826	8.4E-03
Eya4	-2.672	4.9E-03		Cd200r4	-1.823	3.8E-03
C2cd4b	-2.667	5.3E-03		Actn2	-1.822	2.5E-02
Tfpi2	-2.655	2.0E-02		A130071D04Rik	-1.803	3.2E-02
Stfa1	-2.644	6.0E-05		Gm14286	-1.800	2.3E-03
Skint3	-2.636	1.3E-02		6330409D20Rik	-1.797	1.0E-02
Gm16531	-2.636	1.5E-02		Bace1	-1.789	3.4E-06
Igkv3-9	-2.607	2.5E-02		Tead2	-1.786	4.1E-04
Rims2	-2.600	3.3E-05		C1qtnf6	-1.777	3.3E-02
Myl9	-2.599	2.0E-02		C77080	-1.759	1.8E-02
Akr1c12	-2.596	1.3E-04		Slc35g2	-1.737	2.9E-05
Gpr27	-2.583	9.4E-03		Hoxb6	-1.721	3.6E-02
Gm13154	-2.555	1.5E-03		Gm17055	-1.719	3.0E-02
Muc20	-2.550	1.4E-02		Gm38142	-1.715	1.4E-02
BC026585	-2.545	4.3E-05		Fbxo17	-1.696	1.3E-02
Il4	-2.545	2.2E-03		Eno2	-1.691	1.1E-02
Cpvl	-2.540	2.2E-02		Socs2	-1.641	1.5E-02
BC117090	-2.522	3.3E-03		Pde3b	-1.635	1.3E-02
Krt18	-2.519	1.3E-02		Hoxb8	-1.627	2.8E-02
Fzd1	-2.512	5.6E-03		Gm26804	-1.626	3.8E-02
Gm26790	-2.495	1.1E-02		Nnat	-1.623	4.2E-02

Gene	FC	q-value		Gene	FC	q-value
Hs6st2	-2.490	3.6E-02		Mboat4	-1.610	1.6E-02
Gm26581	-2.487	1.3E-02		Erdr1	-1.606	4.4E-03
Cd200r3	-2.478	1.8E-02		Notch3	-1.588	3.5E-02
Prg3	-2.476	2.0E-02		Gm19345	-1.587	1.0E-02
Gm21814	-2.472	3.5E-02		Kdm6bos	-1.577	4.4E-02
Mmrn1	-2.468	2.8E-02		Tec	-1.574	2.8E-03
Igkv3-4	-2.468	3.0E-02		Plcl1	-1.550	1.5E-02
Igkv4-91	-2.451	3.5E-02		C530050E15Rik	-1.548	6.1E-04
Gm24801	-2.448	1.2E-02		Gm15856	-1.544	1.0E-02
Ighv1-4	-2.447	2.8E-02		Gng11	-1.541	2.9E-03
Ighv1-53	-2.431	5.0E-03		Gm21967	-1.539	1.0E-04
Igkv8-30	-2.429	9.7E-03		Sytl3	-1.531	1.3E-02
Rassf6	-2.417	1.1E-02		Gm37939	-1.511	1.5E-07
Apob	-2.408	4.3E-02		Fap	-1.507	4.7E-02

Table 6.14 3w vs >52w-AML, up in 3w

Gene	FC	q-value		Gene	FC	q-value
Prdm16	5.426	3.9E-25		BC147527	2.191	1.4E-03
Kctd4	4.738	2.0E-12		Tac4	2.190	1.6E-02
Camkv	4.681	3.7E-15		Zfp697	2.185	1.8E-02
Klk1b27	4.489	1.4E-09		Aif1	2.180	3.0E-03
Stox2	4.464	5.9E-10		B3galt5	2.179	1.1E-03
Abca9	4.447	5.6E-10		Aim1	2.166	1.8E-04
Rasgrf2	4.399	7.5E-38		Adora3	2.164	4.6E-03
Klk1	4.239	6.0E-08		Fam26f	2.161	6.1E-06
Slc15a2	4.106	6.2E-14		Sowahc	2.159	3.3E-03
Cd209a	4.101	1.0E-07		Il6ra	2.149	9.2E-03
Hpse	4.066	8.7E-10		Sh3rf1	2.147	9.1E-07
Lalba	3.897	1.2E-05		Gm12161	2.147	2.9E-02
Hspd1-ps4	3.892	1.5E-05		Nrp1	2.139	1.9E-03
Apba1	3.890	3.1E-08		Ms4a6c	2.135	6.3E-03
Gm13564	3.797	1.9E-06		Hopx	2.127	9.3E-03
Dntt	3.757	1.0E-10		Selm	2.126	7.9E-04
Hpgd	3.738	2.2E-10		Gm16299	2.117	3.0E-02
Ppfia4	3.737	1.7E-07		Myo7a	2.113	5.8E-05
Tifab	3.714	5.2E-09		Nxpe5	2.110	2.5E-03
Gm15503	3.700	4.1E-10		Hebp2	2.098	4.6E-02
Irf8	3.687	1.7E-11		Rab7b	2.098	9.3E-03
Cds1	3.645	2.4E-07		Gm17767	2.096	1.3E-02
Gm21857	3.615	8.4E-06		Dusp3	2.096	2.6E-05
Mx1	3.608	1.4E-06		Rapgefl1	2.092	4.1E-03
Myadml2os	3.587	3.1E-05		D830039M14Rik	2.090	1.7E-02
Arhgef37	3.584	1.2E-05		Gm15987	2.089	1.1E-03
Depdc7	3.560	1.5E-08		Coch	2.087	4.5E-02
Upk1b	3.534	4.6E-05		Psap	2.083	1.9E-03
Arsi	3.529	1.2E-05		Cxcl10	2.082	9.1E-03
Plxnb2	3.524	5.7E-09		Mag	2.081	7.6E-03
Ptpro	3.509	6.8E-06		Penk	2.077	2.9E-02
Afap1	3.493	7.0E-06		Ip6k3	2.075	1.9E-02
F13a1	3.479	3.6E-05		Ldhb	2.075	5.7E-04
Gpnmb	3.445	8.9E-05		Ccdc102a	2.072	1.6E-02
Cx3cr1	3.441	1.0E-06		Rgs9	2.069	3.4E-02
Pld4	3.418	2.2E-10		Car12	2.064	6.6E-03
Cysltr1	3.415	2.6E-06		Gm7609	2.063	1.2E-03
Nostrin	3.413	1.8E-08		Adap2	2.063	5.3E-03
AI607873	3.404	2.0E-05		Gm7582	2.061	1.8E-03
Tns4	3.402	6.8E-06		Phf11a	2.048	7.0E-03
Drc7	3.382	4.3E-13		Gm15515	2.046	3.1E-02
Notumos	3.376	2.7E-04		Vis1	2.046	4.4E-02
P2ry6	3.375	6.8E-06		Ptpn5	2.045	4.8E-02
Gm2635	3.374	1.3E-05		Klrb1f	2.043	1.0E-02
Ly86	3.354	5.9E-09		Gpr35	2.038	1.4E-02

Gene	FC	q-value		Gene	FC	q-value
Apcdd1	3.310	2.4E-05		Tfec	2.035	2.8E-02
Adam3	3.279	2.1E-04		Olfm1	2.033	1.7E-02
Nr0b2	3.275	1.5E-04		Raph1	2.030	7.5E-04
Myadml2	3.231	2.4E-05		Ctsc	2.029	5.5E-04
Mx2	3.215	2.2E-05		Fam105a	2.025	1.6E-03
Fam78b	3.207	1.6E-04		Nlrp1c-ps	2.020	1.6E-02
Kcnt1	3.162	1.4E-04		Gm4070	2.019	4.5E-03
Plekhh2	3.161	4.0E-05		Gm16602	2.016	2.0E-02
Nlrp1a	3.155	1.1E-05		Rnase2b	2.015	5.0E-02
Glis3	3.146	1.0E-04		Dusp22	2.013	1.0E-02
Atf3	3.145	8.2E-05		Mid1	2.013	3.6E-04
Ak8	3.145	6.2E-08		Clec4a3	2.006	2.1E-02
Rspo1	3.144	1.4E-05		Trim30c	1.988	2.9E-02
Pdzd4	3.143	6.6E-10		Pde8b	1.987	3.7E-03
Tlr9	3.115	4.1E-09		Tmem221	1.984	8.6E-03
Gm9581	3.101	2.9E-06		Mrc2	1.982	9.3E-03
Lmo1	3.084	1.2E-05		Mefv	1.982	1.4E-02
Gm5960	3.066	4.0E-04		Ugt1a7c	1.979	1.6E-02
Galnt9	3.064	3.4E-04		Cox4i2	1.978	1.9E-02
Nrg1	3.044	1.5E-04		Gria3	1.975	1.2E-03
Pyhin1	3.038	6.0E-06		Rasal2	1.971	3.8E-02
Phf11d	3.032	2.1E-05		Il6st	1.968	1.5E-02
Rnd3	3.032	1.9E-05		Oas1a	1.967	5.6E-03
Pkdcc	3.030	1.1E-04		Evpl	1.966	4.5E-02
Matn2	3.018	2.7E-05		6330403L08Rik	1.966	3.8E-02
Arhgef10l	3.011	1.1E-07		Frmd4b	1.962	1.3E-03
Mycl	3.008	9.5E-06		Tmem144	1.958	7.9E-03
Rassf4	3.007	1.1E-07		Dse	1.955	4.1E-03
Pcdh17	2.983	1.7E-03		1700026L06Rik	1.950	1.3E-03
Ifi30	2.981	5.7E-09		Tifa	1.936	3.9E-06
Slamf8	2.978	2.9E-06		Gm17518	1.936	3.1E-02
Slc4a8	2.974	7.3E-06		Dusp7	1.929	6.8E-04
Ier5l	2.935	2.6E-08		Prr5	1.920	4.2E-05
Gm13814	2.931	4.3E-04		Sdc3	1.919	9.1E-03
Aldh1b1	2.923	4.2E-05		Cd93	1.917	2.5E-03
C1galt1c1	2.922	9.8E-06		Tmem119	1.916	2.8E-02
Klk1b11	2.912	2.9E-03		Pdlim4	1.915	1.8E-03
4933424M12Rik	2.903	3.2E-05		Zeb2	1.914	2.0E-07
Rasa4	2.898	3.8E-11		Tmem173	1.909	1.6E-04
Siglech	2.896	1.3E-04		Il10ra	1.908	6.6E-05
Gm5431	2.893	1.8E-04		Gm3912	1.907	3.8E-02
4930455G09Rik	2.884	3.1E-04		Irf7	1.906	1.4E-02
Trio	2.883	3.7E-08		Spsb4	1.903	3.2E-03
Kmo	2.872	1.4E-09		Ctsz	1.903	3.3E-05
Phf11b	2.872	4.6E-05		Spr-ps1	1.903	1.0E-05
Ckb	2.867	5.9E-09		Zfp62	1.903	4.5E-13

Gene	FC	q-value		Gene	FC	q-value
Mnda	2.861	7.8E-04		Tlr7	1.900	1.4E-02
Adgre1	2.804	1.3E-05		Gm9920	1.896	7.9E-04
Itga1	2.801	1.1E-03		Gm12709	1.887	5.0E-02
Gm8093	2.796	1.1E-03		Ccdc152	1.886	4.1E-02
Ctss	2.782	1.7E-05		Cd68	1.879	3.6E-04
Trbv29	2.779	1.8E-03		Ablim2	1.872	2.2E-02
Pik3c2a	2.772	1.0E-06		Trem2	1.872	2.3E-02
Lpar5	2.766	6.0E-08		BC035044	1.864	5.4E-04
Xist	2.764	6.0E-06		Enc1	1.863	3.9E-03
Sema4c	2.764	2.3E-09		Mafb	1.859	1.4E-02
Zeb2os	2.763	2.9E-06		Chdh	1.859	1.9E-02
Ifi204	2.761	1.4E-03		Lpl	1.857	3.2E-02
Ms4a4c	2.757	2.7E-04		Ccdc109b	1.848	2.5E-02
Sdk1	2.751	5.5E-04		Mfap3l	1.834	5.0E-02
Mst1r	2.748	1.2E-04		Fam129b	1.834	6.4E-04
Fam49a	2.747	1.6E-18		NA	1.832	5.0E-02
Gdf9	2.745	3.6E-05		Gm29395	1.827	4.6E-02
Upb1	2.732	2.2E-10		Cacna1f	1.824	3.8E-02
Asgr2	2.725	1.3E-03		Ddr1	1.823	3.6E-02
Csf1r	2.724	2.4E-04		Ncr1	1.823	4.6E-02
Lifr	2.698	1.4E-03		Tspan17	1.820	8.3E-03
Cryba4	2.697	1.5E-04		Plekhg1	1.819	4.3E-02
Cdr2l	2.694	3.8E-04		Nrg4	1.815	4.4E-02
Rhbdl3	2.693	3.0E-05		Cd28	1.810	2.3E-02
Nucb2	2.687	1.5E-05		Ifit1	1.809	2.8E-02
Clec9a	2.686	1.9E-05		Trgv2	1.808	2.6E-02
Gm20431	2.684	6.3E-03		Grb10	1.805	4.4E-02
Gm12250	2.683	6.4E-05		Camk1d	1.804	1.7E-03
Gm10645	2.668	7.3E-04		2310040G24Rik	1.796	3.3E-05
Mpeg1	2.652	7.9E-04		Cyp39a1	1.795	2.0E-02
Serpinf1	2.650	2.4E-08		Ehd4	1.794	3.4E-06
Ceacam19	2.642	7.3E-04		Ptgr1	1.784	4.0E-02
Cyp2ab1	2.640	8.5E-04		Apof	1.784	2.0E-03
Shisa2	2.640	2.2E-03		Slc29a3	1.783	1.7E-04
Chit1	2.638	7.5E-03		Inpp5j	1.780	4.6E-02
Gm33142	2.637	3.4E-03		Ccdc154	1.779	5.0E-02
Tmem106a	2.625	8.4E-06		B4galt5	1.777	1.6E-03
Lrp1	2.625	9.3E-04		Cp	1.766	8.0E-03
Tctex1d1	2.616	6.8E-03		Sh3tc1	1.761	2.2E-02
Cd180	2.610	1.1E-09		Gamt	1.759	1.0E-04
Gm37820	2.609	1.0E-05		Lima1	1.758	3.4E-02
Gm18853	2.609	9.4E-05		Ednrb	1.755	3.7E-02
Itga8	2.602	1.5E-03		H2-DMa	1.749	6.1E-06
Gbp3	2.588	2.9E-06		Tnfsfm13	1.748	2.6E-02
AF067063	2.582	8.4E-03		C1ra	1.729	1.0E-02
Slfn5	2.560	8.9E-04		Siglec1	1.727	4.7E-02

Gene	FC	q-value		Gene	FC	q-value
Ptprf	2.558	3.5E-03		Snx24	1.720	4.6E-02
Cd300c	2.558	4.0E-04		Oasl1	1.720	2.3E-02
Slc2a5	2.552	1.0E-02		Gvin1	1.717	6.9E-03
Notum	2.533	1.3E-02		Tmem51	1.716	1.4E-02
S100a4	2.526	1.9E-03		Gm26822	1.716	2.3E-02
Gm7592	2.523	8.4E-04		Hmgb1-ps5	1.714	3.7E-02
Sh2d6	2.514	3.3E-03		Tlr12	1.710	1.1E-02
Ctsh	2.499	5.8E-05		Cd7	1.704	7.8E-03
Ticam2	2.496	6.8E-06		Cndp2	1.704	2.3E-05
Gm17944	2.492	8.9E-03		Wfs1	1.703	1.7E-03
Ripk4	2.482	1.4E-02		1110002J07Rik	1.698	3.4E-02
Gm15433	2.470	5.2E-05		Gm1123	1.693	2.1E-02
Cd300lg	2.463	3.4E-03		Unc93b1	1.692	5.4E-03
Disc1	2.461	7.0E-06		Bag3	1.687	8.6E-04
Gm13147	2.453	1.2E-03		Kifc3	1.680	6.1E-04
Zcchc24	2.451	1.9E-05		Clcn5	1.670	2.5E-04
Scpep1	2.443	2.1E-08		Sec24d	1.668	9.7E-04
Irf5	2.435	1.7E-04		Xxylt1	1.666	1.0E-09
Mmp28	2.433	4.6E-03		B3gnt8	1.662	1.0E-02
Stard9	2.427	2.8E-04		Rgs10	1.655	3.1E-10
AA414768	2.425	3.7E-04		Itgb3	1.654	1.7E-03
Cbs	2.424	1.9E-02		Plpp2	1.653	1.2E-03
2810047C21Rik1	2.422	1.9E-02		Nckipsd	1.652	1.8E-06
Cyp4f37	2.422	1.3E-02		Thbd	1.652	3.2E-02
Gm20482	2.412	4.1E-03		Nlrp1b	1.640	3.1E-02
Inppl1	2.411	2.3E-06		Kcnk6	1.640	1.4E-02
Mfsd7a	2.403	1.9E-04		Mmp19	1.639	3.3E-02
8430423G03Rik	2.401	1.6E-02		Rundc3b	1.639	2.2E-03
Dab2	2.397	5.5E-04		Bmf	1.635	4.7E-02
1700012B09Rik	2.392	5.3E-03		Pvrl4	1.635	9.5E-04
Hip1	2.388	1.2E-04		Trim66	1.624	3.2E-02
Gm13373	2.385	1.3E-02		Gm1966	1.620	2.8E-02
Csrp2	2.381	1.4E-03		Mef2c	1.618	1.2E-03
Ahnak	2.380	5.2E-05		Ass1	1.615	8.2E-03
Gm4955	2.377	8.1E-04		Tep1	1.615	4.9E-04
Arl14epl	2.376	1.4E-02		Plekha1	1.614	4.1E-03
Klf4	2.365	1.8E-03		Ahcyl2	1.614	7.3E-06
Gm26947	2.360	4.5E-04		Fkbp1b	1.612	1.3E-02
Tmprss4	2.357	1.8E-02		Slc7a7	1.612	1.5E-05
Cacna1d	2.352	1.7E-03		Guca1a	1.611	9.3E-03
Klri1	2.351	1.6E-02		Tmem109	1.608	3.2E-04
Gm12551	2.339	2.3E-02		Dbndd2	1.606	2.7E-02
Abcb1a	2.337	7.7E-05		Alpk1	1.604	5.4E-03
Rapgef4	2.337	1.4E-03		Cd48	1.604	7.4E-05
Ccr8	2.337	1.3E-02		Zbp1	1.597	4.1E-02
Six1	2.337	2.6E-02		Fam20c	1.593	4.8E-02

Gene	FC	q-value		Gene	FC	q-value
F10	2.333	4.2E-03		Asah1	1.592	9.0E-03
Gtsf1	2.330	1.5E-04		Tmem243	1.591	1.4E-03
Tlr11	2.326	2.1E-02		Clmp	1.588	3.2E-02
Hs3st3b1	2.318	7.3E-04		Cd160	1.584	2.5E-02
Plekho1	2.314	7.6E-07		Ctsa	1.584	3.0E-05
Capn9	2.313	2.5E-02		Cdk5rap1	1.581	3.4E-07
Capn13	2.304	2.4E-02		Pou2f2	1.578	7.9E-05
Tnfsf12	2.295	2.8E-05		Zc3h12d	1.576	1.1E-03
F7	2.293	1.0E-02		Satb2	1.568	1.9E-02
Gm28527	2.292	2.3E-02		Fam102b	1.566	1.5E-03
Arl5c	2.289	3.9E-05		Adam15	1.562	2.9E-02
Bpi	2.286	3.5E-03		Layn	1.561	2.5E-02
Nap1l2	2.283	3.0E-02		Lamp1	1.561	7.6E-04
D430040D24Rik	2.281	5.7E-03		Mdfic	1.560	3.9E-04
Plekhh3	2.279	3.4E-03		Tnfrsf13b	1.559	6.5E-04
Plekhm3	2.275	6.8E-09		Gbp2b	1.559	4.2E-02
Tmem171	2.265	1.7E-02		Gm12896	1.556	4.8E-05
Trex1	2.256	2.6E-06		Pkib	1.548	1.0E-02
Ldlrad3	2.248	2.9E-03		Slc36a1	1.546	2.9E-03
Ldlrad4	2.247	8.5E-05		Bst2	1.542	6.5E-03
Ccr2	2.234	1.4E-03		Plxdc1	1.540	3.2E-02
Pydc4	2.224	5.7E-03		Jup	1.529	2.5E-02
Atrnl1	2.223	1.1E-02		Klhl41	1.528	5.3E-03
Gm7281	2.220	3.0E-02		Trafd1	1.527	2.8E-04
Aox2	2.217	9.2E-03		Sh2d1b1	1.526	2.3E-02
Capn2	2.216	1.8E-05		Ly9	1.524	1.9E-03
Cfb	2.214	9.2E-03		9930111J21Rik1	1.524	3.5E-02
Ifi27l2a	2.210	1.8E-02		Lair1	1.522	2.4E-02
Ifit3	2.210	1.4E-02		Gpr18	1.519	1.8E-02
Bmp8a	2.202	3.4E-02		Otogl	1.519	2.1E-02
Crybg3	2.200	3.5E-05		Scarb1	1.514	7.1E-09
Met	2.197	1.4E-02		Fam234a	1.510	3.9E-02
Trim36	2.196	2.4E-05		Slfn8	1.510	1.3E-02
Rwdd2a	2.195	1.5E-05		Slc12a9	1.502	3.1E-03
Ctnnd2	2.191	1.1E-02				

Table 6.15 3w vs >52w-AML, up in >52w

Gene	FC	q-value		Gene	FC	q-value
Eif2s3y	-9.490	5.0E-94		Dkk3	-2.296	1.7E-02
Ddx3y	-8.747	3.2E-96		Cpt1c	-2.292	1.8E-02
BC018473	-7.048	6.2E-27		Sh3tc2	-2.290	1.5E-02
Rims2	-6.805	2.5E-34		Spon2	-2.288	2.3E-02
Mab21l2	-6.617	2.2E-20		Fgf11	-2.276	7.2E-03
Adcyap1r1	-6.465	1.7E-16		1300017J02Rik	-2.275	1.5E-02
Slc4a10	-6.379	1.2E-17		Nuak1	-2.262	2.5E-04
Eya4	-6.185	4.9E-17		Cd55	-2.259	3.1E-03
St6galnac1	-5.996	2.2E-20		Tulp3	-2.257	5.9E-03
Pik3c2g	-5.966	6.0E-15		Aldh1a1	-2.255	1.5E-02
Gm11735	-5.719	7.5E-16		Slc26a1	-2.254	6.5E-03
Uty	-5.543	5.6E-56		Gm3488	-2.252	3.4E-02
Ncam2	-5.437	4.9E-15		Lama5	-2.252	3.0E-02
Neo1	-5.295	2.0E-18		Gm6634	-2.250	2.2E-02
Cpvl	-5.214	4.1E-10		Fgfrl1	-2.249	5.7E-03
Pgm5	-4.859	8.4E-11		C530008M17Rik	-2.247	7.5E-03
Prkg1	-4.840	2.8E-12		Ank1	-2.242	1.5E-02
Jsrp1	-4.810	1.4E-09		Gramd1c	-2.241	1.5E-03
Ramp2	-4.571	4.3E-10		Gm15707	-2.235	5.1E-05
Chga	-4.533	1.1E-07		Apol8	-2.234	1.5E-02
Gm29650	-4.401	2.1E-08		Ccnjl	-2.234	3.1E-02
Msrb3	-4.350	2.3E-11		Akr1c12	-2.231	7.6E-04
Olfr248	-4.348	4.3E-07		Gm29669	-2.224	9.9E-03
Rec8	-4.303	1.3E-07		Soat2	-2.222	1.1E-03
Zfp57	-4.273	6.6E-08		4931431F19Rik	-2.221	1.9E-02
Tmem252	-4.267	1.4E-08		Cd79a	-2.218	2.5E-03
Pcdh7	-4.267	3.6E-08		Sptb	-2.212	1.7E-02
Sema3a	-4.239	6.8E-07		Gm26669	-2.210	7.5E-03
Defb40	-4.184	1.4E-07		Igkv4-80	-2.210	2.6E-02
B230118H07Rik	-4.178	1.2E-08		Sorbs3	-2.209	3.3E-03
Pde3b	-4.132	2.1E-17		Auts2	-2.207	1.1E-02
Mycn	-4.062	1.8E-09		Snap47	-2.206	9.8E-05
Hnmt	-4.003	2.2E-08		Gm28857	-2.205	1.8E-02
Arrdc4	-3.983	1.5E-13		Fzd1	-2.204	9.6E-03
Zan	-3.950	3.9E-06		Igkv3-9	-2.202	3.9E-02
Atp8b5	-3.949	1.5E-08		Nkd1	-2.202	3.1E-02
Myct1	-3.882	1.4E-07		Cenpv	-2.201	7.7E-05
Mpp4	-3.819	4.1E-06		Car1	-2.200	3.1E-02
Mmp14	-3.796	3.5E-07		Angpt1	-2.197	1.1E-02
Cr2	-3.782	2.9E-09		Ighv1-72	-2.196	1.8E-02
Plg	-3.779	3.9E-05		Ighd	-2.193	2.0E-05
Gpha2	-3.749	4.5E-05		BC016579	-2.191	4.1E-02
Rab40b	-3.720	3.6E-05		Hes1	-2.178	3.0E-03
Arhgef25	-3.714	6.0E-06		Ccdc39	-2.175	2.2E-02
Ctf1	-3.711	5.3E-05		Add2	-2.175	2.4E-02

Gene	FC	q-value		Gene	FC	q-value
9330132A10Rik	-3.688	3.0E-05		Ndrg2	-2.174	9.8E-03
Cib3	-3.688	1.9E-05		Tet1	-2.171	5.3E-03
Spin4	-3.683	2.3E-06		Ccdc8	-2.166	9.3E-04
Ybx2	-3.571	5.8E-05		5730460C07Rik	-2.163	1.8E-02
Rcvrn	-3.561	4.8E-05		Pla2g4c	-2.162	8.2E-03
Htr1b	-3.517	1.9E-05		Xrcc5	-2.162	7.8E-03
Frmpd4	-3.476	1.8E-04		Mboat4	-2.161	3.1E-04
Scin	-3.470	7.4E-05		Tmem120b	-2.160	8.2E-03
Map9	-3.464	1.0E-05		Ppm1l	-2.159	4.4E-04
Csrp3	-3.462	1.7E-04		Odf3b	-2.157	3.0E-02
Patl2	-3.458	7.0E-05		Gm11879	-2.156	1.8E-03
Gsta4	-3.443	4.3E-06		Ccdc74a	-2.156	1.8E-02
Slc30a10	-3.410	5.8E-05		Gm16325	-2.151	3.1E-02
1110032F04Rik	-3.396	1.7E-04		Gm2830	-2.147	1.4E-02
1700017G19Rik	-3.393	1.3E-04		Gm867	-2.146	2.7E-02
Calml4	-3.389	1.1E-05		Ebf1	-2.145	2.1E-03
Cox6b2	-3.384	9.0E-05		4930412C18Rik	-2.144	8.9E-03
Shank3	-3.350	1.3E-04		Gm3696	-2.142	3.8E-02
D430036J16Rik	-3.349	3.8E-04		Sorl1	-2.142	2.2E-02
Arhgef40	-3.346	2.7E-07		Gm8989	-2.141	4.5E-02
BC051537	-3.340	1.7E-04		Cecr2	-2.140	1.0E-02
C77080	-3.331	1.1E-08		Hcn3	-2.137	6.9E-04
Zfp521	-3.328	4.3E-04		Rnf39	-2.137	2.3E-02
Sphk1	-3.325	7.2E-05		Hba-a1	-2.136	2.5E-02
Cacna2d3	-3.320	2.4E-04		Chrnb1	-2.133	1.5E-03
Lama3	-3.318	2.5E-04		Mcam	-2.133	2.2E-02
Samd13	-3.317	1.8E-05		Gpr27	-2.132	2.3E-02
Dmwd	-3.316	1.8E-05		Igkv5-48	-2.132	1.5E-02
Kdm5d	-3.264	2.9E-35		Pkd1l1	-2.130	4.5E-02
Gpc4	-3.233	6.5E-04		Acmsd	-2.129	1.1E-02
Sema3e	-3.228	5.1E-09		Trim47	-2.129	2.0E-02
Shroom4	-3.222	3.6E-06		Slc6a20a	-2.128	4.5E-02
Tfr2	-3.215	8.4E-05		Ccdc79	-2.123	3.4E-02
Phyhip	-3.213	1.6E-04		Dock7	-2.122	2.3E-07
1700048O20Rik	-3.201	1.9E-08		1700029J07Rik	-2.121	1.4E-02
Igkv15-103	-3.192	3.4E-04		Gfap	-2.119	3.9E-02
Bfsp2	-3.178	1.4E-05		Meiob	-2.118	4.6E-02
Med12l	-3.171	1.3E-06		Col14a1	-2.116	3.2E-02
Tmem108	-3.168	1.5E-04		Zfp711	-2.115	4.6E-02
Cyp11a1	-3.166	2.2E-04		0610043K17Rik	-2.114	3.2E-02
Gm37192	-3.137	4.4E-04		St6galnac2	-2.114	4.5E-02
Lrrc23	-3.137	6.5E-04		Acyp2	-2.113	4.4E-02
5830418P13Rik	-3.131	3.6E-04		Trim10	-2.104	2.9E-02
Ppp4r4	-3.126	1.1E-03		Epb42	-2.101	2.6E-02
Vill	-3.117	4.6E-04		Zbed5	-2.097	1.3E-02
Gm37915	-3.113	3.1E-06		B3gnt7	-2.097	7.9E-03

Gene	FC	q-value		Gene	FC	q-value
Eya2	-3.103	5.1E-05		Clec2f	-2.095	8.8E-03
Ighv1-9	-3.102	3.4E-11		BC021767	-2.091	3.3E-02
1700020N18Rik	-3.100	1.1E-03		Alox15	-2.091	4.0E-02
Gm973	-3.091	1.4E-03		Maged1	-2.091	5.2E-03
Kcnc1	-3.057	1.4E-03		Klhdc8b	-2.088	1.7E-03
Tnip3	-3.054	9.5E-05		Dhcr24	-2.087	2.7E-04
Epor	-3.054	1.6E-04		Faah	-2.083	1.0E-04
Gng11	-3.044	4.5E-11		Gm15816	-2.080	4.5E-02
Tfpi2	-3.025	1.6E-03		Synm	-2.079	4.7E-02
Galm	-3.009	3.2E-07		Gm3383	-2.079	9.1E-03
Rassf10	-3.007	1.9E-03		NA	-2.079	5.9E-03
2410021H03Rik	-2.999	1.2E-03		Hyal3	-2.076	3.1E-03
Gata2	-2.998	4.9E-04		Afp	-2.073	1.8E-03
Cldn12	-2.996	2.3E-07		Cxx1c	-2.072	5.4E-03
Adam11	-2.989	6.1E-06		Wfikkn2	-2.069	3.8E-02
2700046G09Rik	-2.937	1.6E-03		Tmem45a2	-2.066	3.6E-02
2900052L18Rik	-2.933	1.1E-03		Phka1	-2.065	1.7E-02
Sox6	-2.928	9.6E-04		Sptbn4	-2.056	1.6E-07
Btbd3	-2.926	3.9E-04		Cachd1	-2.055	5.7E-03
Gm16252	-2.913	3.1E-03		Hist3h2ba	-2.054	8.9E-03
Spire1	-2.910	7.3E-04		2610307P16Rik	-2.050	3.5E-02
Krba1	-2.904	2.0E-04		Ighv5-4	-2.047	1.7E-02
Pdia2	-2.899	1.4E-03		Gm25193	-2.046	4.8E-02
Clec11a	-2.895	4.6E-04		Fam234b	-2.045	8.3E-04
Galnt3	-2.894	2.0E-08		Armc9	-2.041	7.3E-04
Nxf7	-2.891	1.7E-03		Arxes2	-2.040	2.4E-02
Shroom1	-2.890	6.6E-04		Adgrl1	-2.040	4.0E-03
Tmem121	-2.889	8.7E-04		Slc2a4	-2.039	4.6E-02
Smim1	-2.882	1.0E-03		Reep6	-2.038	3.2E-02
Cxx1a	-2.879	7.8E-06		Zscan18	-2.033	2.3E-02
Il4	-2.879	1.4E-04		Prg2	-2.030	3.3E-02
Entpd3	-2.867	2.5E-03		Hmgb3	-2.028	4.7E-03
Actn2	-2.866	2.2E-05		Nxpe2	-2.026	2.6E-02
Ms4a2	-2.863	2.5E-03		Gprasp2	-2.026	2.9E-02
Arntl2	-2.850	5.8E-04		4930556M19Rik	-2.021	1.0E-02
Gstm5	-2.850	1.3E-03		AB041806	-2.020	4.6E-02
Klf1	-2.845	7.6E-04		Bcl11a	-2.020	1.1E-02
Zfp2	-2.843	4.0E-04		Mapk12	-2.019	1.5E-04
Hemgn	-2.839	2.5E-04		Rab3il1	-2.015	2.0E-02
Mboat2	-2.838	2.4E-03		Rcn3	-2.012	5.6E-03
Atp8b1	-2.838	1.3E-04		March3	-2.012	1.7E-02
Ccdc120	-2.836	2.5E-03		Pla2g7	-2.008	4.5E-02
Tal1	-2.823	8.3E-04		Zfp820	-2.005	2.9E-02
Car2	-2.822	7.9E-04		Cgn	-2.005	2.9E-02
Glb1l2	-2.822	3.8E-03		Gm37151	-2.002	1.2E-02
Ighv1-5	-2.817	1.2E-03		Arvcf	-2.002	4.2E-03

Gene	FC	q-value		Gene	FC	q-value
Adgrg6	-2.810	7.3E-04		Gm29560	-2.001	3.6E-02
Mcf2	-2.806	4.8E-03		Eid2	-1.999	4.5E-02
Sept8	-2.805	1.1E-03		Nhlrc4	-1.998	4.7E-02
Gpr34	-2.805	1.0E-03		Il1rl1	-1.997	1.1E-02
Cd200r3	-2.801	1.7E-03		Magi3	-1.993	1.6E-05
Abat	-2.800	1.6E-04		Grm1	-1.993	1.5E-03
Rab4a	-2.799	6.8E-04		Muc20	-1.986	4.4E-02
Tspo2	-2.797	5.8E-04		Mir8116	-1.981	4.3E-02
Gm37527	-2.796	5.4E-04		C030037D09Rik	-1.981	3.4E-02
Gata1	-2.792	1.2E-03		Ctse	-1.980	2.4E-02
A730089K16Rik	-2.791	1.3E-03		Vopp1	-1.979	1.6E-02
Crip2	-2.789	9.5E-04		Zfpm1	-1.979	1.7E-02
Epdr1	-2.788	1.3E-03		Gm15657	-1.977	3.4E-02
Pnck	-2.777	3.4E-03		Tmem9	-1.976	8.5E-03
Cited4	-2.776	4.7E-04		Rnd2	-1.976	9.2E-03
Epb41l1	-2.775	9.9E-05		Pla2g12a	-1.975	2.2E-02
Mmp15	-2.756	7.1E-04		Actn3	-1.975	1.9E-02
Ermap	-2.754	1.5E-03		Gp5	-1.973	3.8E-02
Gfi1b	-2.752	1.1E-03		Rbpms	-1.971	3.4E-08
A930038B10Rik	-2.744	3.8E-04		Nipa1	-1.970	1.4E-02
E130309D14Rik	-2.742	3.6E-03		Gm15856	-1.967	2.1E-04
Slc22a3	-2.741	6.2E-03		Gm10913	-1.966	3.9E-02
Gm16617	-2.741	5.6E-03		1700061G19Rik	-1.966	1.3E-04
Il6	-2.739	3.0E-03		Gpsm2	-1.961	3.3E-03
Gm17641	-2.736	6.1E-03		Rbm11	-1.958	1.8E-03
Hoxb6	-2.732	1.5E-05		Klk8	-1.957	8.3E-03
Icam4	-2.728	4.6E-04		Tie1	-1.953	3.0E-03
Pdzk1ip1	-2.724	2.3E-03		Scarf1	-1.947	3.1E-03
Gm29050	-2.724	3.7E-03		Nudt12	-1.946	1.8E-02
2010109A12Rik	-2.719	1.4E-03		2010204K13Rik	-1.941	5.0E-02
Adcy6	-2.717	1.3E-03		Catsperd	-1.940	4.5E-02
Hpn	-2.711	2.6E-03		Wdr60	-1.939	1.1E-02
Perp	-2.697	1.5E-03		C030014I23Rik	-1.938	1.8E-02
Adgra3	-2.697	1.2E-03		Gm27896	-1.936	1.9E-02
Mtap7d3	-2.687	5.1E-03		Ak1	-1.936	1.0E-02
Kif7	-2.684	1.5E-03		Gm5577	-1.936	4.8E-03
Scd1	-2.684	4.2E-03		Amigo2	-1.932	2.7E-02
Abcg4	-2.684	1.9E-03		9130008F23Rik	-1.931	6.9E-03
Spns2	-2.676	4.1E-04		Igf1os	-1.931	1.3E-02
Armcx1	-2.661	1.9E-04		E130102H24Rik	-1.927	1.0E-05
Enkur	-2.656	2.8E-04		Stxbp1	-1.926	2.1E-02
Clstn3	-2.655	1.9E-04		Tert	-1.924	1.6E-02
1110028F11Rik	-2.652	2.2E-03		Tbx2	-1.920	3.1E-02
Slc38a5	-2.651	3.0E-03		Gm3194	-1.919	3.6E-02
4933406I18Rik	-2.644	3.4E-03		Hipk4	-1.919	3.8E-02
Pkhd1l1	-2.635	4.0E-03		Gm37397	-1.913	5.7E-03

Gene	FC	q-value		Gene	FC	q-value
4933431E20Rik	-2.635	2.7E-03		Prkca	-1.911	1.9E-02
Zfhx4	-2.631	8.3E-03		E130215H24Rik	-1.908	2.0E-02
Aknad1	-2.629	1.5E-03		Cpox	-1.905	1.4E-02
Abcb4	-2.621	1.7E-03		Ddx25	-1.902	4.3E-02
Hnf4a	-2.621	6.2E-03		Rassf6	-1.900	3.6E-02
Snx31	-2.621	3.4E-03		Zfp867	-1.899	1.3E-03
E330017A01Rik	-2.616	5.2E-03		Gm26513	-1.899	1.9E-02
Gm3512	-2.616	5.1E-03		Gm14703	-1.897	3.0E-02
Thsd1	-2.613	8.6E-04		Mgst3	-1.888	1.2E-02
Sdsl	-2.609	3.0E-03		Nrip1	-1.882	9.2E-03
Cntd1	-2.607	5.9E-06		A330023F24Rik	-1.881	7.5E-03
Ighv1-4	-2.592	6.7E-03		Igkv8-30	-1.878	3.8E-02
Cacnb2	-2.592	1.6E-05		Cerkl	-1.874	4.8E-02
Dkkl1	-2.590	1.9E-03		Mt2	-1.868	3.6E-02
Gm11992	-2.586	1.9E-04		Gna14	-1.867	4.6E-02
Tmem56	-2.582	6.3E-03		Stard10	-1.861	2.2E-02
Aqp1	-2.582	2.5E-03		Phldb2	-1.859	3.3E-02
Zfp354c	-2.573	5.2E-04		Epb41l4b	-1.857	2.8E-02
Procr	-2.573	5.5E-04		H2-Oa	-1.854	1.2E-03
Gm15674	-2.563	4.3E-03		Msi2	-1.852	1.9E-02
Dmpk	-2.563	1.9E-03		Aqp11	-1.850	3.1E-02
Platr27	-2.562	7.2E-03		St3gal5	-1.845	3.4E-03
Cuedc1	-2.560	1.2E-03		Tmem151b	-1.844	3.3E-02
Sec14l2	-2.557	3.6E-03		NA	-1.841	1.1E-02
Btnl10	-2.549	3.7E-03		Etl4	-1.836	3.8E-02
Rnf217	-2.546	8.9E-03		Gm29017	-1.830	3.8E-02
Meis1	-2.545	4.1E-03		Nynrin	-1.827	7.4E-03
Rhd	-2.544	2.7E-03		Blvrb	-1.827	2.6E-02
Paqr9	-2.540	5.3E-03		Arl4a	-1.825	1.5E-02
Slc22a23	-2.539	3.6E-03		Bcar3	-1.819	2.2E-03
Fbn1	-2.538	7.3E-06		Gm26756	-1.813	4.6E-02
Slc36a4	-2.528	7.3E-04		Gm19569	-1.813	4.6E-02
Cdkl1	-2.527	5.3E-03		Zfp93	-1.811	5.7E-03
Cldn13	-2.526	5.2E-03		Erc1	-1.811	9.0E-03
Selp	-2.522	4.0E-03		Zfp248	-1.811	1.7E-02
Rhag	-2.517	4.8E-03		Spatc1	-1.805	1.5E-02
Pklr	-2.516	6.4E-03		Slc14a1	-1.804	2.1E-02
2310069B03Rik	-2.513	1.4E-02		Smim10l2a	-1.804	2.0E-02
Tspan33	-2.512	3.4E-03		Hmbs	-1.803	1.8E-02
Flywch2	-2.512	2.8E-04		Galnt6	-1.797	2.2E-02
Gm11767	-2.508	1.1E-02		Igkv5-39	-1.796	3.9E-02
Ttc39a	-2.508	8.0E-03		Zfp30	-1.793	3.7E-03
Cxx1b	-2.504	2.3E-04		Alad	-1.792	2.0E-02
Hsd11b2	-2.500	5.0E-03		Acss2	-1.791	7.6E-04
Gm15491	-2.499	1.9E-03		Rbp1	-1.791	2.1E-02
Ifitm1	-2.498	3.3E-03		Ighv6-3	-1.791	2.3E-03

Gene	FC	q-value		Gene	FC	q-value
Farp1	-2.496	7.5E-03		Poln	-1.787	2.7E-02
Mfsd2b	-2.495	4.1E-03		Golm1	-1.786	1.9E-02
Ctla2a	-2.492	3.5E-04		Hist1h2br	-1.786	2.0E-03
Adamdec1	-2.492	1.5E-02		Nfia	-1.786	2.8E-02
Tmem184a	-2.486	8.0E-03		Fsd1l	-1.785	1.9E-02
B930095G15Rik	-2.484	1.0E-02		Aqp9	-1.781	2.6E-02
Gja5	-2.479	1.5E-02		Nrgn	-1.781	3.1E-02
Dapk1	-2.475	9.8E-05		Chchd10	-1.779	1.2E-02
2210408I21Rik	-2.475	2.0E-03		Traf4	-1.778	2.1E-02
Lmna	-2.473	3.0E-03		Abca1	-1.776	1.9E-04
Hrh4	-2.473	1.6E-02		1300002E11Rik	-1.776	2.0E-02
6030468B19Rik	-2.470	4.8E-03		Optn	-1.775	2.3E-02
Arx	-2.470	8.1E-03		Nedd4	-1.763	1.4E-02
Zg16	-2.466	1.7E-02		Hdac9	-1.761	2.8E-02
D930020B18Rik	-2.464	4.5E-03		Igkv4-59	-1.758	1.4E-02
Ces2g	-2.462	7.1E-03		Gm27177	-1.752	1.1E-02
Clcn2	-2.461	5.5E-05		Gm38224	-1.750	3.6E-02
Atp1b2	-2.459	6.9E-03		Stau2	-1.747	3.4E-02
Dpf3	-2.456	3.7E-03		Kif3a	-1.740	3.2E-03
Gm13842	-2.455	1.1E-02		Pdcd1lg2	-1.739	5.9E-03
Agmat	-2.453	1.3E-02		Mrap	-1.732	4.8E-03
1500009L16Rik	-2.453	4.6E-03		Zfp941	-1.731	4.5E-02
Samd14	-2.451	5.7E-03		Dyrk3	-1.729	1.3E-02
Tek	-2.450	5.7E-03		Gdpd1	-1.728	4.3E-02
Mylk3	-2.444	7.5E-03		Gm5111	-1.727	3.9E-02
Cnga1	-2.444	1.0E-02		Fads2	-1.723	3.4E-02
Gm12649	-2.444	1.2E-02		Sh3yl1	-1.721	1.1E-02
Hoxd3os1	-2.441	1.8E-02		Kcnip4	-1.720	3.1E-02
Dmtn	-2.438	6.3E-03		Prr36	-1.719	7.4E-04
Samd11	-2.433	5.0E-03		Zfp580	-1.718	1.9E-02
Otub2	-2.432	2.0E-03		Bpgm	-1.716	2.1E-02
4930426D05Rik	-2.431	1.4E-02		C530050E15Rik	-1.711	6.4E-05
Gm14198	-2.423	1.1E-02		Gm38102	-1.688	2.7E-02
Cdh1	-2.422	1.2E-02		Clcf1	-1.685	1.2E-04
Arhgap6	-2.421	1.1E-03		Gm14286	-1.684	2.6E-03
Cpa2	-2.419	8.5E-03		Bmpr2	-1.680	1.5E-03
Gm14490	-2.408	1.0E-02		Gpr155	-1.679	4.5E-03
Syde2	-2.405	6.7E-03		Dab2ip	-1.676	1.2E-04
Hebp1	-2.405	1.8E-02		Slc7a8	-1.672	1.5E-04
Art4	-2.404	7.4E-03		Rgs12	-1.669	6.0E-03
Tspan15	-2.401	1.3E-04		Mns1	-1.668	2.9E-02
Slc43a1	-2.399	2.6E-03		1700086O06Rik	-1.666	4.4E-02
Asb17os	-2.399	1.4E-02		Aldh7a1	-1.659	5.8E-03
Muc13	-2.398	2.3E-03		Ubac1	-1.659	2.4E-02
Kel	-2.396	8.7E-03		Lypd6b	-1.656	3.8E-02
Ighv1-19	-2.393	3.5E-03		Apoe	-1.651	3.3E-02

Gm15697	-2.390	1.8E-02		Gm14340	-1.650	1.6E-05
Gm11770	-2.388	1.9E-02		Fap	-1.640	1.1E-02
Zc2hc1a	-2.386	1.1E-03		Il18r1	-1.639	1.5E-03
Popdc2	-2.376	5.5E-03		Csf1	-1.637	3.7E-02
Spta1	-2.374	1.0E-02		Pfkm	-1.635	5.3E-03
D330045A20Rik	-2.371	1.0E-02		Rasgef1b	-1.634	2.4E-02
Begain	-2.367	1.9E-02		Cyth3	-1.634	4.9E-02
C1qtnf4	-2.367	1.5E-02		Vsig10	-1.633	1.2E-02
Atp7b	-2.366	9.2E-03		Vamp5	-1.626	3.3E-02
AI427809	-2.366	7.5E-03		Hmgn1	-1.626	9.1E-03
Lrrc34	-2.364	2.2E-02		A230050P20Rik	-1.619	1.8E-02
Prss28	-2.362	2.3E-02		Vwa7	-1.614	5.2E-03
Cadm1	-2.359	1.8E-02		Gm28187	-1.607	2.2E-03
Gnb4	-2.357	1.4E-02		Uros	-1.607	2.9E-02
Ccdc27	-2.356	2.0E-02		Gm10286	-1.606	1.4E-02
Gypa	-2.355	1.1E-02		Tmem64	-1.606	2.8E-02
Eno2	-2.351	3.3E-05		Vcam1	-1.604	4.5E-02
Notch3	-2.351	1.5E-04		Nefh	-1.603	4.8E-02
2810410L24Rik	-2.346	7.0E-05		Exoc3l2	-1.590	1.5E-02
NA	-2.340	1.5E-02		1700012L04Rik	-1.587	2.9E-02
Stap2	-2.340	3.9E-03		Mtfp1	-1.586	4.2E-02
Ache	-2.338	7.0E-03		Gimap1	-1.583	5.7E-03
Foxh1	-2.337	2.3E-02		Lat	-1.576	2.9E-02
1700063H04Rik	-2.330	2.3E-02		2700081O15Rik	-1.576	3.1E-02
Mpl	-2.327	2.9E-03		Stab2	-1.576	1.5E-02
C2cd4b	-2.326	9.6E-03		Kcnn4	-1.575	1.3E-02
Lpar4	-2.323	1.1E-02		Heg1	-1.573	2.9E-02
Adgrg1	-2.321	4.5E-03		Rapgef3	-1.560	2.3E-02
Hgfac	-2.321	1.4E-05		Btnl9	-1.554	7.4E-05
Ighv1-31	-2.318	2.5E-02		Slc22a18	-1.554	3.5E-02
Mex3a	-2.318	5.2E-03		Ccdc88a	-1.549	1.7E-02
Rnf212	-2.317	1.7E-02		Vmn1r-ps128	-1.549	2.9E-02
Ccdc149	-2.316	1.4E-02		Fam210b	-1.547	4.5E-02
Plpp1	-2.314	1.1E-02		Chst3	-1.544	5.0E-02
Mdfi	-2.311	3.4E-03		Slc25a23	-1.544	2.2E-02
Acot6	-2.310	1.4E-04		Ggact	-1.544	2.1E-02
Pxdc1	-2.310	3.6E-03		Fn3krp	-1.540	2.8E-02
Fer	-2.306	1.0E-02		A230056P14Rik	-1.536	1.8E-02
Olfr414	-2.306	2.7E-02		Gm38142	-1.529	1.9E-02
S1pr1	-2.302	1.4E-03		Gm15706	-1.518	1.5E-03
Dpys	-2.301	2.7E-02		Ccdc40	-1.517	8.9E-03
Plekha5	-2.301	1.7E-03		Tcp11	-1.515	4.5E-02
Gm36948	-2.300	3.8E-03		C920006O11Rik	-1.514	2.6E-02
Ighv14-3	-2.300	5.5E-03		Tmem176b	-1.509	6.9E-03
Thsd7b	-2.297	3.6E-04		NA	-1.507	2.3E-02
Snx22	-2.297	9.1E-04		Msantd1	-1.505	8.8E-03
Igkv6-15	-2.297	2.4E-04		Ptdss2	-1.504	3.7E-02

Publications

List of publications:

“Insights into cell ontogeny, age, and acute myeloid leukemia”
S. Chaudhury, J. K. Morison, B. E. Gibson, K. Keeshan
Experimental Hematology. 2015 Sep;43(9):745-55.
DOI: 10.1016/j.exphem.2015.05.008

“Co-operative leukemogenesis in acute myeloid leukemia and acute promyelocytic leukemia reveals C/EBPalpha as a common target of TRIB1 and PML/RARA”
K. Keeshan, P. Vieugue, S. Chaudhury,L. Rishi, C. Gaillard, L. Liang, E. Garcia, T. Nakamura, N. Omidvar, S. C. Kogan
Haematologica. 2016 Oct;101(10):1228-1236.
DOI: 10.3324/haematol.2015.138503

References

ADAMS, G. B., CHABNER, K. T., ALLEY, I. R., OLSON, D. P., SZCZEPIORKOWSKI, Z. M., POZNANSKY, M. C., KOS, C. H., POLLAK, M. R., BROWN, E. M. & SCADDEN, D. T. 2006. Stem cell engraftment at the endosteal niche is specified by the calcium-sensing receptor. *Nature,* 439**,** 599-603.

ADOLFSSON, J., MANSSON, R., BUZA-VIDAS, N., HULTQUIST, A., LIUBA, K., JENSEN, C. T., BRYDER, D., YANG, L., BORGE, O. J., THOREN, L. A., ANDERSON, K., SITNICKA, E., SASAKI, Y., SIGVARDSSON, M. & JACOBSEN, S. E. 2005. Identification of Flt3+ lympho-myeloid stem cells lacking erythro-megakaryocytic potential a revised road map for adult blood lineage commitment. *Cell,* 121**,** 295-306.

AHMED, M., STERNBERG, A., HALL, G., THOMAS, A., SMITH, O., O'MARCAIGH, A., WYNN, R., STEVENS, R., ADDISON, M., KING, D., STEWART, B., GIBSON, B., ROBERTS, I. & VYAS, P. 2004. Natural history of GATA1 mutations in Down syndrome. *Blood,* 103**,** 2480-9.

AKASHI, K., TRAVER, D., MIYAMOTO, T. & WEISSMAN, I. L. 2000. A clonogenic common myeloid progenitor that gives rise to all myeloid lineages. *Nature,* 404**,** 193-7.

AL-KASIM, F., DOYLE, J. J., MASSEY, G. V., WEINSTEIN, H. J., ZIPURSKY, A. & PEDIATRIC ONCOLOGY, G. 2002. Incidence and treatment of potentially lethal diseases in transient leukemia of Down syndrome: Pediatric Oncology Group Study. *J Pediatr Hematol Oncol,* 24**,** 9-13.

ALLSOPP, R. C., MORIN, G. B., DEPINHO, R., HARLEY, C. B. & WEISSMAN, I. L. 2003. Telomerase is required to slow telomere shortening and extend replicative lifespan of HSCs during serial transplantation. *Blood,* 102**,** 517-20.

AMORIM, S., STATHIS, A., GLEESON, M., IYENGAR, S., MAGAROTTO, V., LELEU, X., MORSCHHAUSER, F., KARLIN, L., BROUSSAIS, F., REZAI, K., HERAIT, P., KAHATT, C., LOKIEC, F., SALLES, G., FACON, T., PALUMBO, A., CUNNINGHAM, D., ZUCCA, E. & THIEBLEMONT, C. 2016. Bromodomain inhibitor OTX015 in patients with lymphoma or multiple myeloma: a dose-escalation, open-label, pharmacokinetic, phase 1 study. *Lancet Haematol,* 3**,** e196-204.

ANDREEFF, M., RUVOLO, V., GADGIL, S., ZENG, C., COOMBES, K., CHEN, W., KORNBLAU, S., BARON, A. E. & DRABKIN, H. A. 2008. HOX expression patterns identify a common signature for favorable AML. *Leukemia,* 22**,** 2041-7.

ANTONCHUK, J., SAUVAGEAU, G. & HUMPHRIES, R. K. 2002. HOXB4-induced expansion of adult hematopoietic stem cells ex vivo. *Cell,* 109**,** 39-45.

ARAI, F., HIRAO, A., OHMURA, M., SATO, H., MATSUOKA, S., TAKUBO, K., ITO, K., KOH, G. Y. & SUDA, T. 2004. Tie2/angiopoietin-1 signaling regulates hematopoietic stem cell quiescence in the bone marrow niche. *Cell,* 118**,** 149-61.

ARBER, D. A., ORAZI, A., HASSERJIAN, R., THIELE, J., BOROWITZ, M. J., LE BEAU, M. M., BLOOMFIELD, C. D., CAZZOLA, M. & VARDIMAN, J. W. 2016. The 2016 revision to the World Health Organization classification of myeloid neoplasms and acute leukemia. *Blood,* 127**,** 2391-405.

ARMSTRONG, S. A., STAUNTON, J. E., SILVERMAN, L. B., PIETERS, R., DEN BOER, M. L., MINDEN, M. D., SALLAN, S. E., LANDER, E. S., GOLUB, T. R. & KORSMEYER, S. J. 2002. MLL translocations specify a distinct gene expression profile that distinguishes a unique leukemia. *Nat Genet,* 30**,** 41-7.

ARORA, N., WENZEL, P. L., MCKINNEY-FREEMAN, S. L., ROSS, S. J., KIM, P. G., CHOU, S. S., YOSHIMOTO, M., YODER, M. C. & DALEY, G. Q. 2014. Effect of developmental stage of HSC and recipient on transplant outcomes. *Dev Cell*, 29, 621-8.

BAIN, G., MAANDAG, E. C., IZON, D. J., AMSEN, D., KRUISBEEK, A. M., WEINTRAUB, B. C., KROP, I., SCHLISSEL, M. S., FEENEY, A. J., VAN ROON, M. & ET AL. 1994. E2A proteins are required for proper B cell development and initiation of immunoglobulin gene rearrangements. *Cell,* 79, 885-92.

BALGOBIND, B. V., HOLLINK, I. H., ARENTSEN-PETERS, S. T., ZIMMERMANN, M., HARBOTT, J., BEVERLOO, H. B., VON BERGH, A. R., CLOOS, J., KASPERS, G. J., DE HAAS, V., ZEMANOVA, Z., STARY, J., CAYUELA, J. M., BARUCHEL, A., CREUTZIG, U., REINHARDT, D., PIETERS, R., ZWAAN, C. M. & VAN DEN HEUVEL-EIBRINK, M. M. 2011a. Integrative analysis of type-I and type-II aberrations underscores the genetic heterogeneity of pediatric acute myeloid leukemia. *Haematologica,* 96, 1478-87.

BALGOBIND, B. V., RAIMONDI, S. C., HARBOTT, J., ZIMMERMANN, M., ALONZO, T. A., AUVRIGNON, A., BEVERLOO, H. B., CHANG, M., CREUTZIG, U., DWORZAK, M. N., FORESTIER, E., GIBSON, B., HASLE, H., HARRISON, C. J., HEEREMA, N. A., KASPERS, G. J., LESZL, A., LITVINKO, N., NIGRO, L. L., MORIMOTO, A., PEROT, C., PIETERS, R., REINHARDT, D., RUBNITZ, J. E., SMITH, F. O., STARY, J., STASEVICH, I., STREHL, S., TAGA, T., TOMIZAWA, D., WEBB, D., ZEMANOVA, Z., ZWAAN, C. M. & VAN DEN HEUVEL-EIBRINK, M. M. 2009. Novel prognostic subgroups in childhood 11q23/MLL-rearranged acute myeloid leukemia: results of an international retrospective study. *Blood,* 114, 2489-96.

BALGOBIND, B. V., VAN DEN HEUVEL-EIBRINK, M. M., DE MENEZES, R. X., REINHARDT, D., HOLLINK, I. H., ARENTSEN-PETERS, S. T., VAN WERING, E. R., KASPERS, G. J., CLOOS, J., DE BONT, E. S., CAYUELA, J. M., BARUCHEL, A., MEYER, C., MARSCHALEK, R., TRKA, J., STARY, J., BEVERLOO, H. B., PIETERS, R., ZWAAN, C. M. & DEN BOER, M. L. 2011b. Evaluation of gene expression signatures predictive of cytogenetic and molecular subtypes of pediatric acute myeloid leukemia. *Haematologica,* 96, 221-30.

BARABE, F., KENNEDY, J. A., HOPE, K. J. & DICK, J. E. 2007. Modeling the initiation and progression of human acute leukemia in mice. *Science,* 316, 600-4.

BARKER, J. E. 1997. Early transplantation to a normal microenvironment prevents the development of Steel hematopoietic stem cell defects. *Exp Hematol,* 25, 542-7.

BASSO, G., RONDELLI, R., COVEZZOLI, A. & PUTTI, M. 1994. The role of immunophenotype in acute lymphoblastic leukemia of infant age. *Leuk Lymphoma,* 15, 51-60.

BECKER, H., MARCUCCI, G., MAHARRY, K., RADMACHER, M. D., MROZEK, K., MARGESON, D., WHITMAN, S. P., WU, Y. Z., SCHWIND, S., PASCHKA, P., POWELL, B. L., CARTER, T. H., KOLITZ, J. E., WETZLER, M., CARROLL, A. J., BAER, M. R., CALIGIURI, M. A., LARSON, R. A. & BLOOMFIELD, C. D. 2010. Favorable prognostic impact of NPM1 mutations in older patients with cytogenetically normal de novo acute myeloid leukemia and associated gene- and microRNA-expression signatures: a Cancer and Leukemia Group B study. *J Clin Oncol,* 28, 596-604.

BECKER, P. S., KOPECKY, K. J., WILKS, A. N., CHIEN, S., HARLAN, J. M., WILLMAN, C. L., PETERSDORF, S. H., STIREWALT, D. L., PAPAYANNOPOULOU, T. & APPELBAUM, F. R. 2009. Very late antigen-4 function of myeloblasts

correlates with improved overall survival for patients with acute myeloid leukemia. *Blood,* 113**,** 866-74.

BEERMAN, I., BHATTACHARYA, D., ZANDI, S., SIGVARDSSON, M., WEISSMAN, I. L., BRYDER, D. & ROSSI, D. J. 2010. Functionally distinct hematopoietic stem cells modulate hematopoietic lineage potential during aging by a mechanism of clonal expansion. *Proc Natl Acad Sci U S A,* 107**,** 5465-70.

BEERMAN, I., SEITA, J., INLAY, M. A., WEISSMAN, I. L. & ROSSI, D. J. 2014. Quiescent hematopoietic stem cells accumulate DNA damage during aging that is repaired upon entry into cell cycle. *Cell Stem Cell,* 15**,** 37-50.

BENNETT, J. M., CATOVSKY, D., DANIEL, M. T., FLANDRIN, G., GALTON, D. A., GRALNICK, H. R. & SULTAN, C. 1976. Proposals for the classification of the acute leukaemias. French-American-British (FAB) co-operative group. *Br J Haematol,* 33**,** 451-8.

BENZ, C., COPLEY, M. R., KENT, D. G., WOHRER, S., CORTES, A., AGHAEEPOUR, N., MA, E., MADER, H., ROWE, K., DAY, C., TRELOAR, D., BRINKMAN, R. R. & EAVES, C. J. 2012. Hematopoietic stem cell subtypes expand differentially during development and display distinct lymphopoietic programs. *Cell Stem Cell,* 10**,** 273-83.

BEPPU, H., KAWABATA, M., HAMAMOTO, T., CHYTIL, A., MINOWA, O., NODA, T. & MIYAZONO, K. 2000. BMP type II receptor is required for gastrulation and early development of mouse embryos. *Dev Biol,* 221**,** 249-58.

BERENSON, R. J., ANDREWS, R. G., BENSINGER, W. I., KALAMASZ, D., KNITTER, G., BUCKNER, C. D. & BERNSTEIN, I. D. 1988. Antigen CD34+ marrow cells engraft lethally irradiated baboons. *J Clin Invest,* 81**,** 951-5.

BEROUKHIM, R., MERMEL, C. H., PORTER, D., WEI, G., RAYCHAUDHURI, S., DONOVAN, J., BARRETINA, J., BOEHM, J. S., DOBSON, J., URASHIMA, M., MC HENRY, K. T., PINCHBACK, R. M., LIGON, A. H., CHO, Y. J., HAERY, L., GREULICH, H., REICH, M., WINCKLER, W., LAWRENCE, M. S., WEIR, B. A., TANAKA, K. E., CHIANG, D. Y., BASS, A. J., LOO, A., HOFFMAN, C., PRENSNER, J., LIEFELD, T., GAO, Q., YECIES, D., SIGNORETTI, S., MAHER, E., KAYE, F. J., SASAKI, H., TEPPER, J. E., FLETCHER, J. A., TABERNERO, J., BASELGA, J., TSAO, M. S., DEMICHELIS, F., RUBIN, M. A., JANNE, P. A., DALY, M. J., NUCERA, C., LEVINE, R. L., EBERT, B. L., GABRIEL, S., RUSTGI, A. K., ANTONESCU, C. R., LADANYI, M., LETAI, A., GARRAWAY, L. A., LODA, M., BEER, D. G., TRUE, L. D., OKAMOTO, A., POMEROY, S. L., SINGER, S., GOLUB, T. R., LANDER, E. S., GETZ, G., SELLERS, W. R. & MEYERSON, M. 2010. The landscape of somatic copy-number alteration across human cancers. *Nature,* 463**,** 899-905.

BERTHON, C., RAFFOUX, E., THOMAS, X., VEY, N., GOMEZ-ROCA, C., YEE, K., TAUSSIG, D. C., REZAI, K., ROUMIER, C., HERAIT, P., KAHATT, C., QUESNEL, B., MICHALLET, M., RECHER, C., LOKIEC, F., PREUDHOMME, C. & DOMBRET, H. 2016. Bromodomain inhibitor OTX015 in patients with acute leukaemia: a dose-escalation, phase 1 study. *Lancet Haematol,* 3**,** e186-95.

BHARDWAJ, G., MURDOCH, B., WU, D., BAKER, D. P., WILLIAMS, K. P., CHADWICK, K., LING, L. E., KARANU, F. N. & BHATIA, M. 2001. Sonic hedgehog induces the proliferation of primitive human hematopoietic cells via BMP regulation. *Nat Immunol,* 2**,** 172-80.

BHATIA, M., BONNET, D., WU, D., MURDOCH, B., WRANA, J., GALLACHER, L. & DICK, J. E. 1999. Bone morphogenetic proteins regulate the developmental program of human hematopoietic stem cells. *J Exp Med,* 189**,** 1139-48.

BHATIA, M., WANG, J. C., KAPP, U., BONNET, D. & DICK, J. E. 1997. Purification of primitive human hematopoietic cells capable of repopulating immune-deficient mice. *Proc Natl Acad Sci U S A,* 94**,** 5320-5.

BISIO, V., PIGAZZI, M., MANARA, E., MASETTI, R., TOGNI, M., ASTOLFI, A., MECUCCI, C., ZAPPAVIGNA, V., SALSI, V., MERLI, P., RIZZARI, C., FAGIOLI, F., LOCATELLI, F. & BASSO, G. 2014. NUP98 Fusion Proteins Are Recurrent Aberrancies in Childhood Acute Myeloid Leukemia: A Report from the AIEOP AML-2001-02 Study Group. *Blood,* 124**,** 1025.

BLAIR, A., HOGGE, D. E., AILLES, L. E., LANSDORP, P. M. & SUTHERLAND, H. J. 1997. Lack of expression of Thy-1 (CD90) on acute myeloid leukemia cells with long-term proliferative ability in vitro and in vivo. *Blood,* 89**,** 3104-12.

BLAIR, A., HOGGE, D. E. & SUTHERLAND, H. J. 1998. Most acute myeloid leukemia progenitor cells with long-term proliferative ability in vitro and in vivo have the phenotype CD34(+)/CD71(-)/HLA-DR. *Blood,* 92**,** 4325-35.

BLAIR, A. & SUTHERLAND, H. J. 2000. Primitive acute myeloid leukemia cells with long-term proliferative ability in vitro and in vivo lack surface expression of c-kit (CD117). *Exp Hematol,* 28**,** 660-71.

BLANK, U., KARLSSON, G. & KARLSSON, S. 2008. Signaling pathways governing stem-cell fate. *Blood,* 111**,** 492-503.

BONIG, H., PRIESTLEY, G. V., NILSSON, L. M., JIANG, Y. & PAPAYANNOPOULOU, T. 2004. PTX-sensitive signals in bone marrow homing of fetal and adult hematopoietic progenitor cells. *Blood,* 104**,** 2299-306.

BONNET, D. & DICK, J. E. 1997. Human acute myeloid leukemia is organized as a hierarchy that originates from a primitive hematopoietic cell. *Nat Med,* 3**,** 730-7.

BORROW, J., SHEARMAN, A. M., STANTON, V. P., JR., BECHER, R., COLLINS, T., WILLIAMS, A. J., DUBE, I., KATZ, F., KWONG, Y. L., MORRIS, C., OHYASHIKI, K., TOYAMA, K., ROWLEY, J. & HOUSMAN, D. E. 1996. The t(7;11)(p15;p15) translocation in acute myeloid leukaemia fuses the genes for nucleoporin NUP98 and class I homeoprotein HOXA9. *Nat Genet,* 12**,** 159-67.

BORTHAKUR, G., OFRAN, Y., NAGLER, A., ROWE, J. M., FORAN, J. M., UY, G. L., DIPERSIO, J. F., ALTMAN, J. K., FRANKFURT, O., TALLMAN, M. S., PELED, A., PEREG, Y., VAINSTEIN, A., AHARON, A., ALRAWI, A., MCQUEEN, T., PEMMARAJU, N., BUESO-RAMOS, C. E., CORTES, J. E. & ANDREEFF, M. 2015. The Peptidic CXCR4 Antagonist, BL-8040, Significantly Reduces Bone Marrow Immature Leukemia Progenitors By Inducing Differentiation, Apoptosis and Mobilization: Results of the Dose Escalation Clinical Trial in Acute Myeloid Leukemia. *Blood,* 126**,** 2546.

BORZILLO, G. V., ASHMUN, R. A. & SHERR, C. J. 1990. Macrophage lineage switching of murine early pre-B lymphoid cells expressing transduced fms genes. *Mol Cell Biol,* 10**,** 2703-14.

BOWIE, M. B., KENT, D. G., COPLEY, M. R. & EAVES, C. J. 2007a. Steel factor responsiveness regulates the high self-renewal phenotype of fetal hematopoietic stem cells. *Blood,* 109**,** 5043-8.

BOWIE, M. B., KENT, D. G., DYKSTRA, B., MCKNIGHT, K. D., MCCAFFREY, L., HOODLESS, P. A. & EAVES, C. J. 2007b. Identification of a new intrinsically timed developmental checkpoint that reprograms key hematopoietic stem cell properties. *Proc Natl Acad Sci U S A,* 104**,** 5878-82.

BOWIE, M. B., MCKNIGHT, K. D., KENT, D. G., MCCAFFREY, L., HOODLESS, P. A. & EAVES, C. J. 2006. Hematopoietic stem cells proliferate until after birth and show a reversible phase-specific engraftment defect. *J Clin Invest,* 116**,** 2808-16.

BRAY, N. L., PIMENTEL, H., MELSTED, P. & PACHTER, L. 2016. Near-optimal probabilistic RNA-seq quantification. *Nat Biotechnol,* 34**,** 525-7.

BRUCE, W. R. & VAN DER GAAG, H. 1963. A Quantitative Assay for the Number of Murine Lymphoma Cells Capable of Proliferation in Vivo. *Nature,* 199**,** 79-80.

BUCHHOLZ, F., REFAELI, Y., TRUMPP, A. & BISHOP, J. M. 2000. Inducible chromosomal translocation of AML1 and ETO genes through Cre/loxP-mediated recombination in the mouse. *EMBO Rep,* 1**,** 133-9.

BULLINGER, L., DOHNER, K., BAIR, E., FROHLING, S., SCHLENK, R. F., TIBSHIRANI, R., DOHNER, H. & POLLACK, J. R. 2004. Use of gene-expression profiling to identify prognostic subclasses in adult acute myeloid leukemia. *N Engl J Med,* 350**,** 1605-16.

BUMGARNER, R. 2013. Overview of DNA microarrays: types, applications, and their future. *Curr Protoc Mol Biol,* Chapter 22**,** Unit 22 1.

BURNETT, A. K., RUSSELL, N. H., HILLS, R. K., HUNTER, A. E., KJELDSEN, L., YIN, J., GIBSON, B. E., WHEATLEY, K. & MILLIGAN, D. 2013. Optimization of chemotherapy for younger patients with acute myeloid leukemia: results of the medical research council AML15 trial. *J Clin Oncol,* 31**,** 3360-8.

BUSQUE, L., PATEL, J. P., FIGUEROA, M. E., VASANTHAKUMAR, A., PROVOST, S., HAMILOU, Z., MOLLICA, L., LI, J., VIALE, A., HEGUY, A., HASSIMI, M., SOCCI, N., BHATT, P. K., GONEN, M., MASON, C. E., MELNICK, A., GODLEY, L. A., BRENNAN, C. W., ABDEL-WAHAB, O. & LEVINE, R. L. 2012. Recurrent somatic TET2 mutations in normal elderly individuals with clonal hematopoiesis. *Nat Genet,* 44**,** 1179-81.

CABEZAS-WALLSCHEID, N., BUETTNER, F., SOMMERKAMP, P., KLIMMECK, D., LADEL, L., THALHEIMER, F. B., PASTOR-FLORES, D., ROMA, L. P., RENDERS, S., ZEISBERGER, P., PRZYBYLLA, A., SCHONBERGER, K., SCOGNAMIGLIO, R., ALTAMURA, S., FLORIAN, C. M., FAWAZ, M., VONFICHT, D., TESIO, M., COLLIER, P., PAVLINIC, D., GEIGER, H., SCHROEDER, T., BENES, V., DICK, T. P., RIEGER, M. A., STEGLE, O. & TRUMPP, A. 2017. Vitamin A-Retinoic Acid Signaling Regulates Hematopoietic Stem Cell Dormancy. *Cell,* 169**,** 807-823 e19.

CABEZAS-WALLSCHEID, N., EICHWALD, V., DE GRAAF, J., LOWER, M., LEHR, H. A., KREFT, A., ESHKIND, L., HILDEBRANDT, A., ABASSI, Y., HECK, R., DEHOF, A. K., OHNGEMACH, S., SPRENGEL, R., WORTGE, S., SCHMITT, S., LOTZ, J., MEYER, C., KINDLER, T., ZHANG, D. E., KAINA, B., CASTLE, J. C., TRUMPP, A., SAHIN, U. & BOCKAMP, E. 2013. Instruction of haematopoietic lineage choices, evolution of transcriptional landscapes and cancer stem cell hierarchies derived from an AML1-ETO mouse model. *EMBO Mol Med,* 5**,** 1804-20.

CABEZAS-WALLSCHEID, N., KLIMMECK, D., HANSSON, J., LIPKA, D. B., REYES, A., WANG, Q., WEICHENHAN, D., LIER, A., VON PALESKE, L., RENDERS, S., WUNSCHE, P., ZEISBERGER, P., BROCKS, D., GU, L., HERRMANN, C., HAAS, S., ESSERS, M. A., BRORS, B., EILS, R., HUBER, W., MILSOM, M. D., PLASS, C., KRIJGSVELD, J. & TRUMPP, A. 2014. Identification of regulatory networks in HSCs and their immediate progeny via integrated proteome, transcriptome, and DNA methylome analysis. *Cell Stem Cell,* 15**,** 507-22.

CALVI, L. M., ADAMS, G. B., WEIBRECHT, K. W., WEBER, J. M., OLSON, D. P., KNIGHT, M. C., MARTIN, R. P., SCHIPANI, E., DIVIETI, P., BRINGHURST, F. R., MILNER, L. A., KRONENBERG, H. M. & SCADDEN, D. T. 2003. Osteoblastic cells regulate the haematopoietic stem cell niche. *Nature,* 425**,** 841-6.

CALVO, K. R., SYKES, D. B., PASILLAS, M. P. & KAMPS, M. P. 2002. Nup98-HoxA9 immortalizes myeloid progenitors, enforces expression of Hoxa9, Hoxa7 and Meis1, and alters cytokine-specific responses in a manner similar to that induced by retroviral co-expression of Hoxa9 and Meis1. *Oncogene,* 21**,** 4247-56.

CAMPISI, J. 2005. Senescent cells, tumor suppression, and organismal aging: good citizens, bad neighbors. *Cell,* 120**,** 513-22.

CANCER GENOME ATLAS RESEARCH, N., LEY, T. J., MILLER, C., DING, L., RAPHAEL, B. J., MUNGALL, A. J., ROBERTSON, A., HOADLEY, K., TRICHE, T. J., JR., LAIRD, P. W., BATY, J. D., FULTON, L. L., FULTON, R., HEATH, S. E., KALICKI-VEIZER, J., KANDOTH, C., KLCO, J. M., KOBOLDT, D. C., KANCHI, K. L., KULKARNI, S., LAMPRECHT, T. L., LARSON, D. E., LIN, L., LU, C., MCLELLAN, M. D., MCMICHAEL, J. F., PAYTON, J., SCHMIDT, H., SPENCER, D. H., TOMASSON, M. H., WALLIS, J. W., WARTMAN, L. D., WATSON, M. A., WELCH, J., WENDL, M. C., ALLY, A., BALASUNDARAM, M., BIROL, I., BUTTERFIELD, Y., CHIU, R., CHU, A., CHUAH, E., CHUN, H. J., CORBETT, R., DHALLA, N., GUIN, R., HE, A., HIRST, C., HIRST, M., HOLT, R. A., JONES, S., KARSAN, A., LEE, D., LI, H. I., MARRA, M. A., MAYO, M., MOORE, R. A., MUNGALL, K., PARKER, J., PLEASANCE, E., PLETTNER, P., SCHEIN, J., STOLL, D., SWANSON, L., TAM, A., THIESSEN, N., VARHOL, R., WYE, N., ZHAO, Y., GABRIEL, S., GETZ, G., SOUGNEZ, C., ZOU, L., LEISERSON, M. D., VANDIN, F., WU, H. T., APPLEBAUM, F., BAYLIN, S. B., AKBANI, R., BROOM, B. M., CHEN, K., MOTTER, T. C., NGUYEN, K., WEINSTEIN, J. N., ZHANG, N., FERGUSON, M. L., ADAMS, C., BLACK, A., BOWEN, J., GASTIER-FOSTER, J., GROSSMAN, T., LICHTENBERG, T., WISE, L., DAVIDSEN, T., DEMCHOK, J. A., SHAW, K. R., SHETH, M., SOFIA, H. J., YANG, L., DOWNING, J. R., et al. 2013. Genomic and epigenomic landscapes of adult de novo acute myeloid leukemia. *N Engl J Med,* 368**,** 2059-74.

CANCER RESEARCH UK. 2014. *Acute myeloid leukaemia (AML) incidence statistics* [Online]. London: Cancer Research UK. Available: http://www.cancerresearchuk.org/cancer-info/cancerstats/types/leukaemia-aml/incidence/ [Accessed 5th September 2014 2014].

CANCER RESEARCH UK. 2016. *Acute lymphoblastic leukaemia (ALL) incidence by age* [Online]. London: Cancer Research UK. Available: http://www.cancerresearchuk.org/health-professional/cancer-statistics/statistics-by-cancer-type/leukaemia-all/incidence#heading-One [Accessed 10th August 2017 2017].

CAPELSON, M., LIANG, Y., SCHULTE, R., MAIR, W., WAGNER, U. & HETZER, M. W. 2010. Chromatin-bound nuclear pore components regulate gene expression in higher eukaryotes. *Cell,* 140**,** 372-83.

CHAMBERS, S. M., SHAW, C. A., GATZA, C., FISK, C. J., DONEHOWER, L. A. & GOODELL, M. A. 2007. Aging hematopoietic stem cells decline in function and exhibit epigenetic dysregulation. *PLoS Biol,* 5**,** e201.

CHAUDHURY, S. S., MORISON, J. K., GIBSON, B. E. & KEESHAN, K. 2015. Insights into cell ontogeny, age, and acute myeloid leukemia. *Exp Hematol,* 43**,** 745-55.

CHEN, W., KUMAR, A. R., HUDSON, W. A., LI, Q., WU, B., STAGGS, R. A., LUND, E. A., SAM, T. N. & KERSEY, J. H. 2008. Malignant transformation initiated by Mll-AF9: gene dosage and critical target cells. *Cancer Cell,* 13**,** 432-40.

CHEN, W., O'SULLIVAN, M. G., HUDSON, W. & KERSEY, J. 2011. Modeling human infant MLL leukemia in mice: leukemia from fetal liver differs from that originating in postnatal marrow. *Blood,* 117**,** 3474-5.

CHESI, M., ROBBIANI, D. F., SEBAG, M., CHNG, W. J., AFFER, M., TIEDEMANN, R., VALDEZ, R., PALMER, S. E., HAAS, S. S., STEWART, A. K., FONSECA, R., KREMER, R., CATTORETTI, G. & BERGSAGEL, P. L. 2008. AID-dependent activation of a MYC transgene induces multiple myeloma in a conditional mouse model of post-germinal center malignancies. *Cancer Cell,* 13**,** 167-80.

CHESSELLS, J. M. 1992. Leukaemia in the young child. *Br J Cancer Suppl,* 18**,** S54-7.

CHOI, Y., ELAGIB, K. E., DELEHANTY, L. L. & GOLDFARB, A. N. 2006. Erythroid inhibition by the leukemic fusion AML1-ETO is associated with impaired acetylation of the major erythroid transcription factor GATA-1. *Cancer Res,* 66**,** 2990-6.

CHOU, W. C., CHEN, C. Y., HOU, H. A., LIN, L. I., TANG, J. L., YAO, M., TSAY, W., KO, B. S., WU, S. J., HUANG, S. Y., HSU, S. C., CHEN, Y. C., HUANG, Y. N., TSENG, M. H., HUANG, C. F. & TIEN, H. F. 2009. Acute myeloid leukemia bearing t(7;11)(p15;p15) is a distinct cytogenetic entity with poor outcome and a distinct mutation profile: comparative analysis of 493 adult patients. *Leukemia,* 23**,** 1303-10.

CHRISTENSEN, J. L. & WEISSMAN, I. L. 2001. Flk-2 is a marker in hematopoietic stem cell differentiation: a simple method to isolate long-term stem cells. *Proc Natl Acad Sci U S A,* 98**,** 14541-6.

CHUNG, K. Y., MORRONE, G., SCHURINGA, J. J., PLASILOVA, M., SHIEH, J. H., ZHANG, Y., ZHOU, P. & MOORE, M. A. 2006. Enforced expression of NUP98-HOXA9 in human CD34(+) cells enhances stem cell proliferation. *Cancer Res,* 66**,** 11781-91.

CIVIN, C. I., STRAUSS, L. C., BROVALL, C., FACKLER, M. J., SCHWARTZ, J. F. & SHAPER, J. H. 1984. Antigenic analysis of hematopoiesis. III. A hematopoietic progenitor cell surface antigen defined by a monoclonal antibody raised against KG-1a cells. *J Immunol,* 133**,** 157-65.

CIVINI, S., JIN, P., REN, J., SABATINO, M., CASTIELLO, L., JIN, J., WANG, H., ZHAO, Y., MARINCOLA, F. & STRONCEK, D. 2013. Leukemia cells induce changes in human bone marrow stromal cells. *J Transl Med,* 11**,** 298.

COBALEDA, C., JOCHUM, W. & BUSSLINGER, M. 2007. Conversion of mature B cells into T cells by dedifferentiation to uncommitted progenitors. *Nature,* 449**,** 473-7.

COLMONE, A., AMORIM, M., PONTIER, A. L., WANG, S., JABLONSKI, E. & SIPKINS, D. A. 2008. Leukemic cells create bone marrow niches that disrupt the behavior of normal hematopoietic progenitor cells. *Science,* 322**,** 1861-5.

CONLON, R. A. 1995. Retinoic acid and pattern formation in vertebrates. *Trends Genet,* 11**,** 314-9.

COPLEY, M. R., BABOVIC, S., BENZ, C., KNAPP, D. J., BEER, P. A., KENT, D. G., WOHRER, S., TRELOAR, D. Q., DAY, C., ROWE, K., MADER, H., KUCHENBAUER, F., HUMPHRIES, R. K. & EAVES, C. J. 2013. The Lin28b-let-7-Hmga2 axis determines the higher self-renewal potential of fetal haematopoietic stem cells. *Nat Cell Biol,* 15**,** 916-25.

CORCES-ZIMMERMAN, M. R., HONG, W. J., WEISSMAN, I. L., MEDEIROS, B. C. & MAJETI, R. 2014. Preleukemic mutations in human acute myeloid leukemia affect epigenetic regulators and persist in remission. *Proc Natl Acad Sci U S A,* 111**,** 2548-53.

CORCORAN, A. E., RIDDELL, A., KROOSHOOP, D. & VENKITARAMAN, A. R. 1998. Impaired immunoglobulin gene rearrangement in mice lacking the IL-7 receptor. *Nature,* 391**,** 904-7.

CORRAL, J., LAVENIR, I., IMPEY, H., WARREN, A. J., FORSTER, A., LARSON, T. A., BELL, S., MCKENZIE, A. N., KING, G. & RABBITTS, T. H. 1996. An Mll-AF9 fusion gene made by homologous recombination causes acute leukemia in chimeric mice: a method to create fusion oncogenes. *Cell,* 85**,** 853-61.

COZZIO, A., PASSEGUE, E., AYTON, P. M., KARSUNKY, H., CLEARY, M. L. & WEISSMAN, I. L. 2003. Similar MLL-associated leukemias arising from self-renewing stem cells and short-lived myeloid progenitors. *Genes Dev,* 17**,** 3029-35.

CREUTZIG, U., VAN DEN HEUVEL-EIBRINK, M. M., GIBSON, B., DWORZAK, M. N., ADACHI, S., DE BONT, E., HARBOTT, J., HASLE, H., JOHNSTON, D., KINOSHITA, A., LEHRNBECHER, T., LEVERGER, G., MEJSTRIKOVA, E., MESHINCHI, S., PESSION, A., RAIMONDI, S. C., SUNG, L., STARY, J., ZWAAN, C. M., KASPERS, G. J., REINHARDT, D. & GROUP, A. M. L. C. O. T. I. B. S. 2012. Diagnosis and management of acute myeloid leukemia in children and adolescents: recommendations from an international expert panel. *Blood,* 120**,** 3187-205.

CREUTZIG, U., ZIMMERMANN, M., BOURQUIN, J. P., DWORZAK, M. N., FLEISCHHACK, G., GRAF, N., KLINGEBIEL, T., KREMENS, B., LEHRNBECHER, T., VON NEUHOFF, C., RITTER, J., SANDER, A., SCHRAUDER, A., VON STACKELBERG, A., STARY, J. & REINHARDT, D. 2013. Randomized trial comparing liposomal daunorubicin with idarubicin as induction for pediatric acute myeloid leukemia: results from Study AML-BFM 2004. *Blood,* 122**,** 37-43.

CRISAN, M., KARTALAEI, P. S., VINK, C. S., YAMADA-INAGAWA, T., BOLLEROT, K., VAN, I. W., VAN DER LINDEN, R., DE SOUSA LOPES, S. M., MONTEIRO, R., MUMMERY, C. & DZIERZAK, E. 2015. BMP signalling differentially regulates distinct haematopoietic stem cell types. *Nat Commun,* 6**,** 8040.

DAKIC, A., METCALF, D., DI RAGO, L., MIFSUD, S., WU, L. & NUTT, S. L. 2005. PU.1 regulates the commitment of adult hematopoietic progenitors and restricts granulopoiesis. *J Exp Med,* 201**,** 1487-502.

DANG, C. V. 2012. MYC on the path to cancer. *Cell,* 149**,** 22-35.

DE GUZMAN, C. G., WARREN, A. J., ZHANG, Z., GARTLAND, L., ERICKSON, P., DRABKIN, H., HIEBERT, S. W. & KLUG, C. A. 2002. Hematopoietic stem cell expansion and distinct myeloid developmental abnormalities in a murine model of the AML1-ETO translocation. *Mol Cell Biol,* 22**,** 5506-17.

DE HAAN, G., NIJHOF, W. & VAN ZANT, G. 1997. Mouse strain-dependent changes in frequency and proliferation of hematopoietic stem cells during aging: correlation between lifespan and cycling activity. *Blood,* 89**,** 1543-50.

DE HAAN, G. & PLOEMACHER, R. 2002. The Cobblestone-Area-Forming Cell Assay. *In:* KLUG, C. A. & JORDAN, C. T. (eds.) *Hematopoietic Stem Cell Protocols.* Totowa, NJ: Humana Press.

DE HAAN, G. & VAN ZANT, G. 1999. Dynamic changes in mouse hematopoietic stem cell numbers during aging. *Blood,* 93**,** 3294-301.

DEN BESTEN, W., KUO, M. L., WILLIAMS, R. T. & SHERR, C. J. 2005. Myeloid leukemia-associated nucleophosmin mutants perturb p53-dependent and independent activities of the Arf tumor suppressor protein. *Cell Cycle,* 4**,** 1593-8.

DICK, J. E. 1996. Normal and leukemic human stem cells assayed in SCID mice. *Semin Immunol,* 8**,** 197-206.

DICK, J. E. 2008. Stem cell concepts renew cancer research. *Blood,* 112**,** 4793-807.

DING, L., LEY, T. J., LARSON, D. E., MILLER, C. A., KOBOLDT, D. C., WELCH, J. S., RITCHEY, J. K., YOUNG, M. A., LAMPRECHT, T., MCLELLAN, M. D., MCMICHAEL, J. F., WALLIS, J. W., LU, C., SHEN, D., HARRIS, C. C., DOOLING, D. J., FULTON, R. S., FULTON, L. L., CHEN, K., SCHMIDT, H., KALICKI-VEIZER, J., MAGRINI, V. J., COOK, L., MCGRATH, S. D., VICKERY, T. L., WENDL, M. C., HEATH, S., WATSON, M. A., LINK, D. C., TOMASSON, M. H., SHANNON, W. D., PAYTON, J. E., KULKARNI, S., WESTERVELT, P., WALTER, M. J., GRAUBERT, T. A., MARDIS, E. R., WILSON, R. K. & DIPERSIO, J. F. 2012. Clonal evolution in relapsed acute myeloid leukaemia revealed by whole-genome sequencing. *Nature,* 481**,** 506-10.

DOHNER, H., ESTEY, E. H., AMADORI, S., APPELBAUM, F. R., BUCHNER, T., BURNETT, A. K., DOMBRET, H., FENAUX, P., GRIMWADE, D., LARSON, R. A., LO-COCO, F., NAOE, T., NIEDERWIESER, D., OSSENKOPPELE, G. J., SANZ, M. A., SIERRA, J., TALLMAN, M. S., LOWENBERG, B., BLOOMFIELD, C. D. & EUROPEAN, L. 2010. Diagnosis and management of acute myeloid leukemia in adults: recommendations from an international expert panel, on behalf of the European LeukemiaNet. *Blood,* 115**,** 453-74.

DORANTES-ACOSTA, E. & PELAYO, R. 2012. Lineage switching in acute leukemias: a consequence of stem cell plasticity? *Bone Marrow Res,* 2012**,** 406796.

DUBOULE, D. & DOLLE, P. 1989. The structural and functional organization of the murine HOX gene family resembles that of Drosophila homeotic genes. *EMBO J,* 8**,** 1497-505.

DUBRIDGE, R. B., TANG, P., HSIA, H. C., LEONG, P. M., MILLER, J. H. & CALOS, M. P. 1987. Analysis of mutation in human cells by using an Epstein-Barr virus shuttle system. *Mol Cell Biol,* 7**,** 379-87.

DUNCAN, A. W., RATTIS, F. M., DIMASCIO, L. N., CONGDON, K. L., PAZIANOS, G., ZHAO, C., YOON, K., COOK, J. M., WILLERT, K., GAIANO, N. & REYA, T. 2005. Integration of Notch and Wnt signaling in hematopoietic stem cell maintenance. *Nat Immunol,* 6**,** 314-22.

DUTTA, S. & SENGUPTA, P. 2016. Men and mice: Relating their ages. *Life Sci,* 152**,** 244-8.

DYKSTRA, B., KENT, D., BOWIE, M., MCCAFFREY, L., HAMILTON, M., LYONS, K., LEE, S. J., BRINKMAN, R. & EAVES, C. 2007. Long-term propagation of distinct hematopoietic differentiation programs in vivo. *Cell Stem Cell,* 1**,** 218-29.

DYKSTRA, B., OLTHOF, S., SCHREUDER, J., RITSEMA, M. & DE HAAN, G. 2011. Clonal analysis reveals multiple functional defects of aged murine hematopoietic stem cells. *J Exp Med,* 208**,** 2691-703.

EFFICACE, F., MANDELLI, F., AVVISATI, G., COTTONE, F., FERRARA, F., DI BONA, E., SPECCHIA, G., BRECCIA, M., LEVIS, A., SICA, S., FINIZIO, O., KROPP, M. G., FIORITONI, G., CERQUI, E., VIGNETTI, M., AMADORI, S., SCHLENK, R. F., PLATZBECKER, U. & LO-COCO, F. 2014. Randomized phase III trial of retinoic acid and arsenic trioxide versus retinoic acid and chemotherapy in patients with acute promyelocytic leukemia: health-related quality-of-life outcomes. *J Clin Oncol,* 32**,** 3406-12.

EL-MIR, M. Y., NOGUEIRA, V., FONTAINE, E., AVERET, N., RIGOULET, M. & LEVERVE, X. 2000. Dimethylbiguanide inhibits cell respiration via an indirect effect targeted on the respiratory chain complex I. *J Biol Chem,* 275**,** 223-8.

EPPERT, K., TAKENAKA, K., LECHMAN, E. R., WALDRON, L., NILSSON, B., VAN GALEN, P., METZELER, K. H., POEPPL, A., LING, V., BEYENE, J., CANTY, A. J., DANSKA, J. S., BOHLANDER, S. K., BUSKE, C., MINDEN, M. D., GOLUB, T. R., JURISICA, I., EBERT, B. L. & DICK, J. E. 2011. Stem cell gene expression programs influence clinical outcome in human leukemia. *Nat Med,* 17**,** 1086-93.

EVANS, J. M., DONNELLY, L. A., EMSLIE-SMITH, A. M., ALESSI, D. R. & MORRIS, A. D. 2005. Metformin and reduced risk of cancer in diabetic patients. *BMJ,* 330**,** 1304-5.

FLACH, J., BAKKER, S. T., MOHRIN, M., CONROY, P. C., PIETRAS, E. M., REYNAUD, D., ALVAREZ, S., DIOLAITI, M. E., UGARTE, F., FORSBERG, E. C., LE BEAU, M. M., STOHR, B. A., MENDEZ, J., MORRISON, C. G. & PASSEGUE, E. 2014. Replication stress is a potent driver of functional decline in ageing haematopoietic stem cells. *Nature,* 512**,** 198-202.

FLEMING, H. E., JANZEN, V., LO CELSO, C., GUO, J., LEAHY, K. M., KRONENBERG, H. M. & SCADDEN, D. T. 2008. Wnt signaling in the niche enforces hematopoietic stem cell quiescence and is necessary to preserve self-renewal in vivo. *Cell Stem Cell,* 2**,** 274-83.

FLURKEY, K., M. CURRER, J. & HARRISON, D. E. 2007. Chapter 20 - Mouse Models in Aging Research A2 - Fox, James G. *In:* DAVISSON, M. T., QUIMBY, F. W., BARTHOLD, S. W., NEWCOMER, C. E. & SMITH, A. L. (eds.) *The Mouse in Biomedical Research (Second Edition)*. Burlington: Academic Press.

FORD, A. M., RIDGE, S. A., CABRERA, M. E., MAHMOUD, H., STEEL, C. M., CHAN, L. C. & GREAVES, M. 1993. In utero rearrangements in the trithorax-related oncogene in infant leukaemias. *Nature,* 363**,** 358-60.

FORSBERG, E. C., PASSEGUE, E., PROHASKA, S. S., WAGERS, A. J., KOEVA, M., STUART, J. M. & WEISSMAN, I. L. 2010. Molecular signatures of quiescent, mobilized and leukemia-initiating hematopoietic stem cells. *PLoS One,* 5**,** e8785.

FRANKE, K., VILNE, B., PRAZERES DA COSTA, O., RUDELIUS, M., PESCHEL, C., OOSTENDORP, R. A. & KELLER, U. 2015. In vivo hematopoietic Myc activation directs a transcriptional signature in endothelial cells within the bone marrow microenvironment. *Oncotarget,* 6**,** 21827-39.

FREHLICK, L. J., EIRIN-LOPEZ, J. M. & AUSIO, J. 2007. New insights into the nucleophosmin/nucleoplasmin family of nuclear chaperones. *Bioessays,* 29**,** 49-59.

FRIEDMAN, A. D. 2002. Transcriptional regulation of granulocyte and monocyte development. *Oncogene,* 21**,** 3377-90.

GALE, K. B., FORD, A. M., REPP, R., BORKHARDT, A., KELLER, C., EDEN, O. B. & GREAVES, M. F. 1997. Backtracking leukemia to birth: identification of clonotypic gene fusion sequences in neonatal blood spots. *Proc Natl Acad Sci U S A,* 94**,** 13950-4.

GALY, A., TRAVIS, M., CEN, D. & CHEN, B. 1995. Human T, B, natural killer, and dendritic cells arise from a common bone marrow progenitor cell subset. *Immunity,* 3**,** 459-73.

GAMIS, A. S., ALONZO, T. A., GERBING, R. B., HILDEN, J. M., SORRELL, A. D., SHARMA, M., LOEW, T. W., ARCECI, R. J., BARNARD, D., DOYLE, J., MASSEY, G., PERENTESIS, J., RAVINDRANATH, Y., TAUB, J. & SMITH, F. O. 2011. Natural history of transient myeloproliferative disorder clinically diagnosed in Down syndrome neonates: a report from the Children's Oncology Group Study A2971. *Blood,* 118**,** 6752-9.

GAMIS, A. S., ALONZO, T. A., MESHINCHI, S., SUNG, L., GERBING, R. B., RAIMONDI, S. C., HIRSCH, B. A., KAHWASH, S. B., HEEREMA-MCKENNEY, A., WINTER, L., GLICK, K., DAVIES, S. M., BYRON, P., SMITH, F. O. & APLENC, R. 2014. Gemtuzumab ozogamicin in children and adolescents with De Novo acute myeloid leukemia improves event-free survival by reducing relapse risk: results from the randomized phase III Children's Oncology Group trial AAML0531. *J Clin Oncol,* 32**,** 3021-32.

GEKAS, C., DIETERLEN-LIEVRE, F., ORKIN, S. H. & MIKKOLA, H. K. 2005. The placenta is a niche for hematopoietic stem cells. *Dev Cell,* 8**,** 365-75.

GENOVESE, G., KAHLER, A. K., HANDSAKER, R. E., LINDBERG, J., ROSE, S. A., BAKHOUM, S. F., CHAMBERT, K., MICK, E., NEALE, B. M., FROMER, M., PURCELL, S. M., SVANTESSON, O., LANDEN, M., HOGLUND, M., LEHMANN, S., GABRIEL, S. B., MORAN, J. L., LANDER, E. S., SULLIVAN, P. F., SKLAR, P., GRONBERG, H., HULTMAN, C. M. & MCCARROLL, S. A. 2014. Clonal hematopoiesis and blood-cancer risk inferred from blood DNA sequence. *N Engl J Med,* 371**,** 2477-87.

GENTLES, A. J., PLEVRITIS, S. K., MAJETI, R. & ALIZADEH, A. A. 2010. Association of a leukemic stem cell gene expression signature with clinical outcomes in acute myeloid leukemia. *JAMA,* 304**,** 2706-15.

GEORGOPOULOS, K., BIGBY, M., WANG, J. H., MOLNAR, A., WU, P., WINANDY, S. & SHARPE, A. 1994. The Ikaros gene is required for the development of all lymphoid lineages. *Cell,* 79**,** 143-56.

GEYH, S., RODRIGUEZ-PAREDES, M., JAGER, P., KHANDANPOUR, C., CADEDDU, R. P., GUTEKUNST, J., WILK, C. M., FENK, R., ZILKENS, C., HERMSEN, D., GERMING, U., KOBBE, G., LYKO, F., HAAS, R. & SCHROEDER, T. 2016. Functional inhibition of mesenchymal stromal cells in acute myeloid leukemia. *Leukemia,* 30**,** 683-91.

GIBSON, B. E., WEBB, D. K., HOWMAN, A. J., DE GRAAF, S. S., HARRISON, C. J., WHEATLEY, K., UNITED KINGDOM CHILDHOOD LEUKAEMIA WORKING, G. & THE DUTCH CHILDHOOD ONCOLOGY, G. 2011. Results of a randomized trial in children with Acute Myeloid Leukaemia: medical research council AML12 trial. *Br J Haematol,* 155**,** 366-76.

GILLILAND, D. G. & GRIFFIN, J. D. 2002. The roles of FLT3 in hematopoiesis and leukemia. *Blood,* 100**,** 1532-42.

GOARDON, N., MARCHI, E., ATZBERGER, A., QUEK, L., SCHUH, A., SONEJI, S., WOLL, P., MEAD, A., ALFORD, K. A., ROUT, R., CHAUDHURY, S., GILKES, A., KNAPPER, S., BELDJORD, K., BEGUM, S., ROSE, S., GEDDES, N., GRIFFITHS, M., STANDEN, G., STERNBERG, A., CAVENAGH, J., HUNTER, H., BOWEN, D., KILLICK, S., ROBINSON, L., PRICE, A., MACINTYRE, E., VIRGO, P., BURNETT, A., CRADDOCK, C., ENVER, T., JACOBSEN, S. E., PORCHER, C. & VYAS, P. 2011. Coexistence of LMPP-like and GMP-like leukemia stem cells in acute myeloid leukemia. *Cancer Cell,* 19**,** 138-52.

GODDARD, A. D., BORROW, J., FREEMONT, P. S. & SOLOMON, E. 1991. Characterization of a zinc finger gene disrupted by the t(15;17) in acute promyelocytic leukemia. *Science,* 254**,** 1371-4.

GOLUB, T. R., SLONIM, D. K., TAMAYO, P., HUARD, C., GAASENBEEK, M., MESIROV, J. P., COLLER, H., LOH, M. L., DOWNING, J. R., CALIGIURI, M. A., BLOOMFIELD, C. D. & LANDER, E. S. 1999. Molecular classification of cancer: class discovery and class prediction by gene expression monitoring. *Science,* 286**,** 531-7.

GOTHERT, J. R., GUSTIN, S. E., HALL, M. A., GREEN, A. R., GOTTGENS, B., IZON, D. J. & BEGLEY, C. G. 2005. In vivo fate-tracing studies using the Scl stem cell enhancer: embryonic hematopoietic stem cells significantly contribute to adult hematopoiesis. *Blood,* 105**,** 2724-32.

GOTHOT, A., PYATT, R., MCMAHEL, J., RICE, S. & SROUR, E. F. 1997. Functional heterogeneity of human CD34(+) cells isolated in subcompartments of the G0 /G1 phase of the cell cycle. *Blood,* 90**,** 4384-93.

GOUGH, S. M., SLAPE, C. I. & APLAN, P. D. 2011. NUP98 gene fusions and hematopoietic malignancies: common themes and new biologic insights. *Blood,* 118**,** 6247-57.

GOYAMA, S. & MULLOY, J. C. 2011. Molecular pathogenesis of core binding factor leukemia: current knowledge and future prospects. *Int J Hematol,* 94**,** 126-33.

GRAHAM, F. L., SMILEY, J., RUSSELL, W. C. & NAIRN, R. 1977. Characteristics of a human cell line transformed by DNA from human adenovirus type 5. *J Gen Virol,* 36**,** 59-74.

GRCEVIC, D., MARUSIC, A., GRAHOVAC, B., JAKSIC, B. & KUSEC, R. 2003. Expression of bone morphogenetic proteins in acute promyelocytic leukemia

before and after combined all trans-retinoic acid and cytotoxic treatment. *Leuk Res,* 27**,** 731-8.

GREEN, C. L., KOO, K. K., HILLS, R. K., BURNETT, A. K., LINCH, D. C. & GALE, R. E. 2010. Prognostic significance of CEBPA mutations in a large cohort of younger adult patients with acute myeloid leukemia: impact of double CEBPA mutations and the interaction with FLT3 and NPM1 mutations. *J Clin Oncol,* 28**,** 2739-47.

GREENBAUM, A., HSU, Y. M., DAY, R. B., SCHUETTPELZ, L. G., CHRISTOPHER, M. J., BORGERDING, J. N., NAGASAWA, T. & LINK, D. C. 2013. CXCL12 in early mesenchymal progenitors is required for haematopoietic stem-cell maintenance. *Nature,* 495**,** 227-30.

GRIFFIN, J. D., LINCH, D., SABBATH, K., LARCOM, P. & SCHLOSSMAN, S. F. 1984. A monoclonal antibody reactive with normal and leukemic human myeloid progenitor cells. *Leuk Res,* 8**,** 521-34.

GRIMWADE, D., HILLS, R. K., MOORMAN, A. V., WALKER, H., CHATTERS, S., GOLDSTONE, A. H., WHEATLEY, K., HARRISON, C. J., BURNETT, A. K. & NATIONAL CANCER RESEARCH INSTITUTE ADULT LEUKAEMIA WORKING, G. 2010. Refinement of cytogenetic classification in acute myeloid leukemia: determination of prognostic significance of rare recurring chromosomal abnormalities among 5876 younger adult patients treated in the United Kingdom Medical Research Council trials. *Blood,* 116**,** 354-65.

GRIMWADE, D., WALKER, H., OLIVER, F., WHEATLEY, K., HARRISON, C., HARRISON, G., REES, J., HANN, I., STEVENS, R., BURNETT, A. & GOLDSTONE, A. 1998. The Importance of Diagnostic Cytogenetics on Outcome in AML: Analysis of 1,612 Patients Entered Into the MRC AML 10 Trial. *Blood,* 92**,** 2322-2333.

GRISENDI, S., MECUCCI, C., FALINI, B. & PANDOLFI, P. P. 2006. Nucleophosmin and cancer. *Nat Rev Cancer,* 6**,** 493-505.

GRISOLANO, J. L., O'NEAL, J., CAIN, J. & TOMASSON, M. H. 2003. An activated receptor tyrosine kinase, TEL/PDGFbetaR, cooperates with AML1/ETO to induce acute myeloid leukemia in mice. *Proc Natl Acad Sci U S A,* 100**,** 9506-11.

GROSSO, L. E. & PITOT, H. C. 1985. Transcriptional regulation of c-myc during chemically induced differentiation of HL-60 cultures. *Cancer Res,* 45**,** 847-50.

GRUBER, T. A., LARSON GEDMAN, A., ZHANG, J., KOSS, C. S., MARADA, S., TA, H. Q., CHEN, S. C., SU, X., OGDEN, S. K., DANG, J., WU, G., GUPTA, V., ANDERSSON, A. K., POUNDS, S., SHI, L., EASTON, J., BARBATO, M. I., MULDER, H. L., MANNE, J., WANG, J., RUSCH, M., RANADE, S., GANTI, R., PARKER, M., MA, J., RADTKE, I., DING, L., CAZZANIGA, G., BIONDI, A., KORNBLAU, S. M., RAVANDI, F., KANTARJIAN, H., NIMER, S. D., DOHNER, K., DOHNER, H., LEY, T. J., BALLERINI, P., SHURTLEFF, S., TOMIZAWA, D., ADACHI, S., HAYASHI, Y., TAWA, A., SHIH, L. Y., LIANG, D. C., RUBNITZ, J. E., PUI, C. H., MARDIS, E. R., WILSON, R. K. & DOWNING, J. R. 2012. An Inv(16)(p13.3q24.3)-encoded CBFA2T3-GLIS2 fusion protein defines an aggressive subtype of pediatric acute megakaryoblastic leukemia. *Cancer Cell,* 22**,** 683-97.

GURALNIK, J. M., EISENSTAEDT, R. S., FERRUCCI, L., KLEIN, H. G. & WOODMAN, R. C. 2004. Prevalence of anemia in persons 65 years and older in the United States: evidence for a high rate of unexplained anemia. *Blood,* 104**,** 2263-8.

GURBUXANI, S., VYAS, P. & CRISPINO, J. D. 2004. Recent insights into the mechanisms of myeloid leukemogenesis in Down syndrome. *Blood,* 103**,** 399-406.

GUZMAN, M. L., NEERING, S. J., UPCHURCH, D., GRIMES, B., HOWARD, D. S., RIZZIERI, D. A., LUGER, S. M. & JORDAN, C. T. 2001. Nuclear factor-kappaB is constitutively activated in primitive human acute myelogenous leukemia cells. *Blood,* 98**,** 2301-7.

HAFERLACH, T., KOHLMANN, A., WIECZOREK, L., BASSO, G., KRONNIE, G. T., BENE, M. C., DE VOS, J., HERNANDEZ, J. M., HOFMANN, W. K., MILLS, K. I., GILKES, A., CHIARETTI, S., SHURTLEFF, S. A., KIPPS, T. J., RASSENTI, L. Z., YEOH, A. E., PAPENHAUSEN, P. R., LIU, W. M., WILLIAMS, P. M. & FOA, R. 2010. Clinical utility of microarray-based gene expression profiling in the diagnosis and subclassification of leukemia: report from the International Microarray Innovations in Leukemia Study Group. *J Clin Oncol,* 28**,** 2529-37.

HAHNEL, P. S., ENDERS, B., SASCA, D., ROOS, W. P., KAINA, B., BULLINGER, L., THEOBALD, M. & KINDLER, T. 2014. Targeting components of the alternative NHEJ pathway sensitizes KRAS mutant leukemic cells to chemotherapy. *Blood,* 123**,** 2355-66.

HAO, Q. L., ZHU, J., PRICE, M. A., PAYNE, K. J., BARSKY, L. W. & CROOKS, G. M. 2001. Identification of a novel, human multilymphoid progenitor in cord blood. *Blood,* 97**,** 3683-90.

HARRISON, C. J., HILLS, R. K., MOORMAN, A. V., GRIMWADE, D. J., HANN, I., WEBB, D. K., WHEATLEY, K., DE GRAAF, S. S., VAN DEN BERG, E., BURNETT, A. K. & GIBSON, B. E. 2010. Cytogenetics of childhood acute myeloid leukemia: United Kingdom Medical Research Council Treatment trials AML 10 and 12. *J Clin Oncol,* 28**,** 2674-81.

HARRISON, D. E. & ASTLE, C. M. 1982. Loss of stem cell repopulating ability upon transplantation. Effects of donor age, cell number, and transplantation procedure. *J Exp Med,* 156**,** 1767-79.

HAYAKAWA, F., TOWATARI, M., KIYOI, H., TANIMOTO, M., KITAMURA, T., SAITO, H. & NAOE, T. 2000. Tandem-duplicated Flt3 constitutively activates STAT5 and MAP kinase and introduces autonomous cell growth in IL-3-dependent cell lines. *Oncogene,* 19**,** 624-31.

HAYLOCK, D. N., WILLIAMS, B., JOHNSTON, H. M., LIU, M. C., RUTHERFORD, K. E., WHITTY, G. A., SIMMONS, P. J., BERTONCELLO, I. & NILSSON, S. K. 2007. Hemopoietic stem cells with higher hemopoietic potential reside at the bone marrow endosteum. *Stem Cells,* 25**,** 1062-9.

HE, S., KIM, I., LIM, M. S. & MORRISON, S. J. 2011. Sox17 expression confers self-renewal potential and fetal stem cell characteristics upon adult hematopoietic progenitors. *Genes Dev,* 25**,** 1613-27.

HEALD, B., HILDEN, J. M., ZBUK, K., NORTON, A., VYAS, P., THEIL, K. S. & ENG, C. 2007. Severe TMD/AMKL with GATA1 mutation in a stillborn fetus with Down syndrome. *Nat Clin Pract Oncol,* 4**,** 433-8.

HIGUCHI, M., O'BRIEN, D., KUMARAVELU, P., LENNY, N., YEOH, E. J. & DOWNING, J. R. 2002. Expression of a conditional AML1-ETO oncogene bypasses embryonic lethality and establishes a murine model of human t(8;21) acute myeloid leukemia. *Cancer Cell,* 1**,** 63-74.

HILLS, R. K., CASTAIGNE, S., APPELBAUM, F. R., DELAUNAY, J., PETERSDORF, S., OTHUS, M., ESTEY, E. H., DOMBRET, H., CHEVRET, S., IFRAH, N., CAHN, J. Y., RECHER, C., CHILTON, L., MOORMAN, A. V. & BURNETT, A. K. 2014. Addition of gemtuzumab ozogamicin to induction chemotherapy in adult patients with acute myeloid leukaemia: a meta-analysis of individual patient data from randomised controlled trials. *Lancet Oncol,* 15**,** 986-96.

HIYAMA, K., HIRAI, Y., KYOIZUMI, S., AKIYAMA, M., HIYAMA, E., PIATYSZEK, M. A., SHAY, J. W., ISHIOKA, S. & YAMAKIDO, M. 1995. Activation of telomerase

in human lymphocytes and hematopoietic progenitor cells. *J Immunol,* 155**,** 3711-5.

HO, P. A., ALONZO, T. A., GERBING, R. B., POLLARD, J., STIREWALT, D. L., HURWITZ, C., HEEREMA, N. A., HIRSCH, B., RAIMONDI, S. C., LANGE, B., FRANKLIN, J. L., RADICH, J. P. & MESHINCHI, S. 2009. Prevalence and prognostic implications of CEBPA mutations in pediatric acute myeloid leukemia (AML): a report from the Children's Oncology Group. *Blood,* 113**,** 6558-66.

HO, P. A., KUTNY, M. A., ALONZO, T. A., GERBING, R. B., JOAQUIN, J., RAIMONDI, S. C., GAMIS, A. S. & MESHINCHI, S. 2011. Leukemic mutations in the methylation-associated genes DNMT3A and IDH2 are rare events in pediatric AML: a report from the Children's Oncology Group. *Pediatr Blood Cancer,* 57**,** 204-9.

HOCK, H., HAMBLEN, M. J., ROOKE, H. M., SCHINDLER, J. W., SALEQUE, S., FUJIWARA, Y. & ORKIN, S. H. 2004a. Gfi-1 restricts proliferation and preserves functional integrity of haematopoietic stem cells. *Nature,* 431**,** 1002-7.

HOCK, H., MEADE, E., MEDEIROS, S., SCHINDLER, J. W., VALK, P. J., FUJIWARA, Y. & ORKIN, S. H. 2004b. Tel/Etv6 is an essential and selective regulator of adult hematopoietic stem cell survival. *Genes Dev,* 18**,** 2336-41.

HOEBEKE, I., DE SMEDT, M., STOLZ, F., PIKE-OVERZET, K., STAAL, F. J., PLUM, J. & LECLERCQ, G. 2007. T-, B- and NK-lymphoid, but not myeloid cells arise from human CD34(+)CD38(-)CD7(+) common lymphoid progenitors expressing lymphoid-specific genes. *Leukemia,* 21**,** 311-9.

HOFMANN, I., STOVER, E. H., CULLEN, D. E., MAO, J., MORGAN, K. J., LEE, B. H., KHARAS, M. G., MILLER, P. G., CORNEJO, M. G., OKABE, R., ARMSTRONG, S. A., GHILARDI, N., GOULD, S., DE SAUVAGE, F. J., MCMAHON, A. P. & GILLILAND, D. G. 2009. Hedgehog signaling is dispensable for adult murine hematopoietic stem cell function and hematopoiesis. *Cell Stem Cell,* 4**,** 559-67.

HOFMANN, J. W., ZHAO, X., DE CECCO, M., PETERSON, A. L., PAGLIAROLI, L., MANIVANNAN, J., HUBBARD, G. B., IKENO, Y., ZHANG, Y., FENG, B., LI, X., SERRE, T., QI, W., VAN REMMEN, H., MILLER, R. A., BATH, K. G., DE CABO, R., XU, H., NERETTI, N. & SEDIVY, J. M. 2015. Reduced expression of MYC increases longevity and enhances healthspan. *Cell,* 160**,** 477-88.

HOLLAND, I. B. & BLIGHT, M. A. 1999. ABC-ATPases, adaptable energy generators fuelling transmembrane movement of a variety of molecules in organisms from bacteria to humans. *J Mol Biol,* 293**,** 381-99.

HOLLINK, I. H., FENG, Q., DANEN-VAN OORSCHOT, A. A., ARENTSEN-PETERS, S. T., VERBOON, L. J., ZHANG, P., DE HAAS, V., REINHARDT, D., CREUTZIG, U., TRKA, J., PIETERS, R., VAN DEN HEUVEL-EIBRINK, M. M., WANG, J. & ZWAAN, C. M. 2012. Low frequency of DNMT3A mutations in pediatric AML, and the identification of the OCI-AML3 cell line as an in vitro model. *Leukemia,* 26**,** 371-3.

HOLLINK, I. H., VAN DEN HEUVEL-EIBRINK, M. M., ARENTSEN-PETERS, S. T., PRATCORONA, M., ABBAS, S., KUIPERS, J. E., VAN GALEN, J. F., BEVERLOO, H. B., SONNEVELD, E., KASPERS, G. J., TRKA, J., BARUCHEL, A., ZIMMERMANN, M., CREUTZIG, U., REINHARDT, D., PIETERS, R., VALK, P. J. & ZWAAN, C. M. 2011. NUP98/NSD1 characterizes a novel poor prognostic group in acute myeloid leukemia with a distinct HOX gene expression pattern. *Blood,* 118**,** 3645-56.

HOLLINK, I. H., ZWAAN, C. M., ZIMMERMANN, M., ARENTSEN-PETERS, T. C., PIETERS, R., CLOOS, J., KASPERS, G. J., DE GRAAF, S. S., HARBOTT, J.,

CREUTZIG, U., REINHARDT, D., VAN DEN HEUVEL-EIBRINK, M. M. & THIEDE, C. 2009. Favorable prognostic impact of NPM1 gene mutations in childhood acute myeloid leukemia, with emphasis on cytogenetically normal AML. *Leukemia,* 23**,** 262-70.

HOLYOAKE, T. L., NICOLINI, F. E. & EAVES, C. J. 1999. Functional differences between transplantable human hematopoietic stem cells from fetal liver, cord blood, and adult marrow. *Exp Hematol,* 27**,** 1418-27.

HOPE, K. J., JIN, L. & DICK, J. E. 2004. Acute myeloid leukemia originates from a hierarchy of leukemic stem cell classes that differ in self-renewal capacity. *Nat Immunol,* 5**,** 738-43.

HORAK, C. E. & SNYDER, M. 2002. ChIP-chip: a genomic approach for identifying transcription factor binding sites. *Methods Enzymol,* 350**,** 469-83.

HORTON, S. J., JAQUES, J., WOOLTHUIS, C., VAN DIJK, J., MESURACA, M., HULS, G., MORRONE, G., VELLENGA, E. & SCHURINGA, J. J. 2013. MLL-AF9-mediated immortalization of human hematopoietic cells along different lineages changes during ontogeny. *Leukemia,* 27**,** 1116-26.

HOUSSAINT, E. 1981. Differentiation of the mouse hepatic primordium. II. Extrinsic origin of the haemopoietic cell line. *Cell Differ,* 10**,** 243-52.

HOWLADER N, N. A., KRAPCHO M, GARSHELL J, MILLER D, ALTEKRUSE SF, KOSARY CL, YU M, RUHL J, TATALOVICH Z,MARIOTTO A, LEWIS DR, CHEN HS, FEUER EJ, CRONIN KA (EDS). 2014. *SEER Cancer Statistics Review, 1975-2011* [Online]. Bethesda, MD: National Cancer Institute. . Available: http://seer.cancer.gov/csr/1975_2011/ [Accessed 5th September 2014 2014].

HUANG DA, W., SHERMAN, B. T. & LEMPICKI, R. A. 2009a. Systematic and integrative analysis of large gene lists using DAVID bioinformatics resources. *Nat Protoc,* 4**,** 44-57.

HUANG DA, W., SHERMAN, B. T., ZHENG, X., YANG, J., IMAMICHI, T., STEPHENS, R. & LEMPICKI, R. A. 2009b. Extracting biological meaning from large gene lists with DAVID. *Curr Protoc Bioinformatics,* Chapter 13**,** Unit 13 11.

HUANG, S. Y., TANG, J. L., LIANG, Y. J., WANG, C. H., CHEN, Y. C. & TIEN, H. F. 1997. Clinical, haematological and molecular studies in patients with chromosome translocation t(7;11): a study of four Chinese patients in Taiwan. *Br J Haematol,* 96**,** 682-7.

HUNTLY, B. J., SHIGEMATSU, H., DEGUCHI, K., LEE, B. H., MIZUNO, S., DUCLOS, N., ROWAN, R., AMARAL, S., CURLEY, D., WILLIAMS, I. R., AKASHI, K. & GILLILAND, D. G. 2004. MOZ-TIF2, but not BCR-ABL, confers properties of leukemic stem cells to committed murine hematopoietic progenitors. *Cancer Cell,* 6**,** 587-96.

IKUTA, K. & WEISSMAN, I. L. 1992. Evidence that hematopoietic stem cells express mouse c-kit but do not depend on steel factor for their generation. *Proc Natl Acad Sci U S A,* 89**,** 1502-6.

INABA, H., RUBNITZ, J. E., COUSTAN-SMITH, E., LI, L., FURMANSKI, B. D., MASCARA, G. P., HEYM, K. M., CHRISTENSEN, R., ONCIU, M., SHURTLEFF, S. A., POUNDS, S. B., PUI, C. H., RIBEIRO, R. C., CAMPANA, D. & BAKER, S. D. 2011. Phase I pharmacokinetic and pharmacodynamic study of the multikinase inhibitor sorafenib in combination with clofarabine and cytarabine in pediatric relapsed/refractory leukemia. *J Clin Oncol,* 29**,** 3293-300.

ISHIKAWA, F., YOSHIDA, S., SAITO, Y., HIJIKATA, A., KITAMURA, H., TANAKA, S., NAKAMURA, R., TANAKA, T., TOMIYAMA, H., SAITO, N., FUKATA, M., MIYAMOTO, T., LYONS, B., OHSHIMA, K., UCHIDA, N., TANIGUCHI, S., OHARA, O., AKASHI, K., HARADA, M. & SHULTZ, L. D. 2007. Chemotherapy-resistant

human AML stem cells home to and engraft within the bone-marrow endosteal region. *Nat Biotechnol*, 25**,** 1315-21.

ITO, S., BARRETT, A. J., DUTRA, A., PAK, E., MINER, S., KEYVANFAR, K., HENSEL, N. F., REZVANI, K., MURANSKI, P., LIU, P., LAROCHELLE, A. & MELENHORST, J. J. 2015. Long term maintenance of myeloid leukemic stem cells cultured with unrelated human mesenchymal stromal cells. *Stem Cell Res,* 14**,** 95-104.

IVANOVA, N. B., DIMOS, J. T., SCHANIEL, C., HACKNEY, J. A., MOORE, K. A. & LEMISCHKA, I. R. 2002. A stem cell molecular signature. *Science,* 298**,** 601-4.

IVEY, A., HILLS, R. K., SIMPSON, M. A., JOVANOVIC, J. V., GILKES, A., GRECH, A., PATEL, Y., BHUDIA, N., FARAH, H., MASON, J., WALL, K., AKIKI, S., GRIFFITHS, M., SOLOMON, E., MCCAUGHAN, F., LINCH, D. C., GALE, R. E., VYAS, P., FREEMAN, S. D., RUSSELL, N., BURNETT, A. K., GRIMWADE, D. & GROUP, U. K. N. C. R. I. A. W. 2016. Assessment of Minimal Residual Disease in Standard-Risk AML. *N Engl J Med,* 374**,** 422-33.

IWASAKI, H., MIZUNO, S., ARINOBU, Y., OZAWA, H., MORI, Y., SHIGEMATSU, H., TAKATSU, K., TENEN, D. G. & AKASHI, K. 2006. The order of expression of transcription factors directs hierarchical specification of hematopoietic lineages. *Genes Dev,* 20**,** 3010-21.

IWASAKI, M., KUWATA, T., YAMAZAKI, Y., JENKINS, N. A., COPELAND, N. G., OSATO, M., ITO, Y., KROON, E., SAUVAGEAU, G. & NAKAMURA, T. 2005. Identification of cooperative genes for NUP98-HOXA9 in myeloid leukemogenesis using a mouse model. *Blood,* 105**,** 784-93.

JAISWAL, S., FONTANILLAS, P., FLANNICK, J., MANNING, A., GRAUMAN, P. V., MAR, B. G., LINDSLEY, R. C., MERMEL, C. H., BURTT, N., CHAVEZ, A., HIGGINS, J. M., MOLTCHANOV, V., KUO, F. C., KLUK, M. J., HENDERSON, B., KINNUNEN, L., KOISTINEN, H. A., LADENVALL, C., GETZ, G., CORREA, A., BANAHAN, B. F., GABRIEL, S., KATHIRESAN, S., STRINGHAM, H. M., MCCARTHY, M. I., BOEHNKE, M., TUOMILEHTO, J., HAIMAN, C., GROOP, L., ATZMON, G., WILSON, J. G., NEUBERG, D., ALTSHULER, D. & EBERT, B. L. 2014. Age-related clonal hematopoiesis associated with adverse outcomes. *N Engl J Med,* 371**,** 2488-98.

JAN, M., SNYDER, T. M., CORCES-ZIMMERMAN, M. R., VYAS, P., WEISSMAN, I. L., QUAKE, S. R. & MAJETI, R. 2012. Clonal evolution of preleukemic hematopoietic stem cells precedes human acute myeloid leukemia. *Sci Transl Med,* 4**,** 149ra118.

JANZER, A., GERMAN, N. J., GONZALEZ-HERRERA, K. N., ASARA, J. M., HAIGIS, M. C. & STRUHL, K. 2014. Metformin and phenformin deplete tricarboxylic acid cycle and glycolytic intermediates during cell transformation and NTPs in cancer stem cells. *Proc Natl Acad Sci U S A,* 111**,** 10574-9.

JARRIAULT, S., BROU, C., LOGEAT, F., SCHROETER, E. H., KOPAN, R. & ISRAEL, A. 1995. Signalling downstream of activated mammalian Notch. *Nature,* 377**,** 355-8.

JIANG, H., LIN, J., SU, Z. Z., COLLART, F. R., HUBERMAN, E. & FISHER, P. B. 1994. Induction of differentiation in human promyelocytic HL-60 leukemia cells activates p21, WAF1/CIP1, expression in the absence of p53. *Oncogene,* 9**,** 3397-406.

JIN, L., HOPE, K. J., ZHAI, Q., SMADJA-JOFFE, F. & DICK, J. E. 2006. Targeting of CD44 eradicates human acute myeloid leukemic stem cells. *Nat Med,* 12**,** 1167-74.

JOHNSON, J. J., CHEN, W., HUDSON, W., YAO, Q., TAYLOR, M., RABBITTS, T. H. & KERSEY, J. H. 2003. Prenatal and postnatal myeloid cells demonstrate

stepwise progression in the pathogenesis of MLL fusion gene leukemia. *Blood,* 101**,** 3229-35.

JOHNSON, P. F. 2005. Molecular stop signs: regulation of cell-cycle arrest by C/EBP transcription factors. *J Cell Sci,* 118**,** 2545-55.

JORDAN, C. T., UPCHURCH, D., SZILVASSY, S. J., GUZMAN, M. L., HOWARD, D. S., PETTIGREW, A. L., MEYERROSE, T., ROSSI, R., GRIMES, B., RIZZIERI, D. A., LUGER, S. M. & PHILLIPS, G. L. 2000. The interleukin-3 receptor alpha chain is a unique marker for human acute myelogenous leukemia stem cells. *Leukemia,* 14**,** 1777-84.

JULIUSSON, G., ANTUNOVIC, P., DEROLF, A., LEHMANN, S., MOLLGARD, L., STOCKELBERG, D., TIDEFELT, U., WAHLIN, A. & HOGLUND, M. 2009. Age and acute myeloid leukemia: real world data on decision to treat and outcomes from the Swedish Acute Leukemia Registry. *Blood,* 113**,** 4179-87.

KALVERDA, B., PICKERSGILL, H., SHLOMA, V. V. & FORNEROD, M. 2010. Nucleoporins directly stimulate expression of developmental and cell-cycle genes inside the nucleoplasm. *Cell,* 140**,** 360-71.

KANNAN, S., SUTPHIN, R. M., HALL, M. G., GOLFMAN, L. S., FANG, W., NOLO, R. M., AKERS, L. J., HAMMITT, R. A., MCMURRAY, J. S., KORNBLAU, S. M., MELNICK, A. M., FIGUEROA, M. E. & ZWEIDLER-MCKAY, P. A. 2013. Notch activation inhibits AML growth and survival: a potential therapeutic approach. *J Exp Med,* 210**,** 321-37.

KASPER, L. H., BRINDLE, P. K., SCHNABEL, C. A., PRITCHARD, C. E., CLEARY, M. L. & VAN DEURSEN, J. M. 1999. CREB binding protein interacts with nucleoporin-specific FG repeats that activate transcription and mediate NUP98-HOXA9 oncogenicity. *Mol Cell Biol,* 19**,** 764-76.

KASPERS, G. J., ZIMMERMANN, M., REINHARDT, D., GIBSON, B. E., TAMMINGA, R. Y., ALEINIKOVA, O., ARMENDARIZ, H., DWORZAK, M., HA, S. Y., HASLE, H., HOVI, L., MASCHAN, A., BERTRAND, Y., LEVERGER, G. G., RAZZOUK, B. I., RIZZARI, C., SMISEK, P., SMITH, O., STARK, B. & CREUTZIG, U. 2013. Improved outcome in pediatric relapsed acute myeloid leukemia: results of a randomized trial on liposomal daunorubicin by the International BFM Study Group. *J Clin Oncol,* 31**,** 599-607.

KATAYAMA, Y., BATTISTA, M., KAO, W. M., HIDALGO, A., PEIRED, A. J., THOMAS, S. A. & FRENETTE, P. S. 2006. Signals from the sympathetic nervous system regulate hematopoietic stem cell egress from bone marrow. *Cell,* 124**,** 407-21.

KELLY, L. M., LIU, Q., KUTOK, J. L., WILLIAMS, I. R., BOULTON, C. L. & GILLILAND, D. G. 2002. FLT3 internal tandem duplication mutations associated with human acute myeloid leukemias induce myeloproliferative disease in a murine bone marrow transplant model. *Blood,* 99**,** 310-8.

KENT, D., DYKSTRA, B. & EAVES, C. 2007. Isolation and assessment of long-term reconstituting hematopoietic stem cells from adult mouse bone marrow. *Curr Protoc Stem Cell Biol,* Chapter 2**,** Unit 2A 4.

KENT, D. G., COPLEY, M. R., BENZ, C., WOHRER, S., DYKSTRA, B. J., MA, E., CHEYNE, J., ZHAO, Y., BOWIE, M. B., ZHAO, Y., GASPARETTO, M., DELANEY, A., SMITH, C., MARRA, M. & EAVES, C. J. 2009. Prospective isolation and molecular characterization of hematopoietic stem cells with durable self-renewal potential. *Blood,* 113**,** 6342-50.

KESSEL, M. & GRUSS, P. 1990. Murine developmental control genes. *Science,* 249**,** 374-9.

KIEL, M. J., YILMAZ, O. H., IWASHITA, T., TERHORST, C. & MORRISON, S. J. 2005. SLAM family receptors distinguish hematopoietic stem and progenitor cells and reveal endothelial niches for stem cells. *Cell,* 121**,** 1109-21.

KIHARA, R., NAGATA, Y., KIYOI, H., KATO, T., YAMAMOTO, E., SUZUKI, K., CHEN, F., ASOU, N., OHTAKE, S., MIYAWAKI, S., MIYAZAKI, Y., SAKURA, T., OZAWA, Y., USUI, N., KANAMORI, H., KIGUCHI, T., IMAI, K., UIKE, N., KIMURA, F., KITAMURA, K., NAKASEKO, C., ONIZUKA, M., TAKESHITA, A., ISHIDA, F., SUZUSHIMA, H., KATO, Y., MIWA, H., SHIRAISHI, Y., CHIBA, K., TANAKA, H., MIYANO, S., OGAWA, S. & NAOE, T. 2014. Comprehensive analysis of genetic alterations and their prognostic impacts in adult acute myeloid leukemia patients. *Leukemia,* 28**,** 1586-95.

KIKUCHI, K. & KONDO, M. 2006. Developmental switch of mouse hematopoietic stem cells from fetal to adult type occurs in bone marrow after birth. *Proc Natl Acad Sci U S A,* 103**,** 17852-7.

KILBORN, S. H., TRUDEL, G. & UHTHOFF, H. 2002. Review of growth plate closure compared with age at sexual maturity and lifespan in laboratory animals. *Contemp Top Lab Anim Sci,* 41**,** 21-6.

KIM, I., SAUNDERS, T. L. & MORRISON, S. J. 2007. Sox17 dependence distinguishes the transcriptional regulation of fetal from adult hematopoietic stem cells. *Cell,* 130**,** 470-83.

KIYOI, H., TOWATARI, M., YOKOTA, S., HAMAGUCHI, M., OHNO, R., SAITO, H. & NAOE, T. 1998. Internal tandem duplication of the FLT3 gene is a novel modality of elongation mutation which causes constitutive activation of the product. *Leukemia,* 12**,** 1333-7.

KLIMMECK, D., HANSSON, J., RAFFEL, S., VAKHRUSHEV, S. Y., TRUMPP, A. & KRIJGSVELD, J. 2012. Proteomic cornerstones of hematopoietic stem cell differentiation: distinct signatures of multipotent progenitors and myeloid committed cells. *Mol Cell Proteomics,* 11**,** 286-302.

KLUSMANN, J. H., CREUTZIG, U., ZIMMERMANN, M., DWORZAK, M., JORCH, N., LANGEBRAKE, C., PEKRUN, A., MACAKOVA-REINHARDT, K. & REINHARDT, D. 2008. Treatment and prognostic impact of transient leukemia in neonates with Down syndrome. *Blood,* 111**,** 2991-8.

KOCABAS, F., ZHENG, J., THET, S., COPELAND, N. G., JENKINS, N. A., DEBERARDINIS, R. J., ZHANG, C. & SADEK, H. A. 2012. Meis1 regulates the metabolic phenotype and oxidant defense of hematopoietic stem cells. *Blood,* 120**,** 4963-72.

KODE, A., MANAVALAN, J. S., MOSIALOU, I., BHAGAT, G., RATHINAM, C. V., LUO, N., KHIABANIAN, H., LEE, A., MURTY, V. V., FRIEDMAN, R., BRUM, A., PARK, D., GALILI, N., MUKHERJEE, S., TERUYA-FELDSTEIN, J., RAZA, A., RABADAN, R., BERMAN, E. & KOUSTENI, S. 2014. Leukaemogenesis induced by an activating beta-catenin mutation in osteoblasts. *Nature,* 506**,** 240-4.

KOHLER, A., SCHMITHORST, V., FILIPPI, M. D., RYAN, M. A., DARIA, D., GUNZER, M. & GEIGER, H. 2009. Altered cellular dynamics and endosteal location of aged early hematopoietic progenitor cells revealed by time-lapse intravital imaging in long bones. *Blood,* 114**,** 290-8.

KOHLER, G. & MILSTEIN, C. 1975. Continuous cultures of fused cells secreting antibody of predefined specificity. *Nature,* 256**,** 495-7.

KOLLET, O., DAR, A., SHIVTIEL, S., KALINKOVICH, A., LAPID, K., SZTAINBERG, Y., TESIO, M., SAMSTEIN, R. M., GOICHBERG, P., SPIEGEL, A., ELSON, A. & LAPIDOT, T. 2006. Osteoclasts degrade endosteal components and promote mobilization of hematopoietic progenitor cells. *Nat Med,* 12**,** 657-64.

KONDO, M., SCHERER, D. C., MIYAMOTO, T., KING, A. G., AKASHI, K., SUGAMURA, K. & WEISSMAN, I. L. 2000. Cell-fate conversion of lymphoid-committed progenitors by instructive actions of cytokines. *Nature,* 407**,** 383-6.

KONI, P. A., JOSHI, S. K., TEMANN, U. A., OLSON, D., BURKLY, L. & FLAVELL, R. A. 2001. Conditional vascular cell adhesion molecule 1 deletion in mice: impaired lymphocyte migration to bone marrow. *J Exp Med,* 193**,** 741-54.

KOTTARIDIS, P. D., GALE, R. E., FREW, M. E., HARRISON, G., LANGABEER, S. E., BELTON, A. A., WALKER, H., WHEATLEY, K., BOWEN, D. T., BURNETT, A. K., GOLDSTONE, A. H. & LINCH, D. C. 2001. The presence of a FLT3 internal tandem duplication in patients with acute myeloid leukemia (AML) adds important prognostic information to cytogenetic risk group and response to the first cycle of chemotherapy: analysis of 854 patients from the United Kingdom Medical Research Council AML 10 and 12 trials. *Blood,* 98**,** 1752-9.

KOZBOR, D. & CROCE, C. M. 1984. Amplification of the c-myc oncogene in one of five human breast carcinoma cell lines. *Cancer Res,* 44**,** 438-41.

KRISHNAMURTHY, P., ROSS, D. D., NAKANISHI, T., BAILEY-DELL, K., ZHOU, S., MERCER, K. E., SARKADI, B., SORRENTINO, B. P. & SCHUETZ, J. D. 2004. The stem cell marker Bcrp/ABCG2 enhances hypoxic cell survival through interactions with heme. *J Biol Chem,* 279**,** 24218-25.

KRIVTSOV, A. V., FIGUEROA, M. E., SINHA, A. U., STUBBS, M. C., FENG, Z., VALK, P. J., DELWEL, R., DOHNER, K., BULLINGER, L., KUNG, A. L., MELNICK, A. M. & ARMSTRONG, S. A. 2013. Cell of origin determines clinically relevant subtypes of MLL-rearranged AML. *Leukemia,* 27**,** 852-60.

KRIVTSOV, A. V., TWOMEY, D., FENG, Z., STUBBS, M. C., WANG, Y., FABER, J., LEVINE, J. E., WANG, J., HAHN, W. C., GILLILAND, D. G., GOLUB, T. R. & ARMSTRONG, S. A. 2006. Transformation from committed progenitor to leukaemia stem cell initiated by MLL-AF9. *Nature,* 442**,** 818-22.

KROON, E., THORSTEINSDOTTIR, U., MAYOTTE, N., NAKAMURA, T. & SAUVAGEAU, G. 2001. NUP98-HOXA9 expression in hemopoietic stem cells induces chronic and acute myeloid leukemias in mice. *EMBO J,* 20**,** 350-61.

KUMARAVELU, P., HOOK, L., MORRISON, A. M., URE, J., ZHAO, S., ZUYEV, S., ANSELL, J. & MEDVINSKY, A. 2002. Quantitative developmental anatomy of definitive haematopoietic stem cells/long-term repopulating units (HSC/RUs): role of the aorta-gonad-mesonephros (AGM) region and the yolk sac in colonisation of the mouse embryonic liver. *Development,* 129**,** 4891-9.

KVINLAUG, B. T., CHAN, W. I., BULLINGER, L., RAMASWAMI, M., SEARS, C., FOSTER, D., LAZIC, S. E., OKABE, R., BENNER, A., LEE, B. H., DE SILVA, I., VALK, P. J., DELWEL, R., ARMSTRONG, S. A., DOHNER, H., GILLILAND, D. G. & HUNTLY, B. J. 2011. Common and overlapping oncogenic pathways contribute to the evolution of acute myeloid leukemias. *Cancer Res,* 71**,** 4117-29.

KWONG, Y. L. & PANG, A. 1999. Low frequency of rearrangements of the homeobox gene HOXA9/t(7;11) in adult acute myeloid leukemia. *Genes Chromosomes Cancer,* 25**,** 70-4.

LAIOSA, C. V., STADTFELD, M., XIE, H., DE ANDRES-AGUAYO, L. & GRAF, T. 2006. Reprogramming of committed T cell progenitors to macrophages and dendritic cells by C/EBP alpha and PU.1 transcription factors. *Immunity,* 25**,** 731-44.

LAVAU, C., SZILVASSY, S. J., SLANY, R. & CLEARY, M. L. 1997. Immortalization and leukemic transformation of a myelomonocytic precursor by retrovirally transduced HRX-ENL. *EMBO J,* 16**,** 4226-37.

LAWRENCE, H. J., HELGASON, C. D., SAUVAGEAU, G., FONG, S., IZON, D. J., HUMPHRIES, R. K. & LARGMAN, C. 1997. Mice bearing a targeted interruption of the homeobox gene HOXA9 have defects in myeloid, erythroid, and lymphoid hematopoiesis. *Blood,* 89**,** 1922-30.

LEE, B. H., TOTHOVA, Z., LEVINE, R. L., ANDERSON, K., BUZA-VIDAS, N., CULLEN, D. E., MCDOWELL, E. P., ADELSPERGER, J., FROHLING, S., HUNTLY, B. J., BERAN, M., JACOBSEN, S. E. & GILLILAND, D. G. 2007. FLT3 mutations confer enhanced proliferation and survival properties to multipotent progenitors in a murine model of chronic myelomonocytic leukemia. *Cancer Cell,* 12**,** 367-80.

LEE, B. H., WILLIAMS, I. R., ANASTASIADOU, E., BOULTON, C. L., JOSEPH, S. W., AMARAL, S. M., CURLEY, D. P., DUCLOS, N., HUNTLY, B. J., FABBRO, D., GRIFFIN, J. D. & GILLILAND, D. G. 2005. FLT3 internal tandem duplication mutations induce myeloproliferative or lymphoid disease in a transgenic mouse model. *Oncogene,* 24**,** 7882-92.

LEEMHUIS, T., YODER, M. C., GRIGSBY, S., AGUERO, B., EDER, P. & SROUR, E. F. 1996. Isolation of primitive human bone marrow hematopoietic progenitor cells using Hoechst 33342 and Rhodamine 123. *Exp Hematol,* 24**,** 1215-24.

LEY, T. J., DING, L., WALTER, M. J., MCLELLAN, M. D., LAMPRECHT, T., LARSON, D. E., KANDOTH, C., PAYTON, J. E., BATY, J., WELCH, J., HARRIS, C. C., LICHTI, C. F., TOWNSEND, R. R., FULTON, R. S., DOOLING, D. J., KOBOLDT, D. C., SCHMIDT, H., ZHANG, Q., OSBORNE, J. R., LIN, L., O'LAUGHLIN, M., MCMICHAEL, J. F., DELEHAUNTY, K. D., MCGRATH, S. D., FULTON, L. A., MAGRINI, V. J., VICKERY, T. L., HUNDAL, J., COOK, L. L., CONYERS, J. J., SWIFT, G. W., REED, J. P., ALLDREDGE, P. A., WYLIE, T., WALKER, J., KALICKI, J., WATSON, M. A., HEATH, S., SHANNON, W. D., VARGHESE, N., NAGARAJAN, R., WESTERVELT, P., TOMASSON, M. H., LINK, D. C., GRAUBERT, T. A., DIPERSIO, J. F., MARDIS, E. R. & WILSON, R. K. 2010. DNMT3A mutations in acute myeloid leukemia. *N Engl J Med,* 363**,** 2424-33.

LEY, T. J., MARDIS, E. R., DING, L., FULTON, B., MCLELLAN, M. D., CHEN, K., DOOLING, D., DUNFORD-SHORE, B. H., MCGRATH, S., HICKENBOTHAM, M., COOK, L., ABBOTT, R., LARSON, D. E., KOBOLDT, D. C., POHL, C., SMITH, S., HAWKINS, A., ABBOTT, S., LOCKE, D., HILLIER, L. W., MINER, T., FULTON, L., MAGRINI, V., WYLIE, T., GLASSCOCK, J., CONYERS, J., SANDER, N., SHI, X., OSBORNE, J. R., MINX, P., GORDON, D., CHINWALLA, A., ZHAO, Y., RIES, R. E., PAYTON, J. E., WESTERVELT, P., TOMASSON, M. H., WATSON, M., BATY, J., IVANOVICH, J., HEATH, S., SHANNON, W. D., NAGARAJAN, R., WALTER, M. J., LINK, D. C., GRAUBERT, T. A., DIPERSIO, J. F. & WILSON, R. K. 2008. DNA sequencing of a cytogenetically normal acute myeloid leukaemia genome. *Nature,* 456**,** 66-72.

LI, L., PILOTO, O., KIM, K. T., YE, Z., NGUYEN, H. B., YU, X., LEVIS, M., CHENG, L. & SMALL, D. 2007. FLT3/ITD expression increases expansion, survival and entry into cell cycle of human haematopoietic stem/progenitor cells. *Br J Haematol,* 137**,** 64-75.

LI, L., PILOTO, O., NGUYEN, H. B., GREENBERG, K., TAKAMIYA, K., RACKE, F., HUSO, D. & SMALL, D. 2008. Knock-in of an internal tandem duplication mutation into murine FLT3 confers myeloproliferative disease in a mouse model. *Blood,* 111**,** 3849-58.

LIANG, D. C., LIU, H. C., YANG, C. P., JAING, T. H., HUNG, I. J., YEH, T. C., CHEN, S. H., HOU, J. Y., HUANG, Y. J., SHIH, Y. S., HUANG, Y. H., LIN, T. H. & SHIH, L. Y. 2013. Cooperating gene mutations in childhood acute myeloid leukemia with special reference on mutations of ASXL1, TET2, IDH1, IDH2, and DNMT3A. *Blood,* 121**,** 2988-95.

LIANG, Y., VAN ZANT, G. & SZILVASSY, S. J. 2005. Effects of aging on the homing and engraftment of murine hematopoietic stem and progenitor cells. *Blood,* 106**,** 1479-87.

LIESCHKE, G. J., GRAIL, D., HODGSON, G., METCALF, D., STANLEY, E., CHEERS, C., FOWLER, K. J., BASU, S., ZHAN, Y. F. & DUNN, A. R. 1994. Mice lacking granulocyte colony-stimulating factor have chronic neutropenia, granulocyte and macrophage progenitor cell deficiency, and impaired neutrophil mobilization. *Blood,* 84**,** 1737-46.

LO CELSO, C., FLEMING, H. E., WU, J. W., ZHAO, C. X., MIAKE-LYE, S., FUJISAKI, J., COTE, D., ROWE, D. W., LIN, C. P. & SCADDEN, D. T. 2009. Live-animal tracking of individual haematopoietic stem/progenitor cells in their niche. *Nature,* 457**,** 92-6.

LO-COCO, F., AVVISATI, G., VIGNETTI, M., THIEDE, C., ORLANDO, S. M., IACOBELLI, S., FERRARA, F., FAZI, P., CICCONI, L., DI BONA, E., SPECCHIA, G., SICA, S., DIVONA, M., LEVIS, A., FIEDLER, W., CERQUI, E., BRECCIA, M., FIORITONI, G., SALIH, H. R., CAZZOLA, M., MELILLO, L., CARELLA, A. M., BRANDTS, C. H., MORRA, E., VON LILIENFELD-TOAL, M., HERTENSTEIN, B., WATTAD, M., LUBBERT, M., HANEL, M., SCHMITZ, N., LINK, H., KROPP, M. G., RAMBALDI, A., LA NASA, G., LUPPI, M., CICERI, F., FINIZIO, O., VENDITTI, A., FABBIANO, F., DOHNER, K., SAUER, M., GANSER, A., AMADORI, S., MANDELLI, F., DOHNER, H., EHNINGER, G., SCHLENK, R. F., PLATZBECKER, U., GRUPPO ITALIANO MALATTIE EMATOLOGICHE, D. A., GERMAN-AUSTRIAN ACUTE MYELOID LEUKEMIA STUDY, G. & STUDY ALLIANCE, L. 2013. Retinoic acid and arsenic trioxide for acute promyelocytic leukemia. *N Engl J Med,* 369**,** 111-21.

LUGTHART, S., VAN DRUNEN, E., VAN NORDEN, Y., VAN HOVEN, A., ERPELINCK, C. A., VALK, P. J., BEVERLOO, H. B., LOWENBERG, B. & DELWEL, R. 2008. High EVI1 levels predict adverse outcome in acute myeloid leukemia: prevalence of EVI1 overexpression and chromosome 3q26 abnormalities underestimated. *Blood,* 111**,** 4329-37.

LUKASIK, S. M., ZHANG, L., CORPORA, T., TOMANICEK, S., LI, Y., KUNDU, M., HARTMAN, K., LIU, P. P., LAUE, T. M., BILTONEN, R. L., SPECK, N. A. & BUSHWELLER, J. H. 2002. Altered affinity of CBF beta-SMMHC for Runx1 explains its role in leukemogenesis. *Nat Struct Biol,* 9**,** 674-9.

LYMPERI, S., ERSEK, A., FERRARO, F., DAZZI, F. & HORWOOD, N. J. 2011. Inhibition of osteoclast function reduces hematopoietic stem cell numbers in vivo. *Blood,* 117**,** 1540-9.

LYONS, A. B. & PARISH, C. R. 1994. Determination of lymphocyte division by flow cytometry. *J Immunol Methods,* 171**,** 131-7.

MA, Q., JONES, D., BORGHESANI, P. R., SEGAL, R. A., NAGASAWA, T., KISHIMOTO, T., BRONSON, R. T. & SPRINGER, T. A. 1998. Impaired B-lymphopoiesis, myelopoiesis, and derailed cerebellar neuron migration in CXCR4- and SDF-1-deficient mice. *Proc Natl Acad Sci U S A,* 95**,** 9448-53.

MACKAREHTSCHIAN, K., HARDIN, J. D., MOORE, K. A., BOAST, S., GOFF, S. P. & LEMISCHKA, I. R. 1995. Targeted disruption of the flk2/flt3 gene leads to deficiencies in primitive hematopoietic progenitors. *Immunity,* 3**,** 147-61.

MAGEE, J. A., IKENOUE, T., NAKADA, D., LEE, J. Y., GUAN, K. L. & MORRISON, S. J. 2012. Temporal changes in PTEN and mTORC2 regulation of hematopoietic stem cell self-renewal and leukemia suppression. *Cell Stem Cell,* 11**,** 415-28.

MALLO, M., WELLIK, D. M. & DESCHAMPS, J. 2010. Hox genes and regional patterning of the vertebrate body plan. *Dev Biol,* 344**,** 7-15.

MAN, N., SUN, X. J., TAN, Y., GARCIA-CAO, M., LIU, F., CHENG, G., HATLEN, M., XU, H., SHAH, R., CHASTAIN, N., LIU, N., HUANG, G., ZHOU, Y., SHENG, M., SONG, J., YANG, F. C., BENEZRA, R., NIMER, S. D. & WANG, L. 2016. Differential role of Id1 in MLL-AF9-driven leukemia based on cell of origin. *Blood,* 127**,** 2322-6.

MANESIA, J. K., XU, Z., BROEKAERT, D., BOON, R., VAN VLIET, A., EELEN, G., VANWELDEN, T., STEGEN, S., VAN GASTEL, N., PASCUAL-MONTANO, A., FENDT, S. M., CARMELIET, G., CARMELIET, P., KHURANA, S. & VERFAILLIE, C. M. 2015. Highly proliferative primitive fetal liver hematopoietic stem cells are fueled by oxidative metabolic pathways. *Stem Cell Res,* 15**,** 715-21.

MANSSON, R., HULTQUIST, A., LUC, S., YANG, L., ANDERSON, K., KHARAZI, S., AL-HASHMI, S., LIUBA, K., THOREN, L., ADOLFSSON, J., BUZA-VIDAS, N., QIAN, H., SONEJI, S., ENVER, T., SIGVARDSSON, M. & JACOBSEN, S. E. 2007. Molecular evidence for hierarchical transcriptional lineage priming in fetal and adult stem cells and multipotent progenitors. *Immunity,* 26**,** 407-19.

MANZ, M. G., MIYAMOTO, T., AKASHI, K. & WEISSMAN, I. L. 2002. Prospective isolation of human clonogenic common myeloid progenitors. *Proc Natl Acad Sci U S A,* 99**,** 11872-7.

MANZ, M. G., TRAVER, D., AKASHI, K., MERAD, M., MIYAMOTO, T., ENGLEMAN, E. G. & WEISSMAN, I. L. 2001. Dendritic cell development from common myeloid progenitors. *Ann N Y Acad Sci,* 938**,** 167-73; discussion 173-4.

MARDIS, E. R., DING, L., DOOLING, D. J., LARSON, D. E., MCLELLAN, M. D., CHEN, K., KOBOLDT, D. C., FULTON, R. S., DELEHAUNTY, K. D., MCGRATH, S. D., FULTON, L. A., LOCKE, D. P., MAGRINI, V. J., ABBOTT, R. M., VICKERY, T. L., REED, J. S., ROBINSON, J. S., WYLIE, T., SMITH, S. M., CARMICHAEL, L., ELDRED, J. M., HARRIS, C. C., WALKER, J., PECK, J. B., DU, F., DUKES, A. F., SANDERSON, G. E., BRUMMETT, A. M., CLARK, E., MCMICHAEL, J. F., MEYER, R. J., SCHINDLER, J. K., POHL, C. S., WALLIS, J. W., SHI, X., LIN, L., SCHMIDT, H., TANG, Y., HAIPEK, C., WIECHERT, M. E., IVY, J. V., KALICKI, J., ELLIOTT, G., RIES, R. E., PAYTON, J. E., WESTERVELT, P., TOMASSON, M. H., WATSON, M. A., BATY, J., HEATH, S., SHANNON, W. D., NAGARAJAN, R., LINK, D. C., WALTER, M. J., GRAUBERT, T. A., DIPERSIO, J. F., WILSON, R. K. & LEY, T. J. 2009. Recurring mutations found by sequencing an acute myeloid leukemia genome. *N Engl J Med,* 361**,** 1058-66.

MARJANOVIC, I., KOSTIC, J., STANIC, B., PEJANOVIC, N., LUCIC, B., KARAN-DJURASEVIC, T., JANIC, D., DOKMANOVIC, L., JANKOVIC, S., VUKOVIC, N. S., TOMIN, D., PERISIC, O., RAKOCEVIC, G., POPOVIC, M., PAVLOVIC, S. & TOSIC, N. 2016. Parallel targeted next generation sequencing of childhood and adult acute myeloid leukemia patients reveals uniform genomic profile of the disease. *Tumour Biol,* 37**,** 13391-13401.

MARSHALL, C. J., KINNON, C. & THRASHER, A. J. 2000. Polarized expression of bone morphogenetic protein-4 in the human aorta-gonad-mesonephros region. *Blood,* 96**,** 1591-3.

MASSEY, G. V., ZIPURSKY, A., CHANG, M. N., DOYLE, J. J., NASIM, S., TAUB, J. W., RAVINDRANATH, Y., DAHL, G., WEINSTEIN, H. J. & CHILDREN'S ONCOLOGY, G. 2006. A prospective study of the natural history of transient leukemia (TL) in neonates with Down syndrome (DS): Children's Oncology Group (COG) study POG-9481. *Blood,* 107**,** 4606-13.

MATSUNAGA, T., TAKEMOTO, N., SATO, T., TAKIMOTO, R., TANAKA, I., FUJIMI, A., AKIYAMA, T., KURODA, H., KAWANO, Y., KOBUNE, M., KATO, J., HIRAYAMA, Y., SAKAMAKI, S., KOHDA, K., MIYAKE, K. & NIITSU, Y. 2003. Interaction between leukemic-cell VLA-4 and stromal fibronectin is a decisive factor for minimal residual disease of acute myelogenous leukemia. *Nat Med,* 9**,** 1158-65.

MATSUZAKI, H., LOI, H., DONG, S., TSAI, Y. Y., FANG, J., LAW, J., DI, X., LIU, W. M., YANG, G., LIU, G., HUANG, J., KENNEDY, G. C., RYDER, T. B., MARCUS, G. A., WALSH, P. S., SHRIVER, M. D., PUCK, J. M., JONES, K. W. &

MEI, R. 2004. Parallel genotyping of over 10,000 SNPs using a one-primer assay on a high-density oligonucleotide array. *Genome Res,* 14**,** 414-25.
MATUTES, E., PICKL, W. F., VAN'T VEER, M., MORILLA, R., SWANSBURY, J., STROBL, H., ATTARBASCHI, A., HOPFINGER, G., ASHLEY, S., BENE, M. C., PORWIT, A., ORFAO, A., LEMEZ, P., SCHABATH, R. & LUDWIG, W. D. 2011. Mixed-phenotype acute leukemia: clinical and laboratory features and outcome in 100 patients defined according to the WHO 2008 classification. *Blood,* 117**,** 3163-71.
MAYOTTE, N., ROY, D. C., YAO, J., KROON, E. & SAUVAGEAU, G. 2002. Oncogenic interaction between BCR-ABL and NUP98-HOXA9 demonstrated by the use of an in vitro purging culture system. *Blood,* 100**,** 4177-84.
MCKINNEY-FREEMAN, S., CAHAN, P., LI, H., LACADIE, S. A., HUANG, H. T., CURRAN, M., LOEWER, S., NAVEIRAS, O., KATHREIN, K. L., KONANTZ, M., LANGDON, E. M., LENGERKE, C., ZON, L. I., COLLINS, J. J. & DALEY, G. Q. 2012. The transcriptional landscape of hematopoietic stem cell ontogeny. *Cell Stem Cell,* 11**,** 701-14.
MEAD, A. J., KHARAZI, S., ATKINSON, D., MACAULAY, I., PECQUET, C., LOUGHRAN, S., LUTTEROPP, M., WOLL, P., CHOWDHURY, O., LUC, S., BUZA-VIDAS, N., FERRY, H., CLARK, S. A., GOARDON, N., VYAS, P., CONSTANTINESCU, S. N., SITNICKA, E., NERLOV, C. & JACOBSEN, S. E. 2013. FLT3-ITDs instruct a myeloid differentiation and transformation bias in lymphomyeloid multipotent progenitors. *Cell Rep,* 3**,** 1766-76.
MEDVINSKY, A. & DZIERZAK, E. 1996. Definitive hematopoiesis is autonomously initiated by the AGM region. *Cell,* 86**,** 897-906.
MEJSTRIKOVA, E., VOLEJNIKOVA, J., FRONKOVA, E., ZDRAHALOVA, K., KALINA, T., STERBA, J., JABALI, Y., MIHAL, V., BLAZEK, B., CERNA, Z., PROCHAZKOVA, D., HAK, J., ZEMANOVA, Z., JAROSOVA, M., OLTOVA, A., SEDLACEK, P., SCHWARZ, J., ZUNA, J., TRKA, J., STARY, J. & HRUSAK, O. 2010. Prognosis of children with mixed phenotype acute leukemia treated on the basis of consistent immunophenotypic criteria. *Haematologica,* 95**,** 928-35.
MENDEZ-FERRER, S., LUCAS, D., BATTISTA, M. & FRENETTE, P. S. 2008. Haematopoietic stem cell release is regulated by circadian oscillations. *Nature,* 452**,** 442-7.
MESHINCHI, S., WOODS, W. G., STIREWALT, D. L., SWEETSER, D. A., BUCKLEY, J. D., TJOA, T. K., BERNSTEIN, I. D. & RADICH, J. P. 2001. Prevalence and prognostic significance of Flt3 internal tandem duplication in pediatric acute myeloid leukemia. *Blood,* 97**,** 89-94.
MEYER, C., HOFMANN, J., BURMEISTER, T., GROGER, D., PARK, T. S., EMERENCIANO, M., POMBO DE OLIVEIRA, M., RENNEVILLE, A., VILLARESE, P., MACINTYRE, E., CAVE, H., CLAPPIER, E., MASS-MALO, K., ZUNA, J., TRKA, J., DE BRAEKELEER, E., DE BRAEKELEER, M., OH, S. H., TSAUR, G., FECHINA, L., VAN DER VELDEN, V. H., VAN DONGEN, J. J., DELABESSE, E., BINATO, R., SILVA, M. L., KUSTANOVICH, A., ALEINIKOVA, O., HARRIS, M. H., LUND-AHO, T., JUVONEN, V., HEIDENREICH, O., VORMOOR, J., CHOI, W. W., JAROSOVA, M., KOLENOVA, A., BUENO, C., MENENDEZ, P., WEHNER, S., ECKERT, C., TALMANT, P., TONDEUR, S., LIPPERT, E., LAUNAY, E., HENRY, C., BALLERINI, P., LAPILLONE, H., CALLANAN, M. B., CAYUELA, J. M., HERBAUX, C., CAZZANIGA, G., KAKADIYA, P. M., BOHLANDER, S., AHLMANN, M., CHOI, J. R., GAMEIRO, P., LEE, D. S., KRAUTER, J., CORNILLET-LEFEBVRE, P., TE KRONNIE, G., SCHAFER, B. W., KUBETZKO, S., ALONSO, C. N., ZUR STADT, U., SUTTON, R., VENN, N. C., IZRAELI, S., TRAKHTENBROT, L., MADSEN, H. O., ARCHER, P., HANCOCK, J., CERVEIRA, N., TEIXEIRA, M. R., LO NIGRO, L.,

MORICKE, A., STANULLA, M., SCHRAPPE, M., SEDEK, L., SZCZEPANSKI, T., ZWAAN, C. M., COENEN, E. A., VAN DEN HEUVEL-EIBRINK, M. M., STREHL, S., DWORZAK, M., PANZER-GRUMAYER, R., DINGERMANN, T., KLINGEBIEL, T. & MARSCHALEK, R. 2013. The MLL recombinome of acute leukemias in 2013. *Leukemia,* 27**,** 2165-76.

MEYER, S. E., QIN, T., MUENCH, D. E., MASUDA, K., VENKATASUBRAMANIAN, M., ORR, E., SUAREZ, L., GORE, S. D., DELWEL, R., PAIETTA, E., TALLMAN, M. S., FERNANDEZ, H., MELNICK, A., LE BEAU, M. M., KOGAN, S., SALOMONIS, N., FIGUEROA, M. E. & GRIMES, H. L. 2016. DNMT3A Haploinsufficiency Transforms FLT3ITD Myeloproliferative Disease into a Rapid, Spontaneous, and Fully Penetrant Acute Myeloid Leukemia. *Cancer Discov,* 6**,** 501-15.

MILLER, B. G. & STAMATOYANNOPOULOS, J. A. 2010. Integrative meta-analysis of differential gene expression in acute myeloid leukemia. *PLoS One,* 5**,** e9466.

MILLER, C. L. & EAVES, C. J. 2002. Long-Term Culture-Initiating Cell Assays for Human and Murine Cells. *In:* KLUG, C. A. & JORDAN, C. T. (eds.) *Hematopoietic Stem Cell Protocols.* Totowa, NJ: Humana Press.

MILLER, R. A., CHRISP, C. & GALECKI, A. 1997. CD4 memory T cell levels predict life span in genetically heterogeneous mice. *FASEB J,* 11**,** 775-83.

MILNE, T. A., MARTIN, M. E., BROCK, H. W., SLANY, R. K. & HESS, J. L. 2005. Leukemogenic MLL fusion proteins bind across a broad region of the Hox a9 locus, promoting transcription and multiple histone modifications. *Cancer Res,* 65**,** 11367-74.

MISHINA, Y., SUZUKI, A., UENO, N. & BEHRINGER, R. R. 1995. Bmpr encodes a type I bone morphogenetic protein receptor that is essential for gastrulation during mouse embryogenesis. *Genes Dev,* 9**,** 3027-37.

MIZUNO, S., CHIJIWA, T., OKAMURA, T., AKASHI, K., FUKUMAKI, Y., NIHO, Y. & SASAKI, H. 2001. Expression of DNA methyltransferases DNMT1, 3A, and 3B in normal hematopoiesis and in acute and chronic myelogenous leukemia. *Blood,* 97**,** 1172-9.

MOCHIZUKI-KASHIO, M., MISHIMA, Y., MIYAGI, S., NEGISHI, M., SARAYA, A., KONUMA, T., SHINGA, J., KOSEKI, H. & IWAMA, A. 2011. Dependency on the polycomb gene Ezh2 distinguishes fetal from adult hematopoietic stem cells. *Blood,* 118**,** 6553-61.

MOEHRLE, B. M., NATTAMAI, K., BROWN, A., FLORIAN, M. C., RYAN, M., VOGEL, M., BLIEDERHAEUSER, C., SOLLER, K., PROWS, D. R., ABDOLLAHI, A., SCHLEIMER, D., WALTER, D., MILSOM, M. D., STAMBROOK, P., PORTEUS, M. & GEIGER, H. 2015. Stem Cell-Specific Mechanisms Ensure Genomic Fidelity within HSCs and upon Aging of HSCs. *Cell Rep,* 13**,** 2412-24.

MOHRIN, M., BOURKE, E., ALEXANDER, D., WARR, M. R., BARRY-HOLSON, K., LE BEAU, M. M., MORRISON, C. G. & PASSEGUE, E. 2010. Hematopoietic stem cell quiescence promotes error-prone DNA repair and mutagenesis. *Cell Stem Cell,* 7**,** 174-85.

MOHYELDIN, A., GARZON-MUVDI, T. & QUINONES-HINOJOSA, A. 2010. Oxygen in stem cell biology: a critical component of the stem cell niche. *Cell Stem Cell,* 7**,** 150-61.

MONTECINO-RODRIGUEZ, E., BERENT-MAOZ, B. & DORSHKIND, K. 2013. Causes, consequences, and reversal of immune system aging. *J Clin Invest,* 123**,** 958-65.

MORRISON, S. J., HEMMATI, H. D., WANDYCZ, A. M. & WEISSMAN, I. L. 1995. The purification and characterization of fetal liver hematopoietic stem cells. *Proc Natl Acad Sci U S A,* 92**,** 10302-6.

MORRISON, S. J., PROWSE, K. R., HO, P. & WEISSMAN, I. L. 1996a. Telomerase activity in hematopoietic cells is associated with self-renewal potential. *Immunity,* 5**,** 207-16.

MORRISON, S. J., WANDYCZ, A. M., AKASHI, K., GLOBERSON, A. & WEISSMAN, I. L. 1996b. The aging of hematopoietic stem cells. *Nat Med,* 2**,** 1011-6.

MORRISON, S. J., WANDYCZ, A. M., HEMMATI, H. D., WRIGHT, D. E. & WEISSMAN, I. L. 1997. Identification of a lineage of multipotent hematopoietic progenitors. *Development,* 124**,** 1929-39.

MORRISON, S. J. & WEISSMAN, I. L. 1994. The long-term repopulating subset of hematopoietic stem cells is deterministic and isolatable by phenotype. *Immunity,* 1**,** 661-73.

MORTAZAVI, A., WILLIAMS, B. A., MCCUE, K., SCHAEFFER, L. & WOLD, B. 2008. Mapping and quantifying mammalian transcriptomes by RNA-Seq. *Nat Methods,* 5**,** 621-8.

MULLIGHAN, C. G., PHILLIPS, L. A., SU, X., MA, J., MILLER, C. B., SHURTLEFF, S. A. & DOWNING, J. R. 2008. Genomic analysis of the clonal origins of relapsed acute lymphoblastic leukemia. *Science,* 322**,** 1377-80.

MULLOY, J. C., CAMMENGA, J., BERGUIDO, F. J., WU, K., ZHOU, P., COMENZO, R. L., JHANWAR, S., MOORE, M. A. & NIMER, S. D. 2003. Maintaining the self-renewal and differentiation potential of human CD34+ hematopoietic cells using a single genetic element. *Blood,* 102**,** 4369-76.

MULLOY, J. C., CAMMENGA, J., MACKENZIE, K. L., BERGUIDO, F. J., MOORE, M. A. & NIMER, S. D. 2002. The AML1-ETO fusion protein promotes the expansion of human hematopoietic stem cells. *Blood,* 99**,** 15-23.

NA NAKORN, T., TRAVER, D., WEISSMAN, I. L. & AKASHI, K. 2002. Myeloerythroid-restricted progenitors are sufficient to confer radioprotection and provide the majority of day 8 CFU-S. *J Clin Invest,* 109**,** 1579-85.

NAKAMURA, T., LARGAESPADA, D. A., LEE, M. P., JOHNSON, L. A., OHYASHIKI, K., TOYAMA, K., CHEN, S. J., WILLMAN, C. L., CHEN, I. M., FEINBERG, A. P., JENKINS, N. A., COPELAND, N. G. & SHAUGHNESSY, J. D., JR. 1996. Fusion of the nucleoporin gene NUP98 to HOXA9 by the chromosome translocation t(7;11)(p15;p15) in human myeloid leukaemia. *Nat Genet,* 12**,** 154-8.

NAKANO, T., KODAMA, H. & HONJO, T. 1994. Generation of lymphohematopoietic cells from embryonic stem cells in culture. *Science,* 265**,** 1098-101.

NAKIELNY, S. & DREYFUSS, G. 1999. Transport of proteins and RNAs in and out of the nucleus. *Cell,* 99**,** 677-90.

NERVI, B., RAMIREZ, P., RETTIG, M. P., UY, G. L., HOLT, M. S., RITCHEY, J. K., PRIOR, J. L., PIWNICA-WORMS, D., BRIDGER, G., LEY, T. J. & DIPERSIO, J. F. 2009. Chemosensitization of acute myeloid leukemia (AML) following mobilization by the CXCR4 antagonist AMD3100. *Blood,* 113**,** 6206-14.

NG, S. W., MITCHELL, A., KENNEDY, J. A., CHEN, W. C., MCLEOD, J., IBRAHIMOVA, N., ARRUDA, A., POPESCU, A., GUPTA, V., SCHIMMER, A. D., SCHUH, A. C., YEE, K. W., BULLINGER, L., HEROLD, T., GORLICH, D., BUCHNER, T., HIDDEMANN, W., BERDEL, W. E., WORMANN, B., CHEOK, M., PREUDHOMME, C., DOMBRET, H., METZELER, K., BUSKE, C., LOWENBERG, B., VALK, P. J., ZANDSTRA, P. W., MINDEN, M. D., DICK, J. E. & WANG, J. C. 2016. A 17-gene stemness score for rapid determination of risk in acute leukaemia. *Nature,* 540**,** 433-437.

NIE, Y., HAN, Y. C. & ZOU, Y. R. 2008. CXCR4 is required for the quiescence of primitive hematopoietic cells. *J Exp Med,* 205**,** 777-83.

NIEWERTH, D., CREUTZIG, U., BIERINGS, M. B. & KASPERS, G. J. 2010. A review on allogeneic stem cell transplantation for newly diagnosed pediatric acute myeloid leukemia. *Blood,* 116**,** 2205-14.

NILSSON, S. K., JOHNSTON, H. M. & COVERDALE, J. A. 2001. Spatial localization of transplanted hemopoietic stem cells: inferences for the localization of stem cell niches. *Blood,* 97**,** 2293-9.

NILSSON, S. K., JOHNSTON, H. M., WHITTY, G. A., WILLIAMS, B., WEBB, R. J., DENHARDT, D. T., BERTONCELLO, I., BENDALL, L. J., SIMMONS, P. J. & HAYLOCK, D. N. 2005. Osteopontin, a key component of the hematopoietic stem cell niche and regulator of primitive hematopoietic progenitor cells. *Blood,* 106**,** 1232-9.

NOTTA, F., ZANDI, S., TAKAYAMA, N., DOBSON, S., GAN, O. I., WILSON, G., KAUFMANN, K. B., MCLEOD, J., LAURENTI, E., DUNANT, C. F., MCPHERSON, J. D., STEIN, L. D., DROR, Y. & DICK, J. E. 2016. Distinct routes of lineage development reshape the human blood hierarchy across ontogeny. *Science,* 351**,** aab2116.

NOWELL, P. C. 1976. The clonal evolution of tumor cell populations. *Science,* 194**,** 23-8.

NUTT, S. L., HEAVEY, B., ROLINK, A. G. & BUSSLINGER, M. 1999. Commitment to the B-lymphoid lineage depends on the transcription factor Pax5. *Nature,* 401**,** 556-62.

NYGREN, J. M., BRYDER, D. & JACOBSEN, S. E. 2006. Prolonged cell cycle transit is a defining and developmentally conserved hemopoietic stem cell property. *J Immunol,* 177**,** 201-8.

O'RIORDAN, M. & GROSSCHEDL, R. 1999. Coordinate regulation of B cell differentiation by the transcription factors EBF and E2A. *Immunity,* 11**,** 21-31.

OGAWA, M. & LIVINGSTON, A. G. 2002. Hematopoietic Colony-Forming Cells. *In:* KLUG, C. A. & JORDAN, C. T. (eds.) *Hematopoietic Stem Cell Protocols.* Totowa, NJ: Humana Press.

OKUDA, T., CAI, Z., YANG, S., LENNY, N., LYU, C. J., VAN DEURSEN, J. M., HARADA, H. & DOWNING, J. R. 1998. Expression of a knocked-in AML1-ETO leukemia gene inhibits the establishment of normal definitive hematopoiesis and directly generates dysplastic hematopoietic progenitors. *Blood,* 91**,** 3134-43.

OWENS, P., PICKUP, M. W., NOVITSKIY, S. V., GILTNANE, J. M., GORSKA, A. E., HOPKINS, C. R., HONG, C. C. & MOSES, H. L. 2015. Inhibition of BMP signaling suppresses metastasis in mammary cancer. *Oncogene,* 34**,** 2437-49.

PABST, T., MUELLER, B. U., HARAKAWA, N., SCHOCH, C., HAFERLACH, T., BEHRE, G., HIDDEMANN, W., ZHANG, D. E. & TENEN, D. G. 2001a. AML1-ETO downregulates the granulocytic differentiation factor C/EBPalpha in t(8;21) myeloid leukemia. *Nat Med,* 7**,** 444-51.

PABST, T., MUELLER, B. U., ZHANG, P., RADOMSKA, H. S., NARRAVULA, S., SCHNITTGER, S., BEHRE, G., HIDDEMANN, W. & TENEN, D. G. 2001b. Dominant-negative mutations of CEBPA, encoding CCAAT/enhancer binding protein-alpha (C/EBPalpha), in acute myeloid leukemia. *Nat Genet,* 27**,** 263-70.

PALIS, J., ROBERTSON, S., KENNEDY, M., WALL, C. & KELLER, G. 1999. Development of erythroid and myeloid progenitors in the yolk sac and embryo proper of the mouse. *Development,* 126**,** 5073-84.

PANG, W. W., PRICE, E. A., SAHOO, D., BEERMAN, I., MALONEY, W. J., ROSSI, D. J., SCHRIER, S. L. & WEISSMAN, I. L. 2011. Human bone marrow

hematopoietic stem cells are increased in frequency and myeloid-biased with age. *Proc Natl Acad Sci U S A,* 108**,** 20012-7.

PAPAEMMANUIL, E., GERSTUNG, M., BULLINGER, L., GAIDZIK, V. I., PASCHKA, P., ROBERTS, N. D., POTTER, N. E., HEUSER, M., THOL, F., BOLLI, N., GUNDEM, G., VAN LOO, P., MARTINCORENA, I., GANLY, P., MUDIE, L., MCLAREN, S., O'MEARA, S., RAINE, K., JONES, D. R., TEAGUE, J. W., BUTLER, A. P., GREAVES, M. F., GANSER, A., DOHNER, K., SCHLENK, R. F., DOHNER, H. & CAMPBELL, P. J. 2016. Genomic Classification and Prognosis in Acute Myeloid Leukemia. *N Engl J Med,* 374**,** 2209-2221.

PARK, C. H., BERGSAGEL, D. E. & MCCULLOCH, E. A. 1971. Mouse myeloma tumor stem cells: a primary cell culture assay. *J Natl Cancer Inst,* 46**,** 411-22.

PARK, D. J., CHUMAKOV, A. M., VUONG, P. T., CHIH, D. Y., GOMBART, A. F., MILLER, W. H., JR. & KOEFFLER, H. P. 1999. CCAAT/enhancer binding protein epsilon is a potential retinoid target gene in acute promyelocytic leukemia treatment. *J Clin Invest,* 103**,** 1399-408.

PARK, I. K., QIAN, D., KIEL, M., BECKER, M. W., PIHALJA, M., WEISSMAN, I. L., MORRISON, S. J. & CLARKE, M. F. 2003. Bmi-1 is required for maintenance of adult self-renewing haematopoietic stem cells. *Nature,* 423**,** 302-5.

PASSEGUE, E., WAGERS, A. J., GIURIATO, S., ANDERSON, W. C. & WEISSMAN, I. L. 2005. Global analysis of proliferation and cell cycle gene expression in the regulation of hematopoietic stem and progenitor cell fates. *J Exp Med,* 202**,** 1599-611.

PEAR, W. S., MILLER, J. P., XU, L., PUI, J. C., SOFFER, B., QUACKENBUSH, R. C., PENDERGAST, A. M., BRONSON, R., ASTER, J. C., SCOTT, M. L. & BALTIMORE, D. 1998. Efficient and rapid induction of a chronic myelogenous leukemia-like myeloproliferative disease in mice receiving P210 bcr/abl-transduced bone marrow. *Blood,* 92**,** 3780-92.

PELED, A., PETIT, I., KOLLET, O., MAGID, M., PONOMARYOV, T., BYK, T., NAGLER, A., BEN-HUR, H., MANY, A., SHULTZ, L., LIDER, O., ALON, R., ZIPORI, D. & LAPIDOT, T. 1999. Dependence of human stem cell engraftment and repopulation of NOD/SCID mice on CXCR4. *Science,* 283**,** 845-8.

PEREL, Y., AUVRIGNON, A., LEBLANC, T., MICHEL, G., REGUERRE, Y., VANNIER, J. P., DALLE, J. H., GANDEMER, V., SCHMITT, C., MECHINAUD, F., LEJARS, O., PIGUET, C., COUILLAUD, G., PAUTARD, B., LANDMAN-PARKER, J., THURET, I., ALADJIDI, N., BARUCHEL, A., LEVERGER, G. & FRENCH, L. C. G. 2005. Treatment of childhood acute myeloblastic leukemia: dose intensification improves outcome and maintenance therapy is of no benefit--multicenter studies of the French LAME (Leucemie Aigue Myeloblastique Enfant) Cooperative Group. *Leukemia,* 19**,** 2082-9.

PERK, J., IAVARONE, A. & BENEZRA, R. 2005. Id family of helix-loop-helix proteins in cancer. *Nat Rev Cancer,* 5**,** 603-14.

PESCHON, J. J., MORRISSEY, P. J., GRABSTEIN, K. H., RAMSDELL, F. J., MARASKOVSKY, E., GLINIAK, B. C., PARK, L. S., ZIEGLER, S. F., WILLIAMS, D. E., WARE, C. B., MEYER, J. D. & DAVISON, B. L. 1994. Early lymphocyte expansion is severely impaired in interleukin 7 receptor-deficient mice. *J Exp Med,* 180**,** 1955-60.

PEVNY, L., SIMON, M. C., ROBERTSON, E., KLEIN, W. H., TSAI, S. F., D'AGATI, V., ORKIN, S. H. & COSTANTINI, F. 1991. Erythroid differentiation in chimaeric mice blocked by a targeted mutation in the gene for transcription factor GATA-1. *Nature,* 349**,** 257-60.

PIETERS, R., SCHRAPPE, M., DE LORENZO, P., HANN, I., DE ROSSI, G., FELICE, M., HOVI, L., LEBLANC, T., SZCZEPANSKI, T., FERSTER, A., JANKA, G., RUBNITZ,

J., SILVERMAN, L., STARY, J., CAMPBELL, M., LI, C. K., MANN, G., SUPPIAH, R., BIONDI, A., VORA, A. & VALSECCHI, M. G. 2007. A treatment protocol for infants younger than 1 year with acute lymphoblastic leukaemia (Interfant-99): an observational study and a multicentre randomised trial. *Lancet,* 370**,** 240-50.

PIETRAS, E. M., WARR, M. R. & PASSEGUE, E. 2011. Cell cycle regulation in hematopoietic stem cells. *J Cell Biol,* 195**,** 709-20.

PINE, S. R., GUO, Q., YIN, C., JAYABOSE, S., DRUSCHEL, C. M. & SANDOVAL, C. 2007. Incidence and clinical implications of GATA1 mutations in newborns with Down syndrome. *Blood,* 110**,** 2128-31.

PINEAULT, N., HELGASON, C. D., LAWRENCE, H. J. & HUMPHRIES, R. K. 2002. Differential expression of Hox, Meis1, and Pbx1 genes in primitive cells throughout murine hematopoietic ontogeny. *Exp Hematol,* 30**,** 49-57.

PINTER, O., BEDA, Z., CSABA, Z. & GERENDAI, I. 2007. Differences in the onset of puberty in selected inbred mouse strains. *In:* ENDOCRINOLOGY, E. C. O. (ed.) *European Congress of Endocrinology*. Budapest, Hungary: Endocrine Abstracts.

POLLAK, M. 2012. The insulin and insulin-like growth factor receptor family in neoplasia: an update. *Nat Rev Cancer,* 12**,** 159-69.

PRIESTLEY, G. V., ULYANOVA, T. & PAPAYANNOPOULOU, T. 2007. Sustained alterations in biodistribution of stem/progenitor cells in Tie2Cre+ alpha4(f/f) mice are hematopoietic cell autonomous. *Blood,* 109**,** 109-11.

PUI, C. H., KANE, J. R. & CRIST, W. M. 1995. Biology and treatment of infant leukemias. *Leukemia,* 9**,** 762-9.

QUERE, R., ANDRADOTTIR, S., BRUN, A. C., ZUBAREV, R. A., KARLSSON, G., OLSSON, K., MAGNUSSON, M., CAMMENGA, J. & KARLSSON, S. 2011. High levels of the adhesion molecule CD44 on leukemic cells generate acute myeloid leukemia relapse after withdrawal of the initial transforming event. *Leukemia,* 25**,** 515-26.

RAAIJMAKERS, M. H., MUKHERJEE, S., GUO, S., ZHANG, S., KOBAYASHI, T., SCHOONMAKER, J. A., EBERT, B. L., AL-SHAHROUR, F., HASSERJIAN, R. P., SCADDEN, E. O., AUNG, Z., MATZA, M., MERKENSCHLAGER, M., LIN, C., ROMMENS, J. M. & SCADDEN, D. T. 2010. Bone progenitor dysfunction induces myelodysplasia and secondary leukaemia. *Nature,* 464**,** 852-7.

RAMALHO-SANTOS, M. & WILLENBRING, H. 2007. On the origin of the term "stem cell". *Cell Stem Cell,* 1**,** 35-8.

RAMALHO-SANTOS, M., YOON, S., MATSUZAKI, Y., MULLIGAN, R. C. & MELTON, D. A. 2002. "Stemness": transcriptional profiling of embryonic and adult stem cells. *Science,* 298**,** 597-600.

RAVANDI, F., CORTES, J. E., JONES, D., FADERL, S., GARCIA-MANERO, G., KONOPLEVA, M. Y., O'BRIEN, S., ESTROV, Z., BORTHAKUR, G., THOMAS, D., PIERCE, S. R., BRANDT, M., BYRD, A., BEKELE, B. N., PRATZ, K., LUTHRA, R., LEVIS, M., ANDREEFF, M. & KANTARJIAN, H. M. 2010. Phase I/II study of combination therapy with sorafenib, idarubicin, and cytarabine in younger patients with acute myeloid leukemia. *J Clin Oncol,* 28**,** 1856-62.

REBEL, V. I., MILLER, C. L., EAVES, C. J. & LANSDORP, P. M. 1996. The repopulation potential of fetal liver hematopoietic stem cells in mice exceeds that of their liver adult bone marrow counterparts. *Blood,* 87**,** 3500-7.

REGL, G., KASPER, M., SCHNIDAR, H., EICHBERGER, T., NEILL, G. W., PHILPOTT, M. P., ESTERBAUER, H., HAUSER-KRONBERGER, C., FRISCHAUF, A. M. & ABERGER, F. 2004. Activation of the BCL2 promoter in response to

Hedgehog/GLI signal transduction is predominantly mediated by GLI2. *Cancer Res,* 64**,** 7724-31.

REINISCH, A., ETCHART, N., THOMAS, D., HOFMANN, N. A., FRUEHWIRTH, M., SINHA, S., CHAN, C. K., SENARATH-YAPA, K., SEO, E. Y., WEARDA, T., HARTWIG, U. F., BEHAM-SCHMID, C., TRAJANOSKI, S., LIN, Q., WAGNER, W., DULLIN, C., ALVES, F., ANDREEFF, M., WEISSMAN, I. L., LONGAKER, M. T., SCHALLMOSER, K., MAJETI, R. & STRUNK, D. 2015. Epigenetic and in vivo comparison of diverse MSC sources reveals an endochondral signature for human hematopoietic niche formation. *Blood,* 125**,** 249-60.

REYA, T., DUNCAN, A. W., AILLES, L., DOMEN, J., SCHERER, D. C., WILLERT, K., HINTZ, L., NUSSE, R. & WEISSMAN, I. L. 2003. A role for Wnt signalling in self-renewal of haematopoietic stem cells. *Nature,* 423**,** 409-14.

RHOADES, K. L., HETHERINGTON, C. J., HARAKAWA, N., YERGEAU, D. A., ZHOU, L., LIU, L. Q., LITTLE, M. T., TENEN, D. G. & ZHANG, D. E. 2000. Analysis of the role of AML1-ETO in leukemogenesis, using an inducible transgenic mouse model. *Blood,* 96**,** 2108-15.

RICHTER, A., SCHWAGER, C., HENTZE, S., ANSORGE, W., HENTZE, M. W. & MUCKENTHALER, M. 2002. Comparison of fluorescent tag DNA labeling methods used for expression analysis by DNA microarrays. *Biotechniques,* 33**,** 620-8, 630.

ROMANA, S. P., RADFORD-WEISS, I., BEN ABDELALI, R., SCHLUTH, C., PETIT, A., DASTUGUE, N., TALMANT, P., BILHOU-NABERA, C., MUGNERET, F., LAFAGE-POCHITALOFF, M., MOZZICONACCI, M. J., ANDRIEU, J., LAI, J. L., TERRE, C., RACK, K., CORNILLET-LEFEBVRE, P., LUQUET, I., NADAL, N., NGUYEN-KHAC, F., PEROT, C., VAN DEN AKKER, J., FERT-FERRER, S., CABROL, C., CHARRIN, C., TIGAUD, I., POIREL, H., VEKEMANS, M., BERNARD, O. A., BERGER, R. & GROUPE FRANCOPHONE DE CYTOGENETIQUE, H. 2006. NUP98 rearrangements in hematopoietic malignancies: a study of the Groupe Francophone de Cytogenetique Hematologique. *Leukemia,* 20**,** 696-706.

ROMBOUTS, E. J., PAVIC, B., LOWENBERG, B. & PLOEMACHER, R. E. 2004. Relation between CXCR-4 expression, Flt3 mutations, and unfavorable prognosis of adult acute myeloid leukemia. *Blood,* 104**,** 550-7.

ROSE, M., SCHUBERT, C., DIERICHS, L., GAISA, N. T., HEER, M., HEIDENREICH, A., KNUCHEL, R. & DAHL, E. 2014. OASIS/CREB3L1 is epigenetically silenced in human bladder cancer facilitating tumor cell spreading and migration in vitro. *Epigenetics,* 9**,** 1626-40.

ROSNET, O., BUHRING, H. J., MARCHETTO, S., RAPPOLD, I., LAVAGNA, C., SAINTY, D., ARNOULET, C., CHABANNON, C., KANZ, L., HANNUM, C. & BIRNBAUM, D. 1996. Human FLT3/FLK2 receptor tyrosine kinase is expressed at the surface of normal and malignant hematopoietic cells. *Leukemia,* 10**,** 238-48.

ROSS, M. E., MAHFOUZ, R., ONCIU, M., LIU, H. C., ZHOU, X., SONG, G., SHURTLEFF, S. A., POUNDS, S., CHENG, C., MA, J., RIBEIRO, R. C., RUBNITZ, J. E., GIRTMAN, K., WILLIAMS, W. K., RAIMONDI, S. C., LIANG, D. C., SHIH, L. Y., PUI, C. H. & DOWNING, J. R. 2004. Gene expression profiling of pediatric acute myelogenous leukemia. *Blood,* 104**,** 3679-87.

ROSSI, D. J., BRYDER, D., SEITA, J., NUSSENZWEIG, A., HOEIJMAKERS, J. & WEISSMAN, I. L. 2007a. Deficiencies in DNA damage repair limit the function of haematopoietic stem cells with age. *Nature,* 447**,** 725-9.

ROSSI, D. J., BRYDER, D., ZAHN, J. M., AHLENIUS, H., SONU, R., WAGERS, A. J. & WEISSMAN, I. L. 2005. Cell intrinsic alterations underlie hematopoietic stem cell aging. *Proc Natl Acad Sci U S A,* 102**,** 9194-9.

ROSSI, D. J., SEITA, J., CZECHOWICZ, A., BHATTACHARYA, D., BRYDER, D. & WEISSMAN, I. L. 2007b. Hematopoietic stem cell quiescence attenuates DNA damage response and permits DNA damage accumulation during aging. *Cell Cycle,* 6**,** 2371-6.

ROZHOK, A. I. & DEGREGORI, J. 2015. Toward an evolutionary model of cancer: Considering the mechanisms that govern the fate of somatic mutations. *Proc Natl Acad Sci U S A,* 112**,** 8914-21.

RUBE, C. E., FRICKE, A., WIDMANN, T. A., FURST, T., MADRY, H., PFREUNDSCHUH, M. & RUBE, C. 2011. Accumulation of DNA damage in hematopoietic stem and progenitor cells during human aging. *PLoS One,* 6**,** e17487.

RUBNITZ, J. E., ONCIU, M., POUNDS, S., SHURTLEFF, S., CAO, X., RAIMONDI, S. C., BEHM, F. G., CAMPANA, D., RAZZOUK, B. I., RIBEIRO, R. C., DOWNING, J. R. & PUI, C. H. 2009. Acute mixed lineage leukemia in children: the experience of St Jude Children's Research Hospital. *Blood,* 113**,** 5083-9.

RUFER, N., BRUMMENDORF, T. H., KOLVRAA, S., BISCHOFF, C., CHRISTENSEN, K., WADSWORTH, L., SCHULZER, M. & LANSDORP, P. M. 1999. Telomere fluorescence measurements in granulocytes and T lymphocyte subsets point to a high turnover of hematopoietic stem cells and memory T cells in early childhood. *J Exp Med,* 190**,** 157-67.

SAMOKHVALOV, I. M., SAMOKHVALOVA, N. I. & NISHIKAWA, S. 2007. Cell tracing shows the contribution of the yolk sac to adult haematopoiesis. *Nature,* 446**,** 1056-61.

SANGER, F. & COULSON, A. R. 1975. A rapid method for determining sequences in DNA by primed synthesis with DNA polymerase. *J Mol Biol,* 94**,** 441-8.

SAUER, B. & HENDERSON, N. 1988. Site-specific DNA recombination in mammalian cells by the Cre recombinase of bacteriophage P1. *Proc Natl Acad Sci U S A,* 85**,** 5166-70.

SCHLEIERMACHER, G., RUBIE, H., HARTMANN, O., BERGERON, C., CHASTAGNER, P., MECHINAUD, F., MICHON, J. & NEUROBLASTOMA STUDY GROUP OF THE FRENCH SOCIETY OF PAEDIATRIC, O. 2003. Treatment of stage 4s neuroblastoma--report of 10 years' experience of the French Society of Paediatric Oncology (SFOP). *Br J Cancer,* 89**,** 470-6.

SCHMITT, T. M., CIOFANI, M., PETRIE, H. T. & ZUNIGA-PFLUCKER, J. C. 2004. Maintenance of T cell specification and differentiation requires recurrent notch receptor-ligand interactions. *J Exp Med,* 200**,** 469-79.

SCHNEIDER, F., HOSTER, E., SCHNEIDER, S., DUFOUR, A., BENTHAUS, T., KAKADIA, P. M., BOHLANDER, S. K., BRAESS, J., HEINECKE, A., SAUERLAND, M. C., BERDEL, W. E., BUECHNER, T., WOERMANN, B. J., FEURING-BUSKE, M., BUSKE, C., CREUTZIG, U., THIEDE, C., ZWAAN, M. C., VAN DEN HEUVEL-EIBRINK, M. M., REINHARDT, D., HIDDEMANN, W. & SPIEKERMANN, K. 2012. Age-dependent frequencies of NPM1 mutations and FLT3-ITD in patients with normal karyotype AML (NK-AML). *Ann Hematol,* 91**,** 9-18.

SCHOCH, C., KOHLMANN, A., SCHNITTGER, S., BRORS, B., DUGAS, M., MERGENTHALER, S., KERN, W., HIDDEMANN, W., EILS, R. & HAFERLACH, T. 2002. Acute myeloid leukemias with reciprocal rearrangements can be distinguished by specific gene expression profiles. *Proc Natl Acad Sci U S A,* 99**,** 10008-13.

SCHOFIELD, R. 1978. The relationship between the spleen colony-forming cell and the haemopoietic stem cell. *Blood Cells* 4, 75-25.

SCHOLL, C., BANSAL, D., DOHNER, K., EIWEN, K., HUNTLY, B. J., LEE, B. H., RUCKER, F. G., SCHLENK, R. F., BULLINGER, L., DOHNER, H., GILLILAND, D. G. & FROHLING, S. 2007. The homeobox gene CDX2 is aberrantly expressed

in most cases of acute myeloid leukemia and promotes leukemogenesis. *J Clin Invest,* 117**,** 1037-48.

SCHWIEGER, M., LOHLER, J., FRIEL, J., SCHELLER, M., HORAK, I. & STOCKING, C. 2002. AML1-ETO inhibits maturation of multiple lymphohematopoietic lineages and induces myeloblast transformation in synergy with ICSBP deficiency. *J Exp Med,* 196**,** 1227-40.

SCOTT, E. W., SIMON, M. C., ANASTASI, J. & SINGH, H. 1994. Requirement of transcription factor PU.1 in the development of multiple hematopoietic lineages. *Science,* 265**,** 1573-7.

SEEDHOUSE, C. H., HUNTER, H. M., LLOYD-LEWIS, B., MASSIP, A. M., PALLIS, M., CARTER, G. I., GRUNDY, M., SHANG, S. & RUSSELL, N. H. 2006. DNA repair contributes to the drug-resistant phenotype of primary acute myeloid leukaemia cells with FLT3 internal tandem duplications and is reversed by the FLT3 inhibitor PKC412. *Leukemia,* 20**,** 2130-6.

SHANG, Y., SMITH, S. & HU, X. 2016. Role of Notch signaling in regulating innate immunity and inflammation in health and disease. *Protein Cell,* 7**,** 159-74.

SHAW, A. C., GOLDSTEIN, D. R. & MONTGOMERY, R. R. 2013. Age-dependent dysregulation of innate immunity. *Nat Rev Immunol,* 13**,** 875-87.

SHIBA, N., YOSHIDA, K., SHIRAISHI, Y., OKUNO, Y., YAMATO, G., HARA, Y., NAGATA, Y., CHIBA, K., TANAKA, H., TERUI, K., KATO, M., PARK, M. J., OHKI, K., SHIMADA, A., TAKITA, J., TOMIZAWA, D., KUDO, K., ARAKAWA, H., ADACHI, S., TAGA, T., TAWA, A., ITO, E., HORIBE, K., SANADA, M., MIYANO, S., OGAWA, S. & HAYASHI, Y. 2016. Whole-exome sequencing reveals the spectrum of gene mutations and the clonal evolution patterns in paediatric acute myeloid leukaemia. *Br J Haematol,* 175**,** 476-489.

SHIVDASANI, R. A., FUJIWARA, Y., MCDEVITT, M. A. & ORKIN, S. H. 1997. A lineage-selective knockout establishes the critical role of transcription factor GATA-1 in megakaryocyte growth and platelet development. *EMBO J,* 16**,** 3965-73.

SHLUSH, L. I., ZANDI, S., MITCHELL, A., CHEN, W. C., BRANDWEIN, J. M., GUPTA, V., KENNEDY, J. A., SCHIMMER, A. D., SCHUH, A. C., YEE, K. W., MCLEOD, J. L., DOEDENS, M., MEDEIROS, J. J., MARKE, R., KIM, H. J., LEE, K., MCPHERSON, J. D., HUDSON, T. J., CONSORTIUM, H. P.-L. G. P., BROWN, A. M., YOUSIF, F., TRINH, Q. M., STEIN, L. D., MINDEN, M. D., WANG, J. C. & DICK, J. E. 2014. Identification of pre-leukaemic haematopoietic stem cells in acute leukaemia. *Nature,* 506**,** 328-33.

SIDOROV, I., KIMURA, M., YASHIN, A. & AVIV, A. 2009. Leukocyte telomere dynamics and human hematopoietic stem cell kinetics during somatic growth. *Exp Hematol,* 37**,** 514-24.

SIKORA, K., CHAN, S., EVAN, G., GABRA, H., MARKHAM, N., STEWART, J. & WATSON, J. 1987. c-myc oncogene expression in colorectal cancer. *Cancer,* 59**,** 1289-95.

SIMINOVITCH, L., TILL, J. E. & MCCULLOCH, E. A. 1964. Decline in Colony-Forming Ability of Marrow Cells Subjected to Serial Transplantation into Irradiated Mice. *J Cell Comp Physiol,* 64**,** 23-31.

SIMS-MOURTADA, J., IZZO, J. G., AJANI, J. & CHAO, K. S. 2007. Sonic Hedgehog promotes multiple drug resistance by regulation of drug transport. *Oncogene,* 26**,** 5674-9.

SIMSEK, T., KOCABAS, F., ZHENG, J., DEBERARDINIS, R. J., MAHMOUD, A. I., OLSON, E. N., SCHNEIDER, J. W., ZHANG, C. C. & SADEK, H. A. 2010. The distinct metabolic profile of hematopoietic stem cells reflects their location in a hypoxic niche. *Cell Stem Cell,* 7**,** 380-90.

SINGBRANT, S., KARLSSON, G., EHINGER, M., OLSSON, K., JAAKO, P., MIHARADA, K., STADTFELD, M., GRAF, T. & KARLSSON, S. 2010. Canonical BMP signaling is dispensable for hematopoietic stem cell function in both adult and fetal liver hematopoiesis, but essential to preserve colon architecture. *Blood,* 115**,** 4689-98.

SIPKINS, D. A., WEI, X., WU, J. W., RUNNELS, J. M., COTE, D., MEANS, T. K., LUSTER, A. D., SCADDEN, D. T. & LIN, C. P. 2005. In vivo imaging of specialized bone marrow endothelial microdomains for tumour engraftment. *Nature,* 435**,** 969-73.

SITNICKA, E., BRAKEBUSCH, C., MARTENSSON, I. L., SVENSSON, M., AGACE, W. W., SIGVARDSSON, M., BUZA-VIDAS, N., BRYDER, D., CILIO, C. M., AHLENIUS, H., MARASKOVSKY, E., PESCHON, J. J. & JACOBSEN, S. E. 2003. Complementary signaling through flt3 and interleukin-7 receptor alpha is indispensable for fetal and adult B cell genesis. *J Exp Med,* 198**,** 1495-506.

SITNICKA, E., BRYDER, D., THEILGAARD-MONCH, K., BUZA-VIDAS, N., ADOLFSSON, J. & JACOBSEN, S. E. 2002. Key role of flt3 ligand in regulation of the common lymphoid progenitor but not in maintenance of the hematopoietic stem cell pool. *Immunity,* 17**,** 463-72.

SLANY, R. K. 2009. The molecular biology of mixed lineage leukemia. *Haematologica,* 94**,** 984-93.

SLANY, R. K., LAVAU, C. & CLEARY, M. L. 1998. The oncogenic capacity of HRX-ENL requires the transcriptional transactivation activity of ENL and the DNA binding motifs of HRX. *Mol Cell Biol,* 18**,** 122-9.

SOLOMON, M. J., LARSEN, P. L. & VARSHAVSKY, A. 1988. Mapping protein-DNA interactions in vivo with formaldehyde: evidence that histone H4 is retained on a highly transcribed gene. *Cell,* 53**,** 937-47.

SOMERVAILLE, T. C. & CLEARY, M. L. 2006. Identification and characterization of leukemia stem cells in murine MLL-AF9 acute myeloid leukemia. *Cancer Cell,* 10**,** 257-68.

SPANGRUDE, G. J., HEIMFELD, S. & WEISSMAN, I. L. 1988. Purification and characterization of mouse hematopoietic stem cells. *Science,* 241**,** 58-62.

STAAL, F. J. & CLEVERS, H. C. 2005. WNT signalling and haematopoiesis: a WNT-WNT situation. *Nat Rev Immunol,* 5**,** 21-30.

STANLEY, E., LIESCHKE, G. J., GRAIL, D., METCALF, D., HODGSON, G., GALL, J. A., MAHER, D. W., CEBON, J., SINICKAS, V. & DUNN, A. R. 1994. Granulocyte/macrophage colony-stimulating factor-deficient mice show no major perturbation of hematopoiesis but develop a characteristic pulmonary pathology. *Proc Natl Acad Sci U S A,* 91**,** 5592-6.

STEVENS, R. F., HANN, I. M., WHEATLEY, K. & GRAY, R. G. 1998. Marked improvements in outcome with chemotherapy alone in paediatric acute myeloid leukemia: results of the United Kingdom Medical Research Council's 10th AML trial. MRC Childhood Leukaemia Working Party. *Br J Haematol,* 101**,** 130-40.

STIER, S., KO, Y., FORKERT, R., LUTZ, C., NEUHAUS, T., GRUNEWALD, E., CHENG, T., DOMBKOWSKI, D., CALVI, L. M., RITTLING, S. R. & SCADDEN, D. T. 2005. Osteopontin is a hematopoietic stem cell niche component that negatively regulates stem cell pool size. *J Exp Med,* 201**,** 1781-91.

STONE, R. M., MANDREKAR, S. J., SANFORD, B. L., LAUMANN, K., GEYER, S., BLOOMFIELD, C. D., THIEDE, C., PRIOR, T. W., DOHNER, K., MARCUCCI, G., LO-COCO, F., KLISOVIC, R. B., WEI, A., SIERRA, J., SANZ, M. A., BRANDWEIN, J. M., DE WITTE, T., NIEDERWIESER, D., APPELBAUM, F. R., MEDEIROS, B. C., TALLMAN, M. S., KRAUTER, J., SCHLENK, R. F., GANSER, A., SERVE, H., EHNINGER, G., AMADORI, S., LARSON, R. A. & DOHNER, H. 2017. Midostaurin

plus Chemotherapy for Acute Myeloid Leukemia with a FLT3 Mutation. *N Engl J Med,* 377**,** 454-464.

STUCKI, A., RIVIER, A. S., GIKIC, M., MONAI, N., SCHAPIRA, M. & SPERTINI, O. 2001. Endothelial cell activation by myeloblasts: molecular mechanisms of leukostasis and leukemic cell dissemination. *Blood,* 97**,** 2121-9.

SUBRAMANIAN, A., TAMAYO, P., MOOTHA, V. K., MUKHERJEE, S., EBERT, B. L., GILLETTE, M. A., PAULOVICH, A., POMEROY, S. L., GOLUB, T. R., LANDER, E. S. & MESIROV, J. P. 2005. Gene set enrichment analysis: a knowledge-based approach for interpreting genome-wide expression profiles. *Proc Natl Acad Sci U S A,* 102**,** 15545-50.

SUDO, K., EMA, H., MORITA, Y. & NAKAUCHI, H. 2000. Age-associated characteristics of murine hematopoietic stem cells. *J Exp Med,* 192**,** 1273-80.

SUGIYAMA, T., KOHARA, H., NODA, M. & NAGASAWA, T. 2006. Maintenance of the hematopoietic stem cell pool by CXCL12-CXCR4 chemokine signaling in bone marrow stromal cell niches. *Immunity,* 25**,** 977-88.

SUN, D., LUO, M., JEONG, M., RODRIGUEZ, B., XIA, Z., HANNAH, R., WANG, H., LE, T., FAULL, K. F., CHEN, R., GU, H., BOCK, C., MEISSNER, A., GOTTGENS, B., DARLINGTON, G. J., LI, W. & GOODELL, M. A. 2014. Epigenomic Profiling of Young and Aged HSCs Reveals Concerted Changes during Aging that Reinforce Self-Renewal. *Cell Stem Cell,* 14**,** 673-88.

SUZUKI, S., RACINE, R. R., MANALO, N. A., CANTOR, S. B. & RAFFEL, G. D. 2017. Impairment of fetal hematopoietic stem cell function in the absence of Fancd2. *Exp Hematol,* 48**,** 79-86.

SWERDLOW, S. H., INTERNATIONAL AGENCY FOR RESEARCH ON CANCER. & WORLD HEALTH ORGANIZATION. 2008. *WHO classification of tumours of haematopoietic and lymphoid tissues,* Lyon, France, International Agency for Research on Cancer.

TAICHMAN, R. S. & EMERSON, S. G. 1994. Human osteoblasts support hematopoiesis through the production of granulocyte colony-stimulating factor. *J Exp Med,* 179**,** 1677-82.

TAKEDA, A., GOOLSBY, C. & YASEEN, N. R. 2006. NUP98-HOXA9 induces long-term proliferation and blocks differentiation of primary human CD34+ hematopoietic cells. *Cancer Res,* 66**,** 6628-37.

TASKESEN, E., BULLINGER, L., CORBACIOGLU, A., SANDERS, M. A., ERPELINCK, C. A., WOUTERS, B. J., VAN DER POEL-VAN DE LUYTGAARDE, S. C., DAMM, F., KRAUTER, J., GANSER, A., SCHLENK, R. F., LOWENBERG, B., DELWEL, R., DOHNER, H., VALK, P. J. & DOHNER, K. 2011. Prognostic impact, concurrent genetic mutations, and gene expression features of AML with CEBPA mutations in a cohort of 1182 cytogenetically normal AML patients: further evidence for CEBPA double mutant AML as a distinctive disease entity. *Blood,* 117**,** 2469-75.

TAUSSIG, D. C., MIRAKI-MOUD, F., ANJOS-AFONSO, F., PEARCE, D. J., ALLEN, K., RIDLER, C., LILLINGTON, D., OAKERVEE, H., CAVENAGH, J., AGRAWAL, S. G., LISTER, T. A., GRIBBEN, J. G. & BONNET, D. 2008. Anti-CD38 antibody-mediated clearance of human repopulating cells masks the heterogeneity of leukemia-initiating cells. *Blood,* 112**,** 568-75.

TAUSSIG, D. C., VARGAFTIG, J., MIRAKI-MOUD, F., GRIESSINGER, E., SHARROCK, K., LUKE, T., LILLINGTON, D., OAKERVEE, H., CAVENAGH, J., AGRAWAL, S. G., LISTER, T. A., GRIBBEN, J. G. & BONNET, D. 2010. Leukemia-initiating cells from some acute myeloid leukemia patients with mutated nucleophosmin reside in the CD34(-) fraction. *Blood,* 115**,** 1976-84.

TAVOR, S., PETIT, I., POROZOV, S., AVIGDOR, A., DAR, A., LEIDER-TREJO, L., SHEMTOV, N., DEUTSCH, V., NAPARSTEK, E., NAGLER, A. & LAPIDOT, T.

2004. CXCR4 regulates migration and development of human acute myelogenous leukemia stem cells in transplanted NOD/SCID mice. *Cancer Res,* 64**,** 2817-24.

TERSKIKH, A. V., MIYAMOTO, T., CHANG, C., DIATCHENKO, L. & WEISSMAN, I. L. 2003. Gene expression analysis of purified hematopoietic stem cells and committed progenitors. *Blood,* 102**,** 94-101.

THIEDE, C., KOCH, S., CREUTZIG, E., STEUDEL, C., ILLMER, T., SCHAICH, M. & EHNINGER, G. 2006. Prevalence and prognostic impact of NPM1 mutations in 1485 adult patients with acute myeloid leukemia (AML). *Blood,* 107**,** 4011-20.

THOL, F., DAMM, F., LUDEKING, A., WINSCHEL, C., WAGNER, K., MORGAN, M., YUN, H., GOHRING, G., SCHLEGELBERGER, B., HOELZER, D., LUBBERT, M., KANZ, L., FIEDLER, W., KIRCHNER, H., HEIL, G., KRAUTER, J., GANSER, A. & HEUSER, M. 2011a. Incidence and prognostic influence of DNMT3A mutations in acute myeloid leukemia. *J Clin Oncol,* 29**,** 2889-96.

THOL, F., HEUSER, M., DAMM, F., KLUSMANN, J. H., REINHARDT, K. & REINHARDT, D. 2011b. DNMT3A mutations are rare in childhood acute myeloid leukemia. *Haematologica,* 96**,** 1238-40.

THORSTEINSDOTTIR, U., KROON, E., JEROME, L., BLASI, F. & SAUVAGEAU, G. 2001. Defining roles for HOX and MEIS1 genes in induction of acute myeloid leukemia. *Mol Cell Biol,* 21**,** 224-34.

TIE, R., ZHANG, T., FU, H., WANG, L., WANG, Y., HE, Y., WANG, B., ZHU, N., FU, S., LAI, X., SHI, J. & HUANG, H. 2014. Association between DNMT3A mutations and prognosis of adults with de novo acute myeloid leukemia: a systematic review and meta-analysis. *PLoS One,* 9**,** e93353.

TILL, J. E. & MCCULLOCH, E. 1961. A direct measurement of the radiation sensitivity of normal mouse bone marrow cells. *Radiat Res,* 14**,** 213-22.

TING, C. N., OLSON, M. C., BARTON, K. P. & LEIDEN, J. M. 1996. Transcription factor GATA-3 is required for development of the T-cell lineage. *Nature,* 384**,** 474-8.

TODARO, G. J. & GREEN, H. 1963. Quantitative studies of the growth of mouse embryo cells in culture and their development into established lines. *J Cell Biol,* 17**,** 299-313.

TOPIC, I., IKIC, M., IVCEVIC, S., KOVACIC, N., MARUSIC, A., KUSEC, R. & GRCEVIC, D. 2013. Bone morphogenetic proteins regulate differentiation of human promyelocytic leukemia cells. *Leuk Res,* 37**,** 705-12.

TOTHOVA, Z. & GILLILAND, D. G. 2007. FoxO transcription factors and stem cell homeostasis: insights from the hematopoietic system. *Cell Stem Cell,* 1**,** 140-52.

TRAVER, D., AKASHI, K., MANZ, M., MERAD, M., MIYAMOTO, T., ENGLEMAN, E. G. & WEISSMAN, I. L. 2000. Development of CD8alpha-positive dendritic cells from a common myeloid progenitor. *Science,* 290**,** 2152-4.

TRAVER, D., MIYAMOTO, T., CHRISTENSEN, J., IWASAKI-ARAI, J., AKASHI, K. & WEISSMAN, I. L. 2001. Fetal liver myelopoiesis occurs through distinct, prospectively isolatable progenitor subsets. *Blood,* 98**,** 627-35.

TSANG, A. P., FUJIWARA, Y., HOM, D. B. & ORKIN, S. H. 1998. Failure of megakaryopoiesis and arrested erythropoiesis in mice lacking the GATA-1 transcriptional cofactor FOG. *Genes Dev,* 12**,** 1176-88.

TULJAPURKAR, S. R., MCGUIRE, T. R., BRUSNAHAN, S. K., JACKSON, J. D., GARVIN, K. L., KESSINGER, M. A., LANE, J. T., BJ, O. K. & SHARP, J. G. 2011. Changes in human bone marrow fat content associated with changes in hematopoietic stem cell numbers and cytokine levels with aging. *J Anat,* 219**,** 574-81.

TZENG, Y. S., LI, H., KANG, Y. L., CHEN, W. C., CHENG, W. C. & LAI, D. M. 2011. Loss of Cxcl12/Sdf-1 in adult mice decreases the quiescent state of hematopoietic stem/progenitor cells and alters the pattern of hematopoietic regeneration after myelosuppression. *Blood,* 117**,** 429-39.

UCHIDA, N., DYKSTRA, B., LYONS, K., LEUNG, F., KRISTIANSEN, M. & EAVES, C. 2004. ABC transporter activities of murine hematopoietic stem cells vary according to their developmental and activation status. *Blood,* 103**,** 4487-95.

VALK, P. J., VERHAAK, R. G., BEIJEN, M. A., ERPELINCK, C. A., BARJESTEH VAN WAALWIJK VAN DOORN-KHOSROVANI, S., BOER, J. M., BEVERLOO, H. B., MOORHOUSE, M. J., VAN DER SPEK, P. J., LOWENBERG, B. & DELWEL, R. 2004. Prognostically useful gene-expression profiles in acute myeloid leukemia. *N Engl J Med,* 350**,** 1617-28.

VAN GOSLIGA, D., SCHEPERS, H., RIZO, A., VAN DER KOLK, D., VELLENGA, E. & SCHURINGA, J. J. 2007. Establishing long-term cultures with self-renewing acute myeloid leukemia stem/progenitor cells. *Exp Hematol,* 35**,** 1538-49.

VANGALA, R. K., HEISS-NEUMANN, M. S., RANGATIA, J. S., SINGH, S. M., SCHOCH, C., TENEN, D. G., HIDDEMANN, W. & BEHRE, G. 2003. The myeloid master regulator transcription factor PU.1 is inactivated by AML1-ETO in t(8;21) myeloid leukemia. *Blood,* 101**,** 270-7.

VARDIMAN, J. W., THIELE, J., ARBER, D. A., BRUNNING, R. D., BOROWITZ, M. J., PORWIT, A., HARRIS, N. L., LE BEAU, M. M., HELLSTROM-LINDBERG, E., TEFFERI, A. & BLOOMFIELD, C. D. 2009. The 2008 revision of the World Health Organization (WHO) classification of myeloid neoplasms and acute leukemia: rationale and important changes. *Blood,* 114**,** 937-51.

VARNUM-FINNEY, B., PURTON, L. E., YU, M., BRASHEM-STEIN, C., FLOWERS, D., STAATS, S., MOORE, K. A., LE ROUX, I., MANN, R., GRAY, G., ARTAVANIS-TSAKONAS, S. & BERNSTEIN, I. D. 1998. The Notch ligand, Jagged-1, influences the development of primitive hematopoietic precursor cells. *Blood,* 91**,** 4084-91.

VAS, V., SENGER, K., DORR, K., NIEBEL, A. & GEIGER, H. 2012a. Aging of the microenvironment influences clonality in hematopoiesis. *PLoS One,* 7**,** e42080.

VAS, V., WANDHOFF, C., DORR, K., NIEBEL, A. & GEIGER, H. 2012b. Contribution of an aged microenvironment to aging-associated myeloproliferative disease. *PLoS One,* 7**,** e31523.

VENEZIA, T. A., MERCHANT, A. A., RAMOS, C. A., WHITEHOUSE, N. L., YOUNG, A. S., SHAW, C. A. & GOODELL, M. A. 2004. Molecular signatures of proliferation and quiescence in hematopoietic stem cells. *PLoS Biol,* 2**,** e301.

VERHAAK, R. G., WOUTERS, B. J., ERPELINCK, C. A., ABBAS, S., BEVERLOO, H. B., LUGTHART, S., LOWENBERG, B., DELWEL, R. & VALK, P. J. 2009. Prediction of molecular subtypes in acute myeloid leukemia based on gene expression profiling. *Haematologica,* 94**,** 131-4.

VORA, A., GOULDEN, N., WADE, R., MITCHELL, C., HANCOCK, J., HOUGH, R., ROWNTREE, C. & RICHARDS, S. 2013. Treatment reduction for children and young adults with low-risk acute lymphoblastic leukaemia defined by minimal residual disease (UKALL 2003): a randomised controlled trial. *Lancet Oncol,* 14**,** 199-209.

WALKLEY, C. R., OLSEN, G. H., DWORKIN, S., FABB, S. A., SWANN, J., MCARTHUR, G. A., WESTMORELAND, S. V., CHAMBON, P., SCADDEN, D. T. & PURTON, L. E. 2007a. A microenvironment-induced myeloproliferative syndrome caused by retinoic acid receptor gamma deficiency. *Cell,* 129**,** 1097-110.

WALKLEY, C. R., SHEA, J. M., SIMS, N. A., PURTON, L. E. & ORKIN, S. H. 2007b. Rb regulates interactions between hematopoietic stem cells and their bone marrow microenvironment. *Cell,* 129**,** 1081-95.

WALTER, D., LIER, A., GEISELHART, A., THALHEIMER, F. B., HUNTSCHA, S., SOBOTTA, M. C., MOEHRLE, B., BROCKS, D., BAYINDIR, I., KASCHUTNIG, P., MUEDDER, K., KLEIN, C., JAUCH, A., SCHROEDER, T., GEIGER, H., DICK, T. P., HOLLAND-LETZ, T., SCHMEZER, P., LANE, S. W., RIEGER, M. A., ESSERS, M. A., WILLIAMS, D. A., TRUMPP, A. & MILSOM, M. D. 2015. Exit from dormancy provokes DNA-damage-induced attrition in haematopoietic stem cells. *Nature,* 520**,** 549-52.

WALTER, R. B., ALONZO, T. A., GERBING, R. B., HO, P. A., SMITH, F. O., RAIMONDI, S. C., HIRSCH, B. A., GAMIS, A. S., FRANKLIN, J. L., HURWITZ, C. A., LOKEN, M. R. & MESHINCHI, S. 2010. High expression of the very late antigen-4 integrin independently predicts reduced risk of relapse and improved outcome in pediatric acute myeloid leukemia: a report from the children's oncology group. *J Clin Oncol,* 28**,** 2831-8.

WANG, G. G., PASILLAS, M. P. & KAMPS, M. P. 2005. Meis1 programs transcription of FLT3 and cancer stem cell character, using a mechanism that requires interaction with Pbx and a novel function of the Meis1 C-terminus. *Blood,* 106**,** 254-64.

WANG, Y., KRIVTSOV, A. V., SINHA, A. U., NORTH, T. E., GOESSLING, W., FENG, Z., ZON, L. I. & ARMSTRONG, S. A. 2010. The Wnt/beta-catenin pathway is required for the development of leukemia stem cells in AML. *Science,* 327**,** 1650-3.

WANG, Z., GERSTEIN, M. & SNYDER, M. 2009. RNA-Seq: a revolutionary tool for transcriptomics. *Nat Rev Genet,* 10**,** 57-63.

WARNER, N. L., MOORE, M. A. & METCALF, D. 1969. A transplantable myelomonocytic leukemia in BALB-c mice: cytology, karyotype, and muramidase content. *J Natl Cancer Inst,* 43**,** 963-82.

WEBBER, B. A., CUSHING, M. M. & LI, S. 2008. Prognostic significance of flow cytometric immunophenotyping in acute myeloid leukemia. *Int J Clin Exp Pathol,* 1**,** 124-33.

WEI, J., WUNDERLICH, M., FOX, C., ALVAREZ, S., CIGUDOSA, J. C., WILHELM, J. S., ZHENG, Y., CANCELAS, J. A., GU, Y., JANSEN, M., DIMARTINO, J. F. & MULLOY, J. C. 2008. Microenvironment determines lineage fate in a human model of MLL-AF9 leukemia. *Cancer Cell,* 13**,** 483-95.

WEINBERG, O. K. & ARBER, D. A. 2010. Mixed-phenotype acute leukemia: historical overview and a new definition. *Leukemia,* 24**,** 1844-51.

WELCH, J. S., LEY, T. J., LINK, D. C., MILLER, C. A., LARSON, D. E., KOBOLDT, D. C., WARTMAN, L. D., LAMPRECHT, T. L., LIU, F., XIA, J., KANDOTH, C., FULTON, R. S., MCLELLAN, M. D., DOOLING, D. J., WALLIS, J. W., CHEN, K., HARRIS, C. C., SCHMIDT, H. K., KALICKI-VEIZER, J. M., LU, C., ZHANG, Q., LIN, L., O'LAUGHLIN, M. D., MCMICHAEL, J. F., DELEHAUNTY, K. D., FULTON, L. A., MAGRINI, V. J., MCGRATH, S. D., DEMETER, R. T., VICKERY, T. L., HUNDAL, J., COOK, L. L., SWIFT, G. W., REED, J. P., ALLDREDGE, P. A., WYLIE, T. N., WALKER, J. R., WATSON, M. A., HEATH, S. E., SHANNON, W. D., VARGHESE, N., NAGARAJAN, R., PAYTON, J. E., BATY, J. D., KULKARNI, S., KLCO, J. M., TOMASSON, M. H., WESTERVELT, P., WALTER, M. J., GRAUBERT, T. A., DIPERSIO, J. F., DING, L., MARDIS, E. R. & WILSON, R. K. 2012. The origin and evolution of mutations in acute myeloid leukemia. *Cell,* 150**,** 264-78.

WELNER, R. S., PELAYO, R., NAGAI, Y., GARRETT, K. P., WUEST, T. R., CARR, D. J., BORGHESI, L. A., FARRAR, M. A. & KINCADE, P. W. 2008. Lymphoid

precursors are directed to produce dendritic cells as a result of TLR9 ligation during herpes infection. *Blood,* 112**,** 3753-61.

WILPSHAAR, J., FALKENBURG, J. H., TONG, X., NOORT, W. A., BREESE, R., HEILMAN, D., KANHAI, H., ORSCHELL-TRAYCOFF, C. M. & SROUR, E. F. 2000. Similar repopulating capacity of mitotically active and resting umbilical cord blood CD34(+) cells in NOD/SCID mice. *Blood,* 96**,** 2100-7.

WILSON, A., LAURENTI, E., OSER, G., VAN DER WATH, R. C., BLANCO-BOSE, W., JAWORSKI, M., OFFNER, S., DUNANT, C. F., ESHKIND, L., BOCKAMP, E., LIO, P., MACDONALD, H. R. & TRUMPP, A. 2008. Hematopoietic stem cells reversibly switch from dormancy to self-renewal during homeostasis and repair. *Cell,* 135**,** 1118-29.

WINNIER, G., BLESSING, M., LABOSKY, P. A. & HOGAN, B. L. 1995. Bone morphogenetic protein-4 is required for mesoderm formation and patterning in the mouse. *Genes Dev,* 9**,** 2105-16.

WONG, D. J., LIU, H., RIDKY, T. W., CASSARINO, D., SEGAL, E. & CHANG, H. Y. 2008. Module map of stem cell genes guides creation of epithelial cancer stem cells. *Cell Stem Cell,* 2**,** 333-44.

WU, H., LIU, X., JAENISCH, R. & LODISH, H. F. 1995. Generation of committed erythroid BFU-E and CFU-E progenitors does not require erythropoietin or the erythropoietin receptor. *Cell,* 83**,** 59-67.

XIE, H., YE, M., FENG, R. & GRAF, T. 2004. Stepwise reprogramming of B cells into macrophages. *Cell,* 117**,** 663-76.

XIE, M., LU, C., WANG, J., MCLELLAN, M. D., JOHNSON, K. J., WENDL, M. C., MCMICHAEL, J. F., SCHMIDT, H. K., YELLAPANTULA, V., MILLER, C. A., OZENBERGER, B. A., WELCH, J. S., LINK, D. C., WALTER, M. J., MARDIS, E. R., DIPERSIO, J. F., CHEN, F., WILSON, R. K., LEY, T. J. & DING, L. 2014. Age-related mutations associated with clonal hematopoietic expansion and malignancies. *Nat Med,* 20**,** 1472-8.

XIE, Y., YIN, T., WIEGRAEBE, W., HE, X. C., MILLER, D., STARK, D., PERKO, K., ALEXANDER, R., SCHWARTZ, J., GRINDLEY, J. C., PARK, J., HAUG, J. S., WUNDERLICH, J. P., LI, H., ZHANG, S., JOHNSON, T., FELDMAN, R. A. & LI, L. 2009. Detection of functional haematopoietic stem cell niche using real-time imaging. *Nature,* 457**,** 97-101.

YAGI, T., MORIMOTO, A., EGUCHI, M., HIBI, S., SAKO, M., ISHII, E., MIZUTANI, S., IMASHUKU, S., OHKI, M. & ICHIKAWA, H. 2003. Identification of a gene expression signature associated with pediatric AML prognosis. *Blood,* 102**,** 1849-56.

YAMAZAKI, S., EMA, H., KARLSSON, G., YAMAGUCHI, T., MIYOSHI, H., SHIODA, S., TAKETO, M. M., KARLSSON, S., IWAMA, A. & NAKAUCHI, H. 2011. Nonmyelinating Schwann cells maintain hematopoietic stem cell hibernation in the bone marrow niche. *Cell,* 147**,** 1146-58.

YAN, L., PING, N., ZHU, M., SUN, A., XUE, Y., RUAN, C., DREXLER, H. G., MACLEOD, R. A., WU, D. & CHEN, S. 2012. Clinical, immunophenotypic, cytogenetic, and molecular genetic features in 117 adult patients with mixed-phenotype acute leukemia defined by WHO-2008 classification. *Haematologica,* 97**,** 1708-12.

YAN, M., BUREL, S. A., PETERSON, L. F., KANBE, E., IWASAKI, H., BOYAPATI, A., HINES, R., AKASHI, K. & ZHANG, D. E. 2004. Deletion of an AML1-ETO C-terminal NcoR/SMRT-interacting region strongly induces leukemia development. *Proc Natl Acad Sci U S A,* 101**,** 17186-91.

YAN, M., KANBE, E., PETERSON, L. F., BOYAPATI, A., MIAO, Y., WANG, Y., CHEN, I. M., CHEN, Z., ROWLEY, J. D., WILLMAN, C. L. & ZHANG, D. E. 2006. A

previously unidentified alternatively spliced isoform of t(8;21) transcript promotes leukemogenesis. *Nat Med,* 12**,** 945-9.

YE, M., ZHANG, H., AMABILE, G., YANG, H., STABER, P. B., ZHANG, P., LEVANTINI, E., ALBERICH-JORDA, M., ZHANG, J., KAWASAKI, A. & TENEN, D. G. 2013. C/EBPa controls acquisition and maintenance of adult haematopoietic stem cell quiescence. *Nat Cell Biol,* 15**,** 385-94.

YERGEAU, D. A., HETHERINGTON, C. J., WANG, Q., ZHANG, P., SHARPE, A. H., BINDER, M., MARIN-PADILLA, M., TENEN, D. G., SPECK, N. A. & ZHANG, D. E. 1997. Embryonic lethality and impairment of haematopoiesis in mice heterozygous for an AML1-ETO fusion gene. *Nat Genet,* 15**,** 303-6.

YIP, B. H. & SO, C. W. 2013. Mixed lineage leukemia protein in normal and leukemic stem cells. *Exp Biol Med (Maywood),* 238**,** 315-23.

YOSHIHARA, H., ARAI, F., HOSOKAWA, K., HAGIWARA, T., TAKUBO, K., NAKAMURA, Y., GOMEI, Y., IWASAKI, H., MATSUOKA, S., MIYAMOTO, K., MIYAZAKI, H., TAKAHASHI, T. & SUDA, T. 2007. Thrombopoietin/MPL signaling regulates hematopoietic stem cell quiescence and interaction with the osteoblastic niche. *Cell Stem Cell,* 1**,** 685-97.

YUAN, Y., ZHOU, L., MIYAMOTO, T., IWASAKI, H., HARAKAWA, N., HETHERINGTON, C. J., BUREL, S. A., LAGASSE, E., WEISSMAN, I. L., AKASHI, K. & ZHANG, D. E. 2001. AML1-ETO expression is directly involved in the development of acute myeloid leukemia in the presence of additional mutations. *Proc Natl Acad Sci U S A,* 98**,** 10398-403.

ZENG, Z., SHI, Y. X., SAMUDIO, I. J., WANG, R. Y., LING, X., FROLOVA, O., LEVIS, M., RUBIN, J. B., NEGRIN, R. R., ESTEY, E. H., KONOPLEV, S., ANDREEFF, M. & KONOPLEVA, M. 2009. Targeting the leukemia microenvironment by CXCR4 inhibition overcomes resistance to kinase inhibitors and chemotherapy in AML. *Blood,* 113**,** 6215-24.

ZHANG, D. E., ZHANG, P., WANG, N. D., HETHERINGTON, C. J., DARLINGTON, G. J. & TENEN, D. G. 1997a. Absence of granulocyte colony-stimulating factor signaling and neutrophil development in CCAAT enhancer binding protein alpha-deficient mice. *Proc Natl Acad Sci U S A,* 94**,** 569-74.

ZHANG, H. & BRADLEY, A. 1996. Mice deficient for BMP2 are nonviable and have defects in amnion/chorion and cardiac development. *Development,* 122**,** 2977-86.

ZHANG, J., NIU, C., YE, L., HUANG, H., HE, X., TONG, W. G., ROSS, J., HAUG, J., JOHNSON, T., FENG, J. Q., HARRIS, S., WIEDEMANN, L. M., MISHINA, Y. & LI, L. 2003. Identification of the haematopoietic stem cell niche and control of the niche size. *Nature,* 425**,** 836-41.

ZHANG, P., IWASAKI-ARAI, J., IWASAKI, H., FENYUS, M. L., DAYARAM, T., OWENS, B. M., SHIGEMATSU, H., LEVANTINI, E., HUETTNER, C. S., LEKSTROM-HIMES, J. A., AKASHI, K. & TENEN, D. G. 2004. Enhancement of hematopoietic stem cell repopulating capacity and self-renewal in the absence of the transcription factor C/EBP alpha. *Immunity,* 21**,** 853-63.

ZHANG, S., FUKUDA, S., LEE, Y., HANGOC, G., COOPER, S., SPOLSKI, R., LEONARD, W. J. & BROXMEYER, H. E. 2000. Essential role of signal transducer and activator of transcription (Stat)5a but not Stat5b for Flt3-dependent signaling. *J Exp Med,* 192**,** 719-28.

ZHANG, Y. W., BAE, S. C., HUANG, G., FU, Y. X., LU, J., AHN, M. Y., KANNO, Y., KANNO, T. & ITO, Y. 1997b. A novel transcript encoding an N-terminally truncated AML1/PEBP2 alphaB protein interferes with transactivation and blocks granulocytic differentiation of 32Dcl3 myeloid cells. *Mol Cell Biol,* 17**,** 4133-45.

ZHOU, S., SCHUETZ, J. D., BUNTING, K. D., COLAPIETRO, A. M., SAMPATH, J., MORRIS, J. J., LAGUTINA, I., GROSVELD, G. C., OSAWA, M., NAKAUCHI, H. & SORRENTINO, B. P. 2001. The ABC transporter Bcrp1/ABCG2 is expressed in a wide variety of stem cells and is a molecular determinant of the side-population phenotype. *Nat Med,* 7**,** 1028-34.